

DISSERTATION ZUR ERLANGUNG DES DOKTORGRADES
DER FAKULTÄT CHEMIE UND PHARMAZIE
DER LUDWIG-MAXIMILIANS UNIVERSITÄT MÜNCHEN

**ADVANCED ENERGETIC MATERIALS:
STRATEGIES AND COMPOUNDS**



DAVIN GLENN PIERCEY

AUS

RED DEER, KANADA

2012

Erklärung

Diese Dissertation wurde im Sinne von § 7 der Promotionsordnung vom 28. November 2011 von Prof. Dr. Thomas M. Klapötke betreut.

Eidesstattliche Versicherung

Diese Dissertation wurde eigenständig und ohne unerlaubte Hilfsmittel erarbeitet.

München, den 11.12.2012

.....

(Davin Piercey)

Dissertation eingereicht am:

1. Gutachter Prof. Dr. Thomas M. Klapötke

2. Gutachter Prof. Dr. Konstantin Karaghiosoff

Mündliche Prüfung am06.02.2013.....

*It is not death that a man should fear,
but he should fear never beginning to live.*

-Marcus Aurelius

Acknowledgements:

Firstly, Prof. Dr. Thomas M. Klapötke must be thanked for the incredible experience the past three years have been. Not only for the opportunity to carry out my PhD work in your group, but also for the freedom to work on topics of my choice, for many calculations, conference travel, many useful discussions, and for going above and beyond helping me deal with German bureaucracy.

Next I must thank Prof. Dr. Konstantin Karaghiosoff for countless enthusiastic late-night and weekend crystal structure measurements, for being there to discuss NMR results, and finally being the second corrector of this thesis.

I would like to thank Dr. Jörg Stierstorfer for all the support provided; the solution of crystal structures and calculation of heats of formation and energetic performances would not have been possible without you.

The whole research group, and especially my lab must be thanked for providing a great working environment becoming good friends, and the constant (if unsuccessful) reminders to speak German. Dennis Fischer, thank you for the endless chemical discussions, your enthusiasm and knowledge in all things explosive, and hilarious conversations about home chemistry. Niko Fischer, thank you for providing many precursor compounds, weisswurst eating competitions, and finding a place for me to live. Susanne Scheutzow thanks for assistance with time consuming detonation tests. "St." Stefan Huber, thanks for the hundreds of sensitivity measurements and chemical orders. Richard Moll and Norbert Mayr, thanks for the extensive computer help.

All of my Bachelor, F-praktikum, and Masters students are acknowledged for help in my research; Andi, Martin, Michael ("Hasi"), Flo, Angie, Franzi, Max, Jan, Chris, Stefanie, and Christin.

Ms. Irene Scheckenbach is thanked for being a great secretary and helping me get settled when I first moved here.

Everyone associated with LMU analytical services (NMR, mass spectrometry, elemental analyses) is thanked for their contributions.

Everyone else who assisted with this work, or making my stay here pleasurable is also thanked.

Finally and above all, my parents are extensively thanked for their continuous support in every aspect of my life, for believing in me, and for tolerating my basement lab and chemistry experiments for years. My father is especially thanked for telling tales of blackpowder and firecrackers to me as a child likely sparking this lifelong interest in energetic materials.

Table of Contents

1. Introduction	
1.1 History of Explosives.....	1
1.2 Background and Definitions.....	3
1.3 Considerations in the Development of Modern Explosives.....	6
1.4 Strategies in Energetic Materials Design.....	11
1.5 References.....	19
1.6 Bibliography and Disclosure.....	21
2. Synthesis and Characterization of Energetic Salts of the $C_4N_{12}^{2-}$ Dianion.....	24
3. Copper Salts of Halo Tetrazoles: Laser-Ignitable Primary Explosives.....	32
4. Method for Preparation of a Lead-Free Primary Explosive.....	47
5. Improved Preparation of Sodium Nitrotetrazolate Dihydrate: Suitable for DBX-1 Preparation.....	56
6. Amination of Energetic Anions: High-Performing Energetic Materials	60
7. The 1,3-Diamino-1,2,3-Triazolium Cation: A Highly Energetic Moiety.....	69
8. The 1,4,5-Triaminotetrazolium Cation ($CN_7H_6^+$): A Highly Nitrogen-Rich Moiety.....	78
9. 1,1'-Azobis(tetrazole): A Highly Energetic Nitrogen-Rich Compound with a N10 Chain.....	85
9.1 Supporting Information.....	88
10. The 1,3-Bis(nitroimido)-1,2,3-triazolate Anion, the <i>N</i> -Nitroimide Moiety, and the Strategy of Alternating Positive and Negative Charges in the Design of Energetic Materials.....	98
11. The Synthesis and Energetic Properties of 5,7-Dinitrobenzo-1,2,3,4-tetrazine-1,3-dioxide (DNBTDO).....	108
12. Hydroxylammonium 5-Nitriminotetrazolates	117
13. Nitrotetrazolate-2 <i>N</i> -Oxides and the Strategy of <i>N</i> -Oxide Introduction.....	126
13.1 Supporting Info.....	137
13.2 Addition/Correction.....	144

14. Synthesis and Characterization of Alkaline and Alkaline Earth Salts of the Nitrotetrazolate-2 <i>N</i> -oxide Anion.....	145
15. The Taming of CN_7^- : The Azidotetrazolate-2-Oxide Anion.....	152
16. A Study of Cyanotetrazole Oxides and Derivatives Thereof.....	162
17. Pushing the Limits of Energetic Performance – The Synthesis and Characterization of Dihydroxylammonium 5,5'-Bistetrazolate-1,1'-diolate.....	174
17.1 Supporting Information.....	179
18. The Facile Synthesis and Energetic Properties of an Energetic Furoxan Lacking Traditional “Explosophore” Moieties: (E,E)-3,4-bis(oximomethyl)furoxan (DPX1).....	198
19. Curriculum Vitae.....	206

1. Introduction:

1.1 History of Explosives

Around 220 BC Chinese alchemists were attempting to separate gold from silver via extraction from the ore with potassium nitrate and sulfur in a furnace, however they neglected to add charcoal early in the process and tried to make up for it later. The heated mixture of potassium nitrate, sulfur, and charcoal, the mixture currently known as black powder, albeit in differing proportions, proceeded to explode. Despite the initial lack of exploitation, this marked the first known instance of humanity's experience with explosives. Knowledge of blackpowder in Western Europe was a considerably later, when the first description was by the monk, Roger Bacon, in England in 1249 AD. Between these times, there is mention of the use of black powder, and mixtures assumed to be black powder, for exploding war devices and fireworks by the Romans, Greeks, and Arabs between the 4th and 9th century. In 14th century Europe, the first crude firearm was described by a German monk, Berthold Schwarz; an iron tube capable of throwing stones, while the broad adoption of firearms in warfare took until the end of the 15th century, by which time crude grenades had also been invented. The composition of black powder was inconsistent across time and location until the 16th century when the composition stabilized, similar to the mix of today, at a 75:15:10 mixture of KNO_3 : Charcoal : Sulfur. Further developments were solely in the realm of processing techniques such as corning and pressing, and modification of charcoal types. The use of black powder in mining for blasting can be traced to 1627 by the Hungarian engineer Kaspar Weindl near the town of Selmeczbanya, and was introduced to England in 1670.^{1,2}

While the earliest development in explosives chemistry, blackpowder, found practical use in large quantities, the next significant discovery, that of fulminating gold,³ from dissolving gold oxide in ammonia, possessed such high sensitivity that it never found significant practical use. The German alchemist Sebald Schwaertzer mentions it in 1585 and this marks the discovery of the world's first high explosive (blackpowder is a low explosive and these distinctions will be explained further in the next section). Despite fulminating gold being known in the 16th century, its nature was not understood until the present, and even now the best description is that it is a mixture of polymeric compounds, incapable of being represented by a simple formula, where the partial hydrolysis of $[\text{Au}_2(\mu\text{-NH}_2)(\mu_3\text{-NH})_2]\text{Cl}$ is closest to reality.⁴ Mercury fulminate ($\text{Hg}(\text{CNO})_2$) followed soon after in 1630 by van Drebbel, and again was not fully characterized until modern times.³

The next major milestone came with the development of nitroglycerine (NG) in 1847 by Ascanio Sobrero, an Italian. Despite nitration attempts being made on glycerine since the 1830s, Sobrero was the first to cool the reaction allowing the formation of nitroglycerine instead of oxidation products. The explosive properties were noticed very soon after its discovery however NG was initially only used as heart medicine.⁵ Attempts were made to use nitroglycerine as a filling in shells, however the material's high sensitivity precluded this. Alfred Nobel patented its preparation and used NG in place of blackpowder for mining purposes, despite accidents in manufacture, transport, and initiation. Blackpowder filled detonators were initially used to detonate nitroglycerine, but these were later replaced by mercury fulminate filled blasting caps. The next major advancement in explosive science came in 1867 when 75 parts of nitroglycerin were mixed with 25 parts kieselguhr forming a dough-like material, dynamite, which far less sensitive and easier to handle than pure nitroglycerin. This invention was patented in 1867 and within a year a dozen factories for NG and dynamite existed in the world due to the popularity of the produced explosive. While Nobel is widely credited for the discovery of desensitizing nitroglycerine with kieselguhr, it is noteworthy that concurrently Russian chemist N. N. Zinin had been desensitizing NG with powdered magnesite and the produced "Magnesial'nyi" was being used for blasting Siberian gold mines in 1867. Dynamites at this point in time suffered from two major problems precluding military adoption, the first being the percentage of inert materials, and secondly, the tendency to exude nitroglycerin. The first was solved by the ammonia dynamites where nitroglycerin was mixed with ammonium nitrate and charcoal.⁶ The second was never worked around and nitroglycerin based explosives never found extensive military adoption, however in the civil sector they enjoyed wide use. In the 1950s ammonium nitrate based mixtures lacking nitroglycerin came into vogue and largely supplanted dynamites as the major explosives used in blasting.⁷

Within the military sector, blackpowder was not as easily replaced. Mention of picric acid can be found in the alchemical writings of Glauber as early as 1742 from the action of nitric acid on wool or horn, however it took till 1830 for Welter to suggest the use of picric acid as an explosive. During this time it found extensive use as a dye. Initially it was thought that only salts of picric acid were explosive and by 1871 potassium picrate was used for shell fillings in Great Britain and the USA. In 1873 Sprengel proved that picric acid would detonate under influence of a detonator and by the late 1800s picric acid was accepted as the basic high explosive for military uses.⁸ Unfortunately, picric acid easily forms metal salts

more sensitive than the pure acid, and was too sensitive to be used in armour piercing shells, so trinitrotoluene, first prepared in 1863, had largely replaced picric acid by the outbreak of the First World War.^{7,9}

After the first world war, research into higher performing explosives for military use commenced and by World War II both pentaerythritol tetranitrate (PETN) and cyclotrimethylenetrinitramine (RDX) were investigated. Of the two, RDX found greater use because it is less sensitive and more powerful than PETN, however PETN is still often found in niche uses due to higher performance in small charges. It is interesting to note that both PETN and RDX already had been used in medicine prior to adoption as an explosive, as a result of nitrates and nitramines being NO donors. While other major explosives have been developed for specialized uses such as higher performance or a high degree of insensitivity, none have enjoyed as wide use as RDX in the 20th century.

The final advancement in the 20th century in explosives science that will be mentioned is the process of plasticization whereby coating grains of an explosive such as RDX with a polymer matrix desensitizes the explosive.⁷

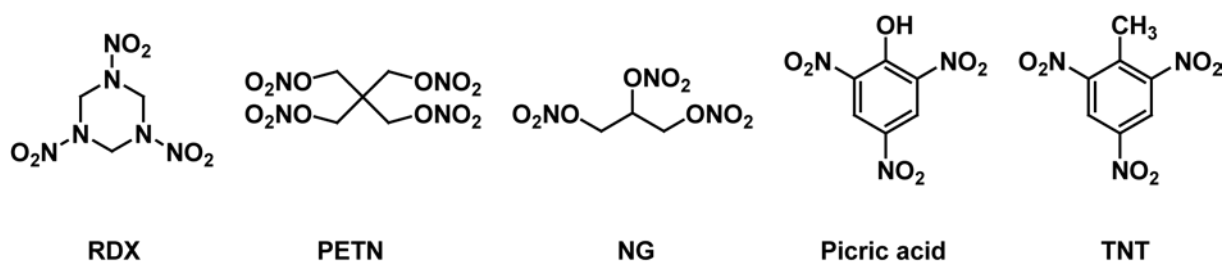


Figure 1. Common explosives and their structures

1.2 Background and Definitions

The Chemistry of Powder and Explosives defines an explosion as: “a loud noise and the sudden going away of things from the place where they have been.”¹⁰ While nuclear and physical explosions are known in addition to chemical, this work solely focuses on chemical explosives. Naturally, an explosive is a pure substance or mixture capable of causing an explosion, and explosives belong to the broader class of energetic materials. Energetic materials are defined by the American Society for Testing and Materials as “chemical compositions or compositions that contain both fuel and oxidizer and rapidly react to release energy and gas”¹¹ and is subdivided based on use into propellants, explosives, and

pyrotechnics based on whether the material is used for thrust generation, explosive effect, or visual properties (smoke, light). I, however, take issue with their definition (but not their subdivisions!) by saying an energetic material must possess both fuel and oxidizer, and release gas. The first criticism is based on the existence of high-nitrogen compounds that are most definitely explosive, while containing no oxidizing species, and also by 'oxidizer only' explosives such as ozone which is known to detonate upon solidification. Stating that an energetic material must also release gas is just as incorrect and easily disproven by the existence of cuprous acetylide Cu_2C_2 , which detonates forming only solid detonation products, the explosive effect resulting from the sudden heat release causing rapid expansion of nearby air. A better definition of energetic material would be "a metastable compound or mixture capable of the rapid release of stored potential energy." In this work we are mostly interested in new explosive materials, but due to the dual-use nature of energetic materials (for example, RDX is explosive, but is also capable of being used in propellants), attention at times may briefly turn to the application of these materials in propellants or pyrotechnics.

We have already distinguished that this thesis deals with chemical explosives; however, these can be divided into broad groups, low explosives and high explosives. In the simplest sense these can be differentiated based on the velocity and mechanism of reaction propagation. While traditional combustion requires atmospheric oxygen, reaction within explosive materials progress by either deflagration or detonation, neither of which require any external oxidant. In the case of deflagration, the mechanism consists of a very rapid auto combustion of energetic particles as a surface-only phenomenon via diffusion of heat and mass, and this will always occur at a rate lower than the speed of sound in the material. In a detonation, the reaction zone progresses faster than the speed of sound in the material. Due to the speed of reaction, a shockwave develops in the material which sustains the detonation by compressing material ahead of the reaction, heating it beyond its decomposition point. While it is noteworthy that a high explosive can deflagrate under appropriate conditions, it is not possible for a low explosive (such as black powder) to detonate as the reaction zone can only proceed by diffusion of heat and mass and reaction must occur at the interfaces of distinct particles. In contrast, a high explosive is a pure compound, and as such the necessity of reaction between particles is no longer needed, and a shockwave can trigger decomposition (and thus reaction propagation) within grains and not merely on the surface. Based on the distinct mechanisms of reaction in low vs. high explosives, as a low explosive is compressed and approaches maximum density, solid-solid instead of solid-gas reactions begin to

dominate during deflagration, and reaction rates decrease with increasing density. High, detonating, explosives show an increase in detonation velocity as density increases towards the maximum density because as sound travels faster in solids than gasses, as density increases, air spaces within the bulk explosive decrease. As a result of detonations progressing at at least the speed of sound in the material, and deflagrations relying on mass and heat flow, detonation reactions are far more rapid than deflagrations. Typical reaction speeds are on the order of 10^2 ms^{-1} for deflagrations and 10^4 m s^{-1} for detonations. This thesis is concerned with high explosives, pure chemical compounds capable of undergoing detonation.

A detonation can arise by two processes, a shock to detonation transition (SDT) or a deflagration to detonation transition (DDT). The simpler of the two is the SDT where an impinging shockwave will compress the explosive particles. The compressed explosive has its temperature raised adiabatically above the decomposition temperature, and the exothermic decomposition accelerates the shockwave. The process by which a DDT occurs is more complex and is not completely understood yet. Current thinking suggests that as a confined explosive deflagrates, hot combustion products intrude into the unreacted explosive increasing the deflagration rate until the material ahead of the explosive is compressed allowing compressive heating to occur, and when sufficient compression waves coalesce ahead of the deflagration zone, detonation breaks out once the critical shock initiation pressure of the explosive is exceeded.¹²

High explosives are grouped into two major classes, primary and secondary. When one considers an explosive device, a flame, spark or hot wire ignites a primary explosive, which undergoes a deflagration to detonation transition, and the shock wave produced is transmitted to a secondary explosive which detonates providing the bulk of the explosive work for the device. The classification of a primary vs. secondary is based on their position in the explosive sequence. Unfortunately, in the case of primary explosives, the ability to undergo a deflagration to detonation transition is a very unique phenomenon, and few materials are capable of undergoing this on a milligram scale, and those that are able are generally sensitive to mechanical stimuli making handling dangerous. For this reason they are often confined in blasting caps or detonators where they are shielded from friction and impact. There is a much wider variety of secondary explosives, and their relative insensitivity means their initiation must be with a shockwave of sufficient power, which is where the primary explosive comes in. Beyond their use in initiating secondary explosives, primaries also find

use for the ignition of propellants such as in firearm cartridges. The firing pin of a firearm impacts the primary containing primer on the round of ammunition, and the impact causes the primary to detonate, and the detonation is used to initiate a deflagration in the propellant powder.

1.3 Considerations in the development of modern explosives

Before we can begin to discuss new explosive materials, we must mention their characterization, beyond standard chemical characterization such as nuclear and vibrational spectroscopy. Explosive characterization can be broken into categories; performance characterization and safety characterization.

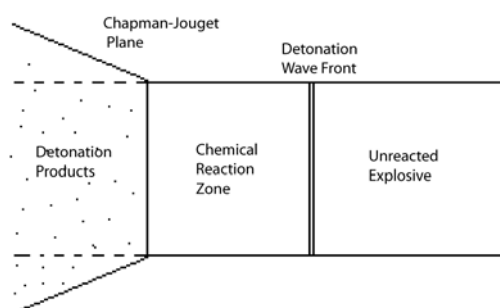


Figure 2. Schematic representation of the detonation process. The detonation wave moves from left to right.

Performance of explosive materials is most simply notated by the detonation velocity (V), and detonation pressure (p_{cj}). The detonation velocity is the speed at which the shockwave and chemical reaction zone propagates the reaction within an explosive material. The detonation pressure is calculated at the *Chapman-Jouguet* plane, the hypothetical plane behind the shockwave front that separates the zone following the chemical reaction zone immediately after the wavefront, and the zone where chemical reaction products are free to expand. (Figure 2) Detonation velocities of explosives can reach over 10000 m s^{-1} and detonation pressures can exceed 400 kbar. (for examples see Table 1) Unfortunately, while detonation velocities can be measured experimentally, detonation pressures cannot be, however pressure can be qualitatively correlated to experimental measures of the brisance. Brisance is the shattering power of an explosive, and can be relatively correlated to detonation pressure based on the cutting, denting, or fragmentation of a metal object by an explosive. In this thesis, detonation velocities and pressures have been calculated with the computer program EXPLO5. Detonation velocities and pressures are more relevant for the

discussion of secondary explosives, where these will accurately describe the performance of a bulk explosive. In the case of a primary explosive, the detonation velocity especially becomes less relevant for inter-explosive comparisons because of multiple types of primary explosives. In the first, metal free primary explosives such as cyanuric triazide ($(\text{CNN}_3)_3$) or tetracene, (Fig. 3) higher detonation velocities can be correlated with higher initiation abilities, however this group cannot be compared with the metal-containing primaries such as lead azide ($\text{Pb}(\text{N}_3)_2$) or silver fulminate (AgCNO) as the presence of a heavy metal slows the detonation wave. Despite the slower detonation velocities of heavy-metal containing primary explosives, many are excellent initiators, requiring far less mass for the initiation of a secondary when compared to a metal-free primary. Table 1 gives several primary and secondary explosives and their detonation parameters.

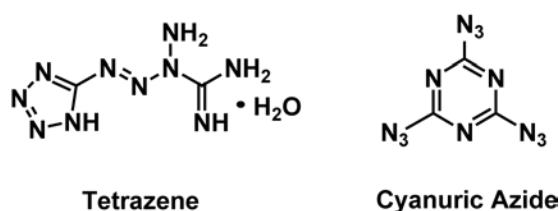
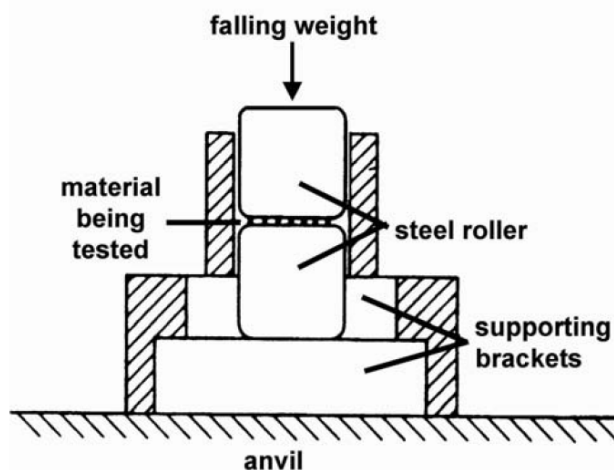


Figure 3. Tetrazene and Cyanuric azide: metal-free primary explosives



Figures 4 and 5. Drophammer and close-up of the sample holder

The safety characterization of explosive materials is described in terms of their sensitivity towards mechanical, thermal, and electrostatic stimuli. Mechanical sensitivity is divided into sensitivity towards impact and frictional forces. The impact sensitivity is

measured in Joules and is determined by the dropping of masses from various heights upon an explosive confined within a steel sleeve between two rollers.(Figure 4) The energy at which 1/6 samples will give an audible or visible decomposition is recorded as the sensitivity (BAM method). In the case of the measurement of sensitivity towards friction, a small quantity of explosive is placed between two ceramic pieces of controlled frictional coefficients. (Figure 5) A weight is applied to the upper ceramic unit, and the lower plate is scraped under this. The force (in Newtons) at which 1/6 samples gives an audible or visible decomposition is recorded as the sensitivity. Table 1 gives the mechanical sensitivities of various primary and secondary explosives, and an important trend can be noticed; generally primary explosives are far more sensitive than secondary explosives. Thermal stability measurements of explosives are measured by differential scanning calorimetry; a sample of explosive is heated at a known rate (in this work $5\text{ }^{\circ}\text{C min}^{-1}$ unless otherwise noted), and the temperature of the explosive is measured relative to a reference. Endothermic events such as melting point or loss of hydration waters, and exothermic events such as decomposition are both easily determined. Some mechanical and thermal stabilities are given in Table 1. Finally, electrostatic sensitivity is measured by sending a spark of known electrical energy through a sample of explosive, and the minimal energy for decomposition is recorded. (Figure 7) Energy release is controlled by varying the capacitance and voltage of the electrostatic spark machine by $E=1/2CV^2$. Electrostatic sensitivity is very dependent on particle size and shape; the smaller the particle size, the more sensitive. For the laboratory investigation of explosives, it is important that the electrostatic sensitivity of the compound be less sensitive than 25 mJ, as the human body can easily generate this. For an industrially-produced compound, far higher energies are capable of being generated by manufacturing processes so the measured value will determine the margin of safety available.

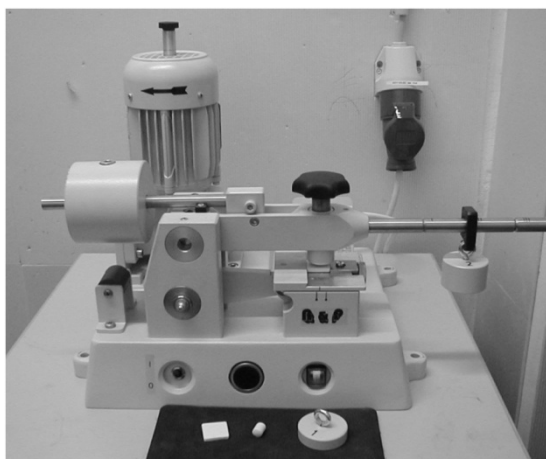


Figure 6. Friction tester



Figure 7. Electrostatic test equipment

Table 1. Common explosives and their properties

Explosive	Primary	Secondary	ρ (g cm ⁻³)	T_{dec} (°C)	Impact sensitivity (J)	Friction Sensitivity (N)	V_{det} (m s ⁻¹)	p_{cj} (kbar)
NG		X	1.59	200	0.2	<5	7800	260
TNT		X	1.65	300	15	353	7300	220
RDX		X	1.82	210	7.5	120	8900	340
PETN		X	1.78	150	3	60	8300	320
Pb(N ₃) ₂	X		4.71	350	<1	<5	5400 ¹³	-
Ag(CNO)	X		3.94	170	<1	<5	1700 ¹⁴	-
(CNN ₃) ₃	X		1.74	94	<1	<5	8300	280
Tetrazene	X		1.68	160	1	<5	5900	110

We have previously mentioned the two uses of primary explosives, for initiation of a secondary in an explosive device, and for the ignition of a propellant in a round of ammunition. Each use mandates a slightly different primary; for the initiation of a secondary, the production of a high-strength shockwave from a DDT is the end goal, whereas for ignition of a propellant, the strength of the SDT is not as important as the hot particles produced which ignite the propellant. This means that in, for example, a firearm primer, the primary explosive used does not need to be as effective as in a primary intended for detonation of a secondary. This is seen in the compounds used, lead azide, often used to initiate a secondary is capable of initiating TNT with only 160 mg¹⁵ whereas even 1.0 g of lead styphnate, the primary used in firearm primers, will not initiate PETN,¹⁶ and PETN is easier to initiate than TNT! In this thesis, when we discuss primary explosives, we are

generally relating to the first class, those capable of initiating a detonation wave in a secondary explosive when only small amounts of primary are used.

Secondary explosives also show a range of uses. Firstly, those used in mining are usually ammonium nitrate mixtures. Ammonium nitrate mixtures show very slow detonation velocities ($\sim 5000 \text{ m s}^{-1}$) and possess low detonation pressures and brisances. For mining this is desirable; a slow heaving effect is more desired to break ore into manageable chunks. If a brisant explosive was used the rocks would be powdered and blown away instead of fragmented and moved. The topic of ammonium nitrate mixtures is beyond the scope of this thesis, as mining explosives are more of a technological topic instead of chemical as the cheapness of ammonium nitrate precludes any major change in base chemical being used. The next major high explosive use is military TNT and TNT-type explosives and formulations. These generally possess higher detonation velocities on the order of $6000\text{-}8000 \text{ m s}^{-1}$, and are used as melt-castable fillings for bombs and grenades. The brisance of these explosives is higher than AN mixtures, however it is not sufficient for the cutting of metal. For cutting explosives, the RDX mixtures are the standard, with HMX (cyclotetramethylene tetranitramine) being used if higher performance in a smaller package is desired. PETN also finds use due to its ability to outperform RDX in small charges. The higher sensitivity of these brisant explosives mean that they are often desensitized with lower-sensitivity explosives such as TNT, or non energetic binders like polyisobutylene in the case of C4 plastic explosive. Finally, there, is the use of thermally stable explosives for mining and oilfield uses; HNS (hexanitrostilbene (Figure 8)) is used for the perforation of oil wells deep underground where other explosives would decompose before the appropriate time.

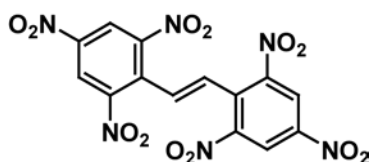


Figure 8. Hexanitrostilbene

This brings us to the next topic, the multitude of areas of research in explosive materials.

- ✓ RDX replacements: RDX, despite being relatively cheap, easy to make, and powerful however its replacement is being driven by its high environmental cost; it is both toxic and carcinogenic. An RDX replacement should be stable above $180 \text{ }^{\circ}\text{C}$, possess

comparable or higher performances, be of comparable or lower sensitivity, and of course, be of lower toxicity.

- ✓ Pushing the limits of energetic performance: working to develop materials that are more powerful than anything known, while possessing adequate sensitivity and thermal stability properties.
- Insensitive munitions: High explosives that are extremely insensitive to mechanical stimuli for use in the most demanding environments.
- HNS replacements: Thermally stable high explosive that is less toxic and more thermally stable than HNS for underground use.
- ✓ Lead azide replacements: lead azide is the most commonly used initiating primary explosive, however the toxicity of lead means finding a replacement with comparable sensitivity, thermal and initiatory properties is desired. Similar to this is the development of primaries for the replacement of cadmium azide, the primary used when extreme thermal stability is mandated.
- TNT replacements: a melt-castable high explosive with performance comparable to TNT that is significantly less toxic.
- ✓ Academic research: work with novel energetic systems to determine factors affecting stability and performance and to bring new strategies into explosive design.
- Lead styphnate replacements: lead has shown to be a major contaminant of firing ranges so a lead-free drop-in replacement for firearm primers is desired.

In this work, most important is the exploration of new or exotic synthetic strategies or functional groups for the tailored design of energetic materials of desired properties. In various capacities, all checkmarked items in the list above are covered.

1.4 Strategies in energetic materials design.

There are three major methods of imparting potentially explosive energy into a molecule; fuel and oxidizer being contained in the same molecule, compounds possessing ring or cage strain, and high heat of formation compounds. These generally are used combined giving explosives with energy content resulting from multiple sources. In an explosive possessing both fuel and oxidizer, the separation of fuel (carbon) and oxidizer (oxygen) creates a thermodynamic downhill slope, and thus energy content, towards the formation of oxidized species upon detonation. When a caged or cyclic explosive compound possesses bond strain resulting from the geometry of the compound, this stored energy

contributes to the energy released upon detonation. Similarly, nitrogen atoms in an explosive are at a higher potential energy compared to nitrogen gas as a result of the higher thermodynamic stability of a nitrogen-nitrogen triple vs. single or double bond, thus the formation of nitrogen gas from a nitrogenous explosive can create explosive energy release. The case of nitrogen is unique where higher bond order results in greater stability, carbon shows the opposing trend and small molecules containing carbon-carbon triple bonds such as acetylene and acetylides are explosive solely based on heat of formation!

For example, consider a cube of eight carbon atoms with a nitro upon each; octanitrocubane. Upon detonation the bond strain in the heavily strained cubane is released, the eight carbon atoms are fully oxidized to CO₂ by the oxygen within the nitro groups, and the nitrogen in the nitro groups forms nitrogen gas; all three strategies in explosive design contribute to explosive output.

In the design of new energetic materials for practical use, one needs to consider the performance, sensitivities, environmental and personal toxicities, and cost of production. Of all the driving forces driving energetics research, environmental concerns are one of the most powerful. Unfortunately for the chemist, this excludes many of the very traditional explosophoric groups useful for the design of energetic materials such as aromatic nitro, or nitramino, or in the case of primaries, the heavy metals often paired with energetic anions such as lead or cadmium. First, aromatic nitro groups often give highly toxic compounds unless the material is totally insoluble, for example extensively used TNT has been demonstrated to have carcinogenic effects in rats, contaminates water at munitions sites, and affects male fertility.¹⁷ RDX, HMX, CL-20 and other nitramine-containing explosives are no better, being possible human carcinogens.¹⁸ Due to these toxicity concerns, two of the largest classes of compounds within explosives, nitramines and aromatic nitro compounds have been precluded for use in new environmentally-friendly explosives! Luckily, explosives based on nitrogen-rich compounds are generally less toxic. In the case of primary explosives, the production of finely divided lead aerosols from the use of lead azide or lead styphnate has been the cause of multiple health concerns.¹⁹ Lead and other heavy metals are often used in primaries as the deflagration to detonation transition proceeds more readily when compared with less toxic alkali or alkali earth salts for a reason that is not well understood, but can be qualitatively correlated with both the covalent nature of the metal-anion bond and the ionization potential of the metal cation.²⁰

The backbone of new energetic materials relying significantly on heat of formation for energy content is often a five or six membered nitrogen heterocycle. In both the five and six membered rings from pyrrole to pentazole, and the six membered rings from pyridine to hexazine there is a spectrum of energy content and stabilities. Unfortunately, there is a limit on the energy content before the system becomes generally unstable. For the five membered heterocycles, this limit is tetrazole, after which pentazoles, while known are not stable at room temperature.²¹ In the case of six-membered heterocycles, this limit comes at tetrazines, where pentazines and hexazines are not known. In this work, many energetic materials based on high-nitrogen backbones such as tetrazoles, triazoles, and tetrazines, have been prepared.

Chapter 2 details the preparation of a series of nitrogen-rich salts of the $C_4N_{12}^{2-}$ anion, (Figure 9) these compounds were found to be thermally stable, however their performance as secondary explosives was low due to hydration waters and poor oxygen balances. The silver salt, proved far more interesting, exhibiting a deflagration to detonation transition when even the smallest amount was introduced to a flame, while being thermally stable with sensitivity parameters comparable to lead azide. For primary explosives, simply the heat of formation of the compound can be correlated to initiating ability, and this was seen with the silver salt being able to initiate RDX.

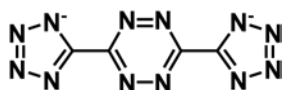


Figure 9. The $C_4N_{12}^{2-}$ dianion

Other heavy metal salts of tetrazoles were investigated as primary explosives. Chapter 3 describes the investigation of the copper (II) salts of chloro- and bromotetrazoles as primary explosives. (Figure 10) The chloro was found to be the better performer of the two, while both exhibited adequate sensitivities and thermal stabilities to be lead azide replacements. Within primary explosive research, copper (I) nitrotetrazolate (DBX1) (Figure 11) has proven to be a more than capable “drop in” lead azide replacement and was developed by *Pacific Scientific Energetic Materials Company*.²² The explosive and sensitivity properties of DBX1 are so similar to lead azide that it can replace lead azide in explosive devices with no re-engineering. During the synthesis of DBX1, 5-aminotetrazole must first be converted to sodium nitrotetrazolate, and then the copper (I) salt prepared in a two-pot process. In chapter 4, a new, patented, one pot preparation from 5-aminotetrazole for this (amazing) primary explosive is presented. Following this, Chapter 5, is an improved

procedure for the preparation of sodium nitrotetrazolate from 5-aminotetrazole. This procedure avoids the intermediate step of handling a highly-sensitive explosive intermediate (the acid salt of copper (II) nitrotetrazolate) involved in previous “state of the art” procedures.²³

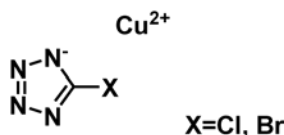


Figure 10. Copper (II) salts of chloro- and bromo tetrazoles

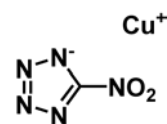


Figure 11. Copper (I) nitrotetrazolate, DBX1

Returning to secondary explosives, we utilized a facile method of increasing the nitrogen content and energetic performances of nitrogen heterocycles: *N*-amination. Using *N*-amination, an energetic anion can be transformed into a neutral explosive, and the amination of a neutral explosive gave nitrogen rich energetic cations. In chapter 6, stable neutral energetic materials were created by the amination of 5-nitrotetrazolate, 3,5-dinitro-1,2,4-triazolate, 1,1'-bistetrazolate, and tetrazolate. (Figure 12) Of these, the 1-amino-3,5-dinitro-1,2,4-triazolate shows promise as a melt-castable high explosive with performances comparable to RDX.

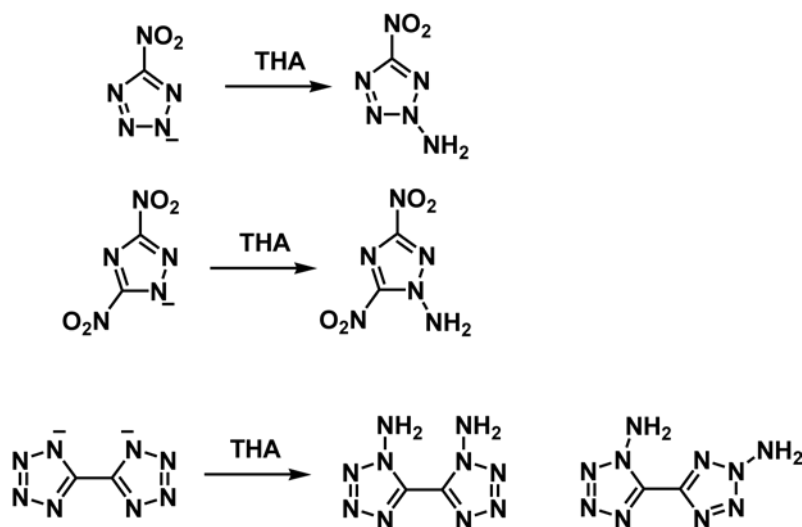


Figure 12. Amination of energetic anions (THA: *O*-tosylhydroxylamine)

Chapter 7 details the amination of 1-amino-1,2,3-triazole giving the 1,3-diamino-1,2,3-triazolium cation, salts of which are stable, high performing energetic materials that

would be capable RDX replacements if not for their high sensitivity towards impact and friction. (Figure 13) The 5-membered chain of nitrogen atoms is already pushing the limits of how much energy can be stored in a heterocycle based solely on heat of formation, while remaining thermally stable. In Chapter 8, we have exceeded all reasonable stabilities by the amination of 1,5-diaminotetrazole to the 1,4,5-triaminotetrazolium cation (CN_7H_6^+). (Figure 13) This cation, salts of which possess RDX like explosive performances, possessed the mechanical sensitivities of primary explosives, making handling difficult, and all decomposed below 100°C , rendering them useless.

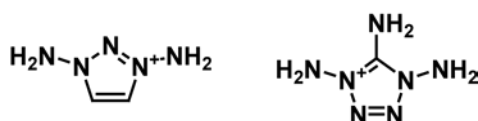


Figure 13. The 1,3-diamino-1,2,3-triazolium and 1,4,5-triaminotetrazolium cations: five and six membered contiguous chains of nitrogen atoms

For further study of the properties of explosive materials with high heat of formations and nitrogen contents, two azo compounds with eight (Chapter 6) and ten canted nitrogen atoms (Chapter 9) were prepared. (Figure 13) Both possess very high sensitivities, often exploding without reason, precluding handling on scales above several dozen milligrams, while their explosive performances are very high.

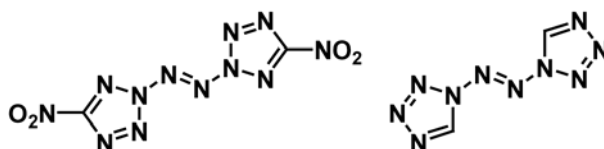


Figure 14. 2,2'-azobis(5-nitrotetrazole) and 1,1'-azobis(tetrazole) with eight and ten contiguous nitrogen atoms respectively: compounds that prefer to explode rather than sit quietly.

At this point we have pushed the limits of explosives based solely on heats of formation to their limits; only so much nitrogen can be incorporated into a molecule before the molecule is so thermodynamically unstable that any stimulus will initiate detonation. The reason that high nitrogen systems are often unstable is that while a nitrogen atom can be considered isoelectronic to a CH group, the lone pair of electrons on the nitrogen atom can donate into adjacent σ^* orbitals destabilizing the system.²⁴ This is the reason while benzene (C_6H_6) is stable, hexazine (N_6) is not; current thought is that the design of stable nitrogen

rich systems must adequately separate the σ and π electron systems.²⁵ Tartakovsky has reviewed several of these methods in a most excellent report,²⁶ and they are also briefly described in chapter 10. Most relevant to this work is removal of lone pair electron density on (preferably alternating) nitrogen atoms within a nitrogen rich system. This effect of stabilization is most readily seen in the 1,2,3,4-tetrazines; by themselves they are highly unstable with only one example being known,²⁷ and even that decomposes below 100 °C. (Figure 15) When the 1,2,3,4-tetrazine system is oxidized once to the 1,2,3,4-tetrazine-1-oxides, stability is seen to increase and there is a wide variety of benzo-annulated 1,2,3,4-tetrazine-1-oxides known.²⁸ The stability increase when another oxide is added is far more pronounced; as a rule the 1,2,3,4-tetrazine-1,3-dioxides are stable to over 200 °C as a result of lone pair electron density being removed on alternate atoms. Chapter 11 details the properties of a RDX-like high explosive based on this theory: 5,7-dinitrobenzo-1,2,3,4-tetrazine-1,3,-dioxide. (Figure 15)

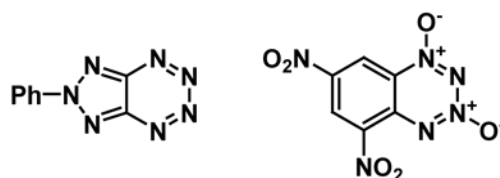


Figure 15. A unstable 1,2,3,4-tetrazine and a stable 1,2,3,4-tetrazine-1,3-dioxide.

Beyond the ability of *N*-oxidation to stabilize nitrogen systems, they also have the advantages that they can increase the oxygen balance of an otherwise oxidizer-poor high explosive, and increase the density of the explosive. The zwitterionic nature of the *N*-oxide increases the density of the explosive by allowing more extensive intermolecular bonding, which can result in very positive gains in detonation velocity and pressure as both are heavily dependent on density. (Chapter 12 details the preparation of dense hydroxylammonium salts of nitriminetrazoles where the significant density advantage of hydroxylammonium compared to triaminoguanidinium results in superior explosive performance.) The increase in interactions can also be advantageous from the sensitivity standpoint, as less sensitive explosives often possess extensive inter- and intramolecular interactions. A significant portion of this thesis (chapters 13-17) explores the oxidation of tetrazoles to their oxides. Nitro, cyano, azido, and bistetrazoles have all been oxidized to their respective oxides in this work, (Figure 16) and energetic salts characterized. Significant insights gained by this work

are that tetrazole *N*-oxidation increases density, and performance, while decreasing sensitivity. Unfortunately, thermal stabilities were seen to decrease, however in the case of the 5,5'-bistetrazolate-1,1'-dioxides, the hydroxylammonium salt (TKX50, Chapter 17, Figure 17) this decrease was not to the degree of precluding practical use, and is of such high performance and low sensitivity that it is being considered as a low-toxicity HMX replacement! Another useful insight gained from tetrazole oxidation is that while the silver salts of the parent tetrazoles are high-efficiency primary explosives, the silver salts of the corresponding tetrazole oxides are far less sensitive and some do not even undergo a deflagration to detonation on gram-scale! This may be the result of there being more metal-oxygen bonds in the oxide vs. the parent tetrazole, leading to more ionic instead of covalent interactions. As mentioned earlier, the covalent/ionic nature of metal-anion bonds in primary explosives can determine their efficiencies and ability to undergo a DDT as primary explosives.

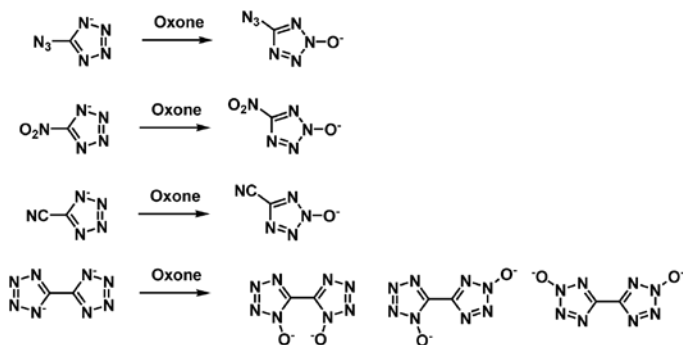


Figure 16. Oxidation of energetic tetrazoles to their oxides

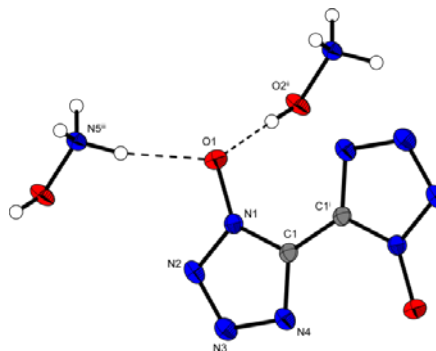


Figure 17. TKX-50. Most useful compound produced from tetrazole oxidations

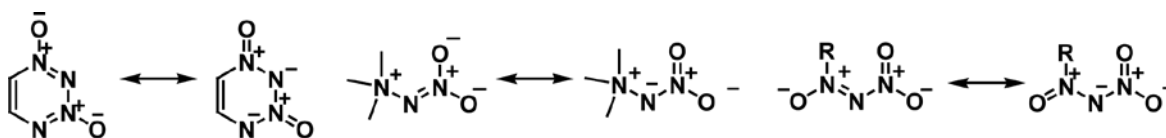


Figure 18. APNC resonance forms in tetrazine dioxides, nitroimides, and nitrodiazine oxides.

Of interest is the ability of unique nitrogen-rich stable systems such as 1,2,3,4-tetrazine-1,3-dioxides, nitrodiazine oxides, and *N*-nitroimides to be represented by the “alternating positive negative charge” (APNC) theory,²⁹ where one potential resonance form possesses positive and negative charges on alternating atoms. (Figure 18) This representation is useful to explain the properties seen by such systems, such as high stabilities and densities and can be useful for the prediction of stability in novel compounds and

systems. In chapter **10** we investigate an extreme example of this class of compound, salts of the 1,3-di(nitroimide)-1,2,3-triazolate anion, which is capable of being represented with *NINE (!)* alternating positive and negative charges. (Figure 19) Computational work confirmed the significance of this resonance form, and experimental results suggested that the APNC strategy can form dense explosives of exceedingly high performance which are thermally stable, unfortunately, they remained highly sensitive to mechanical stimuli. The silver salt is a potentially useful primary explosive.

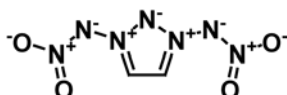


Figure 19. APNC resonance forms in tetrazine dioxides, nitroimides, and nitrodiazine oxides.

Details of all these strategies and compounds are presented in extensive detail in their respective chapters.

1.5 References:

1. B. T. Federoff, O. E. Sheffield, *Encyclopedia of Explosives and Related Items*, VII, Picatinny Arsenal, Dover, NJ. **1975**, H117-H131.
2. B. T. Federoff, O. E. Sheffield, *Encyclopedia of Explosives and Related Items*, II, Picatinny Arsenal, Dover, NJ. **1962**, B166-B169.
3. T. Urbański, *Chemistry and Technology of Explosives*, III, Pergamon Press, **1967**, 129-131.
4. G. Steinhauser, J. Evers, S. Jakob, T. M. Klapötke, G. Oehlinger, *Gold. Bull.* **2008**, *41*, 305-307.
5. T. Urbański, *Chemistry and Technology of Explosives*, II, Pergamon Press, **1965**, 32-34.
6. B. T. Federoff, O. E. Sheffield, *Encyclopedia of Explosives and Related Items*, III, Picatinny Arsenal, Dover, NJ. **1966**, D1584-1588
7. T. M. Klapötke, *Chemistry of High-Energy Materials*, De Gruyter, Berlin, **2011**, 3-7
8. T. Urbański, *Chemistry and Technology of Explosives*, I, Pergamon Press, **1964**, 472-474.
9. S. M. Kaye, *Encyclopedia of Explosives and Related Items*, IIX, Picatinny Arsenal, Dover, NJ. **1978**, P285-P286.
10. T. L. Davis, *The Chemistry of Powder and Explosives*, Angriff Press, 1941, 1.
11. www.astm.org
12. P. M. Dickson, J. E. Field, *Proc. R. Soc. Lond. A.* **1993**, *441*, 359-375.
13. B. T. Federoff, H. A. Asronson, E. F. Reese, O. E. Sheffield, G. D. Clift, *Encyclopedia of Explosives and Related Items*, I, Picatinny Arsenal, Dover, NJ. **1960**, A549.
14. F. P. Bowden, H. T. Williams, *Proc. Roy. Soc. Lond. A* **208**, **1951**, 176-188.
15. T. Urbański, *Chemistry and Technology of Explosives*, III, Pergamon Press, **1967**, 204.
16. T. Urbański, *Chemistry and Technology of Explosives*, III, Pergamon Press, **1967**, 218.
17. P. Richter-Torres, A. Dorsey, C. S. Hodes, *Toxicological Profile for 2,4,6-Trinitrotoluene*, US Department of Health and Human Services, Public Health Service, Agency for Toxic Substances and Disease Registry, **1995**.

18. W. McLellan, W. R. Hartley, M. Brower, *Health advisory for hexahydro-1,3,5-trinitro-1,3,5-triazine*. Technical report PB90-273533; Office of Drinking Water, U.S. Environmental Protection Agency: Washington, DC, **1988**.
19. M. E. Barsan, A. Miller, *Lead Health Hazard Evaluation*. 1996. HETA Report No. 91-0346-2573.
20. C. M. Tarver, T. C. Goodale, M. Cowperthwaite, M. E. Hill, *Structure/Property Correlations in Primary Explosives*. Report on Project SF3354-317, SRI International: Menlo Park, CA for US Naval Sea Systems Command, **1977**, contract no. N00024-76-C-5329.
21. Carlqvist, P.; Ostmark, H.; Brinck, T. *J. Phys. Chem. A* **2004**, *108*, 7463-7467.
22. J. W. Fronabarger, M. D. Williams, W. B. Sanborn, J. G. Bragg, D. A. Parrish, M. Bichay, *Propellants, Explos. Pyrotech.* **2011**, *36*, 541-550
23. W. H. Gilligan, M. J. Kamlet, US Patent 4093623, **1978**.
24. S. Inagake, N. Goto, *J. Am. Chem. Soc.* **1987**, *109*, 3234-3240.
25. M. Noyman, S. Zilberg, Y. Haas, *J. Phys. Chem. A*. **2009**. *113*, 7376-7382.
26. V. A. Tartakovsky, *Mat. Res. Soc. Symp. Proc. Vol 418*. **1996**, 15-24.
27. T. Kaihoh, T. Itoh, K. Yamaguchi, A. Ohsawa, *J. Chem. Soc., Chem. Commun.*, **1988**, 1608-1609.
28. A. M. Churakov, V. A. Tartakovsky, *Chem. Rev.* **2004**, *104*, 2601-2616.
29. H. Shechter, M. Venugopal, D. Srinivasulu, *Synthesis of 1,2,3,4-Tetrazine Di-N-Oxides, Pentazole Derivatives, Pentazine Poly-N-oxides and Nitroacetylenes*. Project 746566, Grant No FA 9550-40-1-0410. USAF AFRL Arlington, Virginia, **2006**.

1.6 Bibliography and Disclosure

The chapters in this thesis are reproductions with permission from the journals in which the work was originally published. Licenses have been obtained in cases where the journal requires it. In the cases of articles in the review process or patents in the process of being filed, the most recent draft or attorney docket is used respectively. Below are the sources or intended publication locations by chapter.

2. Thomas M. Klapötke, **Davin G. Piercey**, Florian Rohrbacher, Jörg Stierstorfer. "Synthesis and Characterization of Energetic Salts of the $C_4N_{12}^{2-}$ Dianion" *Zeitschrift fuer Anorganische und Allgemeine Chemie*. **2012**, 638, 2235-2242.
3. Denis Fischer, Thomas M. Klapötke, **Davin G. Piercey**, Jörg Stierstorfer. "Copper salts of halotetrazoles: laser-ignitable primary explosives" *Journal of Energetic Materials*. **2012**, 30 [1] 40-54.
4. Thomas M. Klapötke, **Davin G. Piercey**, John W. Fronabarger, Michael D. Williams "A Simple One-Pot Synthesis of Copper (I) nitrotetrazolate from 5-aminotetrazole" **2012**, Patent in Progress, provisional patent number 61/680766.
5. Thomas M. Klapötke, Neha Mehta, Karl D. Oyler, Davin G. Piercey. "Improved Preparation of Sodium Nitrotetrazolate Dihydrate: Suitable for DBX-1 Preparation" Not yet submitted for publication, will be submitted to *Zeitschrift fuer Anorganische und Allgemeine Chemie*.
6. Thomas M. Klapötke, **Davin G. Piercey**, Jörg Stierstorfer. "Amination of Energetic Anions: High-Performing Energetic Materials" *Dalton Transactions*. **2012**, 41, 9451-9459.
7. Thomas M. Klapötke, **Davin G. Piercey**, Jörg Stierstorfer. "The 1,3-Diamino-1,2,3-triazolium Cation: A Highly Energetic Moiety." *European Journal of Inorganic Chemistry*, **2012**, accepted, DOI:10.1002/ejic.201201237.
8. Thomas M. Klapötke, **Davin G. Piercey**, Jörg Stierstorfer. "The 1,4,5-Triaminotetrazolium Cation: A Highly Nitrogen Rich Moiety" *European Journal of Inorganic Chemistry*. **2012**, DOI: 10.1002/ejic.201200964, Early View.

9. Thomas M. Klapötke, **Davin G. Piercey**. “1,1’-azobis(tetrazole):A Highly Energetic Nitrogen-Rich Compound with a N10 Chain” *Inorganic Chemistry*. **2011**, 50 [7] 2732-2734.
10. Thomas M. Klapötke, Christian Petermeyer, **Davin G. Piercey**, Jörg Stierstorfer. “The 1,3-Bis(nitroimido)-1,2,3-triazolate Anion, the *N*-Nitroimide Moiety, and the Strategy of Alternating Positive and Negative Charges in the Design of Energetic Materials” *Journal of the American Chemical Society*. Accepted ja310384y
11. Thomas M. Klapötke, **Davin G. Piercey**, Jörg Stierstorfer, Michael Weyrauther. “The Synthesis and Energetic Properties of 5,7-Dinitrobenzotetrazine-1,3-Dioxide.” *Propellants, Explosives, Pyrotechnics*, **2012**, 37, 527-535.
12. Niko Fischer, Thomas M. Klapötke, **Davin G. Piercey**, Jörg Stierstorfer. “Hydroxylammonium 5-Nitriminotetrazolates” *Zeitschrift fuer Anorganische und Allgemeine Chemie*. **2012**, 638 [2], 302-310.
13. Michael Göbel, Konstantin Karaghisoff, Thomas M. Klapötke, **Davin G. Piercey**, Jörg Stierstorfer. “Nitrotetrazolate-2*N*-oxides, and the Strategy of *N*-oxide Introduction” *Journal of the American Chemical Society*. **2010**, 132 (48), 17216-17226.
14. Martin Härtel, Thomas M. Klapötke, **Davin G. Piercey** and Jörg Stierstorfer. “Synthesis and Characterization of Alkaline and Alkaline Earth Salts of the Nitrotetrazolate-2*N*-oxide Anion”. *Zeitschrift fuer Anorganische und Allgemeine Chemie*. **2012**, 638, 2008-2014.
15. Thomas M. Klapötke, **Davin G. Piercey**, Jörg Stierstorfer. “The Taming of CN7: The Azidotetrazolate-2-Oxide Anion. *Chemistry a European Journal*. **2011**, 17 [46] 13068-13077.
16. Franziska Boneberg, Angie Kirchner, Thomas M. Klapötke, **Davin G. Piercey**, Jörg Stierstorfer. “A Study of Cyanotetrazole Oxides and Derivatives Thereof” *Chemistry An Asian Journal*. **2012**, Early view, DOI 10.1002/asia.201200903.
17. Dennis Fischer, Niko Fischer, Thomas M. Klapötke, **Davin G. Piercey**, Jörg Stierstorfer. “Pushing the Limits of Energetic Performance – The Synthesis and

Characterization of Dihydroxylammonium 5,5'-Bistetrazolate-1,1'-diolate" *Journal of Materials Chemistry* **2012**, 22, 20418-20422.

18. Thomas M. Klapötke, **Davin G. Piercey**, Jörg Stierstorfer. "The Facile Synthesis and Energetic Properties of an Energetic Furoxan Lacking Traditional 'Explosophore' Moieties: (E,E)-3,4-bis(oximomethyl)furoxan (DPX1)" *Propellants, Explosives, Pyrotechnics*. **2011**, 36 [2], 160-167.

Synthesis and Characterization of Energetic Salts of the (C₄N₁₂²⁻) Dianion

Thomas M. Klapötke,^{*,[a]} Davin G. Piercey,^[a] Florian Rohrbacher,^[a] and Jörg Stierstorfer^[a]

Dedicated to Professor Hanns-Peter Boehm on the Occasion of His 85th Birthday

Keywords: Tetrazoles; Tetrazines; High energy density materials; Nitrogen-rich compounds; Energetic materials

Abstract. 3,6-Bis(tetrazol-5-yl)-1,2,4,5-tetrazine is a nitrogen-rich energetic compound readily prepared and a strong dibasic acid. By the reaction with energetic bases such including hydroxylamine, triamino-guanidine, hydrazine, and diaminourea, multiple ionic energetic materials were prepared and characterized for the first time. Both chemical (multinuclear NMR, Infrared, Raman, MS, etc) as well as explosive

(Impact, Friction, Static sensitivities) properties are reported. The materials prepared, with the exception of the silver salt, which is a primary explosive, fall into the classification of low-sensitivity energetic materials due to desensitizing hydration waters. Calculated explosive performances using the EXPLO5 computer code are also reported.

Introduction

Nitrogen-rich compounds play an important role in the design of all types of energetic materials: propellants, explosives, and pyrotechnics.^[1–3] Driving this strategy in energetic materials design is the desire for compounds and formulations that are both highly energetic and environmentally friendly. Unlike traditional energetic materials such as RDX and TNT (1,3,5-trinitro-1,3,5-triazinane and 2,4,6-trinitrotoluene, respectively), which rely on the oxidation of a carbon backbone by oxygen atoms in nitro groups, nitrogen rich compounds derive their energetic properties from the high heats of formation of N–N bonds and their thermodynamic driving force towards the formation of nitrogen gas.^[4,5] However, this strategy is limited by the fact that when nitrogen content and associated heats of formation get excessively high, the stabilities decrease.^[5] Conversely, when nitrogen content decreases, the stability of the compound does increase, however the energetic performances concurrently decrease. For example, when the series of five- and six-membered nitrogen heterocycles are considered, tetrazoles and tetrazines occupy the “middle ground” on the stability versus performance continuum, where heterocycles with additional nitrogen are too unstable, and heterocycles with less nitrogen are of lacklustre performance.^[6,7]

The tetrazole heterocycle, depending on ring substituents and anion/cation pairing has demonstrated its ability to form

energetic materials of a wide range of properties, such as being used in the preparation of new high-performing primary and secondary explosives with variable mechanical and thermal stabilities. For example, DBX-1, copper(I) nitrotetrazolate, is a next generation high-performance primary explosive that will replace lead azide, and hydroxylammonium nitriminetetrazolate is a prospective RDX replacement.^[8,9] The 1,2,4,5-tetrazine ring has also enjoyed comparable successes and illustratable tailorability in the energetic materials field. 3,6-Diazido-1,2,4,5-tetrazine is a high performing primary explosive, whereas 3,6-diamino-1,2,4,5-tetrazine-1,4-dioxide has been studied as an RDX replacement.^[10,11]

In this work the tetrazole and tetrazine energetic units were combined into the same molecule giving salts of 3,6-bis(tetrazol-5-ylate)-1,2,4,5-tetrazine after deprotonation with energetic bases. The nitrogen-rich salts are insensitive energetic materials and the disilver salt is a high-sensitivity primary explosive.

Results and Discussion

Synthesis

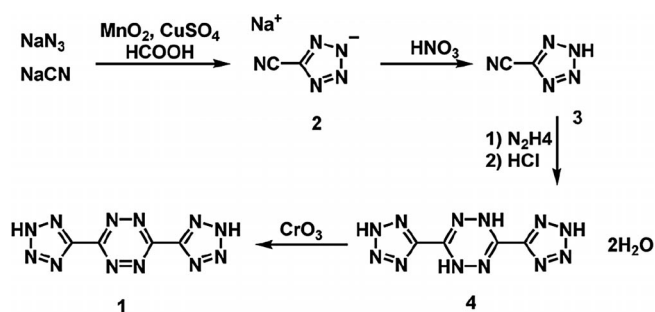
The parent compound 3,6-bis(tetrazol-5-yl)-1,2,4,5-tetrazine (**1**) was prepared according to the literature procedures.^[12] This procedure begins with the reaction of sodium azide and sodium cyanide in the presence of copper(II) sulfate and manganese dioxide in a cycloaddition reaction forming sodium cyanotetrazolate sesquihydrate (**2**). After protonation, free acid 5-cyanotetrazole (**3**) is reacted with hydrazine in dry ethanol yielding 3,6-bis(2*H*-tetrazol-5-yl)-1,4-dihydro-1,2,4,5-tetrazine dihydrate (**4**) after protonation. Finally, the oxidation of **4** with

* Prof. Dr. T. M. Klapötke
Fax: +49-89-2180-77492
E-Mail: tmk@cup.uni-muenchen.de

[a] Department of Chemistry
Energetic Materials Research
Ludwig-Maximilian University
Butenandtstr. 5–13 (D)
81377 München, Germany

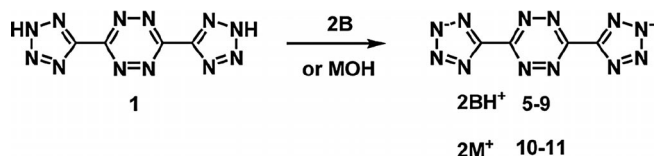
ARTICLE

aqueous acidic chromium trioxide yields **1** in 92% yield. (Scheme 1)



Scheme 1. Synthesis of 3,6-bis(tetrazol-5-yl)-1,2,4,5-tetrazine.^[12]

The reaction of **1** with aqueous bases hydrazine, hydroxylamine, ammonia, diaminourrea, triaminoguanidine, sodium hydroxide, and cesium hydroxide yielded red solids of the corresponding salt **5–11** with varying amounts of hydration water after evaporation in a stream of nitrogen and drying under high vacuum (Scheme 2).



Scheme 2. Synthesis of salts of the $C_4N_{12}^{2-}$ anion. Where B is any of N_2H_4 (**5**), NH_2OH (**6**), NH_3 (**7**), $CO(NHNH_2)_2$ (**8**), $C(NHNH_2)_3$ (**9**), and MOH is NaOH (**10**), or CsOH (**11**).

The hydrazinium salt **5** after drying under high vacuum was found to be anhydrous, however, due to low organic solvent solubility, crystallization had to be performed in water, yielding hydrazinium 3,6-bis(tetrazol-5-ylate)-1,2,4,5-tetrazine as the trihydrate (**5·3H₂O**).

After evaporation and drying under high vacuum, the hydroxylammonium salt was obtained as the trihydrate (**6·3H₂O**). This salt was slightly soluble in methanol, and crystals grown from methanol were found to correspond to the dihydrate (**6·2H₂O**).

The ammonium salt **7** proved to be anhydrous after drying under high vacuum and crystals lacking hydration water were surprisingly could be grown from aqueous solution.

The diaminouronium salt was found to be the dihydrate after drying under high vacuum, and this hydration level persisted after recrystallization from MeOH (**8·2H₂O**).

After drying under high vacuum, the triaminoguanidinium salt **9** was found to be anhydrous, however despite repeated attempts at crystallization from aqueous and non-aqueous solvents **9** failed to form measurable crystals.

After drying under high vacuum, the sodium salt was identified to be the pentahydrate by elemental analysis (**10·5H₂O**). After diffusing ether into a methanol solution of the pentahydrate, the compound was isolated as the hexahydrate (**10·6H₂O**).

The silver salt **12** precipitated anhydrously upon adding a solution of silver nitrate to an aqueous solution of **1**.

Spectroscopy

Multinuclear NMR spectroscopy, especially ^{13}C and ^{15}N spectroscopy proved to be a useful tool for the characterization of the energetic anion. The $C_4N_{12}^{2-}$ anion exhibits two unique resonances in the carbon spectrum, the first appears near 160 ppm for the tetrazole carbons, and the second appears near 157 ppm for the tetrazine carbons. These shifts are all in the vicinity of those calculated for this anion (MPW1PW91/aug-cc-pVDZ, Gaussian 09^[13]). When compared to the protonated species **1**, with chemical shifts of 157.6 and 153.1 ppm for the tetrazole and tetrazine carbons, respectively, the anion has the resonances shifted slightly downfield. In the ^{15}N spectrum the downfield most shift is at $\delta = 15.3$ ppm for the beta-nitrogen atoms of the tetrazole rings. The tetrazine nitrogen atoms resonate at -1.6 ppm and the alpha-tetrazole nitrogens at -55.5 ppm. As with the carbon spectra, assignment was based on comparison with a calculated spectrum.

The IR and Raman spectra of all compounds were collected and assigned using frequency analysis from an optimized structure (B3LYP/cc-pVDZ using Gaussian09 software^[13]). All calculations were performed at the DFT level of theory; the gradient-corrected hybrid three-parameter B3LYP^[14,15] functional theory was used with a correlation consistent pVDZ basis set.^[16–19] All salts of the $C_4N_{12}^{2-}$ anion show three major bands in the infrared. The first of these ranges from 1520 to 1546 cm^{-1} and the calculated value for this band is 1537 cm^{-1} ; it arises from asymmetric C–C stretching. The next major band, calculated to arise at 1198 cm^{-1} from tetrazole ring expansion, ranges from 1158–1196 cm^{-1} . The last band arises from symmetric N2–N3 tetrazole ring stretching at 1030–1051 cm^{-1} , while the calculated value for this band is 1028 cm^{-1} . The Raman spectra of the salts of the $C_4N_{12}^{2-}$ anion also have three diagnostic bands. The first band corresponds to a C–C symmetric stretch and occurs in the range of 1503–1524 cm^{-1} (calcd. 1518 cm^{-1}). The second occurs at 1042–1096 cm^{-1} (calcd. 1048 cm^{-1}) from tetrazole ring breathing with N2–N3 symmetric stretching. The final diagnostic band ranges from 1012–1035 cm^{-1} (calcd. 1029 cm^{-1}) and is caused by tetrazole and tetrazine ring deformation.

Mass Spectrometry

The $C_4N_{12}^{2-}$ anion, present in all species, was either detected by FAB-Ionization technique as either $[M + 1H]$ or $[M+3H]$ signals. This indicates that the $C_4N_{12}^{2-}$ anion can be reduced under the ionization conditions to salts of the corresponding dihydrotetrazine **4**.

Single Crystal X-ray Analysis

With the exception of triaminoguanidinium salt **9** and silver salt **12**, all compounds were characterized by X-ray crystallography. Table 1 summarizes a selection of crystallographic data and refinement details. Additionally, precursor compound **1** was also crystallized and characterized by evaporating an aqueous solution yielding dihydrated crystals (**1·2H₂O**). All

Table 1. Crystallographic data and structure refinement details for **1·2H₂O**, **5·3H₂O**, **6·2H₂O**, **6·3H₂O**, **7**, **8·2H₂O**, **10·6H₂O**, and **11·4H₂O**.

	1·2H₂O	5·3H₂O	6·2H₂O	6·3H₂O	7	8·2H₂O	10·6H₂O	11·4H₂O
Formula	C ₄ H ₆ N ₁₂ O ₂	C ₄ H ₁₆ N ₁₆ O ₃	C ₄ H ₁₂ N ₁₄ O ₄	C ₄ H ₁₄ N ₁₄ O ₅	C ₄ H ₈ N ₁₄	C ₆ H ₁₈ N ₂₀ O ₄	C ₄ H ₁₂ N ₁₂ O ₆ Na ₂	C ₄ H ₈ N ₁₂ O ₄ CS ₂
FW /g mol ⁻¹	254.17	336.27	320.23	338.29	252.20	434.34	370.19	554.00
Crystal system	monoclinic	orthorhombic	monoclinic	orthorhombic	monoclinic	monoclinic	monoclinic	orthorhombic
Space group	<i>P2₁/n</i>	<i>Cmcm</i>	<i>P2₁/n</i>	<i>Pccn</i>	<i>C2/m</i>	<i>C2/c</i>	<i>C2/m</i>	<i>Pbca</i>
<i>a</i> /Å	10.4971(15)	14.3341(6)	10.8330(8)	6.5858(5)	9.5043(19)	17.803(4)	6.9114(4)	14.3842(4)
<i>b</i> /Å	4.8574(5)	6.7190(3)	8.0732(5)	13.4659(9)	11.6050(12)	11.533(5)	14.2740(7)	6.7709(2)
<i>c</i> /Å	10.5978(14)	15.1220(6)	15.5764(11)	15.5861(10)	5.8734(11)	9.849(6)	7.1941(4)	14.6419(4)
<i>a</i> /°	90	90	90	90	90	90	90	90
<i>β</i> /°	113.664(16)	90	107.297(8)	90	126.42(3)	118.503(5)	92.315(5)	90
<i>γ</i> /°	90	90	90	90	90	90	90	90
<i>V</i> /Å ³	494.93	1456.41(11)	1300.6(16)	1382.23(17)	521.3(3)	1777.1(3)	709.14(7)	1426.03(7)
<i>Z</i>	2	4	4	4	2	4	2	4
<i>ρ</i> _{calcd.} /g·cm ⁻³	1.706	1.534	1.636	1.626	1.607	1.624	1.734	2.581
<i>T</i> /K	173	173	173	173	173	173	173	173
<i>R</i> ₁ / <i>wR</i> ₂ (all data)	0.0493 /0.0636	0.0348 /0.0869	0.0656 /0.0683	0.0482 /0.0665	0.0656 /0.0683	0.0716 /0.0499	0.0272 /0.0661	0.0223 /0.0428
<i>R</i> ₁ / <i>wR</i> ₂ (<i>I</i> > 2σ)	0.0296 /0.0598	0.0316 /0.0855	0.0336 /0.0642	0.0308 /0.0636	0.0336 /0.0642	0.0305 /0.0458	0.0236 /0.0651	0.0180 /0.0419
<i>S</i> ^c	0.885	1.097	0.800	0.876	0.800	0.721	1.083	0.969
CCDC	894465	894464	894469	894463	894466	894467	894468	894598

compounds exhibit standard tetrazole^[20] and tetrazine^[21] bond lengths and angles. All structures are dominated by a strong hydrogen bond network

1·2H₂O, displayed in Figure 1, crystallizes in the monoclinic space group *P2₁/n* with two formula units in the unit cell. Its density of 1.706 g·cm⁻³ is the highest observed in this work. Both protons were found to be connected to the N1 nitrogen atoms of the tetrazole rings.

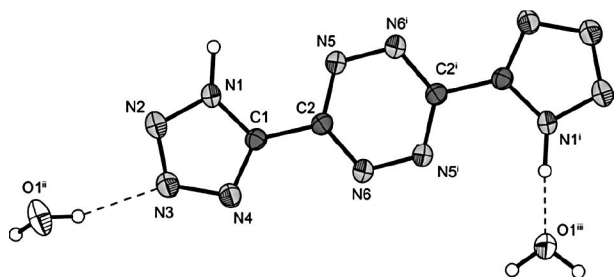


Figure 1. Molecular unit of **1·2H₂O**. Ellipsoids are drawn at the 50% probability level. Symmetry codes: (i) $-x, 1-y, -z$; (ii) $1-x, 1-y, 1-z$; (iii) $-0.5+x, 0.5-y, -0.5+z$.

5·3H₂O crystallizes in the orthorhombic space group *Cmcm* with four formula units in the unit cell. The density of 1.534 g·cm⁻³ is significantly lower than that of the corresponding hydroxylammonium structure **6·2H₂O**. The molecular moiety is shown in Figure 2. All protons of the hydrazinium cations and water molecules participate in an extensive hydrogen bond network.

6·2H₂O, shown in Figure 3, crystallizes in the monoclinic space group *P2₁/n* with four formula units in the unit cell and a density of 1.636 g·cm⁻³.

6·3H₂O crystallizes in the orthorhombic space group *Pccn*. The density of 1.626 g·cm⁻³ is slightly lower than observed for the dihydrate (1.636 g·cm⁻³) which follows a general trend of decreasing densities by increasing content of crystal water. The

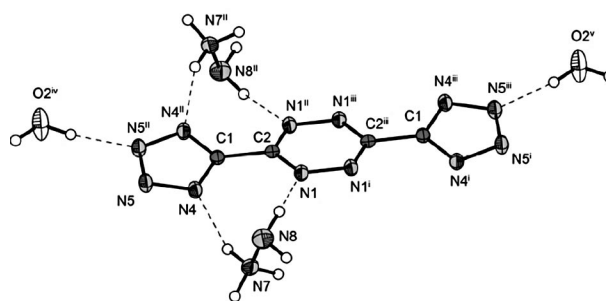


Figure 2. Molecular unit of **5·3H₂O**. Ellipsoids are drawn at the 50% probability level. Symmetry codes: (i) $1-x, y, z$; (ii) $x, -y, 1-z$; (iii) $1-x, -y, 1-z$; (iv) $-0.5+x, -0.5-y, 1-z$; (v) $0.5+x, -0.5-y, 1-z$.

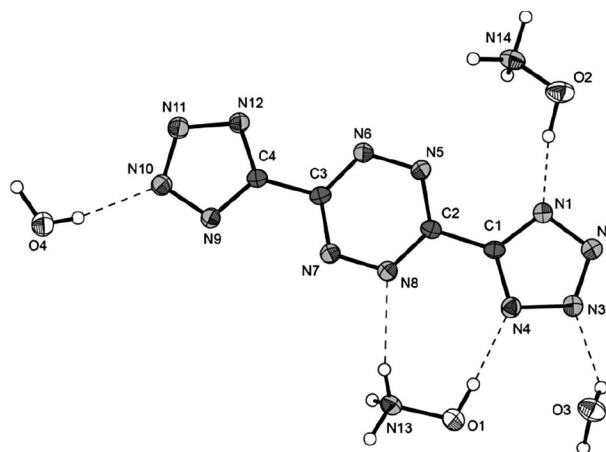


Figure 3. Molecular unit of **6·2H₂O**. Ellipsoids are drawn at the 50% probability level.

molecular moiety is shown in Figure 4. The structure of the hydroxylammonium cations in both structure are comparable to literature values.^[22]

ARTICLE

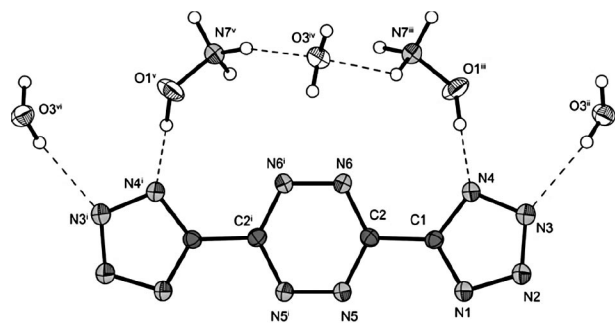


Figure 4. Molecular unit of $6 \cdot 3\text{H}_2\text{O}$. Ellipsoids are drawn at the 50% probability level. Symmetry codes: (i) $0.5-x, 1.5-y, z$; (ii) $0.5-x, 0.5-y, z$; (iii) $1-x, 0.5+y, 0.5-z$; (iv) $-x, 0.5+y, 0.5-z$; (v) $-0.5+x, 1-y, 0.5-z$; (vi) $x, 1+y, z$.

The only crystal structure without inclusion of water was obtained for **7** and is depicted in Figure 5. It crystallizes in the monoclinic space group $C2/m$ with two formula units in the unit cell and slightly lower density of $1.607 \text{ g}\cdot\text{cm}^{-3}$ in comparison to both hydroxylammonium salts.

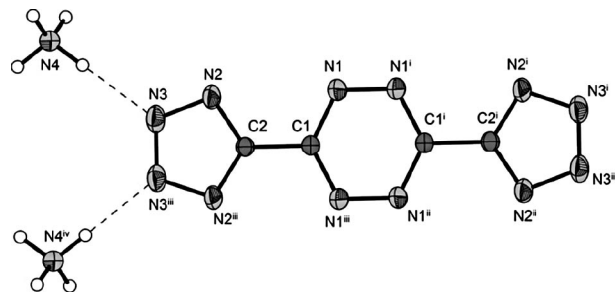


Figure 5. Molecular unit of **7**. Ellipsoids are drawn at the 50% probability level. Symmetry codes: (i) $1-x, y, 3-z$; (ii) $1-x, -y, 3-z$; (iii) $x, -y, z$; (iv) $-x, -y, -z$.

$8 \cdot 2\text{H}_2\text{O}$ crystallizes in the monoclinic space group $C2/c$ with four formula units in the unit cell and a density of $1.624 \text{ g}\cdot\text{cm}^{-3}$ (Figure 6). The diaminouronium cation is monoprotonated and its zigzag-like structure is similar to that described for diaminouronium nitrate.^[23]

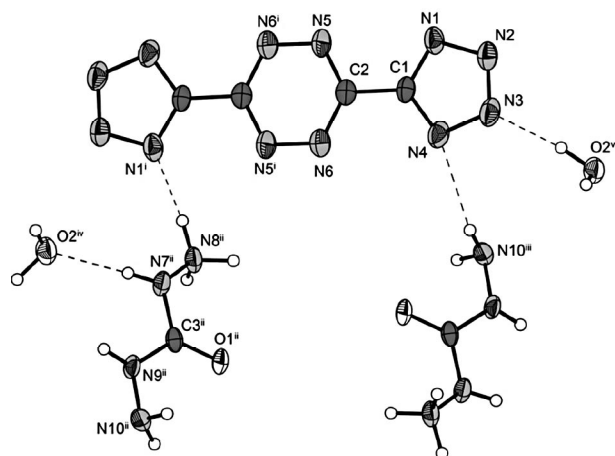


Figure 6. Molecular unit of $8 \cdot 2\text{H}_2\text{O}$. Ellipsoids are drawn at the 50% probability level. Symmetry codes: (i) $-x, -y, -z$; (ii) $-0.5+x, 0.5-y, -0.5+z$; (iii) $0.5-x, 0.5+y, 0.5-z$; (iv) $-x, y, -0.5-z$; (v) $0.5-x, 0.5-y, 1-z$.

$10 \cdot 6\text{H}_2\text{O}$ crystallizes in the monoclinic space group $C2/m$ with two formula units in the unit cell and a density of $1.734 \text{ g}\cdot\text{cm}^{-3}$. The sodium cations are coordinated octahedrally by four water oxygen and two tetrazole nitrogen atoms, indicated in Figure 7. The two remaining water molecules are not coordinated to the central sodium atoms, but also participate in hydrogen bonding.

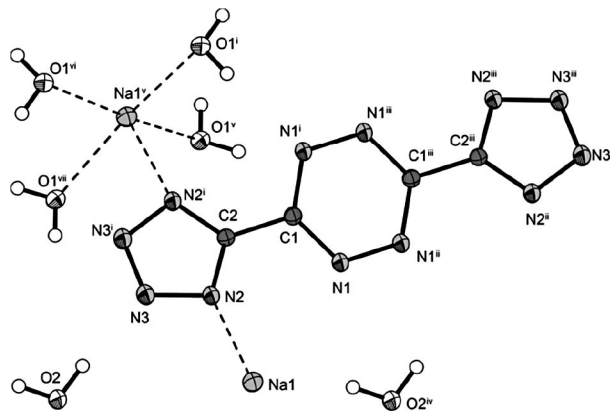


Figure 7. Molecular unit of $10 \cdot 6\text{H}_2\text{O}$. Ellipsoids are drawn at the 50% probability level. (i) $-x, y, 1-z$; (ii) $x, -y, z$; (iii) $1-x, -y, 1-z$; (iv) $0.5+x, -0.5+y, z$; (v) $x, y, 1+z$; (vi) $-0.5+x, 0.5-y, 1+z$; (vii) $0.5-x, 0.5-y, 1-z$.

The cesium salt **11**, shown in Figure 8, crystallizes with inclusion of four crystal water molecules in the orthorhombic space group $Pbca$ with four formula units in the unit cell and of course the highest density of $2.581 \text{ g}\cdot\text{cm}^{-3}$.

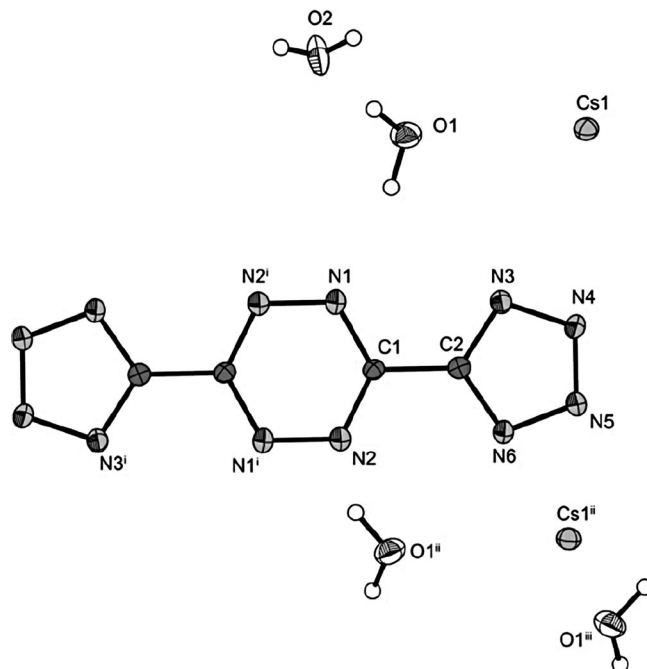


Figure 8. Molecular unit of $11 \cdot 4\text{H}_2\text{O}$. Ellipsoids are drawn at the 50% probability level. Symmetry codes: (i) $-x, 1-y, 1-z$; (ii) $x, 0.5-y, 0.5+z$; (iii) $0.5-x, 1-y, 0.5+z$.

Table 2. Energetic properties for all prepared energetic compounds.

	1	1·2H₂O	5	5·3H₂O	6·2H₂O	6·3H₂O	7	8·2H₂O	9
Formula	C ₄ H ₂ N ₁₂	C ₄ H ₆ N ₁₂ O ₂	C ₄ H ₁₀ N ₁₆	C ₄ H ₁₆ N ₁₆ O ₃	C ₄ H ₁₂ N ₁₄ O ₄	C ₄ H ₁₄ N ₁₄ O ₅	C ₄ H ₈ N ₁₄	C ₆ H ₁₈ N ₂₀ O ₄	C ₆ H ₁₈ N ₂₄
FW /g·mol ⁻¹	218.14	254.17	282.23	336.27	320.23	338.29	252.20	434.34	426.36
Impact sensitivity ^{a)} /J	6	ND ^{o)}	40	ND	40	40	40	40	35
Friction sensitivity ^{b)} /N	72	ND ^{o)}	360	ND	288	360	360	360	288
ESD test ^{c)} /J	0.200	ND ^{o)}	0.500	ND	0.500	0.500	0.700	0.700	0.250
N ^{d)} /%	77.05	66.13	79.40	66.64	61.24	57.97	77.75	64.50	78.84
Ω ^{e)} /%	-66.0	-56.65	-73.69	-61.85	-54.75	-51.57	-76.12	-62.62	-78.79
T _{dec} ^{f)} /°C	226	ND ^{o)}	198	ND ^{o)}	ND ^{o)}	171	256	172	157
Density ^{g)} /g·cm ⁻³	1.75* ^{o)}	1.706	1.57* ^{o)}	1.534	1.635	1.626	1.607	1.624	1.64* ^{o)}
Δ _f H ^o /kJ·kg ⁻¹	4975.5	2399.2	4196.1	893.8	1227.7	268.8	3360.4	1344.6	3994.9
EXPLO5.05 Values									
-Δ _{Ex} U ^o /kJ·kg ⁻¹	5077	4379	4646	3455	4691	4312	3771	3870	4516
T _{det} ^{j)} /K	3900	3299	3125	2528	3181	2978	2783	2759	2967
P _{CJ} ^{k)} /kbar	281	257	293	202	258	246	223	234	275
V _{Det} ^{l)} /m·s ⁻¹	8295	8071	8639	7584	8205	8063	7768	7934	8485
V _o ^{m)} /L·kg ⁻¹	853	736	772	846	819	844	745	811	795
I _S ⁿ⁾ /s	238	216	238	190	214	205	214	198	235

a) Impact sensitivity [BAM drophammer (1 of 6)]. b) Friction sensitivity (BAM friction tester [1 of 6]). c) Electrostatic discharge device (OZM research). d) Nitrogen content. e) Oxygen balance ($\Omega = (xO - 2yC - 1/2zH)M/1600$). f) Decomposition temperature from DSC ($\beta = 5^\circ\text{C}$). g) From X-ray diffraction. h) Calculated energy of formation. i) Energy of explosion. j) Explosion temperature. k) Detonation pressure. l) Detonation velocity. m) Volume of detonation gases (assuming only gaseous products). n) Specific impulse using isobaric (60 bar) conditions. o) * Estimated; ND not determined.

Energetic Properties

Heat of formation calculations of all nitrogen rich compounds were performed using the atomization method based on CBS-4M enthalpies described recently in detail in the literature.^[24] The results are depicted in Table 2. The gas phase heat of formation [$\Delta_f H^o(\text{g}, \text{M})$] was converted into the solid state heat of formation [$\Delta_f H^o(\text{s})$] using the Jenkins and Glasser equations.^[25,26] All compounds are formed endothermically. Of course, higher values were calculated for the anhydrous species. Compound **1** shows an extremely positive energy of formation of 4976 kJ·kg⁻¹, which can be explained by its high nitrogen content of above 77%.

The calculation of the detonation parameters was performed with the program EXPLO5.05^[27,28] using the crystallographically determined densities, with the exception of **1**, **5**, and **9**, in which an estimated density is used. The results are summarized in Table 2. For all hydrated compounds, it can be rationally assumed for the detonation velocities to be lowered compared to the anhydrous material. For compounds **1** and **5** this effect is most important, as the material can be isolated anhydrous, so the materials were calculated with an estimated density slightly higher than that for the hydrated materials.

With respect to their detonation performance the best values were obtained for anhydrous **5** ($V_{\text{Det}} = 8639 \text{ m}\cdot\text{s}^{-1}$, $P_{\text{CJ}} = 293 \text{ kbar}$), which are higher than those of trinitrotoluene (TNT), and pentaerythritol tetranitrate (PETN) but lower than those of the commonly used military explosives like hexogen (RDX) and octogen (HMX).

We also calculated the specific impulse I_S (using the pure compound at 60 bar isobaric rocket conditions), which can be related to the potential use as propellant ingredient. The highest I_S was computed for compounds **1** and **5** (238 s) followed by the triaminoguanidinium salt **8** (235 s).

The sensitivities of all compounds (except for **1·2H₂O**, **5·3H₂O**, and **12**, which were obtained only in very small quan-

ties) towards impact, friction, and electrostatic discharge were determined by standard methods (see Experimental Section). Beside **1** and **12**, which was measured to be sensitive towards impact and friction all compounds are of very low sensitivity or insensitive towards impact and friction.^[29] Also the electrostatic discharge sensitivities are well within the range considered safe. The most sensitive salt is the silver salt **12**, which detonates when placed in a flame. Along with the sensitivities, this behavior indicates the silver salt may be a prospective primary explosive.

Conclusions

The reaction of 3,6-bis(tetrazol-5-yl)-1,2,4,5-tetrazine (**1**) with energetic bases gave a series of ionic energetic materials that were synthesized from commonly-available precursors and characterized for the first time. Multinuclear NMR, IR, and Raman spectroscopy proved to be valuable methods for characterization. Prepared energetic salts were characterized by X-ray crystallography showing standard heterocyclic systems and the experimentally-determined densities allowed computation of explosive performances. The energetic performances range from 7584 m·s⁻¹ to 8639 m·s⁻¹, approaching, but slightly lower than RDX performance at maximum. The sensitivities of all nitrogen rich salts are extremely low, classified as insensitive, and pose no risk for handling in the laboratory. Unfortunately, many of the salts are hydrated, precluding use, however the anhydrous hydrazinium salt due to low sensitivities, high energetic performances and a high decomposition temperature is a promising energetic material. The other promising material is the silver salt, having the behavior and sensitivities of a primary explosive.

Experimental Section

All reagents and solvents were used as received (Sigma-Aldrich, Fluka, Acros Organics) if not stated otherwise. 3,6-Bis(tetrazol-5-yl)-

ARTICLE

1,2,4,5-tetrazine was prepared according to the literature procedure.^[12] Melting and decomposition points were measured with a Linseis PT10 DSC using heating rates of 5 °C·min⁻¹. ¹H and ¹³C NMR spectra were measured with a JEOL instrument. All chemical shifts are quoted in ppm relative to TMS (¹H, ¹³C). Infrared spectra were measured with a Perkin-Elmer FT-IR Spectrum BXII instrument equipped with a Smith Dura SAMP-IR II ATR-unit. Transmittance values are described as strong (s), medium (m), and weak (w). Mass spectra were measured with a JEOL MSstation JMS 700 instrument. Raman spectra were measured with a Perkin-Elmer Spektrum 2000R NIR FT-Raman instrument equipped with a Nd:YAG laser (1064 nm). The intensities are reported as percentages of the most intensive peak and are given in parentheses. Elemental analyses were performed with a Netzsch STA 429 simultaneous thermal analyzer. Sensitivity data were determined using a BAM drophammer and a BAM friction tester. The electrostatic sensitivity tests were carried out with an Electric Spark Tester ESD 2010 EN (OZM Research) operating with the "Winspark 1.15" software package.

CAUTION! The described compounds are energetic materials with sensitivity to various stimuli. While we encountered no issues in the handling of these materials, proper protective measures (face shield, ear protection, body armor, Kevlar gloves, and earthened equipment) should be used at all times. Silver salt **12** is a very sensitive primary explosive and requires exceedingly careful manipulation.

Sodium 5-Cyanotetrazolate Sesquihydrate (2·1.5H₂O): To a solution of sodium cyanide (50.0 g, 1.02 mol) and sodium azide (32.5 g, 500 mmol) in distilled water (400 mL), manganese dioxide (50.0 g, 57.5 mmol) was added. A mixture of sulfuric acid (50%, 100 mL, 96.3 mmol), formic acid (49.1 mL, 60 g, 1.30 mol) and copper(II) sulfate pentahydrate (1.00 g, 4.00 mmol) was added dropwise over 45 min. The temperature was kept between 38 and 42 °C by cooling with an ice bath. After the addition the mixture was stirred for 2 h at 60 °C. The mixture was allowed to cool down to room temperature and was filtered through Celite®. Sodium carbonate (106 g, 1.00 mol) was added to the filtrate until a pH of 10 was reached. The mixture was filtered and the filtrate was neutralized with formic acid (4 mL, 4.88 g, 106 mmol) (pH 7). The solvent was evaporated under reduced pressure. Acetone (900 mL) was added to the residue and the mixture was stirred for 18 h at room temperature. The insoluble solid was removed by gravity filtration and the solvent was evaporated under reduced pressure yielding a yellow solid, which was recrystallized from 50/50 ethanol/water yielding 13.5 g (93.7 mmol, 19%) of sodium 5-cyanotetrazolate sesquihydrate. Elemental analysis for C₂N₅Na·1.5H₂O (144.07): calcd. C 16.67; N 48.61; H 2.10%; found C 16.97; N 48.61; H 2.01%. **DSC** (5 K·min⁻¹): 100 °C (-H₂O), 126 °C, (-H₂O), 264 °C (dec). **IR:** $\tilde{\nu}$ = 3509 (m), 3400 (m), 3287 (m), 2459 (w), 2258 (m), 2126 (w), 2079 (w), 1702 (m), 1617 (s), 1509 (w), 1417 (w), 1378 (s), 1364 (s), 1327 (w), 1293 (w), 1261 (w), 1195 (m), 1149 (m), 1082 (w), 1047 (w), 979 (w), 950 (w), 895 (w), 860 (w), 737 (m), 727 (m) cm⁻¹. **Raman** (1064 nm): $\tilde{\nu}$ = 3315 (2), 2266 (100), 2261 (81), 1422 (58), 1418 (58), 1376 (1), 1148 (4), 1085 (3), 1055 (11), 1048 (16), 738 (5), 603 (11), 499 (18), 236 (7), 209 (9) cm⁻¹. **¹³C NMR** ([D₆]DMSO): δ = 137.7 (s, CN₄), 115.1 (s, CN) ppm. **MS:** m/z : (FAB⁻) 94.0 (C₂N₅); m/z : (FAB⁺) 23.0 (Na). **BAM impact:** 40 J. **BAM friction:** 108 N. **ESD:** 0.280 J.

5-Cyanotetrazole (3): A solution of sodium 5-cyanotetrazolate sesquihydrate (5.00 g, 34.7 mmol) in distilled water (25 mL) was cooled in an ice bath and nitric acid (2 M, 18.5 mL, 37.0 mmol) was added. After stirring for 20 min the solvent was evaporated under reduced pressure and the residue was dried in vacuo. The residue was suspended in ethanol (100 mL) and stirred for 5 min. The insoluble salts

were removed by gravity filtration. The solvent was removed under vacuum and the residue was dried in vacuo yielding 3.30 g (34.7 mmol, 100%) of **3**. **Mp:** 94 °C. **Elem. analysis** C₂N₅H (95.06): calcd. C 25.27; N 73.67; H 1.06%; found C 24.44; N 73.67; H 1.18%. **IR:** $\tilde{\nu}$ = 3461 (w), 3158 (m), 2979 (w), 2881 (w), 2781 (w), 2680 (w), 2548 (w), 2278 (w), 2266 (w), 2153 (w), 1947 (w), 1788 (w), 1686 (m), 1560 (w), 1513 (w), 1466 (w), 1438 (w), 1414 (w), 1393 (w), 1372 (w), 1323 (m), 1294 (s), 1222 (w), 1209 (w), 1184 (w), 1170 (m), 1112 (m), 1044 (s), 1022 (s), 976 (w), 871 (w), 834 (s), 741 (m), 697 (w) cm⁻¹. **Raman** (1064 nm): $\tilde{\nu}$ = 3165 (2), 2280 (100), 1468 (14), 1439 (14), 1413 (34), 1386 (3), 1297 (4), 1221 (7), 1173 (10), 1110 (26), 1068 (15), 1024 (10), 744 (4), 725 (3), 608 (13), 542 (4), 494 (15), 214 (23) cm⁻¹. **¹H NMR** ([D₆]DMSO): δ = 13.09 (s, 1 H, C₂N₅H) ppm. **¹³C NMR** ([D₆]DMSO): δ = 139.2 (s, CN₄), 113.1 (s, CN) ppm. **MS:** (DEI⁺), 70 eV): m/z (%) = 95.05 (44) [M⁺]. **BAM impact:** 6 J. **BAM friction:** 240 N. **ESD:** 0.500 J.

3,6-Bis(2H-tetrazol-5-yl)-1,4-dihydro-1,2,4,5-tetrazine Dihydrate (4):^[12] 5-Cyanotetrazole (6.02 g, 63.3 mmol) was dissolved in dry ethanol (65 mL). The solution was cooled in an ice bath while hydrazine hydrate (100%, 12.3 mL, 12.7 g, 253 mmol) was added dropwise. A colorless precipitate was formed. The mixture was refluxed for 2 h and the precipitate turned yellow. Further hydrazine hydrate (100%, 12.3 mL, 12.7 g, 253 mmol) was added and the mixture was refluxed for 18 h. The precipitate was collected by suction filtration, washed with ethanol (50 mL) and dried in vacuo. The dry precipitate was dissolved in hot water (250 mL) and purified by hot filtration. The filtrate was cooled to 0 °C and concentrated hydrochloric acid (8 mL) was added. The yellow precipitate was collected by suction filtration, washed with 20 mL of cold water, and dried under high vacuum to yield 4.76 g (18.6 mmol, 59%) of **4**. **Mp:** 220 °C. **Elem. analysis** C₄N₁₂H₄·2H₂O (256.19): calcd. C 18.75; N 65.61; H 3.15%; found: C 19.90; N 64.59; H 3.14%. **IR:** $\tilde{\nu}$ = 3533 (w), 3340 (w), 3243 (s), 2596 (w), 2441 (w), 2343 (w), 1896 (w), 1650 (w), 1623 (w), 1577 (m), 1459 (m), 1411 (m), 1241 (w), 1210 (s), 1129 (w), 1088 (m), 1009 (s), 864 (s), 788 (s) cm⁻¹. **Raman** (1064 nm): $\tilde{\nu}$ = 3244 (11), 1671 (100), 1589 (57), 1521 (9), 1500 (8), 1419 (27), 1243 (25), 1175 (8), 1146 (6), 1130 (6), 1096 (11), 1046 (31), 1012 (2), 972 (11), 862 (7), 783 (4), 752 (11), 634 (14), 553 (9), 543 (9), 451 (10), 372 (11), 348 (13), 281 (10) cm⁻¹. **¹H NMR** ([D₆]DMSO): δ = 9.75 (s, 2 H) ppm, two further acidic protons were not detectable, because of a proton exchange with the solvent. **¹³C NMR** ([D₆]DMSO): δ = 149.1 (s, 2C, -CHN₄), 138.1 (s, 2C, -C₂H₂N₄-) ppm. **MS:** m/z : (FAB⁻) 219.0 (C₄N₁₂ -H). **BAM impact:** 40 J. **BAM friction:** 288 N. **ESD:** 100 mJ.

3,6-Bis(2H-tetrazol-5-yl)-1,2,4,5-tetrazine (1):^[12] CrO₃ (6.79 g, 67.9 mmol) was dissolved in a mixture of concentrated sulfuric acid (97%, 6.8 mL) and water (68 mL) at -10 °C. **4** (1.23 g, 4.80 mmol) was added and the mixture was stirred at -5 °C for 0.5 h. A red precipitate was formed, which was collected by suction filtration. The precipitate was washed with diluted hydrochloric acid (8 mL, 2 M) and dried under reduced pressure to yield 959 mg (4.40 mmol, 92%) of **1**. **DSC** (5 K·min⁻¹): 226 °C (dec). **Elem. analysis** C₄N₁₂H₂ (218.14): calcd. C 22.02; N 77.05; H 0.92%; found: C 22.36; N 76.39; H 1.07%. **IR:** $\tilde{\nu}$ = 3476 (m), 3063 (w), 2944 (m), 2743 (m), 2538 (m), 2361 (m), 2171 (w), 1603 (w), 1543 (w), 1467 (m), 1452 (m), 1425 (m), 1270 (m), 1246 (s), 1144 (m), 1098 (m), 1083 (m), 1041 (m), 1021 (s), 916 (s), 848 (m), 743 (w) cm⁻¹. **Raman** (1064 nm): $\tilde{\nu}$ = 1864 (4), 1584 (100), 1538 (12), 1473 (81), 1244 (1), 1226 (14), 1162 (10), 1091 (17), 1015 (12), 1005 (2), 829 (2), 814 (6), 662 (2), 429 (5), 277 (2) cm⁻¹. **¹H NMR** ([D₆]DMSO): δ = 7.23 (s, 2 H) ppm. **¹³C NMR** ([D₆]DMSO): δ = 157.6 (s, 2C, -CHN₄), 153.1 (s, 2C, -C₂N₄-) ppm. **MS:** m/z (DEI⁺) = 218.1 (M⁺). **BAM impact:** 6 J. **BAM friction:** 72 N. **ESD:** 200 mJ.

Hydrazinium 3,6-Bis(tetrazol-5-ylate)-1,2,4,5-tetrazine (5): Compound **1** (200 mg, 917 μmol) was dissolved in distilled water (20 mL) with heating. Hydrazine hydrate (91.8 mg, 1.83 mmol) was added at room temperature and the solution stirred for 5 min. The solvent was evaporated by blowing a nitrogen flow over the liquid surface and the obtained red solid was dried under high vacuum yielding 176 mg (624 μmol, 68 %) of **5**. DSC (5 K·min⁻¹): 198 °C (dec). Elem. analysis C₄N₁₆H₁₀ (282.23): calcd. C 17.02; N 79.41; H 3.57%; found: C 16.78; N 75.89; H 3.52%. **IR:** $\tilde{\nu}$ = 3350 (m), 3245 (m), 3071 (m), 2983 (m), 2837 (m), 2712 (m), 2630 (m), 1656 (m), 1604 (w), 1540 (s), 1414 (m), 1259 (s), 1187 (s), 1117 (s), 1100 (s), 1079 (m), 1067 (m), 1053 (m), 1045 (m), 943 (s), 921 (s), 686 (w) cm⁻¹. **Raman** (1064 nm): $\tilde{\nu}$ = 1861 (1), 1521 (100), 1428 (4), 1139 (3), 1096 (29), 1024 (4), 818 (1) 796 (1) cm⁻¹. **¹H NMR** ([D₆]DMSO): δ = 7.18 (s, 5 H, N₂H₅⁺) ppm. **¹³C NMR** ([D₆]DMSO): δ = 160.0 (s, 2C, -CN₄), 157.0 (s, 2C, -C₂N₄⁻) ppm. **MS:** *m/z*: (FAB⁻) 217.0 (C₄N₁₂ + H); *m/z*: (FAB⁺) 33.0 (N₂H₅). BAM impact: 40 J. BAM friction: 360 N. ESD: 500 mJ.

Hydroxylammonium 3,6-Bis(tetrazol-5-ylate)-1,2,4,5-tetrazine Trihydrate (6·3H₂O): 1 (200 mg, 917 μmol) was dissolved in distilled water (20 mL) with heating. An aqueous solution of hydroxylamine (121 mg, 1.83 mmol, 50 %) was added at room temperature and stirred for 5 min. The solvent was evaporated by blowing a nitrogen flow over the liquid surface and the obtained red solid was dried under high vacuum yielding 225 mg (702 μmol, 76 %) of **6·3H₂O**. DSC (5 K·min⁻¹): 100 °C (-H₂O) 171 °C (dec). Elem. analysis C₄N₁₄H₈·3H₂O (338.24): calcd. C 14.20; N 57.97; H 4.17%; found: C 14.70; N 58.44; H 3.95%. **IR:** $\tilde{\nu}$ = 3217 (s), 2949 (s), 2824 (s), 2701 (s), 2363 (m), 2340 (m), 2134 (w), 2012 (w), 1687 (w), 1608 (m), 1541 (s), 1526 (s), 1435 (m), 1418 (s), 1376 (w), 1271 (s), 1263 (s), 1210 (m), 1183 (s), 1160 (m), 1090 (w), 1070 (m), 1057 (m), 1053 (m), 1048 (m), 1011 (m), 1000 (m), 920 (m), 789 (w), 732 (w) cm⁻¹. **Raman** (1064 nm): $\tilde{\nu}$ = 1524 (100), 1434 (5), 1145 (4), 1081 (27), 1029 (5), 798 (2), 438 (1) cm⁻¹. **¹H NMR** ([D₆]DMSO): δ = 10.26 (s, 4 H, NH₄O⁺) ppm. **¹³C NMR** ([D₆]DMSO): δ = 160.3 (s, 2C, -CN₄), 157.3 (s, 2C, -C₂N₄⁻) ppm. **MS:** *m/z*: (FAB⁻) 217.0 (C₄N₁₂ + 1 H); *m/z*: (FAB⁺) 34.0 (NH₄O). BAM impact: 40 J. BAM friction: 288 N. ESD: 500 mJ.

Ammonium 3,6-Bis(tetrazol-5-ylate)-1,2,4,5-tetrazine (7): 1 (200 mg, 917 μmol) was dissolved in distilled water (20 mL) with heating. An aqueous solution of ammonia (0.92 mL, 1.83 mmol, 2 M) was added at room temperature and the solution stirred for 5 min. The solvent was evaporated by blowing a nitrogen flow over the liquid surface and the obtained red solid was dried under high vacuum yielding 169 mg (670 μmol, 73 %) of **7**. DSC (5 K·min⁻¹): 256 °C (dec). Elem. analysis C₄N₁₄H₈ (252.20): calcd. C 19.05; N 77.75; H 3.20%; found: C 19.27; N 76.23; H 3.06%. **IR:** $\tilde{\nu}$ = 3179 (w), 2957 (m), 2843 (m), 2360 (w), 2339 (w), 2102 (w), 1905 (w), 1769 (w), 1708 (w), 1535 (m), 1449 (s), 1427 (s), 1409 (s), 1255 (s), 1176 (s), 1159 (s), 1078 (w), 1053 (m), 1048 (m), 1037 (m), 917 (m), 757 (w) cm⁻¹. **Raman** (1064 nm): $\tilde{\nu}$ = 1854 (1), 1515 (100), 1427 (4), 1130 (3), 1063 (37), 1017 (5), 793 (1) cm⁻¹. **¹H NMR** ([D₆]DMSO): δ = 7.31 (s, 4 H, NH₄⁺) ppm. **¹³C NMR** ([D₆]DMSO): δ = 160.0 (s, 2C, -CN₄), 157.0 (s, 2C, -C₂N₄⁻) ppm. **MS:** *m/z*: (FAB⁻) 219.0 (C₄N₁₂ + 3 H); *m/z*: (FAB⁺) 17.0 (NH₄). BAM impact: 40 J. BAM friction: 360 N. ESD: 700 mJ.

Diaminouronium 3,6-Bis(tetrazol-5-ylate)-1,2,4,5-tetrazine Dihydrate (8·2H₂O): 1 (200 mg, 917 μmol) was dissolved in distilled water (20 mL) with heating. Diaminouronium (165 mg, 1.83 mmol) was added at room temperature and the solution stirred for 5 min. The solvent was evaporated by blowing a nitrogen flow over the liquid surface and the obtained red solid was dried under high vacuum yielding 254 mg

(586 μmol, 63 %) of **8·2H₂O**. DSC (5 K·min⁻¹): 104 °C (-H₂O), 157 °C (dec). Elem. analysis C₆H₁₄N₂₀O₂·2H₂O (434.18): calcd. C 16.58; N 64.50; H 4.18%; found: C 17.01; N 63.77; H 3.54%. **IR:** $\tilde{\nu}$ = 3277 (m), 3221 (m), 2991 (m), 2671 (m), 2360 (m), 2332 (w), 2090 (w), 1667 (s), 1628 (s), 1582 (s), 1520 (s), 1410 (m), 1380 (m), 1370 (m), 1317 (m), 1261 (m), 1176 (m), 1151 (m), 1109 (m), 1051 (m), 1030 (m), 670 (m), 851 (w), 763 (w), 695 (w) cm⁻¹. **Raman** (1064 nm): $\tilde{\nu}$ = 1626 (5), 1514 (100), 1423 (3), 1135 (4), 1070 (24), 1044 (9), 1024 (3), 813 (2), 512 (1), 428 (1) cm⁻¹. **¹H NMR** ([D₆]DMSO): δ = 8.16 (s, broad, 8H -NH -NH₂ -NH₃⁺) ppm. **¹³C NMR** ([D₆]DMSO): δ = 159.9 (s, 2C, -CN₄), 159.8 (s, C(O)(NHNH₂)(NHNH₃⁺), 156.8 (s, 2C, -C₂N₄⁻) ppm. **MS:** *m/z*: (FAB⁻) 219.0 (C₄N₁₂ + 3 H); *m/z*: (FAB⁺) 90.0 (CH₆N₄O). BAM impact: 40 J. BAM friction: 360 N. ESD: 700 mJ.

Triaminoguanidinium 3,6-Bis(tetrazol-5-ylate)-1,2,4,5-tetrazine (9): 1 (200 mg, 917 μmol) was dissolved in distilled water (20 mL) with heating. Triaminoguanidine (210 mg, 1.83 mmol) was added at room temperature and the solution stirred for 5 min. The solvent was evaporated by blowing a nitrogen flow over the liquid surface and the obtained red solid was dried under high vacuum yielding 347 mg (815 μmol, 89 %) of **9**. DSC (5 K·min⁻¹): 183 °C (dec). Elem. analysis C₄H₁₈N₂₄ (426.37): calcd. C 16.90; N 78.84; H 4.26%; found: C 17.26; N 77.86; H 4.03%. **IR:** $\tilde{\nu}$ = 3346 (w), 3179 (m), 3098 (m), 3013 (w), 2361 (m), 2337 (m), 1668 (s), 1575 (m), 1531 (m), 1401 (w), 1360 (m), 1301 (w), 1250 (m), 1166 (m), 1134 (s), 1032 (m), 1012 (m), 953 (m), 925 (s) cm⁻¹. **Raman** (1064 nm): $\tilde{\nu}$ = 3258 (1), 1511 (100), 1427 (3), 1197 (1), 1121 (3), 1045 (32), 1035 (4), 1012 (8), 879 (1), 814 (2), 507 (1) cm⁻¹. **¹H NMR** ([D₆]DMSO): δ = 8.60 (s, broad, 3H C NH NH₂), 4.52 (s, broad, 6H NH NH₂) ppm. **¹³C NMR** ([D₆]DMSO): δ = 160.1 (s, 2C, -CN₄), 157.0 (s, 2C, -C₂N₄⁻) ppm. **MS:** *m/z*: (FAB⁻) 219.0 (C₄N₁₂ + 3 H); *m/z*: (FAB⁺) 105.1 (CN₈H₆). BAM impact: 35 J. BAM friction: 288 N. ESD: 500 mJ.

Sodium 3,6-Bis(tetrazol-5-ylate)-1,2,4,5-tetrazine Hexahydrate (10·6H₂O): 1 (200 mg, 917 μmol) was dissolved in distilled water (20 mL) with heating. A solution of sodium hydroxide (274 mg, 1.83 mmol) in water (10 mL) was added at room temperature and the solution stirred for 5 min. The solvent was evaporated by blowing a nitrogen flow over the liquid surface and the obtained orange-red solid was dried under high vacuum yielding 236 mg (671 μmol, 73 %) of **10·6H₂O**. DSC (5 K·min⁻¹): 80 °C (-H₂O), 136 °C, (-H₂O), 270 °C (dec). Elem. analysis C₄N₁₂Na₂·6H₂O (370.19): calcd. C 12.98; N 45.40; H 3.27%; found: C 13.81; N 44.89; H 2.85%. **IR:** $\tilde{\nu}$ = 3541 (m), 3452 (m), 3393 (m), 3201 (m), 2144 (w), 1649 (w), 1627 (s), 1557 (w), 1536 (s), 1477 (w), 1411 (w), 1390 (m), 1336 (w), 1261 (s), 1241 (m), 1283 (s), 1162 (m), 1076 (m), 1043 (m), 990 (w), 931 (m), 824 (w) cm⁻¹. **Raman** (1064 nm): $\tilde{\nu}$ = 1881 (1), 1625 (3), 1518 (100), 1432 (2), 1137 (3), 1088 (19), 1023 (4), 811 (2) cm⁻¹. **¹³C NMR** ([D₆]DMSO): δ = 160.1 (s, 2C, -CN₄), 157.0 (s, 2C, -C₂N₄⁻) ppm. **¹⁵N NMR** ([D₆]DMSO): δ = 15.3 (s, 4N), -1.6 (s, 4N), -55.5 (s, 4N) ppm. **MS:** *m/z*: (FAB⁻) 219.0 (C₄N₁₂ + 3 H); *m/z*: (FAB⁺) 23.0 (Na). BAM impact: 40 J. BAM friction: 360 N. ESD: 1 J.

Cesium 3,6-Bis(tetrazol-5-ylate)-1,2,4,5-tetrazine Monohydrate (11·1H₂O): 1 (200 mg, 917 μmol) was dissolved in distilled water (20 mL) with heating. A solution of cesium hydroxide (274 mg, 1.83 mmol) in water (10 mL) was added at room temperature and the solution stirred for 5 min. The solvent was evaporated by blowing a nitrogen flow over the liquid surface and the obtained red/black solid was dried under high vacuum yielding 311 mg (622 μmol, 68 %) of **11·1H₂O**. Elem. analysis C₄N₁₂Cs₂·H₂O (499.95): calcd. C 9.61; N 33.62; H 0.40%; found: C 9.73; N 31.21; H 0.43%. **IR:** $\tilde{\nu}$ = 3462 (w), 3351 (w), 2359 (m), 2332 (m), 1663 (m), 1570 (m), 1525 (m), 1473

ARTICLE

(w), 1399 (w), 1382 (m), 1309 (w), 1246 (s), 1158 (m), 1075 (w), 1036 (s), 913 (m), 813 (w), 674 (w) cm^{-1} . **Raman** (1064 nm): $\tilde{\nu} = 1503$ (100), 1423 (2), 1119 (4), 1042 (32), 1012 (7), 814 (2), 438 (2), 834 (2), 788 (2) cm^{-1} . **^{13}C NMR** ($[\text{D}_6]\text{DMSO}$): $\delta = 160.1$ (s, 2C, $-\text{CN}_4$), 157.0 (s, 2C, $-\text{C}_2\text{N}_4-$) ppm. **MS**: m/z : (FAB $-$) 219.0 ($\text{C}_4\text{N}_{12} + 3\text{H}$); m/z : (FAB $+$) 133.0 (Cs). BAM impact: 40 J. BAM friction: 360 N; ESD: 1 J.

Silver 3,6-Bis(tetrazol-5-ylate)-1,2,4,5-tetrazine (12): **1** (100 mg, 458 μmol) was dissolved in distilled water (20 mL) under heating. A solution of silver nitrate was added dropwise until no more precipitate was formed. The purple precipitate was collected by suction filtration and dried under high vacuum yielding 179 mg (414 μmol , 90%) of **12**. DSC (5 $\text{K}\cdot\text{min}^{-1}$): 219 $^\circ\text{C}$ (dec). **IR**: $\tilde{\nu} = 3374$ (w), 1620 (w), 1546 (m), 1410 (m), 1299 (m), 1272 (s), 1186 (m), 1070 (m), 1052 (m), 926 (m), 816 (w), 723 (w) cm^{-1} . BAM impact: <1 J. BAM friction: <5 N. ESD: 70 mJ.

Crystallographic data (excluding structure factors) for the structures in this paper have been deposited with the Cambridge Crystallographic Data Centre, CCDC, 12 Union Road, Cambridge CB21EZ, UK. Copies of the data can be obtained free of charge on quoting the depository numbers CCDC-894465, -894464, -894469, -894463, -894466, -894467, -894468, and 894598 (for **1**·2 H_2O , **5**·3 H_2O , **6**·2 H_2O , **6**·3 H_2O , **7**, **8**·2 H_2O , **10**·6 H_2O , and **11**·4 H_2O , respectively) (Fax: +44-1223-336-033; E-Mail: deposit@ccdc.cam.ac.uk, <http://www.ccdc.cam.ac.uk>)

Acknowledgments

Financial support of this work by the Ludwig-Maximilian University of Munich (LMU), the U.S. Army Research Laboratory (ARL), the Armament Research, Development and Engineering Center (ARDEC), the Strategic Environmental Research and Development Program (SERDP) and the Office of Naval Research (ONR Global, title: "Synthesis and Characterization of New High Energy Dense Oxidizers (HEDO) – NICOP Effort") under contract nos. W911NF-09-2-0018 (ARL), W911NF-09-1-0120 (ARDEC), W011NF-09-1-0056 (ARDEC) and 10 WPSEED01-002 / WP-1765 (SERDP) is gratefully acknowledged. The authors acknowledge collaborations with *Dr. Mila Krupka* (OZM Research, Czech Republic) in the development of new testing and evaluation methods for energetic materials and with *Dr. Muhamed Sucesca* (Brodarski Institute, Croatia) in the development of new computational codes to predict the detonation and propulsion parameters of novel explosives. We are indebted to and thank *Drs. Betsy M. Rice* and *Brad Forch* (ARL, Aberdeen, Proving Ground, MD) and *Mr. Gary Chen* (ARDEC, Picatinny Arsenal, NJ) for many helpful and inspired discussions and support of our work. The authors want to thank *Stefan Huber* for measuring the sensitivities.

References

- [1] M. Göbel, K. Karaghiosoff, T. M. Klapötke, D. G. Piercec, J. Stierstorfer, *J. Am. Chem. Soc.* **2010**, *132*, 17216–17226.
- [2] T. M. Klapötke, D. G. Piercec, J. Stierstorfer, *Chem. Eur. J.* **2011**, *17*, 13068–13077.
- [3] M. A. C. Härtel, T. M. Klapötke, D. G. Piercec, J. Stierstorfer, *Z. Anorg. Allg. Chem.* **2012**; published online, DOI: 10.1002/zaac.201200049.
- [4] Y.-C. Li, C. Qi, S.-H. Li, H.-J. Zhang, C.-H. Sun, Y.-Z. Yu, S.-P. Pang, *J. Am. Chem. Soc.* **2010**, *132*, 12172–12173.

- [5] T. M. Klapötke, D. G. Piercec, *Inorg. Chem.* **2011**, *50*, 2732–2734.
- [6] P. Carlqvist, H. Östmark, T. Brinck, *J. Phys. Chem. A* **2004**, *108*, 7463–7467.
- [7] T. Schroer, R. Haiges, S. Schneider, K. O. Christie, *Chem. Commun.* **2005**, 1607–1609.
- [8] J. Fronabarger, M. D. Williams, W. B. Sanborn, J. G. Bragg, D. A. Parrish, M. Bichay, *Propellants Explos. Pyrotech.* **2011**, *36*, 541–550.
- [9] N. Fischer, T. M. Klapötke, D. G. Piercec, J. Stierstorfer, *Z. Anorg. Allg. Chem.* **2012**, *638*, 302–310.
- [10] M. H. V. Huynh, M. A. Hiskey, D. E. Chavez, R. D. Gilardi, *J. Am. Chem. Soc.* **2005**, *127*, 12537–12543.
- [11] M. D. Coburn, M. A. Hiskey, K. Y. Lee, D. G. Ott, M. M. Stinecipher, *J. Heterocycl. Chem.* **1993**, *30*, 1593–1595.
- [12] J. Sauer, G. R. Pabst, U. Holland, H.-S. Kim, S. Loebbecke, *Eur. J. Org. Chem.* **2001**, *4*, 697–706.
- [13] Gaussian 09, Revision A.1, M. J. Frisch, G. W. Trucks, H. B. Schlegel, G. E. Scuseria, M. A. Robb, J. R. Cheeseman, G. Scalmani, V. Barone, B. Mennucci, G. A. Petersson, H. Nakatsuji, M. Caricato, X. Li, H. P. Hratchian, A. F. Izmaylov, J. Bloino, G. Zheng, J. L. Sonnenberg, M. Hada, M. Ehara, K. Toyota, R. Fukuda, J. Hasegawa, M. Ishida, T. Nakajima, Y. Honda, O. Kitao, H. Nakai, T. Vreven, J. A. Montgomery Jr., J. E. Peralta, F. Ogliaro, M. Bearpark, J. J. Heyd, E. Brothers, K. N. Kudin, V. N. Staroverov, R. Kobayashi, J. Normand, K. Raghavachari, A. Rendell, J. C. Burant, S. S. Iyengar, J. Tomasi, M. Cossi, N. Rega, J. M. Millam, M. Klene, J. E. Knox, J. B. Cross, V. Bakken, C. Adamo, J. Jaramillo, R. Gomperts, R. E. Stratmann, O. Yazyev, A. J. Austin, R. Cammi, C. Pomelli, J. W. Ochterski, R. L. Martin, K. Morokuma, V. G. Zakrzewski, G. A. Voth, P. Salvador, J. J. Dannenberg, S. Dapprich, A. D. Daniels, Ö. Farkas, J. B. Foresman, J. V. Ortiz, J. Cioslowski, and D. J. Fox, Gaussian, Inc., Wallingford CT, 2009.
- [14] A. D. Becke, *J. Chem. Phys.* **1993**, *98*, 5648–5652.
- [15] C. Lee, W. Yang, R. G. Parr, *Phys. Rev. B* **1988**, *37*, 785–789.
- [16] D. E. Woon, T. H. Dunning Jr., R. J. Harrison, *J. Chem. Phys.* **1993**, *98*, 1358–1371.
- [17] R. A. Kendall, T. H. Dunning Jr., R. J. Harrison, *J. Chem. Phys.* **1992**, *96*, 6796–6806.
- [18] T. H. Dunning Jr., *J. Chem. Phys.* **1989**, *90*, 1007–1023.
- [19] K. A. Peterson, D. E. Woon, T. H. Dunning Jr., *J. Chem. Phys.* **1994**, *100*, 7410–7415.
- [20] V. A. Ostrovskii, G. I. Koldobskii, R. E. Trifonov, *Compr. Heterocycl. Chem. III* **2008**, *6*, 257–423.
- [21] B. Stanovnik, U. Groselj, J. Svete, *Compr. Heterocycl. Chem. III* **2008**, *9*, 641–714.
- [22] N. Fischer, T. M. Klapötke, D. G. Piercec, J. Stierstorfer, *Z. Anorg. Allg. Chem.* **2012**, *638*, 302–310.
- [23] N. Fischer, T. M. Klapötke, J. Stierstorfer, *Propellants Explos. Pyrotech.* **2011**, *36*, 225–232.
- [24] T. Altenburg, T. M. Klapötke, A. Penger, J. Stierstorfer, *Z. Anorg. Allg. Chem.* **2010**, *636*, 463–471.
- [25] H. D. B. Jenkins, H. K. Roobottom, J. Passmore, L. Glasser, *Inorg. Chem.* **1999**, *38*, 3609–3620.
- [26] H. D. B. Jenkins, D. Tudela, L. Glasser, *Inorg. Chem.* **2002**, *41*, 2364–2367.
- [27] M. Sucska, *EXPLO5.05 Program*, Zagreb, Croatia, **2010**.
- [28] M. Sucska, *Mater. Sci. Forum* **2004**, *465–466*, 325–330.
- [29] Impact: Insensitive > 40 J, less sensitive ≥ 35 J, sensitive ≥ 4 J, very sensitive ≤ 3 J; Friction: Insensitive > 360 N, less sensitive = 360 N, sensitive < 360 N and > 80 N, very sensitive ≤ 80 N, extremely sensitive ≤ 10 N. According to the UN Recommendations on the Transport of Dangerous Goods.

Received: August 7, 2012

Published Online: September 27, 2012

Copper Salts of Halo Tetrazoles: Laser-Ignitable Primary Explosives

DENNIS FISCHER,¹ THOMAS
M. KLAPÖTKE,^{1,2} DAVIN G. PIERCEY,¹
and JÖRG STIERSTORFER¹

¹Department of Chemistry, Energetic Materials
Research, Ludwig-Maximilian University of Munich,
Munich, Germany

²Department of Mechanical Engineering,
Center for Energetic Concepts Development,
University of Maryland, College Park, Maryland

Syntheses of the primary explosives copper (II) 5-chlorotetrazolate and copper (II) bromotetrazolate are described. The physical and thermal stabilities of both compounds were determined, and their explosive ability was characterized. Additionally, the first reported X-ray structure of a 5-chlorotetrazole is reported.

Keywords: laser ignition, primer, sensitivity, tetrazole

Dedicated to Professor Peter Klüfers on the occasion of his 60th birthday.

Address correspondence to Thomas M. Klapötke, Department of Chemistry, Energetic Materials Research, Ludwig-Maximilian University of Munich, Butenandstr. 5-13, D-81377 Munich, Germany. E-mail: tmk@cup.uni-muenchen.de

Introduction

Primary explosives are the highly sensitive explosives that upon ignition undergo a deflagration-to-detonation transition (DDT), generating a shockwave capable of initiating detonation in a secondary explosive. Though secondary explosives are well known and common, with dozens of examples having found extensive practical use, primary explosives are less numerous due to the uniqueness of the materials that can undergo a DDT. In the initial stages of the deflagration of a primary explosive, propagation of the combustion wave is entirely thermal, and grains of primary explosives combust from the outside inwards. The pressure released during this combustion is thought to compress unreacted primary explosives ahead of the combustion front while simultaneously heating it via compression and friction to temperatures above its decomposition point, leading to the propagation of a detonation wave [1]. The relative rarity of such a process means that very few materials are suitable for use as primary explosives.

The first primary initiating explosive that found widespread use was mercury fulminate, the use of which was pioneered by Nobel [2], prior to which common black powder (75% KNO_3 , 15% C, 10% S_8) was used to initiate secondary explosives in a very unreliable fashion [3]. During the last century the use of mercury fulminate has been supplanted by the more powerful and less toxic lead azide, the use of which continues to the present day. Though many other initiating primaries have been used on smaller scales, lead azide remains the current primary of choice despite possessing extensive drawbacks.

Beyond the unacceptable personal and environmental toxicity of lead [4], lead azide is also highly sensitive in the pure state, requiring dextrination to reduce sensitivity [5]. Lead azide also needs protection from carbon dioxide or decomposition ensues [6], can detonate during synthesis if conditions are not rigorously controlled [7] (lead azide is not manufactured in the United States for this reason [8]), and requires

a relatively large mass of material in order to initiate a secondary (relative to very vigorous initiators such as silver nitrotetrazolate: 5 mg vs. 20 mg for tetryl initiation) [5].

A lead azide replacement needs to possess the following properties: (1) insensitivity to light; (2) sensitivity to detonation but not too sensitive to handle and transport; (3) stable to at least 200°C; (4) stable upon storage for long periods of time; (5) free of toxic metals; (6) free of toxic perchlorate [9]. Compounds including diazodinitrophenol (DDNP) [10], 3,6-diaza-1,2,4,5-tetrazine [11], 1,3,5-triazido-2,4,6-trinitrobenzene (TATNB) [12] or tetraamine bis(nitrotetrazolato- N^2)cobalt (III) perchlorate [13], and complex nitrotetrazole primaries [9,14] have all been considered as lead azide replacements; however, their instability to light, heat, mechanical stimuli, or toxic perchlorate content preclude this use. Additionally, the use of nitrotetrazolate ions or ligands in primary explosives can be hazardous due to the synthesis of nitrotetrazole involving a very sensitive intermediate product [15].

Laser ignitability in a primary explosive offers a distinct advantage over simple electrical ignition (whether hot wire, slapper, or exploding bridge wire [EBW]) for the distance-separated ignition of blasting caps. In all detonating systems based on electric signal transmission over great distances, exceedingly long wires and cables are used. Unfortunately, the length of such conductors allows ambient electromagnetic fields to induce currents in the electrical conductor, increasing the possibility of the generation of an accidental detonation signal from electromagnetic field generators such as lightning, radio transmitters, or microwaves. The use of optical fibers instead of wires for the transmission of the detonation signal offers a distinct increase in the safety of an initiation system. Naturally, to use such optical fibers, a laser-sensitive primary explosive must be used [16].

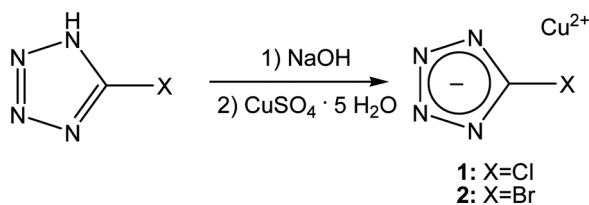
The low toxicity of copper and the known photosensitivity of energetic copper salts and complexes led us to investigate the use of copper (II) chlorotetrazolate (**1**) and copper (II) bromotetrazolate (**2**) as laser-ignitable primary explosives.

Results and Discussion

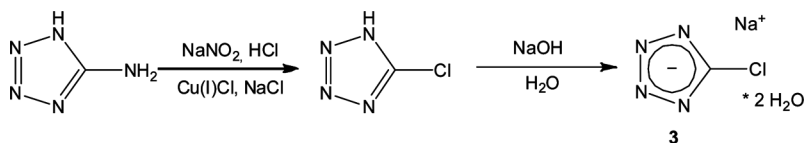
The reaction of copper (II) sulfate pentahydrate with the sodium salt of 5-chloro or 5-bromotetrazole in aqueous solution led to the instantaneous precipitation of the copper (II) chlorotetrazolate (**1**) or copper (II) bromotetrazolate (**2**) as a very fine precipitate (Scheme 1). Attempts at filtration of the halotetrazolates proved that the particle size is too small for conventional filter paper or 450-nm cellulose acetate filters, so isolation was achieved by centrifugation of the reaction mixture. Both **1** and **2** were isolated in almost quantitative yield.

5-Chloro-2*H*-tetrazole is formed by the reaction of 5-amino-tetrazole with sodium nitrite, a mixture of Cu(I)Cl and NaCl in diluted hydrochloric acid (Scheme 2). A basic workup using sodium hydroxide yielded sodium 5-chlorotetrazolate dihydrate (**3**). Acidification and extraction into ethyl acetate yielded free chlorotetrazole after evaporation. An analogous procedure was used for the preparation of the bromotetrazole.

Single crystals of **3** were grown from a water: ethanol mixture. The crystals were analyzed by low-temperature X-ray diffraction on an Oxford Xcalibur3 diffractometer using a Spellman generator (voltage 50 kV, current 40 mA) and a



Scheme 1. Synthesis of copper halotetrazolates (**1** and **2**).



Scheme 2. Synthesis of sodium 5-chlorotetrazolate dihydrate (**3**).

KappaCCD detector. A suitable single crystal was picked from the crystallization mixture and mounted in Kel-F oil on a glass fiber on the goniometer head, which was transferred to the N₂ stream (200 K) of the diffractometer (Agilent Technologies). Data collection was undertaken using CrysAlis CCD software [17] and data reduction was performed with CrysAlis RED software [18]. The structure was solved with SIR-97 [19]. The data set was refined with SHELXL-97 [20] implemented in the program package WinGX [21] and finally checked using the Platon software [22]. Structural data and X-ray parameters are summarized in Table 1.

The present structure represents the first containing the 5-chlorotetrazole moiety. Sodium 5-chlorotetrazolate dihydrate (**3**) crystallizes as a dihydrate in the orthorhombic space group *Pnma* with four molecular formula in the unit cell and a density of 1.830 g cm⁻³. The extended structure is similar to that seen for sodium tetrazolate [23]. The sodium cations have a distorted octahedral coordination sphere, which is shown in Fig. 1. Due to this coordination mode, chains are formed along the *a* axis (Fig. 2).

Compounds **1** and **2** underwent thermal and explosive sensitivity tests. The thermal stability of each (~1 mg) was investigated by differential scanning calorimetry using a Linseis PT10 (Linseis Messgeräte GmbH, Germany) differential scanning calorimeter (DSC) at a heating rate of 5°C min⁻¹. Compound **1** exhibited superior thermal stability with an onset of exothermic decomposition beginning at 275°C and a peak exotherm at 300°C. Compound **2** possessed a slightly lower onset of exothermic decomposition beginning at 265°C and a peak exotherm at 292°C. The DSC traces of both are given in Fig. 3. The decomposition of each was also observed in a standard melting point apparatus (heating rate 5°C min⁻¹) whereby darkening of the blue materials occurred at 278 and 269°C for **1** and **2**, respectively. By 300 or 285°C for **1** and **2** the samples had either detonated or turned black (CuO formation) during the multiple trials performed.

For initial safety testing, the impact, friction, and electrostatic discharge sensitivities were determined [24]. The impact sensitivity tests were carried out according to STANAG 4489

Table 1
X-ray diffraction data and parameters

	3	3
Formula	CH ₄ CIN ₄ NaO ₂	631
Form. weight (g mol ⁻¹)	162.52	0.033
Crystal system	Orthorhombic	586
Space group	<i>Pnma</i> (62)	61
Color/habit	Colorless blocks	0.0295
Size (mm)	0.08 × 0.09 × 0.13	0.0781
<i>a</i> (Å)	6.882(1)	1.14
<i>b</i> (Å)	6.964(1)	-0.27, 0.27
<i>c</i> (Å)	12.306(2)	Oxford Xcalibur3 CCD
$\lambda_{\text{MoK}\alpha}$ (Å)	0.71073	SIR-97
<i>T</i> (K)	200	SHELXL-97
Theta min-max (°)	4.4, 26.0	Multi-scan
Data set (h; k; l)	-6:8; -8:8; -15:15	791757
Reflection collected	2,877	
		Independent reflection
		R_{int}
		Observed reflection
		No. parameters
		R_1 (obs)
		w R_2 (all data)
		<i>S</i>
		Min.-max. resd. (e Å ⁻³)
		Device type
		Solution
		Refinement
		Absorption correction
		CCDC No.

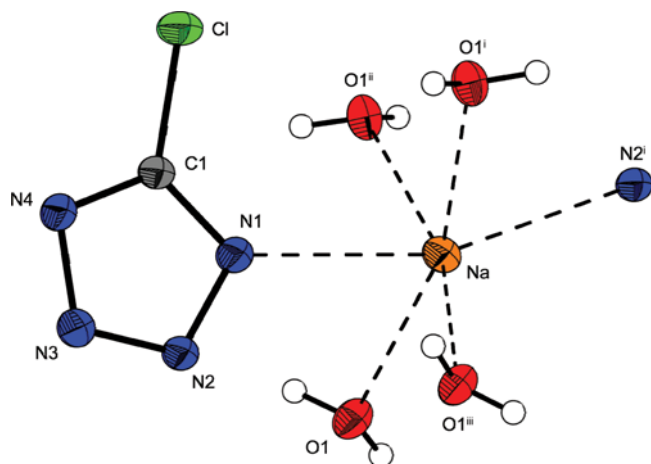


Figure 1. Molecular structure and coordination sphere of the sodium atoms in the structure of **3**. Thermal ellipsoids are drawn at the 50% probability level, and H atoms are shown as spheres of arbitrary radii. Selected distances (Å): Cl–C1 = 1.706(2), Na–O1 = 2.419(1), Na–O1ⁱⁱⁱ = 2.419(1), Na–O1ⁱ = 2.428(1), Na–O1ⁱⁱ = 2.428(1), Na–N1 = 2.574(2), N2–N3 = 1.314(3), N2–N1 = 1.350(3), N3–N4 = 1.349(3), N1–C1 = 1.331(3), N4–C1 = 1.319(3); (i) 0.5 + x, 0.5 – y, 1.5 – z; (ii) 0.5 + x, y, 1.5 – z; (iii) x, 0.5 – y, z (color figure available online).

[25] and were modified according to instruction [26] using a Bundesanstalt für Materialforschung (BAM [27]) drop hammer (Deichel & Partner GmbH, Germany) [28]. The friction

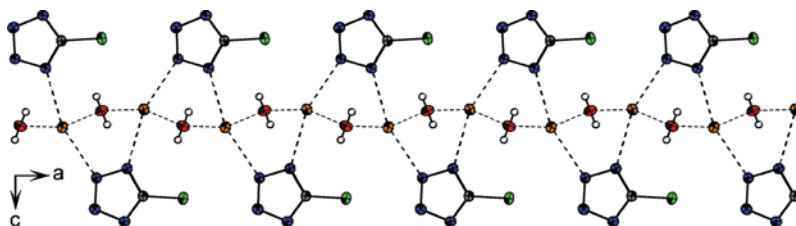


Figure 2. Formation of chains along the *a* axis in the structure of **3**. View along the *b* axis (color figure available online).

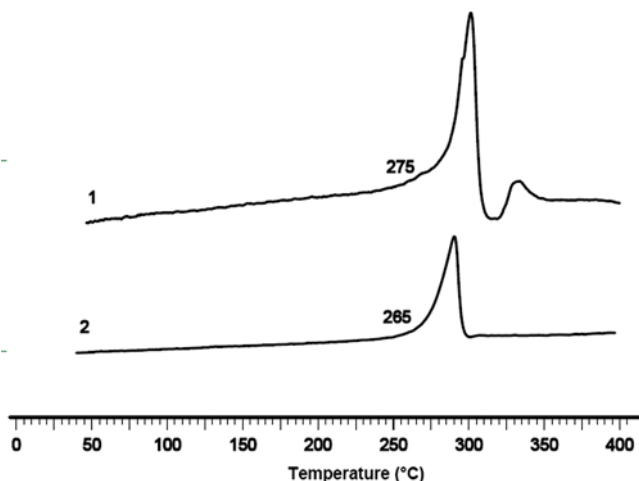


Figure 3. DSC plots of **1** and **2** at a heating rate of $5^{\circ}\text{C min}^{-1}$ (Exo up). T_{dec} ($^{\circ}\text{C}$): **1**, 275; **2**, 265 (color figure available online).

sensitivities were carried out according to STANAG 4487 [29] and were modified according to instruction [30] using a BAM friction tester. Electrostatic sensitivity tests were carried out on a small-scale electric spark tester ESD 2010EN (OZM Research, Czech Republic) operating with the Winspark 1.15 Software Package [31] Both **1** and **2** are classified as “very sensitive” according to the *UN Recommendations on the Transport of Dangerous Goods* [32] in terms of both friction and impact sensitivity (impact: insensitive $>40\text{ J}$, less sensitive $\geq 35\text{ J}$, sensitive $\geq 4\text{ J}$, very sensitive $\leq 3\text{ J}$; friction: insensitive $>360\text{ N}$, less sensitive $= 360\text{ N}$, sensitive $<360\text{ N} > 80\text{ N}$, very sensitive $\leq 80\text{ N}$, extremely sensitive $\leq 10\text{ N}$). Both **1** and **2** are slightly more sensitive than lead azide in terms of impact and comparable within the limits of our instrumentation in friction sensitivities [33]. The advantages of **1** or **2** relative to lead azide become apparent when comparing the sensitivities toward electrostatic discharge (ESD). Lead azide has an ESD sensitivity of only 3 mJ [34], a value easily achieved by the human body, making handling extremely hazardous, whereas **1** and **2** are

only sensitive to 25 and 20 mJ, respectively. These values are at the upper limit of what the human body can generate (~ 25 mJ), offering a distinct margin of safety present compared to the use of lead azide. Table 2 presents the sensitivities of **1** and **2** compared to lead azide.

Flame test results of **1** and **2** provided similar results, with smaller amounts crackling with the presence of a blue-green flame and larger amounts detonating. To characterize the ability of the materials to detonate, plate dent tests [24] were performed with each compound. Into a 0.6-cm-ID copper detonator body 0.12 g of each primary explosive was lightly pressed to a density of 0.85 g cm^{-3} . Using a commercial electric igniter type A (Schäffler & Co. KG, Austria) the samples were detonated against a 1-mm-thick aluminum plate. Compound **1** gave a dent in the plate comparable to the vigorous initiator silver acetylide-nitrate double salt [5], whereas **2** was noticeably less energetic, with a decreased dent in the aluminum plate. Figure 4 shows the remnants of the copper tube detonator bodies where the banana peeling of the copper is noticeably more significant for **1** compared to **2**.

The ability of small amounts of **1** and **2** to explode under the influence of laser ignition was determined by confining several milligrams of each primary explosive in a glass melting point tube and illuminating each with a 658-nm, 200-mW red laser. Both compounds exploded instantly upon illumination. A video of the laser initiation of **1** is available online at <http://www.cup.uni-muenchen.de/ac/klapoetke/content/supplementary/videos/LaserIgnition5.wmv>.

Table 2
Sensitivities of **1** and **2** compared to lead azide

	1	2	Pb(N ₃) ₂
Impact (J)	<1	<1	2.5 ³³
Friction (N)	<5	<5	0.1 ³³
ESD (mJ)	25	20	3 ³⁴



Figure 4. Detonator bodies after detonation of 100 mg of **1** and **2** (color figure available online).

Experimental

All reagents and solvents were used as received (Sigma-Aldrich, Fluka, Germany) if not stated otherwise. Chlorotetrazole and bromotetrazole were prepared according to the literature procedures [35]. Decomposition points were measured with a Linseis PT10 DSC using a heating rate of $5^{\circ}\text{C min}^{-1}$ and were checked with a Büchi Melting Point B-450 apparatus. Infrared spectra were recorded using a Perkin-Elmer Spectrum One Fourier transform infrared (FTIR) instrument. Elemental analyses were performed with a Netsch STA 429 simultaneous thermal analyzer. The impact and friction sensitivity data was determined using a BAM drop hammer and a BAM friction tester, and electrostatic sensitivity was determined using a electric spark tester ESD 2010EN (OZM Research, Czech Republic) operating the Winspark 1.15 software package.

CAUTION: Copper (II) halotetrazolates **1** and **2** are primary explosives of high sensitivity toward various stimuli. Proper personal protective equipment should be used at all times (face shield, goggles, ear protection,

body armor, conductive equipment, Kevlar gloves and arm shields).

Copper (II) Chlorotetrazolate (1)

Copper sulfate (0.40 g, 1.6 mmol) was dissolved in 5 mL distilled water. To this was added a solution of 0.42 g (3.2 mmol) of chlorotetrazole and 1.6 mL 2 M NaOH. The resulting blue precipitate was centrifuged and resuspended in 5 mL distilled water followed by centrifugation. This process was repeated three times to obtain 0.42 g (91%) of **1**. $T_{\text{dec}} = 275^{\circ}\text{C}$; IR (cm^{-1}) $\nu = 3200$ (w, broad), 1442 (w), 1390 (m), 1376 (s), 1358 (s), 1246 (w), 1202 (w), 1182 (w), 1088 (w), 1068 (w), 1038 (w), 721 (w) cm^{-1} ; EA ($\text{CuC}_2\text{N}_8\text{Cl}_2$, 246.51). Calcd.: C, 8.88; N, 41.42. Found: C, 9.21; N, 40.24. BAM impact: <1 J, BAM friction: <5 N; ESD: 25 mJ.

Copper (II) Bromotetrazolate (2)

Copper sulfate (0.20 g, 0.80 mmol) was dissolved in 5 mL distilled water. To this was added a solution of 0.62 g (1.6 mmol) of bromotetrazole and 0.8 mL 2 M NaOH. The resulting blue precipitate was centrifuged and resuspended in 5 mL distilled water followed by centrifugation. This process was repeated three times to obtain 0.26 g (90%) of **2**. $T_{\text{dec}} = 265^{\circ}\text{C}$; IR (cm^{-1}) $\nu = 1436$ (w), 1356 (m), 1335 (s), 1240 (w), 1190 (w), 1173 (w), 1062 (w), 1031 (m), 713 (w) cm^{-1} ; EA ($\text{CuC}_2\text{N}_8\text{Br}_2$, 359.43). Calcd.: C, 6.68, N, 31.18%. Found: C, 6.62; N, 31.37%. BAM impact: <1 J, BAM friction: <5 N; ESD: 20 mJ.

Sodium 5-Chlorotetrazolate Dihydrate (3)

Chlorotetrazole (0.42 g, 3.2 mmol) was dissolved in 1.6 mL of 2 M NaOH and the solution was allowed to evaporate, yielding 0.48 g (92%) of **3** as colorless crystals. $T_{\text{dec}} = 315^{\circ}\text{C}$; IR (cm^{-1}) $\nu = 3507$ (m), 3407 (m), 3251 (w), 1664 (w), 1624 (m), 1458 (w), 1376 (m), 1353 (s), 1195 (m), 1126 (m), 1093 (w), 1044 (m), 1012 (w), 724 (m); ^{13}C NMR (DMSO d_6) δ (ppm) = 150.8

(s, 1C, CN₄Cl); EA (Na₂CN₄Cl(H₂O)₂, 162.51). Calcd.: C, 7.39; N, 34.48; H, 2.48%. Found: C, 7.31; N, 34.36; H, 2.45%.

Conclusions

From this experimental work, the following conclusions can be drawn:

- Copper (II) chloro and bromotetrazolates are easily prepared from the corresponding halotetrazole and a copper salt in high yield.
- The impact and friction sensitivities of the copper halotetrazolates are comparable to (friction) or slightly higher (impact) than those of lead azide; however, the ESD sensitivity of each is lower than lead azide.
- Copper (II) chlorotetrazolate exhibits performance similar to other primaries in the plate dent test. Copper (II) bromotetrazolate exhibits inferior performance.
- Both copper (II) chloro and bromotetrazolates are laser-ignitable primary explosives.
- The chlorotetrazolate anion adopts a similar structure to that of cesium cyanotetrazolate anion.

Acknowledgments

Susanne Scheutzow is gratefully thanked for assistance during testing of the detonators. Financial support of this work by the Ludwig-Maximilian University of Munich (LMU); the U.S. Army Research Laboratory (ARL); the Armament Research, Development and Engineering Center (ARDEC); the Strategic Environmental Research and Development Program (SERDP); and the Office of Naval Research (ONR Global, title: "Synthesis and Characterization of New High Energy Dense Oxidizers (HEDO)—NICOP Effort") under contract nos. W911NF-09-2-0018 (ARL), W911NF-09-1-0120 (ARDEC), W011NF-09-1-0056 (ARDEC), and 10 WPSEED01-002/WP-1765 (SERDP) is gratefully acknowledged. The authors acknowledge collaborations with Dr. Mila Krupka (OZM Research, Czech Republic)

in the development of new testing and evaluation methods for energetic materials and with Dr. Muhamed Sucesca (Brodarski Institute, Croatia) in the development of new computational codes to predict the detonation and propulsion parameters of novel explosives. We are indebted to and thank Drs. Betsy M. Rice and Brad Forch (ARL, Aberdeen, Proving Ground, MD) and Gary Chen (ARDEC, Picatinny Arsenal, NJ) for many helpful and inspired discussions and support of our work.

References

- [1] Dickson, P. M. and J. E. Field. 1993. Initiation and propagation in primary explosives. *Proceedings of the Royal Society A*, 441: 359–375.
- [2] Kaye, S. M. 1978. *Encyclopedia of Explosives and Related Items*, Vol. 8. Dover, NJ: ARRADCOM.
- [3] Urbanski, T. 1967. *Chemistry and Technology of Explosives*, Vol. 4. Oxford: MacMillan Publishing Company.
- [4] Barsan, M. E. and A. Miller. 1996. Lead health hazard evaluation. CDC, HETA Report No. 91-0346-2573.
- [5] Federoff, B. T., H. A. Aaronson, E. F. Reese, O. E. Sheffield, and G. D. Clift. 1960. *Encyclopedia of Explosives and Related Items*, Vol. 1. Picatinny Arsenal, NJ.
- [6] Urbanski, T. 1967. *Chemistry and Technology of Explosives*, Vol. 4. Oxford: Macmillan Publishing Company.
- [7] Fair, H. D. and R. F. Walker. 1977. *Physics and Chemistry of the Inorganic Azides*, Vol 1. New York: Plenum Press.
- [8] Fronabarger, J. W., M. D. Williams, and M. Bichay. 2007. Environmentally acceptable alternatives to lead azide and lead styphnate. In Proceedings of the 43rd AIAA/ASME/SAE/ASEE Joint Propulsion Conference and Exhibit, July 8–11, Cincinnati, Ohio.
- [9] Huynh, M. H. V., M. A. Hiskey, T. J. Meyer, and M. Wetzler. 2006. Green primaries: Environmentally friendly energetic complexes. *Proceedings of the National Academy of Science*, 103: 5409–5412.
- [10] Clark, L. V. 1933. Diazodinitrophenol, a detonating explosive. *Industrial and Engineering Chemistry*, 25: 663–669.
- [11] Huynh, M. H. V., M. A. Hiskey, J. G. Archuleta, E. L. Roemer, and R. D. Gilardi. 2004. 3,6-Diazido-1,2,4,5-tetrazine: A precursor

- for the preparation of carbon nanospheres and nitrogen-rich carbon nitrides. *Angewandte Chemie International Edition*, 43: 5658–5661.
- [12] Davis, T. L. 1943. *The Chemistry of Powder and Explosives, Coll. Vol.* Los Angeles: Angriff Press.
- [13] Zhilin, A. Yu., M. A. Ilyushin, I. V. Tselinskii, and A. S. Brykov. 2001. Synthesis of a high-energy-capacity compound, tetraamine-cis-bis(nitro2H-tetrazolate-N²)cobalt(III) perchlorate. *Russ. J. Appl. Chem.*, 76: 572–576.
- [14] Huynh, M. H. V., M. D. Coburn, T. J. Meyer, and M. Wetzler. 2006. Green primary explosives: 5-Nitrotetrazolato-N²-ferrate hierarchies. *Proceedings of the National Academy of Science*, 103: 10322–10327.
- [15] Gilligan, W. H. and M. J. Kamlet. 1978. *Method of Preparing the Acid Copper Salt of 5-Nitrotetrazole*. U.S. Patent No. 4093623.
- [16] Harkoma, M. 2008. *Laser Detonator*. European Patent No. 1443297 B1.
- [17] CrysAlisPro Oxford Diffraction Ltd. 2009. Version 171.33.41: CrysAlis CCD, v. 1.171.27p5 beta. Oxford Diffraction Ltd.
- [18] CrysAlisPro Oxford Diffraction Ltd. 2009. Version 171.33.41: CrysAlis RED, v. 1.171.27p5 beta. Oxford Diffraction Ltd.
- [19] Altomare, A., M. C. Burla, M. Camalli, G. L. Cascarano, C. Giacovazzo, A. Guagliardi, A. G. G. Moliterni, G. Polidori, and R. Spagna. 1999. A program for crystal structure solution, SIR-92. *Journal of Applied Crystallography*, 32: 115–119.
- [20] Sheldrick, G. M. 1994. *SHELXL-97, Program for the Refinement of Crystal Structures*. Göttingen, Germany: University of Göttingen.
- [21] Farrugia, L. J. 1999. WinGX Suite for single crystal small molecule crystallography. *Journal of Applied Crystallography*, 32: 837–838.
- [22] Spek, A. L. 1999. *Platon, a Multipurpose Crystallographic Tool*. Utrecht, The Netherlands: Utrecht University.
- [23] Klapöte, T. M., M. Stein, and J. Stierstorfer. 2008. Salts of 1H-tetrazole—Synthesis, characterization and properties. *Zeitschrift für Anorganische und Allgemeine Chemie*, 634: 1711–1723.
- [24] Sućeska, M. 1995. *Test Methods for Explosives*. New York: Springer.
- [25] NATO Standardization Agreement (STANAG) on Explosives. 1999. Impact sensitivity tests, no. 4489, 1st ed.

- [26] WIWEB-Standardarbeitsanweisung 4-5.1.02, Ermittlung der Explosionsgefährlichkeit, hier der Schlagempfindlichkeit mit dem Fallhammer, Nov. 8, 2002.
- [27] Available at: <http://www.bam.de> (accessed September 7, 2011).
- [28] Available at: <http://www.reichel-partner.de> (accessed September 7, 2011).
- [29] NATO Standardization Agreement (STANAG) on Explosives. 2002. Friction sensitivity tests, no. 4487, 1st ed.
- [30] WIWEB-Standardarbeitsanweisung 4-5.1.03, Ermittlung der Explosionsgefährlichkeit oder der Reibeempfindlichkeit mit dem Reibeapparat, Nov. 8, 2002.
- [31] Available at: <http://www.ozm.cz/testinginstruments/small-scale-electrostatic-discharge-tester.htm> (accessed September 7, 2011).
- [32] UN Recommendations on the Transport of Dangerous Goods. 2007. ST/SG/AC.10/1/Rev.15, 5th ed., available at: <http://live.unece.org/trans/danger/danger.html> (accessed September 7, 2011).
- [33] Geisberger, G., T. M. Klapötke, and J. Stierstorfer. 2007. Copper bis(1-methyl-5-nitriminotetrazolate): A promising new primary explosive. *European Journal of Inorganic Chemistry*, 30: 4743–4750.
- [34] Hariharanath, B., K. S. Chandrabhanu, A. G. Rajendran, M. Ravindran, and C. B. Kartha. 2006. Detonator using nickel hydrazine nitrate as primary explosive. *Defence Science Journal*, 56: 383–389.
- [35] Stolle, R., E. Schick, F. Henke-Stark, and L. Krauss. 1929. 5-Aminotetrazole. *Berichte der Deutschen Chemischen Gesellschaft*, 62B: 1118–1126.

Inventors: Thomas Klapoetke, Davin Piercey, John Fronabarger, Michael Williams

Attorney Docket No.

METHOD FOR PREPARATION OF A LEAD-FREE PRIMARY EXPLOSIVE

FIELD OF THE INVENTION

[01] This invention relates to explosives, and in particular to a method for preparation of copper(I) 5-nitrotetrazolate “DBX-1”, a lead-free primary explosive under consideration as a replacement for lead azide.

BACKGROUND OF THE INVENTION

[02] The design of new, environmentally friendly, primary explosives to replace lead azide has been a major topic in the research of energetic materials for many years. The unacceptable toxicity of lead azide and its detonation products mandates replacement for both ecological and personal health reasons.

[03] However, finding a suitable replacement for lead azide is complicated by the fact that very few materials have properties which make them useful as primary explosives: the combination of a material that will undergo a deflagration to detonation transition upon ignition, while still being relatively safe to handle is quite rare in chemistry, with relatively few initiatory primary explosives known.

[04] Recently, only one compound has been shown to be a “drop in” replacement for lead azide; requiring no redesign of initiatory devices (detonators or blasting caps) with simple replacement of lead azide by the new material. This new material was created by Pacific Scientific Energetic Materials Company (“PSEMC”) and is copper(I) nitrotetrazolate or “DBX1”. DBX-1 is described in U.S. Patent Nos. 7,833,330 (“the ‘330 patent”); 8,071,784 (“the ‘784 patent”); and 8,163,786 (“the ‘786 patent”) and U.S. Publication Nos. 2012-0024178 (“the ‘178 publication”) and 2012-0077983 (“the ‘983 publication”), all of which are currently assigned to PSEMC. The ‘330, ‘784, and ‘786 patents and the ‘178 and ‘983 publications are hereby incorporated in their entireties herein by this reference. All the explosive requirements of DBX1 are comparable to that of RD1333 grade lead azide in that it is of comparable sensitivity and as such, safety, and also of comparable initiating performance allowing for a material that possesses all the characteristics of lead azide without the associated toxicity.

SUMMARY OF THE INVENTION

[05] The current synthesis of DBX-1 involves preparation and isolation of sodium 5-nitrotetrazolate, which is not commercially available, from 5-aminotetrazole followed by a second reaction step which reacts sodium 5-nitrotetrazolate directly with Cu(I) (U.S. Patent No. 8,071,784) or with Cu(II) and a in-situ reductant (U.S. Patent No. 8,163,786) to produce copper(I) 5-nitrotetrazolate.

[06] There is a need to improve the efficiency of the chemical process by providing a method for preparation of DBX-1 directly from 5-aminotetrazole via a single reactor process which may eliminate the step of isolating the sodium 5-nitrotetrazolate intermediate, a potentially explosive intermediate step. The process delineated in this invention provides a method for converting commercially available 5-aminotetrazole directly to DBX-1 via a single reactor process.

[07] A further advantage of this method is the efficiency in terms of copper. A reaction, commonly known in the industry as the Sandmeyer reaction and used to produce a 5-nitrotetrazolate, utilizes copper(II) to enhance substitution of the reactive diazonium intermediate. This copper is removed and discarded as copper oxide during isolation of the sodium 5-nitrotetrazolate. Additional copper(II) is then used to convert the sodium 5-nitrotetrazolate to DBX-1. The process employed in this invention utilizes the copper(II) associated with the Sandmeyer reaction as a reactant for the formation of DBX-1.

[08] This invention provides a single reactor process for the synthesis of DBX-1 starting from 5-aminotetrazole and which converts it, via a Sandmeyer reaction, to the acid copper(II) salt of 5-nitrotetrazolate. Excess nitrite is then destroyed with nitric acid or urea and the solution is heated. An aqueous solution of sodium ascorbate is then added and the copper(I) nitrotetrazolate is precipitated from solution in the form of a precipitate.

[09] As an example, copper(II) sulfate pentahydrate and sodium nitrite may be dissolved in distilled water and a solution containing 5-aminotetrazole, nitric acid and copper(II) sulfate, also in distilled water, may be added dropwise. The reaction temperature during the addition may be maintained between 15-18 °C. The mixture may then be stirred for 30 minutes followed by addition of nitric acid or urea (to decompose excess nitrite) and then stirring for an additional 1 hour. The solution may be heated to 100 °C and maintained at that temperature for 5 minutes at which time an aqueous sodium ascorbate solution may be added dropwise. The DBX-1 forms

during addition of the sodium ascorbate and may be filtered off and washed with water to afford the product in >80 % yield from 5-aminotetrazole.

DETAILED DESCRIPTION OF THE INVENTION

One aspect of the present subject matter is preparation of the compound copper(I) 5-nitrotetrazolate "DBX-1".

[010] Methods for preparing DBX-1 are contemplated in the present application. DBX-1 may be prepared by reacting copper(II) sulfate pentahydrate, sodium nitrite, 5-aminotetrazole and nitric acid and/or urea in water.

[011] The components may be reacted under conditions suitable to synthesize DBX-1. Alternatively, the components may be reacted by mixing copper(II) sulfate pentahydrate and sodium nitrite in water and then adding a solution containing 5-aminotetrazole, nitric acid and copper(II) sulfate, also in water. The mixture may be maintained in the temperature range of about 0 °C to about 90 °C., alternatively in the temperature range of about 0 °C to about 25 °C, alternatively to about 16 °C. The duration of the temperature control step may be a duration that is greater than about 5 minutes, alternatively greater than about 1 hour, alternatively, about 30 minutes. Nitric acid (or urea) may be added to the reaction and the mixture may be stirred for an additional period which may be greater than 5 minutes, alternatively greater than about 2 hours, alternatively, about 1 hour. The mixture may be heated to 100 °C, alternatively greater than 90 °C, and an aqueous solution of sodium ascorbate may be added at such a rate that DBX-1 begins to precipitate. Once DBX-1 has begun to precipitate, sodium ascorbate may be added at such a rate as to form crystalline DBX-1. Once DBX-1 has formed, the reaction may be stirred for about 30 minutes at elevated temperature, alternatively it may be stirred for 5 minutes at elevated temperature. The DBX-1 precipitate may be isolated by filtration or by a suitable method known to those of skill in the art. The product may be washed either a single time or multiple times with water. Alternatively, the product may be washed a single time or multiple times with an alcohol, for example, isopropanol. Alternatively, the product may be washed with in multiple steps and in any order with both water and alcohol.

[012] It will be understood that DBX-1 may be prepared by reacting any suitable copper(II) salt or combination of copper(II) salts. Suitable copper(II) salts may include, but are not limited to, copper(II) sulfate or copper(II) nitrate. Likewise any suitable reducing agent or combination of

reducing agents may be employed. Suitable reducing agents include, but are not limited to, sodium ascorbate. Likewise, any suitable solvent or combination of solvents may be used. Suitable solvents include, but are not limited to, water.

[013] Regarding quantities of the components employed, sodium nitrite may be supplied in a molar ratio of about 2 moles to about 6 moles per mole of copper(II) sulfate pentahydrate. 5-Aminotetrazole may be supplied in a molar ratio of about 0.8 moles to about 1.2 moles per mole of copper(II) sulfate pentahydrate. Nitric acid may be supplied in a molar ratio of about 1 mole to about 6 moles per mole of copper(II) sulfate pentahydrate. For example, sodium nitrite may be supplied in a molar ratio of about 3 moles per mole of copper(II) sulfate pentahydrate, 5-aminotetrazole may be supplied in a molar ratio of about 1 mole per mole of copper(II) sulfate pentahydrate, while 2 moles of nitric acid may be supplied per mole of copper(II) sulfate pentahydrate. If used for decomposition of excess nitrite, urea may be supplied in a molar ratio of 0.5 moles per mole of excess nitrite added.

[014] A solvent may be supplied in an amount that is suitable to effectuate the reaction between copper(II) sulfate pentahydrate, sodium nitrate, nitric acid and 5-aminotetrazole. As a more specific example, water (or other solvent) may be supplied in an amount that is suitable to effectuate the reaction between copper(II) sulfate pentahydrate, sodium nitrate, nitric acid and 5-aminotetrazole.

[015] The reaction components may be combined in any order or sequence suitable to effectuate the reaction. By way of non-limiting example, the reaction of copper(II) sulfate pentahydrate, sodium nitrite, 5-aminotetrazole, nitric acid and sodium ascorbate may be carried out by adding a mixture of 5-aminotetrazole, nitric acid and copper(II) sulfate as an aqueous solution to an aqueous solution of copper(II) sulfate pentahydrate and sodium nitrite and adding nitric acid or urea followed by an aqueous solution of sodium ascorbate.

[016] The products contemplated and made by the methods of the present application (in at least some aspects of the present subject matter, DBX-1) may be found suitable for use as explosives and, in particular, as an intermediate for primary explosives. Thus, the present application also contemplates methods for preparing compounds suitable for use as primary explosives, and explosive devices employing such compounds. Benefits include ease of preparation and low toxicity waste streams and health benefits for both military and commercial applications.

[017] The foregoing is provided for purposes of illustrating, explaining and describing embodiments of the present invention. Further modifications and adaptations to these embodiments will be apparent to those skilled in the art and may be made without departing from the scope or spirit of the invention.

EXAMPLES

[018] The following examples demonstrate the preparation and characterization of a material as taught herein.

Example 1

[019] To a solution of 1.54 g of copper(II) sulfate pentahydrate and 1.3 g sodium nitrite in 20 mL distilled water was added dropwise a second solution composed of 0.53 g 5-aminotetrazole, 0.75 mL 65% nitric acid, and 0.015 g of copper(II) sulfate pentahydrate in 15 mL distilled water. The temperature during addition was maintained at 15-18 °C. After addition the solution was stirred for 30 minutes followed by the addition of 1 mL 65% nitric acid and stirring for a further 1 hour. The solution was then heated to 100°C, maintained there for 5 minutes, followed by the addition of 10 mL of freshly-prepared 1M sodium ascorbate dropwise also at 100°C. Initially, the precipitated species re-dissolve during which time the addition can be at the rate of 2-3 drops per second. Once the DBX-1 precipitate begins to remain after addition, the dropping proceeds ideally when 5 drops are added at the rate of one per second, the solution is allowed to stir for 10 seconds, then 5 more drops are added. After addition is complete the solution is stirred for 5 minutes at 100°C, filtered while hot and rinsed with hot water. The filter cake is dried at 75°C overnight. The yield is 0.98 g. (88%)

Example 2

[020] To a solution of 1.43 g (6.17 mmol) of copper(II) nitrate and 1.3 g (18.84 mmol) sodium nitrite in 20 mL distilled water was added dropwise a second solution composed of 0.53 g (6.23 mmol) 5-aminotetrazole, 0.75 mL 65% nitric acid, and 0.013 g of copper(II) nitrate in 15 mL distilled water. The temperature during addition was maintained at 14-15 °C. After addition the solution was stirred for 38 minutes followed by the addition of 0.19 g (6.38 mmol) urea and stirring for an additional 5 minutes. The solution was then heated to 100°C, maintained there for 5 minutes, followed by the addition of 10 mL of freshly-prepared 1M sodium ascorbate dropwise also at 100°C. Initially, the precipitated species re-dissolve during which time the addition can be at the rate of 2-3 drops per second. Once the DBX-1 precipitate begins to remain after

addition, the dropping proceeds ideally when 5 drops are added at the rate of one per second, the solution is allowed to stir for 10 seconds, then 5 more drops are added. After addition is complete the solution is stirred for 5 minutes at 100°C, filtered while hot and rinsed with hot water. The filter cake is dried at 75°C overnight.

What is claimed is:

1. A method of preparing copper(I) 5-nitrotetrazolate.
2. The reaction product of:
 - (a) a copper(II) salt;
 - (b) sodium nitrite,
 - (c) nitric acid,
 - (d) 5-aminotetrazole,
 - (e) sodium ascorbate, and
 - (f) water.
3. A method for preparing copper(I) 5-nitrotetrazolate, comprising the steps of:
 - (a) providing an aqueous solution of copper(II) sulfate pentahydrate and sodium nitrite;
 - (b) adding an aqueous solution of 5-aminotetrazole, nitric acid and copper(II) sulfate pentahydrate;
 - (c) combining said solutions to form a mixture while cooling the mixture;
 - (d) adding additional nitric acid to the mixture; and
 - (e) adding an aqueous solution of 1M sodium ascorbate to the mixture.;
4. A method for preparing copper(I) 5-nitrotetrazolate, comprising the steps of:
 - (a) providing an aqueous solution of copper(II) sulfate pentahydrate and sodium nitrite;
 - (b) adding an aqueous solution of 5-aminotetrazole, nitric acid and copper(II) sulfate pentahydrate;
 - (c) combining said solutions to form a mixture while cooling the mixture;

- (d) adding urea to the mixture; and
- (e) adding an aqueous solution of 1M sodium ascorbate to the mixture.

Abstract

Described are methods for preparing copper(I) 5-nitrotetrazolate.

DOI: 10.1002/zaac.200((will be filled in by the editorial staff))

Improved Preparation of Sodium Nitrotetrazolate Dihydrate: Suitable for DBX-1 Preparation

Thomas M. Klapötke,^[*,a] Neha Mehta^[b], Karl D. Oyler,^[b] Davin G. Piercey,^[a]

Keywords: tetrazoles; tetrazines, high energy density materials; nitrogen-rich compounds; energetic materials

Sodium nitrotetrazolate dihydrate is a useful precursor compound for the synthesis of lead-free primary explosives. In this work we report an improved procedure for its preparation avoiding the handling of acid copper(II) nitrotetrazolate, a highly sensitive explosive intermediate. 5-Aminotetrazole is diazotized with sodium nitrite, cupric sulfate, and nitric acid.

Copper is precipitated as its oxide and the aqueous solution evaporated. After soxhlet extraction with acetone, large crystals of sodium nitrotetrazolate dihydrate are obtained. The prepared material is suitable for preparation of lead azide replacement DBX-1 (copper(I) nitrotetrazolate) as evidenced by use in a M55 stab detonator.

* Prof. Dr. T. M. Klapötke

Fax: +49-89-2180-77492

E-Mail: tmk@cup.uni-muenchen.de

- [a] Department of Chemistry
Energetic Materials Research
Ludwig-Maximilian University
Butenandtstr. 5-13 (D)
81377 München, Germany
- [b] US Army TACOM-ARDEC
Picatinny Arsenal
NJ 07806, United States

While a variety of new energetic materials have been studied as prospective lead azide replacements including calcium nitriminotetrazolate, copper chlorotetrazolate, diazodinitrophenol (DDNP), and copper(II) coordination complexes of the nitrotetrazolate anion, all of them have limitations preventing their use. Copper (I) nitrotetrazolate or DBX1 differs in that it is a ‘drop-in’ replacement for lead azide, requiring no redesign to manufactured explosive devices beyond the use of DBX1 instead of lead azide. As a result of possessing these similar safety and initiation abilities compared to lead azide, DBX1 is one of the most promising lead azide replacements to date.^[5,6]

Introduction

The research of new primary explosives for the replacement of lead azide has been very significant in recent years. The major driving force for this work is the high personal and environmental toxicity of lead, and as such, a green primary explosive is sought. Primary explosives are the highly-sensitive explosives used to initiate a larger mass of secondary explosive such as TNT (2,4,6-trinitrotoluene). The phenomena unique to a primary explosive is the ability to undergo a deflagration-to-detonation transition (DDT) whereby a reaction front propagated by conduction and convection (deflagration) develops into a shockwave-propagated reaction. Secondary explosives can undergo a DDT as well, however the difference is that a primary will undergo a DDT on a far smaller scale, often on the order of several milligrams, than a secondary which would simply burn or deflagrate at these small masses.^[1]

Lead azide has been commonly used as a primary since it replaced mercury fulminate in the early 20th century, and has limitations beyond the high toxicity of lead. Lead azide is also degraded by carbon dioxide and can detonate during synthesis if conditions are not rigorously controlled.^[2-4]

DBX-1 is prepared from sodium nitrotetrazolate dihydrate, a copper (II) salt, and a reducing agent; unfortunately sodium nitrotetrazolate dihydrate is not commercially available and must be produced from 5-aminotetrazole.^[7-9] This is done via a sandmeyer reaction in the presence of a copper (II) salt and this produces a very explosive intermediate, copper (II) nitrotetrazolate, acid salt, $\text{Cu}(\text{NT}_2)\text{HNT}$ ($\text{NT} = \text{nitrotetrazolate}, \text{CN}_5\text{O}_2^-$). This copper salt is filtered off, and if dried is very sensitive towards impact and friction, although while wet the sensitivities are reduced. This wet filtercake is then resuspended in water and heated with sodium hydroxide yielding copper (II) oxide and a aqueous solution of sodium nitrotetrazolate which crystallizes as the dihydrate. (NaNT) The limiting step in this procedure is the handling of the copper salt, beyond this material being a sensitive explosive, this precipitate filtration step would lead to increased industrial costs and potentially lower yields due to transfer losses. Another major challenge of the NaNT synthesis is the lack of purity of the resulting NaNT . Raw NaNT solutions made from the current procedure do not successfully produce DBX-1 directly, but first require further purification through

controlled laboratory titration to remove impurities such as unreacted 5-aminotetrazole.

In this work, we report a safer and simplified procedure for the preparation of sodium nitrotetrazolate dihydrate and demonstrate that the produced material is of sufficient purity to be used for the preparation of DBX-1. The DBX-1 prepared from this NaNT functions comparably to current state-of-the-art DBX-1 in stab detonators and is of comparable sensitivity.

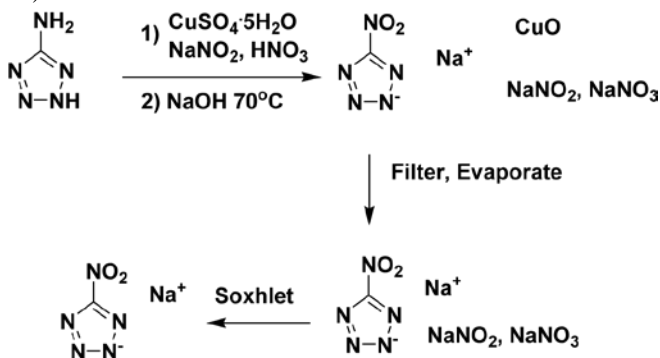
Results and Discussion

SYNTHESIS. An aqueous solution of 5-aminotetrazole, nitric acid, and a trace of copper (II) sulphate pentahydrate is added dropwise to a pre-chilled (5- 10 °C) solution of sodium nitrite and copper (II) sulphate. During addition the temperature of the solution is allowed to raise to 15- 18 °C. Once this temperature range is reached, the addition is continued at a slightly slower rate and the flask immersed in a water bath. The temperature of the reaction is maintained by the raising or lowering of the flask within the water bath, and by the addition of small chunks of ice to the water bath. By following this procedure exactly, we have never observed a single microdetonation as has been known for this reaction.^[7-9] We were, however, able to force microdetonations by the rapid addition of aminotetrazole solution to the reaction under strong cooling. It appears that the key factor preventing microdetonations is a very slow addition rate. After addition is completed, the solution is allowed to stir for thirty minutes and dilute nitric acid is added, followed by the warming of the solution to room temperature and stirring for another hour. An aqueous solution of sodium hydroxide is then added until pH eight is reached and the solution is heated to 70 °C where it is maintained for two hours. The precipitated copper oxide is filtered off through kieselguhr and the aqueous filtrate evaporated under vacuum at a temperature no higher than 35 °C. The solid residue is soxhlet extracted with acetone and the acetone slowly evaporated yielding crystals of sodium nitrotetrazolate dihydrate in over 80% yield. Crystals are isolated by filtration through a Buchner funnel without paper, or a pasta strainer, as small amounts of a non-crystalline solid occasionally precipitates as the nitrotetrazolate crystallizes. The NaNT crystals are often greater than half a centimetre in dimension and the non crystalline solid can easily be removed by this type of filtration. The NaNT can be recrystallized from acetone. Scheme 1 illustrates this process.

Infrared and Raman spectroscopic results were identical to those in the literature, as were proton and carbon NMR spectra.

USE OF NANT FOR THE PREPARATION OF DBX-1. We have synthesized two small scale batches (KO-6 and KO-9) of 2-3 grams each and one intermediate scale batch (KO-12) of 8-10 grams of DBX-1 from our NaNT. The procedure used to synthesize DBX-1 was based on literature methods.^[5,6] For each batch, sensitivity tests, thermal stability by differential scanning calorimetry (DSC) and performance tests were performed and compared to the standard DBX-1 that was obtained from PSEMC (Pacific

Scientific Energetic Materials Company, inventors of DBX-1).



Scheme 1. Synthesis of NaNT

Table 1. Sensivity Data of PSEMC and ARDEC DBX-1

Name	Ball Drop Impact (in)	BAM Friction (N)	ESD (J)
PSEMC DBX1	NG @ 30"	GO @ 0.1N	NG @ 0.0016J
KO-6	NG @ 8"	GO @ 0.1N	NG @ 0.0025J
KO-9	NG @ 30"	GO @ 0.1N	NG @ 0.0020J
KO-12	NG @ 4"	GO @ 0.1N	NG @ 0.0025J

There seems to be a noticeable difference in the Ball Drop Impact results and this could be attributed to the inherent error associated with this relatively crude test; for instance, the manner and precise location at which the steel ball impacts the explosive particles can vary and lead to inconsistent results. Friction and electrostatic sensitivity was consistent across all of our batches of DBX1 as well as PSEMC DBX-1. (Table 1) In terms of determining the effectiveness of a primary explosive, sensitivity tests results are generally only predictive in how to safely handle the material; in order to determine if the explosive is practical or not, performance tests need to be done to see how well the material behaves in actual items, such as detonators.

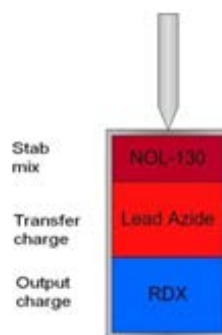


Figure 1. M55 Stab Detonator

Performance tests consisted of loading DBX-1 as a transfer charge in U.S. Army M55 stab detonators. Standard M55 detonators consist of three separate explosive layers, pressed sequentially into a metal detonator cup as shown in Figure 1. The first layer is 15 mg of the stab initiation mix (NOL-130); it is a combination of lead azide, lead styphnate, barium nitrate, antimony sulfide and tetrazene (1-(5-tetrazolyl)-3-guanyltetrazene hydrate), pressed at 70,000 psi. The second layer is 51 mg of transfer charge, lead azide,

pressed at 10,000 psi. Lastly, the third layer is 19 mg of output charge, RDX, pressed at 15,000 psi.

To measure DBX-1 performance, lead azide was replaced with DBX-1 in the loaded M55's. Only 40 mg of DBX-1 was used compared to 51mg of lead azide due to the inherent density differences between the two materials. M55 detonators were loaded using Arbor hand presses (Figure

2a) and tested for performance (Figure 2b-2c). The M55 detonator was placed in a plastic fixture, as shown in Figure 3b and a 0.25 oz ball was dropped onto the firing pin from a height of 3 inches. For a standard M55 detonator, the exploding item creates a dent of greater than 0.01" on a steel plate. Dent depths were measured using a laser profilometer (Figure 2d).

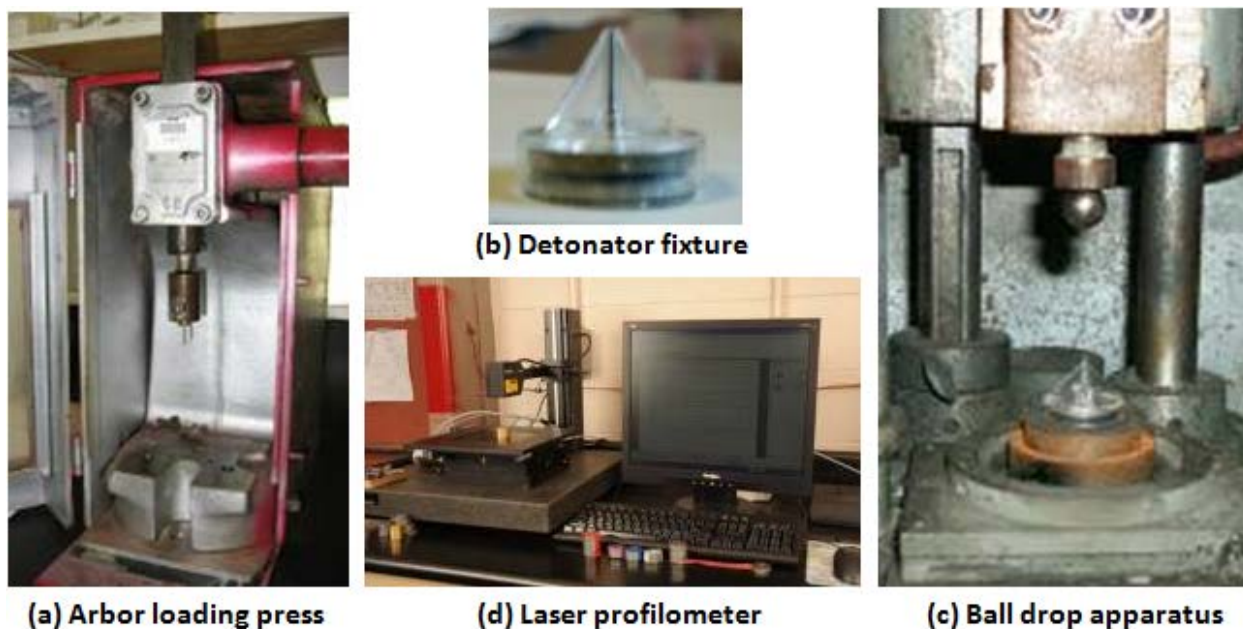


Figure 2. Detonator Loading and Testing Equipment

Table 2. Energetic properties for all prepared energetic compounds.

Batch	Initiation Method	# tests	# >0.01"
PSEMC DBX-1	Stab	10	10
KO-9	Stab	10	9
KO-12	Stab	10	10
KO-6	Stab	10	4
KO-6	electric	9	9

All M55 detonators prepared with PSEMC DBX-1 created dents of the requisite depth. Both batches KO-9 and KO-12 were prepared using a seed crystal from one PSEMC batch of DBX-1 and KO-6 was created using a seed crystal from an older batch of PSEMC DBX-1. All detonators prepared with KO-9 met the dent depth requirement except for one. This could be attributed to an operator error. Since batch KO-9 produced successful results, a larger batch of 10 grams (KO-12) was made. KO-12 also produced successful results and all 10/10 detonators functioned.

For KO-6 only 4 of 10 detonators met the specifications of dent depth greater than 0.01". Other detonators would initiate but would not go high order (e.g. the RDX output charge did not appear to detonate). This could be attributed to a density problem or a run up distance issue. Before making any decisions, it was decided to see if DBX-1 could initiate RDX electrically using a nichrome wire. This test was successful and all nine detonators functioned. Figure 3 shows the electrical ignition setup. There could be a possibility of not having the correct particle size as we desired with this batch or some impurities with this batch.



Figure 3. Setup of electrically initiating M55 detonators

The unusual behaviour of KO-6 prompted us to study it by DSC (Differential Scanning Calorimetry). Two samples each of KO-6 and PSEMC DBX-1 were studied by DSC ($5\text{ }^{\circ}\text{C min}^{-1}$). KO-6 samples had DSC onsets at 305.9 and $307.0\text{ }^{\circ}\text{C}$ while PSEMC DBX-1 had onsets at 304.0 and $305.0\text{ }^{\circ}\text{C}$. The peak temperature in the DSC was 312.4 and 313.0 , and 309.5 and $311.5\text{ }^{\circ}\text{C}$ for KO-6 and PSEMC DBX-1 respectively.

Conclusions

Our new method of isolating sodium nitrotetrazolate dihydrate produces material in high yield, without the intermediate handling of sensitive explosive compounds. This produced NaNT is of sufficient purity for the preparation of DBX-1 of the quality that is required to replace lead azide. It does, however, appear that the DBX used as a seed crystal in the synthesis of DBX-1 influences the behaviour of the end product.

Experimental Section

All reagents and solvents were used as received (*Sigma-Aldrich*) if not stated otherwise. NOL-130 stab initiation mix (Lot # 070601B) and preformed, 19 mg graphite-blended 1,3,5-trinitro-1,3,5-triazacyclohexane (RDX) pellets (Lot # HOL91H600-042) were purchased from Day & Zimmerman (DZI). Scanning electron microscopy (SEM) images and energy dispersive spectroscopy (EDS) spectra were collected on an EVEX mini-SEM SX3000. Differential scanning calorimetry (DSC) data were obtained with a heating rate of 5°C/min by Henry Grau, ARDEC. Sensitivity tests consisted of Ball Drop Impact, BAM Friction and Electrostatic Discharge (ESD). For each test trial 30 mg of explosives were used. The Ball Drop Impact test for primary explosives is described in MIL-STD-1751A, Method 1016, (20 August 1982). The Ball Drop Impact test apparatus, subjects a primary explosive to an impact of a free-falling steel ball weighing 28.35 g (1 oz). The small BAM Friction test method is described in STANAG 4487 "Explosives, Friction Sensitivity Tests." The BAM Small Friction test determines the friction sensitivity of the sample. The Electrostatic Sensitivity Test methodology is given in AOP-7 "Manual of Data Requirements and Tests for the Qualification of Explosive Materials for Military Use".

CAUTION! *Sodium nitrotetrazolate dihydrate is an energetic material with sensitivity to various stimuli. While we encountered no issues in the handling of this material, proper protective measures (face shield, ear protection, body armor, Kevlar gloves, and earthened equipment) should be used at all times.*

Sodium Nitrotetrazolate dihydrate (NaNT)

8.48 g (0.10 mol) of anhydrous aminotetrazole and 0.2 g (0.8 mmol) of copper sulfate pentahydrate was added to a solution of 9 mL 65% nitric acid in 60 mL distilled water. This was added to a pre-cooled solution of 20.8 g (0.30 mol) sodium nitrite and 11 g (0.044 mol) cupric sulfate pentahydrate in 100 mL distilled water. The solution is maintained at 15 to 18 °C during the addition by means of a cool water bath. After addition, the solution is stirred for 30 minutes at the same temperature followed by the addition of 14 mLs of 65% nitric acid diluted to 20 mLs. The solution is allowed to warm to room temperature and is stirred there for one hour. Under vigorous stirring, 50% aqueous sodium hydroxide is added until the pH of the solution reaches 8, and the temperature is then raised to 70 °C where it is maintained for two hours. The pH is checked and adjusted to 8 again if necessary, and then filtered through celite. The filtrate is then evaporated to

dryness (using a 30 °C water bath) and soxhlet extracted overnight with acetone. The acetone is allowed to slowly evaporate and is filtered through a Buchner funnel lacking filter paper or a pasta strainer yielding 13.76 g (0.080 mol) of large colorless-to-light-yellow crystals of sodium nitrotetrazolate dihydrate. The analysis is identical to the literature.^[9]

Acknowledgement

Financial support of this work by the Ludwig-Maximilian University of Munich (LMU), the U.S. Army Research Laboratory (ARL), the Armament Research, Development and Engineering Center (ARDEC), the Strategic Environmental Research and Development Program (SERDP) and the Office of Naval Research (ONR Global, title: "Synthesis and Characterization of New High Energy Dense Oxidizers (HEDO) - NICOP Effort ") under contract nos. W911NF-09-2-0018 (ARL), W911NF-09-1-0120 (ARDEC), W011NF-09-1-0056 (ARDEC) and 10 WPSEED01-002 / WP-1765 (SERDP) is gratefully acknowledged. The authors acknowledge collaborations with Dr. Mila Krupka (OZM Research, Czech Republic) in the development of new testing and evaluation methods for energetic materials and with Dr. Muhamed Suceca (Brodarski Institute, Croatia) in the development of new computational codes to predict the detonation and propulsion parameters of novel explosives. We are indebted to and thank Drs. Betsy M. Rice and Brad Forch (ARL, Aberdeen, Proving Ground, MD) and Mr. Gary Chen (ARDEC, Picatinny Arsenal, NJ) for many helpful and inspired discussions and support of our work. The authors want to thank St. Huber for measuring the sensitivities.

References

- [1] D. Fischer, T. M. Klapötke, D. G. Piercey, J. Stierstorfer, *J. Energ. Mat.* **2012**, *30*, 40-54.
- [2] M. E. Barsan, A. Miller, *Lead Health Hazard Evaluation*. **1996**. HETA Report No. 91-0346-2573.
- [3] T. Urbanski, **1967**. *Chemistry and Technology of Explosives Vol 4* Oxford: Macmillan Publishing Company . p171.
- [4] H. D. Fair, R. F. Walker, **1977**. *Physics and Chemistry of the Inorganic Azides, Vol 1*. Plenum Press: New York.
- [5] J. W. Fronabarger, M. D. Williams, W. B. Sanborn, J. G. Bragg, D. A. Parrish, M. Bichay, *Propellants Explos. Pyrotech.* **2011**, *36*, 541-550.
- [6] J. W. Fronabarger, M. D. Williams, W. B. Sanborn, US Patent 7,833,330. **2010**.
- [7] E. Von Herz, US Patent 2,066,954, **1937**.
- [8] W. H. Gilligan, M. J. Kamlet, US Patent 4,093,623, **1978**.
- [9] T. M. Klapötke, C. M. Sabaté, J. M. Welch, *Eur. J. Inorg. Chem.* **2009**, *6*, 769-776.

Received: ((will be filled in by the editorial staff))
Published online: ((will be filled in by the editorial staff))

Cite this: *Dalton Trans.*, 2012, **41**, 9451

www.rsc.org/dalton

PAPER

Amination of energetic anions: high-performing energetic materials†

Thomas M. Klapötke,* Davin G. Piercey and Jörg Stierstorfer

Received 26th March 2012, Accepted 22nd May 2012

DOI: 10.1039/c2dt30684k

The new energetic materials 2-amino-5-nitrotetrazole (ANT, **1**), 1-amino-3,4-dinitro-1,2,4-triazole (ADNT, **2**), and both 1,1'-diamino-5,5'-bistetrazole and 1,2'-diamino-5,5'-bistetrazole (11DABT, **3** and 12DABT, **4**) have been prepared by the amination of the parent anion with *O*-tosylhydroxylamine. The 5-*H*-tetrazolate anion has also been aminated using hydroxylamine *O*-sulfonic acid to both 1-aminotetrazole and 2-aminotetrazole (1AT, **5** and 2AT, **6**). The prepared materials have been characterized chemically (XRD (**1–4**, **6**·AtNO₂, **8**), multinuclear NMR, IR, Raman) and as explosives (mechanical and electrostatic sensitivity) and their explosive performances calculated using the EXPLO5 computer code. The prepared *N*-amino energetic materials, which can also be used as new ligands for high energy-capacity transition metal complexes, exhibit high explosive performances (in the range of hexogen and octogen) and a range of sensitivities from low to extremely high.

Introduction

The design of new energetic materials is an intensely-pursued research area in the chemical sciences, with a historical following including such scientists as Liebig, Berzelius, and Gay-Lussac.^{1–8} The field of energetic materials research possesses a unique combination of both academic and practical interest, where working with metastable molecules on the edge of existence is both valued militarily and industrially for their value as explosives, and by scientists for their value in predicting factors affecting molecular stability, and the unique synthetic reactions that are mandated. Beyond these factors, one of the driving forces of modern energetic materials research is that the produced materials must be “green” by not causing an environmental or toxicological hazard, while simultaneously increasing performance.^{9,10}

Traditional energetic materials including quintessential explosives such as RDX (1,3,5-trinitro-1,3,5-triazinane) and TNT (2,4,6-trinitrotoluene) are based on the oldest strategy in energetic materials design: the presence of fuel and oxidizer in the same molecule. New strategies in energetic materials research include high-nitrogen/high heat of formation compounds, those possessing ring or cage strain, and combinations of all three strategies.^{3,11,12}

Possessing high heats of formation and ring strain, triazoles and tetrazoles have been used for the preparation of high-performance primary¹³ and secondary explosives.¹⁴ Triazoles and tetrazoles occupy an intermediate position on the ‘stability versus heat of formation’ continuum, where pyrazoles are stable

but possess a poor heat of formation, but pentazoles, while possessing a high heat of formation, are thermally unstable with most members of this class of compound decomposing below room temperature.¹⁵

The *N*-amination of both electron-rich triazoles¹⁶ and tetrazoles¹⁷ has been known for some time, using the commercially available hydroxylamine-*O*-sulfonic acid (HOSA), however HOSA aminations unfortunately do not extend to electron poor systems. The addition of an amino group to an energetic molecule is advantageous in terms of stability, for example amino-nitro compounds such as 1,3,5-triamino-2,4,6-trinitrobenzene (TATB) or diaminodinitroethylene (FOX-7) are low-sensitivity-high-performance explosives that are the standard for insensitive explosives¹⁸ (Fig. 1). *N*-Amino compounds have the further advantage that their heats of formation (and as such explosive performance) increase as a result of the additional N–N single bond. In addition, new donor sites and functionalities are introduced by the NH₂ groups yielding (for example) new potential nitrogen ligands for high energy-capacity transition metal complexes.

O-Tosylhydroxylamine (THA)^{19,20} is a powerful amination agent well known to aminate electron-poor systems. We have used this reagent to aminate the electron poor 5-nitrotetrazolate, 3,5-dinitro-1,2,4-triazolate, and 5,5'-bistetrazolate anions yielding 2-amino-5-nitrotetrazole (ANT, **1**), 1-amino-3,4-dinitro-1,2,4-triazole (ADNT, **2**), and both 1,1'-diamino-5,5'-bistetrazole

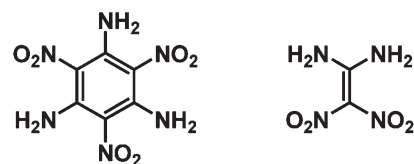


Fig. 1 The structures of TATB and FOX-7.

Butenandstrasse 5-13 (Haus D), D-81377 Munich, Germany.
E-mail: tmk@cup.uni-muenchen.de; Fax: +892180 77492

†CCDC 871736, 871737, 871738, 871739, 871734 and 871735. For ESI and crystallographic data in CIF or other electronic format see DOI: 10.1039/c2dt30684k

and 1,2'-diamino-5,5'-bistetrazole (11DABT, **3** and 12DABT, **4**). ANT and ADNT have been mentioned in the literature,²¹ but no full synthetic procedure is available. The compounds were characterized by X-ray diffraction, infrared and Raman spectroscopy, multinuclear NMR spectroscopy, elemental analysis, and DSC. Computational calculations confirming the high energetic performance were also performed. We furthermore repeat the literature synthesis¹⁷ of 1-amino (**5**) and 2-aminotetrazoles (**6**) with HOSA and report the full chemical and energetic properties. Three derivatives of *N*-amino energetic heterocycles have also been prepared: the azo coupling product of **1**, 2,2'-azobis-(5-nitrotetrazole), **7**, a compound of astounding sensitivity and performance; the condensation product of **5** with trinitroethanol, 1-(trinitroethylamino)tetrazole (**8**); and a cocrystal of **6** with nitriminotetrazole (**6**·ATNO₂). Compound **7** has been mentioned²² in a patent, however no characterization was mentioned, not even the exceedingly high sensitivity that we determined.

Experimental

All reagents and solvents were used as received (Sigma-Aldrich, Fluka, Acros Organics) if not stated otherwise. Ethyl-*O*-*p*-tolylsulphonylacetoxyhydroximate, ammonium nitrotetrazolate hemihydrate, ammonium dinitrotriazolate, 5,5'-bistetrazole and trinitroethanol were prepared according to the literature procedures.^{19,23–25} Melting and decomposition points were measured with a Linseis PT10 DSC using heating rates of 5 °C min⁻¹, which were checked with a Büchi Melting Point B-450 apparatus. ¹H, ¹³C and ¹⁵N NMR spectra were measured with a JEOL Eclipse 270, a JEOL EX 400, or a JEOL Eclipse 400 instrument. All chemical shifts are quoted in ppm relative to TMS (¹H, ¹³C) or nitromethane (¹⁵N). Infrared spectra were measured with a Perkin-Elmer Spektrum One FT-IR instrument. Raman spectra were measured with a Perkin-Elmer Spektrum 2000R NIR FT-Raman instrument equipped with a Nd-YAG laser (1064 nm). Elemental analyses were performed with a Netsch STA 429 simultaneous thermal analyser. Sensitivity data were determined using a BAM drophammer and a BAM friction tester (method: 1 of 6). The electrostatic sensitivity tests were carried out using an Electric Spark Tester ESD 2010 EN (OZM Research) operating with the “Winspark 1.15” software package.

Electronic energies (CBS-4M method) were calculated with the Gaussian09 (Revision A.02) software.²⁶ Gas phase enthalpies of formation were computed using the atomization method numerously described recently.²⁷ The gas phase enthalpies of formation were converted to the solid state enthalpies of formation by subtraction of sublimation enthalpy calculated according to Trouton's rule ($\Delta H_{\text{sub}} = 188T_{\text{m}}$, $\Delta H_{\text{vap}} = 108T_{\text{b}}$).²⁸ Detonation parameters were calculated with the EXPLO5.04 computer code.²⁹

XRD was performed on an Oxford Xcalibur3 diffractometer with a Spellman generator (voltage 50 kV, current 40 mA) and a KappaCCD detector. The data collection and reduction was carried out using the CRYSLISPRO software.³⁰ The structures were solved either with SIR-92³¹ or SHELXS-97,³² refined with SHELXL-97³³ and finally checked using the PLATON³⁴ software integrated in the WINGX³⁵ software suite. The non-hydrogen atoms were refined anisotropically and the hydrogen atoms were

located and freely refined. The absorptions were corrected by a Scale3 Abspack multi-scan method.³⁶

CAUTION! *All the following compounds are energetic materials with sensitivity to various stimuli. While compounds 1–6 and 8 were handled without incident, proper protective measures (face shield, ear protection, body armour, Kevlar® gloves and earthed equipment) should be used at all times. Compound 7 is exceedingly sensitive and can spontaneously detonate even when damp. Extreme caution is advised.*

2-Amino-5-nitrotetrazole (ANT, **1**)

0.95 g (3.69 mmol) of freshly prepared pulverized ethyl *O*-*p*-tolylsulphonylacetoxyhydroximate was added to 7.5 mL of 60% perchloric acid at room temperature and stirred under ambient conditions for 2 h. The now-free tosylhydroxylamine suspension was poured into 80 mL of ice/water slurry and after the ice was melted the mixture was extracted with 7 × 10 mL portions of dichloromethane. The combined dichloromethane extracts were dried over sodium sulfate and then added in one portion to a solution of 0.50 g (3.54 mmol) of ammonium nitrotetrazolate hemihydrate in 250 mL of acetonitrile. The solution was stirred for two days under ambient conditions, evaporated to dryness, and resuspended in ethyl acetate. The suspension was filtered and the filtrate evaporated and purified by silica chromatography using 4 : 4 : 2 ethyl acetate–hexane–benzene as the eluent yielding 0.230 g (50%) of 2-amino-5-nitrotetrazole. DSC (5 °C min⁻¹): 102 (*T*_m), 140 (*T*_{dec}); IR (cm⁻¹) $\tilde{\nu}$ = 3340 (m), 3255 (w), 3191 (w), 2945 (w), 2921 (w), 1729 (w), 1678 (w), 1622 (m), 1563 (s), 1529 (m), 1495 (m), 1473 (s), 1454 (w), 1418 (m), 1340 (w), 1319 (s), 1249 (m), 1227 (w), 1190 (m), 1174 (m), 1154 (m), 1144 (m), 1119 (m), 1049 (m), 1073 (m), 1030 (m), 954 (s), 912 (m), 893 (m), 840 (s), 711 (w), 696 (w), 652 (w). Raman (1064 nm, cm⁻¹) $\tilde{\nu}$ = 3343 (5), 3258 (3), 3195 (8), 2985 (1), 2939 (3), 2915 (1), 1722 (2), 1679 (1), 1617 (4), 1567 (14), 1528 (2), 1497 (20), 1475 (31), 1457 (6), 1420 (100), 1394 (14), 1322 (16), 1252 (3), 1159 (19), 1074 (10), 1030 (86), 842 (8), 772 (11), 762 (3), 746 (17), 663 (1), 569 (8), 455 (8), 419 (6), 332 (3), 229 (6); ¹H NMR (DMSO-*d*₆) δ (ppm) = 8.98; ¹³C NMR (DMSO-*d*₆) δ (ppm) = 163.1 (s, 1C); *m/z*: (DCI+) 131.07 (M + H) (CH₂O₂N₆); EA (CH₂O₂N₆, 130.07 g mol⁻¹) calcd: C 9.23%, N 64.61%, H 1.55%, found: too sensitive for measurement; BAM impact: <1 J; BAM friction: <5 N; ESD: 250 mJ.

1-Amino-3,5-dinitro-1,2,4-triazole (ADNT, **2**)

0.80 g (3.11 mmol) of freshly prepared pulverized ethyl *O*-*p*-tolylsulphonylacetoxyhydroximate was added to 7.5 mL of 60% perchloric acid at room temperature and stirred under ambient conditions for 2 h. The now-free tosylhydroxylamine suspension was poured into 80 mL of ice/water slurry and after the ice was melted the mixture was extracted with 7 × 10 mL portions of dichloromethane. The combined dichloromethane extracts were dried over sodium sulfate and then added in one portion to a solution of 0.50 g (2.84 mmol) of ammonium dinitrotriazolate in 250 mL of acetonitrile. The solution was stirred for two days under ambient conditions, evaporated to dryness,

and resuspended in ethyl acetate. The suspension was filtered and the filtrate evaporated and purified by silica chromatography using 4 : 4 : 2 ethyl acetate–hexane–benzene as the eluent yielding 0.319 g (65%) of 1-amino-3,5-dinitro-1,2,4-triazole. DSC (5 °C min⁻¹): 118 (*T_m*), 165 (*T_{dec}*); IR (cm⁻¹) $\tilde{\nu}$ = 3333 (m), 3278 (w), 3208 (w), 2924 (w), 1612 (w), 1578 (m), 1562 (s), 1512 (s), 1449 (w), 1425 (w), 1392 (w), 1375 (w), 1338 (m), 1321 (s), 1256 (w), 1132 (m), 1032 (w), 991 (w), 974 (w), 934 (m), 883 (w), 856 (s), 828 (s), 771 (w), 755 (w), 731 (w), 673 (w); Raman (1064 nm, cm⁻¹) $\tilde{\nu}$ = 3344 (2), 3280 (5), 3222 (1), 1914 (1), 1799 (1), 1621 (1), 1569 (10), 1518 (3), 1447 (100), 1393 (10), 1382 (30), 1345 (18), 1324 (9), 1281 (9), 1135 (9), 1033 (19), 993 (2), 937 (1), 862 (3), 831 (14), 772 (4), 757 (5), 734 (6), 477 (7), 394 (2), 383 (1), 357 (9), 318 (2), 250 (1), 221 (2); ¹H NMR (DMSO-*d*₆) δ (ppm) = 8.26; ¹³C NMR (DMSO-*d*₆) δ (ppm) = 153.3 (s, 1C), 145.9 (s, 1C); *m/z*: (DEI+) 174.1 (M+) (C₂H₂O₄N₆); EA (C₂H₂O₄N₆, 174.08 g mol⁻¹) calcd: C 13.80%, N 48.29%, H 1.16%, found: C 14.19%, N 47.97%, H 1.08%; BAM impact: 30 J; BAM friction: 240 N; ESD: 500 mJ.

5,5'-Bistetrazole amination

5,5'-Bistetrazole (1.00 g, 7.2 mmol) was dissolved in 20 mL of distilled water, and to this was added 4.34 g (14.5 mmol) of CsOH solution (50 wt%); the solution was then evaporated and the resulting residue was dissolved in 250 mL of acetonitrile and 100 mL of distilled water. 4.4 g (17.1 mmol) of ethyl *O-p*-tolylsulphonylacetohydroximate was added to 40 mL of perchloric acid, stirred for 2 h at rt, poured on 100 mL of iced water and stirred until the ice melted. Subsequently this mixture was extracted with dichloromethane (5 × 10 mL). The extract was added to the solution of bistetrazole and stirred overnight under ambient conditions. The solution was evaporated and extracted with ethyl acetate. The extract was filtered and the filtrate was evaporated and purified by column chromatography (ethyl acetate–benzene–petroleum ether = 3 : 1 : 1) to yield 124 mg (10%) of 1,1'-diamino-5,5'-bistetrazole and 72 mg (6%) of 1,2'-diamino-5,5'-diaminobistetrazole.

1,1'-Diamino-5,5'-bistetrazole (3). DSC (5 °C min⁻¹): 145 °C (mp), 185 °C (dec); IR (cm⁻¹) $\tilde{\nu}$ = 3292 (w), 3249 (w), 3140 (m), 2361 (w), 2200 (w), 1612 (m), 1459 (w), 1406 (w), 1385 (w), 1330 (w), 1303 (w), 1274 (w), 1213 (w), 1193 (w), 1131 (m), 1065 (w), 1032 (s), 1008 (m), 973 (s), 956 (s), 924 (s), 816 (w), 716 (w), 705 (w), 681 (w), 666 (w); Raman (1064 nm): $\tilde{\nu}$ = 3330 (1), 3256 (1), 3177 (4), 2937 (1), 2859 (2), 2026 (1), 1626 (100), 1613 (10), 1502 (2), 1392 (1), 1334 (1), 1278 (27), 1206 (1), 1181 (2), 1130 (1), 1082 (26), 1044 (11), 983 (5), 927 (1), 752 (4), 742 (22), 706 (1), 579 (1), 550 (1), 406 (4), 388 (7), 324 (1), 290 (1), 256 (10); ¹H NMR (DMSO-*d*₆) δ (ppm) = 7.40 (s, 4H); ¹³C NMR (DMSO-*d*₆) δ (ppm) = 141.7 (s, 2C); *m/z*: (DCI+) 169.2 (C₂H₅N₁₀); EA (C₂H₄N₁₀, 168.12) calcd: C 14.29, H 2.40, N 83.31%, found: C 14.70, H 2.33, N 51.03%; BAM impact: 3 J; BAM friction: 10 N; ESD: 0.25 J.

1,2'-Diamino-5,5'-bistetrazole (4). DSC (5 °C min⁻¹): 90 °C (mp), 170 °C (dec); IR (cm⁻¹) $\tilde{\nu}$ = 3299 (w), 3224 (w), 3143 (m), 1634 (w), 1602 (m), 1591 (m), 1499 (w), 1429 (w), 1398 (w), 1348 (w), 1326 (w), 1216 (w), 1184 (m), 1114 (w), 1093 (w), 1064 (m), 993 (s), 953 (s), 822 (w), 733 (w), 718 (w),

704 (m), 682 (w); Raman (1064 nm): $\tilde{\nu}$ = 3229 (5), 3147 (3), 2944 (1), 2859 (2), 1635 (100), 1609 (4), 1501 (2), 1460 (10), 1434 (4), 1395 (7), 1364 (1), 1348 (1), 1327 (7), 1221 (21), 1189 (10), 1126 (13), 1092 (1), 1062 (8), 1030 (43), 993 (3), 950 (4), 755 (5), 736 (1), 708 (7), 682 (1), 543 (1), 454 (2), 417 (3), 366 (9), 320 (5), 269 (4); ¹H NMR (DMSO-*d*₆) δ (ppm) = 8.59 (s, 2H), 7.35 (s, 2H); ¹³C NMR (DMSO-*d*₆) δ (ppm) = 150.5 (s, 1C), 143.7 (s, 1C); *m/z*: (DCI+) 169.2 (C₂H₅N₁₀); EA (C₂H₄N₁₀, 168.12) calcd: C 14.29, H 2.40, N 83.31%, found: C 14.70, H 2.33, N 51.03%; BAM impact: 3 J; BAM friction: 10 N; ESD: 0.25 J.

5H-Tetrazole amination¹⁹

14.0 g (0.200 mol) of tetrazole was dissolved in 150 mL of water and 23.2 g (0.219 mol) of sodium carbonate was added followed by heating to 75 °C. 27.2 g (0.240 mol) of hydroxylamine-*O*-sulfonic acid in 120 mL of water was added dropwise over 20 min while maintaining the pH between 7 and 8 by periodic addition of a saturated solution of sodium bicarbonate. Following addition the solution was refluxed for 30 min and then evaporated to 125 mL. This solution was continuously extracted with ethyl acetate overnight, evaporation of the extract gave a mixture of 1- and 2-aminotetrazoles, of which the 2-isomer could be distilled at 2.2 × 10⁻² mbar and 47 °C yielding a pure distillate of 1.92 g (11%) 2-aminotetrazole, and a pure residue of 4.11 g (24%) 1-aminotetrazole.

1-Aminotetrazole (1AT, 5). DSC (5 °C min⁻¹): 130 °C (*T_{vap, onset}*); IR (cm⁻¹) $\tilde{\nu}$ = 3326 (m), 3282 (m), 3195 (m), 3144 (m), 1625 (m), 1491 (w), 1430 (w), 1348 (w), 1286 (w), 1273 (w), 1184 (s), 1097 (s), 1013 (m), 962 (s), 871 (m), 723 (w), 694 (w), 643 (s); Raman (1064 nm, cm⁻¹): $\tilde{\nu}$ = 3275 (5), 3212 (2), 3148 (24), 1622 (7), 1491 (11), 1430 (21), 1363 (1), 1342 (4), 1272 (42), 1187 (49), 1102 (18), 1016 (40), 957 (7), 723 (2), 697 (100), 646 (4), 422 (12), 270 (7); ¹H NMR (DMSO-*d*₆) δ (ppm) = 9.14 (s, 1H, C-*H*), 7.02 (s, 2H, NH₂); ¹³C NMR (DMSO-*d*₆) δ (ppm) = 143.3 (s, 1C, CN₄); *m/z*: (FAB+) 86.0 (M + H⁺); EA (CN₅H₃, 85.07 g mol⁻¹) calcd: C 14.12, N 82.33, H 3.55%, found: C 14.46, N 82.33, H 3.48%; BAM impact: <1 J; BAM friction: 64 N.

2-Aminotetrazole (2AT, 6). DSC (5 °C min⁻¹): 100 °C (*T_{vap, onset}*); IR (cm⁻¹) ν = 3319 (m), 3271 (m), 3178 (m), 3147 (m), 3003 (w), 1611 (m), 1453 (m), 1386 (m), 1285 (s), 1218 (m), 1178 (m), 1138 (s), 1023 (s), 1006 (s), 948 (s), 883 (s), 703 (s), 667 (s); Raman (1064 nm, cm⁻¹): 3263 (12), 3147 (54), 1610 (7), 1452 (13), 1387 (37), 1286 (100), 1214 (5), 1182 (18), 1141 (36), 1026 (62), 1008 (22), 724 (82), 455 (9), 277 (6); ¹H NMR (DMSO-*d*₆) δ (ppm) = 8.64 (s, 1H, C-*H*), 7.97 (s, 2H, NH₂); ¹³C NMR (DMSO-*d*₆) δ (ppm) = 151.5 (s, 1C, CN₄); *m/z*: (FAB+) 86.0 (M + H⁺); EA (CN₅H₃, 85.07 g mol⁻¹) calcd: C 14.12, N 82.33, H 3.55%, found: C 14.30, N 81.15, H 3.54%; BAM impact: <1 J; BAM friction: 36 N.

2,2'-Azobis(5-nitrotetrazole) (7). 0.13 g (1.00 mmol) of ANT (1) was dissolved in 4 mL of acetonitrile and cooled to 0 °C. To this was added dropwise a solution of 0.225 g (0.88 mmol) of sodium dichloroisocyanurate dehydrate in 8 mL of water containing 0.25 mL of acetic acid. The solution instantly turned

yellow and was stirred in the ice bath for 30 min followed by pouring into 100 mL of 2% aqueous sodium bicarbonate solution. The precipitate was then filtered, during which time the filtercake spontaneously detonated. Raman (1064 nm): $\tilde{\nu} = 3073$ (7), 2970 (3), 2910 (1), 2875 (1), 1604 (3), 1575 (4), 1530 (100), 1495 (44), 1395 (37), 1296 (23), 1257 (5), 1225 (3), 1176 (48), 1113 (3), 1062 (7), 1005 (27), 932 (62), 889 (4), 833 (3), 776 (8), 707 (3), 638 (2), 554 (1), 464 (1), 372 (1), 341 (4), 249 (2). (very wet measurement) m/z : (FAB⁻) 256 (M⁻), 114 (CN₅O₂⁻).

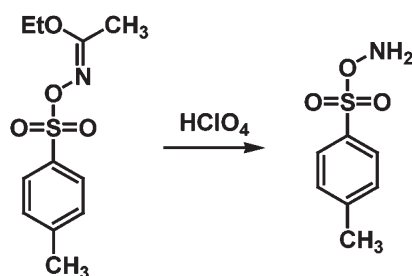
1-(2,2,2-Trinitroethylamino)tetrazole (8). 0.25 g of 1-amino-tetrazole (2.9 mmol) was dissolved in 10 mL of distilled water and to this was added 0.60 g of 1-(2,2,2-trinitroethylamino)-tetrazole (3.3 mmol) and the resultant solution was stirred overnight. After filtration 0.52 g (72%) of colorless 2,2,2-trinitroethanol was obtained.

DSC (5 °C min⁻¹): 116 °C ($T_{dec, onset}$); IR (cm⁻¹) $\nu = 3203$ (w), 3159 (w), 2991 (w), 2949 (w), 1597 (s), 1586 (s), 1512 (w), 1467 (w), 1422 (w), 1386 (w), 1350 (w), 1300 (m), 1190 (w), 1182 (w), 1088 (m), 1039 (w), 999 (w), 956 (w), 907 (w), 889 (w), 856 (w), 833 (w), 803 (s), 776 (m), 719 (w), 672 (w); Raman (1064 nm, cm⁻¹) $\tilde{\nu} = 3212$ (4), 3159 (25), 2991 (25), 2953 (38), 2731 (2), 1609 (36), 1513 (5), 1466 (9), 1430 (36), 1389 (20), 1353 (36), 1304 (14), 1286 (47), 1184 (23), 1150 (4), 1116 (3), 1088 (15), 1041 (13), 997 (49), 957 (17), 906 (6), 858 (99), 807 (6), 778 (3), 724 (10), 674 (7), 640 (21), 547 (10), 496 (10), 418 (25), 396 (15), 380 (81), 322 (14), 278 (16), 237 (11); ¹H NMR (DMSO-d₆) δ (ppm) = 9.18 (s, 1H, tz C-H), 8.24 (t, 1H, N-H, ³J = 6.0 Hz), 5.47 (d, 2H, CH₂, ³J = 6 Hz); ¹³C NMR (acetone-d₆) δ (ppm) = 143.4 (s, 1C, CN₄), 127.1 (s, 1C, C(NO₂)₃), 53.1 (s, 1C, CH₂); m/z : (FAB⁺) 249.0 (M + H⁺); EA (C₃N₈O₆H₄, 248.11 g mol⁻¹) calcd: C 14.52, N 46.16, H 1.63%, found: C 14.81, N 44.72, H 1.56%; BAM impact: 1 J; BAM friction: 20 N; ESD 0.080 J.

Results and discussion

Synthesis

O-Tosylhydroxylamine is unfortunately not stable in storage so before each reaction it was prepared from ethyl *O*-*p*-tolylsulfonylacetohydroxamate by hydrolysis with 60% perchloric acid (Scheme 1). After hydrolysis it was poured into ice water, extracted with dichloromethane, and the dichloromethane solution was dried over sodium sulfate. This solution of *O*-tosylhydroxylamine was then added to an acetonitrile solution of ammonium 5-nitrotetrazolate hemihydrate or ammonium



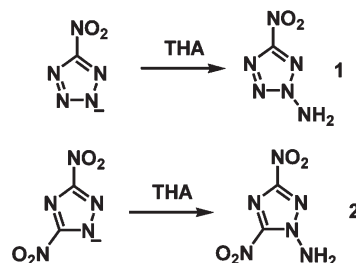
Scheme 1 Synthesis of *O*-tosylhydroxylamine (THA) from ethyl-*O*-*p*-tolylsulfonylacetohydroxamate.

dinitrotriazolate. Salts of 5,5'-bistetrazole are of very low solubility in acetonitrile, so acetonitrile–water was used as the solvent (Scheme 2). The amination reactions were stirred for two days under ambient conditions, evaporated to dryness and extracted with ethyl acetate. After purification of the ethyl acetate extract by column chromatography, 2-amino-5-nitrotetrazole (ANT, **1**), 1-amino-3,4-dinitro-1,2,4-triazole (ADNT, **2**), and both 1,1'-diamino-5,5'-bistetrazole and 1,2'-diamino-5,5'-bistetrazole (11DABT, **3** and 12DABT, **4**) were obtained. Crystals of all four compounds were obtained by slow evaporation of the desired column fractions.

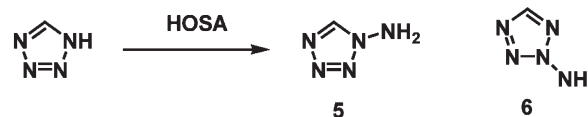
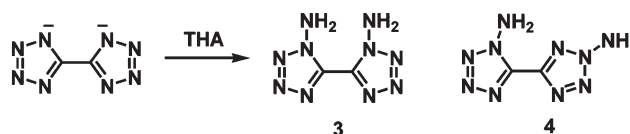
5*H*-Tetrazole was aminated according to the literature procedure by refluxing the anionic tetrazolate with HOSA in water for 30 min (Scheme 3). After reaction the solution was subjected to continuous ethyl acetate extraction overnight followed by distillation of **6** away from **5** under high vacuum (behind a blast shield). Low temperature crystallization proved unsuccessful so densities were measured *via* gas pycnometry.

Crystallization of **6** was achieved as a cocrystal by evaporating a solution of **6** with 5-nitriminotetrazole yielding a 1-to-1 cocrystal (**6**·ATNO₂).

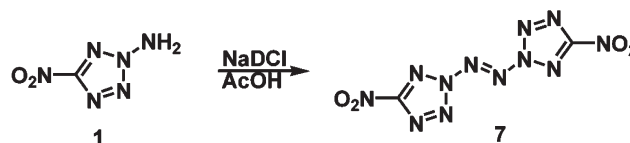
We have previously described the azo coupling of **5** using sodium dichloroisocyanurate and acetic acid.³ **1** was dissolved in acetonitrile and cooled, followed by adding an acidic solution of sodium dichloroisocyanurate in water (Scheme 4). After stirring for 30 min and quenching the reaction in an aqueous sodium bicarbonate solution, a light yellow precipitate (**7**) was obtained.



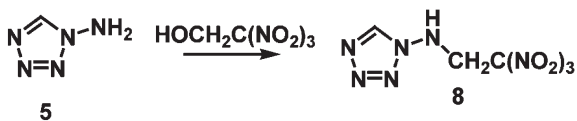
Scheme 2 Amination of energetic heterocycles with THA.



Scheme 3 Amination of 5*H*-tetrazole with HOSA.



Scheme 4 Azo coupling of **1** to **7**.



Scheme 5 Condensation of **5** with trinitroethanol to **8**.

During filtration the compound exploded while wet, sending explosive-contaminated fragments of filter paper around the fume hood. As the fragments of filter paper dried, several spontaneously re-exploded, and all would explode when touched with even the lightest force. Compound **7**, while having a lower number of catenated nitrogen atoms (**8**) than our previously reported 1,1'-azobis(tetrazole) with ten nitrogen atoms, is even more difficult to handle, for the measurement of Raman spectra, a very wet sample had to be used. The only mention of **7** in a patent does not mention this extremely high sensitivity.²²

5 was dissolved in water and trinitroethanol added. After stirring overnight 1-(trinitroethylamino)tetrazole (**8**) had precipitated (Scheme 5). Compounds **1**, **2** and **6** were also all attempted to be reacted with trinitroethanol under these conditions, however only **5** yielded a product. Evaporation of a tetrachloroethylene solution yielded crystals of **8**.

Spectroscopy

Multinuclear NMR spectroscopy (¹H, ¹³C) was used to characterize all compounds with the exception of **7** which decomposed with gas release in all solvents attempted (d₆-DMSO, d₆-acetone, CDCl₃).

The amine protons of ANT (**1**) resonate at 8.98 ppm and in the ¹³C spectra the single carbon at 163.1 ppm. This is in contrast to the nitrotetrazolate anion where the ¹³C signal lies around 169 ppm depending on the counterion.

The amine protons of ADNT (**2**) resonate at 8.26 ppm, slightly upfield compared to those of **1**. In the ¹³C spectrum the previously symmetrical dinitrotriazolate anion's resonance at around 163 ppm is shifted upfield to 153.3 and 145.9 ppm for carbons C2 and C1 respectively.

11DABT possesses ¹H NMR resonances at 7.40 ppm, however in 12DABT the four amino protons are no longer equivalent and are split into two equivalent resonances at 7.35 ppm for the 1-amino protons and at 8.59 ppm for the 2-amino protons. The ¹³C NMR of 11DABT shows an upfield shift to 141.7 ppm from the ~155 ppm shift in the bistetrazolate anion, however the 12DABT carbon resonances are not equivalent at 150.5 and 143.7 ppm for the 1- and 2-substituted tetrazole rings within.

1AT possesses resonances in the ¹H NMR at 9.14 ppm for the CH and at 7.02 ppm for the NH₂ protons. 2AT possesses resonances in the ¹H NMR at 8.64 ppm for the CH and at 7.97 ppm for the NH₂ protons. The CH protons of both **1** and **2AT** are downfield compared to the CH of tetrazole at 8.36, with the change less for **2AT** as the structures would predict. In the ¹³C NMR the resonances of 1AT and 2AT occur at 143.3 and 151.5 ppm compared to the resonance of the tetrazolate anion at ~150 ppm.

8 possesses three resonances in the proton spectrum. The first at 9.18 ppm arises from the tetrazole CH, the second at

8.24 ppm from the NH proton, and finally at 5.47 ppm for the CH₂ of the trinitroethyl moiety. In the carbon spectrum three resonances are also observed: at 143.4 ppm for the tetrazole carbon, at 127.1 ppm for the trinitromethyl carbon, and at 53.1 ppm for the CH₂ group.

Compound **7**, 2,2'-azobis(5-nitrotetrazole), was characterized extensively *via* Raman spectroscopy. The observed spectrum was assigned using frequency analysis from an optimized structure (B3LYP/cc-pVDZ, using Gaussian09 software). All calculations were performed at the DFT level of theory; the gradient-corrected hybrid three-parameter B3LYP^{37,38} functional theory has been used with a correlation-consistent cc-pVDZ basis set.^{39–42} The experimental (calculated) spectrum of **7** possesses five high intensity peaks at 1530 (1603), 1395 (1428), 1176 (1202), 1005 (972) and 776 (871) cm⁻¹. However, the presence of several significant additional peaks (ex. 1495, 1257, 1062 cm⁻¹) in the experimental spectrum suggests partial decomposition. The azo N=N stretch occurs at 1530 cm⁻¹, N3–N4 tetrazole ring deformation at 1395 cm⁻¹, N2–N3 tetrazole ring deformation (with minor N2–azo stretching) at 1176 cm⁻¹, tetrazole N1–N2–N3 asymmetric stretching at 1005 cm⁻¹, and N2–N3 stretching (with minor C–NO₂ symmetric stretching) at 776 cm⁻¹.

Energetic calculations

Bomb calorimetric measurements have not been carried out due to the high nitrogen content of the compounds which oftentimes leads to incorrect values due to explosion and incomplete combustion. The heats of formation were calculated by the atomization eqn (1) using CBS-4M enthalpies.

$$\Delta_f H^\circ_{(\text{g}, \text{M}, 298)} = H_{(\text{M}, 298)} - \sum H^\circ_{(\text{Atoms}, 298)} + \sum \Delta_f H^\circ_{(\text{Atoms}, 298)} \quad (1)$$

The results are summarized in Table 1. All compounds are formed endothermically with the highest value of 1092 kJ mol⁻¹ calculated for **7**. Due to the highly energetic character of the compounds their detonation performance was computed with the EXPLO5.04 computer code.²⁹ The input is based on the sum formula, heats of formation (see the Experimental section) and the maximum densities according to their crystal structures at low temperatures. EXPLO5.04 is based on the chemical equilibrium, steady state model of detonation. It uses Becker–Kistiakowsky–Wilson's equation of state (BKW EOS) for gaseous detonation products and Cowan–Fickett's equation of state for solid carbon. Compound **7** is also the one with the highest sensitivities within this work. Of interest is its exceptional high nitrogen–oxygen (%N + %O) content of 90.62%. Its calculated detonation parameters are the highest calculated for **1–8**. The lowest detonation parameters were calculated for the liquids **5** and **6** because of their low density. All of the other compounds show detonation velocities comparable to those observed for RDX. Although academically interesting the practical use of **1–8** is limited due to their low decomposition temperature, the highest being observed for **3** (185 °C).

The detonation parameters of the aminated compounds are higher than their corresponding methylated derivatives

Table 1 Explosive and detonation parameters of **1–8**

	1	2	3	4	5	6	7	8	RDX
Formula	CN ₆ O ₂ H ₂	C ₂ H ₂ N ₆ O ₄	C ₂ H ₄ N ₁₀	C ₂ H ₄ N ₁₀	CH ₃ N ₅	CH ₃ N ₅	C ₂ N ₁₂ O ₄	C ₃ H ₄ N ₈ O ₆	C ₃ H ₆ N ₆ O ₇
FW/g mol ⁻¹	130.07	174.08	168.12	168.12	85.09	85.09	256.10	248.11	222.12
IS ^a /J	<1	30	3	3	<1	<1	<<<1	1	7.5
FS ^b /N	<5	240	10	10	64	36	<<<5	20	120
ESD ^c /J	0.25	0.5	0.5	0.25	N/A	N/A	ND	0.080	0.1–0.2
N ^d /%	64.61	48.28	83.31	83.31	82.32	82.32	65.63	45.16	37.84
Ω ^e /%	-12.30	-9.19	-57.09	-57.09	-65.82	-65.82	0	-12.9	-21.61
T _{Dec} ^f /°C	102 (T _m)	118 (T _m)	145 (mp),	90 (mp),	130 (T _{vap})	100 (T _{vap})	50 (mp)	116	205 ⁴³
	140 (T _d)	165 (T _d)	185 (dec)	175 (dec)					
ρ ^g /g cm ⁻³	1.791	1.885	1.759	1.762	1.413	1.387	1.80 ^r	1.825	1.858 (90 K) ⁴⁴
H ^o _{CBS4M} ^h /H	517.444682	705.719973	625.146143	625.145978	313.152993	313.165237	1032.454643	1004.479332	896.346781
Δ _f H ^o (g ^o)/kJ mol ⁻¹	446.9	331.8	176.5	176.9	449.0	416.8	1153.0	450.7	176.2
Δ _{sub} H ^o /kJ mol ⁻¹	70.5	73.5	78.6	68.3	43.5 ^f	40.3 ^f	60.8	53.0	89.9
Δ _f H ^o _m ^o /kJ mol ⁻¹	376.4	258.3	797.9	808.7	405.5	376.5	1092.2	397.7	86.3 ^s
Δ _f U ^o /kJ kg ⁻¹	2988.4	1569.1	4847.9	4912.0	4881.7	4541.7	4341.6	1692.6	489.0 ^s
EXPLOS.04 values:									
-Δ _{Ex} U ^o _m /kJ kg ⁻¹	6236	6188	5144	5208	5329	4996	6931	6606	6190
T _{det} ⁿ /K	4698	4706	3611	3639	3571	3428	5855	4830	4232
P _{CJ} ^o /kbar	368	382	326	329	216	200	390	373	380
V _{Det} ^p /m s ⁻¹	9087	8981	8898	8934	7846	7629	9184	8938	8983
V _o ^q /L kg ⁻¹	772	701	759	759	799	799	707	711	734

^a Impact sensitivity (BAM drophammer, 1 of 6). ^b Friction sensitivity (BAM friction tester, 1 of 6). ^c Sensitivity towards electrical discharge. ^d Nitrogen content. ^e Oxygen balance ($\Omega = (xO - 2yC - 1/2zH)M/1600$). ^f Temperature of decomposition. ^g Density. ^h CBS4M electronic enthalpy. ⁱ Gas phase enthalpy of formation. ^j Enthalpy of sublimation according to Trouton's rule. ^k Heat of formation. ^l Energy of formation. ^m Heat of explosion. ⁿ Temperature of detonation. ^o Detonation pressure according to Chapman–Jouguet. ^p Velocity of detonation. ^q Volume of detonation gases. ^r Estimated. ^s Calculated (CBS-4M). ^t Enthalpy of vaporization.

(e.g. $V_{Det}(\text{ANT})$: 9087 m s⁻¹; $V_{Det}(\text{2-methyl-5-nitrotetrazole})$: 8109 m s⁻¹).⁴⁵ This is the reason for (i) a higher density (e.g. $\rho(\text{ANT})$: 1.791 g cm⁻³; $\rho(\text{2-methyl-5-nitrotetrazole})$: 1.668 g cm⁻³) and (ii) a higher heat of formation (e.g. $\Delta_f H_m^o(\text{ANT})$: 376 kJ mol⁻¹; $\Delta_f H_m^o(\text{2-methyl-5-nitrotetrazole})$: 247 kJ mol⁻¹). Comparison of ANT with neutral 5-nitrotetrazole shows (i) a lower density for the aminated compound ($\rho(\text{5-nitrotetrazole})$: 1.899 g cm⁻³),⁴⁵ (ii) a higher heat of formation for ANT ($\Delta_f H_m^o(\text{5-nitrotetrazole})$: 281 kJ mol⁻¹) and (iii) a lower detonation velocity ($V_{Det}(\text{5-nitrotetrazole})$: 9457 m s⁻¹). In comparison to the 2-hydroxy-5-nitrotetrazole¹ the amino compound shows lower values, however it must be mentioned that the neutral 2-hydroxy-5-nitrotetrazole and 5-nitrotetrazole are strongly acidic and deliquescent and cannot be used as single compounds at ambient conditions.

Single crystal X-ray structure analysis

Compounds **1–4**, **6-AtNO₂**, and **8** were characterized by low temperature (173 K) single crystal X-ray diffraction. Selected data and parameters of the X-ray determinations are given in Table 2.

ANT (**1**) crystallizes in the orthorhombic space group $Pna2_1$ with four formula units in the unit cell and a density of 1.791 g cm⁻³. The molecular unit is depicted in Fig. 2. Comparison to the methylated sister compound 2-methyl-5-nitrotetrazole⁴⁵ yields no significant difference. The hydrazine bond N2–N6 is shorter (1.40 Å) than the corresponding methyl bond (1.46 Å).⁴⁵ Of course all tetrazole and triazole rings show planar geometry due to their aromaticity. The ANT molecules are arranged in planar chains along the *b* axis formed by the

bifurcated hydrogen bonds N6–H6a...O1ⁱ and N6–H6b...O1ⁱ. The planar chains are connected orthogonally by the hydrogen bonds N6–H6a...N4ⁱⁱ and N6–H6b...O1ⁱⁱⁱ; symmetry codes: (i) $x, -1 + y, z$, (ii) $1.5 - x, -0.5 + y, -0.5 + z$, (iii) $2 - x, -y, 0.5 + z$.

ADNT(**2**) crystallizes in the non-centrosymmetric triclinic space group $P\bar{1}$ with eight (!) different molecules in the unit cell and a density of 1.885 g cm⁻³. One molecular unit is shown in Fig. 3. The molecular structure is very similar to 1-methyl-3,5-dinitrotriazole.⁴⁶ The structure is dominated by numerous nitrogen–oxygen (mostly nitro–nitro) interactions,⁴⁷ which must be the reason for the extraordinarily large asymmetric unit. These interactions may also cause the highest density of 1.885 g cm⁻³ observed in this work.

11DABT (**3**) crystallizes in the triclinic space group $P\bar{1}$ with four formula units in the unit cell and a density of 1.759 g cm⁻³. Both planar tetrazole rings are twisted slightly (N1–C1–C2–N9 = -14.8(4)°) to each other. The C1–C2 bond length (1.45 Å) is slightly shorter than a typical C–C single bond at 1.54 Å. The amino hydrogen atoms are directed to the other ring systems by two intramolecular bifurcated hydrogen bonds (e.g. N5–H5B...N9: 0.85(2) Å, 2.73(2) Å, 3.08(2) Å, 106(3)°). The crystal structure is strongly dominated by several classical hydrogen bonds involving the NH groups (Fig. 4).

12DABT (**4**), which is shown in Fig. 5, crystallizes in the orthorhombic space group $Pbca$ with eight formula units in the unit cell and a density of 1.762 g cm⁻³. Interestingly both amino groups are directed to one side of the bistetrazole backbone. Although having only one (but slightly stronger) intramolecular hydrogen bond (N5–H5B...N6: 0.89(2) Å, 2.53(2) Å, 2.955(1) Å, 110(2)°), the rings are planar to each other (angle of torsion N1–C1–C2–N6 = -0.12(18)°). The C1–C2 bond length

Table 2 X-ray data and parameters of materials 1–4 as well as 6 and 8

Compound	ANT (1)	ADNT (2)	11DABT (3)	12DABT (4)	2AT·ATNO ₂ (6·ATNO ₂)	1ATTNE (8)
Formula	CH ₂ N ₆ O ₂	C ₂ H ₂ N ₆ O ₄	C ₂ H ₄ N ₁₀	C ₂ H ₄ N ₁₀	CH ₃ N ₅ ·CH ₂ N ₆ O ₂	C ₃ H ₄ N ₈ O ₆
Temperature/K	173	173	173	173	173	173
Crystal system	Orthorhombic	Triclinic	Triclinic	Orthorhombic	Monoclinic	Monoclinic
Space group	<i>Pna</i> 2 ₁	<i>P</i> $\bar{1}$	<i>P</i> $\bar{1}$	<i>Pbca</i>	<i>P</i> 2 ₁ / <i>c</i>	<i>P</i> 2 ₁ / <i>c</i>
<i>a</i> /Å	9.855(6)	8.3125(7)	6.2087(6)	10.2063(3)	13.0616(9)	9.9097(5)
<i>b</i> /Å	78.082(4)	11.4102(8)	9.9845(10)	6.2946(2)	8.8579(6)	7.7761(4)
<i>c</i> /Å	6.059 (4)	13.5629(16)	10.6782(14)	19.7287(6)	6.9023(5)	117 846(6)
α /°	90	78.074(8)	90.106(9)	90	90	90
β /°	90	77.335(8)	90.874(9)	90	90.859(17)	96.124(5)
γ /°	90	89.873(6)	106.336(9)	90	90	90
Volume/Å ³	482.6(5)	1226.8	635.14(9)	1267.46(7)	798.49(10)	902.92(8)
Formula Z	4	8	4	8	4	4
Space group Z	4	8	4	8	4	4
Density calc./g cm ⁻³	1.791	1.885	1.759	1.762	1.790	1.825
μ /mm ⁻¹	0.162	0.177	0.139	0.140	0.154	0.172
<i>F</i> (000)	264	704	344	688	440	504
θ min–max/°	4.1, 26.5	4.3, 26.5	4.3, 26.5	4.1, 26.5	4.6, 26.0	4.4, 25.0
Dataset [<i>h</i> ; <i>k</i> ; <i>l</i>]	–12 : 7; –10 : 9; –6 : 7	–10 : 10; –14 : 13; –17 : 15	–7 : 7; –7 : 12; –13 : 13	–12 : 12; –7 : 7; –24 : 24	–15 : 16; –10 : 10; –8 : 8	–7 : 11; –9 : 9; –14 : –13
Reflections collected	2405	9699	3443	12 017	4024	4041
Independent reflections	543	5066	2592	1300	1565	1574
<i>R</i> _{int}	0.130	0.030	0.024	0.032	0.029	0.022
Observed reflections	398	4379	2034	1103	1133	1139
No. parameters	90	913	249	126	156	170
<i>R</i> ₁ / <i>wR</i> ₂ [all data]	0.0699/0.0984	0.0442/0.0769	0.0719/0.1370	0.0363/0.0813	0.0496/0.0656	0.0510/0.0862
<i>R</i> ₁ / <i>wR</i> ₂ [<i>I</i> > 2 σ (<i>I</i>)]	0.0477/0.0861	0.0344/0.0709	0.0539/0.01260	0.0291/0.0770	0.0302/0.0625	0.0348/0.0819
<i>S</i>	1.001	1.024	1.104	1.055	0.898	0.973
CCDC	871736	871737	871738	871739	871734	871735

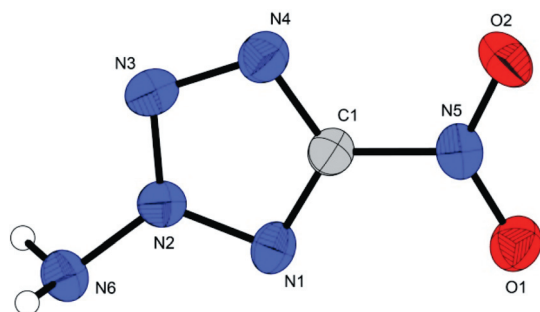


Fig. 2 ORTEP plot of **1**, non-hydrogen atom displacement parameters are at the 50% level. Selected bond distances [Å]: O2–N5 1.224(5), O1–N5 1.239(5), N1–C1 1.328(5), N1–N2 1.334(5), N4–C1 1.328(6), N4–N3 1.329(5), N6–N2 1.396(5), N5–C1 1.439(5), N2–N3 1.322(5); selected bond angles [°]: C1–N1–N2 98.1(4), C1–N4–N3 104.6(4), O2–N5–O1 124.5(4), O2–N5–C1 117.3(4), N3–N2–N1 115.9(4), N3–N2–N6 124.1(4), N1–N2–N6 120.0(4), N4–C1–N1 116.2(4).

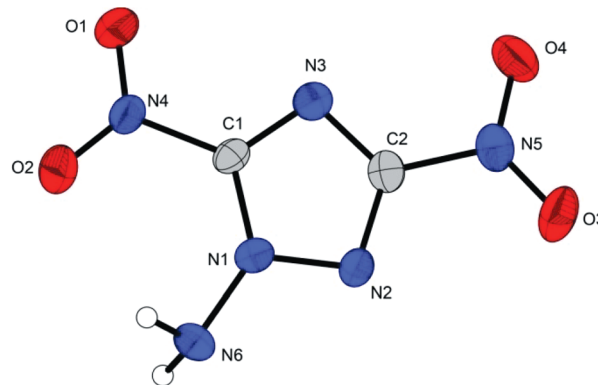


Fig. 3 ORTEP plot of **2**, non-hydrogen atom displacement parameters are at the 50% level. Selected bond distances [Å]: O1–N4 1.208(4), O2–N4 1.229(4), O3–N5 1.213(4), O4–N5 1.232(4), N1–N2 1.339(4), N1–C1 1.352(3), N1–N6 1.405(3), N2–C2 1.348(3), N3–C1 1.300(3), N3–C2 1.325(3), N4–C1 1.454(3), N5–C2 1.451(3); selected bond angles [°]: N2–N1–N6 118.0(2), C1–N1–N6 133.2(2), C1–N3–C2 101.17(18), O1–N4–O2 125.7(3), O3–N5–O4 124.7(3), O3–N5–C2 119.2(3), O4–N5–C2 116.1(3), N3–C1–N1 112.31(17), N3–C1–N4 123.73(17), N1–C1–N4 123.96(17), N3–C2–N2 116.90(17), N3–C2–N5 122.88(18).

is in the same range (1.45 Å) as observed for **3**. The bond lengths and angles within the tetrazole rings of **3** and **4** are similar to those observed for 5,5-bistetrazole salts recently published.⁴⁸

Since 1- and 2-aminotetrazole are liquids at room temperature and their structure could not be determined even at lower temperature, they were derivatized with other energetic compounds in order to provide structural data. Fig. 6 depicts the molecular moiety of the adduct 2AT·ATNO₂ (**6·ATNO₂**). It crystallizes in the monoclinic space group *P*2₁/*c* with four formula units in the unit cell and a density of 1.790 g cm⁻³. The 5-nitriminotetrazole

molecule follows the structure observed for the parent compound described in the literature.⁴⁹ The hydrazine bond length N8–N11 (1.39 Å) is again shorter than a typical N–N bond (1.45 Å).

Single crystals of 1ATTNE (**8**), shown in Fig. 7, were obtained from tetrachloroethylene. It crystallizes in the monoclinic space group *P*2₁/*c* with four formula units in the unit cell and a density of 1.825 g cm⁻³. The trinitromethyl moiety is comparable to

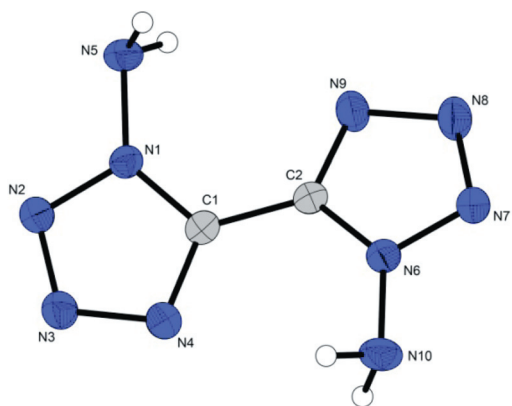


Fig. 4 ORTEP plot of **3**, non-hydrogen atom displacement parameters are at the 50% level. Selected bond distances [Å]: N1–C1 1.343(3), N1–N2 1.345(3), N1–N5 1.404(3), N6–N7 1.335(3), N6–C2 1.343(3), N6–N10 1.396(3), N7–N8 1.293(3), N4–C1 1.314(3), N4–N3 1.370(3), N3–N2 1.301(3), N8–N9 1.371(3), N9–C2 1.317(3), C2–C1 1.458(3); selected bond angles [°]: C1–N1–N5 133.4(2), N2–N1–N5 118.23(19), N7–N6–N10 119.3(2), C2–N6–N10 132.1(2).

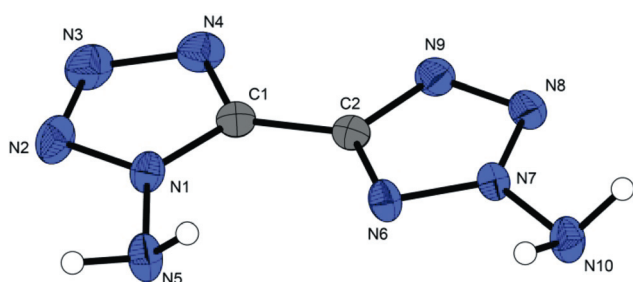


Fig. 5 ORTEP plot of **4**, non-hydrogen atom displacement parameters are at the 50% level. Selected bond distances [Å]: N1–N2 1.3360(15), N1–C1 1.3415(15), N1–N5 1.4025(14), N2–N3 1.3131(16), N3–N4 1.3487(16), N4–C1 1.3267(15), N6–N7 1.3204(13), N6–C2 1.3410(15), N7–N8 1.3175(14), N7–N10 1.3936(13), N8–N9 1.3350(14), N9–C2 1.3383(15), C1–C2 1.4514(17); selected bond angles [°]: N2–N1–N5 121.96(10), C1–N1–N5 128.64(10), N8–N7–N10 122.54(9), N6–N7–N10 121.93(9).

corresponding derivatives described in the literature forming weak nitro–nitro-group interactions.⁴⁷

Sensitivities

For initial safety testing, the impact, friction and electrostatic discharge sensitivity tests of the prepared compounds were carried out.⁵⁰ The impact sensitivity tests were carried out according to STANAG 4489⁵² and were modified according to instructions⁵³ using a BAM (Bundesanstalt für Materialforschung⁵¹) drophammer.⁵⁴ The friction sensitivity tests were carried out according to STANAG 2287⁵⁵ and were modified according to instructions⁵⁶ using a BAM friction tester. Compound **7** could not be measured according to these protocols as it spontaneously detonates when dry. Compounds **1**, **5**, **6**, **7**, **8** are classified as “very sensitive” (**2**) according to the UN Recommendations on the Transport of Dangerous Goods⁵⁷ whereas **3** and **4** are “sensitive” and **2** is “less sensitive”. It is likely that the insensitivity of **2** results from

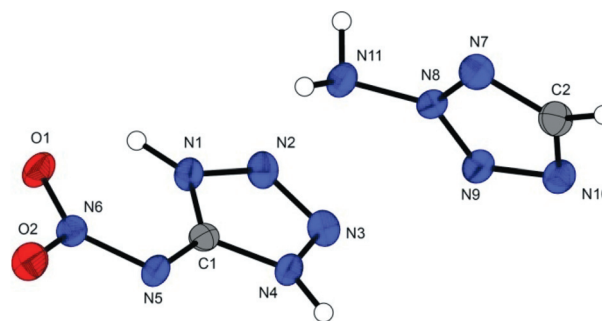


Fig. 6 ORTEP plot of **6·ATNO2**, non-hydrogen atom displacement parameters are at the 50% level. Selected bond distances [Å]: N4–C1 1.3311(19), N4–N3 1.3502(17), C2–N7 1.317(2), C2–N10 1.346(2), N8–N9 1.3099(17), N8–N7 1.3289(17), N8–N11 1.3868(18), O1–N6 1.2350(15), O2–N6 1.2505(15), N3–N2 1.2783(17), N2–N1 1.3549(17), N5–N6 1.3444(17), N5–C1 1.3457(18), N9–N10 1.3252(17), N1–C1 1.3333(19).

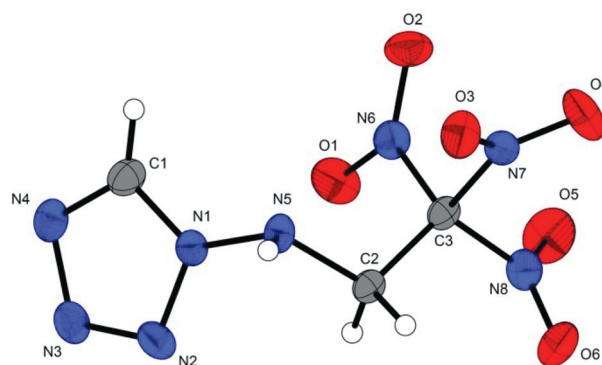


Fig. 7 ORTEP plot of **8**, non-hydrogen atom displacement parameters are at the 50% level. Selected bond distances [Å]: O5–N8 1.213(2), O6–N8 1.211(2), O4–N7 1.211(2), O3–N7 1.209(2), O2–N6 1.215(2), O1–N6 1.217(2), N8–C3 1.516(2), N7–C3 1.529(2), N6–C3 1.517(2), N5–N1 1.399(2), N5–C2 1.459(2), N1–C1 1.327(2), N1–N2 1.350(2), N2–N3 1.297(2), N3–N4 1.367(2), N4–C1 1.307(2), C3–C2 1.512(2); selected bond angles [°]: N1–N5–C2 114.23(15), C2–C3–N8 110.92(15), C2–C3–N6 111.73(14), N8–C3–N6 107.40(14), C2–C3–N7 114.17(15), N8–C3–N7 105.72(13), N6–C3–N7 106.48(14), N5–C2–C3 111.44(15).

the low melting point and amino–nitro group interactions. Electrostatic sensitivity tests were performed on all materials using a small scale electric spark tester ESD2010EN (OZM Research⁵⁸) operating with the “Winspark 1.15” software package.⁵⁹ The human body can generate up to 0.025 J of static energy which all measured compounds are insensitive towards (**3** and **4** cannot be measured as they are liquids). Compound **7** was so sensitive that ESD measurement was impossible.

Conclusions

From this combined experimental and theoretical study, the following conclusions can be drawn.

Amination of nitrogen-rich anionic heterocycles with *O*-tosylhydroxylamine yields the corresponding amino derivative, and the molecular structures of these materials have been determined for the first time. These amino derivatives generally have a

higher density and heat of formation than their methylated versions, which is lower in both compared to the protonated versions. The *N*-amino energetic derivatives are not acidic or hygroscopic unlike their *N*-H or *N*-OH analogues. These amino-energetic materials have the ability to be thermally-stable energetic materials with a range of mechanical sensitivities (ranging from sensitive to less-sensitive energetic materials). These compounds are new nitrogen-rich ligands with multiple donor sites for use in *e.g.* novel high energy-capacity transition metal complexes. The azo coupling of **1** yielding **7** has been achieved, however the 2,2'-azobis(5-nitrotetrazole) is EXCEEDINGLY sensitive and was only characterized by Raman spectroscopy and mass spectra. This compound is among the most sensitive compounds we have handled exceeding our previously-reported compound with exceedingly high sensitivity.³ **1** and 2-Aminotetrazoles (**5**, **6**) have been structurally characterized for the first time as their trinitroethyl condensation product (**8**) and nitriminotetrazole cocrystal respectively (**6**·ATNO₂).

References

- M. Göbel, K. Karaghiosoff, T. M. Klapötke, D. G. Piercey and J. Stierstorfer, *J. Am. Chem. Soc.*, 2010, **132**, 17216–17226.
- H. Gao and J. M. Shreeve, *Chem. Rev.*, 2011, **111**, 7377–7436.
- T. M. Klapötke and D. G. Piercey, *Inorg. Chem.*, 2011, **50**, 2732–2734.
- T. M. Klapötke, D. G. Piercey and J. Stierstorfer, *Chem.–Eur. J.*, 2011, **17**, 13068–13077.
- V. Thottempudi and J. M. Shreeve, *J. Am. Chem. Soc.*, 2011, **133**, 19982–19992.
- J. L. Gay-Lussac, *Ann. Chim. Phys.*, 1824, **27**, 199.
- J. Berzelius, *Justus Liebigs Ann. Chem.*, 1844, **50**, 426–429.
- J. L. Gay-Lussac and J. Leibig, *Kastners Archiv.*, 1824, **II**, 58–91.
- P. Y. Robidoux, J. Hawari, G. Bardai, L. Paquet, G. Ampelman, S. Thiboutot and G. Sunahara, *Arch. Environ. Contam. Toxicol.*, 2002, **43**, 379–388.
- T. Altenburg, T. M. Klapötke, A. Penger and J. Stierstorfer, *Z. Anorg. Allg. Chem.*, 2010, **636**, 463–471.
- M.-X. Zhang, P. E. Eaton and R. Gilardi, *Angew. Chem., Int. Ed.*, 2000, **39**, 401–404.
- R. A. Carboni, J. C. Kauer, J. E. Castle and H. E. Simmons, *J. Am. Chem. Soc.*, 1967, **89**, 2618–2625.
- M. H. V. Huynh, M. A. Hiskey, T. J. Meyer and M. Wetzler, *Proc. Natl. Acad. Sci. U. S. A.*, 2006, **103**, 5409–5412.
- R. Boese, T. M. Klapötke, P. Meyer and V. Verma, *Propellants, Explos., Pyrotech.*, 2006, **31**, 263–268.
- P. Carlqvist, H. Ostmark and T. J. Brinck, *J. Phys. Chem. A*, 2004, **108**, 7463–7467.
- L. Salazar, M. Espada, C. Avendaño and J. Elguero, *J. Heterocycl. Chem.*, 1990, **27**, 1109–1110.
- R. Raap, *Can. J. Chem.*, 1969, **47**, 3677–3681.
- W. A. Trzcinski, S. Cudzilo, Z. Chylek and L. Szymańczyk, *J. Hazard. Mater.*, 2008, **157**, 605–612.
- E. E. Glover and K. T. Rowbottom, *J. Chem. Soc., Perkin Trans. 1*, 1976, 367–371.
- L. A. Carpino, *J. Am. Chem. Soc.*, 1960, **82**, 3133–3135.
- J. C. Bottaro, M. A. Petrie, P. E. Penwell, A. L. Dodge and R. Malhotra, NANO/HEDM Technology: Late Stage Exploratory Effort. Report No. A466714, SRI International, Menlo Park, CA, 2003, DARPA/AFOSR funded, contract no. F49620-02-C-0030.
- J. C. Bottaro, R. J. Schmitt and P. E. Penwell, US 5889161, 1999.
- T. M. Klapötke, P. Mayer, C. M. Sabaté and J. M. Welch, *Inorg. Chem.*, 2008, **47**, 6014–6027.
- K. Y. Lee, C. B. Storm, M. A. Hiskey and M. D. Coburn, *J. Energ. Mater.*, 1994, **12**, 223–235.
- D. E. Chavez, M. A. Hiskey and D. L. Naud, *J. Pyrotech.*, 1999, **10**, 17–36.
- M. J. Frisch, G. W. Trucks, H. B. Schlegel, G. E. Scuseria, M. A. Robb, J. R. Cheeseman, G. Scalmani, V. Barone, B. Mennucci, G. A. Petersson, H. Nakatsuji, M. Caricato, X. Li, H. P. Hratchian, A. F. Izmaylov, J. Bloino, G. Zheng, J. L. Sonnenberg, M. Hada, M. Ehara, K. Toyota, R. Fukuda, J. Hasegawa, M. Ishida, T. Nakajima, Y. Honda, O. Kitao, H. Nakai, T. Vreven, J. A. Montgomery, Jr., J. E. Peralta, F. Ogliaro, M. Bearpark, J. J. Heyd, E. Brothers, K. N. Kudin, V. N. Staroverov, R. Kobayashi, J. Normand, K. Raghavachari, A. Rendell, J. C. Burant, S. S. Iyengar, J. Tomasi, M. Cossi, N. Rega, J. M. Millam, M. Klene, J. E. Knox, J. B. Cross, V. Bakken, C. Adamo, J. Jaramillo, R. Gomperts, R. E. Stratmann, O. Yazyev, A. J. Austin, R. Cammi, C. Pomelli, J. W. Ochterski, R. L. Martin, K. Morokuma, V. G. Zakrzewski, G. A. Voth, P. Salvador, J. J. Dannenberg, S. Dapprich, A. D. Daniels, Ö. Farkas, J. B. Foresman, J. V. Ortiz, J. Cioslowski and D. J. Fox, *GAUSSIAN 09 (Revision A.02)*, Gaussian, Inc., Wallingford, CT, 2009.
- N. Fischer, T. M. Klapötke, J. Stierstorfer and C. Wiedemann, *Polyhedron*, 2011, **30**, 2374–2386.
- (a) M. S. Westwell, M. S. Searle, D. J. Wales and D. H. Williams, *J. Am. Chem. Soc.*, 1995, **117**, 5013–5015; (b) F. Trouton, *Philos. Mag.*, 1884, **18**, 54–57.
- (a) M. Sucińska, *EXPLO5.4 program*, Zagreb, Croatia, 2010; (b) M. Sucińska, *Mater. Sci. Forum*, 2004, 465–466, 325–330.
- CrysAlisPro Oxford Diffraction, *Version 171.33.41*, Oxford, 2009.
- SIR-92, 1993, A program for crystal structure solution, A. Altomare, G. Casciarano, C. Giacovazzo and A. Guagliardi, *J. Appl. Crystallogr.*, 1993, **26**, 343.
- G. M. Sheldrick, *SHELXS-97, Program for Crystal Structure Solution*, Universität Göttingen, 1997.
- G. M. Sheldrick, *SHELXL-97, Program for the Refinement of Crystal Structures*, University of Göttingen, Germany, 1997.
- A. L. Spek, *PLATON, A Multipurpose Crystallographic Tool*, Utrecht University, Utrecht, The Netherlands, 1999.
- L. J. Farrugia, *J. Appl. Crystallogr.*, 1999, **32**, 837.
- SCALE3 ABSPACK – An Oxford Diffraction Program (1.0.4,gui:1.0.3) (C) 2005 Oxford Diffraction Ltd.
- A. D. Becke, *J. Chem. Phys.*, 1993, **98**, 5648–5652.
- C. Lee, W. Yang and R. G. Parr, *Phys. Rev. B*, 1988, **37**, 785–789.
- D. E. Woon, T. H. Dunning and R. J. Harrison, *J. Chem. Phys.*, 1993, **98**, 1358–1371.
- R. A. Kendall, T. H. Dunning and R. J. Harrison, *J. Chem. Phys.*, 1992, **96**, 6796–6806.
- T. H. Dunning, *J. Chem. Phys.*, 1989, **90**, 1007–1023.
- K. A. Peterson, D. E. Woon and T. H. Dunning, *J. Chem. Phys.*, 1994, **100**, 7410–7415.
- J. P. Agrawal, in *High Energy Materials*, Wiley-VCH, Weinheim, 1st edn, 2010, p. 189.
- P. Hakey, W. Ouellette, J. Zubieta and T. Korter, *Acta Crystallogr., Sect. E: Struct. Rep. Online*, 2008, **E64**, o1428.
- T. M. Klapötke, C. M. Sabaté and J. Stierstorfer, *New J. Chem.*, 2009, **33**, 136–147.
- G. L. Starova, O. V. Frank-Kamenetskaya and M. S. Pevzner, *J. Struct. Chem.*, 1988, **29**, 162–165.
- M. Göbel and T. M. Klapötke, *Adv. Funct. Mater.*, 2009, **19**, 347–365.
- N. Fischer, D. Izsák, T. M. Klapötke, S. Rappenglück and J. Stierstorfer, *Chem.–Eur. J.*, 2012, **18**, 4051–4062.
- T. M. Klapötke and J. Stierstorfer, *Helv. Chim. Acta*, 2007, **90**, 2132–2150.
- M. Sucińska, *Test Methods for Explosives*, Springer, New York, 1995, p. 21 (impact), p. 27 (friction).
- www.bam.de
- NATO standardization agreement (STANAG) on explosives, *impact sensitivity tests*, no. 4489, Ed. 1, Sept. 17, 1999.
- WIWEB-Standardarbeitsanweisung 4-5.1.02, Ermittlung der Explosionsgefährlichkeit, hier der Schlagempfindlichkeit mit dem Fallhammer, Nov. 8, 2002.
- http://www.reichel-partner.de
- NATO standardization agreement (STANAG) on explosives, *friction sensitivity tests*, no. 4487, Ed. 1, Aug. 22, 2002.
- WIWEB-Standardarbeitsanweisung 4-5.1.03, Ermittlung der Explosionsgefährlichkeit oder der Reibeempfindlichkeit mit dem Reibeapparat, Nov. 8, 2002.
- Impact: Insensitive >40 J, less sensitive ≥35 J, sensitive ≥4 J, very sensitive ≤3 J; Friction: insensitive >360 N, less sensitive = 360 N, sensitive <360 N a. >80 N, very sensitive ≤80 N, extremely sensitive ≤10 N. According to the UN Recommendations on the Transport of Dangerous Goods.
- D. Skinner, D. Olson and A. Block-Bolten, *Propellants, Explos., Pyrotech.*, 1998, **23**, 34–42.
- http://www.ozm.cz/testinginstruments/small-scale-electrostatic-discharge-tester.htm

DOI: 10.1002/ (will be filled in by the editorial staff)

The 1,3-Diamino-1,2,3-Triazolium Cation: A Highly Energetic Moiety

Thomas M. Klapötke,^{[*], [a]} Davin G. Piercey,^[a] and Jörg Stierstorfer^[a]

Keywords: 1,2,3-Triazole, N-amination, Crystal Structure; Explosives; N-oxides

The 1,3-diamino-1,2,3-triazolium cation was prepared by the amination of 1-amino-1,2,3-triazole with *O*-tosylhydroxylamine. The cation shows a very positive enthalpy of formation and is therefore highly suitable as the fuel component in new energetic materials. This was then paired with energetic anions nitrate, nitrotetrazolate-2-oxide, 5,5'-bis(1-oxidotetrazolate), 5,5'-azobis(1-oxidotetrazolate), and nitriminotetrazolate and characterized.

All prepared compounds are high-performance energetic materials and when performances are compared to the corresponding triaminoguanidinium salt, those for 1,3-diamino-1,2,3-triazolium are generally superior as calculated by the EXPLO5 computer code. Heats of formation were calculated on the CBS-4M level of theory. The impact, friction, and electrical spark sensitivities of the 1,3-diamino-1,2,3-triazolium salts were measured and found to be easily-initiated energetic materials.

* Prof. Dr. T. M. Klapötke
Fax: +49-89-2180-77492
E-Mail: tmk@cup.uni-muenchen.de

[a] Department of Chemistry
Energetic Materials Research
Ludwig-Maximilian University
Butenandtstr. 5-13 (D)
81377 München, Germany

Introduction

The replacement of currently used energetic materials with novel materials is an intense area of research.^[1-5] Generally, three strategies of imparting explosive properties are employed in the design of a new energetic material. The first and most traditional is the combination of fuel and oxidizer in the same molecule as exemplified in the quintessential explosives TNT (2,4,6-trinitrotoluene) and NG (nitroglycerine). The second strategy is the design of ring and caged strained compounds such as octanitrocubane and TNAZ (trinitroazetidine), where the strained bonds in the system impart energy to the final compound.^[6] Finally, nitrogen-rich compounds possessing a high heat of formation often contain explosive energy content as a result of the energetic favorability of the formation of nitrogen gas.

Of the above strategies, energetic materials based on high heat of formation compounds have been some of the most promising in recent years for the potential of low toxicity materials with reasonably facile syntheses. Within this class of energetic materials, several trends can be noted. The first is the 'stability-vs-performance continuum' of nitrogen rich heterocycles; when the 5-membered azoles from pyrazole to pentazole are considered, the low energetic performances of pyrazoles generally precludes use in energetic materials, whereas pentazoles do not exist at room temperature for extended periods of time.^[7] On this nitrogenous heterocycle continuum, triazoles (1,2,4 and 1,2,3) and tetrazoles are

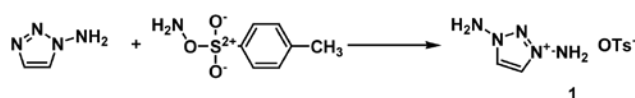
found to occupy the 'sweet spot' of possessing sufficient thermal stabilities for use, while also donating sufficient energy into the material to create explosives of acceptable performance.^[8,9] Another trend also seen is the correlation of mechanical sensitivities, and accordingly the safety to handle, of nitrogen-rich energetic materials. This trend can be dramatically seen when comparing the energetic materials 1,1'-azobis(1,2,3-triazole) with 1,1'-azobis(tetrazole); the extension of the nitrogen chain by two nitrogen atoms from triazole to tetrazole causes the sensitivity to change from a compound that can easily be manipulated, to one that explodes when gently touched or even upon its own accord.^[10,11] Concurrently, thermal stabilities decrease. The final trend that needs mentioning is the possibility for a decrease in density. While not as general (the azo compounds above have their densities increase with an increase in nitrogen content) as the previous two trends, it comes into play when discussing nitrogen rich cations to be paired with an energetic anion. The cations guanidinium, aminoguanidinium, diaminoguanidinium and triaminoguanidinium have long been paired with energetic anions such as nitrotetrazolate,^[12] nitrotetrazolate-2-oxide,^[13] methylnitriminotetrazolate,^[14] hydroxyethyl nitriminotetrazolate,^[15] and others to give salt-based energetic materials. Positively, these salt series show increasing heats of formation, and energetic performances, however, negatively, they also show declining densities, increasing sensitivities, and decreasing thermal stabilities.

As triaminoguanidinium salts (ex. azotetrazolate) have been promising materials for the replacement of currently-used energetics, a cation similar to, but better than, was sought. As a major factor affecting explosive performance is the density, we chose to look at the cyclic 1,3-diamino-1,2,3-triazolium cation as a material with similar heat of formation to, but higher density than triaminoguanidinium salts. This cation has been mentioned in the literature, but never with a detailed preparation.^[16,17] In this work we would like to present a series of energetic salts of 1,3-

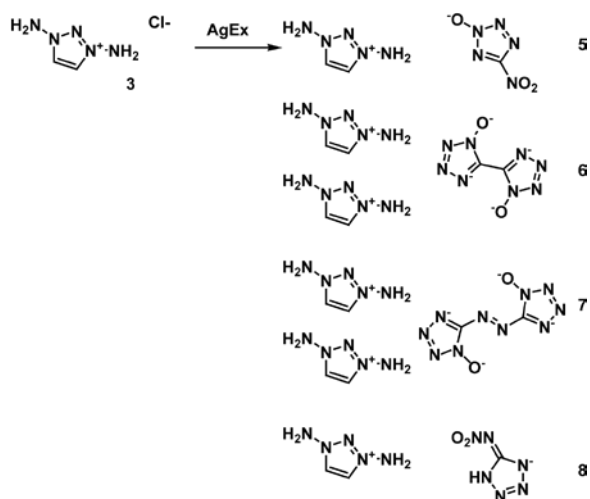
diamino-1,2,3-triazolium anion, and their characterization by X-ray diffraction, infrared and Raman spectroscopy, multinuclear NMR spectroscopy, elemental analysis, and DSC. Computational calculations predicting energetic performance properties confirm the highly energetic nature of these materials.

Results and Discussion

SYNTHESIS. The preparation of 1,3-diamino-1,2,3-triazolium tosylate **1** occurs easily overnight from the reaction of 1-amino-1,2,3-triazole in acetonitrile with a freshly prepared solution of *O*-tosylhydroxylamine in dichloromethane.^[18] (Scheme 1) After evaporation and recrystallization from ethanol the pure tosylate salt **1** was obtained. The tosylate salt **1** was used as the general precursor for the remainder of the salts. By dissolving **1** in minimal ethanol, adding stoichiometric aqueous hydrobromic acid and adding ether, 1,3-diamino-1,2,3-triazolium bromide **2** was precipitated. Chloride salt **3** and nitrate salt **4** were prepared by stirring the tosylate salt overnight with ion exchange resin loaded with chloride and nitrate respectively. The remaining salts, nitrotetrazolate-2-oxide, (**5**) bistetrazolate-1,1'-dioxide, (**6**) azotetrazolate-1,1'-dioxide (**7**) and nitriminotetrazolate (**8**) were all prepared by the reaction of chloride salt **3** with the corresponding silver salt of the desired anion. After filtration of the precipitated silver chloride and evaporation of the aqueous solution the desired compound was obtained in high yield. (Scheme 2) All crystals were obtained by diffusing ether into a methanolic solution of the desired salt.



Scheme 1: Amination of 1-amino-1,2,3-triazole.



Scheme 2: Metathesis reactions of 1,3-diamino-1,2,3-triazolium chloride with silver salts of energetic anions (AgEx).

SPECTROSCOPY All NMR spectra were measured in DMSO-*d*₆. The proton spectrum of the 1,3-diamino-1,2,3-

triazolium cation exhibits two signals. The C–H protons occur as a sharp singlet at ~8.6 ppm and the amine protons as a broad singlet at ~8.0 ppm. In the ¹³C spectrum a lone singlet is seen at ~128 ppm. In the ¹⁵N spectrum three singlet signals are seen. Proton coupled and proton decoupled spectra were taken. At –50 ppm, N2, the middle ring nitrogen atoms resonance occurs. This signal is inverted between coupled and decoupled spectra due to the nuclear overhauser effect. At –132 ppm the signals for N1 and N3, aminated ring nitrogen atoms, occur. Finally, the amine groups, N4 and N5 resonate at –288 ppm. These assignments are based on comparison with a calculated spectrum (MPW1PW91/aug-cc-pVDZ, Gaussian09^[19])

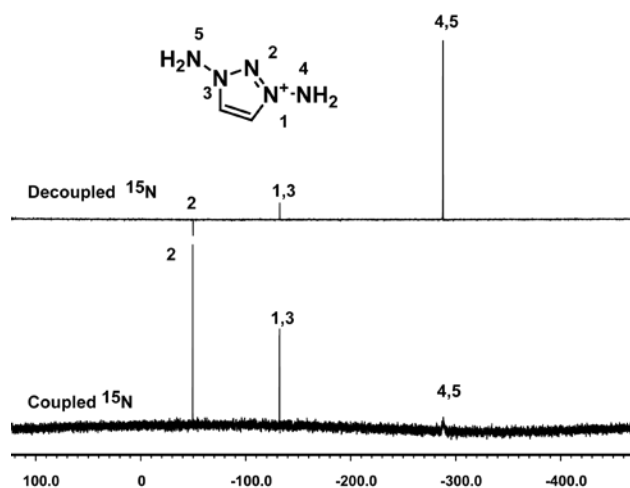


Figure 1: ¹⁵N spectra of 1,3-diamino-1,2,3-triazolium cation both proton coupled and decoupled.

SINGLE CRYSTAL X-RAY ANALYSIS. Compounds **2–7** have been characterized using single crystal X-ray structure determination. Compound **8** proved to be unable to be crystallized in our hands. Table 1 summarizes a selection of crystallographic data and refinement details. In the literature, only the structure of 1,3-diamino-1,2,3-triazolium chloride is known, and our cell parameters agree well with these values.^[17] When the bond lengths within the 1,3-diamino-1,2,3-triazolium cation is compared with those within parent 1-amino-1,2,3-triazole²⁰ slight changes are seen. The C1–C2 bond length stays essentially the same at 1.360 Å, and the NH₂–ring-nitrogen bond lengths are also unchanged at 1.400 Å. The process of amination causes the ring to become symmetric, and this is reflected in the N1–N2 and N2–N3 bond lengths being 1.319 Å in the diaminotriazolium cation, whereas in 1-aminotriazole they are 1.345 and 1.316 Å respectively. A similar effect is seen for C1–N1 and C2–N3 at 1.352 Å in the diaminotriazolium cation, whereas in 1-aminotriazole they are 1.343 and 1.363 Å, respectively. All 1,3-diamino-1,2,3-triazolium salts have a higher density than their known triaminoguanidinium analogues (1.594,^[21] 1.639,^[13] and 1.621^[22] g cm⁻³ for triaminoguanidine analogues of **4**, **5**, **7**, respectively)

1,3-Diamino-1,2,3-triazolium bromide **2** crystallizes in the space group *P*2₁2₁ with four formula units in the unit cell and a density of 1.96 g cm⁻³ (Fig. 2).

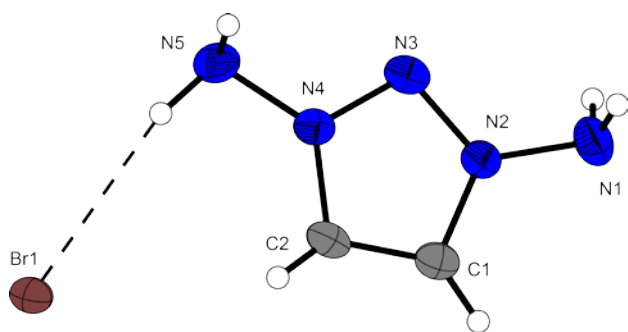


Figure 2. ORTEP representation of the molecular structure of **2**. Displacement ellipsoids are shown at the 50 % probability level.

1,3-Diamino-1,2,3-triazolium chloride **3** crystallizes in the space group $P2_12_12_1$ with four formula units in the unit cell and a density of 1.587 g cm^{-3} , which is significantly lower than that of **2**. The unit cell of **3** is depicted in Figure 3.

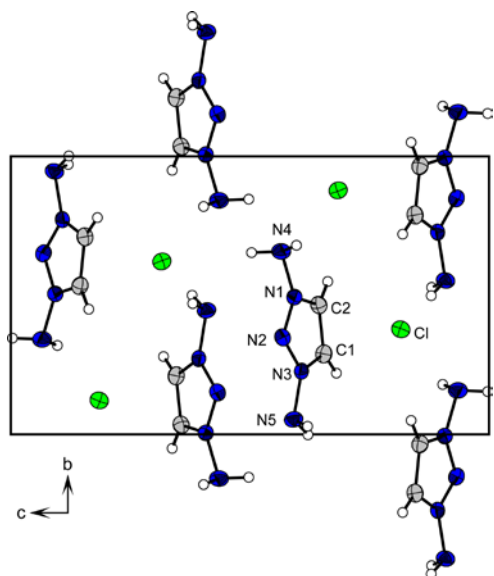


Figure 3. View on the unit cell of **3** along the a axes. Displacement ellipsoids are shown at the 50 % probability level.

1,3-Diamino-1,2,3-triazolium nitrate **4** crystallizes in the space group $P2_1/n$ with four formula units in the unit cell and a density of 1.650 g cm^{-3} . (Fig. 4)

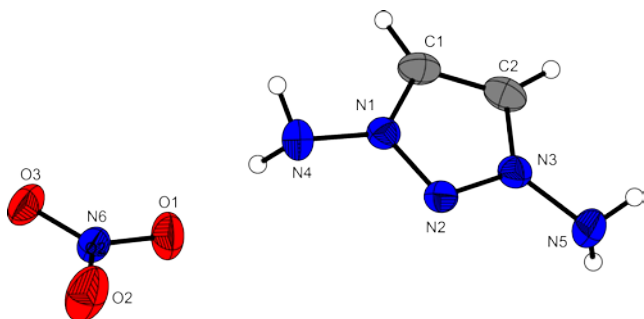


Figure 4. ORTEP representation of the molecular structure of **4**. Displacement ellipsoids are shown at the 50 % probability level.

1,3-Diamino-1,2,3-triazolium nitrotetrazolate-2-oxide **5** crystallizes in the space group $P2_1/n$ with four formula units

in the unit cell and a density of 1.716 g cm^{-3} . (Fig. 5) The structure of the anion is similar to that of its ammonium salt.^[13]

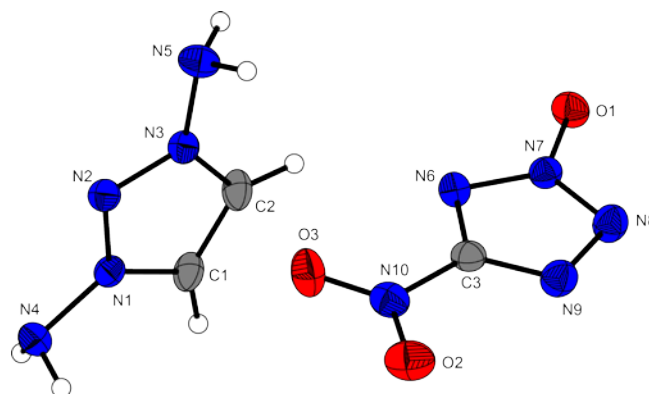


Figure 5. ORTEP representation of the molecular structure of **5**. Displacement ellipsoids are shown at the 50 % probability level.

1,3-Diamino-1,2,3-triazolium 5,5'-bistetrazolate-1,1'-dioxide **6** crystallizes in the space group $P2_1/c$ with two formula units in the unit cell and a density of 1.711 g cm^{-3} . (Fig. 6) The bistetrazolate- N -oxide dianion shows a similar structure to that recently described for its hydroxylammonium salt.^[23]

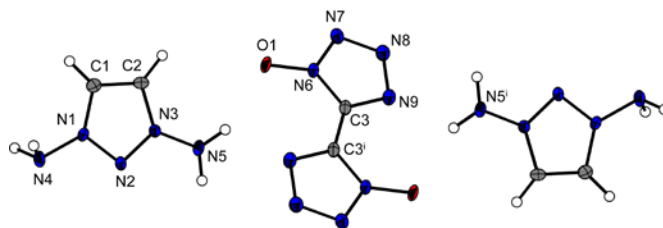


Figure 6. ORTEP representation of the molecular structure of **6**. Displacement ellipsoids are shown at the 50 % probability level. Symmetry codes: (i) $1-x, -y, -z$.

1,3-Diamino-1,2,3-triazolium 5,5'-azotetrazolate-1,1'-dioxide **7** crystallizes in the space group $P2_1/c$ with two formula units in the unit cell and the highest density of 1.739 g cm^{-3} observed in this work (Fig. 7). The azotetrazolate- N -oxide dianion is comparable the planar structure recently discovered.^[22]

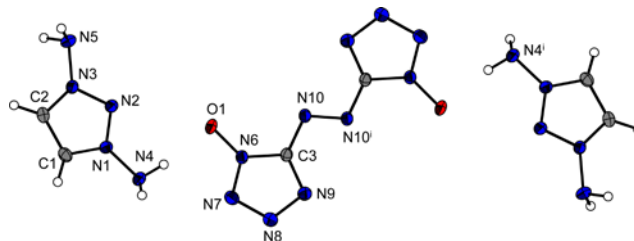


Figure 7. ORTEP representation of the molecular structure of **7**. Displacement ellipsoids are shown at the 50 % probability level. Symmetry code: (i) $-x, 1-y, 1-z$.

Table 1. Crystallographic data and structure refinement details for compounds **2–7**.

	2	3	4	5	6	7
formula	C ₂ H ₆ N ₅ Br	C ₂ H ₆ N ₅ Cl	C ₂ H ₆ N ₅ NO ₃	C ₂ H ₆ N ₅ CN ₅ O ₃	C ₂ H ₆ N ₅ C ₂ N ₈ O ₂	C ₂ H ₆ N ₅ C ₂ N ₁₀ O ₂
formula weight [g mol ⁻¹]	180.03	135.57	162.13	230.18	368.34	396.36
temperature [K]	173	173	173	173	173	173
crystal system	orthorhombic	orthorhombic	monoclinic	monoclinic	monoclinic	monoclinic
space group	<i>P</i> 2 ₁ 2 ₁ 2 ₁	<i>P</i> 2 ₁ 2 ₁ 2 ₁	<i>P</i> 2 ₁ / <i>n</i>	<i>P</i> 2 ₁ / <i>n</i>	<i>P</i> 2 ₁ / <i>c</i>	<i>P</i> 2 ₁ / <i>c</i>
<i>a</i> [Å]	5.7426(4)	5.5505(2)	9.3339(14)	10.6853(6)	5.4212(4)	11.8116(6)
<i>b</i> [Å]	7.8357(5)	7.6983(3)	5.0198(7)	75.1711(2)	12.0353 (7)	6.4824(2)
<i>c</i> [Å]	13.5633(10)	13.2792(6)	13.939(2)	16.9047(9)	11.0317(7)	10.9305(5)
α [°]	90	90	90	90	90	90
β [°]	90	90	92.129(13)	107.504(6)	96.600(6)	115.231(6)
γ [°]	90	90	90	90	90	90
volume [Å ³]	610.37(7)	567.41(4)	652.65(16)	890.81(8)	715.00(8)	757.08(6)
formula Z	4	4	4	4	2	2
space group Z	4	4	4	4	4	4
density calc. [g cm ⁻³]	1.959	1.587	1.650	1.716	1.711	1.739
R ₁ / wR ₂ [all data]	0.0302 / 0.0552	0.0233 / 0.0520	0.0505 / 0.0967	0.444 / 0.0806	0.0670 / 0.1123	0.0416 / 0.0888
R ₁ / wR ₂ [I > 2 σ (I)]	0.0270 / 0.0539	0.0210 / 0.0507	0.0376 / 0.0878	0.0333 / 0.0737	0.0485 / 0.1058	0.0336 / 0.0819
<i>S</i>	1.005	1.081	1.077	1.067	1.111	1.076
CCDC	900682	900687	900683	900684	900685	900686

PHYSICO-CHEMICAL PROPERTIES. Since all materials studied are energetic compounds, the energetic behavior for all were investigated.

THERMAL BEHAVIOR. The thermal behavior of all salts prepared were investigated on a Lenseis PT10 DSC with heating rates of 5 °C using ~1.5 mg of material. (Table 5) The highest decomposition temperature is seen for the bistetrazolate-1,1'-dioxide salt **6** and the lowest decomposition temperatures are seen for nitriminotetrazolate salt **7** and nitrotetrazolate-2-oxide salt **5**. Of particular interest is nitrate salt **4** with a melting point of 45 °C and decomposing at 185 °C, putting it well into the range of an energetic ionic liquid, and making melt cast charges of this material a definite possibility for this material. Comparison of all decomposition temperatures of the diaminotriazolium salts with the decomposition temperatures of the corresponding triaminoguanidinium salt for the respective anions was possible for all compounds. Triaminoguanidinium nitrate decomposes at 216 °C,²⁴ higher than diaminotriazolium compound **4**. Triaminoguanidinium nitrotetrazolate-2-oxide decomposes at 153 °C, slightly lower than **5**.¹³ Triaminoguanidinium bistetrazolate-1,1'-dioxide and azotetrazolate-1,1'-dioxide decompose at 206 and 175 °C respectively,¹²² both lower than **6** and **7** respectively. Finally, triaminoguanidinium nitriminotetrazolate decomposes at 184 °C, higher than compound **8** at 154 °C.¹²⁵

HEATS OF FORMATION. All calculations were carried out using the Gaussian G09W (revision A.02) program package.¹⁹ The heats of formation $\Delta_f H^\circ$ (s) (Table 4) of the investigated compounds **4–8** were calculated with the atomization method (equation 1) using room temperature CBS-4M electronic enthalpies summarized in Table 4.^{126,27}

$$\Delta_f H^\circ_{(g, M, 298)} = H_{(M, 298)} - \sum H^\circ_{(A, 298)} + \sum \Delta_f H^\circ_{(A, 298)} \quad (1)$$

The calculated gas phase enthalpies of formation $\Delta_f H^\circ$ (g) of one ion-pair, which are taken as the respective sums of the non-interacting component ions (Table 3) were converted into the solid state enthalpies of formation (ΔH_m (s)) by using the Jenkins and Glasser equations for

XY and X₂Y salts^[28] based on the molecular volumes V_M (taken from X-ray structures) in order to calculate the lattice energies (ΔE_L) and enthalpies (ΔH_L). Lastly, the molar standard enthalpies of formation ($\Delta_f H_m$) were used to calculate the molar solid state energies of formation (ΔU_m) according to equation (2).

$$\Delta U_m = \Delta H_m - \Delta n RT \quad (2)$$

(Δn being the change of moles of gaseous components)

Table 3. CBS-4M calculation results, molecular volumes taken from X-ray solution and calculated lattice enthalpy.

M	$-H^{298}$ (a.u.) ^a	$\Delta_f H^\circ$ (g,M) (kJ mol ⁻¹) ^b	V _M (nm ³) ^c	$\Delta E_L, \Delta H_L$ (kJ mol ⁻¹) ^d	Δn ^e
C ₂ H ₆ N ₅ ⁺	352.718467	1094.6			
NO ₃ ⁻	280.080446	-313.6			
CN ₅ O ₃ ⁻	536.798772	83.0			
C ₂ N ₈ O ₂ ²⁻	663.687267	587.7			
C ₂ N ₁₀ O ₂ ²⁻	773.024382	766.3			
CN ₆ O ₂ H ⁻	516.973495	150.4			
4		781.0 [#]	0.163	533.1, 538.1	7.5
5		1177.6 [#]	0.223	490.8, 495.8	9.5
6		2776.9 [#]	0.358	1218.6, 1226.1	16
7		2955.5 [#]	0.379	1192.3, 1199.7	17
8		1245.0 [#]	0.256 [°]	473.3, 478.3	10

^a CBS-4M enthalpy at room temperature; ^b calculated gas phase heat of formation by the atomization equation; ^c molecular volume of the molecular moiety in the crystal structure; ^d lattice energy and lattice enthalpy calculated by Jenkins and Glasser equations; ^e change of moles of gaseous components; [#] Gas phase enthalpies of formation of the ionic compounds are taken as the respective sums of the non-interacting component ions; * recalculated from **4** and ammonium 5-nitriminotetrazolate^[29]

The investigated salts **4–8** are formed endothermically. Usually positive heats of formations are yielded by nitrogen-

rich materials, with a large number of N–N single bonds. The lowest heat of formation was calculated for the nitrate salt **2** (243 kJ mol⁻¹), the most positive one for **7** (1756 kJ mol⁻¹), which is high!

Detonation parameters. The calculation of several detonation parameters as well as the specific impuls at 60

bar rocket conditions (Table 4) were performed with the program package EXPLO5 using the version 5.05.^[30] The program is based on the chemical equilibrium, steady-state model of detonation and uses the Becker-Kistiakowsky-Wilson's equation of state (BKW EOS) for gaseous detonation products and Cowan-Fickett's equation of state for solid carbon.

Table 4. Energetic Properties and detonation parameters

	4	5	6	7	8	RDX
Formula	C ₂ H ₆ N ₆ O ₃	C ₃ H ₆ N ₁₀ O ₃	C ₆ H ₁₂ N ₁₈ O ₂	C ₆ H ₁₂ N ₂₀ O ₂	C ₃ H ₇ N ₁₁ O ₂	C ₃ H ₆ N ₆ O ₆
FW (g mol ⁻¹)	162.11	230.14	368.28	396.36	229.16	222.12
IS ^a (J)	6	3	2	1	3	7.5 ^[24]
FS ^b (N)	180	42	14	18	42	120
ESD ^c (J)	1.0	0.3	0.3	0.2	0.5	0.2
N ^d (%)	51.84	60.86	68.46	70.69	67.23	37.84
ℒ ^e (%)	-39.48	-41.71	-69.50	-64.59	-52.63	-21.61
T _{Dec} ^f (°C)	185	155	220	185	154	205
T _m ^f (°C)	45	50	210	165	-	-
ρ ^g (g cm ⁻³)	1.650	1.716	1.711	1.739	1.71(est.)	1.858 (90 K)
Δ _f H _m ^{oh} (kJ mol ⁻¹)	242.9	681.8	1550.9	1755.8	766.7	86.3
Δ _f U ^{oi} (kJ kg ⁻¹)	1612.8	3064.4	4317.8	4535.9	3453.3	489.0
<i>Calculated Values by EXPLO5*</i>						
Δ _{Ex} U ^{oi} (kJ kg ⁻¹)	5981	6116	5854	5967	5699	6190
T _{det} ^k (K)	3949	4191	3770	3865	3831	4232
ρ _{Cl} ^l (kbar)	296	321	319	336	315	380
V _{Det} ^m (m s ⁻¹)	8588	8784	8860	9013	8800	8983
V _o ⁿ (L kg ⁻¹)	523	774	756	759	784	734
I _S ^o (s)	253	255	255	259	250	258

^a BAM Dropphammer. ^b BAM Impact. ^c Electrical Spark Sensitivity. ^d Nitrogen Content. ^e Oxygen Balance. ^f From DSC (5 °C min⁻¹). ^g Density from X-ray diffraction. ^h Calculated molar enthalpy of formation. ⁱ Energy of formation. ^j Total energy of detonation. ^k Explosion temperature. ^l Detonation Pressure. ^m Detonation Velocity. ⁿ Volume of Detonation Products. ^o specific impulse using isobaric (60 bar) conditions. EXPLO5.05.

All salts of the 1,3-diamino-1,2,3-triazolium cation exhibit detonation velocities in the vicinity of RDX, while the detonation pressures are all slightly lowered (due to the lower densities). The highest values (V_{det} 9013 m s⁻¹, ρ_{Cl} 336 kbar) were calculated for the 5,5'-azo-bis(1N-oxidotetrazolate) salt **7**. Of interest is the performance of the nitrate salt **4**, at ~8600 ms⁻¹, to the best of our knowledge this is the energetic ionic liquid with the highest calculated performance known in the literature. Calculated values between 253 and 259 s for the specific impulse are also great for use e.g. in triple base propellant mixtures. When the energetic performances of all diaminotriazolium salts are compared with their corresponding triaminoguanidinium salts, comparable or slightly higher performance is seen.^[13,22]

SENSITIVITIES. For initial safety testing the impact, friction, and electrostatic discharge sensitivity of the prepared nitrogen-rich salts were carried out.^[31,32] The least sensitive salt prepared was nitrate salt **4**, with 6 J impact sensitivity and is classified as “sensitive” the remainder of the salts are between 1 and 3 J, classifying them as very sensitive.^[33] There does not appear to be any trend when the sensitivities are compared with those of the corresponding triaminoguanidinium salts, triaminoguanidinium nitrotetrazolate-2-oxide is far less sensitive at 25 J, whereas triaminoguanidinium nitrate is more sensitive at 4 J.^[13,24] Salts **5-8** all possess friction sensitivities classified as “very sensitive” whereas salt **4** is classified as sensitive. The Electrostatic sensitivities of all compounds are in the range of, or more insensitive than, commonly used secondary explosive RDX.

Conclusions

From this combined experimental and theoretical study the following conclusions can be drawn:

- (i) 1-Amino-1,2,3-triazole can be aminated with tosylhydroxylamine giving 1,3-diamino-1,2,3-triazolium tosylate which can be effectively used as a precursor to a wide range of energetic salts.
- (ii) Multinuclear NMR spectroscopy was a valuable tool in characterizing these salts.
- (iii) Computational calculations indicate that the diaminotriazolium cation has higher heats of formation than the triaminoguanidinium cation.
- (iv) Diaminotriazolium salts have higher densities than the corresponding triaminoguanidinium salt.
- (iv) Due to high experimentally-determined densities, 1,3-diamino-1,2,3-triazolium salts are high-performance energetic materials that are comparable to, or slightly better than the corresponding triaminoguanidinium salt.
- (v) Decomposition temperatures range from 154–220 °C indicating the 1,3-diamino-1,2,3-triazolium cation has the ability to form thermally-stable energetic materials with appropriate anion pairing.
- (vi) Salts of the 1,3-diamino-1,2,3-triazolium cation are generally sensitive or very sensitive energetic materials.

Experimental Part

All reagents and solvents were used as received (Sigma-Aldrich, Fluka, Acros Organics) if not stated otherwise. 1-aminotriazole and ethyl-*O*-*p*-tosylacetohydroximate were prepared according to the literature procedures.^[34,18] Melting and decomposition points were measured with a Linseis PT10 DSC using heating rates of 5 °C min⁻¹, which were checked with a Büchi Melting Point B-450 apparatus. ¹H, ¹³C and ¹⁵N NMR spectra were measured with a JEOL Eclipse 270, JEOL EX 400, or a JEOL Eclipse 400 instrument. All chemical shifts are quoted in ppm relative to TMS (¹H, ¹³C) or nitromethane (¹⁵N). Infrared spectra were measured with a Perkin-Elmer Spektrum One FT-IR instrument. Raman spectra were measured with a Perkin-Elmer Spektrum 2000R NIR FT-Raman instrument equipped with a Nd-YAG laser (1064 nm). Elemental analyses were performed with a Netsch STA 429 simultaneous thermal analyser. The impact sensitivity tests were carried out according to STANAG 4489^[35] and were modified according to instruction^[36] using a BAM (Bundesanstalt für Materialforschung) drophammer.^[37] The friction sensitivity tests were carried out according to STANAG 2287^[38] and were modified according to instruction^[39] using a BAM friction tester. Electrostatic sensitivity tests were performed using a small scale electric spark tester ESD 2010EN (OZM Research^[40]) operating with with “Winspark 1.15” Software package.^[41] XRD was performed on an Oxford Xcalibur3 diffractometer with a Spellman generator (voltage 50 kV, current 40 mA) and a KappaCCD detector using Mo-*K*_α radiation ($\lambda = 0.71073 \text{ \AA}$) at low temperature (173 K). The data collection and reduction was carried out using the CRYSTALIS PRO software^[42]. The structures were solved either with SHELXS-97^[43] or SIR-92^[44], refined with SHELXL-97^[45] and finally checked using the PLATON^[46] software integrated in the WINGX^[47] software suite. All hydrogen atoms were found and freely refined. Friedel pairs of non-centrosymmetric space groups have been merged using the MERG3 command. The absorptions were corrected with a Scale3 Abspack multi-scan method.^[48] Cif files can be obtained free of charge using the CCDC Nos. from the Cambridge Crystallographic Data Centre via www.ccdc.cam.ac.uk/data_request/cif.

CAUTION! All salts are energetic compounds with sensitivity to various stimuli. While we encountered no issues in the handling of these materials, proper protective measures (face shield, ear protection, body armour, Kevlar® gloves and earthed equipment) should be used at all times.

1,3-Diamino-1,2,3-triazolium tosylate (1)

13.00 g (50.5 mmol) of Ethyl *O*-*p*-tolylsulphonylacetohydroximate was added to 150 mL of 60% perchloric acid, stirred for 2 h at room temperature, poured on 500 mL of iced water and stirred until the ice melted. This mixture was extracted with dichloromethane (5 x 100 mL). The extract was added to 1-amino-1,2,3-triazole (3.00 g, 35.7 mmol) in 900 mL of acetonitrile and stirred over night. Afterwards the solution was evaporated and recrystallized from ethanol to yield 8.00 g (83%) of **1**.

IR (cm⁻¹) $\tilde{\nu} = 3559$ (w), 3257 (w), 3140 (m), 3104 (w), 2997 (w), 1919 (w), 1646 (w), 1597 (w), 1547 (w), 1494 (w), 1488 (w), 1464 (w), 1395 (w), 1383 (w), 1271 (w), 1241 (w), 1209 (s), 1188 (m), 1167 (s), 1121 (s), 1109 (m), 1088 (w), 1054 (w), 1044 (w), 1032 (m), 1009 (s), 974 (m), 952 (m), 851 (w), 816 (m), 802 (w), 777 (s), 745 (w), 711 (w), 682 (s), 661 (w); Raman (1064 nm): $\tilde{\nu} = 3246$ (1), 3175 (14), 3143 (11), 3110 (1), 3068 (46),

3046 (8), 3031 (3), 2986 (5), 2927 (35), 2876 (1), 2733 (4), 2579 (3), 1655 (1), 1598 (35), 1575 (3), 1550 (5), 1499 (15), 1489 (4), 1468 (7), 1408 (6), 1378 (18), 1326 (2), 1308 (4), 1273 (4), 1240 (5), 1214 (26), 1192 (5), 1184 (14), 1126 (100), 1086 (24), 1054 (47), 1035 (25), 1012 (26), 990 (2), 859 (2), 823 (6), 804 (84), 747 (5), 712 (2), 686 (9), 665 (4), 637 (37), 571 (9), 557 (1), 515 (6), 494 (3), 399 (12), 374 (3), 358 (6), 332 (1), 294 (48), 233 (22); ¹H NMR (DMSO-*d*₆) δ (ppm) = 8.61 (s, 2H, CH, DATr), 8.06 (s, 4H, NH₂, DATr), 7.48 (d, *J* = 8.0 Hz, 2H, CH, OTs), 7.11 (d, *J* = 7.6 Hz, 2H, CH, OTs), 2.29 (s, 3H, CH₃, OTs); ¹³C NMR (DMSO-*d*₆) δ (ppm) = 146.1 (s, 1C, OTs), 138.3 (s, 1C, OTs), 128.7 (s, 2C, OTs), 128.3 (s, 2C, DATr), 126.0 (s, 2C, OTs), 21.3 (s, 1C, OTs); *m/z*: (FAB⁺) 100.1 (C₂H₆N₅); *m/z*: (FAB⁻) 171.0 (C₇H₇SO₃); EA (C₉H₁₃N₅O₃S, 271.30) calcd: C, 39.84; H, 4.83; N, 25.81%; found: C, 39.65; H, 4.67; N, 25.98%.

1,3-Diamino-1,2,3-triazolium bromide (2)

1 (0.58 g, 2.1 mmol) was dissolved in 20 mL of ethanol, and to this was added 0.5 g of 48% hydrobromic acid. 100 mL of diethyl ether was added and the newly formed precipitate was filtered off and dried to yield 0.37 g (98%) of **2**.

IR (cm⁻¹) $\tilde{\nu} = 3595$ (w), 3235 (m), 3145 (w), 3117 (m), 3083 (m), 2976 (w), 2404 (w), 2269 (w), 1796 (m), 1715 (m), 1614 (m), 1525 (m), 1463 (m), 1392 (m), 1372 (m), 1341 (m), 1267 (m), 1230 (s), 1185 (m), 1082 (m), 1039 (w), 923 (s), 899 (m), 822 (s), 742 (s), 657 (w); Raman (1064 nm): $\tilde{\nu} = 3237$ (2), 3156 (5), 3123 (37), 3090 (8), 1631 (1), 1616 (7), 1527 (26), 1487 (2), 1451 (23), 1390 (16), 1375 (4), 1343 (2), 1313 (4), 1270 (11), 1232 (33), 1187 (16), 1078 (55), 1047 (7), 1037 (100), 935 (11), 904 (2), 822 (3), 743 (24), 644 (25), 620 (3), 514 (29), 367 (19), 316 (10), 250 (4); ¹H NMR (DMSO-*d*₆) δ (ppm) = 8.64 (s, 2H, CH), 8.11 (s, 4H, NH₂); ¹³C NMR (DMSO-*d*₆) δ (ppm) = 128.2 (s, 2C); *m/z*: (FAB⁺) 100.1 (C₂H₆N₅); *m/z*: (FAB⁻) 78.9 (Br); EA (C₂H₆N₅Br, 180.01) calcd: C, 13.34; H, 3.36; N, 38.91%; found: C, 13.37; H, 3.46; N, 38.79%.

1,3-Diamino-1,2,3-triazolium chloride (3)

1 (2.00 g, 7.4 mmol) was dissolved in 400 mL of distilled water, and to this was added 100 g of anion-exchange resin (Amberjet 4200®, Aldrich) loaded with chloride anion; the solution was then stirred over night at room temperature. The resin was filtered off and the solution was evaporated to yield 759 mg (76%) of **3**.

IR (cm⁻¹) $\tilde{\nu} = 3446$ (w), 3223 (m), 3127 (m), 3082 (s), 2976 (w), 2540 (w), 2401 (w), 2268 (w), 2112 (w), 1805 (w), 1722 (w), 1615 (m), 1527 (m), 1464 (m), 1393 (w), 1376 (w), 1341 (w), 1273 (w), 1229 (s), 1185 (m), 1123 (w), 1081 (m), 1045 (w), 1038 (w), 972 (w), 920 (s), 902 (s), 824 (s), 741 (s), 660 (w); Raman (1064 nm): $\tilde{\nu} = 3251$ (1), 3158 (5), 3131 (47), 3097 (13), 3048 (1), 1639 (3), 1620 (7), 1530 (35), 1488 (1), 1455 (31), 1392 (8), 1378 (21), 1345 (2), 1321 (5), 1275 (20), 1232 (39), 1188 (21), 1116 (2), 1078 (64), 1050 (16), 1035 (100), 1003 (3), 937 (15), 908 (2), 825 (4), 744 (23), 694 (2), 660 (3), 644 (34), 622 (5), 518 (23), 378 (13), 327 (9), 254 (4); ¹H NMR (DMSO-*d*₆) δ (ppm) = 8.66 (s, 2H, CH), 8.34 (s, 4H, NH₂); ¹³C NMR (DMSO-*d*₆) δ (ppm) = 127.8 (s, 2C); *m/z*: (FAB⁺) 100.1 (C₂H₆N₅); *m/z*: (FAB⁻) 34.9 (Cl); EA (C₂H₆N₅Cl, 135.56) calcd: C, 17.72; H, 4.46; N, 51.66%; found: C, 17.71; H, 4.35; N, 48.41%.

1,3-Diamino-1,2,3-triazolium nitrate (4)

1 (3.00 g, 11.1 mmol) was dissolved in 400 mL of distilled water, and to this was added 100 g of anion-exchange resin (Amberjet 4200[®], Aldrich) loaded with nitrate anion; the solution was then stirred over night at room temperature. The resin was filtered off and the solution was evaporated to yield 1.77 g (99%) of **4**.

DSC: 45 °C (mp), 185 °C (dec); IR (cm⁻¹) $\tilde{\nu}$ = 3291 (m), 3255 (m), 3172 (m), 3140 (m), 3108 (m), 2428 (w), 2351 (w), 2309 (w), 2268 (w), 1796 (w), 1756 (w), 1715 (w), 1692 (w), 1620 (w), 1525 (w), 1454 (w), 1378 (s), 1304 (s), 1259 (s), 1232 (w), 1218 (s), 1124 (w), 1091 (m), 1043 (m), 1010 (w), 936 (s), 823 (s), 745 (m), 710 (w), 686 (w), 661 (w); Raman (1064 nm): $\tilde{\nu}$ = 3251 (1), 3196 (1), 3159 (7), 3134 (1), 1640 (2), 1618 (1), 1526 (11), 1462 (1), 1454 (1), 1385 (5), 1361 (1), 1349 (1), 1260 (2), 1233 (1), 1214 (1), 1188 (1), 1080 (6), 1068 (7), 1047 (100), 948 (1), 744 (3), 714 (5), 647 (10), 519 (5), 364 (2), 338 (1); ¹H NMR (DMSO-*d*₆) δ (ppm) = 8.61 (s, 2H, CH), 8.09 (s, 4H, NH₂); ¹³C NMR (DMSO-*d*₆) δ (ppm) = 128.3 (s, 2C); *m/z*: (FAB⁺) 100.0 (C₂H₆N₅); *m/z*: (FAB⁻) 62.0 (NO₃); EA (C₂H₆N₆O₃, 162.11) calcd: C, 14.81; H, 3.73; N, 51.84%; found: C, 14.47; H, 3.58; N, 47.30%; BAM impact: 6 J; BAM friction: 180 N; ESD: 1.0 J.

1,3-Diamino-1,2,3-triazolium nitrotetrazolate-2-oxide (5)

3 (285 mg, 2.1 mmol) was added to a suspension of 500 mg (2.1 mmol) of silver 5-nitrotetrazolate-2*N*-oxide in 10 mL of distilled water. The mixture was stirred for 1 h and was filtered in the dark. The filtrate was evaporated to yield 395 mg (82%) of **5**.

DSC: 50 °C (mp), 155 °C (dec); IR (cm⁻¹) $\tilde{\nu}$ = 3340 (w), 3209 (w), 3131 (m), 2962 (w), 2137 (w), 1725 (w), 1691 (w), 1640 (w), 1569 (m), 1542 (m), 1465 (w), 1456 (m), 1416 (s), 1376 (m), 1308 (s), 1268 (m), 1228 (m), 1122 (w), 1090 (m), 1070 (w), 1053 (m), 1019 (m), 999 (m), 967 (w), 844 (m), 793 (m), 774 (s), 701 (w), 656 (w); Raman (1064 nm): $\tilde{\nu}$ = 3157 (6), 3143 (1), 2506 (1), 1843 (1), 1571 (2), 1524 (7), 1424 (100), 1408 (7), 1313 (14), 1272 (6), 1230 (2), 1091 (76), 1055 (10), 1002 (73), 848 (1), 779 (2), 762 (4), 704 (1), 658 (3), 642 (1), 611 (4), 520 (3), 487 (3), 427 (1), 355 (1), 322 (1), 267 (1), 229 (5); ¹H NMR (DMSO-*d*₆) δ (ppm) = 8.59 (s, 2H, CH), 8.02 (s, 4H, NH₂); ¹³C NMR (DMSO-*d*₆) δ (ppm) = 157.8 (s, 1C, NTX), 128.3 (s, 2C, DATr); *m/z*: (FAB⁺) 100.0 (C₂H₆N₅); *m/z*: (FAB⁻) 130.0 (CN₅O₃); EA (C₃H₆N₁₀O₃, 230.15) calcd: C, 15.66; H, 2.63; N, 60.86%; found: C, 15.97; H, 2.47; N, 60.60%; BAM impact: 3 J; BAM friction: 42 N; ESD: 0.3 J.

1,3-Diamino-1,2,3-triazolium bistetrazolate-1,1'-dioxide (6)

3 (536 mg, 4.0 mmol) was added to a suspension of 759 mg (2.0 mmol) of silver bistetrazolate-1,1'-dioxide in 50 mL of distilled water. The mixture was stirred for 1 h and was filtered in the dark. The filtrate was evaporated to yield 600 mg (82%) of **6**.

DSC: 210 °C (mp), 220 °C (dec); IR (cm⁻¹) $\tilde{\nu}$ = 3267 (m), 3146 (m), 3123 (m), 3064 (m), 2939 (m), 2258 (w), 2137 (w), 1751 (w), 1674 (w), 1626 (m), 1545 (w), 1491 (w), 1437 (w), 1417 (w), 1399 (s), 1338 (m), 1319 (m), 1222 (s), 1210 (s), 1161 (m), 1122 (w), 1084 (m), 1055 (m), 1040 (m), 994 (s), 973 (s), 876 (w), 827 (w), 799 (s), 742 (m), 724 (m), 684 (w), 665 (w); Raman (1064 nm): $\tilde{\nu}$ = 3270 (2), 3151 (6), 3128 (2), 3093 (1), 1596 (100), 1547 (3), 1492 (8), 1456 (1), 1440 (2), 1404 (6), 1337 (3), 1322 (1), 1276 (2), 1232 (30), 1108 (9), 1085 (13), 1047 (21), 996 (6), 804 (1), 769 (9), 742 (4), 647 (5), 607 (4), 524 (2), 424 (2), 400 (3), 351 (3), 274 (6), 256 (2); ¹H NMR

(DMSO-*d*₆) δ (ppm) = 8.61 (s, 2H, CH), 8.13 (s, 4H, NH₂); ¹³C NMR (DMSO-*d*₆) δ (ppm) = 134.5 (s, 2C, BTO), 128.1 (s, 2C, DATr); *m/z*: (FAB⁺) 100.0 (C₂H₆N₅); *m/z*: (FAB⁻) 169.0 (C₂H₆N₈O₂); EA (C₆H₁₂N₁₈O₂, 368.28) calcd: C, 19.57; H, 3.28; N, 68.46%; found: C, 19.79; H, 3.19; N, 65.95%; BAM impact: 2 J; BAM friction: 14 N; ESD: 0.3 J.

1,3-Diamino-1,2,3-triazolium azotetrazolate-1,1'-dioxide (7)

3 (519 mg, 3.8 mmol) was added to a suspension of 788 mg (1.9 mmol) of silver azotetrazolate-1,1'-dioxide in 30 mL of distilled water. The mixture was stirred for 30 min with heating (70 °C) and was filtered in the dark. The filtrate was evaporated to yield 630 mg (84%) of **7**.

DSC: 165 °C (mp), 185 °C (dec); IR (cm⁻¹) $\tilde{\nu}$ = 3253 (w), 3152 (m), 3070 (m), 2997 (w), 2802 (w), 2676 (w), 2464 (w), 2148 (w), 1800 (w), 1711 (w), 1694 (w), 1634 (w), 1542 (w), 1470 (m), 1450 (w), 1430 (m), 1331 (w), 1311 (w), 1264 (s), 1224 (m), 1198 (m), 1144 (w), 1082 (m), 1075 (m), 1046 (w), 1010 (w), 976 (s), 875 (w), 807 (s), 776 (s), 734 (m), 722 (m), 667 (w); Raman (1064 nm): $\tilde{\nu}$ = 1465 (3), 1390 (100), 1207 (16), 1150 (6), 1091 (10), 1021 (2), 922 (13), 727 (3), 473 (3), 233 (3); ¹H NMR (DMSO-*d*₆) δ (ppm) = 8.63 (s, 2H, CH), 8.16 (s, 4H, NH₂); ¹³C NMR (DMSO-*d*₆) δ (ppm) = 154.1 (s, 2C, ZTX), 128.2 (s, 2C, DATr); *m/z*: (FAB⁺) 100.0 (C₂H₆N₅); *m/z*: (FAB⁻) 197.0 (C₂H₆N₁₀O₂); EA (C₆H₁₂N₂₀O₂, 396.29) calcd: C, 18.18; H, 3.05; N, 70.69%; found: C, 18.73; H, 2.94; N, 70.48%; BAM impact: 1 J; BAM friction: 18 N; ESD: 0.2 J.

1,3-Diamino-1,2,3-triazolium nitriminotetrazolate (8)

3 (368 mg, 2.7 mmol) was added to a suspension of 643 mg (2.7 mmol) of silver nitriminotetrazolate in 25 mL of distilled water. The mixture was stirred for 30 min under heating and was filtered in the dark. The filtrate was evaporated to yield 406 mg (66%) of **8**.

DSC: 154 °C (dec); IR (cm⁻¹) $\tilde{\nu}$ = 3425 (w), 3231 (m), 3126 (s), 3088 (s), 2397 (w), 2309 (w), 2140 (w), 1802 (w), 1724 (w), 1617 (w), 1528 (m), 1493 (w), 1450 (m), 1374 (s), 1306 (s), 1229 (m), 1216 (m), 1207 (m), 1187 (m), 1142 (w), 1122 (w), 1081 (m), 1050 (m), 1011 (m), 968 (m), 927 (m), 902 (m), 860 (m), 826 (m), 787 (m), 771 (m), 738 (m), 692 (w), 656 (w), 641 (w), 621 (w); Raman (1064 nm): $\tilde{\nu}$ = 3256 (2), 3158 (21), 3131 (5), 3094 (5), 1640 (2), 1619 (3), 1543 (100), 1499 (5), 1455 (35), 1414 (2), 1391 (9), 1378 (3), 1360 (12), 1337 (8), 1317 (33), 1275 (9), 1232 (16), 1188 (11), 1147 (7), 1078 (29), 1051 (36), 1034 (12), 1027 (69), 1005 (19), 971 (2), 942 (4), 863 (6), 745 (16), 644 (22), 517 (16), 481 (3), 417 (16), 373 (4), 325 (6), 250 (9); ¹H NMR (DMSO-*d*₆) δ (ppm) = 8.64 (s, 2H, CH), 8.25 (s, 4H, NH₂); ¹³C NMR (DMSO-*d*₆) δ (ppm) = 161.7 (s, 1C, NATZ), 127.9 (s, 2C, DATr); *m/z*: (FAB⁺) 100.0 (C₂H₆N₅); *m/z*: (FAB⁻) 129.0 (CN₅O₃); BAM impact: 3 J; BAM friction: 42 N; ESD: 0.5 J.

Acknowledgement

Financial support of this work by the Ludwig-Maximilian University of Munich (LMU), the U.S. Army Research Laboratory (ARL), the Armament Research, Development and Engineering Center (ARDEC), the Strategic Environmental Research and Development Program (SERDP) and the Office of Naval Research (ONR Global, title: "Synthesis and Characterization of New High Energy Dense Oxidizers (HEDO) - NICOP Effort") under contract nos. W911NF-09-2-0018 (ARL), W911NF-09-1-0120

(ARDEC), W011NF-09-1-0056 (ARDEC) and 10 WPSEED01-002 / WP-1765 (SERDP) is gratefully acknowledged. The authors acknowledge collaborations with Dr. Mila Krupka (OZM Research, Czech Republic) in the development of new testing and evaluation methods for energetic materials and with Dr. Muhamed Sucesca (Brodarski Institute, Croatia) in the development of new computational codes to predict the detonation and propulsion parameters of novel explosives. We are indebted to and thank Drs. Betsy M. Rice and Brad Forch (ARL, Aberdeen, Proving Ground, MD) and Mr. Gary Chen (ARDEC, Picatinny Arsenal, NJ) for many helpful and inspired discussions and support of our work. The authors want to thank Stefan Huber for measuring the sensitivities. Dennis Fischer is thanked for providing azotetrazolate-1,1'-dioxide and Niko Fischer is thanked for providing bistetrazolate-1,1'-dioxide.

References

- [1] O. S. Bushuyev, P. Brown, A. Maiti, R. H. Gee, G. R. Peterson, B. L. Weeks, J. J. Hope-Weeks, *J. Am. Chem. Soc.* **2012**, *134*, 1422-1425.
- [2] D. E. Chavez, M. A. Hiskey, D. L. Naud, D. Parrish, *Angew. Chem. Int. Ed.* **2008**, *47*, 8307-8309.
- [3] M. H. V. Huynh, M. A. Hiskey, D. E. Chavez, D. L. Naud, R. D. Gilardi, *J. Am. Chem. Soc.* **2005**, *127*, 12537-12543.
- [4] D. E. Chavez, M. A. Hiskey, R. D. Gilardi, *Org. Lett.* **2004**, *6*, 2889-2891.
- [5] J. W. Fronabarger, M. D. Williams, W. B. Sanborn, J. G. Bragg, D. A. Parrish, M. Bichay, *Propellants Explos. Pyrotech.* **2012**, *36*(6), 541-550.
- [6] M.-X. Zhang, P. E. Eaton, R. Gilardi, *Angew. Chem. Int. Ed.* **2000**, *39*, 401-404.
- [7] P. Carlqvist, H. Ostmark, T. Brinck, *J. Phys. Chem. A* **2004**, *108*, 7463-7467.
- [8] Q. -H. Lin, Y. -C. Li, Y. -Y. Li, W. Liu, C. Qi, S. -P. Pang, *J. Mater. Chem.* **2012**, *22*, 666-6674.
- [9] T. M. Klapötke, J. Stierstorfer, *J. Am. Chem. Soc.* **2009**, *131*, 1122-1134.
- [10] Y. -C. Li, C. Qi, S. -H. Li, H. -J. Zhang, C. -H. Sun, Y. -Z. Yu, S. -P. Pang, S.-P. *J. Am. Chem. Soc.* **2010**, *132* (35), 12172-12173.
- [11] T. M. Klapötke, D. G. Piercey, *Inorg. Chem.* **2011**, *50*, 2732-2734.
- [12] T. M. Klapötke, P. Mayer, C. M. Sabaté, J. M. Welch, N. Wiegand, *Inorg. Chem.* **2008**, *47*(13), 6014-6027.
- [13] M. Göbel, K. Karaghiosoff, T. M. Klapötke, D. G. Piercey, J. Stierstorfer, *J. Am. Chem. Soc.* **2010**, *132*, 17216-17226.
- [14] T. Fendt, N. Fischer, T. M. Klapötke, J. Stierstorfer, *J. Inorg. Chem.* **2011**, *50*, 1447-1458.
- [15] N. Fischer, T. M. Klapötke, J. Stierstorfer, *Eur. J. Inorg. Chem.* **2011**, *28*, 4471-4480.
- [16] O. P. Shitov, V. A. Vyazkov, V. A. Tartakovskii, *Izv. Akad. Nauk. SSSR. Ser. Khim.* **1989**, *11*, 2654-2655.
- [17] G. Laus, V. Kahlenberg, D. M. Toebbens, R. K. R. Jetti, U. J. Greisser, J. Schuetz, E. Kristeva, K. Wurst, H. Schottenberger, *Cryst. Growth & Design.* **2006**, *6*, 404-410.
- [18] T. M. Klapötke, D. G. Piercey, J. Stierstorfer, *Dalton. Trans.* **2012**, *41*, 9451-9459.
- [19] Gaussian 09, Revision A.1, M. J. Frisch, G. W. Trucks, H. B. Schlegel, G. E. Scuseria, M. A. Robb, J. R. Cheeseman, G. Scalmani, V. Barone, B. Mennucci, G. A. Petersson, H. Nakatsuji, M. Caricato, X. Li, H. P. Hratchian, A. F. Izmaylov, J. Bloino, G. Zheng, J. L. Sonnenberg, M. Hada, M. Ehara, K. Toyota, R. Fukuda, J. Hasegawa, M. Ishida, T. Nakajima, Y. Honda, O. Kitao, H. Nakai, T. Vreven, J. A. Montgomery, Jr., J. E. Peralta, F. Ogliaro, M. Bearpark, J. J. Heyd, E. Brothers, K. N. Kudin, V. N. Staroverov, R. Kobayashi, J. Normand, K. Raghavachari, A. Rendell, J. C. Burant, S. S. Iyengar, J. Tomasi, M. Cossi, N. Rega, J. M. Millam, M. Klene, J. E. Knox, J. B. Cross, V. Bakken, C. Adamo, J. Jaramillo, R. Gomperts, R. E. Stratmann, O. Yazyev, A. J. Austin, R. Cammi, C. Pomelli, J. W. Ochterski, R. L. Martin, K. Morokuma, V. G. Zakrzewski, G. A. Voth, P. Salvador, J. J. Dannenberg, S. Dapprich, A. D. Daniels, Ö. Farkas, J. B. Foresman, J. V. Ortiz, J. Cioslowski, and D. J. Fox, Gaussian, Inc., Wallingford CT, **2009**.
- [20] G. Kaplan, G. Drake, K. Tollison, L. Hall, T. Hawkins, *J. Het. Chem.* **2005**, *42*, 19-27.
- [21] A. J. Bracuti, *J. Acta. Cryst.* **1979**, *B35*, 760-761.
- [22] D. Fischer, N. Fischer, T. M. Klapötke, J. Stierstorfer, *Unpublished Results*
- [23] N. Fischer, D. Fischer, T. M. Klapötke, D. G. Piercey, J. Stierstorfer, *J. Mater. Chem.* **2012**, *22*, 20418-20422.
- [24] R. Meyer, J. Köhler, A. Homberg, A. *Explosives*, 5th edition, p344, Essen, Germany, **2002**.
- [25] M. Tremblay, *Can. J. Chem.* **1965**, *43*, 1230-1232.
- [26] (a) J. W. Ochterski, G. A. Petersson, J. A. Montgomery Jr., *J. Chem. Phys.* **1996**, *104*, 2598; (b) J. A. Montgomery Jr., M. J. Frisch, J. W. Ochterski, G. A. Petersson, *J. Chem. Phys.* **2000**, *112*, 6532.
- [27] (a) L. A. Curtiss, K. Raghavachari, P. C. Redfern, J. A. Pople, *J. Chem. Phys.* **1997**, *106*(3), 1063; (b) E. F. C. Byrd, B. M. Rice, *J. Phys. Chem. A* **2006**, *110*(3), 1005-1013; (c) B. M. Rice, S. V. Pai, J. Hare, *Comb. Flame* **1999**, *118*(3), 445-458.
- [28] (a) H. D. B. Jenkins, H. K. Roobottom, J. Passmore, L. Glasser, *L. Inorg. Chem.* **1999**, *38*(16), 3609-3620. (b) H. D. B. Jenkins, D. Tudela, L. Glasser, *L. Inorg. Chem.* **2002**, *41*(9), 2364-2367.
- [29] A. D. Vasiliev, A. M. Astakhov, A. A. Nefedov, R. S. Stepanov, *J. Struct. Chem.* **2003**, *44*, 322-325.
- [30] a) M. Sućeska, *Materials Science Forum*, **2004**, 465-466, 325-330. b) M. Sućeska, *Propellants Explos. Pyrotech.* **1999**, *24*, 280-285; c) M. Sućeska, *Propellants Explos. Pyrotech.* **1991**, *16*(4), 197-202.
- [31] M. Sućeska, *Test Methods for Explosives*; Springer: New York, **1995**, p 21 (impact), p 27 (friction).
- [32] www.bam.de
- [33] Impact: Insensitive > 40 J, less sensitive ≥ 35 J, sensitive ≥ 4 J, very sensitive ≤ 3 J; Friction Insensitive > 360 N, less sensitive = 360 N, sensitive < 360 N a. > 80N, very sensitive ≤ 80 N, extremely sensitive ≤ 10 N. According to the UN Recommendations on the Transport of Dangerous Goods.
- [34] G. Kaplan, G. Drake, K. Tollison, L. Hall, T. Hawkins, *Heterocyclic Chem.* **2005**, *42*, 19-27
- [35] NATO standardization agreement (STANAG) on explosives, *impact sensitivity tests*, no. 4489, Ed. 1, Sept. 17, **1999**.
- [36] WIWEB-Standardarbeitsanweisung 4-5.1.02, Ermittlung der Explosionsgefährlichkeit, hier der Schlagempfindlichkeit mit dem Fallhammer, Nov. 8, **2002**.
- [37] <http://www.reichel-partner.de>
- [38] NATO standardization agreement (STANAG) on explosives, *friction sensitivity tests*, no. 4487, Ed. 1, Aug. 22, **2002**.
- [39] WIWEB-Standardarbeitsanweisung 4-5.1.03, Ermittlung der Explosionsgefährlichkeit oder der Reibeempfindlichkeit mit dem Reibeapparat, Nov. 8, **2002**.
- [40] D. Skinner, D. Olson, A. Block-Bolten, A. *Propellants, Explos., Pyrotech.* **1998**, *23*, 34-42.
- [41] <http://www.ozm.cz/testinginstruments/> small-scale-electrostatic-discharge-tester.htm.

- [42] CrysAlisPro, Agilent Technologies, Version 1.171.35.11, **2011**.
- [43] G. M. Sheldrick, SHELXS-97, Program for Crystal Structure Solution, Universität Göttingen, **1997**.
- [44] A. Altomare, G. Cascarano, C. Giacovazzo, A. Guagliardi *A. Appl. Cryst.* **1993**, 26, 343.
- [45] G. M. Sheldrick, Shelxl-97, Program for the Refinement of Crystal Structures, University of Göttingen, Germany, **1994**.
- [46] A. L. Spek, A. Platon, A Multipurpose Crystallographic Tool, Utrecht University, Utrecht, The Netherlands, **1999**.
- [47] L. Farrugia, *J. Appl. Crystallogr.* **1999**, 32, 837–838.
- [48] Empirical absorption correction using spherical harmonics, implemented in SCALE3 ABSPACK scaling algorithm (CrysAlisPro Oxford Diffraction Ltd., Version 171.33.41, **2009**)

Received: ((will be filled in by the editorial staff))
Published online: ((will be filled in by the editorial staff))

The 1,4,5-Triaminotetrazolium Cation (CN_7H_6^+): A Highly Nitrogen-Rich Moiety

Thomas M. Klapötke,^{*[a]} Davin G. Piercey,^[a] and Jörg Stierstorfer^[a]

Dedicated to the memory of Professor Dr. Detlef Schröder

Keywords: Nitrogen heterocycles / Amination / Energetic materials / Structure elucidation

The amination of 1,5-diamino-1,2,3,4-tetrazole with tosyl-hydroxylamine yielded 1,4,5-triaminotetrazolium tosylate. Metathesis reactions yielded energetic bromide, nitrate, and nitrotetrazolate 2-oxide salts. Owing to the exceedingly high nitrogen content of the cation (>84 % !), the calculated heats of formation and the experimental explosive and thermal

sensitivities are exceedingly high. For the first time, the X-ray structure of this energetic cation is reported, as are the standard multinuclear NMR, infrared, and Raman spectroscopic data. Explosive performances (detonation velocity and pressure) have also been calculated for a sample compound.

Introduction

Many scientists are attracted to this field as a result of the unique challenges encountered in synthesis and characterization of these prospective replacements for currently used energetic materials. Within the field of energetic materials, nitrogen-rich compounds are extensively looked at as replacements for currently used energetics because they are higher performing and are more environmentally friendly alternatives.^[1–5]

Traditional energetic materials including TNT (2,4,6-trinitrotoluene) and RDX (1,3,5-trinitro-1,3,5-triazinane) obtain the majority of their energy content by oxidation of their carbon backbones through the presence of an oxidizer in the molecule. With new research in the development of novel energetics, two new classes of explosive materials have been introduced: those containing either ring or cage strain (e.g., energetic cubanes) and those with high heats of formation that are nitrogen rich (e.g., tetrazoles and tetrazines). These strategies have also been combined to make strained, nitrogen-rich heterocycles a promising and well-investigated area of research.^[6–11]

Among the elements, nitrogen occupies a unique position; the strong, short triple bond means that there is a large energetic driving force towards the formation of mo-

lecular nitrogen. In singly and doubly bonded nitrogen systems, this is especially true, where the more contiguous nitrogen atoms in the system leads to higher heats of formation and, as such, higher performances.^[7,8]

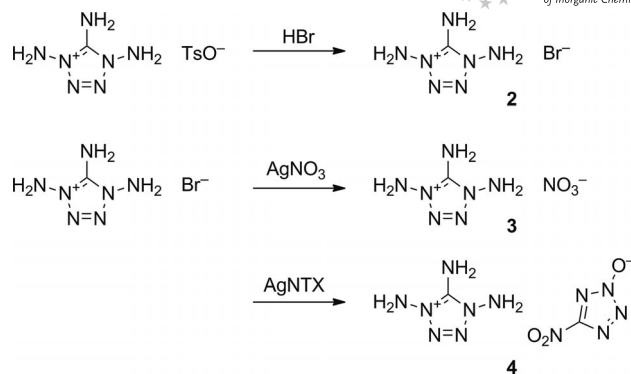
Nitrogen-rich heterocycles, especially tetrazoles, have been the backbones of various new explosive compounds, as the carbon position can be easily tailored. This allows the introduction of various substituents to create compounds that span a range of sensitivities from highly sensitive primary explosives to insensitive secondary explosives.^[11,12] However, the tailoring of substituents on the nitrogen atoms of tetrazole rings is far less investigated. Alkylation reactions are well known;^[13–15] however, the addition of carbon atoms often has negative effects on explosive performance. In our recent work, we reported on a series of *N*-aminated energetic tetrazoles that were the result of aminating energetic anions with hydroxylamine-*O*-sulfonic acid.^[16] The *N*-amination of energetic anions gave neutral *N*-amino species with very high performances, and in this work, we extended this methodology to the amination of a well-known neutral tetrazole species (1,5-diaminotetrazole) to yield the first energetic tetrazolium cation containing three amino groups on the same tetrazole ring.

The 1,4,5-triaminotetrazolium cation, at over 84% nitrogen, belongs to the unique class of compounds containing over 80% nitrogen.^[8,17,18] Beyond use in explosive materials, compounds containing such high nitrogen contents are important in propellant formulations, as lower reaction temperatures and higher N_2/CO ratios in the combustion products result in lower erosivity. It has been shown that lower

[a] Department of Chemistry, Energetic Materials Research, Ludwig-Maximilian University, Butenandtstr. 5–13 (D), 81377 München, Germany
 Fax: +49-89-2180-77492
 E-mail: tmk@cup.uni-muenchen.de
 Homepage: <http://www.cup.uni-muenchen.de/ac/klapoetke/>

erosivity results from the presence of higher concentrations of nitrogen in the combustion gasses of a propellant leading to surface formation of iron nitride instead of iron carbide on the inside of the barrel.^[18]

In this work, we have aminated 1,5-diaminotetrazole with *O*-tosylhydroxylamine to yield 1,4,5-triaminotetrazolium tosylate. Through metathesis reactions, the bromide, nitrate, and nitrotetrazolate 2-oxide salts were all prepared. The compounds were characterized by X-ray diffraction, infrared and Raman spectroscopy, multinuclear NMR spectroscopy, elemental analysis, and differential scanning calorimetry (DSC). Computational calculations confirming the high energetic performance were also performed.

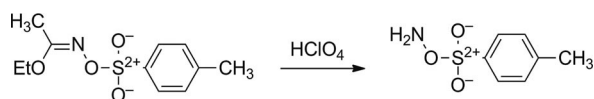


Scheme 3. Metathesis reactions of the 1,4,5-triaminotetrazolium cation.

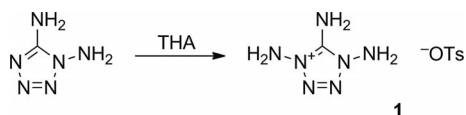
Results and Discussion

Synthesis

O-Tosylhydroxylamine is not stable in storage, so it was prepared from ethyl *O*-*p*-tolylsulfonylethoxyacetimidate by hydrolysis with 60% perchloric acid (Scheme 1) before each reaction. After hydrolysis, it was then poured into ice water and extracted with dichloromethane, and the dichloromethane solution was dried with sodium sulfate.^[16] A solution of *O*-tosylhydroxylamine (THA) was then added to an acetonitrile solution/suspension of 1,5-diaminotetrazole. After reaction for 3 d, the crude 1,4,5-triaminotetrazolium tosylate was obtained (Scheme 2).



Scheme 1. Synthesis of *O*-tosylhydroxylamine (THA) from ethyl-*O*-*p*-tolylsulfonylethoxyacetimidate.



Scheme 2. Synthesis of triaminotetrazolium tosylate.

The as-prepared 1,4,5-triaminotetrazolium tosylate (**1**) was then dissolved in a minimal amount of ethanol, concentrated hydrobromic acid was added, and 1,4,5-triaminotetrazolium bromide (**2**) was precipitated by the addition of diethyl ether. Through metathesis reactions with either silver nitrate or silver nitrotetrazolate 2-oxide, 1,4,5-triaminotetrazolium nitrate (**3**) and 1,4,5-triaminotetrazolium nitrotetrazolate 2-oxide (**4**) were obtained, respectively (Scheme 3). Crystals were grown of all salts, with the exception of **4**, by diffusing ether into a methanolic solution of the salt. Compound **4** was unable to be crystallized despite repeated attempts.

Spectroscopy

Multinuclear NMR spectroscopy proved to be a useful tool for the characterization of the energetic cation and its salts. In the ¹H NMR spectrum, the 1,4,5-triaminotetrazolium cation shows two resonances. The first at $\delta \approx 8.9$ ppm for the amino group attached to the carbon atom of the tetrazole ring, and another at $\delta \approx 6.9$ ppm for the *N*-amino groups, which is double the intensity of the previous resonance. In the ¹³C NMR spectrum, a single peak for the lone carbon atom is observed at $\delta = 147$ ppm.

The IR and Raman spectra of all compounds were collected and assigned by using frequency analysis from an optimized structure (B3LYP/cc-pVDZ using Gaussian09 software^[19]). All calculations were performed at the DFT level of theory; the gradient-corrected hybrid three-parameter B3LYP^[20,21] functional theory has been used with a correlation consistent *p*-VDZ basis set.^[22–25] The infrared spectra of the triaminotetrazolium cation possesses five strong intensity bands that are easily rendered to medium or low intensity when paired with an anion with strong absorbances. As bromide salt **2** only has resonances resulting from the triaminotetrazolium cation, this spectrum was used extensively for comparison. The calculated spectrum shows a strong absorbance at 922 cm⁻¹ resulting from N–NH₂ wagging. In the spectrum of the bromide salt, this peak is visible at 867 cm⁻¹, and in nitrate salt **3**, it appears at 825 cm⁻¹. In the spectra of tosylate **1** and nitrotetrazolate 2-oxide **4**, the presence of other peaks in the area makes assignment unclear. The next high-intensity band occurs at 1787 cm⁻¹ in the calculated spectrum and arises from C–N stretching with symmetric C1–N1/C1–N4 ring deformation. In the observed spectra, this band occurs at 1722, 1715, 1726, and 1717 cm⁻¹ for compounds **1–4**, respectively. The remaining strong bands result from symmetric N–NH₂, symmetric C–NH₂, asymmetric N–NH₂, and asymmetric C–NH₂ N–H stretching at calculated wavenumbers of 3449, 3535, 3537, and 3670 cm⁻¹, respectively. In the observed spectra, these all occur in the range from 3400 to 3000 cm⁻¹ and show a greater deviation between the experimental and calculated values compared to the previous bands. The calculated Raman spectrum of the triaminotetrazolium cation contains one very high-intensity peak at 779 cm⁻¹ resulting

FULL PAPER

from tetrazole ring breathing. In the spectra of **2** and **3**, this signal occurs at 789 and 791 cm^{-1} , respectively. In the spectra of **1** and **4**, the presence of multiple peaks in this region precludes exact assignment.

Single-Crystal X-ray Analysis

With the exception of nitrotetrazolate 2-oxide salt **4**, all compounds were characterized by X-ray crystallography. Table 1 summarizes a selection of crystallographic data and refinement details. Exact bond lengths and angles of the 1,4,5-triaminotetrazolium cations are given in Table 2. The bond lengths and angles within the tetrazole moiety are comparable to those in 1,5-diaminotetrazole,^[26] with several small changes. We will discuss the changes based on bond lengths and angles from salt **1**; however, the trend also holds for salt **3**. The tetrazole ring within 1,5-diaminotetrazole is not symmetric; C1–N1 is longer than C1–N4: 1.345 vs. 1.327 Å, respectively. After amination, these bond lengths, while they become similar at 1.344 and 1.332 Å, respectively, they do not become equivalent, leaving the tetrazole ring slightly distorted. Concurrently, N2–N3 and N3–N4 increase in length from 1.363 to 1.376 Å. Finally, of note is that only the protons of the C1–NH₂ are planar with the ring, indicating electronic communication between the π system of the ring and the p electrons on the N5 amino group. The process of amination reduces electron density within the tetrazole ring, easily explaining why the C1–N5 bond length decreases to 1.314 Å from the 1.334 Å seen in 1,5-diaminotetrazole. The N–NH₂ bond lengths, N1–N6 and N4–N7, do not change appreciably from the N–NH₂ bond length in 1,5-diaminotetrazole.

Table 1. Crystallographic data and structure refinement details for triaminotetrazolium salts.

	1·0.5MeOH	3
Formula	C ₁₇ H ₃₀ N ₁₄ O ₇ S ₂	CH ₆ N ₈ O ₃
FW [g mol ⁻¹]	606.67	320.23
Crystal system	triclinic	orthorhombic
Space Group	P1̄	Pna2 ₁
<i>a</i> [Å]	6.5993(2)	7.7144(18)
<i>b</i> [Å]	13.6361(5)	17.605(4)
<i>c</i> [Å]	15.9896(6)	5.2393(13)
α [°]	90.705(3)	90
β [°]	95.737(3)	90
γ [°]	98.577(3)	90
<i>V</i> [Å ³]	1415.12(9)	711.6(3)
<i>Z</i>	2	4
$\rho_{\text{calcd.}}$ [g cm ⁻³]	1.424	1.663
<i>T</i> [K]	173	173
<i>R</i> ₁ / <i>wR</i> ₂ (all data)	0.0549/0.0969	0.0440/0.0736
<i>R</i> ₁ / <i>wR</i> ₂ (<i>I</i> > 2 σ)	0.0381/0.0881	0.0360/0.0696
<i>S</i> _c	1.048	1.049

Salt **1**·0.5MeOH crystallizes in the triclinic space group P1̄ with four formula units in the unit cell and a density of 1.424 g cm⁻³. The asymmetric unit consists of two anion–cation pairings and one methanol molecule that is shown in Figure 1.

Table 2. Crystallographic bond lengths and angles of the 1,4,5-triaminotetrazolium cations in the structures of **1** and **3**.

	1a	1b	3
A–B length [Å]			
C1–N1	1.344(2)	1.334(2)	1.338(4)
C1–N4	1.332(2)	1.339(2)	1.342(3)
C1–N5	1.314(2)	1.313(2)	1.308(4)
N1–N2	1.376(2)	1.376(2)	1.381(3)
N2–N3	1.277(3)	1.277(3)	1.271(3)
N3–N4	1.376(2)	1.375(2)	1.374(3)
N1–N6	1.386(2)	1.381(2)	1.385(3)
N4–N7	1.384(2)	1.392(2)	1.374(3)
A–B–C angle [°]			
C1–N1–N2	110.33(16)	110.30(17)	110.1(2)
C1–N4–N3	110.85(16)	110.40(17)	110.5(2)
C1–N1–N6	124.36(17)	124.23(17)	122.8(2)
C1–N4–N7	123.82(17)	123.45(17)	124.1(2)
N1–C1–N4	103.79(17)	104.14(17)	103.9(2)
N5–C1–N1	128.60(19)	128.38(19)	127.4(2)
N5–C1–N4	127.61(19)	127.47(19)	128.7(3)

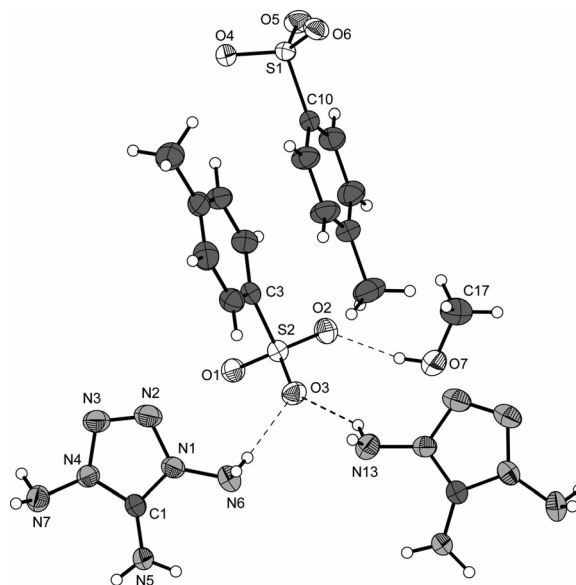


Figure 1. View of the asymmetric unit in the structure of **1**·0.5MeOH. Ellipsoids are drawn at the 50% probability level.

The crystal structure of **2** could not be determined sufficiently due to a hard twinning problem. By using a twin data reduction, two species could be detected and separated. One of them^[27] could be solved and refined to yield a final *wR*₂ value of 23.2%. However, it was not possible to locate any electron density for the hydrogen atoms.

Salt **3** crystallizes in the non-centrosymmetric orthorhombic space group Pna2₁ with four formula units in the unit cell. The molecular moiety is shown in Figure 2. Although an intensive hydrogen-bonding network is formed, the density is only 1.663 g cm⁻³. This is quite low in comparison to other tetrazolium compounds, especially the corresponding 5-aminotetrazolium nitrate (1.847 g cm⁻³)^[28] and 1,5-diaminotetrazolium nitrate (1.727 g cm⁻³)^[29] Inter-

estingly, the density decreases by increasing the number of amino groups connected to the tetrazolium ring nitrogen atoms.

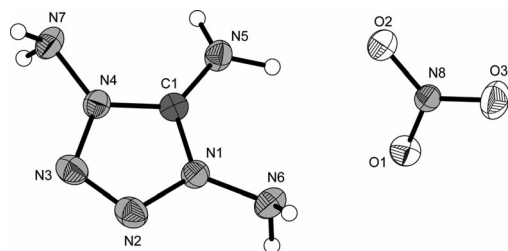


Figure 2. Molecular unit of **3**. Ellipsoids are drawn at the 50% probability level.

Hydrogen bonding takes place at all oxygen atoms of the nitrate anion and all hydrogen atoms of the 1,4,5-triamino-tetrazolium cations, which is indicated in Figure 3.

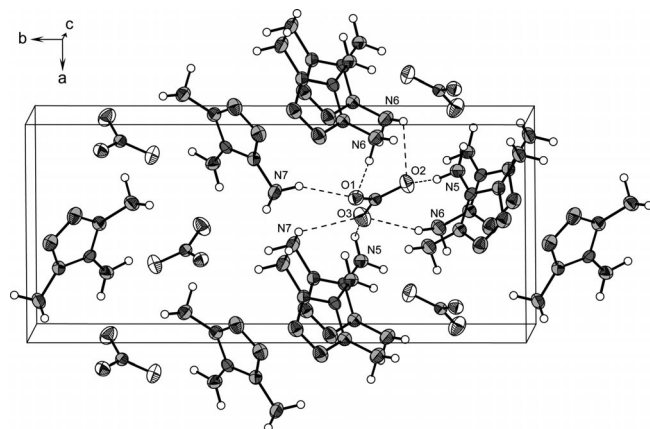


Figure 3. The unit cell of **4**, depicting the important hydrogen bonds of the nitrate anion.

Energetic Properties

Calculation of the heats of formation of compounds **2–4** was performed by using the atomization method based on CBS-4M calculated gas-phase enthalpies and Equation (1) described recently in detail.^[5]

$$\Delta_f H^\circ_{(g,M,298)} = H_{(molecule,298)} - \Sigma H^\circ_{(atoms,298)} + \Sigma \Delta_f H^\circ_{(atoms,298)} \quad (1)$$

The results are depicted in Table 3. The gas-phase heat of formation [$\Delta_f H^\circ(g,M)$] was converted into the solid-state heat of formation [$\Delta_f H^\circ(s)$] (Table 3) by using the Jenkins and Glasser equations for the lattice energies and enthalpies.^[30] The gas-phase enthalpies of formation of Br^- ($-239.5 \text{ kJ mol}^{-1}$) and NO_3^- ($-313.6 \text{ kJ mol}^{-1}$) fit very well to experimentally obtained values published in the literature (Br^- $-233.9 \text{ kJ mol}^{-1}$)^[31] and NO_3^- ($-300.2 \text{ kJ mol}^{-1}$)^[32]

Table 3. CBS-4M results and gas-phase enthalpies.

	Formula	$-H^{298}$ [a.u.]	$\Delta_f H(g)$ [kJ mol ⁻¹]
1,4,5-TAT ⁺	CH_6N_7^+	424.051319	1129.0
Br ⁻	Br^-	2572.763437	-239.5
NO ₃ ⁻	NO_3^-	280.080446	-313.6
NTX ⁻	CN_5O_3^-	536.798772	83.0
2	$\text{CH}_6\text{N}_7\text{Br}$		889.5 ^[a]
3	$\text{CH}_6\text{N}_8\text{O}_3$		815.4 ^[a]
4	$\text{C}_2\text{H}_6\text{N}_{12}\text{O}_3$		1212.0 ^[a]

[a] Gas-phase enthalpies of formation of the ionic compounds are taken as the respective sums of the non-interacting component ions.

These molar standard enthalpies of formation (ΔH_m) were used to calculate the molar solid-state energies of formation (ΔU_m) according to Equation (2) (Table 3).

$$\Delta U_m = \Delta H_m - \Delta nRT \quad (2)$$

where Δn is the change of mol of gaseous components.

As it can be seen from Table 4, compounds **2–4** are formed endothermically. The most positive value of $722.6 \text{ kJ mol}^{-1}$ is obtained for **4** as a result of its highly energetic and endothermic anion. The calculation of the detonation parameters was performed with the program EXPLO5.05^[33] by using the X-ray density for **3** and a helium gas pycnometer density for **4**. The results for **3** and **4** in comparison to those of RDX are gathered in Table 5.

Table 4. Calculation of the solid-state energies of formation ($\Delta_f U^\circ$).

	2	3	4
V_M [nm ³]	0.167	0.178	0.234 ^[a]
U_L [kJ mol ⁻¹]	606.7	520.9	484.5
ΔH_L [kJ mol ⁻¹]	607.9	525.9	489.5
$\Delta_f H^\circ(s)$ [kJ mol ⁻¹]	281.6	289.5	722.6
Δn	6.5	8.5	10.5
$\Delta_f U^\circ(s)$ [kJ kg ⁻¹]	1518.4	1743.2	3040.6

[a] The molecular volume of **4** was recalculated from the X-ray structure of ammonium 5-nitrotetrazolate *N*-oxide^[5] and a literature value for the nitrate anion.^[29]

The detonation parameters of **3** and **4** are slightly lower than those of RDX, which is due to their lower densities. However, the detonation velocities (V_{det}) of 8779 m s^{-1} (for **3**) and 8872 m s^{-1} (for **4**) are much higher than those of TNT ($V_{\text{det}} = 7459 \text{ m s}^{-1}$) and also PETN (pentaerythritol tetranitrate) ($V_{\text{det}} = 8561 \text{ m s}^{-1}$) calculated by using the same approaches. With respect to a potential use as propellant ingredients, **3** and **4** show very high values for the specific impulse (using 60 bar chamber pressure isobaric rocket conditions) of 260 s (for **3**) and 259 s (for **4**).

In addition, the sensitivities towards shock, friction, and electrostatic discharge were carried out for all compounds. Generally, tosylate salt **1** was found to be the least sensitive with 10 J and 240 N friction and impact sensitivities, respectively, classifying it as a “less sensitive”^[36] energetic material. For remaining compounds **2–4**, all impact energies were 2 J or less and all friction sensitivities were below 10 N. Of interest is the very high sensitivities of bromide salt **2**, uncharacteristic for an energetic cation paired with a non-energetic anion; for example, triaminoguanidinium

FULL PAPER

Table 5. Energetic properties of **3** and **4** in comparison to those of RDX.

	3	4	RDX
Formula	CH ₆ N ₈ O ₃	C ₂ H ₆ N ₁₂ O ₃	C ₃ H ₆ N ₆ O ₆
FW [g mol ⁻¹]	178.11	246.15	222.12
Impact sensitivity [J] ^[a]	2	1	7.5 ^[34]
Friction sensitivity [N] ^[b]	5	7	120 ^[34]
ESD-test [J] ^[c]	0.050	0.100	0.2
N [%] ^[d]	62.91	68.28	37.84
Ω [%] ^[e]	-17.96	-26.00	-21.61
T _{dec} [°C] ^[f]	78	84	210
Density [g cm ⁻³] ^[g]	1.663	1.71	1.858 (90 K) ^[35]
Δ _f U ^o [kJ kg ⁻¹] ^[h]	1743.2	3040.6	489.0
<i>EXPLO5.05 Values</i>			
-Δ _{Ex} U ^o [kJ kg ⁻¹] ^[i]	5745	5910	6190
T _{det} [K] ^[j]	4006	4221	4232
P _{Cl} [kbar] ^[k]	311	326	380
V _{det} [m s ⁻¹] ^[l]	8779	8872	8983
V _o [L kg ⁻¹] ^[m]	876	815	734
I _s [s] ^[n]	260	259	258

[a] Impact sensitivity [BAM drophammer (1 of 6)]. [b] Friction sensitivity [BAM friction tester (1 of 6)]. [c] Electrostatic discharge device (OZM research). [d] Nitrogen content. [e] Oxygen balance [$\Omega = (xO - 2yC - 1/2zH)M/1600$]. [f] Decomposition temperature from DSC ($\beta = 5^\circ\text{C}$). [g] From X-ray diffraction. [h] Calculated energy of formation. [i] Energy of explosion. [j] Explosion temperature. [k] Detonation pressure. [l] Detonation velocity. [m] Volume of detonation gases (assuming only gaseous products). [n] Specific impulse using isobaric (60 bar) conditions.

bromide is insensitive.^[37] Bromide salt **2** is highly sensitive towards mechanical stimuli (impact, friction), but with 15 mJ electrostatic sensitivity it is also capable of being initiated by a static charge created by the human body. All these results indicate that the 1,4,5-triaminotetrazolium cation is far too sensitive towards mechanical and electrostatic stimuli to find any practical use as an energetic material.

Finally, compounds **2–4** all decompose in the range from 102 to 78 °C. These thermal stabilities are too low for a practical energetic material; however, it does provide insight that there is a limit on the thermal stability as heats of formation and associated nitrogen content increase.

Conclusions

The amination of 1,5-diaminotetrazole with *O*-tosylhydroxylamine is an effective method of preparing the new energetic 1,4,5-tetrazolium cation. Metathesis reactions allowed easy preparation of the bromide, nitrate, and nitrotetrazolate 2-oxide salts. The crystal structure of this unique cation was determined for the first time, as were its spectral properties. The energetic performances of the nitrate and nitrotetrazolate 2-oxide salts were calculated, illustrating the ability of the triaminotetrazolium cation to form high-performance energetic materials almost on par with RDX. However, the major limitations of the triaminotetrazolium cation are its sensitivities; the mechanical, electrostatic, and thermal sensitivities of this new energetic cation are all far too low to be used in practical energetic materials.

Experimental Section

General Methods: All reagents and solvents were used as received (Sigma–Aldrich, Fluka, Acros Organics) if not stated otherwise. *O*-*p*-Tolylsulfonylacetohydroximate was prepared according to a literature procedure.^[12] Melting and decomposition points were measured with a Linseis PT10 DSC by using heating rates of 5 °C min⁻¹. ¹H NMR and ¹³C NMR spectra were measured with a JEOL instrument. All chemical shifts are quoted in ppm relative to TMS (¹H, ¹³C). Infrared spectra were measured with a Perkin–Elmer FTIR Spektrum BXII instrument equipped with a Smith Dura SAMPiIR II ATR-unit. Transmittance values are described as strong (s), medium (m), and weak (w). Mass spectra were measured with a JEOL MStation JMS 700 instrument. Raman spectra were measured with a Perkin–Elmer Spektrum 2000R NIR FT-Raman instrument equipped with a Nd:YAG laser (1064 nm). The intensities are reported as percentages of the most intensive peak and are given in parentheses. Elemental analyses were performed with a Netsch STA 429 simultaneous thermal analyzer. Sensitivity data were determined by using a BAM drophammer and a BAM friction tester. The electrostatic sensitivity tests were carried out by using an Electric Spark Tester ESD 2010 EN (OZM Research) operating with the “Winspark 1.15” software package.

CCDC-896690 (for **1**·0.5MeOH) and -896691 (for **3**) contain the supplementary crystallographic data for this paper. These data can be obtained free of charge from The Cambridge Crystallographic Data Centre via www.ccdc.cam.ac.uk/data_request/cif.

CAUTION! *The described compounds are energetic materials with sensitivity to various stimuli. Although we encountered no issues in the handling of these materials, proper protective measures (face shield, ear protection, body armor, Kevlar gloves, and earthened equipment) should be used at all times.*

1,4,5-Triaminotetrazolium Tosylate (1): Ethyl *O*-*p*-tolylsulfonylacetohydroximate (3.5 g, 13.6 mmol) was slurried in 60% perchloric acid (40 mL) and stirred for 2 h. The mixture was then poured into ice water (500 mL) and once the ice had melted the solution was extracted with dichloromethane (5 × 50 mL). The dichloromethane solutions were combined and dried with sodium sulfate. This was then added to a solution of 1,5-diaminotetrazole (1.0 g, 9.99 mmol) in acetonitrile (100 mL), and the mixture was stirred for 3 d. The solution was then evaporated to yield the crude triaminotetrazolium tosylate (2.74 g, 95%). IR: $\tilde{\nu} = 3348$ (w), 3278 (m), 3186 (m), 3047 (m), 2861 (w), 1722 (m), 1652 (w), 1625 (w), 1602 (w), 1496 (w), 1403 (w), 1340 (w), 1177 (s), 1123 (s), 1136 (m), 1010 (m), 898 (m), 821 (m), 793 (m), 712 (w), 682 (m) cm⁻¹. Raman (1064 nm) = 3277 (4), 3190 (7), 3066 (49), 3032 (4), 2986 (5), 2924 (15), 2870 (4), 2739 (4), 2698 (4), 2575 (5), 1734 (4), 1599 (34), 1575 (4), 1524 (5), 1495 (3), 1456 (1), 1446 (3), 1391 (20), 1309 (4), 1212 (12), 1192 (20), 1128 (84), 1042 (39), 1015 (16), 902 (4), 802 (98), 687 (9), 638 (38), 616 (11), 555 (9), 492 (6), 400 (14), 367 (3), 348 (7), 314 (3), 296 (35), 230 (17) cm⁻¹. ¹H NMR (400 MHz, [D₆]DMSO): $\delta = 8.95$ (s, 2 H, C-NH₂), 7.47 (d, ³J_{H,H} = 8 Hz, 2 H, Ar C-H OTs-), 7.11 (d, ³J_{H,H} = 8 Hz, 2 H, Ar C-H OTs-), 6.94 (s, 4 H, N-NH₂), 2.28 (s, 3 H, CH₃) ppm. ¹³C NMR (68 MHz, [D₆]DMSO): $\delta = 147.1$ (s, 1 C, CN₇H₆), 146.1, 138.3, 128.6, 126.0, 21.3 (tosylate carbon atoms) ppm. MS (FAB+): *m/z* = 116.1 [CN₇H₆]. MS (FAB-): *m/z* = 170.0 [C₇H₇SO₃]. BAM impact: 10 J. BAM friction: 240 N.

1,4,5-Triaminotetrazolium Bromide (2): To a solution of triaminotetrazolium tosylate (0.25 g, 0.87 mmol) dissolved in a minimal amount of ethanol was added 47% hydrobromic acid (0.21 g). The mixture was stirred for 5 min and then diethyl ether (50 mL) was added, which resulted in the precipitation of triaminotetrazolium

bromide(0.15 g, 88%). DSC: 102 °C (dec.). IR: $\tilde{\nu}$ = 3350 (w), 3210 (m), 3067 (m), 1715 (s), 1685 (m), 1654 (w), 1600 (m), 1576 (w), 1560 (m), 1541 (w), 1394 (w), 1214 (m), 1192 (m), 1134 (w), 1091 (m), 1015 (m), 927 (w), 867 (s), 789 (w), 769 (w), 700 (w), 671 (w) cm^{-1} . Raman (1064 nm) = 3250 (11), 3218 (1), 3202 (1), 3180 (1), 3147 (1), 3117 (1), 1731 (2), 1599 (9), 1521 (2), 1412 (2), 1384 (25), 1319 (1), 1223 (3), 1136 (4), 1093 (12), 1010 (5), 790 (100), 636 (91), 617 (20), 545 (3), 474 (3), 351 (2), 303 (22) cm^{-1} . ^1H NMR (400 MHz, $[\text{D}_6]\text{DMSO}$): δ = 8.96 (s, 2 H, C-NH₂), 6.99 (s, 4 H, N-NH₂) ppm. ^{13}C NMR (68 MHz, $[\text{D}_6]\text{DMSO}$): δ = 147.2 (s, 1 C, CN₇H₆) ppm. MS (FAB+): m/z = 116.1 [CN₇H₆]. MS (FAB-): m/z = 78.9 [Br]. CN₇H₆Br (196.01): calcd: C 6.13, H 3.09, N 50.02; found too sensitive for measurement. BAM impact: <1 J. BAM friction: <5 N. ESD: 0.015 J.

1,4,5-Triaminotetrazolium Nitrate (3): To a solution of triaminotetrazolium bromide (0.300 g, 1.53 mmol) dissolved in distilled water (10 mL) was added a solution of silver nitrate (0.260 g, 1.53 mmol) in distilled water (10 mL). The solution was stirred in the dark at 100 °C for 3 h. After filtration of silver bromide and evaporation of the aqueous filtrate, triaminotetrazolium nitrate (0.250 g, 92%) was obtained. DSC: 78 °C (dec.). IR: $\tilde{\nu}$ = 3325 (m), 3200 (m), 3088 (m), 1726 (m), 1645 (m), 1621 (m), 1374 (s), 1311 (s), 1220 (m), 1125 (w), 1086 (m) 1048 (w), 1033 (w), 1009 (w), 949 (w), 863 (w), 825 (m), 791 (w), 719 (w), 683 (w) cm^{-1} . Raman (1064 nm) = 3325 (1), 3214 (10), 1734 (2), 1620 (6), 1583 (2), 1521 (2), 1413 (1), 1384 (31), 1332 (1), 1231 (1), 1128 (3), 1088 (11), 1050 (100), 1009 (2), 792 (84), 722 (5), 617 (20), 543 (1), 323 (11), 291 (2) cm^{-1} . ^1H NMR (400 MHz, $[\text{D}_6]\text{DMSO}$): δ = 8.97 (s, 2 H, C-NH₂), 7.00 (s, 4 H, N-NH₂) ppm. ^{13}C NMR (68 MHz, $[\text{D}_6]\text{DMSO}$): δ = 147.2 (s, 1C, CN₇H₆) MS (FAB+): m/z = 116.1 [CN₇H₆]. MS (FAB-): m/z = 62.0 [NO₃]. CN₇H₆NO₃ (178.11): calcd: C 6.74, H 3.40, N 62.91; found too sensitive for measurement. BAM impact: 2 J. BAM friction: 5 N. ESD: 0.050 J.

1,4,5-Triaminotetrazolium Nitrotetrazolate 2-Oxide (4): To a solution of triaminotetrazolium bromide (0.200 g, 1.02 mmol) dissolved in distilled water (10 mL) was added silver nitrotetrazolate 2-oxide (0.243 g, 1.02 mmol). The solution was stirred in the dark at 100 °C for 3 h. After filtration of silver bromide and evaporation of the aqueous filtrate, triaminotetrazolium nitrotetrazolate 2-oxide (0.668 g, 67%) was obtained. DSC: 84 °C (dec.). IR: $\tilde{\nu}$ = 3384 (m), 3338 (m), 3188 (m), 2951 (m), 1717 (m), 1636 (w), 1535 (s), 1466 (m), 1457 (m), 1419 (s), 1391 (s), 1311 (s), 1234 (m), 1185 (w), 1129 (w), 1114 (w), 1085 (w), 1051 (w), 1001 (w), 917 (w), 846 (w), 785 (s), 759 (w), 693 (w) cm^{-1} . Raman (1064 nm): = 3382 (1), 3313 (1), 3251 (5), 1831 (1), 1599 (1), 1544 (5), 1522 (2), 1430 (100), 1407 (37), 1317 (19), 1237 (3), 1087 (77), 1059 (21), 1004 (94), 851 (1), 797 (11), 762 (2), 617 (6), 491 (4), 429 (2), 399 (1), 340 (8), 239 (7) cm^{-1} . MS (FAB+): m/z = 116.1 [CN₇H₆]. MS (FAB-): m/z = 62.0 [NO₃]. CN₇H₆CN₅O₃ (246.15): calcd: C 9.76, H 2.46, N 68.28; found too sensitive for measurement. BAM impact: 1 J; BAM friction: 7 N; ESD: 0.100 J.

Acknowledgments

Financial support of this work by the Ludwig-Maximilian University of Munich (LMU), the U.S. Army Research Laboratory (ARL), the Armament Research, Development and Engineering Center (ARDEC), the Strategic Environmental Research and Development Program (SERDP), and the Office of Naval Research (ONR Global, title: "Synthesis and Characterization of New High Energy Dense Oxidizers (HEDO) - NICOP Effort") under contract nos. W911NF-09-2-0018 (ARL), W911NF-09-1-0120

(ARDEC), W011NF-09-1-0056 (ARDEC), and 10 WPSEED01-002/WP1765 (SERDP) is gratefully acknowledged. The authors acknowledge collaborations with Dr. Mila Krupka (OZM Research, Czech Republic) in the development of new testing and evaluation methods for energetic materials and with Dr. Muhamed Sucesca (Brodarski Institute, Croatia) in the development of new computational codes to predict the detonation and propulsion parameters of novel explosives. We are indebted to and thank Drs. Betsy M. Rice and Brad Forch (ARL, Aberdeen, Proving Ground, MD) and Mr. Gary Chen (ARDEC, Picatinny Arsenal, NJ) for many helpful and inspired discussions and support of our work. The authors want to thank St. Huber for measuring the sensitivities.

- [1] K. O. Christie, *Propellants Explos. Pyrotech.* **2007**, *32*, 194–204.
- [2] Y.-H. Joo, J. M. Shreeve, *Angew. Chem.* **2009**, *121*, 572–575; *Angew. Chem. Int. Ed.* **2009**, *48*, 564–567.
- [3] D. E. Chavez, D. A. Parrish, *Propellants Explos. Pyrotech.* **2012**, DOI: 10.1002/prop.201100112.
- [4] O. S. Bushuyev, P. Brown, A. Maiti, R. H. Geen, G. R. Peterson, B. L. Hope-Weeks, L. J. Hope-Weeks, *J. Am. Chem. Soc.* **2012**, *134*, 1422–1425.
- [5] M. Göbel, K. Karaghiosoff, T. M. Klapötke, D. G. Piercy, J. Stierstorfer, *J. Am. Chem. Soc.* **2010**, *132*, 17216–17226.
- [6] T. M. Klapötke, D. G. Piercy, J. Stierstorfer, *Chem. Eur. J.* **2011**, *17*, 13068–13077.
- [7] Y.-C. Li, C. Qi, S.-H. Li, H.-J. Zhang, C.-H. Sun, Y.-Z. Yu, S.-P. Pang, *J. Am. Chem. Soc.* **2010**, *132*, 12172–12173.
- [8] T. M. Klapötke, D. G. Piercy, *Inorg. Chem.* **2011**, *50*, 2732–2734.
- [9] P. Carlqvist, H. Östmark, T. Brinck, *J. Phys. Chem. A* **2004**, *108*, 7463–7467.
- [10] T. Schroer, R. Haiges, S. Schneider, K. O. Christie, *Chem. Commun.* **2005**, 1607–1609.
- [11] J. Fronabarger, M. D. Williams, W. B. Sanborn, J. G. Bragg, D. A. Parrish, M. Bichay, *Propellants Explos. Pyrotech.* **2011**, *36*, 541–550.
- [12] N. Fischer, T. M. Klapötke, D. G. Piercy, J. Stierstorfer, *Z. Anorg. Allg. Chem.* **2012**, *638*, 302–310.
- [13] T. M. Klapötke, C. M. Sabate, J. Stierstorfer, *New J. Chem.* **2009**, *33*, 136–147.
- [14] N. Fischer, K. Karaghiosoff, T. M. Klapötke, J. Stierstorfer, *Z. Anorg. Allg. Chem.* **2010**, *636*, 735–749.
- [15] R. Boese, T. M. Klapötke, P. Mayer, V. Verma, *Propellants Explos. Pyrotech.* **2006**, *31*, 263–268.
- [16] T. M. Klapötke, D. G. Piercy, J. Stierstorfer, *Dalton Trans.* **2012**, *41*, 9451–9459.
- [17] M. H. V. Huynh, M. A. Hiskey, D. E. Chavez, R. D. Gilardi, *J. Am. Chem. Soc.* **2005**, *127*, 12537–12543.
- [18] T. M. Klapötke, J. Stierstorfer, *J. Am. Chem. Soc.* **2009**, *131*, 1122–1134.
- [19] M. J. Frisch, G. W. Trucks, H. B. Schlegel, G. E. Scuseria, M. A. Robb, J. R. Cheeseman, G. Scalmani, V. Barone, B. Mennucci, G. A. Petersson, H. Nakatsuji, M. Caricato, X. Li, H. P. Hratchian, A. F. Izmaylov, J. Bloino, G. Zheng, J. L. Sonnenberg, M. Hada, M. Ehara, K. Toyota, R. Fukuda, J. Hasegawa, M. Ishida, T. Nakajima, Y. Honda, O. Kitao, H. Nakai, T. Vreven, J. A. Montgomery Jr., J. E. Peralta, F. Ogliaro, M. Bearpark, J. J. Heyd, E. Brothers, K. N. Kudin, V. N. Staroverov, R. Kobayashi, J. Normand, K. Raghavachari, A. Rendell, J. C. Burant, S. S. Iyengar, J. Tomasi, M. Cossi, N. Rega, J. M. Millam, M. Klene, J. E. Knox, J. B. Cross, V. Bakken, C. Adamo, J. Jaramillo, R. Gomperts, R. E. Stratmann, O. Yazyev, A. J. Austin, R. Cammi, C. Pomelli, J. W. Ochterski, R. L. Martin, K. Morokuma, V. G. Zakrzewski, G. A. Voth, P. Salvador, J. J. Dannenberg, S. Dapprich, A. D. Daniels, Ö. Farkas, J. B. Foresman, J. V. Ortiz, J. Cioslowski, D. J. Fox, *Gaussian 09*, Revision A.1, Gaussian, Inc., Wallingford, CT, **2009**.
- [20] A. D. Becke, *J. Chem. Phys.* **1993**, *98*, 5648–5652.

- [21] C. Lee, W. Yang, R. G. Parr, *Phys. Rev. B* **1988**, *37*, 785–789.
- [22] D. E. Woon, T. H. Dunning Jr, R. J. Harrison, *J. Chem. Phys.* **1993**, *98*, 1358–1371.
- [23] R. A. Kendall, T. H. Dunning Jr, R. J. Harrison, *J. Chem. Phys.* **1992**, *96*, 6796–6806.
- [24] T. H. Dunning Jr, *J. Chem. Phys.* **1989**, *90*, 1007–1023.
- [25] K. A. Peterson, D. E. Woon, T. H. Dunning Jr, *J. Chem. Phys.* **1994**, *100*, 7410–7415.
- [26] A. S. Lyakhov, P. N. Gaponik, S. V. Voitekhovich, *Acta Crystallogr., Sect. C* **2001**, *57*, 185–186.
- [27] Cell parameters for **2**: $P2_1/n$, $a = 8.178(2) \text{ \AA}$, $b = 5.4205(9) \text{ \AA}$, $c = 15.169(2) \text{ \AA}$, $\beta = 96.225(19)^\circ$, $V = 668.5(2) \text{ \AA}^3$, $Z = 2$, $\rho = 1.888 \text{ g cm}^{-3}$.
- [28] M. von Denffer, T. M. Klapötke, G. Kramer, G. Spieß, J. M. Welch, *Propellants Explos. Pyrotech.* **2005**, *30*, 191–195.
- [29] J. C. Galvez-Ruiz, G. Holl, K. Karaghiosoff, T. M. Klapötke, K. Löhnwitz, P. Mayer, H. Nöth, K. Polborn, C. J. Rohbogner, M. Suter, J. J. Weigand, *Inorg. Chem.* **2005**, *44*, 4237–4253.
- [30] a) H. D. B. Jenkins, H. K. Roobottom, J. Passmore, L. Glasser, *Inorg. Chem.* **1999**, *38*, 3609–3620; b) H. D. B. Jenkins, D. Tudela, L. Glasser, *Inorg. Chem.* **2002**, *41*, 2364–2367; c) H. D. B. Jenkins, L. Glasser, *Inorg. Chem.* **2002**, *41*, 4378–88.
- [31] D. A. Johnson in *Some Thermodynamic Aspects of Inorganic Chemistry*, 2nd ed., Cambridge University Press, Ambridge, **1982**.
- [32] a) J. A. Davidson, F. C. Fehsenfeld, C. J. Howard, *Int. J. Chem. Kinet.* **1977**, *9*, 17; b) D. A. Dixon, D. Feller, C.-G. Zhan, J. S. Francisco, *Int. J. Mass Spectrom.* **2003**, *227*, 421–438.
- [33] a) M. Sućeska, *EXPLO5.05 Program*, Zagreb, Croatia, **2011**; b) M. Sućeska, *Propellants Explos. Pyrotech.* **1991**, *16*, 197–202.
- [34] R. Mayer, J. Köhler, A. Homburg, *Explosives*, 5th ed., Wiley-VCH, Weinheim, **2002**.
- [35] P. Hakey, W. Ouellette, J. Zubietta, T. Korter, *Acta Crystallogr., Sect. E* **2008**, *64*, o1428.
- [36] Impact: Insensitive >40 J, less sensitive ≥ 35 J, sensitive ≥ 4 J, very sensitive ≤ 3 J; friction: insensitive >360 N, less sensitive = 360 N, sensitive <360 and >80 N, very sensitive ≤ 80 N, extremely sensitive ≤ 10 N. According to the UN Recommendations on the Transport of Dangerous Goods.
- [37] T. M. Klapötke, unpublished results.

Received: August 22, 2012

Published Online: October 5, 2012

1,1'-Azobis(tetrazole): A Highly Energetic Nitrogen-Rich Compound with a N₁₀ Chain

Thomas M. Klapötke* and Davin G. Piercey

Department of Chemistry, Energetic Materials Research, Ludwig-Maximilians Universität München, Butenandtstrasse 5-13, D-81377 Munich, Germany

S Supporting Information

ABSTRACT: The reaction of 1-aminotetrazole with acidic sodium dichloroisocyanurate allowed isolation of 1,1'-azobis(tetrazole). The rare chain of 10 nitrogen atoms in this compound was confirmed by X-ray crystallography, and the physical and explosive properties of the azo compound were characterized. The title compound possesses both exceedingly high explosive performance and sensitivity.

Energetic materials research encompassing all propellants, explosives, and pyrotechnics has long attracted intense work in the chemical sciences, with participating scientists including Liebig, Berzelius, and Gay-Lussac.^{1,2} This tradition has led to many chemical advances. For example, work with silver fulminate, which has the same composition as silver cyanate, led to the concept of isomerism.³ Studies of unstable compounds on the borderline of existence and nonexistence allow elucidation of the fundamental properties affecting chemical stability and bonding.^{4–6}

The unique stability of the dinitrogen molecule arising from its strong, short triple bond means that decomposition of compounds containing nitrogen with the formation of nitrogen gas is highly favored energetically.⁷ This is especially true for singly and doubly bonded nitrogen systems where compounds with N–N bonds have even higher positive heats of formation than their counterparts with noncontiguous nitrogen atoms.⁸ For example, comparison of the azotriazoles 1,1'-azobis(1,2,3-triazole) (**1**) and 1,1'-azobis(1,3,4-triazole) (**2**) (Figure 1) reveals that the former possesses a higher, more positive heat of formation than the latter, resulting from the increased number of N–N bonds.⁸

Unfortunately, despite their potential significance^{9,10} to both theory and technology, compounds containing extended chains of nitrogen atoms are not well-known; this arises from both the endothermicities and associated stability problems and the relative scarcity of N–N bond-forming reactions known in the literature (especially when compared with carbon!). For example, the recent publication of **1**⁸ marked the discovery of a surprisingly stable compound containing a chain of eight nitrogen atoms, one of the few^{8,11–13} compounds with such a long nitrogen chain, whereas comparable and longer carbon compounds are plentiful, well-known, and stable.

Azo coupling reactions have been used to prepare useful azo-based energetic materials such as azotetrazoles,¹⁴ triazoles,¹⁵ and furazans¹⁶ and have even allowed the preparation of eight-linked nitrogen compound **1**.⁸ The azo homocoupling of 1-aminotetrazole

(**3**) gave the first fully characterized compound containing 10 linked nitrogen atoms. A search of the literature indicated only one mention¹⁷ of compounds with 10 connected nitrogen atoms, formed from the reaction of 5-Ar-1-dichloroaminotetrazole (Ar = Ph, 1-ClPh, 4-MePh) with potassium iodide. However, only the melting points and a single elemental analysis were reported, and comments on the highly explosive nature of the reaction products were provided, albeit with no proof of the structure.¹⁷

From the treatment of **3** in acetonitrile at 0 °C with an aqueous acidic solution of sodium dichloroisocyanurate, we obtained a precipitate of colorless 1,1'-azobis(tetrazole) (**4**; Figure 2) after dilution with a dilute bicarbonate solution and filtration (Scheme 1). Sodium dichloroisocyanurate was chosen as the azo coupling reagent because it was used successfully for **1**,⁸ and attempted coupling using *t*-BuOCl led only to decomposition. The precipitated N₁₀ compound **4** was not dried in the funnel because attempts to manipulate the dry solid inevitably led to extremely loud explosions and the destruction of labware. Instead, the wet solid was transferred to the desired analytical instrument, the water was allowed to evaporate, and the measurement taken (e.g., loading a Raman tube). Attempts to store the sensitive product in solution led to the slow release of nitrogen gas and decomposition.

We obtained colorless crystals of **4** sufficient for X-ray crystallographic analysis by the overnight evaporation of an acetone solution of **4**. The N₁₀ compound crystallizes in the orthorhombic space group *Pbca* with four formula units in the unit cell and a density of 1.774 g cm⁻³. The structure of **4** about the azo double bond is *trans*, and the azo double bond is 1.178 Å long, shorter than that in the N₈ compound **1** at 1.250 Å.⁸ The tetrazole rings have bond lengths and angles comparable to those of other 1-substituted tetrazoles.¹⁸

The N₁₀ compound **4** has a calculated solid-state heat of formation of +1030.0 kJ mol⁻¹, 68 kJ mol⁻¹ higher than that of the N₈ compound **1**, as a result of the higher nitrogen content, and only 71 kJ mol⁻¹ lower than that of diazidotetrazine,⁵ which has been claimed (in 2005, we were unable to find a higher published material) to have the highest heat of formation for a binary CN compound. The performance properties of **4** were calculated using the experimental density and the EXPLOS.04 (5.03) code. **4** has a very high explosive performance of 9185 (9371) m s⁻¹, which is slightly higher than that of HMX, one of the most powerful explosives in common military use with a detonation velocity of 9058 (9215) m s⁻¹. It is interesting to note

Received: January 12, 2011

Published: March 08, 2011

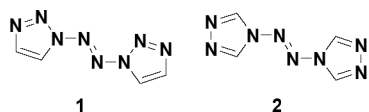
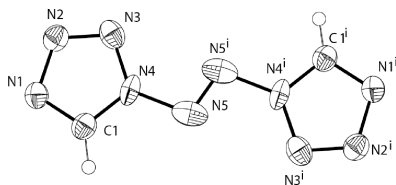
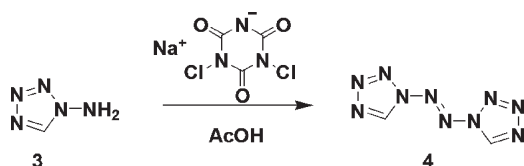


Figure 1. Azotriazoles.

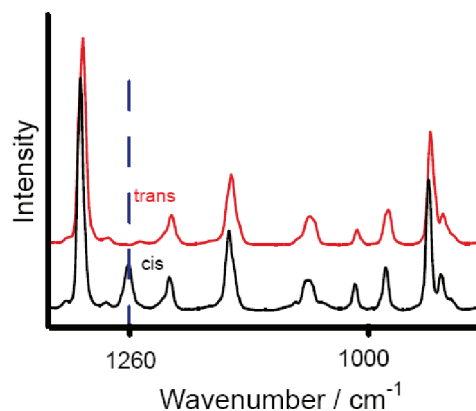
Figure 2. Molecular structure of **4** as it appears in the crystal structure. Non-hydrogen atomic displacement ellipsoids are 50% probability.Scheme 1. Synthesis of **4**

that the previously reported N_8 compound **1**⁸ has a detonation velocity of 8029 (8323) m s^{-1} , making for a significant increase of almost 1000 m s^{-1} , as a result of the addition of two nitrogen atoms in place of CH groups (for complete calculation details of **4**, see the Supporting Information).

The most striking difference between the reported N_8 compound (**1**) and our N_{10} compound (**4**) is the sensitivity; **1** is reported to be insensitive enough for handling, whereas with our N_{10} compound **4**, we experienced several inadvertent explosions during handling such as allowing the dry powder to slide down the inside of a Raman tube or slowing down the rotation rate of a rotary evaporator as **4** crystallized. The material demands the utmost care in handling, and the sensitivities were well below the measurable limit ($\ll 5$ N friction and $\ll 1$ J impact) of our safety characterization equipment; the material violently explodes when impacted with a 150 g hammer at 2 cm (~ 0.03 J). It is among the most sensitive materials that we have handled. The decomposition temperature of **4** is far lower than that of compound **1**,⁸ with an exothermic peak measured by differential scanning calorimetry of 80 °C (193.8 °C for **1**).

The ^1H and ^{13}C resonances for **4** occur at 9.33 and 143.2 ppm respectively in $\text{DMSO-}d_6$. In the ^{14}N spectra broad tetrazole resonances are visible at -5 and -99 ppm, and less broad resonances at -135 , -140 , -146 , and -154 ppm, however due to the instability of **4** in solution, assignment of these peaks is unclear.

The reported⁸ photochromicity of **1** provoked us to study the behavior of **4** under the influence of UV light. Exposure of a Raman tube of the sample to UV light from a commercial thin-layer chromatography plate visualization aid for 3 days led to the sample yellowing slightly and a new $\text{N}=\text{N}$ stretching peak arising at 1260 cm^{-1} (Figure 3), similar to 1259 cm^{-1} as seen for *cis*-**1**. Quantitative conversion to the *cis* compound was not possible even with high-intensity UV light because only the surface of the material reacts. While such photochromic materials do have

Figure 3. Raman spectrum: $\text{N}=\text{N}$ stretch at 1260 cm^{-1} for *cis*-**4** arising from UV illumination.

many applications, the high sensitivity of **4** would preclude application.^{19,20}

In conclusion, we have demonstrated the ability of 1-amino-5H-tetrazole to azocouple, forming 1,1'-azobis(tetrazole), the first well-characterized compound with a chain of 10 nitrogen atoms, including crystallographic proof. This unique material possesses explosive performances comparable to those of the most powerful energetic materials in common use, with the source of this power being the very high heat of formation of this material. Unfortunately, this material is both thermally and physically unstable with a decomposition temperature of 80 °C and undergoes violent explosion when subjected to mild stimuli. Proof of the existence of this N_{10} compound opens the possibility for the discovery of even longer chain nitrogen compounds, although the trend in increasing sensitivity from N_8 to N_{10} compounds may present challenges for isolation.

■ ASSOCIATED CONTENT

Supporting Information. Experimental details, characterization data, a CIF file, and computational details. This material is available free of charge via the Internet at <http://pubs.acs.org>.

■ AUTHOR INFORMATION

Corresponding Author

*E-mail: tmk@cup.uni-muenchen.de.

■ ACKNOWLEDGMENT

Financial support of this work by the Ludwig-Maximilian University of Munich, the U.S. Army Research Laboratory (ARL), the Armament Research, Development and Engineering Center (ARDEC), the Strategic Environmental Research and Development Program (SERDP), and the Office of Naval Research (ONR Global, title "Synthesis and Characterization of New High Energy Dense Oxidizers (HEDO)—NICOP Effort") under Contracts W911NF-09-2-0018 (ARL), W911NF-09-1-0120 and W011NF-09-1-0056 (ARDEC), and 10 WPSEED01-002/WP-1765 (SERDP) is gratefully acknowledged. The authors acknowledge collaborations with Dr. Mila Krupka (OZM Research, Czech Republic) in the development of new testing and evaluation methods for energetic materials and with Dr. Muhamed Suceca (Brodarski Institute, Croatia) in the development of new

computational codes to predict the detonation and propulsion parameters of novel explosives. We are indebted to and thank Drs. Betsy M. Rice and Brad Forch (ARL, Aberdeen, Proving Ground, MD) and Gary Chen (ARDEC, Picatinny Arsenal, NJ) for many helpful and inspired discussions and support of our work. Dr. Burkhard Krumm, Dr. Jörg Stierstorfer, and Fabian Wehnekamp are thanked for assistance with NMR, crystallography and computational work.

REFERENCES

- (1) Gay-Lussac, J. L.; Leibig, J. *Kastners Arch.* **1824**, *II*, 58–91.
- (2) Berzelius, J. *Ann. Chem. Pharm.* **1844**, *L*, 426–429.
- (3) Gay-Lussac, J. L. *Ann. Chim. Phys.* **1824**, *27* (2), 199.
- (4) Klapötke, T. M.; Stierstorfer, J. *J. Am. Chem. Soc.* **2009**, *131*, 1122–1134.
- (5) Huynh, M. H. V.; Hiskey, M. A.; Chavez, D. E.; Gilardi, R. D. *J. Am. Chem. Soc.* **2005**, *127*, 12537–12543.
- (6) Carlqvist, P.; Ostmark, H.; Brinck, T. *J. Phys. Chem. A* **2004**, *108*, 7463–7467.
- (7) Klapötke, T. M. *High Energy Density Materials*; Springer: Berlin, 2007.
- (8) Li, Y.-C.; Qi, C.; Li, S.-H.; Zhang, H.-J.; Sun, C.-H.; Yu, Y.-Z.; Pang, S.-P. *J. Am. Chem. Soc.* **2010**, *132* (35), 12172–12173.
- (9) Benson, F. R. *The High Nitrogen Compounds*; Wiley: New York, 1984.
- (10) Huisgen, R.; Ugi, I. *Angew. Chem.* **1956**, *68*, 705–706.
- (11) Glover, E. E.; Rowbottom, K. T. *J. Chem. Soc., Perkin Trans. 1* **1974**, 1792.
- (12) Behringer, H.; Fischer, H. *J. Chem. Ber.* **1962**, *95*, 2546.
- (13) Minato, H.; Oku, M.; Chan, S. H. *Bull. Chem. Soc. Jpn.* **1966**, *39*, 1049.
- (14) Klapötke, T. M.; Sabaté, C. M. *Chem. Mater.* **2008**, *20*, 1750–1763.
- (15) Naud, D. L.; Hiskey, M. A.; Harry, H. H. *J. Energ. Mater.* **2003**, *21*, 57–62.
- (16) Chavez, D.; Hill, L.; Hiskey, M.; Kinkead, S. *J. Energ. Mater.* **2003**, *18*, 219–236.
- (17) Stolle, R.; Netz, A.; Kramer, O.; Rothschild, S.; Erbe, E.; Schick, O. *J. Prakt. Chem.* **1933**, *138*, 1–17.
- (18) Klapötke, T. M.; Sabaté, C. M.; Stierstorfer, J. *New J. Chem.* **2009**, *33*, 136–147.
- (19) Cheben, P.; del Monte, F.; Worsfold, D. J.; Carlsson, D. J.; Grover, C. P.; Mackenzie, J. D. *Nature* **2000**, *408*, 64–67.
- (20) Koshima, H.; Ojima, N.; Uchimoto, H. *J. Am. Chem. Soc.* **2009**, *131*, 6890–6891.

Supporting Information for:

1,1'-Azobistetrazole: A Highly Energetic Nitrogen Rich Compound With a N₁₀ Chain.

Thomas M. Klapötke and Davin G. Piercey.

Department of Chemistry and Biochemistry, Energetic Materials Research, Ludwig-Maximilian University of Munich, Butenandtstr. 5-13, D-81377 Munich, Germany.

tmk@cup.uni-muenchen.de

Table of Contents Image: From left to right; Buchner funnel after explosion of 100 mg of **4**, glass vial after explosion of ~5-10 mg of **4**, and 50 mL flask after explosion of ~70 mg of **4**.

Experimental:

All reagents and solvents were used as received (Sigma-Aldrich) if not stated otherwise. 1-aminotetrazole was prepared according to the literature procedure.¹ Melting and decomposition points were measured with a Linseis PT10 DSC using heating rates of 5 °C min⁻¹. ¹H, and ¹³C NMR spectra were measured with a JEOL EX 400 instrument. All chemical shifts are quoted in ppm relative to TMS (¹H, ¹³C). Infrared spectra were measured with a Perkin-Elmer Spektrum One FT-IR instrument. Raman spectra were measured with a Perkin-Elmer Spektrum 2000R NIR FT-Raman instrument equipped with a Nd-YAG laser (1064 nm). Sensitivity data were determined using a BAM drophammer and a BAM friction tester. The electrostatic sensitivity tests were carried out using an Electric Spark Tester ESD 2010 EN (OZM Research) operating with the “Winspark 1.15” software package.

CAUTION! 1,1'-azobistetrazole is a highly energetic compound with extreme sensitivity to various stimuli. We encountered several unintended explosions while working with this material, so proper

protective measures (face shield, ear protection, body armour, Kevlar® gloves and earthened equipment) must be used at all times.

Preparation of 1,1'-azobistetrazole

0.17 g (2.0 mmol) of 1-aminotetrazole¹ was dissolved in 4 mL acetonitrile and the solution cooled to 0 °C. To this was added an oxidizing suspension formed by mixing 0.5 mL glacial acetic acid with 8 mL of water containing 0.45 g (2 mmol) of sodium dichloroisocyanurate. The solution instantly yellows and was stirred at 0 °C for 30 minutes followed by pouring this solution into 100 mL of a 2 % sodium bicarbonate solution at 5 °C. The solution was stirred for 5 minutes and was filtered yielding a white precipitate. Approximate yield is 0.12 g or 72%. (Exact yield not determinable due to sensitivity). DSC (5 °C min⁻¹): 80 °C (dec); IR (cm⁻¹) $\tilde{\nu}$ = 3134 (m), 1757 (w), 1465 (m), 1424 (m), 1405 (w), 1364 (w), 1328 (w), 1318 (w), 1305 (w), 1211 (w), 1185 (w), 1173 (m), 1155 (s), 1071 (m), 1054 (s), 982 (m), 951 (s), 910 (s), 878 (m), 776 (w), 720 (w), 702 (s), 640 (s); Raman (1064 nm): $\tilde{\nu}$ = 3135 (12), 1899 (1), 1838 (1), 1688 (1), 1530 (100), 1465 (66), 1405 (11), 1372 (25), 1312 (77), 1216 (11), 1152 (26), 1066 (11), 1015 (6), 982 (13), 936 (43), 922 (4), 872 (4), 706 (1), 627 (1), 375 (3), 291 (8), 245 (7); ¹H NMR (DMSO *d*₆) δ (ppm) = 9.33 (s, 2H, C-H); ¹³C NMR (DMSO *d*₆) δ (ppm) = 143.2 (s, 2C, CN₄). m/z: (DCI+) 167.1 (M+H); EA (C₂H₂N₁₀, 166.10 g mol⁻¹) calcd: C 14.46, N 84.32, H 1.21 %, found: too sensitive for measurement; BAM impact: <<1 J; BAM friction: <<5 N; ESD: 15 mJ.

NMR Note: The spectrum should be collected as soon as possible after dissolving in DMSO, if the solution is allowed to stand, a peak at 86.0 ppm in the carbon spectrum appears, resulting from decomposition products.

X-ray Structure:

Single crystals of **4** suitable for x-ray crystallographic analysis was obtained by evaporation of an acetone solution of **4** overnight. The molecular structure was determined using an Oxford Xcaliber3 diffractometer with a Spellman generator (voltage 50kV, 40mA current) and a KappaCCD detector. The data collection was performed using the CrysAlis CCD software.² Data reduction was performed with the CrysAlis RED software,³ the structure was solved using the SIR-92 program,⁴ refined with SHELXL-97⁵ and finally checked with PLATON software.⁶ The hydrogen atoms were located and refined. Relevant data are given in Table S1.

Table S1: Crystallographic details of 4

compound	1,1'-azobistetrazole
formula	C ₂ H ₂ N ₁₀
formula weight [g mol ⁻¹]	166.10
temperature [K]	100
crystal system	orthorhombic
space group	<i>Pbca</i>
<i>a</i> [Å]	8.177(5)
<i>b</i> [Å]	6.835(5)
<i>c</i> [Å]	11.130(5)
α [°]	90
β [°]	90
γ [°]	90
volume [Å ³]	622.1(7)
formula Z	4
space group Z	8
density calc. [g cm ⁻³]	1.774
R ₁ / wR ₂ [all data]	0.0701 / 0.1362
R ₁ / wR ₂ [I > 2σ(I)]	0.0470 / 0.1259
<i>S</i>	1.072

Sensitivities:

For initial safety testing, impact, friction and electrostatic discharge sensitivities were determined.

Impact sensitivity was carried out according to STANAG 4489⁷ and modified according to instruction⁸ on a BAM drophammer.^{9,10} Friction sensitivity was carried out in accordance with STANAG 4487¹¹ and modified according to instruction.¹² Sensitivity towards electrostatic discharge (ESD) was determined^{13,14} on a small scale electric spark tester ESD 2010EN (OZM Research) operating with the “Winspark 1.15 software package.”¹⁵ **4** has in impact sensitivity of $\ll 1$ J, a friction sensitivity of $\ll 5$ N and electrostatic discharge sensitivity (ESD) of 15 mJ. According to the UN Recommendations on the Transport of Dangerous Goods, **4** is classified as very sensitive.¹⁶ **4** is more sensitive than primary explosives in common use such as lead azide.

Theoretical Calculations

All calculations were carried out using the Gaussian G03W (revision B.03) program package.¹⁷ The enthalpies (H) and free energies (G) were calculated using the complete basis set (CBS) method of Petersson and coworkers in order to obtain very accurate energies. The CBS models use the known asymptotic convergence of pair natural orbital expressions to extrapolate from calculations using a finite

basis set to the estimated complete basis set limit. CBS-4 begins with a HF/3-21G(d) geometry optimization; the zero point energy is computed at the same level. It then uses a large basis set SCF calculation as a base energy, and a MP2/6-31+G calculation with a CBS extrapolation to correct the energy through second order. A MP4(SDQ)/6-31+(d,p) calculation is used to approximate higher order contributions. In this study we applied the modified CBS-4M method (**M** referring to the use of Minimal Population localization) which is a re-parametrized version of the original CBS-4 method and also includes some additional empirical corrections.¹⁸ The enthalpies of the gas-phase species **M** were computed according to the atomization energy method (eq. 1) (Tables S2-S4).¹⁹

$$\Delta_f H^\circ_{(g, M, 298)} = H_{(Molecule, 298)} - \sum H^\circ_{(Atoms, 298)} + \sum \Delta_f H^\circ_{(Atoms, 298)} \quad (1)$$

Table S2. CBS-4M results

	point group	el. state	$-H^{298}$ / a.u.	<i>NIMAG</i>
4	C_{2h}		-621.306973	0
H		$^2A_{1g}$	0.500991	0
C			37.786156	0
N		$^4A_{1g}$	54.522462	0
O			74.991202	0

Table S3. Literature values for atomic $\Delta H_f^\circ{}^{298}$ / kcal mol⁻¹

	NIST ²⁰
H	52.1
C	171.3
N	113.0
O	59.6

Table S4. Enthalpies of the gas-phase species M.

M	M	$\Delta_f H^\circ(\text{g}, \text{M}) / \text{kJ mol}^{-1}$
4	$\text{C}_2\text{H}_2\text{N}_{10}$	+1096.4

The solid state energy of formation (Table S5) of **4** was calculated by subtracting the gas-phase enthalpy with the heat of sublimation obtained by the Trouton rule ($\Delta H_{\text{sub}} = 188 \cdot T_m$ [$T_{\text{dec}} = 80 \text{ }^\circ\text{C}$]).²¹ The molar standard enthalpy of formation (ΔH_m) was used to calculate the molar solid state energy of formation (ΔU_m) according to equation (2) (Table S5).

$$\Delta U_m = \Delta H_m - \Delta n RT \quad (2) \quad (\Delta n \text{ being the change of moles of gaseous components})$$

Table S5. Solid state energies of formation ($\Delta_f U^\circ$)

	$\Delta_f H^\circ(\text{s}) /$ kJ mol ⁻¹	Δn	$\Delta_f U^\circ(\text{s}) /$ kJ mol ⁻¹	M / g mol ⁻¹	$\Delta_f U^\circ(\text{s}) /$ kJ kg ⁻¹
4	1030.0	-5	1044.9	166.10	6290.4

Detonation Parameters

The calculation of the detonation parameters was performed with the program package EXPLO5.04 (5.03)²². The program is based on the chemical equilibrium, steady-state model of detonation. It uses the Becker-Kistiakowsky-Wilson's equation of state (BKW EOS) for gaseous detonation products and

Cowan-Fickett's equation of state for solid carbon²³. The calculation of the equilibrium composition of the detonation products is done by applying modified White, Johnson and Dantzig's free energy minimization technique. The program is designed to enable the calculation of detonation parameters at the CJ point. The BKW equation in the following form was used with the BKWN set of parameters (α , β , κ , θ) as stated below the equations and X_i being the mol fraction of i -th gaseous product, k_i is the molar covolume of the i -th gaseous product:²³

$$pV / RT = 1 + xe^{\beta x} \quad x = (\kappa \sum X_i k_i) / [V (T + \theta)]^\alpha$$

$$\alpha = 0.5, \beta = 0.176, \kappa = 14.71, \theta = 6620. \text{ (EXPLO 5.03)}$$

$$\alpha = 0.5, \beta = 0.96, \kappa = 17.56, \theta = 4950. \text{ (EXPLO 5.04)}$$

The detonation parameters calculated with the EXPLO5.04 (5.03) program using the experimentally determined densities (X-ray) are summarized in Table S6 and compared to HMX.

Table S6: Energetic properties of **4**

	4	HMX
Formula	C ₂ H ₂ N ₁₀	(CH ₂ NNO ₂) ₄
FW (g mol ⁻¹)	166.10	296.16
IS^a (J)	<<1 J	7
FS^b (N)	<<5 N	112
ESD^c (J)	0.015 J	0.210
N^d (%)	84.32	37.84
\mathcal{L}^e (%)	-48.16	-21.61
T_{Dec}^f (°C)	80	275
ρ^g (g cm ⁻³)	1.774	1.905
$\Delta_f H_m^{oh}$ (kJ mol ⁻¹)	1030.0	74.8
$\Delta_f U^{oi}$ (kJ kg ⁻¹)	6290.4	353.0

*Calculated Values by EXPLO5**

$\Delta_{\text{Ex}}U^{\text{oj}}$ (kJ kg ⁻¹)	6427 (6472)	6063 (6159)
$T_{\text{det}}^{\text{k}}$ (K)	4649 (4904)	4117 (4337)
P_{CJ}^{l} (GPa)	36.1 (37.1)	39.2 (37.7)
$V_{\text{Det}}^{\text{m}}$ (m s ⁻¹)	9185 (9371)	9058 (9215)
V_{o}^{n} (L kg ⁻¹)	722 (734)	734 (770)

^a BAM Drophammer. ^b BAM Impact. ^c Electrical Spark Sensitivity. ^d Nitrogen Content. ^e Oxygen Balance. ^f Decomposition temperature from DSC (5 °C min⁻¹). ^g Density from x-ray diffraction. ^h Calculated molar enthalpy of formation. ⁱ Energy of formation. ^j Total energy of detonation. ^k Explosion temperature. ^l Detonation Pressure. ^m Detonation Velocity. ⁿ Volume of Detonation Products,* Explo5.04 (Explo5.03).

References:

1. Raap, R. *Can. J. Chem.* **1969**, 47, 3677-3681.
2. *CrysAlis CCD*, Oxford Diffraction Ltd., Version 1.171.27p5 beta (release 01-04-2005 CrysAlis171.NET)(compiled April 1 2005, 17 : 53 :34).
3. *CrysAlis RED*, Oxford Diffraction Ltd., Version 1.171.27p5 beta (release 01-04-2005 CrysAlis171.NET)(compiled April 1 2005, 17 : 53 :34).
4. Altomare, A.; Cascarano, G.; Giacovazzo, C.; Guagliardi, A. *J. Appl. Cryst.* **1993**, 26, 343.
5. Sheldrick, G. M. *Program for the Refinement of Crystal Structures*, SHELXS-97, University of Göttingen, Germany, **1997**.

6. Spek, A.L. *A Multipurpose Crystallographic Tool*, PLATON, Utrecht University, Utrecht, The Netherlands, **1999**.
7. NATO standardization agreement (STANAG) on explosives, *impact sensitivity tests*, no. 4489, Ed. 1, Brussels, Sept. 17, **1999**.
8. WIWEB-Standardarbeitsanweisung 4-5.1.02, Ermittlung der Explosionsgefährlichkeit, hier der Schlagempfindlichkeit mit dem Fallhammer, Erding, Nov. 8, 2002.
9. <http://www.bam.de>.
10. <http://www.reichel-partner.de>.
11. NATO standardization agreement (STANAG) on explosives, *friction sensitivity tests*, no. 4487, Ed. 1, Brussels, Aug. 22, **2002**.
12. WIWEB-Standardarbeitsanweisung 4-5.1.03, Ermittlung der Explosionsgefährlichkeit oder der Reibeempfindlichkeit mit dem Reibeapparat, Erding, Nov. 8, **2002**.
13. Zeman, S.; Pelikán, V.; Majzlík, J. *Cent. Eur. J. Energ. Mat.* **2006**, 3, 45–51.
14. Skinner, D.; Olson, D.; Block-Bolten, A. *Propellants, Explosives, Pyrotechnics*. **1998**, 23, 34–42.
15. <http://www.ozm.cz/testinginstruments/small-scale-electrostatic-discharge-tester.htm>.
16. Impact: Insensitive > 40 J, less sensitive ≥ 35 J, sensitive ≥ 4 J, very sensitive ≤ 3 J; Friction Insensitive > 360 N, less sensitive = 360 N, sensitive < 360 N a. > 80N, very sensitive ≤ 80 N, extremely sensitive ≤ 10 N. According to: UN Recommendations of the Transport of Dangerous Goods. Manual of Tests and Criteria (Fourth revised ed.), New York and Geneva, United Nations, **2002**, ST/SG/AC.10/11/Rev 4.
17. Frisch, M. J.; Trucks, G. W.; Schlegel, H. B.; Scuseria, G. E.; Robb, M. A.; Cheeseman, J. R.; Montgomery, J. A.; Vreven, J. T.; Kudin, K. N.; Burant, J. C.; Millam, J. M.; Iyengar, S. S.; Tomasi, J.; Barone, V.; Mennucci, B.; Cossi, M.; Scalmani, G.; Rega, N.; Petersson, G. A.; Nakatsuji, H.; Hada, M.; Ehara, M.; Toyota, K.; Fukuda, R.; Hasegawa, J.; Ishida, M.; Nakajima, T.; Honda, Y.; Kitao, O.; Nakai, H.; Klene, M.; Li, X.; Knox, J. E.; Hratchian, H. P.; Cross, J. B.; Adamo, C.; Jaramillo, J.; Gomperts, R.; Stratmann, R. E.; Yazyev, O.; Austin, A. J.; Cammi, R.; Pomelli, C.; Ochterski, J. W.; Ayala, P. Y.; Morokuma, K.; Voth, G. A.; Salvador, P.; Dannenberg, J. J.; Zakrzewski, V. G.; Dapprich, S.; Daniels, A. D.; Strain, M. C.; Farkas, O.; Malick, D. K.; Rabuck, A. D.; Raghavachari, K.; Foresman, J. B.; Ortiz, J. V.; Cui, Q.; Baboul, A. G.; Clifford, S.; Cioslowski, J.; Stefanov, B. B.; Liu, G.; Liashenko, A.; Piskorz, P.; Komaromi, I.; Martin, R. L.; Fox, D. J.; Keith, T.; Al-Laham, M. A.; Peng, C. Y.; Nanayakkara,

A.; Challacombe, M.; Gill, P. M. W.; Johnson, B.; Chen, W.; Wong, M. W.; Gonzalez, C.; Pople, J. A. Gaussian 03, Revision C.03, Gaussian Inc.: Pittsburgh PA, **2003**.

18. (a) Ochterski, J.W.; Petersson, G.A.; Montgomery, J. A. Jr., *J. Chem. Phys.* **1996**, *104*, 2598; (b) Montgomery, J. A. Jr., Frisch, M. J.; Ochterski, J. W.; Petersson, G. A. *J. Chem. Phys.* **2000**, *112*, 6532.
19. (a) Curtiss, L. A.; Raghavachari, K.; Redfern, P.C.; Pople, J.A. *J. Chem. Phys.* **1997**, *106*(3), 1063; (b) Byrd, E. F.C.; Rice, B. M. *J. Phys. Chem. A* **2006**, *110*(3), 1005–1013; (c) Rice, B. M.; Pai, S. V.; Hare, J. *Comb. Flame* **1999**, *118*(3), 445–458.
20. Linstrom, P. J.; Mallard, W. G.; Eds., NIST Chemistry WebBook, NIST Standard Reference Database Number 69, National Institute of Standards and Technology, Gaithersburg MD, 20899, <http://webbook.nist.gov>, (retrieved March 30, 2010).
21. (a) Westwell, M.S.; Searle, M.S.; Wales, D. J.; Williams, D. H. *J. Am. Chem. Soc.* **1995**, *117*, 5013–5015; (b) Trouton, F. *Philos. Mag.* **1884**, *18*, 54–57.
22. (a) Sućeska, M. EXPLO5.03 program, Zagreb, Croatia, **2009**. (b) Sućeska, M EXPLO5.04 program, Zagreb, Croatia, **2010**.
23. (a) Sućeska, M. *Materials Science Forum*, **2004**, 465–466, 325–330. (b) Sućeska, M. *Propellants, Explos., Pyrotech.* **1991**, *16*, 197–202. (c) Sućeska, M. *Propellants, Explos., Pyrotech.* **1999**, *24*, 280–285. (d) Hobbs, M. L.; Baer: M .R. *Proc. of the 10th Symp. (International) on Detonation*, ONR 33395-12, Boston, MA, July 12–16, 1993, p. 409.

1,3-Bis(nitroimido)-1,2,3-triazolate Anion, the *N*-Nitroimide Moiety, and the Strategy of Alternating Positive and Negative Charges in the Design of Energetic Materials

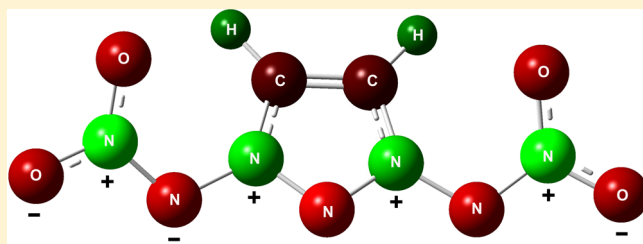
Thomas M. Klapötke,^{*,†,‡} Christian Petermayer,[†] Davin G. Piercey,[†] and Jörg Stierstorfer[†]

[†]Department of Chemistry, Energetic Materials Research, Ludwig-Maximilian University of Munich, Butenandstr. 5–13, D-81377 Munich, Germany

[‡]Center for Energetic Concepts Development, CECD, University of Maryland, UMD, Department of Mechanical Engineering, College Park, Maryland 20742, United States

S Supporting Information

ABSTRACT: This unique study reports on the 1,3-bis(nitroimido)-1,2,3-triazolate anion. This compound provides unique insight into both academic and practical considerations surrounding high-nitrogen systems. The bonding in this energetic anion can be represented multiple ways, one of which includes a chain of alternating positive/negative charges nine atoms long. The validity of this resonance structure is discussed in terms of experimental, computational, and valence bond results. The prepared materials based on this energetic anion were also characterized chemically (infrared, Raman, NMR, X-ray) and as high explosives in terms of their energetic performances (detonation velocity, pressure, etc.) and sensitivities (impact, friction, electrostatic), and the 1,3-bis(nitroimido)-1,2,3-triazolate anion is found to be very high performing with high thermal stabilities while being quite sensitive to mechanical stimuli.



INTRODUCTION

The main challenge in energetic materials chemistry (all of propellants, explosives, and pyrotechnics) is producing a material that will release large amounts of energy when desired but still be safe enough to handle without energetic decomposition.^{1–5} Beyond their practical applications, working with such materials on the borderline of existence and nonexistence allows insight into base properties affecting molecular stability and energy capacity. The practical aspect of energetic materials research is focused on ever higher performing explosives and propellants,⁶ energetics that can be used with greatly reduced toxicological or environmental results,⁷ and materials with increased margins of safe handling.⁸ However, on the molecular level, new insights are necessary to determine methods of ever increasing the energy content while retaining stability.

There are two major strategies for incorporating energetic properties into a molecule, and naturally, they can be combined. The first is simply fuel and oxidizer in the same molecule as is seen in quintessential explosives such as TNT (2,4,6-trinitrotoluene) and RDX (1,3,5-trinitro-1,3,5-triazinane). The second broad category is high heat of formation compounds where high heats of formation are created from either highly strained bonds in the molecule (e.g., cubane energetics)⁹ or the driving force of a nitrogen-rich compound toward forming nitrogen gas (e.g., 1,1'-azobi-1,2,3-triazole).¹⁰ Unfortunately, these strategies all appear to have limits. In the

case of combining fuel and oxidizer in the same molecule using aromatic and aliphatic nitro compounds and nitramines, as the oxygen balance (indicator of ratio of fuels (C,H) to oxidizers (O) in an energetic molecule) improves, the sensitivities toward impact have been shown to increase.¹¹ A similar effect is seen with high heat of formation compounds: when the five-membered azoles from pyrazole to pentazole are considered, as nitrogen content increases, thermal stability decreases (heat of formation concurrently increases), culminating in the pentazole ring, derivatives of which are not stable at ambient conditions.¹² In the case of heavily strained compounds, octanitrocubane has been prepared; however, the synthesis is exceedingly long, precluding use.¹³

Unlike energetic design strategies based on fuel and oxidizer or strained compounds, nitrogen-rich compounds offer some unique chemical properties that can allow stabilization via several distinct methods. One of the reasons high nitrogen systems that possess extended nitrogen chains are not stable, while the corresponding carbonaceous version is stable, is a result of the lone pair of electrons on the nitrogen atoms. While a nitrogen atom can be considered isoelectronic to a CH group, nitrogen's lone pair possesses electron density which can donate into adjacent σ^* orbitals destabilizing the system.¹⁴ This is the reason that materials such as hexazine (cyclic- N_6) are not

Received: October 30, 2012

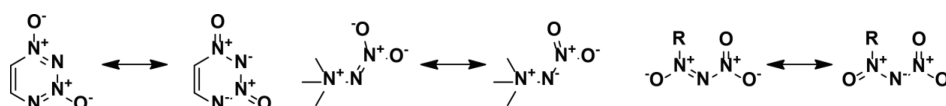


Figure 1. Nitrogen–oxygen APNC systems.

74 stable. The successful design of such nitrogen-rich systems
 75 must adequately separate σ - and π -systems.¹⁵ Tailoring of the
 76 molecular shape can achieve this. In the case of the
 77 nitrohydrazines, a class of compounds generally regarded to
 78 be of low stability, Tartakovsky¹⁶ prepared a bicyclic nitro-
 79 hydrazine of increased stability where the cis-fixed β -nitrogen
 80 lone pair does not possess the flexibility to reach an
 81 antiperiplanar arrangement relative to the N–NO₂, a require-
 82 ment to destabilize the system. Naturally, the placement of
 83 electron-withdrawing substituents on the β -nitrogen of a
 84 nitrohydrazine was also shown by Tartakovsky to increase the
 85 stability of the species,¹⁷ and a similar effect was seen by
 86 delocalization when the β -nitrogen was part of a heterocycle,
 87 preferably where the heterocyclic nitrogen can be assigned a
 88 formal positive charge.¹⁶ In the case of a heterocycle, where
 89 ring shape is fixed, σ and π separation can be achieved by
 90 functionalization. This is best exemplified by the fully
 91 unsaturated 1,2,3,4-tetrazine ring; without ring nitrogen
 92 atoms substitution, it is unstable, with only one low-
 93 decomposing example of one such compound existing.^{18,19} In
 94 the case of the 1,2,3,4-tetrazine-1-oxides, an increase in stability
 95 is seen with many benzo-annulated species known.²⁰ The major
 96 increase in stability is seen with the 1,2,3,4-tetrazine-1,3-
 97 dioxides; generally, members of this class of compounds
 98 decompose above 200 °C.^{20–22} This increase in stability can be
 99 described by the above separation of σ and π systems;¹⁵
 100 however, qualitatively it gives rise to the unique “alternating
 101 positive negative charge” (APNC) theory, whereby stable
 102 nitrogen-rich systems can have one of their resonance forms
 103 illustrated with positive and negative charges on alternating
 104 atoms.^{16,23} Unique nitrogen–oxygen systems, beyond 1,2,3,4-
 105 tetrazine-1,3-dioxides, can all have their resonance forms
 106 illustrated in the APNC form including the nitroimide^{24,25}
 107 and nitrodiazine oxide^{16,26} functionalities (Figure 1). When it is
 108 considered that heterocycle stabilization by an oxide results
 109 from removal of electron density on alternating nitrogen atoms,
 110 there is the potential for heterocycle stabilization by the
 111 nitroimide functionality, where extended APNC systems can be
 112 created.

113 In this work, we have chosen to investigate the nitration
 114 product of the 1,3-diamino-1,2,3-triazolium cation, 1,3-bis-
 115 (nitroimido)-1,2,3-triazolate. When one resonance form is
 116 considered (Figure 2), an alternating positive/negative charge

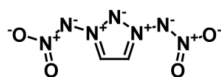


Figure 2. Most charged resonance form of the 1,3-bis(nitroimido)-1,2,3-triazolate anion.

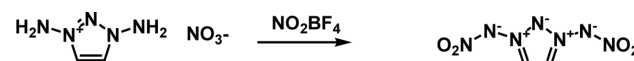
117 system is created that extends over *nine* atoms when the nitro
 118 group resonances are included. This compound was first
 119 prepared by Tartakovsky;²⁷ however, only limited character-
 120 ization was presented, such as the decomposition point of the
 121 potassium salt, and not even a detailed synthesis was presented.
 122 In this work we have prepared a variety of energetic salts of the
 123 1,3-bis(nitroimido)-1,2,3-triazolate anion, and these were

characterized by X-ray diffraction, infrared and Raman
 spectroscopy, multinuclear NMR spectroscopy, elemental
 analysis, and DSC. Computational calculations predicting
 energetic performance properties confirm the exceedingly
 high energetic properties of this class of materials. The
 favorable resonance forms of the APNC system are discussed
 based on crystallographically determined bond lengths as well
 as using computational results (NBO and Mulliken charges and
 valence bond theory). We have exemplarily demonstrated the
 ability of this unique class of compounds to form energetic
 materials of high explosive performance and high thermal
 stability.

RESULTS AND DISCUSSION

Synthesis. The nitration of 1,3-diamino-1,2,3-triazolium
 nitrate with nitronium tetrafluoroborate is performed at 0 °C
 for 30 min followed by allowing the solution to warm to room
 temperature over the next 30 min (Scheme 1). After this time,

Scheme 1. Synthesis of Potassium 1,3-Bis(nitroimido)-1,2,3-triazolate



solid potassium acetate is added and the mixture stirred
 overnight. After filtration of the acetate, acetonitrile is
 evaporated, and acetic acid is removed as the azeotrope with
 benzene. Due to the increased solubility of tetrafluoroborate in
 acetonitrile in the presence of acetic acid, the produced residue
 was extracted with acetonitrile to obtain crude potassium 1,3-
 bis(nitroimido)-1,2,3-triazolate (**1**). Raman and ¹⁹F NMR
 confirmed the presence of tetrafluoroborate in the crude
 material. Crystals were obtained by diffusing ether into a
 solution of **1** in acetonitrile, and these crystals were used for
 DSC as well as crystallographic measurement.

The reaction of crude **1** with aqueous silver nitrate solution
 precipitates the silver salt (**2**) as an off-white solid. Interestingly,
 when a small sample of high purity **1** from multiple EtOH and
 MeOH crystallizations is used to prepare the silver salt, the
 silver salt does not precipitate instantly and instead forms salt-
 like crystals with dimensions over 1 mm. This crystal growth
 process is incredibly slow with very tiny crystals visible after a
 day or two, and 1 mm crystals took over a week. As lower
 purity samples of **1** were used for the synthesis of **2**, the crystal
 shape becomes needle-like and finally simply a powder. The
 powder **2** does not explode but merely deflagrates when
 ignited, whereas the crystalline material explodes with a very
 satisfying report when ignited. Due to the high sensitivity of the
 silver salt, elemental analysis could not be performed to
 determine purity. Raman measurements were also precluded by
 the tendency of explosive silver salts to explode upon Raman
 irradiation.

The silver salt **2** was reacted with ammonium, hydroxylammonium,
 hydrazinium, and triaminoguanidinium halides to
 obtain the corresponding energetic salt and silver halide. After
 filtration of the silver halide and evaporation of the filtrate, the

173 ammonium (3), hydroxylammonium (4), hydrazinium (5), and
174 triaminoguanidinium (6) salts were isolated, and elemental
175 analysis indicated all were pure. Tetrafluoroborate impurities
176 were assumed to be lost during the precipitation of the silver
177 salt, and only minute traces of tetrafluoroborate were detected
178 in the Raman spectra. All of these salts were crystallized by
179 diffusion of ether into a methanolic solution.

180 **Spectroscopy.** The 1,3-bis(nitroimido)-1,2,3-triazolate
181 anion was characterized by proton, carbon-13, and nitrogen-
182 15 NMR in DMSO-*d*₆. In all salts the lone ¹H and ¹³C signals
183 occur at 8.75 and 129.7 ppm. The ¹⁵N spectrum (Figure 3)

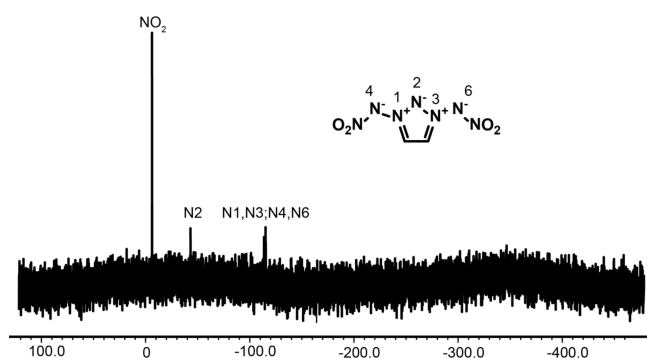


Figure 3. ¹⁵N NMR spectrum of the 1,3-bis(nitroimido)-1,2,3-triazolate anion.

184 possesses four signals, at -6.2, -43.0, -113.6, and -115.3
185 ppm. Assignments were made based on comparison with a
186 calculated spectrum (MPW1PW91/aug-cc-pVDZ, Gaus-
187 sian09²⁸) where calculated values for N5/N7, N2, N1/N3,
188 and N4/N6 were found to be -12.9, -53.7, -106.2, and
189 -108.7 ppm. These values match well with experimental;
190 however, the difference of N1/N3 and N4/N6 being only 2
191 ppm in both the experimental and calculated spectra leaves
192 precise assignment of these similar signals ambiguous.

193 The IR and Raman spectra of all compounds were recorded
194 and assigned using frequency analysis from an optimized
195 structure (B3LYP/cc-pVDZ using the Gaussian 09 software).²⁸

All calculations were performed at the DFT level of theory; the
gradient-corrected hybrid three-parameter B3LYP^{29,30} func-
tional theory has been used with a correlation consistent cc-
pVDZ basis set.³¹⁻³⁴

In the Raman spectra, five major bands are observed. The
first occurs from 1509 to 1520 cm⁻¹ (calcd 1563 cm⁻¹) and
results from the NO₂ asymmetric stretch as well as the
symmetric triazole C-C ring deformation. The next occurs
from 1338 to 1372 cm⁻¹ (calcd 1365 cm⁻¹) and results from
C1-N1 and C2-N3 triazole symmetric stretch in combination
with N1-N4 and N3-N6 stretching. At 1241-1252 cm⁻¹
(calcd 1250 cm⁻¹) is the band resultant from C1-C2, N1-N2,
and N2-N3 triazole ring breathing. Between 1070 and 1091
cm⁻¹ (calcd 1070 cm⁻¹), combined triazole ring breathing with
C-H wagging is observed. The final strong band at 1005-1015
cm⁻¹ (calcd 1059 cm⁻¹) results from a combination of N-NO₂
stretching and C-H wagging. Traces of tetrafluoroborate
impurities (1098, 773, 535, and 359 cm⁻¹) can be seen in
several spectra, however, only in trace quantities as evidenced
by their intensities and the elemental analyses being correct.

In the literature,²⁴ nitroimides tend to have two distinct
bands from nitro group stretching in the infrared spectrum. The
first generally occurs at 1260-1300 cm⁻¹ and the next at
1380-1450 cm⁻¹. For the materials prepared, the first of these
occurs from 1390 to 1455 cm⁻¹ (calcd 1355 cm⁻¹) from N-
NO₂ symmetric nitro stretching in combination with N1-N2
and N2-N3 asymmetric stretching, while the second (obs.
1244-1280 cm⁻¹, calcd 1310 cm⁻¹) arises from the same
vibrations with the addition of asymmetric C-H C-H
wagging.

Single Crystal X-ray Structure Analysis. All compounds
have been fully characterized by single-crystal X-ray structure
determination. Table 1 summarizes a selection of crystallo-
graphic data and refinement details. In the literature,²⁷ mention
is made of the structure of potassium salt being known;
however, no details were presented. Of interest is the rotational
ability of the N2-N3-N6-N7 bond, giving each salt a unique
rotation of the "arms" of the nitroimide functionality relative to
the triazole ring.

Table 1. Crystallographic Data and Structure Refinement Details for Compounds 1-6

compound	1	2	3	4	5	6
formula	KC ₂ H ₂ N ₇ O ₄	AgC ₂ H ₂ N ₇ O ₄	NH ₄ C ₂ H ₂ N ₇ O ₄	NH ₄ OC ₂ H ₂ N ₇ O ₄	N ₂ H ₃ C ₂ H ₂ N ₇ O ₄	CN ₆ H ₉ C ₂ H ₂ N ₇ O ₄
formula weight [g mol ⁻¹]	227.18	295.98	206.15	222.15	221.17	293.25
temperature [K]	173	173	173	173	173	173
crystal system	orthorhombic	orthorhombic	orthorhombic	triclinic	monoclinic	triclinic
space group	<i>Pca</i> 2 ₁	<i>P2</i> ₁ <i>2</i> ₁ <i>2</i> ₁	<i>Pna</i> 2 ₁	<i>P</i> -1	<i>P2</i> ₁ / <i>n</i>	<i>P</i> -1
<i>a</i> [Å]	9.7258 (4)	5.5785(6)	6.4299(2)	5.6251(4)	3.6154(4)	9.6819(14)
<i>b</i> [Å]	19.6056(7)	8.5311(7)	5.6658(2)	7.8446(7)	23.160(2)	9.8267(12)
<i>c</i> [Å]	8.2346(3)	15.4048(11)	20.5491(8)	9.7402(8)	10.0335(9)	12.1787(19)
α [°]	90	90	90	76.794(7)	90	89.446(11)
β [°]	90	90	90	89.114(6)	91.855(11)	88.555(12)
γ [°]	90	90	90	77.979(7)	90	89.845(11)
volume [Å ³]	1570.17	733.13(11)	748.61 (5)	409.03(6)	839.69	1158.3(3)
formula Z	8	4	4	2	4	4
space group Z	4	4	4	2	4	4
density calcd [g cm ⁻³]	1.922	2.682	1.829	1.804	1.749	1.683
R ₁ /wR ₂ [all data]	0.0314/0.0643	0.0276/0.0508	0.0395/0.0999	0.0358/0.0725	0.1029/0.1822	0.1243/0.0827
R ₁ /wR ₂ [<i>I</i> > 2 σ (<i>I</i>)]	0.0277/0.0620	0.0238/0.0492	0.0380/0.0978	0.0286/0.0678	0.0714/0.1682	0.0827/0.1990
<i>S</i>	1.044	1.006	1.152	1.050	1.039	1.034
CCDC	905012	905013	905015	905014	905016	905017

235 Potassium 1,3-bis(nitroimido)-1,2,3-triazolate (**1**) crystallizes
 236 in the orthorhombic space group $Pca2_1$ with four formula units
 237 in the unit cell and a density of 1.922 g cm^{-3} (Figure 4). The

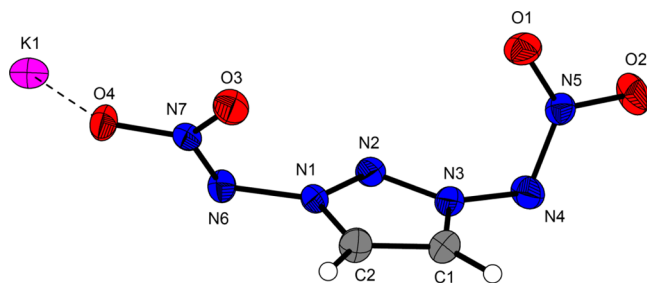


Figure 4. ORTEP representation of the molecular structure of **1**. Displacement ellipsoids are shown at the 50% probability level.

238 anions are arranged in a wavelike structure along the b -axes.
 239 The potassium cations are collocated in layers along the ac -
 240 planes and are coordinated ($<3 \text{ \AA}$) by the atoms O4, O2, O6,
 241 O7, and N6 forming no regular polyhedra.

242 Silver 1,3-bis(nitroimido)-1,2,3-triazolate (**2**) crystallizes in
 243 the orthorhombic space group $P2_12_12_1$ with four formula units
 244 in the unit cell and a density of 2.756 g cm^{-3} . (Figure 5) This
 245 density is in the range of other silver nitroamino-azoles, e.g.,
 246 silver 1-methyl-5-nitriminotetrazolate (2.948 g cm^{-3}) in the
 247 literature.³⁵

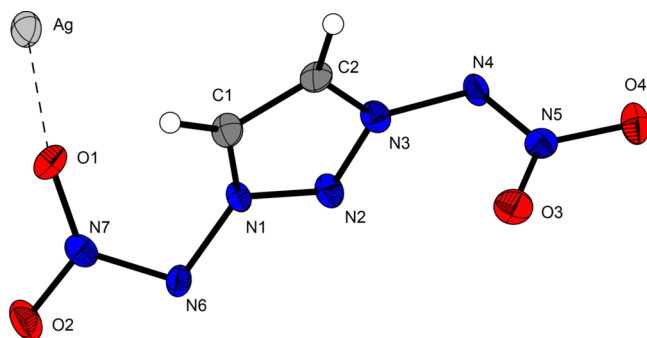


Figure 5. ORTEP representation of the molecular structure of **2**. Displacement ellipsoids are shown at the 50% probability level.

248 Ammonium 1,3-bis(nitroimido)-1,2,3-triazolate (**3**) crystal-
 249 lizes in the orthorhombic space group $Pna2_1$ with four formula
 250 units in the unit cell and a density of 1.829 g cm^{-3} (Figure 6).
 251 The structure is strongly influenced by the formation of
 252 numerous hydrogen bonds using all ammonium protons, e.g.,
 253 $N8-H8A \cdots O3$: $0.82(4), 2.51(4), 3.116(3) \text{ \AA}, 132(4)^\circ$; $N8-$
 254 $H8D \cdots O4$: $0.89(4), 2.37(7), 2.879(3) \text{ \AA}, 116(6)^\circ$; $N8-$
 255 $H8C \cdots O4^i$: $0.84(4), 2.35(5), 3.052(4) \text{ \AA}, 142(6)^\circ$; and $N8-$

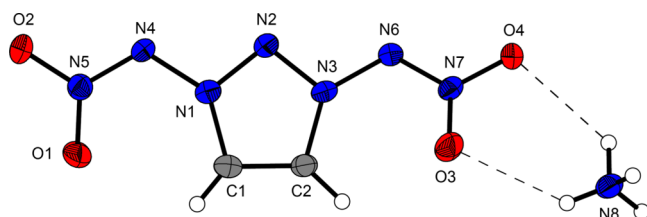


Figure 6. ORTEP representation of the molecular structure of **3**. Displacement ellipsoids are shown at the 50% probability level.

$H8B \cdots O2^{ii}$: $0.87(4), 2.32(7), 2.957(3) \text{ \AA}, 130(7)^\circ$ ((i) $0.5 + x,$
 $-0.5 - y, z$, (ii) $-x, -y, -0.5 + z$).

Hydroxylammonium-1,3-bis(nitroimido)-1,2,3-triazolate (**4**)
 crystallizes in the triclinic space group $P-1$ with two formula
 units in the unit cell and a density of 1.804 g cm^{-3} . Interestingly
 this density is lower than that of the ammonium salt **3**, which is
 usually the other way around. As can be seen from Figure 7, the
 C connected hydrogen atoms participate in nonclassical
 hydrogen bonds to the $O1^i$ and $O3^i$ atoms of a neighbored
 anion, forming a dimer.

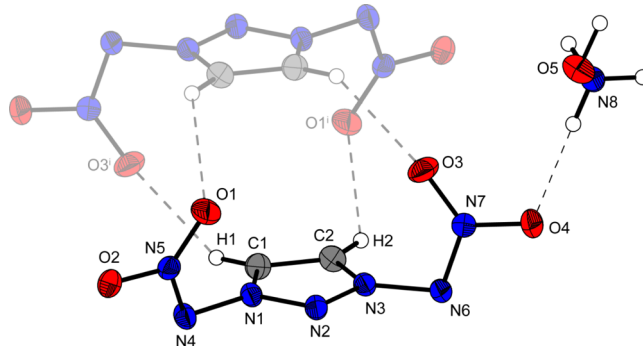


Figure 7. ORTEP representation of the molecular structure of **4** and the formation of nonclassical hydrogen bonds. Displacement ellipsoids are shown at the 50% probability level. Symmetry code: (i) $2 - x, -y, 1 - z$.

Hydrazinium-1,3-bis(nitroimido)-1,2,3-triazolate (**5**) crystal-
 lizes without inclusion of water or hydrazine in the monoclinic
 space group $P2_1/n$ with four formula units in the unit cell and a
 density of 1.749 g cm^{-3} (Figure 8). The anions are arranged in

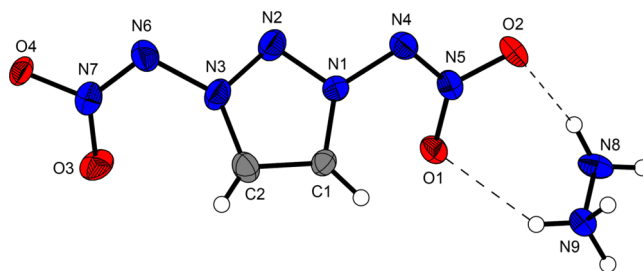


Figure 8. ORTEP representation of the molecular structure of **5**. Displacement ellipsoids are shown at the 50% probability level.

wave-like constitution along the b -axes, interrupted by the
 hydrazinium cations within the ac -planes. All hydrogens of the
 hydrazinium cations participate in hydrogen bonds.

Triaminoguanidinium 1,3-bis(nitroimido)-1,2,3-triazolate
 (**6**) crystallizes in colorless platelets in the triclinic space
 group $P-1$ with four formula units in the unit cell. Half of the
 asymmetric unit is depicted in Figure 9. The density of 1.682 g
 cm^{-3} is the lowest one observed in this work and can be
 explained by a relatively loose 3-dim packing (best observable
 by viewing along the a direction).

Table 2 presents selected torsion angles and bond lengths. As
 the NNO_2 fragments on the compound exhibit a wide range of
 $N2-N1-N4-N5$ and $N2-N3-N6-N7$ torsion angles relative
 to the triazole ring, the $N1-N4$ and $N3-N6$ bonds can
 reasonably be assumed to be single bonds based on their
 rotational freedom. In all compounds, this bond length ranges
 from 1.40 to 1.44 \AA , slightly shorter than the standard (1.48)

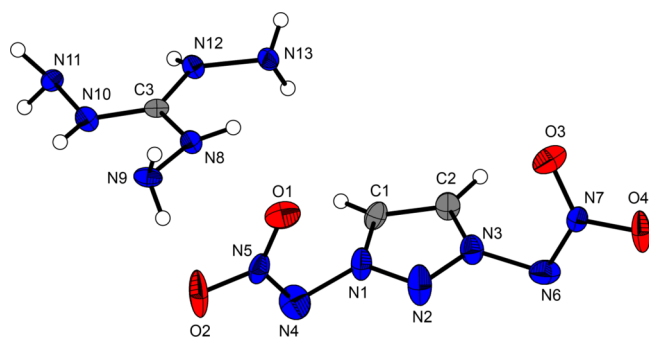


Figure 9. ORTEP representation of the molecular structure of **6**. Displacement ellipsoids are shown at the 50% probability level.



Figure 10. Contributing double bond resonance form.

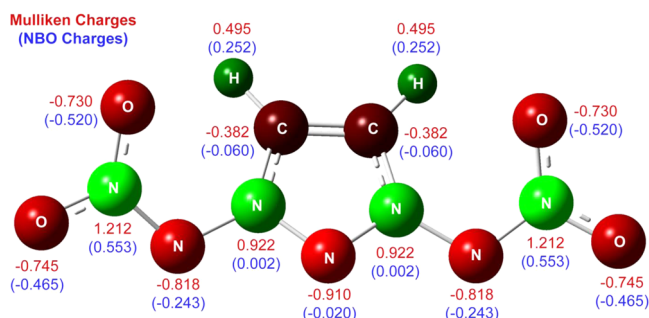


Figure 11. Mulliken and NBO charges on the 1,3-di(nitroimide)-1,2,3-triazolate anion.

287 N–N single bond, consistent with the $N^+–N^-$ fragments as
 288 seen in pyridine-1-nitroimide where this bond length is seen to
 289 be 1.421 \AA ³⁶ or in 1-nitroimido-1,2,3-triazole where this bond is
 290 1.40 \AA .³⁷ Interesting to note is that the corresponding bond in
 291 the precursor diaminotriazolium cation is also 1.40 \AA ,³⁸ again
 292 supporting this bond's single nature. As the NNO_2 fragments
 293 approach planarity with the ring, we expected to see this bond
 294 length decrease due to increased π -system communication;
 295 however, this was not seen. The N–N bond lengths within the
 296 NNO_2 fragments (N4–N5 and N6–N7) are slightly shorter,
 297 ranging from 1.30 to 1.35 \AA , approximately half way between a
 298 double and single bond, illustrating the contributing nature of
 299 the resonance form shown in Figure 10. Within the ring, the
 300 bond lengths are comparable to those found in the precursor
 301 diaminotriazolium cation.³⁸

302 **Computational Structural Considerations.** Unfortu-
 303 nately, crystallographic results are not sufficient evidence for
 304 the highly charged resonance structure presented in Figure 2,
 305 so NBOs (natural bond orbitals) as well as Mulliken charges of
 306 the anion were calculated on the B3LYP/cc-PVTZ level of
 307 theory using the optimized gas-phase structure with the
 308 Gaussian09²⁸ software (Figure 11).

309 First, when the Mulliken charges are considered, a chain of
 310 nine atoms with alternating positive and negative charges is
 311 seen across the system, exactly what was suggested in Figure 2.
 312 NBO charges are considered more reasonable for discussion,

and the same trend is seen within the nitroimide functionalities 313
 on the 1,2,3-triazole ring; however, within the 1,2,3-triazole ring 314
 the charges slightly differ. When NBO charges are considered 315
 vs Mulliken, the majority of the triazole ring's negative charges 316
 is localized on the carbon atoms in NBO, whereas in Mulliken, 317
 the negative charge is located on the central nitrogen atom. The 318
 magnitude of the positive charges on the flanking nitrogen 319
 atoms is also greatly reduced in NBO charges vs Mulliken; 320
 however, when one considers that the triazole ring has negative 321
 charge overall, it is unsurprising that formal positive charges 322
 would be reduced. Overall, both NBO and Mulliken charges 323
 support the contributing nature of the resonance form in Figure 324
 2 in the structure of the 1,3-bis(nitroimido)-1,2,3-triazolate 325
 anion. 326

Next, to judge the contributions of the various resonance 327
 forms, we attempted to calculate the contributions of the 328
 various resonance forms according to valence bond theory 329
 using the program VB2000.^{39,40} Unfortunately, the 1,3- 330
 bis(nitroimido)-1,2,3-triazolate anion is too large for the 331
 program to handle (>14 VB orbitals), so one nitroimide 332
 group was replaced with an *N*-oxide as an “approximate 333
 replacement”; however, the higher electronegativity of the 334

Table 2. Selected Torsion Angles and Bond Lengths

	1	2	3	4	5	6
N2–N1–N4–N5 (°)	–122.9 (2)	–134.0 (3)	160.0 (2)	76.5 (1)	–137.1 (3)	93.3 (5)
° not planar	57.1	46.0	20.0	76.5	42.9	86.7
N2–N3–N6–N7 (°)	82.4 (3)	–93.8 (4)	145.5 (2)	–96.2 (1)	138.5 (3)	–114.6 (5)
° not planar	82.4	86.2	34.5	83.8	41.5	65.4
C1–C2	1.358 (3)	1.351 (5)	1.374 (4)	1.360 (2)	1.368 (6)	1.347 (7)
C1–N1	1.355 (3)	1.349 (5)	1.368 (3)	1.349 (2)	1.363 (5)	1.350 (6)
C2–N3	1.357 (3)	1.351 (5)	1.358 (3)	1.357 (2)	1.373 (5)	1.366 (6)
N1–N2	1.323 (3)	1.323 (4)	1.331 (3)	1.327 (2)	1.323 (4)	1.323 (6)
N2–N3	1.322 (3)	1.328 (4)	1.329 (3)	1.324 (2)	1.330 (4)	1.313 (6)
N1–N4	1.402 (3)	1.404 (4)	1.402 (3)	1.400 (2)	1.403 (4)	1.435 (6)
N3–N6	1.406 (3)	1.397 (5)	1.400 (3)	1.406 (2)	1.441 (5)	1.438 (6)
N4–N5	1.327 (3)	1.349 (5)	1.316 (3)	1.327 (2)	1.341 (4)	1.309 (6)
N6–N7	1.334 (3)	1.338 (5)	1.324 (3)	1.332 (2)	1.298 (4)	1.307 (5)
N5–O1	1.248 (3)	1.241 (4)	1.259 (3)	1.237 (2)	1.254 (4)	1.235 (6)
N5–O2	1.256 (2)	1.244 (6)	1.260 (3)	1.276 (2)	1.260 (4)	1.246 (5)
N7–O3	1.242 (3)	1.266 (4)	1.246 (3)	1.242 (1)	1.282 (4)	1.245 (5)
N7–O4	1.254 (3)	1.235 (4)	1.262 (3)	1.259 (2)	1.260 (4)	1.251 (5)

335 oxygen atom vs a nitrogen was believed to favor the resonance
 336 forms with increased negative charge on the oxide vs the ring.
 337 Figure 12 illustrates the nine resonance forms which were
 338 calculated.

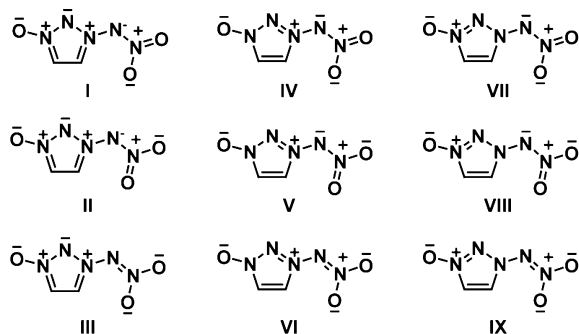


Figure 12. Valence bond resonance forms.

339 The calculated Hiberty Weights (percentage contribution of
 340 each resonance form) is 1.1%, 0%, 0%, 90.8%, 1.0%, 0.1%, 6.9%,
 341 0.2%, and 0% for I–IX, respectively. The first piece of
 342 information that is noteworthy is the insignificant contribution
 343 of the resonance forms III, VI, and IX, those containing a
 344 double bond between the nitrogen atoms of the nitroimide
 345 groups, in interesting contrast to the results in the
 346 crystallography section. The next interesting piece of
 347 information is that when each column of resonance forms is
 348 considered individually, the only difference down a column
 349 being the resonance differences within the nitroimide group,
 350 within the standard NO₂ group resonances there is a distinct
 351 favorability to I, IV, and VII over II, V, and VIII. A potential
 352 explanation for this is that when the adjacent proton on the ring
 353 is considered to be of partial positive charge resonance forms I,
 354 IV, and VII allow the negatively charged oxygen atom to
 355 approach this proton, allowing for a six-membered ring to be
 356 established. Structure IV is the highest contributing resonance
 357 form over I and VII. The major difference between these three
 358 is the location of anionic negative charge, after the cancelling of
 359 charges within zwitterionic groups such as N-oxide, nitro, and
 360 nitroimide, on the ring, on the ring oxygen atom, and on the
 361 nitrimide nitrogen, respectively. When we consider the higher
 362 electronegativity of oxygen compared to nitrogen, it is
 363 unsurprising that resonance form IV is the highest contributor.
 364 In the 1,3-bis(nitroimido)-1,2,3-triazolate anion, this resonance
 365 form is naturally not possible due to the lack of said oxygen
 366 atom, meaning that resonance forms analogous to I and VII
 367 would be of higher contribution. Despite I contributing less
 368 than VII, its contribution would not be insignificant when we
 369 go from the model system above to the actual 1,3-
 370 bis(nitroimido)-1,2,3-triazolate anion, illustrating that while it
 371 may not be the most favored resonance form it is a contributor.

372 **Thermal Behavior.** The thermal behavior of all prepared
 373 compounds (Table 3) was investigated by differential scanning
 374 calorimetry. Only one compound, triaminoguanidinium salt **8**,
 375 melts prior to decomposition. Generally energetic salts of the
 376 1,3-bis(nitroimido)-1,2,3-triazolate anion are of high thermal
 377 stability, decomposing only above 180 °C, a general require-
 378 ment of an any energetic prior to adaptation for practical use.
 379 The only exception to this trend is the hydroxylammonium salt
 380 **5** which decomposes below 150 °C; however, this is often seen
 381 for hydroxylammonium salts of nitro compounds, such as the
 382 hydroxylammonium nitrotetrazolate-2-oxide. The most stable

Table 3. Thermal Behavior of Nitrogen-Rich Salts

compound	<i>T_m</i> (°C)	<i>T_{dec}</i> (°C)
1	-	210
2	-	238
3	-	184
4	-	149
5	-	210
6	145	185

salt is the silver salt **3** which decomposes at almost 240 °C. The
 generally high thermal stability of all salts of the 1,3-
 bis(nitroimido)-1,2,3-triazolate anion is comparable to or
 slightly higher than other known nitroimides.²⁴ These stabilities
 are far higher than for N-nitrimino systems incapable of
 forming APNC systems such as 1-and 2-nitraminotetrazoles,⁴¹
 again supporting the use of APNC theory in the design of
 thermally stable energetic systems.

Heats of Formation. It is commonly accepted that heats of
 formation of energetic materials are calculated theoretically, and
 even superior results are achieved. The calculations were
 carried out using the Gaussian G09W (revision A.02) program
 package.²⁸ The heats of formation $\Delta_f H^\circ(\text{s})$ (Table 5) of the
 investigated compounds **1** and **4–8** (silver cannot be calculated
 by the CBS-4 M method) were calculated with the atomization
 method (eq 1) using room-temperature CBS-4 M electronic
 enthalpies summarized in Table 5.

$$\Delta_f H^\circ_{(\text{g,M},298)} = H_{(\text{Molecule},298)} - \sum H^\circ_{(\text{Atoms},298)} + \sum \Delta_f H^\circ_{(\text{Atoms},298)} \quad (1)$$

The calculated gas-phase enthalpies of formation $\Delta_f H^\circ(\text{g})$
 (Table 4) were converted into the solid state enthalpies of
 formation ($\Delta H_m(\text{s})$) by using the Jenkins and Glasser
 equations for 1:1 salts.⁴⁵ The molecular volumes V_M were
 calculated from the X-ray structures to calculate the lattice
 energies (ΔE_L) and enthalpies (ΔH_L). Lastly, the molar
 standard enthalpies of formation ($\Delta_f H_m$) were used to calculate

Table 4. CBS-4M Calculation Results, Molecular Volumes Taken from X-ray Solution, and Calculated Lattice Enthalpies

M	$-H^{298}$ (au) ^a	$\Delta_f H^\circ(\text{g,M})$ (kJ mol ⁻¹) ^b	V_M (nm ³) ^c	$\Delta E_L, \Delta H_L$ (kJ mol ⁻¹) ^d	Δn^e
K ⁺	599.035967	487.7			
NH ₄ ⁺	56.796608	635.8			
Hx ⁺	131.863229	687.2			
Hy ⁺	112.030523	774.1			
TAG ⁺	371.197775	874.3			
IMY ⁻	760.415222	351.0			9
1		838.7 ^f	0.197	581.4, 582.6	6.5
3		986.8 ^f	0.188	513.9, 518.9	9
4		1038.2 ^f	0.205	502.0, 507.0	9.5
5		1125.1 ^f	0.210	498.6, 503.5	10
6		1225.3 ^f	0.290	458.4, 463.3	14

^aCBS-4 M calculated enthalpy at room temperature. ^bCalculated gas-phase heat of formation by the atomization equation. ^cMolecular volume of the molecular moiety in the crystal structure. ^dLattice energy and lattice enthalpy calculated by Jenkins and Glasser equations. ^eChange of moles of gaseous components. ^fGas-phase enthalpies of formation of the ionic compounds are taken as the respective sums of the noninteracting component ions.

Table 5. Energetic Properties and Detonation Parameters

	1	3	4	5	6	RDX
formula	C ₂ H ₂ KN ₇ O ₄	C ₂ H ₆ N ₈ O ₄	C ₂ H ₆ N ₈ O ₅	C ₂ H ₇ N ₉ O ₄	C ₃ H ₁₁ N ₁₃ O ₄	C ₃ H ₆ N ₆ O ₆
FW (g mol ⁻¹)	227.18	206.12	222.12	221.13	293.20	222.12
IS ^a (J)	1	1	1	5	>5	7.5
FS ^b (N)	20	20	20	6	20	120
ESD ^c (J)	0.020	0.800	0.200	0.100	0.200	0.2
N ^d (%)	43.16	54.36	50.45	57.01	62.10	37.84
Ω ^e (%)	-10.56	-23.28	-14.41	-25.32	-40.92	-21.61
T _{Dec} ^f (°C)	210	184	149	210	185	205
ρ ^g (g cm ⁻³)	1.922	1.829	1.804	1.749	1.683	1.858 (90 K)
Δ _f H _m ^h (kJ mol ⁻¹)	256.1	468.0	531.3	621.6	761.9	86.3
Δ _f U ^o (kJ kg ⁻¹)	1198.0	2378.1	2497.3	2922.6	2716.4	489.0
EXPLO5.05:						
Δ _{Ex} U ^o (kJ kg ⁻¹)	9736 ^q	6711	7342	7068	6109	6190
T _{det} ^k (K)	5552 ^q	4454	4896	4610	3951	4232
ρ _{CJ} ^l (kbar)	319 ^p , 367 ^q	399	407	376	326	380
V _{Det} ^m (m s ⁻¹)	8698 ^p , 8823 ^q	9406	9426	9337	8954	8983
V _o ⁿ (L kg ⁻¹)	600 ^q	805	793	828	841	734
I _s ^o (s)	300 ^q	271	275	277	259	258

^aBAM Droppammer. ^bBAM Impact. ^cElectrical Spark Sensitivity. ^dNitrogen Content. ^eOxygen Balance. ^fDecomposition temperature from DSC (5 °C min⁻¹). ^gDensity from X-ray diffraction. ^hCalculated molar enthalpy of formation. ⁱEnergy of formation ^jTotal energy of detonation. ^kExplosion temperature. ^lDetonation Pressure. ^mDetonation Velocity. ⁿVolume of Detonation Products. ^ospecific impulse using isobaric (60 bar) conditions. ^pCalculated by Dr. Betsy Rice with Cheetah 6. ^qCalculated with EXPLO5.06

408 the molar solid state energies of formation (ΔU_m) (Table 5)
409 according to eq 2.

$$410 \quad \Delta U_m = \Delta H_m - \Delta nRT \quad (2)$$

411 (Δn being the change of moles of gaseous components).

412 Investigated salts **1** and **3–6** are all formed endothermically.
413 Highly positive heats of formations are usually calculated for
414 nitrogen-rich material, with a large number of N–N single
415 bonds. Oxygen-rich energetic materials such as nitro carbons⁴⁶
416 have mostly negative enthalpies of formation. The lowest heat
417 of formation was calculated for the potassium salt **1** (256 kJ
418 mol⁻¹), the most positive one for triaminoguanidinium salt **6**
419 (762 kJ mol⁻¹) showing the largest number of N–N single
420 bonds followed by the hydrazinium salt **5** (622 kJ mol⁻¹),
421 which is also remarkably high. With respect to one kilogram,
422 hydrazinium salt **5** shows the highest value (2923 kJ kg⁻¹)
423 because of its lower molecular mass in comparison to **6**.

424 **Detonation Parameters.** To evaluate the utility of new
425 energetic materials, usually their performance characteristics are
426 calculated by computer codes such as EXPLO5.05⁴⁷ or
427 Cheetah.⁴⁸ In this manuscript the calculation of the most
428 important detonation parameters as well as the specific impulse
429 (at 60 bar rocket conditions) (Table 5) were performed with
430 the program package EXPLO5.05 for the nitrogen-rich salts.
431 Values for the potassium salt were generated with a beta version
432 of EXPLO5.06 (Dr. M. Sućeska) and Cheetah 6 in cooperation
433 with the army research laboratory. The EXPLO5.05 program is
434 based on the chemical equilibrium, steady-state model of
435 detonation and uses the Becker–Kistiakowsky–Wilson equa-
436 tion of state (BKW EOS) for gaseous detonation products and
437 Cowan–Fickett's equation of state for solid carbon. The
438 highest values in terms of detonation performance were
439 observed for compounds **3** and **4** due to their highest density.
440 Their calculated detonation velocity (9406 m s⁻¹ (**3**) and 9426
441 m s⁻¹) but also pressure (399 kbar (**3**) and 407 kbar (**4**)) are
442 much greater than that of RDX. **4** shows also a remarkable high
443 energy of detonation (-7342 kJ mol⁻¹) which is ca. 20% larger

444 than that of RDX. **3–5** show also very promising propulsion
445 values (specific impulse >270 s) which indicates a potential use
446 in e.g. triple base propellant mixtures.

447 **Sensitivities.** For initial safety testing, the impact, friction,
448 and electrostatic discharge sensitivity tests of the prepared salts
449 were carried out.^{49,50} The impact sensitivity tests were carried
450 out according to STANAG 4489⁵¹ and were modified
451 according to instruction⁵² using a BAM (Bundesanstalt für
452 Materialforschung⁵⁰) droppammer.⁵³ The friction sensitivity
453 tests were carried out according to STANAG 2287⁵⁴ and were
454 modified according to instruction⁵⁵ using a BAM friction tester.
455 When the impact sensitivities of all salts are considered, all
456 except **5** and **6** are highly sensitive explosives, well in the range
457 of primary explosives, while **5** and **6** are slightly less sensitive at
458 5 J and are classified as sensitive according the UN
459 recommendations for the transportation of dangerous
460 goods.⁵⁶ The friction sensitivities of **1**, **3**, **4**, and **6** are all 20
461 N, classifying them as very sensitive, while compounds **2** and **5**
462 are 5 and 6 N, respectively, classifying them as extremely
463 sensitive. The electrostatic sensitivities of all salts of nitrogen-
464 rich cations **3–6** are greater than the human body can generate,
465 making for safe laboratory handling. Compounds **1** and **2** are
466 far more sensitive at only 20 mJ, a value easily achievable by the
467 human body mandating extra care with handling. When the
468 sensitivities of all compounds are regarded as a whole, the
469 generalization can be made that energetic materials based on
470 the 1,3-bis(nitroimido)-1,2,3-triazolate anion are highly sensi-
471 tive, indicating that while alternating positive and negative
472 charges in a system can contribute to high thermal stability as
473 seen earlier, correlation toward mechanical sensitivities is less
474 applicable, and as seen in other systems⁵⁷ a large chain of
475 canted nitrogen atoms, as well as compounds with
476 increasingly balanced oxygen balances, can still be generalized¹¹
477 as highly sensitive.

478 ■ CONCLUSIONS

479 It is possible to nitrate the 1,3-diamino-1,2,3-triazoliumtriazolo-
480 lium cation to the 1,3-bis(nitroimido)-1,2,3-triazolate anion,
481 and many energetic salts can be formed through metathesis
482 reactions. The molecular and crystal structures were
483 determined for the first time. Multinuclear NMR, IR, and
484 Raman spectroscopy proved useful for the characterization of
485 these salts. Computational results in terms of Mulliken and
486 NBO charges support this structure as possessing a resonance
487 for containing a chain of nine atoms of alternating positive and
488 negative charges extending over the anion, and valence bond
489 calculations also suggest this resonance form as being a not-
490 insignificant contributor. The experimentally determined high
491 densities, calculated performances, and real thermal stabilities
492 support the use of alternating positive and negative charges and
493 *N*-nitroimides in the design of advanced energetic materials
494 with desirable properties. Unfortunately, the mechanical
495 sensitivities of these materials proved to be too high for
496 practical use, illustrating that while the *N*-nitroimides are useful
497 other molecular features which reduce their sensitivity must be
498 developed.

499 ■ EXPERIMENTAL SECTION

500 All reagents and solvents were used as received (Sigma-Aldrich, Fluka,
501 Acros Organics) if not stated otherwise. Diaminotriazolium nitrate was
502 prepared according to our method.⁵⁸ Melting and decomposition
503 points were measured with a Linseis PT10 DSC using heating rates of
504 5 °C min⁻¹, which were checked with a Büchi Melting Point B-450
505 apparatus. ¹H, ¹³C, and ¹⁵N NMR spectra were measured with a JEOL
506 Eclipse 270, JEOL EX 400, or a JEOL Eclipse 400 instrument. All
507 chemical shifts are quoted in parts per million relative to TMS (¹H,
508 ¹³C) or nitromethane (¹⁵N). Infrared spectra were measured with a
509 Perkin-Elmer Spektrum One FT-IR instrument. Raman spectra were
510 measured with a Perkin-Elmer Spektrum 2000R NIR FT-Raman
511 instrument equipped with a Nd:YAG laser (1064 nm). Elemental
512 analyses were performed with a Netsch STA 429 simultaneous thermal
513 analyzer. Sensitivity data were determined using a BAM drophammer
514 and a BAM friction tester. The electrostatic sensitivity tests were
515 carried out using an Electric Spark Tester ESD 2010 EN (OZM
516 Research).

517 CAUTION! All materials prepared are all energetic compounds with
518 sensitivity to various stimuli. While we encountered no issues in the
519 handling of these materials, proper protective measures (face shield, ear
520 protection, body armor, Kevlar gloves, and earthened equipment) should be
521 used at all times.

522 **Potassium 1,3-Di(nitroimide)-1,2,3-triazolate (1).** To a sol-
523 ution of dried 1,3-diamino-1,2,3-triazolium nitrate (0.40 g, 2.47 mmol)
524 in 100 mL of acetonitrile nitronium tetrafluoroborate (1.00 g, 7.53
525 mmol) was added slowly. The mixture was stirred at 0 °C for 30 min
526 and then allowed to heat to RT over 30 min. The reaction was stopped
527 by the addition of potassium acetate (6.00 g, 61.13 mmol), and the
528 mixture was stirred overnight. The precipitate was filtered off and
529 washed with 500 mL of acetonitrile, and half of the solvent was
530 removed in vacuo. Benzene (500 mL) was added and removed in
531 vacuo, and this process was repeated four times. Removal of the
532 remaining solvent under reduced pressure and extraction of the
533 residue with dry acetonitrile gave 0.32 g (1.81 mmol, 73%) of crude **1**
534 after evaporation of acetonitrile. DSC (5 °C min⁻¹): 210 °C (dec), IR
535 (cm⁻¹) $\tilde{\nu}$ = 3181 (m), 3167 (m), 3141 (m), 2418 (w), 2360 (m), 2341
536 (m), 1772 (w), 1696 (w), 1684 (w), 1635 (w), 1559 (m), 1520 (w),
537 1396 (s), 1364 (s), 1305 (s), 1280 (s), 1249 (m), 1181 (w), 1075 (s),
538 1058 (s), 1042 (s), 1012 (s), 918 (w), 864 (m), 857 (m), 802 (m),
539 771 (s), 720 (w), 687 (w); Raman (1064 nm) $\tilde{\nu}$ = 3169 (17), 3142
540 (15), 2938 (14), 1548 (11), 1519 (38), 1437 (15), 1410 (18), 1364
541 (65), 1252 (62), 1183 (15), 1077 (35), 1046 (26), 1009 (100), 923
542 (10), 870 (19), 803 (10), 775 (15), 735 (11), 722 (12), 697 (10), 661
543 (10), 637 (11), 603 (1), 494 (20), 461 (21), 440 (23), 407 (21), 379

(21), 325 (19); ¹H NMR (DMSO-*d*₆) δ (ppm) = 8.75 (d, 2H, CH); 544
¹³C NMR (DMSO-*d*₆) δ (ppm) = 129.7 (s, 2C, CH); ¹⁵N NMR 545
(DMSO-*d*₆) δ (ppm) = -6.2 (s, 2N, N5, N7, calcd -12.9), -43.0 (s, 546
2N, N1, N3, calcd -53.1), -113.6 (s, 2N, N4, N6, calcd -106.2), 547
-115.3 (s, 1N, N2, calcd -108.1); *m/z* (FAB+) 39.00 (K⁺); *m/z* 548
(FAB-) 188.02 (C₂H₂N₇O₄⁻). EA (C₂H₂N₇O₄K, 227.12) calcd: C, 549
10.57; N, 43.16; H, 0.89. Found: C, 11.46; N, 41.98; H, 0.94. BAM 550
impact: 1 J. BAM friction: 20 N. ESD: 20 mJ. 551

Silver 1,3-Di(nitroimide)-1,2,3-triazolate (2). To a solution of **1** 552
(1.08 g, 4.76 mmol) in 30 mL of distilled water was added a solution 553
of silver nitrate (0.81 g, 4.76 mmol) in 30 mL of distilled water. The 554
precipitate was filtered off, and the remaining solvent in the filtrate was 555
removed under reduced pressure, leaving 0.81 g (2.74 mmol, 58%) of 556
2. DSC (5 °C min⁻¹): 238 °C (dec), IR (cm⁻¹) $\tilde{\nu}$ = 3718 (m), 3163 557
(m), 2710 (w), 2445 (w), 2360 (m), 2341 (m), 2249 (w), 1669 (w), 558
1540 (m), 1517 (m), 1448 (s), 1364 (m), 1319 (m), 1257 (s), 1244 559
(s), 1184 (s), 1174 (s), 1081 (s), 1062 (m), 1040 (m), 1000 (m), 993 560
(m), 888 (m), 865 (m), 795 (s), 768 (m), 763 (m), 743 (m), 720 (m), 561
659 (w). BAM impact: 2 J. BAM friction: 5 N. ESD: 20 mJ. 562

Ammonium 1,3-Di(nitroimide)-1,2,3-triazolate (3). To a 563
suspension of **2** (0.27 g, 0.91 mmol) in 10 mL of distilled water was 564
added a solution of ammonium chloride (0.05 g, 0.91 mmol) in 10 mL 565
of distilled water. The mixture was heated to 80 °C for 3 h; the 566
precipitate was filtered off; and the remaining solvent in the filtrate was 567
removed under reduced pressure, leaving 0.13 g (0.65 mmol, 71%) of 568
3. DSC (5 °C min⁻¹): 184 °C (dec), IR (cm⁻¹) $\tilde{\nu}$ = 3507 (w), 3214 569
(m), 3158 (s), 3137 (s), 3063 (m), 2841 (m), 2271 (w), 1720 (w), 570
1652 (w), 1516 (w), 1390 (s), 1361 (s), 1262 (s), 1247 (s), 1180 (s), 571
1073 (s), 1054 (m), 999 (m), 953 (w), 856 (m), 795 (m), 783 (m), 572
768 (s), 720 (m), 660 (w); Raman (1064 nm) $\tilde{\nu}$ = 3162 (12), 3141 573
(12), 1541 (9), 1517 (32), 1362 (63), 1323 (16), 1251 (63), 1181 574
(10), 1078 (35), 1046 (16), 1008 (100), 870 (16), 774 (7), 735 (6), 575
722 (8), 663 (5), 637 (5), 494 (6), 441 (7), 406 (7), 381 (8), 325 576
(15); ¹H NMR (DMSO-*d*₆) δ (ppm) = 8.75 (d, 2H, CH), 7.12 (s, 577
broad, 4H, NH₄); ¹³C NMR (DMSO-*d*₆) δ (ppm) = 129.7 (s, 2C, 578
CH); *m/z* (FAB+) 18.03 (NH₄⁺); *m/z* (FAB-) 188.02 (C₂H₂N₇O₄⁻). 579
EA (C₂H₂N₇O₄NH₄, 206.12) calcd: C, 11.65; N, 54.36; H, 2.93. 580
Found: C, 11.58; N, 48.18; H, 2.80. BAM impact: 1 J. BAM friction: 581
20 N. ESD: 800 mJ. 582

Hydroxylammonium 1,3-Di(nitroimide)-1,2,3-triazolate (4). 583
To a solution of **2** (0.26 g, 0.88 mmol) in 10 mL of distilled water was 584
added a solution of hydroxylammonium chloride (0.09 g, 0.88 mmol) 585
in 10 mL of distilled water. The precipitate was filtered off, and the 586
remaining solvent in the filtrate was removed under reduced pressure, 587
leaving 0.11 g (0.52 mmol, 69%) of **4** (beige powder). DSC (5 °C 588
min⁻¹): 149 °C (dec), IR (cm⁻¹) $\tilde{\nu}$ = 3155 (m), 3145 (m), 3076 (m), 589
2909 (m), 2759 (m), 2691 (m), 1738 (w), 1624 (m), 1580 (w), 1546 590
(w), 1501 (m), 1430 (s), 1406 (s), 1371 (s), 1298 (s), 1264 (s), 1247 591
(s), 1192 (s), 1158 (s), 1076 (s), 1051 (m), 1008 (s), 867 (s), 791 (s), 592
768 (s), 723 (s), 698 (m), 660 (m); Raman (1064 nm) $\tilde{\nu}$ = 3160 (10), 593
3143 (9), 1669 (9), 1538 (12), 1428 (13), 1372 (44), 1331 (13), 1251 594
(52), 1188 (15), 1186 (25), 1056 (22), 1015 (100), 875 (12), 787 (9), 595
733 (11), 666 (9), 636 (9), 551 (9), 498 (10), 440 (12), 413 (11), 392 596
(11), 334 (18), 240 (17); ¹H NMR (DMSO-*d*₆) δ (ppm) = 9.93 (d, 597
broad, 3H, NH₃), 8.74 (d, 2H, CH), 1.02 (t, 1H, HO); ¹³C NMR 598
(DMSO-*d*₆) δ (ppm) = 129.7 (s, 2C, CH); *m/z* (FAB+) 34.03 599
(NH₄O⁺); *m/z* (FAB-) 188.02 (C₂H₂N₇O₄⁻). EA (C₂H₂N₇O₄NH₄O, 600
222.12) calcd: C, 10.81; N, 50.45; H, 2.72. Found: C, 11.30; N, 48.56; 601
H, 2.66. BAM impact: 1 J. BAM friction: 20 N. ESD: 200 mJ. 602

Hydrazinium 1,3-Di(nitroimide)-1,2,3-triazolate (5). To a 603
solution of **2** (0.62 g, 2.10 mmol) in 20 mL of distilled water was 604
added a solution of hydrazinium bromide (0.24 g, 2.10 mmol) in 20 605
mL of distilled water. The precipitate was filtered off, and the 606
remaining solvent in the filtrate was removed under reduced pressure, 607
leaving 0.46 g (2.08 mmol, 99%) of **5**. DSC (5 °C min⁻¹): 210 °C 608
(dec), IR (cm⁻¹) $\tilde{\nu}$ = 3451 (m), 3320 (s), 3240 (m), 3166 (s), 3145 609
(s), 3013 (s), 2934 (m), 2781 (m), 2707 (m), 2627 (s), 2506 (m), 610
2416 (m), 2274 (m), 2094 (w), 2026 (w), 1749 (w), 1691 (w), 1626 611
(m), 1582 (m), 1537 (m), 1509 (s), 1404 (s), 1385 (s), 1266 (s), 612
1245 (s), 1179 (s), 1085 (s), 1050 (s), 1003 (s), 978 (s), 856 (m), 838 613

614 (m), 785 (s), 760 (s), 727 (m); Raman (1064 nm) $\tilde{\nu}$ = 3282 (7), 3260
 615 (7), 3152 (11), 2827 (7), 2794 (7), 2699 (6), 2458 (4), 1629 (11),
 616 1509 (61), 1435 (13), 1338 (100), 1301 (30), 1249 (77), 1182 (9),
 617 1091 (98), 1047 (47), 1005 (93), 857 (45), 788 (8), 763 (7), 748 (7),
 618 729 (11), 632 (5), 650 (5), 536 (6), 530 (5), 434 (9), 389 (13), 351
 619 (12), 301 (20); ^1H NMR (DMSO- d_6) δ (ppm) = 8.73 (d, 2H, CH),
 620 7.00 (t, broad, 3H, NH₃), 2.47 (q, broad, 2H, NH₂); ^{13}C NMR
 621 (DMSO- d_6) δ (ppm) = 129.7 (s, 2C, CH); m/z (FAB⁺) 33.05
 622 (H₃N₂⁺); m/z (FAB⁻) 188.02 (C₂H₂N₇O₄⁻). EA (C₂H₂N₇O₄H₃N₂,
 623 221.14) calcd: C, 10.86; N, 57.01; H, 3.19. Found: C, 11.28; N, 51.59;
 624 H, 3.47. BAM impact: 5 J. BAM friction: 6 N. ESD: 100 mJ.

625 **Triaminoguanidinium 1,3-Di(nitroimide)-1,2,3-triazolate (6).**
 626 To a solution of **2** (0.69 g, 2.34 mmol) in 20 mL of distilled water was
 627 added a solution of triaminoguanidinium chloride (0.33 g, 2.34 mmol)
 628 in 50 mL of distilled water. The precipitate was filtered off, and the
 629 remaining solvent in the filtrate was removed under reduced pressure,
 630 leaving 0.65 g (2.22 mmol, 95%) of **6**. DSC (5 °C min⁻¹): 145 °C
 631 (mp), 185 °C (dec), IR (cm⁻¹) $\tilde{\nu}$ = 3446 (w), 3361 (m), 3345 (m),
 632 3221 (s), 3176 (m), 3029 (w), 2797 (w), 2707 (w), 2401 (w), 2274
 633 (w), 1912 (w), 1776 (w), 1678 (s), 1596 (w), 1546 (w), 1509 (w),
 634 1422 (m), 1399 (s), 1358 (m), 1290 (s), 1259 (s), 1240 (s), 1195
 635 (m), 1169 (m), 1158 (m), 1132 (m), 1070 (m), 1045 (w), 1001 (w),
 636 958 (m), 926 (s), 868 (m), 789 (m), 770 (m), 726 (w), 713 (w);
 637 Raman (1064 nm) $\tilde{\nu}$ = 3398 (5), 3349 (10), 3280 (15), 3264 (20),
 638 3241 (17), 3206 (13), 3176 (14), 3151 (13), 1681 (29), 1649 (29),
 639 1542 (30), 1512 (46), 1456 (30), 1411 (31), 1358 (61), 1325 (37),
 640 1241 (81), 1171 (32), 1139 (32), 1070 (64), 1048 (53), 1009 (100),
 641 871 (41), 772 (30), 716 (31), 637 (33), 491 (29), 402 (34), 367 (35),
 642 313 (33), 263 (37), 210 (47); ^1H NMR (DMSO- d_6) δ (ppm) = 8.75
 643 (d, 2H, CH), 8.58 (t, broad, 3H, NH), 4.48 (d, broad, 6H, NH₂); ^{13}C
 644 NMR (DMSO- d_6) δ (ppm) = 129.7 (s, 2C, CH); m/z (FAB⁺) 105
 645 (CH₉N₆⁺); m/z (FAB⁻) 188.02 (C₂H₂N₇O₄). EA (C₂H₂N₇O₄CH₉N₆,
 646 222.12) calcd: C, 12.29; N, 62.10; H, 3.78. Found: C, 12.76; N, 61.59;
 647 H, 3.59. BAM impact: >5 J. BAM friction: 20 N. ESD: 200 mJ.

648 ■ ASSOCIATED CONTENT

649 ■ Supporting Information

650 CIF files are available. This material is available free of charge
 651 via the Internet at <http://pubs.acs.org>.

652 ■ AUTHOR INFORMATION

653 Corresponding Author

654 tmk@cup.uni-muenchen.de

655 Notes

656 The authors declare no competing financial interest.

657 ■ ACKNOWLEDGMENTS

658 Financial support of this work by the Ludwig-Maximilian
 659 University of Munich (LMU), the U.S. Army Research
 660 Laboratory (ARL), the Armament Research, Development
 661 and Engineering Center (ARDEC), and the Office of Naval
 662 Research (ONR Global, title: "Synthesis and Characterization
 663 of New High Energy Dense Oxidizers (HEDO) - NICOP
 664 Effort") under contract nos. W911NF-09-2-0018 (ARL),
 665 W911NF-09-1-0120 (ARDEC), W011NF-09-1-0056
 666 (ARDEC), and 10 WPSEED01-002/WP-1765 (SERDP) is
 667 gratefully acknowledged. The authors acknowledge collabo-
 668 rations with Dr. Mila Krupka (OZM Research, Czech
 669 Republic) in the development of new testing and evaluation
 670 methods for energetic materials and with Dr. Muhamed
 671 Sucasca (Brodarski Institute, Croatia) in the development of
 672 new computational codes to predict the detonation and
 673 propulsion parameters of novel explosives. We are indebted
 674 to and thank Drs. Betsy M. Rice and Brad Forch (ARL,
 675 Aberdeen, Proving Ground, MD) and Mr. Gary Chen
 676 (ARDEC, Picatinny Arsenal, NJ) for the Cheetah calculation

and many inspired discussions and support of our work. Last
 but not least the authors thank Mr. St. Huber for the sensitivity
 measurements.

680 ■ REFERENCES

- (1) Zhang, M.-X.; Eaton, P. E.; Gilardi, R. *Angew. Chem., Int. Ed.* **2000**, *39*, 401–404. 681
- (2) Tao, G.-H.; Twamley, B.; Shreeve, J. M. *J. Mater. Chem.* **2009**, *19*, 683
5850–5854. 684
- (3) Klapötke, T. M.; Stierstorfer, J. *J. Am. Chem. Soc.* **2009**, *131*, 685
1122–1134. 686
- (4) Gao, H.; Shreeve, J. M. *Chem. Rev.* **2011**, *111*, 7377–7436. 687
- (5) Wang, R.; Xu, H.; Guo, Y.; Sa, R.; Shreeve, J. M. *J. Am. Chem. Soc.* **2010**, *132*, 11904–11905. 688
- (6) Binnikov, A. N.; Kulikov, A. S.; Makhov, N. N.; Orchinnikov, I. 690
V.; Pivina, T. *30th International Annual Conference of ICT*; Karlsruhe: 691
Germany, June 29–July 2, 1999; pp 58/1–58/10. 692
- (7) Huynh, M. H. V.; Hiskey, M. A.; Meyer, T. J.; Wetzler, M. *Proc.* 693
Natl. Acad. Sci. U.S.A. **2006**, *103*, 5409–5412. 694
- (8) Evers, J.; Klapötke, T. M.; Mayer, P.; Oehlinger, G.; Welch, J. 695
Inorg. Chem. **2006**, *45*, 4996–5007. 696
- (9) Lukin, K.; Li, J.; Gilardi, R.; Eaton, P. E. *Angew. Chem., Int. Ed.* 697
2000, *35*, 864–866. 698
- (10) Li, Y.-C.; Qi, C.; Li, S.-H.; Zhang, H.-J.; Sun, C.-H.; Yu, Y.-Z.; 699
Pang, S.-P. *J. Am. Chem. Soc.* **2010**, *132*, 12172–12173. 700
- (11) Adolph, H. G.; Holden, J. R.; Cichra, D. A. Relationships 701
between the impact sensitivity of high energy compounds and some 702
molecular properties which determine their performance; N, M, and 703
 ρ_0 . *Report No A101203*; Naval Surface Weapons Center, Dahlgren, 704
Virginia, 1981. 705
- (12) Carlqvist, P.; Ostmark, H.; Brinck, T. *J. Phys. Chem. A* **2004**, 706
108, 7463–7467. 707
- (13) Eaton, P. E.; Zhang, M.-X.; Gilardi, R.; Gelber, N.; Iyer, S.; 708
Surapeneni, R. *Propellants, Explos., Pyrotech.* **2001**, *27*, 1–6. 709
- (14) Inagake, S.; Goto, N. *J. Am. Chem. Soc.* **1987**, *109*, 3234–3240. 710
- (15) Noyman, M.; Zilberg, S.; Haas, Y. *J. Phys. Chem. A* **2009**, *113*, 711
7376–7382. 712
- (16) Tartakovsky, V. A. *Mater. Res. Soc. Symp. Proc.* **1996**, *418*, 15– 713
24. 714
- (17) Kalinin, A. V.; Apasov, E. T.; Ioffe, S. L.; Tartakovsky, V. A. *Bull.* 715
Acad. Sci. USSR, Div. Chem. Sci. **1991**, *40*, 988. 716
- (18) Kaihoh, T.; Itoh, T.; Yamaguchi, K.; Ohsawa, A. *J. Chem. Soc.,* 717
Chem. Commun. **1988**, 1608–1609. 718
- (19) Kaihoh, T.; Itoh, T.; Yamaguchi, K.; Ohsawa, A. *J. Chem. Soc.,* 719
Perkin Trans. 1 **1991**, 2045–2048. 720
- (20) Churakov, A. M.; Tartakovsky, V. A. *Chem. Rev.* **2004**, *104*, 721
2601–2616. 722
- (21) Rezhchikova, K. I.; Churakov, A. M.; Burshtein, K. Y.; 723
Shlyapochnikov, V. A.; Tartakovskii, V. A. *Mendeleev Commun.* **1997**, 724
7, 174–175. 725
- (22) Klapötke, T. M.; Piercey, D. G.; Stierstorfer, J.; Weyrauther, M. 726
Propellants, Explos., Pyrotech. **2012**, *37*, 527–535. 727
- (23) Shechter, H.; Venugopal, M.; Srinivasulu, D. Synthesis of 728
1,2,3,4-Tetrazine Di-N-Oxides, Pentazole Derivatives, Pentazine Poly- 729
N-oxides and Nitroacetylenes. *Project 746566, Grant No FA 9550–* 730
40–1-0410; USAF AFRL Arlington: VA, 2006. 731
- (24) Epszajn, J.; Katritzky, A. R.; Lunt, E.; Mitchell, J. W.; Roch, G. *J.* 732
Chem. Soc., Perkin Trans. 1 **1973**, 2622–2624. 733
- (25) Myasnikov, V. A.; Vyazkov, V. A.; Yudin, I. L.; Shitov, O. P.; 734
Tartakovskii, V. A. *Izv. Akad. Nauk SSSR, Ser. Khim.* **1991**, *5*, 1239. 735
- (26) Churakov, A. M.; Ioffe, S. L.; Tartakovskii, V. A. *Mendeleev* 736
Commun. **1996**, *6*, 20–22. 737
- (27) Shitov, O. P.; Vyazkov, V. A.; Tartakovskii, V. A. *Izv. Akad. Nauk* 738
SSSR, Ser. Khim **1989**, *11*, 2654–2655. 739
- (28) Frisch, M. J.; Trucks, G. W.; Schlegel, H. B.; Scuseria, G. E.; 740
Robb, M. A.; Cheeseman, J. R.; Scalmani, G.; Barone, V.; Mennucci, 741
B.; Petersson, G. A.; Nakatsuji, H.; Caricato, M.; Li, X.; Hratchian, H. 742
P.; Izmaylov, A. F.; Bloino, J.; Zheng, G.; Sonnenberg, J. L.; Hada, M.; 743

- 744 Ehara, M.; Toyota, K.; Fukuda, R.; Hasegawa, J.; Ishida, M.; Nakajima,
745 T.; Honda, Y.; Kitao, O.; Nakai, H.; Vreven, T.; Montgomery, Jr., J. A.;
746 Peralta, J. E.; Ogliaro, F.; Bearpark, M.; Heyd, J. J.; Brothers, E.; Kudin,
747 K. N.; Staroverov, V. N.; Kobayashi, R.; Normand, J.; Raghavachari, K.;
748 Rendell, A.; Burant, J. C.; Iyengar, S. S.; Tomasi, J.; Cossi, M.; Rega,
749 N.; Millam, J. M.; Klene, M.; Knox, J. E.; Cross, J. B.; Bakken, V.;
750 Adamo, C.; Jaramillo, J.; Gomperts, R.; Stratmann, R. E.; Yazyev, O.;
751 Austin, A. J.; Cammi, R.; Pomelli, C.; Ochterski, J. W.; Martin, R. L.;
752 Morokuma, K.; Zakrzewski, V. G.; Voth, G. A.; Salvador, P.;
753 Dannenberg, J. J.; Dapprich, S.; Daniels, A. D.; Farkas, Ö.;
754 Foresman, J. B.; Ortiz, J. V.; Cioslowski, J.; Fox, D. J. *Gaussian 09*,
755 Revision A2; Gaussian, Inc.: Wallingford CT, 2009.
- 756 (29) Becke, A. D. *J. Chem. Phys.* **1993**, *98*, 5648–5652.
- 757 (30) Lee, C.; Yang, W.; Parr, R. G. *Phys. Rev. B* **1988**, *37*, 785–789.
- 758 (31) Woon, D. E.; Dunning, T. H., Jr. *J. Chem. Phys.* **1993**, *98*, 1358–
759 1371.
- 760 (32) Kendall, R. A.; Dunning, T. H., Jr.; Harrison, R. J. *J. Chem. Phys.*
761 **1992**, *96*, 6796–6806.
- 762 (33) Dunning, T. H., Jr. *J. Chem. Phys.* **1989**, *90*, 1007–1023.
- 763 (34) Peterson, K. A.; Woon, D. E.; Dunning, T. H., Jr. *J. Chem. Phys.*
764 **1994**, *100*, 7410–7415.
- 765 (35) Klapötke, T. M.; Stierstorfer, J.; Wallek, A. U. *Chem. Mater.*
766 **2008**, *20*, 4519–4530.
- 767 (36) Arriau, J.; Deschamps, J. *Tetrahedron Lett.* **1974**, *44*, 3865–3868.
- 768 (37) Huang, Y.; Gao, H.; Twamley, B.; Shreeve, J. M. *Eur. J. Inorg.*
769 *Chem.* **2008**, 2560–2568.
- 770 (38) Laus, G.; Kahlenberg, V.; Toebbens, D. M.; Jetty, R. K. R.;
771 Greisser, U. J.; Schuetz, J.; Kristeva, E.; Wurst, K.; Schottenberger, H.
772 *Cryst. Growth Des.* **2006**, *6*, 404–410.
- 773 (39) Li, J.; Duke, B.; McWeeny, R. *VB2000*, version 2.1; SciNet
774 Technologies: San Diego, CA, 2009.
- 775 (40) Li, J.; McWeeny, R. *Int. J. Quantum Chem.* **2002**, *89*, 208–216.
- 776 (41) Ilyushin, M. A.; Terpigorev, A. N.; Tselinskii, I. V. *Russ. J. Gen.*
777 *Chem.* **1999**, *69*, 1654–1657.
- 778 (42) Ochterski, J. W.; Petersson, G. A.; Montgomery, J. A., Jr. *J.*
779 *Chem. Phys.* **1996**, *104*, 2598.
- 780 (43) Montgomery, J. A., Jr.; Frisch, M. J.; Ochterski, J. W.; Petersson,
781 G. A. *J. Chem. Phys.* **2000**, *112*, 6532.
- 782 (44) (a) Curtiss, L. A.; Raghavachari, K.; Redfern, P. C.; Pople, J. A. *J.*
783 *Chem. Phys.* **1997**, *106*, 1063. (b) Byrd, E. F. C.; Rice, B. M. *J. Phys.*
784 *Chem. A* **2006**, *110*, 1005–1013. (c) Rice, B. M.; Pai, S. V.; Hare, J.
785 *Combust. Flame* **1999**, *118*, 445–458.
- 786 (45) (a) Jenkins, H. D. B.; Roobottom, H. K.; Passmore, J.; Glasser,
787 L. *Inorg. Chem.* **1999**, *38*, 3609–3620. (b) Jenkins, H. D. B.; Tudela,
788 D.; Glasser, L. *Inorg. Chem.* **2002**, *41*, 2364–2367.
- 789 (46) Nielsen, A. T. *Nitrocarbons*, 1st ed.; Wiley-VCH: Weinheim,
790 1995.
- 791 (47) (a) Sućeska, M. *Mater. Sci. Forum* **2004**, 465–466, 325–330.
792 (b) Sućeska, M. *Propellants, Explos., Pyrotech.* **1999**, *24*, 280–285.
793 (c) Sućeska, M. *Propellants, Explos., Pyrotech.* **1991**, *16*, 197–202.
- 794 (48) Lu, J. P. *Evaluation of the Thermochemical Code—CHEETAH 2.0*
795 *for Modelling Explosives Performance*; DSTO Aeronautical and
796 Maritime Research Laboratory: Edinburgh, 2001.
- 797 (49) Sućeska, M. *Test Methods for Explosives*; Springer: New York,
798 1995; p 21 (impact), p 27 (friction).
- 799 (50) www.bam.de.
- 800 (51) NATO standardization agreement (STANAG) on explosives,
801 impact sensitivity tests, no. 4489, Ed. 1, Sept. 17, 1999.
- 802 (52) WIWEB-Standardarbeitsanweisung 4–5.1.02, Ermittlung der
803 Explosionsgefährlichkeit, hier der Schlagempfindlichkeit mit dem
804 Fallhammer, Nov. 8, 2002.
- 805 (53) <http://www.reichel-partner.de>.
- 806 (54) NATO standardization agreement (STANAG) on explosives,
807 friction sensitivity tests, no. 4487, Ed. 1, Aug. 22, 2002.
- 808 (55) WIWEB-Standardarbeitsanweisung 4–5.1.03, Ermittlung der
809 Explosionsgefährlichkeit oder der Reibeempfindlichkeit mit dem
810 Reibeapparat, Nov. 8, 2002.
- 811 (56) Impact: Insensitive > 40 J, less sensitive ≥ 35 J, sensitive ≥ 4 J,
812 very sensitive ≤ 3 J; Friction Insensitive > 360 N, less sensitive = 360
N, sensitive < 360 N a. > 80N, very sensitive ≤ 80 N, extremely
sensitive ≤ 10 N. According to the UN Recommendations on the
Transport of Dangerous Goods.
(57) Klapötke, T. M.; Piercey, D. G. *Inorg. Chem.* **2011**, *50*, 2732–
2734. 815
817
(58) Klapötke, T. M.; Piercey, D. G.; Stierstorfer, J. *Eur. J. Inorg.*
Chem. **2012**, DOI: 10.1002/ejic.201201237. 818
819

The Synthesis and Energetic Properties of 5,7-Dinitrobenzo-1,2,3,4-tetrazine-1,3-dioxide (DNBTDO)

Thomas M. Klapötke,^{*[a, b]} Davin G. Piercey,^[a] Jörg Stierstorfer,^[a] and Michael Weyrauther^[a]

Abstract: Energetic tetrazine-1,3-dioxide, 5,7-dinitrobenzo-1,2,3,4-tetrazine-1,3-dioxide (**DNBTDO**), was synthesized in 45% yield. **DNBTDO** was characterized as an energetic material in terms of performance (V_{det} 8411 m s^{-1} ; $p_{\text{C-J}}$ 3.3×10^{10} Pa at a density of 1.868 g cm^{-3}), mechanical sensitivity

(impact and friction as a function of grain size), and thermal stability (T_{dec} 204 °C). **DNBTDO** exhibits a sensitivity slightly higher than that of **RDX**, and a performance slightly lower (96% of **RDX**).

Keywords: DNBTDO · Nitrogen heterocycles

1 Introduction

High nitrogen heterocycles are a recurring pattern in the research of highly energetic materials [1–5]. The number of linked nitrogen atoms is directly correlated with the heat of formation of the compound, as a result of the energetically-favored formation of dinitrogen gas. For example 1,1'-azobis(1,2,4-triazole) (676 kJ mol^{-1}) has a lower heat of formation than 1,1'-azobis(1,2,3-triazole) (962 kJ mol^{-1}), both of which have lower heats of formation than 1,1'-azobis(tetrazole) (1030 kJ mol^{-1}) [1,5]. This is in contrast to classical explosives such as 1,3,5-trinitro-1,3,5-triazinane (**RDX**) and 1,3,5,7-tetranitro-1,3,5,7-tetrazocane (**HMX**), which derive their enthalpy of detonation through oxidation of the backbone (Figure 1).

Currently used explosives suffer from problems ranging from high sensitivity to posing an environmental hazard. **RDX** is widely used in formulations with polymeric binders and plasticizers such as PBXN-107 (86/14 **RDX/HTPB**) or C4 (90/10: **RDX/PIB**). This use is despite concerns about the toxicity of **RDX** [6,7]. In order to be considered as a candidate explosive, a nitrogen-rich material requires sufficient performance (comparable to or greater than **RDX**), and sufficient thermal (T_{dec} above 180 °C) and mechanical stability (impact, friction, shock), while having a lower toxicity [8,9].

One of the currently pursued strategies in the development of new advanced energetic materials are 1,2,4,5 and 1,2,3,4-tetrazines (Figure 2). The former class of compounds, as well as their 1,4-dioxides are well known and are high performing energetic materials, including LAX-112 (3,6-dia-



Figure 2. Structures of 1,2,4,5- and 1,2,3,4-tetrazine.

mino-1,2,4,5-tetrazine-1,4-dioxide), which was once considered a prospective **RDX** replacement [10].

In contrast, simple 1,2,3,4-tetrazines are rarely reported in the literature, with only one known example being stable [11a]. However the oxidation product 1,2,3,4-tetrazine-1,3-dioxide moiety, is far more abundant in the literature and compounds with remarkable thermal stability have been reported, some members of this class of compounds decomposing above 200 °C [11b,15]. This stabilization is understood to result from the *N*-oxide removing lone pair electron density (increasing σ - π separation) that would otherwise destabilize the nitrogen system by donating electron density into antibonding orbitals [12–14]. Due to the zwitterionic character of the *N*-oxides, the densities of the 1,2,3,4-tetrazine-1,3-dioxides are often high, with short N–N bond lengths due to what has been termed “Alternating Positive Negative Charge” theory. (Figure 3) Application of 1,2,3,4-tetrazine-1,3-dioxides in theoretical energetic materials has led to materials with calculated properties being



Figure 1. Structures of 1,2,4-triazole, 1,2,3-triazole, and 1,2,3,4-tetrazole, respectively.

[a] T. M. Klapötke, D. G. Piercey, J. Stierstorfer, M. Weyrauther
Energetic Materials Research, Department of Chemistry, Ludwig-Maximilian University Munich, Butenandtstr. 5–13, 81377 Munich, Germany
*e-mail: tmk@cup.uni-muenchen.de

[b] T. M. Klapötke
Center for Energetic Concepts Development, CECD, Department of Mechanical Engineering
University of Maryland, UMD, College Park, MD 20742, USA

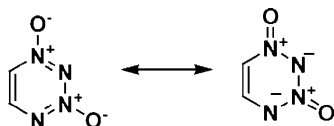


Figure 3. Isomerization as described by APNC Theory.

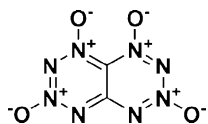
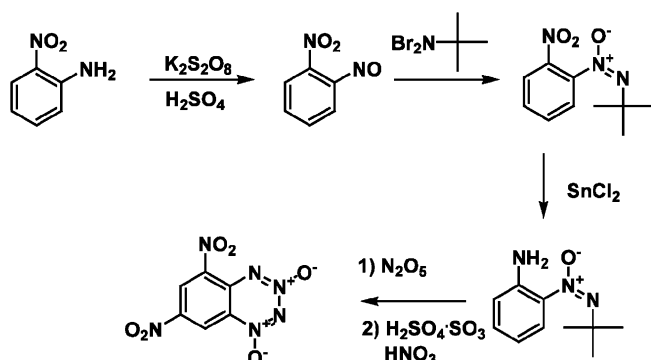


Figure 4. Formula of DTTO.



Scheme 1. Synthesis of DNBDTO.

among the most powerful explosives in existence such as **DTTO** [16] (Figure 4).

Unfortunately, the majority of 1,2,3,4-tetrazine-1,3-dioxides that have been prepared so far bear an annulated benzene ring [11]. However, annulated pyridines and the more explosive furazan are also known [17, 18]. There is only one known non-annulated 1,2,3,4-tetrazine-1,3-dioxide, which is the dicyano derivative [19]. Of the known tetrazine dioxides 5,7-dinitrobenzo-1,2,3,4-tetrazine-1,3-dioxide is one of the most facile prepared from the reaction of 2-*tert*-butyl-1-(2-anilino)-diazine-1-oxide (**BADO**) with N_2O_5 in dichloromethane, followed by nitration with nitric acid and oleum in a one-pot synthesis. The precursor **BADO** is available from 2-nitro-aniline in a three step process (Scheme 1) [20].

In this study we have prepared 5,7-dinitrobenzo-1,2,3,4-tetrazine-1,3-dioxide (**DNBDTO**), by the literature procedure [20] in 45% yield, and we report the full chemical (NMR, IR, Raman, mass spectra, and crystallographic proof) and explosive (impact, friction, static sensitivities and calculated performance) properties.

2 Experimental Section

2.1 General

All reagents and solvents were used as received (Sigma-Aldrich, Fluka, and Acros Organics). 2-*tert*-Butyl-1-(2-anilino)-

diazine-1-oxide was prepared by the literature procedure [20]. Decomposition temperature measurements were performed with a Linseis DSC at a heating rate of 5°C min^{-1} (in air). ^1H , ^{13}C , and ^{15}N NMR spectra were recorded with a Jeol Eclipse 400 instrument. All chemical shifts are in ppm relative to TMS (^1H , ^{13}C) or nitromethane (^{15}N). IR spectra were recorded with a Perkin-Elmer Spectrum One FT-IR instrument. Raman spectra were measured with a Perkin-Elmer Spectrum 2000R NIR FT-Raman instrument equipped with a Nd-YAG laser (1064 nm). Elemental analyses were performed with a Netzsch STA 429 Simultaneous Thermal Analyser.

2.2 Synthesis of 1,2,3,4-Tetrazine-1,3-dioxide: 5,7-Dinitrobenzo-1,2,3,4-tetrazine-1,3-dioxide (DNBDTO)

Caution! The prepared compound is an explosive with sensitivity towards various stimuli. Although we had no problems during synthesis, proper protective equipment (Kevlar gloves and wrist protectors, face shield, ear protection, and thick leather coat) should be worn. Extra precautions should be taken when working on larger scale.

According to the literature procedure, 2-*tert*-butyl-1-(2-anilino)-diazine-1-oxide (0.85 g, 4.4 mmol) was dissolved in dichloromethane (25 mL) and cooled to -20°C . While maintaining this temperature, dinitrogen pentoxide (2.7 g, 25 mmol) was added in a nitrogen atmosphere. The temperature was allowed to rise to 0°C over 1/2 h, and was stirred at this temperature for 15 min. A solution of nitric acid (100%, 4 mL, 95 mmol) in oleum (6 mL, 20%) was added. The mixture was heated to 80°C and the temperature was maintained for 2 h to evaporate the dichloromethane. After cooling to room temperature, the mixture was poured very slowly into an ice/water slurry. Afterwards, it was filtered and rinsed with water, followed by recrystallization from dichloroethane yielding 0.5 g (45%) of **DNBDTO** as yellow crystals. M.p. 204°C (dec.) (DSC, 5°C min^{-1}). IR: $\tilde{\nu}=3099$ (w), 1602 (m), 1541 (s), 1516 (s), 1474 (m), 1435 (m), 1336 (vs), 1267 (w), 1184 (m), 1080 (w), 993 (w), 915 (m), 860 (m), 800 (m), 776 (w), 735 (s), 708 (w), 671 (w) cm^{-1} . Raman (200 mW): 3078 (16), 1622 (83), 1548 (57), 1518 (55), 1477 (52), 1437 (57), 1370 (88), 1346 (100), 1191 (49), 1081 (57), 1056 (53), 992 (49), 938 (50), 756 (45), 711 (45), 330 (49), 99 (70) cm^{-1} . ^1H NMR (acetone- d_6 , 400.18 MHz, 25°C , TMS): $\delta=9.42$ (d, 1 H, $^4J_{\text{HH}}=2.40$ Hz), 9.32 (d, 1 H, $^4J_{\text{HH}}=2.40$ Hz) ppm. ^{13}C NMR (acetone- d_6 , 100.63 MHz, 25°C , TMS): $\delta=146.5$ (1C), 142.0 (1C), 140.0 (1C), 127.3 (1C), 126.4 (1C), 119.2 (1C) ppm. ^{14}N NMR (acetone- d_6 , 40.55 MHz, 25°C , acetone- d_6): $\delta=-17$ (2N, NO_2), -36 (1N, $\text{N}_4\text{-O}$), -41 (1N, $\text{N}_2\text{-O}$) ppm. EA: $\text{C}_6\text{H}_2\text{N}_6\text{O}_6$ (Mw = 254.12 g mol^{-1}): calcd. C 28.36; H 0.79; N 33.07%; found: C 28.05; H 0.83; N 32.96%. MS DEI+ m/z (%) 254.2 (30) [M^+] 209.1 (56) [$\text{M}-\text{NO}_2$], 181.1 (20) [$\text{M}-\text{N}_2\text{O}_3$], 120.1 (54) [$\text{M}-\text{NO}_2-\text{N}_4\text{O}_2$], 62.1 (68) [NO_3], 74.09 (66) [$\text{M}-\text{N}_2\text{O}_2-\text{N}_4\text{O}_2$], 30.1 (100) [NO]; Impact sensitivity: 5 J. Friction Sensitivity: 360 N. Electrostatic Discharge Sensitivity: 0.15 J.

Crystallographic data (excluding structure factors) for the structure in this paper have been deposited with the Cambridge Crystallographic Data Centre, CCDC, 12 Union Road, Cambridge CB21EZ, UK. Copies of the data can be obtained free of charge on quoting the depository number CCDC-854937 (Fax: +44-1223-336-033; E-Mail: deposit@ccdc.cam.ac.uk, <http://www.ccdc.cam.ac.uk>).

3 Results and Discussion

3.1 X-ray Structure

After recrystallization from dichloroethane, crystals of DNBTDO suitable for single-crystal X-ray structure determination were obtained. The molecular structure of the crystalline DNBTDO is shown in Figure 5.

The molecular structure was determined with an Oxford Xcalibur3 diffractometer with a Spellman generator (voltage 50 kV, 40 mA current) and a KappaCCD detector. The data collection and reduction was performed using the CrysAlis Pro software [21,22]. The structure was solved using the SIR-92 program [23], refined with SHELXL-97 [24], and finally checked with PLATON software [25]. The hydrogen atoms were located and refined. Relevant data and parameters of the X-ray measurement and refinement are given in Table 1.

DNBTDO crystallizes in the space group $Pca2_1$, with eight formula units in the unit cell and a density of 1.868 g cm^{-3} . The bond lengths within the tetrazine ring and its N-oxides are as expected and lie between that of a single and double bond, however, the oxide bonds are generally closer to double-bond length and shorter than N–N bond lengths in the tetrazine ring indicating the significant resonance contribution of the "Alternating Positive Negative Charge" resonance form as described above. The wave-like packing arrangement of DNBTDO within the unit cell is

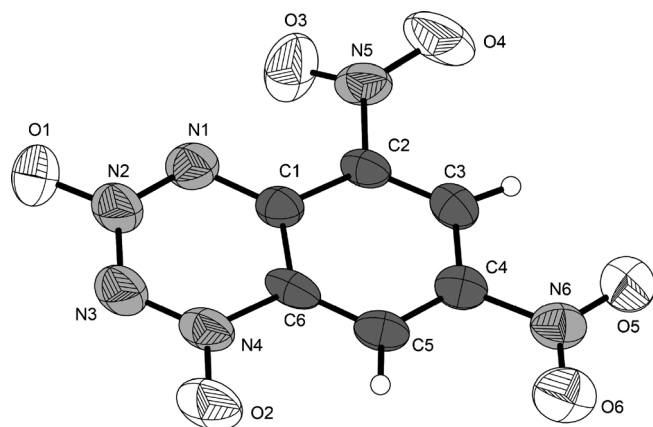


Figure 5. Molecular structure of DNBTDO in the crystalline state. Non-hydrogen displacement ellipsoids are shown at the 50% probability level.

Table 1. Crystal data and structure refinement parameters of DNBTDO.

Formula	$\text{C}_6\text{H}_2\text{N}_6\text{O}_6$
Formula Mass/ g mol^{-1}	254.14
Crystal System	$Pca2_1$
Space group	orthorhombic
a/pm	988.9(2)
b/pm	1785.9(3)
c/pm	1023.4(1)
$\alpha/^\circ$	90
$\beta/^\circ$	90
$\gamma/^\circ$	90
V/pm^3	$1.8075 \times 10^9(5)$
Z	8
$\rho_{\text{calc}}/\text{g cm}^{-3}$	1.868
T/K	173
R_1/wR_2 (all data)	0.0874/0.1586
R_1/wR_2 ($I > 2\sigma$)	0.0583/0.1342
S	1.049
Device type	Oxford Xcalibur3 CCD
Solution	SIR-92
Refinement	SHELXL-97
Absorpt. corr.	Multi-Scan
CCDC No.	854937

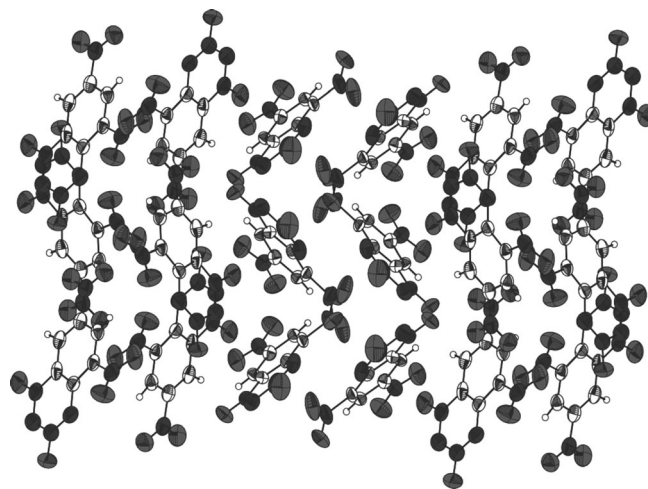


Figure 6. Wave-like packing arrangement of DNBTDO within the unit cell.

shown in Figure 6. These results are in accordance with those in the literature [20].

3.2 Infrared Spectroscopy

DNBTDO was analyzed by infrared spectroscopy. The strongest band occurs at 1333 cm^{-1} and is assigned to symmetric nitro group C–N stretching. The characteristic vibrations of the tetrazine dioxide system occur at 1516 and 1435 cm^{-1} (literature: 1520 and 1432 cm^{-1}) and arise from the synphase and antiphase N=N vibrations [11].

3.3 Mass Spectra

The $M+$ peak was detected at 254.2 m/z during a $DEI+$ experiment. Loss of one nitro group, one nitro group, and the tetrazine dioxide ring, and two nitro groups and the tetrazine dioxide ring are observed at 209.1, 120.1, and 74.09 m/z , respectively.

3.4 NMR Spectroscopy

3.4.1 ^1H NMR

The two protons in **DNBTDO** yield two resonances at $\delta = 9.42$ and 9.32 ppm. The shift difference between the two is too small to be able to definitely assign, which shift belongs to which proton. The coupling constant between the two is 2.40 Hz

3.4.2 ^{13}C NMR

The benzene ring of **DNBTDO** yields six separate peaks. The literature assignments for these carbon atoms are 146.5:C5, 142.0:C3, 140.0:C2, 127.3:C1, 126.4:C4, 119.2:C6 [11].

3.4.3 ^{14}N NMR

The spectrum shows three resonances. The first at $\delta = -17$ ppm ($\Delta\nu_{1/2} = 50$ Hz) corresponds to the nitrogen of the aromatic nitro groups (N5, N6), while the remaining two resonances are resulting from the N-oxides of the tetrazine dioxide -36 ($\Delta\nu_{1/2} = 40$ Hz) and -41 ppm ($\Delta\nu_{1/2} = 40$ Hz) for N4 and N2 respectively [11]. N1 and N3 are not observed.

3.5 Differential Scanning Calorimetry (DSC)

For determination of the decomposition temperature of **DNBTDO**, a differential scanning calorimetry (DSC) experiment was run at a heating rate of 5 K min^{-1} . Exothermic decomposition occurred beginning at 204°C . No melting event was observed prior to decomposition. A manual melting point determination was also performed and again no melting was observed prior to an onset of decomposition at 211.8°C

3.6 Explosive Properties

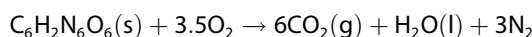
3.6. Experimental Sensitivities

For initial safety testing, impact, friction, and electrostatic discharge sensitivities were determined. Impact sensitivity was carried out according to STANAG 4489 [26] and modified according to Ref. [27] on a BAM drophammer [28,29]. Friction sensitivity was carried out in accordance with STANAG 4487 [30] and modified according to Ref. [31]. Sensitivity towards electrostatic discharge (ESD) was deter-

mined [32,33] on a small scale electric spark tester ESD 2010EN (OZM Research) operating with the "Winspark 1.15 software package" [34]. **DNBTDO** had its sensitivities determined at four particle sizes; $< 100 \mu\text{m}$, $100\text{--}500 \mu\text{m}$, $500\text{--}1000 \mu\text{m}$, and $> 1000 \mu\text{m}$. For these particle sizes the impact sensitivity was determined to be 6, 5, 4 and 4 J, respectively, whereas the friction sensitivity was found to be constant at 360 N for all of these particle sizes. Electrostatic discharge sensitivity (ESD) was determined at $100\text{--}500 \mu\text{m}$ to be 0.15 J. According to the UN Recommendations on the Transport of Dangerous Goods, **DNBTDO** is classified as sensitive [35].

3.6.2 Bomb Calorimetry

The heat of combustion of **DNBTDO** was determined to be 14846 kJ g^{-1} using a Parr 1356 bomb calorimeter. ΔH_f° was calculated at 298.15 K using Hess' law and the following combustion reaction:



The calculated solid state energy of formation for **DNBTDO** is an endothermic $+420 \text{ kJ mol}^{-1}$.

3.6.3 Computational Properties

3.6.3.1 Theoretical Calculations

All calculations were carried out using the Gaussian G09W (revision B.09) program package [36]. The enthalpies (H) and free energies (G) were calculated using the complete basis set (CBS) method of Petersson and co-workers in order to obtain very accurate energies. The CBS models use the known asymptotic convergence of pair natural orbital expressions to extrapolate from calculations using a finite basis set to the estimated complete basis set limit. CBS-4 begins with a HF/3-21G(d) geometry optimization; the zero point energy is computed at the same level. It uses a large basis set SCF calculation as a base energy, and a MP2/6-31+G calculation with a CBS extrapolation to correct the energy through second order. A MP4(SDQ)/6-31+(d,p) calculation is used to approximate higher order contributions. In this study we applied the modified CBS-4 M method (M referring to the use of Minimal Population localization), which is a re-parameterized version of the original CBS-4 method and also includes some additional empirical correc-

Table 2. CBS-4 M results.

	Point group	$-H_f^{298}/\text{a.u.}$
DNBTDO	C_s	1008.059173
H		0.500991
C		37.786156
N		54.522462
O		74.991202

5,7-Dinitrobenzo-1,2,3,4-tetrazine-1,3-dioxide (DNBTDO)

Table 3. Literature values for atomic $\Delta H_f^{298}/\text{kJ mol}^{-1}$.

	NIST [39]
H	218.1
C	717.2
N	473.1
O	249.5

Table 4. Enthalpies of the gas-phase species M.

M	M	$\Delta H_f(\text{g,M})/\text{kJ mol}^{-1}$
DNBTDO	$\text{C}_6\text{H}_2\text{N}_6\text{O}_6$	515.0

Table 5. Solid state energies of formation (ΔU_f°).

	$\Delta H_f(\text{s})$ /kJ mol ⁻¹	Δn	$\Delta U_f(\text{s})$ /kJ mol ⁻¹	M /g mol ⁻¹	$\Delta U_f(\text{s})$ /kJ kg ⁻¹
DNBTDO	475.3	-7	442.7	254.14	1741

tions [37]. The enthalpies of the gas-phase species M were computed according to the atomization energy method (Equation (1)) (Table 2, Table 3, and Table 4) [38].

$$\Delta H_f^\circ(\text{g, M, 298}) = H_{(\text{Molecule, 298})} - \sum H_{(\text{Atoms, 298})}^\circ + \sum \Delta H_f^\circ(\text{Atoms, 298}) \quad (1)$$

The solid state energy of formation (Table 5) of DNBTDO was calculated by subtracting the gas-phase enthalpy with the heat of sublimation (77.9 kJ mol^{-1}) obtained by the Troutman rule ($\Delta H_{\text{sub}} = 188 \cdot T_m$ ($T_m = 204^\circ\text{C}$)) [40]. The molar standard enthalpy of formation (ΔH_m) was used to calculate the molar solid state energy of formation (ΔU_m) according to Equation (2) (Table 5).

$$\Delta U_m = \Delta H_m - \Delta nRT \quad (2)$$

(Δn being the change of moles of gaseous components) The calculated solid state energy of formation of $442.7 \text{ kJ mol}^{-1}$ agrees well with the value determined from bomb calorimetry of 420 kJ mol^{-1} .

3.6.3.2 Detonation Parameters

The calculation of the detonation parameters was performed with the program package EXPLO5 (version 5.04) [41]. The program is based on the chemical equilibrium, steady-state model of detonation. It uses the Becker–Kistia–Wilson's equation of state (BKW EOS) for gaseous detonation products and Cowan–Fickett's equation of state for solid carbon [42]. The calculation of the equilibrium composition of the detonation products is done by applying modified White, Johnson, and Dantzig's free energy minimization technique.

Table 6. Detonation parameters.

	DNBTDO	RDX
$\rho/\text{g cm}^{-3}$	1.868	1.80
$\Omega/\%$	-44.07	-21.61
$Q_v/\text{kJ kg}^{-1}$	-6306.7	-6125
T_{ex}/K	4659	4236
$p_{\text{C-J}}/\text{GPa}$	33.0	34.9
$V_{\text{det}}/\text{m s}^{-1}$	8411	8748
$V_0/\text{L kg}^{-1}$	576	739

The detonation parameters calculated with the EXPLO5 program using the experimentally determined densities (X-ray) are summarized in Table 6.

DNBTDO has a calculated detonation velocity of 8411 m s^{-1} and pressure of 33.0 GPa. These values are both lower than those of RDX, however they are high for energetic materials containing the benzene ring, i.e. when compared to trinitrotoluene (TNT) and triaminotrinitrobenzene (TATB) both of which have detonation velocities below 7500 m s^{-1} . These results confirm the highly energetic nature of the 1,2,3,4-tetrazine-1,3-dioxide moiety.

3.6.3.3 Small-Scale Shock Reactivity Test

The Small-Scale Shock Reactivity Test (SSRT) [43] was introduced by researchers at IHDIV, DSWC (Indian Head Division, Naval Surface Warfare Center). The SSRT measures the shock reactivity (explosiveness) of energetic materials, often well-below critical diameter, without requiring a transition to detonation. The test setup combines the benefits from a lead block test [44] and a gap test [45]. In comparison to gap tests, the advantage is the use of a large smaller sample size of the tested explosive (ca. 500 mg). The sample volume V_s is recommended to be 0.284 mL (284 mm^3). For our test setup, shown in Figure 7a–c, no possible attenuator (between detonator and sample) and air gap (between sample and aluminum block) was used.

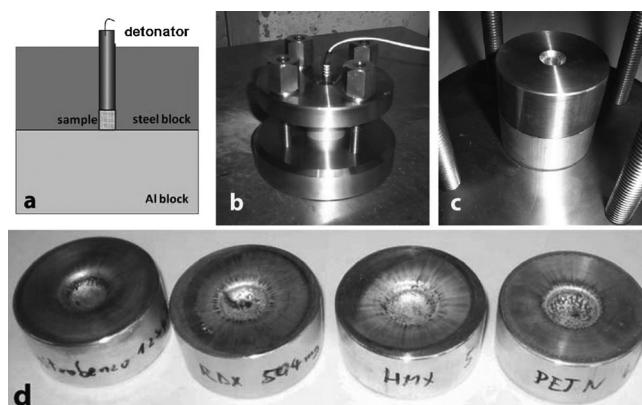


Figure 7. Small Scale Shock Reactivity Test (SSRT). (a) Schematic setup. (b) Picture of the overall setup. (c) Steel cyclinder on top of the aluminum cyclinder (d) Test results.

Table 7. Results from the Small Scale Shock Reactivity Test (SSRT).

Explosive	Weight/mg	Dent/mg SiO ₂
DNBTDO	505	744
RDX	504	589
HMX	534	972
PETN	482	917

The used sample weight m_s (504 mg) was calculated by the formula $V_s \cdot \rho_{\text{Xray}} \cdot 0.95$. Several tests with commonly used explosives such as **PETN**, **RDX**, and **HMX** were performed in order to get different dents within the aluminum plate. The dent sizes were measured by filling them with fine quartz sand and back-calculating the volume from the corresponding SiO₂ mass.

As it can also be seen from Figure 7, the dent resulted from **DNBTDO** is larger than that of **RDX** but smaller than that of **HMX** and **PETN**. Quantitative values were summarized in Table 7. Due to the large dent in the case of **PETN** we conclude that the obtained results also depend from the sensitivity of the explosive and also from the critical diameter. The lower these values, the larger is the impact on the aluminum plate. From the SSRT it can be inferred that the explosiveness of **DNBTDO** is higher than that of **RDX** but lower than those of **HMX** and **PETN**.

3.6.3.4 Cylinder Runs

As was already discussed extensively in the literature, it is not the detonation velocity that determines how quickly metal fragments are ejected from an explosive charge, but the so-called Gurney velocity [46]. This question was investigated in the work of Ronald W. Gurney in 1943 [47]. Gurney suggested that there was a simple dependence relating the mass of the metal confinement (M) and the explosive (C) on the fragment velocity (V). The simple Gurney model developed in Aberdeen (MD) presumes the following:

- (i) The energy released on detonation is essentially completely changed into the kinetic energy of the detonation gases and kinetic energy of the metal fragments;
- (ii) The energy used for the deformation or fragmentation of the confinement material can be essentially ignored;
- (iii) During detonation, the explosive is spontaneously ($\Delta t=0$) transformed into homogeneous, chemically completely changed, gaseous products under high pressure;
- (iv) The gaseous detonation products expand with uniform density and a linear velocity gradient;
- (v) The chemical detonation energy of the explosive is changed into kinetic energy, until the fragments have a steady-state velocity, from which the Gurney velocity can be calculated.

The fragment velocity is largely dependent on the shape of the charge. For cylindrical charges (which are a good approximation for most bomb and missile (rocket) warheads) the following equation is a good approximation:

$$\frac{V}{\sqrt{2E}} = \left(\frac{M}{C} + \frac{1}{2} \right)^{-0.5}$$

The constant $\sqrt{2E}$ is the so-called Gurney velocity (in km s^{-1}), which is dependent on the nature of the explosive. The Gurney velocity $\sqrt{2E}$ is decisive for the performance of the explosive used. It was only in 2002 that A. Koch et al. could show that the Gurney velocity $\sqrt{2E}$ and the detonation velocity (D) of an explosive can be described approximately using the following simple relationship [48]:

$$\sqrt{2E} = \frac{3\sqrt{3}}{16} D \approx \frac{D}{3.08}$$

Of course, the Gurney velocity can also be determined experimentally using the measured fragment velocity V. It can be concluded that the relationship discussed above provides a good approximation, but that the Gurney velocity is also dependent on other factors including, for example, the material of the confinement used (in particular its density).

The cylinder test provides an experimental method to measure the effectiveness of an explosive. The radial expansion on detonation of a metallic cylinder (usually copper) filled with a high explosive is observed [49]. A streak camera or a laser method might be used. The detonation velocity is determined simultaneously. The equation of state (EOS) of the detonation products is derived using Gurney theory.

Using the Cheetah code [50], in the "cylinder runs" output section of the summary sheet, information on the adiabat is given. The term cylinder run is used, because the cylinder test is the best experimental measurement of the adiabat. Relative V/V_0 volumes are shown along with the calculated energy. The energies are compared to **TATB** at 1.83 g cm^{-3} , **PETN** at 1.76 g cm^{-3} , and **HMX** at 1.89 g cm^{-3} . The comparison is given in terms of percentages, 100 percent indicating no difference. We calculated the cylinder energies (E_c) for **DNBTDO** and for **RDX** for comparison (Table 8). It is evident from Table 8 that the cylinder energy for **DNBTDO** is comparable to but slightly larger than that of **RDX**, which is also in accord with the result from the SSRT test (see above).

4 Conclusions

From this combined experimental and theoretical study the following conclusions can be drawn

5,7-Dinitrobenzo-1,2,3,4-tetrazine-1,3-dioxide (DNBTDO)

Table 8. Calculated cylinder energies (E_c) for DNBTDO and for RDX.

Compound	V/V_0	$E_c/\text{kJ cm}^{-3}$	% of Standard			
			TATB	PETN	HMX	CI-20
DNBTDO						
2.2		-7.05	145	111	94	78
RDX						
2.2		-6.94	143	109	93	77

- (i) 1,2,3,4-Tetrazine-1,3-dioxides are high-performance energetic materials even when the explosophoric tetrazine dioxide is "diluted" with low-performing aromatics.
- (ii) 1,2,3,4-Tetrazine-1,3-dioxides have the capability to be used in thermally stable energetic materials.
- (iii) Mechanical sensitivities and explosive performances of DNBTDO are higher than, and lower than those possessed by RDX, respectively.
- (iv) DNBTDO shows a higher explosiveness in the SSRT (small-scale shock reactivity test) than RDX.
- (v) DNBTDO has slightly higher calculated cylinder energy than RDX.

Symbols and Abbreviations:

D	Detonation velocity/ m s^{-1}
δ	Chemical shift (ppm)
DNBTDO	5,7-Dinitrobenzo-1,2,3,4-tetrazine-1,3-dioxide
DTTO	Ditetrazine-tetraoxide
ΔH_f	Heat of formation/ kJ mol^{-1}
ΔU_f	Energy of formation/ kJ kg^{-1}
ΔU_E	Energy of explosion/ kJ kg^{-1}
EA	Elemental analysis
ESD	Electrostatic discharge/J
FS	Friction Sensitivity/N
FW	Formula weight/ g mol^{-1}
H_2O	Water
IS	Impact sensitivity/N
N	Nitrogen content/%
NMR	Nuclear magnetic resonance
Ω	Oxygen balance/%
p_{CJ}	Detonation pressure/kbar
PETN	Nitropenta
RDX	Hexogen
SSRT	Small-Scale Shock Reactivity Test
T_{dec}	Decomposition temperature/ $^{\circ}\text{C}$
T_E	Explosion temperature/ $^{\circ}\text{C}$

Acknowledgments

Financial support of this work by the Ludwig-Maximilian University of Munich (LMU), the Fonds der Chemischen Industrie (FCI), the Eu-

ropean Research Office (ERO) of the U.S. Army Research Laboratory (ARL) and the Armament Research, Development and Engineering Center (ARDEC) under contract nos. W911NF-09-2-0018, W911NF-09-1-0120 and W011NF-09-1-0056 is gratefully acknowledged. The authors acknowledge collaborations with Dr. Mila Krupka (OZM Research, Czech Republic) in the development of new testing and evaluation methods for energetic materials and with Dr. Muhamed Sucesca (Brodarski Institute, Croatia) in the development of new computational codes to predict the detonation and propulsion parameters of novel explosives. We are indebted to and thank Drs. Betsy M. Rice and Brad Forch (ARL, Aberdeen, Proving Ground, MD). Stefan Huber is thanked for assistance with sensitivity measurements. We also like to thank one referee for many helpful comments and suggestions.

References

- [1] T. M. Klapötke, D. G. Piercey, 1,1'-Azobis(tetrazole): A Highly Energetic Nitrogen-Rich Compound with a N_{10} Chain, *Inorg. Chem.* **2011**, *50*, 2732–2734.
- [2] M. Göbel, K. Karaghiosoff, T. M. Klapötke, D. G. Piercey, J. Stierstorfer, Nitrotetrazolate-2-N-oxides and the Strategy of N-Oxide Introduction, *J. Am. Chem. Soc.* **2010**, *132*, 17216–17226.
- [3] T. M. Klapötke, D. G. Piercey, J. Stierstorfer, The Facile Synthesis and Energetic Properties of an Energetic Furoxan Lacking Traditional "Explosophore" Moieties: (E,E)-3,4-Bis(oximomethyl)-furoxan (DPX1), *Propellants Explos. Pyrotech.* **2011**, *36*, 160–167.
- [4] T. M. Klapötke, D. G. Piercey, J. Stierstorfer, The Taming of CN_7^- : The Azidotetrazolate 2-Oxide Anion, *Chem. Eur. J.* **2011**, *17*, 13068–13077.
- [5] Y.-C. Li, C. Qi, S.-H. Li, H.-J. Zhang, C.-H. Sun, Y.-Z. Yu, S.-P. Pang, 1,1'-Azobis-1,2,3-triazole: A High-Nitrogen Compound with Stable N_8 Structure and Photochromism, *J. Am. Chem. Soc.* **2010**, *132*, 12172–12173.
- [6] W. McLellan, W. R. Hartley, M. Brower, *Health Advisory for Hexahydro-1,3,5-trinitro-1,3,5-triazine*, Technical Report PB90-273533; Office of Drinking Water, U. S. Environmental Protection Agency, Washington, D.C., USA, **1988**.
- [7] A. Provatas, *Formulation and Performance Studies of Polymer Bonded Explosives (PBX) Containing Energetic Binder Systems, Part 1*, Weapons Systems Division Systems Sciences Laboratory, Edinburg South Australia, Australia. DSTO-TR-1397, **2003**, AR 012–585.
- [8] T. Altenburg, T. M. Klapötke, A. Penger, J. Stierstorfer, Two Outstanding Explosives Based on 1,2-Dinitroguanidine: Ammonium Dinitroguanidine and 1,7-Diamino-1,7-dinitrimino-2,4,6-trinitro-2,4,6-triazahexane, *Z. Anorg. Allg. Chem.* **2010**, *636*, 463–471.
- [9] T. M. Klapötke, C. M. Sabaté, 5-Aminotetrazolium 5-Aminotetrazolates – New Insensitive Nitrogen-Rich Materials, *Z. Anorg. Allg. Chem.* **2009**, *635*, 1812–1822.
- [10] T. Wei, W. Zhu, X. Zhang, Y.-F. Li, H. Xio, Molecular Design of 1,2,4,5-Tetrazine-Based High-Energy Density Materials, *J. Phys. Chem. A* **2009**, *113*, 9404–9412.
- [11] a) T. Kaihoh, T. Itoh, K. Yamaguchi, A. Ohsawa, First Synthesis of A 1,2,3,4-Tetrazine, *J. Chem. Soc., Chem. Commun.* **1988**, 1608–1609; b) A. M. Churakov, V. A. Tartakovsky, Progress in 1,2,3,4-Tetrazine Chemistry, *Chem. Rev.* **2004**, *104*, 2601–2616.
- [12] M. N. Glukhovtsev, B. Y. Simkin, V. I. Minkin, Stabilization of the Hexaazabenzene Heterocyclic System in Hexazine 1,3,5-Trioxide, *Zh. Organicheskoi Khim.* **1988**, *24*, 2486–2488.

- [13] S. Inagake, N. Goto, Nature of Conjugation in Hydronitrogens and Fluoronitrogens. Excessive Flow of Unshared Electron Pairs into σ -Bonds, *J. Am. Chem. Soc.* **1987**, *109*, 3234–3240.
- [14] M. Noyman, S. Zilberg, Y. Haas, Stability of Polynitrogen Compounds: The Importance of Separating the σ - and π -Electron Systems, *J. Phys. Chem. A* **2009**, *113*, 7376–7382.
- [15] H. Schechter, M. Venugopal, D. Srinivasulu, *Synthesis of 1,2,3,4-Tetrazines, 1,2,3,4-Tetrazine Di-N-oxides, Pentazole Derivatives, Pentazine Poly N-oxides, and Nitroacetylenes*, Ohio State University Research Foundations, DARPA/AFOSR Sponsored, Project 746566. March 8, **2006**.
- [16] X. Song, J. Li, H. Hou, B. Wang, Extensive Theoretical Studies of a New Energetic Material: Tetrazino-tetrazine-tetraoxide, *J. Comput. Chem.* **2009**, *30*, 1816–1820.
- [17] V. A. Tartakovsky, I. E. Filatov, A. M. Churakov, S. L. Ioffe, Y. A. Strelenko, V. S. Kuz'min, G. L. Rusinov, K. I. Pashkevich, Synthesis and Structure of Pyridoannelated 1,2,3,4-Tetrazine 1,3-dioxides, *Izvest. Akad. Nauk. Ser. Khim.* **2004**, *11*, 2471–2477.
- [18] A. M. Churakov, S. L. Ioffe, V. A. Tartakovsky, The First Synthesis of 1,2,3,4-Tetrazine-1,3-di-N-oxides, *Mendeleev Commun.* **1991**, *1*, 101–103.
- [19] A. Y. Tyurin, A. M. Churakov, Y. A. Strelenko, M. O. Ratnikov, V. A. Tartakovsky, Synthesis of First Nonannulated 1,2,3,4-Tetrazine-1,3-dioxides, *Izvest. Akad. Nauk. Ser. Khim.* **2006**, *9*, 1589–1594.
- [20] K. L. Altman, L. H. Merwin, W. P. Norris, W. S. Wilson, R. Gilardi, *High Nitrogen Explosives. Part 2. Dibenzo-1,3a,4,6a-tetraazapentalenes and Benzo-1,2,3,4-tetrazine-1,3-dioxides*, Report NAWCWPNS TP 8277, Naval Air Warfare Center Weapons Division, China Lake, CA, USA, **1996**.
- [21] *CrysAlis Pro*, Oxford Diffraction Ltd., Version 1.171.33.41 beta (release **2009** CrysAlis171.NET).
- [22] *CrysAlis RED*, Oxford Diffraction Ltd., Version 1.171.27p5 beta (release April 01, **2005**, CrysAlis171.NET).
- [23] A. Altomare, G. Cascarano, C. Giacovazzo, A. Guagliardi, A Program for Crystal Structure Solution, SIR-92, *J. Appl. Crystallogr.* **1993**, *26*, 343.
- [24] G. M. Sheldrick, *SHELXS-97*, Program for the Refinement of Crystal Structures, University of Göttingen, Germany, **1997**.
- [25] A. L. Spek, *PLATON*, A Multipurpose Crystallographic Tool, Utrecht University, Utrecht, The Netherlands, **1999**.
- [26] NATO Standardization Agreement (STANAG) on Explosives, *Impact Sensitivity Tests*, No. 4489, Ed. 1, Brussels, Sept. 17, **1999**.
- [27] WIWEB-Standardarbeitsanweisung 4-5.1.02, *Ermittlung der Explosionsgefährlichkeit, hier der Schlagempfindlichkeit mit dem Fallhammer*, Erding, November 8, **2002**.
- [28] <http://www.bam.de>.
- [29] <http://www.reichel-partner.de>.
- [30] NATO Standardization Agreement (STANAG) on Explosives, *Friction Sensitivity Tests*, No. 4487, Ed. 1, Brussels, August 22, **2002**.
- [31] WIWEB-Standardarbeitsanweisung 4-5.1.03, *Ermittlung der Explosionsgefährlichkeit oder der Reibeempfindlichkeit mit dem Reibeapparat*, Erding, November 8, **2002**.
- [32] S. Zeman, V. Pelikán, J. Majzlík, Electric Spark Sensitivity of Nitramines, Part II. A Problem of "Hot Spots", *Cent. Eur. J. Energ. Mater.* **2006**, *3*, 45–51.
- [33] D. Skinner, D. Olson, A. Block-Bolten, Electrostatic Discharge Ignition of Energetic Materials, *Propellants Explos. Pyrotech.* **1998**, *23*, 34–42.
- [34] <http://www.ozm.cz/testinginstruments/small-scale-electrostatic-discharge-tester.htm>.
- [35] According to the UN Recommendations on the Transport of Dangerous Goods. ISBN 92-1-139087-7: Impact: Insensitive >40 J, less sensitive ≥ 35 J, sensitive ≥ 4 J, very sensitive ≤ 3 J; Friction Insensitive >360 N, less sensitive =360 N, sensitive <360 N a. >80N, very sensitive ≤ 80 N, extremely sensitive ≤ 10 N.
- [36] M. J. Frisch, G. W. Trucks, H. B. Schlegel, G. E. Scuseria, M. A. Robb, J. R. Cheeseman, J. A. Montgomery Jr., T. Vreven, K. N. Kudin, J. C. Burant, J. M. Millam, S. S. Iyengar, J. Tomasi, V. Barone, B. Mennucci, M. Cossi, G. Scalmani, N. Rega, G. A. Petersson, H. Nakatsuji, M. Hada, M. Ehara, K. Toyota, R. Fukuda, J. Hasegawa, M. Ishida, T. Nakajima, Y. Honda, O. Kitao, H. Nakai, M. Klene, X. Li, J. E. Knox, H. P. Hratchian, J. B. Cross, V. Bakken, C. Adamo, J. Jaramillo, R. Gomperts, R. E. Stratmann, O. Yazyev, A. J. Austin, R. Cammi, C. Pomelli, J. W. Ochterski, P. Y. Ayala, K. Morokuma, G. A. Voth, P. Salvador, J. J. Dannenberg, V. G. Zakrzewski, S. Dapprich, A. D. Daniels, M. C. Strain, O. Farkas, D. K. Malick, A. D. Rabuck, K. Raghavachari, J. B. Foresman, J. V. Ortiz, Q. Cui, A. G. Baboul, S. Clifford, J. Cioslowski, B. B. Stefanov, G. Liu, A. Liashenko, P. Piskorz, I. Komaromi, R. L. Martin, D. J. Fox, T. Keith, M. A. Al-Laham, C. Y. Peng, A. Nanayakkara, M. Challacombe, P. M. W. Gill, B. Johnson, W. Chen, M. W. Wong, C. Gonzalez, J. A. Pople, *Gaussian 09*, Revision A1, Gaussian, Inc., Wallingford CT, USA, **2009**.
- [37] a) J. W. Ochterski, G. A. Petersson, J. A. Montgomery Jr., A Complete Basis Set Model Chemistry. V. Extensions to Six or More Heavy Atoms, *J. Chem. Phys.* **1996**, *104*, 2598; b) J. A. Montgomery Jr., M. J. Frisch, J. W. Ochterski, G. A. Petersson, A Complete Basis Set Model Chemistry. VII. Use of the Minimum Population Localization Method, *J. Chem. Phys.* **2000**, *112*, 6532.
- [38] a) L. A. Curtiss, K. Raghavachari, P. C. Redfern, J. A. Pople, Assessment of Gaussian-2 and Density Functional Theories for the Computation of Enthalpies of Formation, *J. Chem. Phys.* **1997**, *106*, 1063; b) E. F. C. Byrd, B. M. Rice, Improved Prediction of Heats of Formation of Energetic Materials Using Quantum Chemical Methods, *J. Phys. Chem. A* **2006**, *110*, 1005–1013; c) B. M. Rice, S. V. Pai, J. Hare, Predicting Heats of Formation of Energetic Materials Using Quantum Chemical Calculations, *Combust. Flame* **1999**, *118*, 445–458.
- [39] P. J. Linstrom, W. G. Mallard (Eds.), NIST Chemistry WebBook, NIST Standard Reference Database Number 69, National Institute of Standards and Technology, Gaithersburg MD, 20899, <http://webbook.nist.gov>, (retrieved March 30, 2010).
- [40] a) M. S. Westwell, M. S. Searle, D. J. Wales, D. H. Williams, Empirical Correlations Between Thermodynamic Properties and Intermolecular Forces, *J. Am. Chem. Soc.* **1995**, *117*, 5013–5015; b) F. Trouton, On Molecular Latent Heat, *Philos. Mag.* **1884**, *18*, 54–57.
- [41] M. Sućeska, EXPLO5.3 Program, Zagreb, Croatia, **2009**.
- [42] a) M. Sućeska, Calculation of Detonation Parameters by EXPLO5 Computer Program, *Mater. Sci. Forum*, **2004**, 465–466, 325–330; b) M. Sućeska, Calculation of Detonation Properties of C–H–N–O Explosives, *Propellants Explos. Pyrotech.* **1991**, *16*, 197–202; c) M. Sućeska, Evaluation of Detonation Energy from EXPLO5 Computer Code Results, *Propellants Explos. Pyrotech.* **1999**, *24*, 280–285; d) M. L. Hobbs, M. R. Baer: Calibration of the BKW-EOS with a Large Product Species Data Base and Measured C–J Properties, *10th Symposium (International) on Detonation*, ONR 33395-12, Boston, MA, USA, July 12–16, **1993**, p. 9.
- [43] a) J. E. Felts, H. W. Sandusky, R. H. Granholm, Development of the Smallscale Shock Sensitivity Test (SSST), *16th Conference of the American Physical Society Topical Group on Shock Compress-*

5,7-Dinitrobenzo-1,2,3,4-tetrazine-1,3-dioxide (DNBTDO)

- sion of Condensed Matter*, Nashville, TN, USA, June 28–July 1, **2009**, AIP Conference Proceedings 1195, p. 3; b) H. W. Sandusky, R. H. Granholm, D. G. Bohl, *Small-Scale Shock Reactivity Test (SSRT)*, IHTR 2701, Naval Surface Warfare Center, Indian Head, MD, USA, August 12, **2005**.
- [44] R. Mayer, J. Köhler, A. Homburg, *Explosives*, 5th ed., Wiley VCH, Weinheim, **2002**, pp. 7–200.
- [45] R. Mayer, J. Köhler, A. Homburg, *Explosives*, 5th ed., Wiley VCH, Weinheim, **2002**, p. 8.
- [46] T. M. Klapötke, *Chemistry of High-Energy Materials*, Walter de Gruyter, Berlin, New York, **2011**, Ch. 3.
- [47] R. W. Gurney, *Internal Report BRL-405*, **1943**, Ballistic Research Laboratory, Aberdeen Proving Ground, MD, USA.
- [48] A. Koch, N. Arnold, M. Estermann, A Simple Relation Between the Detonation Velocity of An Explosive and its Gurney Energy, *Propellants Explos. Pyrotech.* **2002**, *27*, 365–368.
- [49] R. Meyer, J. Köhler, A. Homburg, *Explosives*, 6th ed., Wiley-VCH, Weinheim, **2007**.
- [50] *Cheetah 2.0*, Energetic Materials Center, Lawrence Livermore National Laboratory, Livermore, CA, USA, **1998**.

Received: November 24, 2011

Revised: May 10, 2012

DOI: 10.1002/zaac.201100479

Hydroxylammonium 5-Nitriminotetrazolates

Niko Fischer,^[a] Thomas M. Klapötke,*^[a] Davin G. Piercey,^[a] and Jörg Stierstorfer^[a]

Keywords: Tetrazoles; Explosives; X-ray diffraction; Detonation parameters; Sensitivities

Abstract. The hydroxylammonium salts of monodeprotonated 5-nitriminotetrazole (**4**), double deprotonated 5-nitriminotetrazole (**5**), 1-methyl-5-nitriminotetrazole (**6**), and 2-methyl-5-nitraminotetrazole (**7**) have been prepared in high yield from the corresponding 5-nitriminotetrazoles as free acids and an aqueous solution of hydroxylamine or the metathesis reactions of hydroxylammonium hydrochloride with the silver salt of the corresponding nitriminotetrazole, respectively. The

energetic salts **4–7** were fully characterized by single-crystal X-ray diffraction (**4–6**), NMR spectroscopy, IR- and Raman spectroscopy as well as DSC measurements. The sensitivities towards impact, friction and electrical discharge were determined. In addition, several detonation parameters (e.g. heat of explosion, detonation velocity) were computed by the EXPLO5.04 computer code based on calculated (CBS-4M) heats of formation and X-ray densities.

Introduction

The design of new energetic materials encompassing all of propellants, explosives, and pyrotechnics is a modern academic and technological challenge.^[1–3] Intense research is focused on the tailoring of new energetic molecules with performances and stability similar to that of RDX (cyclotrimethylenetrinitramine) to replace this widely-used high explosive. For a novel energetic molecule to find practical application as a high explosive it needs to possess high thermal and mechanical stabilities, while at the same time satisfying the increasing demand for higher performing (high detonation velocity, pressure and heat of explosion) materials.^[4]

One of the most promising energetic backbones for the tailoring of energetic molecules is the tetrazole ring; the carbon on position 5 of the ring allows the facile attachment of various substituents for energetic tailorability, and the high nitrogen content of the heterocycle leads to high energetic performances.^[5] It can be stated that the tetrazole heterocycle occupies the “middle ground” of the stability vs. high performance continuum, where highly stable compounds can be poorly-performing energetics and highly energetic compounds are often unstable. This trend is exemplified in the range of five-membered azoles from pyrazole to pentazole, where pyrazoles are not used in energetics due to low performance, and the few pentazole derivatives known are highly unstable.^[6]

Of the energetic tetrazoles known, nitriminotetrazoles are some of the most promising for practical use as they have some of the highest performances and thermal stabilities. By tailoring substituents and counterions, nitriminotetrazoles have

been shown to illustrate the entire spectrum of sensitivity from insensitive secondary to sensitive primary explosives,^[7,8] while maintaining high thermal stability. High thermal stabilities arise from the aromatic nature of the tetrazole ring, whereas the high performances arise from the high heats of formation of nitriminotetrazoles, the ring strain of the five-membered ring, and good oxygen balances.^[9]

The oxygen balance is a percentage representation of a compound's ability to oxidize all carbon and hydrogen in the molecule to carbon dioxide and water, respectively. When an oxygen balance is at or near zero, explosive performances are high, however deviation into either a negative (fuel rich) or positive (oxygen rich) oxygen balance leads to a loss of performance. For an energetic material containing only CHNO the oxygen balance is easily calculated by the equation $\Omega (\%) = (wO - 2xC - 1/2yH) \cdot 1600/M$ (w : number of oxygen atoms, x : number of carbon atoms, y : number of hydrogen atoms, z : number of sulfur atoms). Nitriminotetrazole itself has an only slightly negative oxygen balance and hence, shows very good detonation performance data. When nitriminotetrazoles are deprotonated to form stable, nitrogen rich salts, the oxygen balance decreases and also the performance compared to the neutral, acidic form. Our recent efforts pairing nitriminotetrazolate anions with the oxygen-containing diammonium cation^[10] illustrated the improvement in performances seen when oxygen balances are improved. In our quest for ever higher performances while maintaining thermal stability, we have paired three nitriminotetrazoles (5-nitriminotetrazole, 1-methyl-5-nitriminotetrazole, 2-methyl-5-nitraminotetrazole) with the hydroxylammonium cation, the synthesis and characterization of which we describe in the following.

Results and Discussion

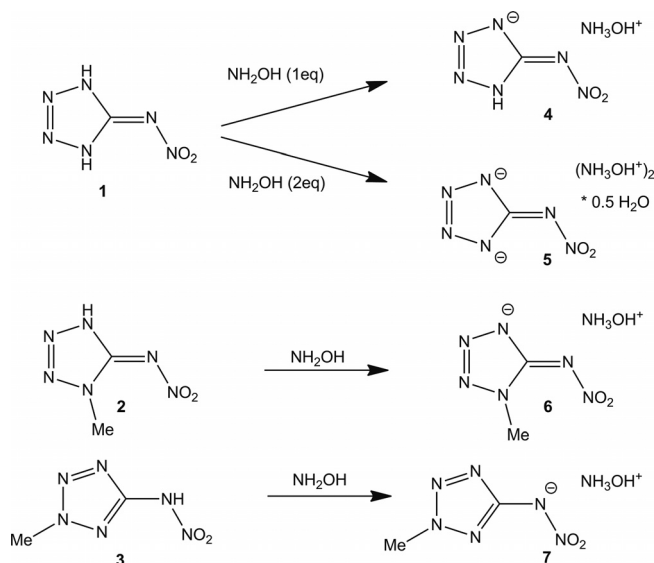
Synthesis

Hydroxylammonium 5-nitriminotetrazolates can be synthesized most easily either from the neutral 5-nitriminotetrazol-

* Prof. Dr. T. M. Klapötke
Fax: +49-89-2180-77492
E-Mail: tmk@cup.uni-muenchen.de

[a] Energetic Materials Research
Department Chemie
Ludwigs-Maximilians Universität München
Butenandtstr. 5–13
81377 München, Germany

ates and an aqueous solution of hydroxylamine or via metathesis reaction using the respective silver salts and hydroxylammonium chloride. The synthesis of the 5-nitriminotetrazolates **4–7** was achieved employing both synthetic routes; the first one is using the neutral compounds, which have been deprotonated with an 50% (w/w) aqueous solution of hydroxylamine as described in Scheme 1. The second route using the silver salts of the corresponding 5-nitriminotetrazoles and hydroxylammonium chloride is working with yields, that are almost as high (80–90%), but the use of expensive starting materials (AgNO_3) and the isolation of the highly friction and impact sensitive silver 5-nitriminotetrazolates make this route disadvantageous compared to the first route described here. Unexpectedly, the solubility of the monodeprotonated 5-nitriminotetrazolate salts **5–7** is very good in water and to a small extend, the salts are even soluble in lower aliphatic alcohols such as methanol. Therefore, they have to be recrystallized from mixtures containing methanol or ethanol and small amounts of water to obtain crystals suitable for X-ray single crystal measurements. In contrast, the solubility of the double deprotonated salt **4** is comparatively low in water, which means, that single crystals for the structure determination have to be grown directly from the aqueous reaction mixture after the addition of hydroxylamine to the free acid. The starting materials 5-nitriminotetrazole as well as the methylated compounds



Scheme 1. Synthesis via Brønsted acid-base reactions of the target molecules presented in this work: hydroxylammonium 5-nitriminotetrazolate (**4**), bishydroxylammonium 5-nitriminotetrazolate semihydrate (**5**), hydroxylammonium 1-methyl-5-nitriminotetrazolate (**6**), hydroxylammonium 2-methyl-5-nitriminotetrazolate (**7**).

1-methyl-5-nitriminotetrazole and 2-methyl-5-nitriminotetrazole were synthesized according to literature.^[11]

Table 1. X-ray data and parameters.

	4	5	6
Formula	$\text{CH}_5\text{N}_7\text{O}_3$	$\text{CH}_6\text{N}_8\text{O}_{4.5}$	$\text{C}_2\text{H}_7\text{N}_7\text{O}_3$
FW / $\text{g}\cdot\text{mol}^{-1}$	163.12	205.16	177.15
Crystal system	monoclinic	monoclinic	orthorhombic
Space Group	$P2_1/c$ (14)	$P2_1/n$ (13)	$Pbca$ (61)
Color / Habit	colorless rod	colorless block	colorless block
Size /mm	$0.12 \times 0.20 \times 0.24$	$0.32 \times 0.34 \times 0.40$	$0.06 \times 0.07 \times 0.13$
a /Å	8.6228(5)	14.7405(10)	7.6060(17)
b /Å	9.2014(5)	3.6447(2)	6.5593(12)
c /Å	7.6673(5)	15.2973(9)	28.995(7)
α /°	90	90	90
β /°	93.768(5)	110.602(7)	90
γ /°	90	90	90
V /Å ³	607.02(6)	769.28(9)	1446.6(5)
Z	4	2	8
$\rho_{\text{calcd.}}$ / $\text{g}\cdot\text{cm}^{-3}$	1.785	1.771	1.627
μ / mm^{-1}	0.164	0.166	0.145
$F(000)$	336	428	736
$\lambda_{\text{Mo-K}\alpha}$ /Å	0.71073	4.8, 26.0	0.71073
T /K	173	173	173
$\theta_{\text{Min-Max}}$ /°	4.3, 26.2	4.8, 26.0	4.2, 26.0
Dataset hkl	–10:10; –11:11; –9: 9	–15:18; –4:4; –18:18	–9:9; –8:8; –35:26
Reflections collected	8996	3633	6409
Independent reflections	1219	1516	1366
R_{int}	0.036	0.019	0.083
Observed reflections	951	1275	720
Parameters	120	160	126
R_1 (obs)	0.0277	0.0285	0.0520
wR_2 (all data)	0.0760	0.0771	0.1191
GooF	0.98	1.03	0.86
Resd. Dens. / $\text{e}\cdot\text{Å}^{-3}$	–0.19, 0.17	–0.20, 0.20	–0.22, 0.40
Device type	Oxford Xcalibur 3	Oxford Xcalibur 3	Oxford Xcalibur 3
Solution	SIR-92	SIR-92	SHELXS-97
Refinement	SHELXL-97	SHELXL-97	SHELXL-97
Absorption correction	semiempirical	semiempirical	semiempirical
CCDC	790986	851203	790987

Crystal Structures

Relevant data and parameters of the crystal structure elucidations are listed in Table 1. Bond lengths and angles are listed in Table 2.

Table 2. Bond lengths and bond angles of **4**, **5** and **6**.

atoms	4	5	6
	<i>d</i> /Å	<i>d</i> /Å	<i>d</i> /Å
O1–N6	1.2493(15)	1.2930(14)	1.234(3)
O2–N6	1.2661(15)	1.2668(14)	1.279(3)
N5–N6	1.3175(16)	1.2873(14)	1.308(3)
N5–C1	1.3657(17)	1.3980(16)	1.375(4)
N1–C1	1.3396(17)	1.3412(15)	1.335(4)
N4–C1	1.3342(19)	1.3382(17)	1.334(4)
N1–N2	1.3436(16)	1.3368(16)	1.352(4)
N2–N3	1.2939(16)	1.3093(16)	1.288(4)
N3–N4	1.3502(16)	1.3463(15)	1.361(4)
N1(N2)–C2			1.466(4)
O3–N7	1.4145(18)	1.4100(17)	1.407(3)
O4–N8		1.4138(16)	
	\angle /°	\angle /°	\angle /°
O1–N6–O2	120.48(11)	118.22(10)	120.3(3)
O2–N6–N5	114.81(11)	125.54(11)	113.8(2)
O1–N6–N5	124.70(11)	116.23(10)	125.9(2)
N6–N5–C1	115.88(11)	117.49(11)	117.2(3)
N3–N4–C1	106.11(11)	104.30(10)	105.6(3)
N2–N1–C1	108.95(11)	105.70(10)	108.8(3)
N1–N2–N3	106.46(11)	108.68(10)	106.4(2)
N2–N3–N4	110.92(11)	110.41(11)	111.1(3)
N4–C1–N5	119.75(12)	132.35(11)	133.7(3)
N1–C1–N4	107.55(11)	110.91(10)	108.1(3)
N1–C1–N5	132.69(13)	116.75(11)	118.0(3)
C1–N1–C2			129.4(3)
N2–N1–C2			121.8(3)

Hydroxylammonium 5-nitriminotetrazolate (**4**) crystallizes in the monoclinic space group $P2_1/c$ with four anion/cation pairs in the unit cell. The asymmetric unit is depicted in Figure 1. Its density of 1.785 g cm^{-3} is quite high in comparison with other tetrazolate salts in literature.^[12,13] The hydroxylammonium cations in all structures described here show equal bond lengths and angles comparable to those found in literature, e.g. for hydroxylammonium azotetrazolate monohydrate.^[14]

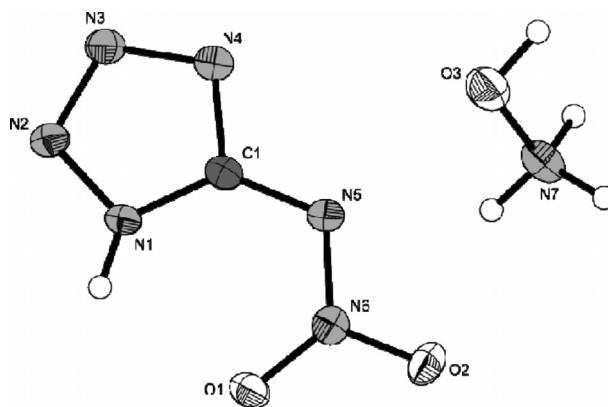


Figure 1. Molecular unit of hydroxylammonium 5-nitriminotetrazolate (**4**). Ellipsoids of non-hydrogen atoms are drawn at the 50% probability level.

Compound **4** crystallizes layer-like along the *b*-axes (Figure 2A). The packing is stabilized by several inter- and intra-

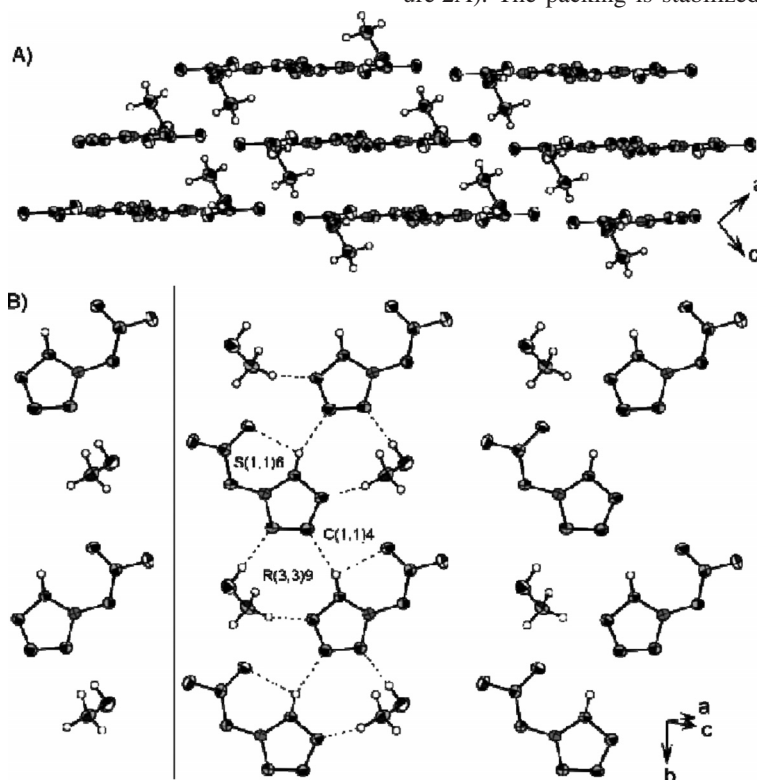


Figure 2. A) View along the *b* axes. B) View on the layers in the structure of **4**. Selected graph sets^[15] are drawn.

molecular hydrogen bridges within the layers (forming strands) on the one hand. On the other hand, the hydroxylammonium cations act as linkers between two layers by forming strong hydrogen bonds.

The double deprotonated salt bis(hydroxylammonium) 5-nitriminotetrazolate (**5**) could only be obtained crystalline as its hemihydrate. Compound **5** crystallizes in the monoclinic space group $P2_1/n$ with four cation/anion pairs as well as two water molecules in the unit cell. Its density of $1.771 \text{ g}\cdot\text{cm}^{-3}$ is only slightly lower than that of **4**. The structure of the dianion is almost planar, which is in accordance to previously published structures e.g. diammonium 5-nitrimino-tetrazolate.^[16] The molecular unit is depicted in Figure 3.

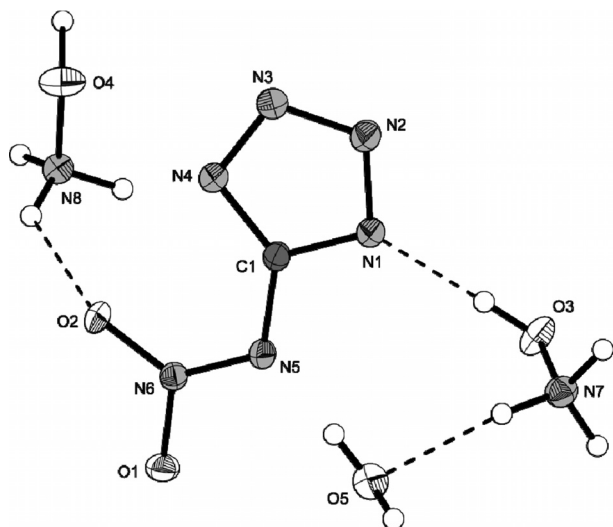


Figure 3. Molecular unit of bis(hydroxylammonium) 5-nitriminotetrazolate semihydrate (**5**). Ellipsoids of non-hydrogen atoms are drawn at the 50% probability level.

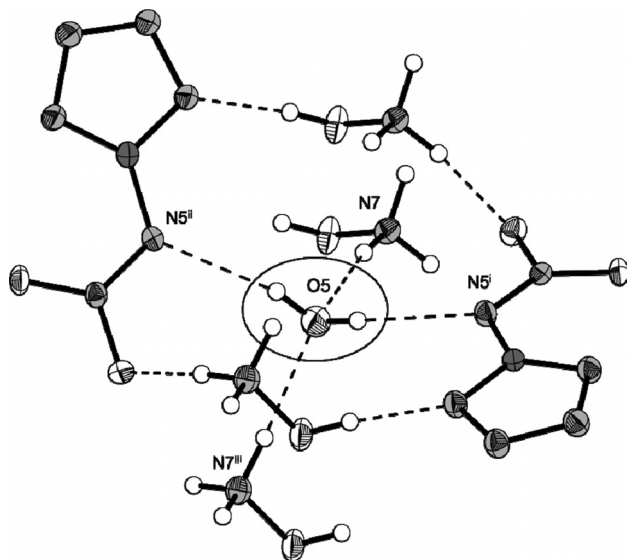


Figure 4. Hydrogen bonds of the crystal water. Symmetry codes: (i) $2.5-x, 1+y, 1.5-z$; (ii) $-1+x, 1+y, z$; (iii) $2.5-x, y, 1.5-z$.

The packing of **5** is dominated by several strong hydrogen bonds. Exemplarily, the coordination of the crystal water is

shown in Figure 4. The water molecules form a tetrahedral coordination sphere, connecting two nitriminotetrazolate anions via the N5 nitrogen atoms.

Hydroxylammonium 1-methyl-5-nitriminotetrazolate (**6**) crystallizes in the orthorhombic space group $Pbca$ with eight anion/cation pairs in the unit cell. The asymmetric unit is shown in Figure 5. Its density of $1.627 \text{ g}\cdot\text{cm}^{-3}$ is significantly lower than that of **4** and **5**. Again a strong hydrogen bond network is formed, which is depicted in Figure 6.

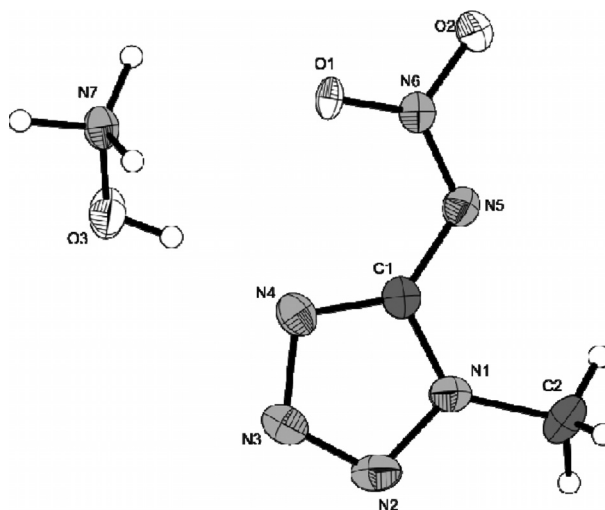


Figure 5. Molecular unit of hydroxylammonium 1-methyl-5-nitriminotetrazolate (**6**). Ellipsoids of non-hydrogen atoms are drawn at the 50% probability level.

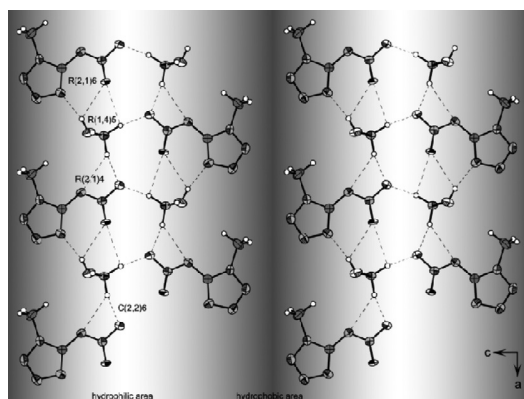


Figure 6. View on the layers in the structure of **6**. Bright regions represent hydrophilic parts, dark regions hydrophobic parts.

Heats of Formation

Usually energetic materials tend to explode in bomb calorimetric measurements. Consequently doubtful combustion energies are obtained. Therefore heats of formation of energetic materials mostly are calculated theoretically. In our group we combine the atomization energy method (Equation (1)) with CBS-4M electronic energies which has been shown suitable in many recently published studies.^[17] CBS-4M energies of the atoms, cations, and anions were calculated with the

Gaussian09 (revision A1) software package^[18] and checked for imaginary frequencies. Values for $\Delta_f H^\circ$ (atoms) were taken from the NIST database.^[19]

$$\Delta_f H^\circ_{(\text{g}, \text{M}, 298)} = H_{(\text{Molecule}, 298)} - \sum H^\circ_{(\text{Atoms}, 298)} + \sum \Delta_f H^\circ_{(\text{Atoms}, 298)} \quad (1)$$

For calculation of the solid state energy of formation (Table 4) of **4–7**, the lattice energies (U_L) and lattice enthalpies (ΔH_L) were calculated from the corresponding molecular volumes (obtained from X-ray elucidations) according to the equations provided by Jenkins et al.^[20] With the calculated lattice enthalpy (Table 4), the CBS-4M based gas-phase enthalpy of formation (Table 3) was converted into the solid state (standard conditions) enthalpy of formation. These molar standard enthalpies of formation (ΔH_m) were used to calculate the molar solid state energies of formation (ΔU_m) according to Equation (2) (Table 4).

$$\Delta U_m = \Delta H_m - \Delta n RT \quad (2)$$

(Δn being the change of moles of gaseous components)

Compounds **4–7** are all formed endothermically. The 2-methyl derivative **7** has the highest value of 352.2 kJ·mol⁻¹. The significantly lower value (63.3 kJ·mol⁻¹) of compound **5**

Table 3. CBS-4M results and gas phase enthalpies.

M	$-H^{298}$ /a.u.	$\Delta_f H$ (g) /kJ·mol ⁻¹
H ₄ NO ⁺ (in 4–7)	131.863229	687.0
CHN ₆ O ₂ ⁻ (in 4)	516.973495	150.5
CN ₆ O ₂ ²⁻ (in 5)	516.294886	399.0
C ₂ H ₃ N ₆ ⁻ (in 6)	556.194636	166.3
C ₂ H ₃ N ₆ ⁻ (in 7)	556.186685	187.2

is based on the inclusion of crystal water on the one hand and the higher lattice enthalpy of a 2:1 salt on the other hand.

Detonation Parameters

The detonation parameters calculated with the EXPLO5 V5.04 computer code^[21] using the experimentally determined densities (X-ray) are summarized in Table 5.

Especially the detonation parameters of compound **4** and **5** show promising values, much higher than those of trinitrotoluene (**TNT**), pentaerythrityl tetranitrate (**PETN**) and hexogen (**RDX**). The most powerful compound in terms of all calculated detonation parameters is the monodeprotonated salt **4**, which has also the highest density. Also compound **5** and **6** exceed the values of **TNT** and **PETN**. The most important criteria of high explosives are their detonation velocity (V_{det}).

Table 4. Calculation of solid state energies of formation ($\Delta_f U^\circ$).

	$\Delta_f H$ (g) /kJ·mol ⁻¹	V_M / nm^3	U_L /kJ·mol ⁻¹	ΔH_L /kJ·mol ⁻¹	$\Delta_f H^\circ(\text{s})$ /kJ·mol ⁻¹	Δn	$\Delta_f U^\circ(\text{s})$ /kJ·mol ⁻¹	M /g·mol ⁻¹	$\Delta_f U^\circ(\text{s})$ /kJ·kg ⁻¹
4	837.7	151.8	543.6	547.1	290.5	7.5	309.1	163.13	1895.1
5	1652.6*	179.8	1578.4	1589.3	63.3	10.75	90.0	205.16	438.6
6	853.5	180.8	518.7	522.2	331.3	8.5	352.4	177.16	1989.0
7	874.4	180.8	518.7	522.2	352.2	8.5	373.3	177.16	2106.9

*Value has been corrected (-120 kJ·mol⁻¹) to hemihydrate formation.

Table 5. Physico-chemical properties of **4–7** in comparison with trinitrotoluene (**TNT**), nitropenta (**PETN**) and hexogen (**RDX**).

	4	5	6	7	TNT*	PETN*	RDX*
Formula	CH ₅ N ₇ O ₃	CH ₆ N ₈ O _{4.5}	C ₂ H ₇ N ₇ O ₃	C ₂ H ₇ N ₇ O ₃	C ₇ H ₅ N ₃ O ₆	C ₅ H ₈ N ₄ O ₁₂	C ₃ H ₆ N ₆ O ₇
FW /g·mol ⁻¹	163.13	205.16	177.12	177.12	227.13	316.14	222.12
IS /J ^{a)}	2	10	8	6	15	3	7.5
FS /N ^{b)}	40	80	144	144	353	60	120
ESD-test /J	0.30	0.30	0.50	0.30	---	---	0.1–0.2
N % ^{c)}	60.1	54.6	40.7	40.7	18.50	17.72	37.8
O % ^{d)}	-14.7	-20.3	-55.4	-55.4	-73.96	-10.1	-21.6
$T_{\text{dec.}}$ /°C ^{e)}	172	166	185	180	>160	202	210
ρ /g·cm ⁻³ ^{f)}	1.785	1.771	1.627	1.627*	1.654	1.778	1.800
$\Delta_f H_m^\circ$ /kJ·mol ⁻¹ ^{g)}	+290	+80	+331	+352	-59	-539	+70
$\Delta_f U^\circ$ /kJ·kg ⁻¹ ^{h)}	1895	520	1989	2107	-185	-1612	417
EXPLO5 values:							
$-\Delta_E U^\circ$ /kJ·kg ⁻¹ ⁱ⁾	6113	5678	6095	6210	5227	6190	6125
T_E /K ^{j)}	4219	3715	3949	4000	3657	4306	4236
p_{C-J} /kbar ^{k)}	371	360	297	300	216	320	349
$V_{\text{Det.}}$ /m·s ⁻¹ ^{l)}	9236	9214	8651	8690	7253	8320	8748
Gas vol. /L·kg ⁻¹ ^{m)}	853	923	842	842	574	688	739

a) Impact sensitivity measured by the BAM drophammer, grain size (75–150 μm); b) Impact sensitivity measured by the BAM friction tester, grain size (75–150 μm); c) Nitrogen content; d) Oxygen balance;^[22] e) Temperature of decomposition by DSC ($\beta = 5^\circ\text{C}$); f) Density from X-ray structure; g) Molar enthalpy of formation; i) Energy of formation; j) Explosion temperature; k) Detonation pressure; l) Detonation velocity; m) Assuming only gaseous products; *Values based on Ref.^[23] and the EXPLO5 database; #: estimated to be equal than **6**.

= **4**: 9236, **5**: 9214, **6**: 8651, **7**: 8690, TNT: 7253, PETN: 8320, RDX: 8748 m·s⁻¹), detonation pressure (p_{C-J} = **4**: 371, **5**: 360; **6**: 297, **7**: 300, TNT: 216, PETN: 320, RDX: 349 kbar) and energy of explosion ($\Delta_E U^\circ$ = **4**: -6113, **5**: -5678, **6**: -6095, **7**: -6210, TNT: -5227, PETN: -6190, RDX: -6125 kJ·kg⁻¹).

Sensitivity Testing

For application of new energetic compounds important values for safety, handling and processing are the sensitivity data. The values for friction and impact sensitivity were determined according to BAM standard methods described in the NATO STANAG 4487, 4489 and 4490 specifications for energetic materials.^[24–30] The sensitivities towards electrical discharge were determined on a small scale electrostatic discharge device.^[31] According to the UN Recommendations on the Transport of Dangerous Goods compound **4** is regarded very sensitive towards impact (2 J), whereas compounds **5–7** are classified as sensitive towards impact (**5**: 10 J, **6**: 8 J, **7**: 6 J).^[32] Also the friction sensitivities vary between very sensitive for **4** and **5** (**4**: 40 N, **5**: 80 N) and sensitive for **6** and **7** (both 144 N). A general trend towards higher sensitivity for the 2-methylated compound compared to the 1-methylated compound, which has also been shown for other nitrogen-rich salts of both nitriminotetrazoles^[9,33] is reconfirmed in this case, if the sensitivity data of **6** and **7** are compared. The sensitivities towards electrostatic discharge are relatively similar being in a range between 0.30 J (**4**, **5**, **7**) and 0.50 J (**6**).

Thermal Stabilities

Thermostability of energetic compounds is considered important especially in processing and storing the material. Because of the diverse use of energetic materials e.g. under extreme climatic conditions like in deserts, for oil drilling or military ammunition high temperature stability is desired. Three of the four introduced compounds (**4–6**) decompose in a two or even three step mechanism, whereas the decomposition of **7** involves only a single step. For a safe handling of the material, certainly the first decomposition step is of major importance. In the following, all decomposition temperatures are given as absolute onset temperatures. For the monodeprotonated salt **4**, a first decomposition at 172 °C is observed and a following at 204 °C. It decomposes without previous melting, which is not the case for compounds **5–7**, indicated by an endothermic step before decomposition. For the double deprotonated salt **5** a more complex decomposition mechanism can be proposed since it involves three exothermic steps at 166 °C, 184 °C and 194 °C, respectively, however for a detailed investigation of the mechanism a thermogravimetric measurement would be necessary. It furthermore loses its crystal water and melts before decomposition indicated by two endothermic steps at 129 °C and 162 °C, respectively. Also the 1-methyl-5-nitriminotetrazolate **6** melts at 180 °C right before it decomposes at 185 °C followed by a second decomposition step at 193 °C. Compound **7**, which has its methyl group in position 2 at the tetrazole ring differs in that it has a significantly lower

melting point 139 °C and a relatively large liquidity range before it decomposes at 180 °C. All DSC plots are depicted in Figure 7.

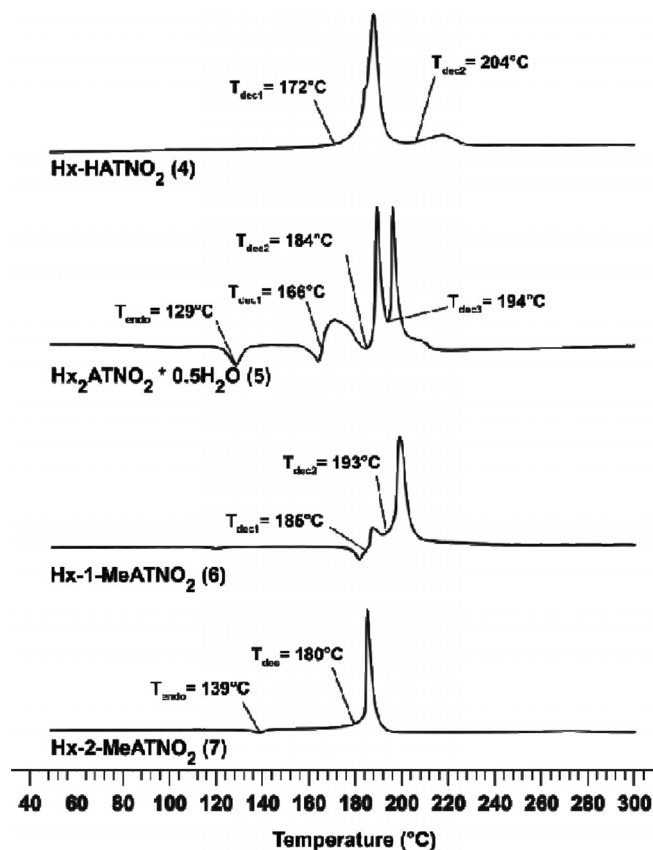


Figure 7. DSC-plots of compounds **4–7** at a heating rate of 5 K·min⁻¹. Exothermic = ↑, endothermic = ↓.

Conclusions

From this combined experimental and theoretical study the following conclusions can be drawn: Four different hydroxylammonium 5-nitriminotetrazolates, namely hydroxylammonium 5-nitriminotetrazolate (**4**), bishydroxylammonium 5-nitriminotetrazolate semihydrate (**5**), hydroxylammonium 1-methyl-5-nitriminotetrazolate (**6**) and hydroxylammonium 2-methyl-5-nitriminotetrazolate (**7**), were synthesized from the corresponding 5-nitriminotetrazoles and aqueous hydroxylamine or via the corresponding silver 5-nitriminotetrazolates and hydroxylammonium chloride in high yields and good purity. All compounds were fully characterized including the structural determination of **4–6**. The detonation performance of these high energy density materials was calculated based on the crystal density and CBS-4M based heats of formation. Unfortunately, the monodeprotonated salt hydroxylammonium 5-nitriminotetrazolate (**4**), which shows the best performance reveals sensitivity data comparable to primary explosives (IS: 2 J, FS: 40 N), whereas the double deprotonated salt **5**, which is less sensitive towards impact and friction (IS: 10 J, FS: 80 N) reveals a poor thermal stability of 166 °C. Both

methyated compounds **6** and **7** show a higher thermal stability whereas having a lower detonation performance. The above mentioned findings again confirm the fact, that highly stable compounds can be poorly-performing energetics and highly energetic compounds are often unstable, which is one of the greatest challenges when synthesizing new high explosives.

Experimental Section

Caution! Nitriminotetrazoles and their salts are highly energetic materials with increased sensitivities towards shock and friction. Therefore, proper security precautions (safety glass, face shield, earthened equipment and shoes, Kevlar® gloves and ear plugs) have to be applied while synthesizing and handling the herein described compounds.

All reagents and solvents were used as received (Sigma–Aldrich, Fluka, Acros Organics) if not stated otherwise. Melting and decomposition points were measured with a Linseis PT10 DSC using heating rates of 5 K·min⁻¹, which were checked with a Büchi Melting Point B-450 apparatus. ¹H, ¹³C and ¹⁵N NMR spectra were measured with a JEOL instrument. All chemical shifts are quoted in ppm relative to TMS (¹H, ¹³C) or nitromethane (¹⁵N). Infrared spectra were measured with a Perkin–Elmer Spektrum One FT-IR instrument. Raman spectra were measured with a Perkin–Elmer Spektrum 2000R NIR FT-Raman instrument equipped with a Nd:YAG laser (1064 nm). Elemental analyses were performed with a Netsch STA 429 simultaneous thermal analyzer. Sensitivity data were determined using a BAM drophammer and a BAM friction tester. The electrostatic sensitivity tests were carried out using an Electric Spark Tester ESD 2010 EN (OZM Research). The X-ray structure determinations were performed on a Oxford Xcalibur3 diffractometer with a Spellman generator (voltage 50 kV, current 40 mA) and a KappaCCD detector using a λ_{Mo-Kα} radiation wavelength of 71.073 pm. All structures were measured at -100 °C. Suitable single crystals of the compounds (**4**–**7**) were picked from the crystallization mixture and mounted in Kel-F oil on a glass fiber on top of the goniometer head. The data collection and data reduction was carried out with the CrysAlisPro software.^[34] The structures were solved with SIR-92^[35] or SHELXS-97^[36] refined with SHELXL-97^[37] and finally checked using the PLATON software^[38] integrated in the WINGX software suite.^[39] The non-hydrogen atoms were refined anisotropically and the hydrogen atoms were located and freely refined. The absorptions were corrected by a SCALE3 ABSPACK multi-scan method.^[40]

Hydroxylammonium 5-Nitriminotetrazolate (**4**)

5-Nitriminotetrazole (1.30 g, 10.0 mmol) was dissolved in cold water (10 mL) and an aqueous solution of hydroxylamine (50% w/w, 1.32 g, 20.0 mmol) was added dropwise. The solvent was removed with a rotary evaporator and the residue was recrystallized from ethanol/water. Yield: 88% (1.44 g, 8.82 mmol).

Alternative route: 5-Nitriminotetrazole (1.59 g, 12.2 mmol) was dissolved in water (a few mL) and a solution of silver nitrate (2.07 g, 12.2 mmol) was added. Silver 5-nitriminotetrazolate precipitated instantly as a colorless solid. It was sucked off and washed with water until free of acid. The colorless solid was resuspended in warm water (50 mL) and treated with a solution of hydroxylammonium chloride (0.84 g, 13.0 mmol) in water (20 mL). The mixture was stirred at 30 °C for 1 h in the dark and the formed silver chloride was filtered off. The filtrate was evaporated and the residue was recrystallized from an

ethanol/water mixture to yield **5** as a colorless solid (1.70 g, 10.4 mmol, 85%).

DSC (5 K·min⁻¹): 172 °C (dec.). **IR** (KBr, cm⁻¹): $\tilde{\nu}$ = 3125 (s), 2958 (s), 2776 (m), 2711 (s), 1617 (m), 1598(m), 1539 (s), 1431 (s), 1383 (m), 1321 (vs), 1244 (m), 1213 (m), 1188 (m), 1153 (m), 1108 (m), 1061 (m), 1039 (m), 1003 (m), 872 (w), 823 (w), 777 (w), 753 (w), 742 (w), 700 (w), 493 (w); **Raman** (1064 nm, 300 mW, 25 °C, cm⁻¹): $\tilde{\nu}$ = 2715 (1), 1541 (100), 1452 (1), 1433 (1), 1381 (4), 1332 (36), 1158 (7), 1110 (4), 1070 (4), 1036 (22), 1014 (85), 875 (8), 744 (14), 695 (1), 494 (3), 427 (4), 413 (15). **¹H NMR** ([D₆]DMSO, 25 °C, ppm): δ = 10.95 (s). **¹³C NMR** ([D₆]DMSO, 25 °C, ppm): δ = 158.3 (CN₄); *m/z* (FAB⁺): 34.0 [NH₃OH⁺]; *m/z* (FAB⁻): 129.1 [HATNO₂⁻]; **EA** (CH₅N₇O₃, 163.10): calcd.: C 7.36, H 3.09, N 60.12%; found: C 7.38, H 3.17, N 57.40%; BAM drophammer: 2 J; friction tester: 40 N; ESD: 0.30 J (at grain size 100–500 μm).

Dihydroxylammonium 5-Nitriminotetrazolate Hemihydrate (**5**)

5-Nitriminotetrazole (2.60 g, 20.0 mmol) was dissolved in cold water (10 mL) and an aqueous solution of hydroxylamine (50% w/w, 2.64 g, 40.0 mmol) was added. After a few minutes, the product began to crystallize in fine needles, which were isolated. For recovery of the remaining material the mother liquor was evaporated and the colorless residue was recrystallized from ethanol/water to give **4** in 90% overall-yield (3.69 g, 18.0 mmol).

DSC (5 K·min⁻¹): 166 °C (weak exo), 184 °C (weak exo), 194 °C (dec., strong exo). **IR** (KBr, cm⁻¹): $\tilde{\nu}$ = 3421 (m), 3217 (m), 3101 (s), 2719 (s), 1612 (m), 1523 (m), 1466 (m), 1418 (s), 1384 (vs), 1338 (s), 1310 (s), 1219 (s), 1171 (m), 1146 (m), 1109 (w), 1099 (w), 1039 (w), 1022 (m), 1003 (s), 871 (m), 757 (m), 757 (w), 748 (w), 737 (w), 486 (w); **Raman** (1064 nm, 300 mW, 25 °C, cm⁻¹): $\tilde{\nu}$ = 1452 (100), 1423 (10), 1395 (3), 1358 (1), 1293 (2), 1236 (6), 1184 (8), 1154 (15), 1109 (3), 1021 (41), 1011 (12), 876 (3), 755 (3), 731 (6), 424 (9), 410 (8). **¹H NMR** ([D₆]DMSO, 25 °C, ppm): δ = 8.83 (s, NH₃OH). **¹³C NMR** ([D₆]DMSO, 25 °C, ppm): δ = 158.4 (CN₄); *m/z* (FAB⁺): 34.0 [NH₃OH⁺]; *m/z* (FAB⁻): 129.0 [CHN₆O₂⁻]; **EA** (CH₈N₈O₄, water-free, 196.13): calcd.: C 6.12, H 4.11, N 57.13%; found: C 6.09, H 3.96, N 57.13%; BAM drophammer: 10 J; friction tester: 80 N; ESD: 0.30 J (at grain size 500–1000 μm).

Hydroxylammonium 1-Methyl-5-nitriminotetrazolate (**6**)

1-Methyl-5-nitriminotetrazole (1.44 g, 10.0 mmol) was dissolved in cold water (20 mL) and an aqueous solution of hydroxylamine (50% w/w, 0.66 g, 10.0 mmol) was added dropwise. The solvent was removed on a rotary evaporator and the residue was recrystallized from ethanol/water. Yield: 88% (1.56 g, 8.81 mmol).

Alternative route: 1-Methyl-5-nitriminotetrazole (1.67 g, 11.6 mmol) was dissolved in water (a few mL) and a solution of silver nitrate (1.97 g, 11.6 mmol) was added. Silver 1-methyl-5-nitriminotetrazolate precipitated instantly as a white solid. It was sucked off and washed with water until free of acid. The white solid was resuspended in warm water (50 mL) and treated with a solution of hydroxylammonium chloride (0.74 g, 11.5 mmol) in water (20 mL). The mixture was stirred at 30 °C for 1 h in the dark and the formed silver chloride was filtered off. The filtrate was evaporated and the residue was recrystallized from ethanol to yield **6** as a colorless solid (1.78 g, 10.0 mmol, 86%).

DSC (5 K·min⁻¹): 180 °C (m.p.), 185 °C (dec.). **IR** (KBr, cm⁻¹): $\tilde{\nu}$ = 3435 (vs), 3099 (m), 2737 (m), 2375 (w), 1627 (m), 1587 (m), 1515

(m), 1470 (m), 1424 (m), 1396 (m), 1385 (m), 1339 (s), 1303 (m), 1278 (m), 1250 (m), 1205 (m), 1106 (m), 1035 (w), 1011 (w), 987 (w), 890 (w), 831 (w), 774 (w), 753 (w), 733 (w), 689 (w); **Raman** (1064 nm, 300 mW, 25 °C, cm^{-1}): $\tilde{\nu}$ = 3026 (6), 2960 (53), 2804 (2), 2728 (2), 1585 (3), 1546 (7), 1520 (64), 1471 (35), 1425 (3), 1407 (13), 1342 (10), 1316 (3), 1304 (47), 1254 (4), 1123 (2), 1110 (15), 1037 (100), 1012 (19), 991 (3), 893 (14), 774 (2), 754 (30), 734 (4), 699 (5), 690 (35), 503 (17), 460 (6), 376 (8), 289 (51). **^1H NMR** ($[\text{D}_6]\text{DMSO}$, 25 °C, ppm): δ = 10.12 (s, NH_3OH^+), 3.67 (s, CH_3). **^{13}C NMR** ($[\text{D}_6]\text{DMSO}$, 25 °C, ppm): δ = 157.5 (CN_4), 33.1 (CH_3); m/z (FAB⁺): 34.0 [NH_3OH^+]; m/z (FAB⁻): 143.0 [1-MeATNO_2^-]; **EA** ($\text{C}_2\text{H}_7\text{N}_7\text{O}_3$, 177.12): calcd.: C 13.56, H 3.98, N 55.36%; found: C 13.70, H 3.73, N 55.08%; BAM drophammer: 8 J; friction tester: 144 N; ESD: 0.50 J (at grain size 500–1000 μm).

Hydroxylammonium 2-Methyl-5-nitraminotetrazolate (7)

2-Methyl-5-nitraminotetrazole (1.44 g, 10.0 mmol) is dissolved in 20 mL of cold water and an aqueous solution of hydroxylamine (50% w/w, 0.66 g, 10.0 mmol) is added dropwise. The solvent was removed on a rotary evaporator and the residue recrystallized from ethanol/water. Yield: 82% (1.45 g, 8.20 mmol).

Alternative route: Ammonium 2-methyl-5-nitraminotetrazolate (4.12 g, 25.6 mmol) was dissolved in 20 mL of water and a solution of silver nitrate (4.34 g, 25.5 mmol) was added. The silver salt of 2-methyl-5-nitraminotetrazolate precipitates as a colorless solid. After being washed until free of ammonium nitrate it is resuspended in 100 mL of water and a solution of hydroxylammonium chloride (1.61 g, 25.0 mmol) is added. The mixture is stirred for 1 h at 30 °C in the dark and the formed silver chloride is filtered off. The filtrate is evaporated and the viscous residue is redissolved in ethanol for recrystallization. **7** crystallizes as a colorless, fluffy precipitate. Yield: 3.96 g, 22.3 mmol, 87%.

DSC (5 $\text{K}\cdot\text{min}^{-1}$): 139 °C (m.p.), 180 °C (dec.). **IR** (KBr, cm^{-1}): $\tilde{\nu}$ = 3433 (m), 3116 (s), 3048 (s), 2802 (m), 2724 (s), 1619 (m), 1506 (m), 1483 (s), 1435 (m), 1405 (s), 1384 (s), 1364 (m), 1329 (vs), 1282 (m), 1232 (m), 1212 (m), 1184 (m), 1118 (w), 1101 (m), 1094 (m), 1035 (m), 1013 (w), 1002 (w), 900 (w), 890 (w), 764 (w), 754 (w), 706 (w), 678 (w); **Raman** (1064 nm, 300 mW, 25 °C, cm^{-1}): $\tilde{\nu}$ = 2965 (17), 2840 (1), 1622 (1), 1603 (1), 1484 (100), 1437 (3), 1420 (3), 1396 (3), 1368 (3), 1290 (1), 1215 (5), 1187 (7), 1119 (3), 1096 (2), 1040 (4), 1030 (47), 1015 (15), 1003 (2), 902 (2), 890 (4), 754 (5), 707 (9), 454 (8), 404 (4). **^1H NMR** ($[\text{D}_6]\text{DMSO}$, 25 °C, ppm): δ = 9.90 (s, NH_3OH^+), 4.20 (s, CH_3). **^{13}C NMR** ($[\text{D}_6]\text{DMSO}$, 25 °C, ppm): δ = 168.0 (CN_4), 39.7 (CH_3); m/z (FAB⁺): 34.0 [NH_3OH^+]; m/z (FAB⁻): 143.0 [2-MeATNO_2^-]; **EA** ($\text{C}_2\text{H}_7\text{N}_7\text{O}_3$, 177.12): calcd.: C 13.56, H 3.98, N 55.36%; found: C 13.25, H 3.88, N 53.47%; BAM drophammer: 6 J; friction tester: 144 N; ESD: 0.30 J (at grain size <100 μm).

Acknowledgments

Financial support of this work by the *Ludwig-Maximilian University of Munich* (LMU), the *U.S. Army Research Laboratory* (ARL), the *Armament Research, Development and Engineering Center* (ARDEC), the *Strategic Environmental Research and Development Program* (SERDP) and the *Office of Naval Research* (ONR Global, title: "Synthesis and Characterization of New High Energy Dense Oxidizers (HEDO) – NICOP Effort") under contract nos. W911NF-09-2-0018 (ARL), W911NF-09-1-0120 (ARDEC), W011NF-09-1-0056

(ARDEC) and 10 WPSEED01-002 / WP-1765 (SERDP) is gratefully acknowledged. The authors acknowledge collaborations with *Dr. Mila Krupka* (OZM Research, Czech Republic) in the development of new testing and evaluation methods for energetic materials and with *Dr. Muhamed Sucesca* (Brodarski Institute, Croatia) in the development of new computational codes to predict the detonation and propulsion parameters of novel explosives. We are indebted to and thank *Drs. Betsy M. Rice* and *Brad Forch* (ARL, Aberdeen, Proving Ground, MD) and *Mr. Gary Chen* (ARDEC, Picatinny Arsenal, NJ) for many helpful and inspired discussions and support of our work.

References

- [1] J. Giles, *Nature* **2004**, *427*, 580.
- [2] D. Carrington, *New Scientist* **2001**, 101.
- [3] T. M. Klapötke, *Tin Moderne Anorganische Chemie* (Ed.: E. Riedel), 3ed., Walter de Gruyter, Berlin, New York, **2007**, pp. 99–104.
- [4] T. M. Klapötke, *High Energy Density Materials*, Springer, **2007**.
- [5] T. M. Klapötke, J. Stierstorfer, *J. Am. Chem. Soc.* **2009**, *131*, 1122.
- [6] P. Carlqvist, H. Ostmark, T. Brinck, *J. Phys. Chem. A* **2004**, *108*, 7463.
- [7] T. M. Klapötke, J. Stierstorfer, *New Trends in the Research of Energetic Materials*, 12th Seminar, Pardubice, Czech Republic, **2009**.
- [8] N. Fischer, T. M. Klapötke, J. Stierstorfer, *Z. Anorg. Allg. Chem.* **2009**, *635*, 271.
- [9] T. M. Klapötke, J. Stierstorfer, A. U. Wallek, *Chem. Mater.* **2008**, *20*, 4519.
- [10] N. Fischer, T. M. Klapötke, D. G. Piercey, S. Scheutzow, J. Stierstorfer, *Z. Anorg. Allg. Chem.* **2010**, *636*, 2357.
- [11] T. M. Klapötke, J. Stierstorfer, *Helv. Chim. Acta* **2007**, *90*, 2132.
- [12] J. Stierstorfer, Dissertation, Ludwig-Maximilians-Universität München, **2009**.
- [13] N. Fischer, T. M. Klapötke, J. Stierstorfer, *Z. Anorg. Allg. Chem.* **2009**, *635*, 271.
- [14] G. Bentivoglio, G. Laus, V. Kahlenberg, G. Nauer, H. Schottenberger, *Z. Kristallogr.* **2008**, *223*, 425.
- [15] J. Bernstein, R. E. Davis, L. Shimoni, N.-L. Chang, *Angew. Chem. Int. Ed. Engl.* **1995**, *34*, 1555.
- [16] A. M. Astakhov, A. D. Vasiliev, M. S. Molokoev, A. M. Sirotnin, L. A. Kruglyakova, R. S. Stepanov, *J. Struct. Chem.* **2004**, *45*, 175.
- [17] T. Altenburg, T. M. Klapötke, A. Penger, J. Stierstorfer, *Z. Anorg. Allg. Chem.* **2010**, *636*, 463.
- [18] *Gaussian 09, Revision A.1*, M. J. Frisch, G. W. Trucks, H. B. Schlegel, G. E. Scuseria, M. A. Robb, J. R. Cheeseman, G. Scalmani, V. Barone, B. Mennucci, G. A. Petersson, H. Nakatsuji, M. Caricato, X. Li, H. P. Hratchian, A. F. Izmaylov, J. Bloino, G. Zheng, J. L. Sonnenberg, M. Hada, M. Ehara, K. Toyota, R. Fukuda, J. Hasegawa, M. Ishida, T. Nakajima, Y. Honda, O. Kitao, H. Nakai, T. Vreven, J. A. Montgomery Jr., J. E. Peralta, F. Ogliaro, M. Bearpark, J. J. Heyd, E. Brothers, K. N. Kudin, V. N. Staroverov, R. Kobayashi, J. Normand, K. Raghavachari, A. Rendell, J. C. Burant, S. S. Iyengar, J. Tomasi, M. Cossi, N. Rega, J. M. Millam, M. Klene, J. E. Knox, J. B. Cross, V. Bakken, C. Adamo, J. Jaramillo, R. Gomperts, R. E. Stratmann, O. Yazyev, A. J. Austin, R. Cammi, C. Pomelli, J. W. Ochterski, R. L. Martin, K. Morokuma, V. G. Zakrzewski, G. A. Voth, P. Salvador, J. J. Dannenberg, S. Dapprich, A. D. Daniels, Ö. Farkas, J. B. Foresman, J. V. Ortiz, J. Cioslowski, D. J. Fox, Gaussian, Inc., Wallingford CT, **2009**.
- [19] *NIST Chemistry WebBook*, NIST Standard Reference Database Number 69 (Eds.: P. J. Linstrom, W. G. Mallard), National Institute of Standards and Technology, Gaithersburg MD, 20899, <http://webbook.nist.gov>, October 27, **2011**.
- [20] a) H. D. B. Jenkins, H. K. Roobottom, J. Passmore, L. Glasser,

- Inorg. Chem.* **1999**, 38, 3609; b) H. D. B. Jenkins, D. Tudela, L. Glasser, *Inorg. Chem.* **2002**, 41, 2364.
- [21] a) M. Sućeska, *EXPLO5.3* program, Zagreb, Croatia, **2009**; b) M. Sućeska, *EXPLO5.4* program, Zagreb, Croatia, **2010**.
- [22] Calculation of oxygen balance: Ω (%) = $(wO - 2xC - 1/2yH - 2zS)/1600/M$. (w : number of oxygen atoms, x : number of carbon atoms, y : number of hydrogen atoms, z : number of sulfur atoms, M : molecular weight).
- [23] J. Köhler, R. Meyer, in: *Explosivstoffe*, 9th Ed., Wiley-VCH, Weinheim, **1998**.
- [24] *NATO standardization agreement (STANAG) on explosives, impact sensitivity tests*, no. 4489, 1st ed., Sept. 17, **1999**.
- [25] *NATO standardization agreement (STANAG) on explosive, friction sensitivity tests*, no. 4487, 1st ed., Aug. 22, **2002**.
- [26] *NATO standardization agreement (STANAG) on explosive, electrostatic discharge sensitivity tests*, no. 4490, 1st ed., Feb. 19, **2001**.
- [27] *WIWEB-Standardarbeitsanweisung 4-5.1.02*, Ermittlung der Explosionsgefährlichkeit, hier der Schlagempfindlichkeit mit dem Fallhammer, Nov. 8, **2002**.
- [28] *WIWEB-Standardarbeitsanweisung 4-5.1.03*, Ermittlung der Explosionsgefährlichkeit or der Reibeempfindlichkeit mit dem Reibeapparat, Nov. 8, **2002**.
- [29] <http://www.bam.de>.
- [30] Impact: Insensitive > 40 J, less sensitive \geq 35 J, sensitive \geq 4 J, very sensitive \leq 3 J; friction: Insensitive > 360 N, less sensitive = 360 N, sensitive < 360 N a. > 80 N, very sensitive \leq 80 N, extreme sensitive \leq 10 N; According to the UN Recommendations on the Transport of Dangerous Goods (+) indicates: not safe for transport.
- [31] a) <http://www.ozm.cz/testing-instruments/small-scale-electrostatic-discharge-tester.htm>; b) V. Pelikán, OZM research, Czech Republic, private communication.
- [32] a) *REICHELTL & PARTNER GmbH*, <http://www.reichelt-partner.de>; b) Test methods according to the *UN Recommendations on the Transport of Dangerous Goods, Manual of Test and Criteria*, fourth revised edition, United Nations Publication, New York and Geneva, **2003**, ISBN 92-1-139087-7, Sales No. E.03.VIII.2; 13.4.2 Test 3a (ii) BAM Fallhammer.
- [33] T. Fendt, N. Fischer, T. M. Klapötke, J. Stierstorfer, *Inorg. Chem.* **2011**, 50, 1447.
- [34] *CrysAlisPro*, Agilent Technologies, Version 1.171.35.11, **2011**.
- [35] *SIR-92*, 1993, A Program for Crystal Structure Solution, A. Altomare, G. Casciarano, C. Giacovazzo, A. Guagliardi, *J. Appl. Crystallogr.* **1993**, 26, 343.
- [36] G. M. Sheldrick *SHELXS-97*, Program for Crystal Structure Solution, Universität Göttingen, **1997**.
- [37] G. M. Sheldrick, *SHELXL-97*, Program for the Refinement of Crystal Structures. University of Göttingen, Germany, **1997**.
- [38] A. L. Spek, *PLATON*, A Multipurpose Crystallographic Tool, Utrecht University, Utrecht, The Netherlands, **1999**.
- [39] L. J. Farrugia, *J. Appl. Crystallogr.* **1999**, 32, 837.
- [40] *SCALE3 ABSPACK* - An Oxford Diffraction Program (1.0.4.gui:1.0.3), Oxford Diffraction Ltd, **2005**.

Received: November 2, 2011
Published Online: January 9, 2012

Nitrotetrazolate-2*N*-oxides and the Strategy of *N*-Oxide Introduction

Michael Göbel,[†] Konstantin Karaghiosoff,[†] Thomas M. Klapötke,^{*,†,‡}
Davin G. Piercey,[†] and Jörg Stierstorfer[†]

Department of Chemistry and Biochemistry, Energetic Materials Research, Ludwig-Maximilian University of Munich, Butenandtstr. 5-13, D-81377 Munich, Germany, and Center for Energetic Concepts Development, CECD, University of Maryland, UMD, Department of Mechanical Engineering, College Park, Maryland 20742, United States

Received August 2, 2010; E-mail: tmk@cup.uni-muenchen.de

Abstract: The first anionic tetrazole-2*N*-oxide has been prepared by mild aqueous oxidation of easily prepared 5-nitrotetrazole with commercially available oxone in high yields. The result of protonating 5-nitrotetrazolate-2*N*-oxide has been identified as a hydroxytetrazole, and the nitrogen-rich salts including ammonium, hydroxylammonium, guanidinium, aminoguanidinium, diaminoguanidinium, and triaminoguanidinium have been prepared and characterized. When compared to the nitrogen-rich salts of nitrotetrazole, the nitrogen-rich salts of nitrotetrazole-2*N*-oxide show superior energetic performance as calculated by the EXPLO5 computer code, using heats of formation calculated using the CBS-4M level of quantum mechanical theory. The impact, friction, and electrical spark sensitivities of the nitrogen-rich nitrotetrazolate-2*N*-oxides were measured and cover the whole range from sensitive to insensitive energetic materials.

Introduction

The design of new energetic materials, encompassing all of propellants, explosives, and pyrotechnics, is a long-standing tradition in the chemical sciences. The chemistry of energetic materials has led to many advances in the chemical sciences, notably the concept of isomerism which was derived from the structural isomers silver fulminate and silver cyanate.¹ Due to the nature of energetic materials being on the borderline between existence and nonexistence, many historical chemists were drawn to this field including Liebig, Berzelius, and Gay-Lussac.^{2,3} Energetic materials chemistry pushes the limits of the unique molecules that can be created, while retaining some semblance of stability. The design of modern energetic materials is a modern scientific challenge.^{4–6} Currently used, outdated, energetics suffer from limitations that can be remedied by the tailoring at the molecular level of new energetic molecules. One of the most important characteristics of new energetic materials is that they can be characterized as “green” by not causing a toxicological problem or an environmental hazard. New energetics must also meet increased performance requirements, where propellants must transport ever-increasing payloads, explosives must become more powerful, and pyrotechnics demands a greater range and purity of spectral emissions.⁷

Exemplifying these problems is the quintessential commonly used explosive, RDX (1,3,5-trinitro-1,3,5-triazinane), a potential carcinogen,⁸ and possessing nitramines it is known to be toxic to vital organisms at the base of the food chain.⁹ In particular, RDX is also sensitive to physical stimuli so for use it must be stabilized.¹⁰ Technical challenges facing today’s synthetic energetic chemists include the preparation of new energetic materials with performance equal to or surpassing that of RDX, while tailoring them for high personal and ecological safety.^{11–13}

Traditional energetic materials such as TNT (2,4,6-trinitrotoluene) and RDX derive the majority of their energy from the oxidation of a carbon backbone and the presence of both fuel and oxidizer in the same molecule. New trends in the research and development of novel energetics have introduced two other classes of energetic materials: high heat of formation, nitrogen-rich materials (e.g., high-nitrogen heterocyclics such as tetrazoles, and tetrazines) and caged and cyclic compounds (e.g., cubane based energetics).⁷ Naturally, these strategies can and have been combined making high-nitrogen, strained, heterocycles an intense area of research.

[†] Ludwig-Maximilian University of Munich.

[‡] University of Maryland.

(1) Gay-Lussac, J. L. *Ann. Chem. Phys.* **1824**, 27 (2), 199.

(2) Gay-Lussac, J. L.; Leibig, J. *Kastners Archiv* **1824**, II, 58–91.

(3) Berzelius, J. *Ann. Chem. Pharm.* **1844**, L, 426–429.

(4) Davis, T. L. *The Chemistry of Powder and Explosives*; Angrif, Los Angeles, 1943; pp 424–430.

(5) De Yong, L. V.; Campanella, J. J. *Hazard Mater.* **1989**, 21, 125–133.

(6) Klapötke, T. M.; Sabaté, C. M. *Heteroatom. Chem.* **2008**, 19, 301–305.

(7) Klapötke, T. M. *High Energy Density Materials*; Springer: 2007.

(8) McLellan, W.; Hartley, W. R.; Brower, M. *Health advisory for hexahydro-1,3,5-trinitro-1,3,5-triazine*. Technical report PB90–273533; Office of Drinking Water, U.S. Environmental Protection Agency: Washington, DC, 1988.

(9) Robidoux, P. Y.; Hawari, J.; Bardai, G.; Paquet, L.; Ampleman, G.; Thiboutot, S.; Sunahara, G. I. *Arch. Environ. Contam. Toxicol.* **2002**, 43, 379–388.

(10) Bowers, R. C.; Romans, J. B.; Zisman, W. A. *Ind. Eng. Chem. Prod. Res. Dev.* **1973**, 12 (1), 2–13.

(11) Altenburg, T.; Klapötke, T. M.; Penger, A.; Stierstorfer, J. *Z. Anorg. Allg. Chem.* **2010**, 636, 463–471.

(12) Klapötke, T. M.; Sabaté, C. M. *Z. Anorg. Allg. Chem.* **2009**, 635, 1812–1822.

(13) Fischer, N.; Karaghiosoff, K.; Klapötke, T. M.; Stierstorfer, J. *Z. Anorg. Allg. Chem.* **2010**, 636, 735–739.

For a nitrogen-rich, endothermic material, possessing ring or cage strain, to find application as a high explosive it needs to possess high thermal and mechanical stabilities, while at the same time satisfying the increasing demand for higher performing materials. Unfortunately, in many cases high performance and low sensitivity appear to be mutually exclusive; many high performing materials are not stable enough to find practical use, and many materials with the desired sensitivity do not possess the performance requirements of a material to replace a commonly used explosive.¹⁴ This trend is exemplified in the range of five-membered azoles from pyrazole to pentazole, where pyrazole is not used in energetics due to low performance, and the few pentazole derivatives known are highly unstable.¹⁵ One of the most promising heterocyclic backbones for the preparation of high-performing energetics is the tetrazole ring.

Possessing high heats of formation resulting from the nitrogen–nitrogen bonds, ring strain, and high density, the tetrazole ring has allowed the preparation of high-performing primary¹⁶ and secondary¹⁷ explosives. Depending on the ring substituents and anion/cation pairing, tetrazole based energetics can be tailored to span the spectrum of sensitivity from insensitive to highly sensitive (primary explosives). The sensitivity of 5-substituted anionic tetrazole based explosive materials decreases in the order of $N_2^+ > N_3 > NO_2 > Cl > NNO_2 > H > NH_2 > CH_3$ as a function of the electron-withdrawing nature of the substituent.¹⁸ Additionally, due to their aromatic ring, tetrazoles are generally thermally stable.¹⁹

Other than the high heats of formation, for a molecule or salt to be a high-performing energetic, a high oxygen balance is required. The oxygen balance is a percentage representation of the oxygen content of a compound, enabling it to oxidize all of its nonoxidizing content to their respective oxides and is easily calculated by the equation $\Omega (\%) = (wO - 2xC - 1/2yH - 2zS) \cdot 1600/M$ (w : number of oxygen atoms, x : number of carbon atoms, y : number of hydrogen atoms, z : number of sulfur atoms). A current limitation of current tetrazole-based energetic materials is the low oxygen balances.^{13,20,21} Anionic tetrazole oxygen balances are limited by the explosophore of choice on position 5 of the ring, the carbon atom. High-performance tetrazole-based energetics often contain nitro,²¹ nitrimino,¹³ or azido²⁰ functionalities upon the carbon of position 5, and at most these contain two oxygen atoms, only sufficient for the oxidation of the tetrazole carbon to carbon dioxide, however, not enough to oxidize any nitrogen-rich, oxygen-lacking energetic cation (e.g., aminoguanidinium, diaminoguanidinium) paired with the energetic tetrazole. There is a pressing need in the energetic materials field to be able to incorporate more oxygen atoms onto derivatives of the already high-performing tetrazole ring. Introducing *N*-oxides onto the tetrazole ring may prove to be a

viable solution to this challenge and may push the limits of well-explored tetrazole chemistry into a new, unexplored, dimension.

Amine *N*-oxides are a strategy of increasing density, stability, and performance of energetic materials and has found use in insensitive explosives.²² Their zwitterionic structure and large dipole moment allow for the formation of compounds with high densities,²³ while simultaneously increasing their oxygen balance compared to the nonoxide amine. For example, comparison of 2,4,6-trinitropyridine to 2,4,6-trinitropyridine-1-oxide shows both a higher density and as such higher energetic performance.²⁴ The stabilizing effects of the *N*-oxide on a nitrogen-rich system is well-known; for example, 1,2,3,4-tetrazines are uncommon in the literature with only a single compound claimed to exist.²⁵ In contrast, the 1,2,3,4-tetrazine-1,3-dioxides are well-known and show remarkably high stabilities, with many members of this highly energetic class of compounds decomposing above 200 °C.²⁵ For high-nitrogen systems, the source of this stabilization has been calculated to be resultant from the *N*-oxide removing lone pair electron density (increasing $\sigma-\pi$ separation) that would otherwise destabilize the nitrogen system by donating electron density into antibonding orbitals.^{26–28}

Tetrazole oxides are uncommon in the literature. The tetrazole 1*N*-oxides are only slightly more common than the 2*N*-oxides with a handful of compounds and preparations known in the literature; the first 2*N*-oxides were only described in 2010. The 1*N*-oxides have been prepared by the rearrangement of 1-alkoxy tetrazoles either by high temperature²⁹ or by means of trifluoroacetic acid.³⁰ Also known is the reaction of toxic HN_3 with nitrolic acids to produce tetrazole 1*N*-oxides.³¹ The tetrazole 2*N*-oxides were not known until earlier this year, where 1,5-disubstituted tetrazoles were successfully oxidized with hypofluorous acid in acetonitrile to give 1,5-disubstituted tetrazole-2*N*-oxides.³² This was the first preparation of a tetrazole oxide by oxidation of the tetrazole ring, widely thought impossible prior as a result of the low HOMO in tetrazoles,³³ where previous attempts at forming oxides on the tetrazole ring only led to hydroxy compounds.^{34,35} To date, anionic tetrazole 2*N*-oxides are unknown in scientific literature.

We have developed a procedure for the mild, aqueous, oxidation of nitrotetrazole to the corresponding nitrotetrazolate-2*N*-oxide. The base nitrotetrazole anion was first synthesized

- (14) Sikder, A. K.; Sikder, N. *J. Hazard. Mater.* **2004**, *112*, 1–15.
- (15) Carlqvist, P.; Östmark, H.; Brinck, T. *J. Phys. Chem. A* **2004**, *108*, 7463–7467.
- (16) Huynh, M. H. V.; Hiskey, M. A.; Meyer, T. J.; Wetzler, M. *Proc. Natl. Acad. Sci. U.S.A.* **2006**, *103* (14), 5409–5412.
- (17) Boese, R.; Klapötke, T. M.; Mayer, P.; Verma, V. *Propellants, Explos., Pyrotech.* **2006**, *31* (4), 263–268.
- (18) Zhao-Xu, C.; Heming, X. *Int. J. Quantum Chem.* **2000**, *79*, 350–357.
- (19) Stierstorfer, J.; Klapötke, T. M.; Hammerl, A.; Chapman, R. D. *Z. Anorg. Allg. Chem.* **2008**, *634*, 1051–1057.
- (20) Klapötke, T. M.; Stierstorfer, J. *J. Am. Chem. Soc.* **2009**, *131*, 1122–1134.
- (21) Klapötke, T. M.; Mayer, P.; Sabaté, C. M.; Welch, J. M.; Wiegand, N. *Inorg. Chem.* **2008**, *47* (13), 6014–6027.

- (22) Zhang, C.; Wang, X.; Huang, H. *J. Am. Chem. Soc.* **2008**, *130* (26), 8359–8365.
- (23) Molchanova, M. S.; Pivina, T. S.; Arnautova, E. A.; Zefirov, N. S. *J. Mol. Struct.* **1999**, *465*, 11–24.
- (24) Jia-Rong, L.; Jian-Min, Z.; Hai-Shan, D. *J. Chem. Crystallogr.* **2005**, *35* (12), 943–948.
- (25) Churakov, A. M.; Tartakovsky, V. A. *Chem. Rev.* **2004**, *104*, 2601–2616.
- (26) Glukhovtsev, M. N.; Simkin, B. Y.; Minkin, V. I. *Zh. Organicheskoi Khim.* **1988**, *24* (12), 2486–2488.
- (27) Inagake, S.; Goto, N. *J. Am. Chem. Soc.* **1987**, *109*, 3234–3240.
- (28) Noyman, M.; Zilberg, S.; Haas, Y. *J. Phys. Chem. A* **2009**, *113*, 7376–7382.
- (29) Plenkiewicz, J.; Roszkiewicz, A. *Pol. J. Chem.* **1993**, *67* (10), 1767–1778.
- (30) Liepa, A. J.; Jones, D. A.; McCarthy, T. D.; Nearn, R. H. *Aust. J. Chem.* **2000**, *53* (7), 619–622.
- (31) Maffei, S.; Bettinetti, G. F. *Ann. Chim. (Rome, Italy)* **1956**, *46*, 812–815.
- (32) Harel, T.; Rozen, S. *J. Org. Chem.* **2010**, *75*, 3141–3143.
- (33) Eicher, T.; Hauptman, S. *The Chemistry of Heterocycles*, 2nd ed.; Wiley: 2003; p 212.
- (34) Begtrup, M.; Vedsoe, P. *J. Chem. Soc., Perkin Trans. 1* **1995**, 243–247.
- (35) Giles, R. G.; Lewis, N. J.; Oxley, P. X.; Quick, J. K. *Tetrahedron Lett.* **1999**, *40*, 6093–6094.

Scheme 1. Oxidation of Nitrotetrazolate to the Nitrotetrazolate-2*N*-oxide Anion

over 75 years ago by von Herz and has enjoyed the ability to form next-generation “green” primary explosives.¹⁶ Additionally, the nitrogen-rich salts²¹ and covalent compounds¹⁷ of nitrotetrazole are potential green replacements of currently used secondary explosives. Possessing a wide spectrum of fully characterized compounds with various properties, nitrotetrazole proved to be an ideal candidate for oxidation to the nitrotetrazole-2*N*-oxide allowing comparison of the properties of our newly prepared nitrogen-rich nitrotetrazolate-2*N*-oxides with the corresponding nitrotetrazolates.

Beyond application as energetic materials, tetrazole oxides may find application for medicinal purposes as both *N*-oxides^{36,37} and tetrazoles have known biological activity.³⁸

Herein we report on the synthesis and characterization of a series of highly energetic nitrogen- and oxygen-rich salts containing the nitrotetrazolate 2*N*-oxide anion. The compounds prepared were characterized by X-ray diffraction, infrared and Raman spectroscopy, multinuclear NMR spectroscopy, elemental analysis, and DSC. Computational calculations predicting energetic performance properties confirm the initial hypothesis that oxidation of tetrazoles to tetrazole oxides is indeed an effective method of improving energetic performance. We expand the field of tetrazole chemistry by offering the first synthesis of an anionic tetrazole 2*N*-oxide in a high-yielding, aqueous synthesis starting from the parent tetrazole. We have exemplarily demonstrated the ability of this new class of compounds to form high performance, energetic materials based on nitrogen-rich salts of the nitrotetrazolate-2*N*-oxide moiety.

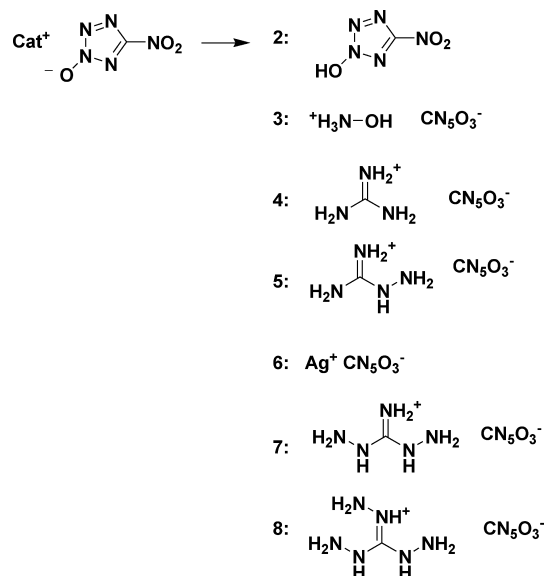
Results and Discussion

Synthesis. The most facile synthesis of the nitrotetrazolate-2*N*-oxide anion is by the oxidation of ammonium 5-nitrotetrazolate hemihydrate in a saturated oxone solution at 40 °C (Scheme 1).

The free acid **2** and salts **3–6** were prepared from the ammonium salt by simple acid–base chemistry and metathesis reactions with either acid or (amino) guanidinium (bi) carbonate, while salts **7** and **8** were prepared from the silver salt **6** and the corresponding substituted guanidinium halide (Scheme 2). Salt **3** was prepared by ion exchange.

CAUTION. 5-Nitrotetrazole-2*N*-oxide (**2**) and its salts (**1**, **3–8**) are all energetic compounds with sensitivity to various stimuli. While we encountered no issues in the handling of these materials, proper protective measures (face shield, ear protection, body armor, Kevlar gloves, and earthened equipment) should be used at all times.

The oxidation of ammonium nitrotetrazolate hemihydrate in a saturated aqueous Oxone solution proceeds smoothly at 40 °C over three days. Acidification of the reaction liquors allowed separation of the crude protonated nitrotetrazolate-2*N*-oxide,

Scheme 2. Prepared Salts of Nitrotetrazolate-2*N*-oxide

which after reaction with dilute, aqueous ammonia yielded ammonium nitrotetrazolate-2*N*-oxide. The ammonium salt (ANTX, **1**) was purified by recrystallization from acetonitrile yielding crystals suitable for X-ray diffraction. The free acid 5-nitrotetrazole-2*N*-oxide (**2**) was extracted from an acidic solution of the aqueous ammonium salt with ether; it is extremely deliquescent, dissolving itself in absorbed water after only a few minutes of exposure to air. Crystals of **2** were grown by slow evaporation of an ether/toluene solution under vacuum. The hydroxylammonium salt (HxNTX, **3**) was prepared by ion-exchanging the ammonium salt and recrystallizing from acetonitrile. The crystals grown this way contained a molecule of acetonitrile which was lost upon drying under high vacuum; crystals suitable for X-ray diffraction were grown from slow evaporation of an ethyl acetate solution. Guanidinium (GNTX, **4**) and aminoguanidinium (AGNTX, **5**) salts were prepared by refluxing an ethanolic solution of **1** with the corresponding carbonate or bicarbonate. After 24 h the aminoguanidinium salt was isolated as crystals suitable for X-ray diffraction upon cooling; however, the guanidinium salt required ether diffusion into a methanolic solution in order to obtain crystals. Preparation of diaminoguanidinium (DAGNTX, **7**) and triaminoguanidinium (TAGNTX, **8**) nitrotetrazolate-2*N*-oxide required the preparation of silver nitrotetrazolate-2*N*-oxide from the ammonium salt and aqueous silver nitrate in stoichiometric quantities. The silver salt (**6**) precipitates as a flocculent precipitate slightly soluble in water. The silver salt (**6**) is not a sensitive primary explosive unlike silver nitrotetrazolate²¹ and can be safely handled. **6** was easily reacted with aqueous diaminoguanidinium iodide or triaminoguanidinium chloride, which after filtration of the precipitated silver halide, and evaporation of water, yielded pure diaminoguanidinium nitrotetrazolate-2*N*-oxide (**7**) and triaminoguanidinium nitrotetrazolate-2*N*-oxide (TAGNTX, **8**), after recrystallization from ethanol. Crystals suitable for X-ray diffraction were grown for both **7** and **8** by the slow diffusion of ether into a methanolic solution of the material.

Spectroscopy. Multinuclear NMR spectroscopy, especially ¹³C and ¹⁵N spectroscopy, proved to be a valuable tool for the characterization of the tetrazole and tetrazolates. With the exception of the free acid **2**, all NMR spectra were performed in DMSO-*d*₆. The extreme acidity of **2** mandated NMR

(36) Pyatakova, N. V.; Khropov, Y. V.; Churakov, A. M.; Tarasova, N. I.; Serezhnikov, V. A.; Vanin, A. F.; Tartakovskiy, V. A.; Severina, I. S. *Biokhimiya* **2002**, *67* (3), 396–402.

(37) Boiani, M.; Cerecetto, H.; González, M.; Risso, M.; Olea-Azar, C.; Piro, O. E.; Castellano, E. E.; Ceráin, A. L.; Ezpeleta, O.; Monge-Vega, A. *Eur. J. Med. Chem.* **2001**, *36*, 771–782.

(38) Jin, T.; Kamijo, S.; Yamamoto, Y. *Tetrahedron Lett.* **2004**, *45*, 9435–9437.

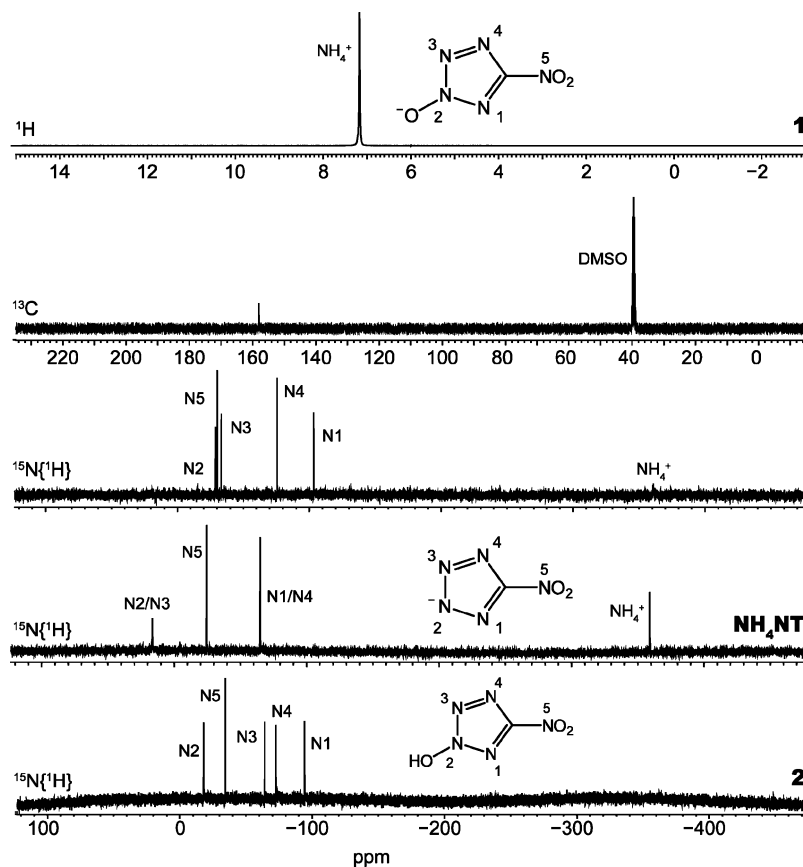


Figure 1. Multinuclear (^1H , ^{13}C , and ^{15}N) spectra of ANTX (**1**) compared to ^{15}N spectra of ammonium nitrotetrazolate (NH_4NT) and free acid (**2**).

experiments to be performed in $\text{THF-}d_8$; spectra could not be measured in $\text{DMSO-}d_6$ as **2** is a strong acid, protonating DMSO , and attempts to perform NMR in $\text{acetone-}d_6$ led to polymerization of the acetone. In all anionic nitrotetrazolate-2*N*-oxides the single ^{13}C carbon shift for the CN_5O_3^- anion lies near 158 ppm. In the free acid (**2**) the ^{13}C shift for $\text{CN}_5\text{O}_3\text{H}$ shifts downfield to 162 ppm. Figure 1 illustrates the ^1H , ^{13}C , and ^{15}N NMR spectra of ANTX (**1**). The ammonium protons occur as a broad singlet at ~ 7.4 ppm, similar to that in ammonium nitrotetrazolate,²¹ and the ^{13}C shift of 158.4 ppm is approximately 10 ppm upfield compared with the ^{13}C shift of 169.5 ppm in ammonium nitrotetrazolate.²¹ When the ^{15}N spectrum of ANTX (**1**) is compared with that of ammonium nitrotetrazolate (Figure 1), a loss of nitrogen equivalency is seen between N1 and N4 and between N2 and N3. The largest change in chemical shift for a ring nitrogen between the nitrotetrazolate ion and the nitrotetrazolate-2*N*-oxide ion is for N2, where in nitrotetrazolate N2's chemical shift occurs at 16.4 ppm, but in nitrotetrazolate-2*N*-oxide this peak has shifted to -33.3 ppm. The remainder of the peak assignments were made after the determination that the largest peak shift would belong to the nitrogen onto which the *N*-oxide has been added (Figure 1). Protonation of the nitrotetrazolate-2*N*-oxide anion yields highly acidic **2**, with a proton resonance at 12.99 ppm. This is out of the range for an acidic N–H proton, as even 5-nitrotetrazole with a $\text{p}K_a$ of -0.8 ³⁹ has its proton shift at 6.29 ppm.⁴⁰ This

high ^1H shift along with the ^{15}N NMR (Figure 1), where the largest N shift compared to that of the nitrotetrazolate-2*N*-oxide anion is for N2 led to the determination that the nitrotetrazolate-2*N*-oxide protonates forming a 2-hydroxy-5-nitrotetrazole. Lack of N–H coupling in the ^{15}N spectrum supports this conclusion. ^{15}N signal assignments (Figure 1) were made based on comparison with our ^{15}N spectra of nitrotetrazolate-2*N*-oxide and with the ^{15}N spectrum of 5-nitrotetrazole.⁴⁰

The IR and Raman spectra of all compounds were recorded and assigned using frequency analysis from an optimized structure (B3LYP/cc-pVDZ using the Gaussian 03 software).⁴¹ All calculations were performed at the DFT level of theory; the gradient-corrected hybrid three-parameter B3LYP^{42,43} functional theory has been used with a correlation consistent cc-pVDZ basis set.^{44–47} The anionic nitrotetrazolate-2*N*-oxides generally contain a strong, diagnostic band in the infrared ranging from 1531 to 1551 cm^{-1} . The calculated value for this band is 1549 cm^{-1} , and it arises from the N–O stretch, with a minor constitution of asymmetric NO_2 stretching and the N1–N2–N3 symmetric tetrazole ring in phase deformation. The Raman spectra of all salts of nitrotetrazolate-2*N*-oxide all adopt

(39) Koldobskii, G. I.; Soldatenko, D. S.; Gerasimova, E. S.; Khokryakova, N. R.; Shcherbinin, M. B.; Lebedev, V. P.; Ostrovskii, V. A. *Russ. J. Org. Chem.* **1997**, *33* (12), 1771–1783.

(40) Klapötke, T. M.; Sabaté, C. M.; Stierstorfer, J. *New J. Chem.* **2009**, *33*, 136–147.

(41) Frisch, M. J. *Gaussian 03*, revision C.03; see ref 1 in the Supporting Information

(42) Becke, A. D. *J. Chem. Phys.* **1993**, *98*, 5648–5652.

(43) Lee, C.; Yang, W.; Parr, R. G. *Phys. Rev. B* **1988**, *37*, 785–789.

(44) Woon, D. E.; Dunning, T. H., Jr. *J. Chem. Phys.* **1993**, *98*, 1358–1371.

(45) Kendall, R. A.; Dunning, T. H., Jr.; Harrison, R. J. *J. Chem. Phys.* **1992**, *96*, 6796–6806.

(46) Dunning, T. H., Jr. *J. Chem. Phys.* **1989**, *90*, 1007–1023.

(47) Peterson, K. A.; Woon, D. E.; Dunning, T. H., Jr. *J. Chem. Phys.* **1994**, *100*, 7410–7415.

Table 1. Relative Energies of Protonation Sites on the Nitrotetrazolate-2*N*-oxide Anion

	N1-H	N3-H	N4-H	O-H
Point group	C _s	C _s	C _s	C _s
- <i>E</i> (a.u.)	537.930 995	537.936 350	537.935 818	537.943 076
El. state	¹ A'	¹ A'	¹ A'	¹ A'
NIMAG	0	0	0	0
zpe (kcal/mol)	33.1	33.5	33.5	33.3
<i>E</i> _{rel} (kcal/mol)	7.6	4.2	4.6	0.0

a diagnostic pattern of three bands of high intensity. The first of these occurs in the range of 1407–1421 cm⁻¹ (calcd 1431 cm⁻¹) and corresponds to a combined C–NO₂ stretch and an asymmetric C1–N4–N3 in a phase tetrazole ring stretch. The next of these occurs at 1048–1112 cm⁻¹ (calcd 1060 cm⁻¹) and corresponds to N1–N2 stretching, in-phase tetrazole ring deformation, and C–NO₂ stretching. The final diagnostic stretch at 984–1010 cm⁻¹ (calcd 918 cm⁻¹) corresponds to N2–N3

stretching with a small component of NO₂ asymmetric stretching. Due to its deliquescent nature, the acid (2), Raman proved to be a far more effective method of characterization compared to IR, as the water present resulted in broad bands in the IR, whereas in the Raman bands were sharp. The intense peak at 1423 (1433 calcd) cm⁻¹ is a combination of a symmetric NO₂ stretch and an asymmetric, in-phase, N1–C5–N4 stretch. The next most intense Raman band at 1037 (1040 calcd) cm⁻¹ is an in-plane asymmetric stretch of the tetrazole ring. The N–O stretch of the tetrazole oxide occurs at 761 (751 calcd) cm⁻¹ with a significant component of this motion being the symmetric N1–N2–N3 deformation of the tetrazole ring. At 412 (402 calcd) cm⁻¹ is the in-plane rocking of the N–O and the C–NO₂. These assignments supported the assignment of compound 2, resulting from the protonation of nitrotetrazolate-2*N*-oxide, as being a hydroxytetrazole as opposed to being a ring-protonated species.

Table 2. Crystallographic Data and Structure Refinement Details for Compounds 1–5 and 7–8

compound	ANTX (1)	HNTX (2)	HxNTX (3)	GNTX (4)	AGNTX (5)	DAGNTX (7)	TAGNTX (8)
formula	C ₁ H ₄ N ₆ O ₃	C ₁ H ₁ N ₅ O ₃	C ₁ H ₄ N ₆ O ₄	C ₂ H ₆ N ₈ O ₃	C ₂ H ₇ N ₉ O ₃	C ₂ H ₈ N ₁₀ O ₃	C ₂ H ₉ N ₁₁ O ₃
formula weight [g mol ⁻¹]	148.10	131.07	164.10	190.15	205.17	220.18	235.20
temperature [K]	100	173	173	173	173	173	173
crystal system	orthorhombic	monoclinic	monoclinic	triclinic	monoclinic	triclinic	monoclinic
space group	<i>Pbca</i>	<i>Cc</i>	<i>P2₁/c</i>	<i>P1</i>	<i>P2₁/c</i>	<i>P1</i>	<i>P2₁/c</i>
<i>a</i> [Å]	9.3989(4)	7.9946(6)	8.489(5)	6.0610(8)	7.812(3)	6.4344(6)	10.267(3)
<i>b</i> [Å]	7.9263(3)	9.1402(6)	12.341(5)	7.5528(9)	15.783(2)	8.0055(7)	12.622(2)
<i>c</i> [Å]	15.2618(6)	6.2269(4)	5.626(5)	8.2886(9)	6.619(3)	8.5160(8)	7.370(3)
α [deg]	90	90	90	79.360(10)	90	90.218(7)	90
β [deg]	90	99.584(6)	91.221(5)	89.576(10)	100.194(5)	94.461(7)	93.724(5)
γ [deg]	90	90	90	85.918(11)	90	97.519(7)	90
volume [Å ³]	1136.98(8)	448.66(5)	589.3(7)	371.96(8)	803.2(5)	433.53(7)	953.1(5)
formula <i>Z</i>	8	4	4	2	4	2	4
space group <i>Z</i>	8	4	4	2	4	2	4
density calcd [g cm ⁻³]	1.7304(1)	1.9404(2)	1.850(2)	1.6978(4)	1.6967(17)	1.6867(3)	1.6391(15)
<i>R</i> ₁ / <i>wR</i> ₂ [all data]	0.0336/0.0659	0.0270/0.0437	0.0349/0.0592	0.1166/0.2089	0.0795/0.0582	0.0800/0.0887	0.0607/0.0753
<i>R</i> ₁ / <i>wR</i> ₂ [<i>I</i> > 2σ(<i>I</i>)]	0.0259/0.0638	0.0220/0.0428	0.0246/0.0571	0.0760/0.1943	0.0359/0.0538	0.0383/0.0799	0.0332/0.0699
<i>S</i>	0.958	0.921	0.928	0.906	0.842	0.861	0.99
CCDC	783 533	783 532	783 534	783 535	783 536	783 537	783 538

Table 3. Comparison of Selected Bond Lengths and Angles of Compounds 1–5 and 7–8 to the Corresponding 5-Nitro-2*H*-tetrazol Derivatives^a

	Bond lengths/Å					Bond angles (deg)					ρ/Δ	
	N1–N2	N2–N3	N3–N4	N4–C1	C1–N1	C1–N1–N2	N1–N2–N3	N2–N3–N4	N3–N4–C1	N4–C1–N1		N2–O1
1 ANTX	1.33	1.34	1.34	1.32	1.33	99.4	114.9	105.2	105.0	115.6	1.301	1.730/+0.09
3 HxNTX	1.32	1.33	1.34	1.32	1.33	99.1	115.4	105.2	104.3	116.0	1.306	1.850/+0.13
4 GNTX	1.34	1.34	1.35	1.32	1.33	99.3	114.3	105.5	104.3	116.7	1.286	1.698/+0.05
5 AGNTX	1.33	1.34	1.35	1.32	1.33	99.7	114.1	105.6	104.5	116.1	1.288	1.697/+0.04
7 DAGNTX	1.32	1.34	1.35	1.32	1.34	99.4	114.9	105.9	105.2	114.5	1.273	1.687/+0.09
8 TAGNTX	1.33	1.33	1.34	1.32	1.34	99.3	114.3	106.0	104.3	116.1	1.293	1.639/+0.04
Average	1.33	1.34	1.34	1.32	1.33	99.4	114.6	105.5	104.5	116.1	1.295	1.717/+0.07
10 ANT ²¹	1.33	1.33	1.34	1.32	1.32	103.7	109.3	109.7	103.2	114.1	–	1.637/–0.09
11 HyNT ²¹	1.34	1.32	1.34	1.32	1.32	103.0	109.5	109.9	102.8	114.8	–	1.72/–0.13
12 GNT ²¹	1.34	1.33	1.34	1.33	1.34	102.5	110.0	110.0	102.5	115.2	–	1.644/–0.05
13 AGNT ²¹	1.34	1.32	1.34	1.31	1.32	102.8	109.7	109.7	103.1	114.8	–	1.661/–0.04
14 DAGNT ²¹	1.34	1.32	1.34	1.31	1.31	102.9	109.6	109.5	102.8	115.3	–	1.595/–0.09
15 TAGNT ²¹	1.35	1.34	1.35	1.33	1.33	102.9	109.7	109.3	103.1	114.9	–	1.601/–0.04
Average	1.34	1.33	1.34	1.32	1.32	103.0	109.6	109.7	102.9	114.9	–	1.643/–0.07
2 HNTX	1.31	1.32	1.32	1.34	1.32	98.9	115.5	104.5	105.0	115.1	1.344	1.940/+0.04
9 HNT ⁴⁰	1.32	1.32	1.32	1.34	1.31	98.9	115.5	105.5	104.2	115.9	–	1.899/–0.04

^a HNT = 5-nitro-2*H*-tetrazol; ANT = ammonium 5-nitro-2*H*-tetrazolate; HyNT = hydrazinium 5-nitro-2*H*-tetrazolate; GNT = guanidinium 5-nitro-2*H*-tetrazolate, AGNT = aminoguanidinium 5-nitro-2*H*-tetrazolate; DAGNT = diaminoguanidinium 5-nitro-2*H*-tetrazolate; TAGNT = triaminoguanidinium 5-nitro-2*H*-tetrazolate; ρ = calculated crystal density/g cm⁻³, Δ = difference to corresponding structure containing/missing the *N*-oxide moiety.

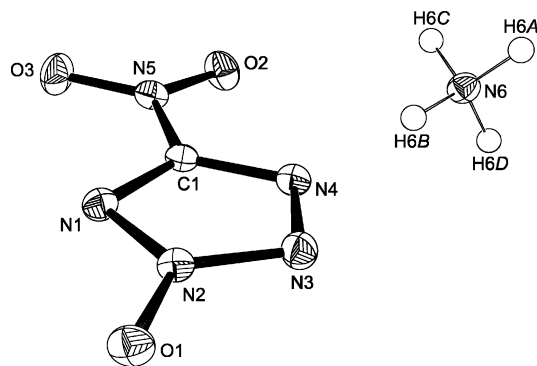


Figure 2. ORTEP representation of the molecular structure of **1** (ANTX, ammonium 5-nitrotetrazolate-2*N*-oxide) in the crystalline state. Displacement ellipsoids are shown at the 50% probability level.

Relative Energy. To support the NMR data in that the nitrotetrazolate-2*N*-oxide anion is protonated on the oxygen forming 2-hydroxy-5-nitrotetrazole, the relative energies of N1–H, N3–H, and N4–H ring-protonated species were calculated. The calculations performed were in accordance with the same software, theory, and basis set as described in the vibrational spectroscopy section. The relative energies calculated indicate that the 2-hydroxy-5-nitrotetrazole is the lowest energy species formed from the protonation of the nitrotetrazolate-2*N*-oxide anion (Table 1).

Single Crystal X-ray Structure Analysis. Compounds **1–5** as well as **7–8** have been characterized using single crystal X-ray structure determination. Table 2 summarizes a selection of crystallographic data and refinement details. A comparison of selected bond length and angles of compounds **1–5** and **7–8** and to the corresponding compounds **9–15** bearing no *N*-oxide moiety is given in Table 3. The data reveal that bond length values of both groups of anions are comparable within the limits of error in contrast to their bond angles. The average N₁–N₂–N₃ bond angle of the *N*-oxide anions has a value of 114.6° as compared to an average value of 109.6° of the *N*-oxide free nitrotetrazolate anions (Table 3) indicative of the higher sp² type hybridization of the *N*-oxide nitrogen atom. In contrast, the two neighboring angles (C₁–N₁–N₂ *N*-oxide: 99.4°/parent compound: 103.0°, N₂–N₃–N₄ *N*-oxide: 105.5°/parent compound: 109.7°) have smaller values yielding a slightly distorted tetrazole moiety in the 5-nitrotetrazolate-2*N*-oxide anions compared to the symmetric structure of the tetrazole in the parent nitrotetrazolate anions. This difference is not observed in the case of the corresponding free acids. Both 5-nitro-2*H*-tetrazole (**9**, HNT)

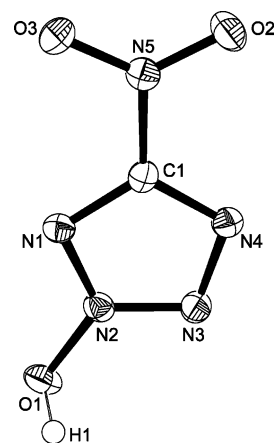


Figure 4. ORTEP representation of the molecular structure of **2** (2-hydroxy-5-nitrotetrazole, HNTX) in the crystalline state. Displacement ellipsoids are shown at the 50% probability level.

and 2-hydroxy-5-nitrotetrazole (**2**, HNTX) share comparable bond lengths and angles (cf. Table 3). The most striking difference between the *N*-oxide containing compounds and their parent relatives is observed in their extended structures. Each of the compounds **1–5** and **7–8** has a higher crystal density compared to the corresponding *N*-oxide free compound as a consequence of the *N*-oxide being involved in multiple intermolecular bonding interactions as exemplified in the case of **1** and **2** (cf. Figures 3 and 5).

The structure of **1** (ANTX, ammonium 5-nitrotetrazolate-2*N*-oxide) at 100 K has orthorhombic (*Pbca*) symmetry. The asymmetric unit consists of one molecule (Figure 2).

The extended structure of **1** consists of two-dimensional ribbons of 5-nitrotetrazolate-2*N*-oxide anions interconnected via hydrogen bonding (N–H⋯O_{*N*-oxide}, N–H⋯O_{nitro group}, N–H⋯N_{ring}) through each of the hydrogen atoms of the ammonium cations. Additionally, one of the oxygen atoms of the nitro group is involved in an interaction with the π electrons of the tetrazole ring (Figure 3).

The structure of **2** (2-hydroxy-5-nitrotetrazole, HNTX) at 173 K has monoclinic (*Cc*) symmetry. The asymmetric unit consists of one molecule (Figure 4).

The remarkably high density of 1.9404(2) g cm^{–3} can be rationalized in terms of intermolecular interactions. Hydrogen bonding of the hydroxyl group to one ring nitrogen atom takes place along with a nitro group π interaction yielding two-dimensional ribbons similar to the structure of **1**. However, in

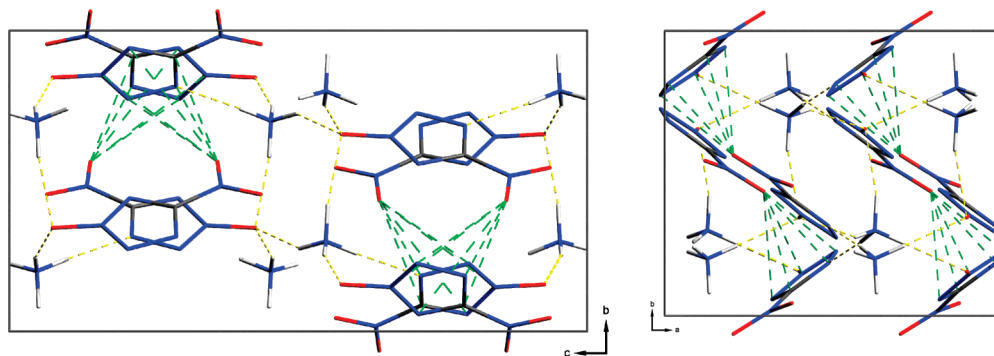


Figure 3. Unit cell packing of **1** (ANTX, ammonium 5-nitrotetrazolate-2*N*-oxide), viewed along the *a* axis (left) and *c* axis (right). Yellow dashed lines indicate intermolecular hydrogen bonding (N6–H6A⋯O1ⁱ, N6–H6A⋯N2ⁱ, N6–H6B⋯N4ⁱⁱ, N6–H6C⋯O1ⁱⁱⁱ, N6–H6D⋯O1). The green dashed lines indicate the interaction between the O3-oxygen atom of the nitro group and the π electrons of the tetrazole ring (contact distance: 3.4022(10) Å [O3⋯Cg(π_{Ring})^{iv}]); Symmetry code: (i) 1/2 – *x*, 1/2 + *y*, *z*; (ii) –1/2 + *x*, *y*, 1/2 – *z*; (iii) –1/2 + *x*, 1/2 – *y*, –*z*; (iv) –1/2 + *x*, *y*, 1/2 – *z*.

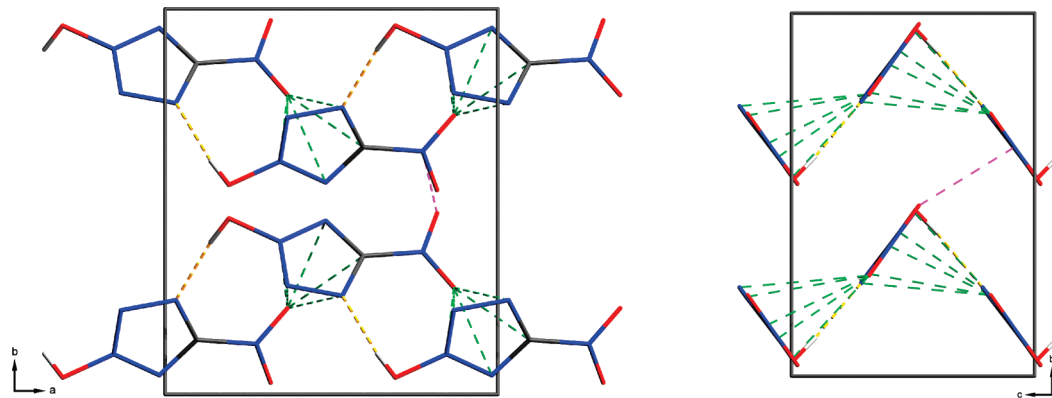


Figure 5. Unit cell packing of **2** (5-nitro-2-hydroxy-tetrazole, HNTX), viewed along the *c* axis (left) and *a* axis (right). Yellow dashed lines indicate intermolecular hydrogen bonding ($\text{O1-H1}\cdots\text{N4}$). The pink dashed line represents a dipolar nitro group interactions between two neighboring N5/O2/O3 nitro groups (contact distance: 2.8200(17) Å [$\text{N5}\cdots\text{O3}^{\text{ii}}$]; 2.966(4) Å [$\text{O6}\cdots\text{O15}^{\text{ii}}$]). The green dashed lines indicate the interaction between the O2-oxygen atom of the nitro group and the π electrons of the tetrazole ring (contact distance: 2.8897(13) Å [$\text{O2}\cdots\text{Cg}(\pi_{\text{Ring}})$]); Symmetry code: (i) $-\frac{1}{2} + x, \frac{1}{2} - y, -\frac{1}{2} + z$; (ii) $x, -y, -\frac{1}{2} + z$; (iii) $\frac{1}{2} + x, \frac{1}{2} - y, \frac{1}{2} + z$.

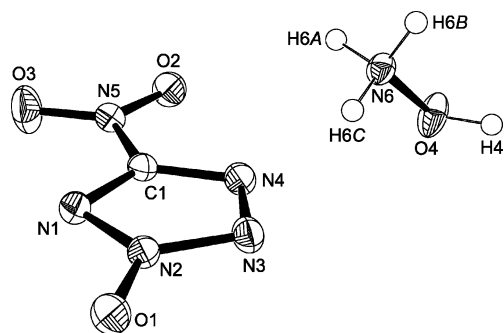


Figure 6. ORTEP representation of the molecular structure of **3** (HxNTX, hydroxylammonium 5-nitrotetrazolate-2*N*-oxide) in the crystalline state. Displacement ellipsoids are shown at the 50% probability level.

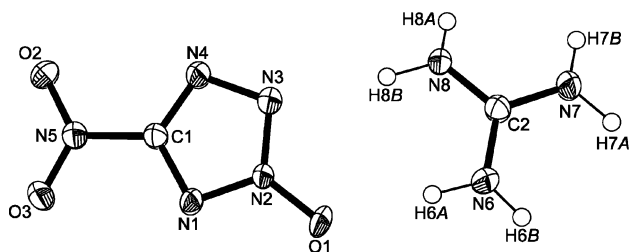


Figure 7. ORTEP representation of the molecular structure of **4** (GNTX, guanidinium 5-nitrotetrazolate-2*N*-oxide) in the crystalline state. Displacement ellipsoids are shown at the 50% probability level.

the case of the free acid, these ribbons are interconnected through a dipolar nitro group interaction (Figure 5).

The structure of **3** (HxNTX, hydroxylammonium 5-nitrotetrazolate-2*N*-oxide) at 173 K has monoclinic ($P2_1/c$) symmetry. The asymmetric unit consists of one molecule (Figure 6). **3** displays a high density of 1.850(2) g cm⁻³.

The structure of **4** (GNTX, guanidinium 5-nitrotetrazolate-2*N*-oxide) at 173 K has triclinic ($P\bar{1}$) symmetry. The asymmetric unit consists of one molecule (Figure 7).

The structure of **5** (AGNTX, aminoguanidinium 5-nitrotetrazolate-2*N*-oxide) at 173 K has monoclinic ($P2_1/c$) symmetry. The asymmetric unit consists of one molecule (Figure 8).

The structure of **6** (DAGNTX, diaminoguanidinium 5-nitrotetrazolate-2*N*-oxide) at 173 K has triclinic ($P\bar{1}$) symmetry. The asymmetric unit consists of one molecule (Figure 9). The nitrotetrazolate-2*N*-oxide anion is disordered such that 31% of anions are rotated 180° around the center of gravity. In Figure 9 only one orientation is shown.

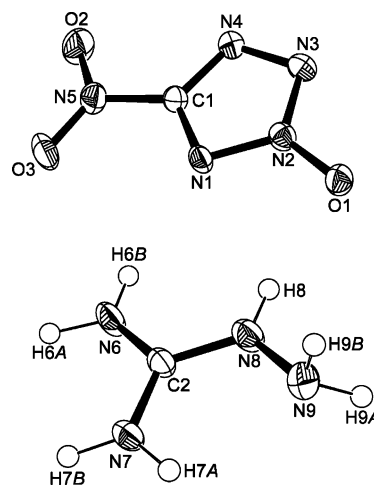


Figure 8. ORTEP representation of the molecular structure of **5** (AGNTX, aminoguanidinium 5-nitrotetrazolate-2*N*-oxide) in the crystalline state. Displacement ellipsoids are shown at the 50% probability level.

The structure of **8** (TAGNTX, triaminoguanidinium 5-nitrotetrazolate-2*N*-oxide) at 173 K has monoclinic ($P2_1/c$) symmetry. The asymmetric unit consists of one molecule (Figure 10).

Physicochemical Properties. Since all the materials studied are energetic compounds, their energetic behaviors were investigated.

Thermal Behavior. The thermal behaviors of all the nitrogen-rich salts prepared were investigated on a Linseis PT10 DSC with heating rates of 5 °C min⁻¹ using ~1.5 mg of material. Many of the compounds decompose violently, especially ANTXX and HxNTX which rupture the DSC pans. The triaminoguanidinium salt shows the lowest decomposition temperature of 153 °C, and the highest decomposition temperature is shown by the guanidinium salt with at 211 °C. Large liquid ranges are seen for DAGNTX and TAGNTX making them potential melt-cast explosives. Table 4 contains the decomposition temperatures and melting points for nitrogen-rich materials **1**, **3–5**, and **7–8**. The substituted guanidinium salts show decreased thermal stability with an increased number of amino substituents on the guanidinium cation. To compare the decomposition temperatures with the nitrogen-rich nitrotetrazolates DSC experiments were also carried out with a heating rate of 10 °C min⁻¹ as was used for the nitrotetrazolates in the literature²¹ (Table 4). The use of

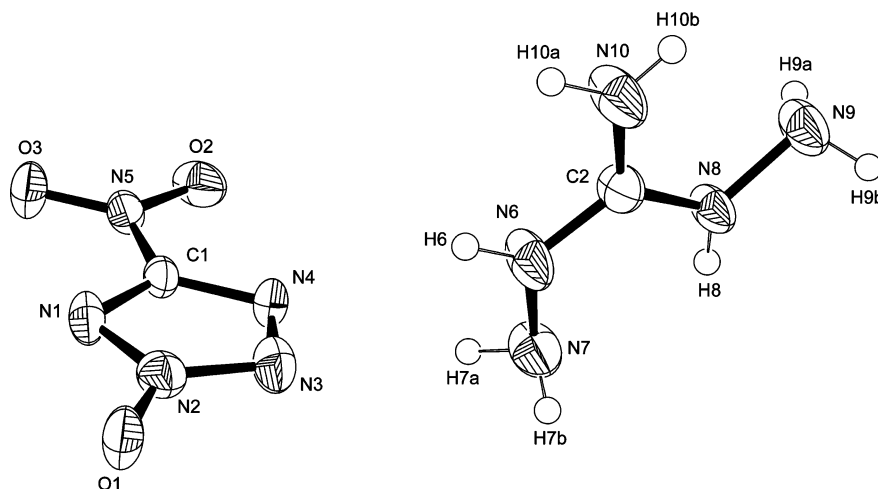


Figure 9. ORTEP representation of the molecular structure of **6** (DAGNTX, 1,3-diaminoguanidinium 5-nitrotetrazolate-2*N*-oxide) in the crystalline state. Displacement ellipsoids are shown at the 50% probability level.

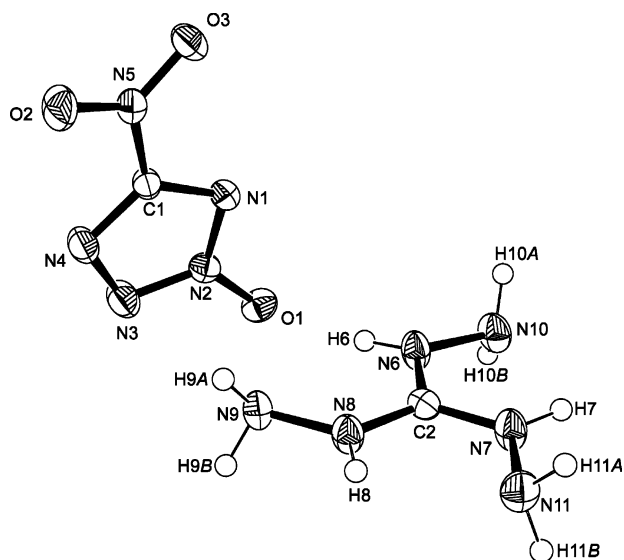


Figure 10. ORTEP representation of the molecular structure of **8** (TAGNTX, triaminoguanidinium 5-nitrotetrazolate-2*N*-oxide) in the crystalline state. Displacement ellipsoids are shown at the 50% probability level.

Table 4. Thermal Behavior of Nitrogen-Rich Salts

Compound	Abbreviation	T_m (°C) (5 °C min ⁻¹)	T_{dec} (°C) (5 °C min ⁻¹)	T_{dec} (°C) (10 °C min ⁻¹)
1	ANTX	165	173	179
3	HxNTX	149	157	164
4	GNTX	198	211	219
5	AGNTX	167	185	196
7	DAGNTX	83	174	184
8	TAGNTX	82	153	162

a faster heating rate is known to give higher decomposition temperatures.⁴⁸ When the decomposition temperatures are compared to those possessed by the nitrogen-rich nitrotetrazolates²¹ the nitrogen-rich nitrotetrazolate-2*N*-oxides generally decompose at a lower temperature with the exception of **4** which is comparable. The high decomposition temperature for the guanidinium salt (**4**) indicates the nitrotetrazolate-2*N*-oxide anion is capable of forming highly thermally stable salts with the

appropriate cation pairing; unfortunately, many of the cations we paired with the nitrotetrazolate-2*N*-oxide anion proved to have lower thermal stability.

Heats of Formation. For a complete discussion on the methods used please see the Supporting Information. When compared to the corresponding heats of formation of the nitrogen-rich nitrotetrazolates¹⁷ all the nitrotetrazolate-2*N*-oxides possess lower heats of formation. For example, the ammonium salt shows a decrease from 191.4 to 152.0 kJ mol⁻¹ and the triaminoguanidinium salt shows a decrease from 601.8 to 471.5 kJ mol⁻¹ between nitrotetrazolate and nitrotetrazolate-2*N*-oxide. However, the acid (**2**) has an increased heat of formation of 308.6 kJ mol⁻¹ in contrast to the lower heat of formation of 281.0 kJ mol⁻¹ in free nitrotetrazole³⁵ as a consequence of the proton lying on oxygen as opposed to a nitrogen atom. For a summary of the heat of formation results please see Table 5.

Detonation Parameters. Calculations of the detonation parameters (Table 5) were performed with the program package EXPLO5 using the version 5.03⁴⁹ as well as version 5.04⁵⁰ (values in brackets), in which several parameters have been modified. The input was made using the sum formula, energy of formation, and the experimentally determined densities (X-ray). The program is based on the chemical equilibrium, steady-state model of detonation. It uses the Becker–Kistiakowsky–Wilson’s equation of state (BKW EOS) for gaseous detonation products and Cowan–Fickett’s equation of state for solid carbon.^{51–54} The calculation of the equilibrium composition of the detonation products is done by applying modified White, Johnson, and Dantzig’s free energy minimization technique. The program is designed to enable the calculation of detonation parameters at the CJ point. The BKW equation in the following form was used with the BKWN set of parameters (α , β , κ , θ) as stated below the equations, X_i being the molar fraction of i -th gaseous product, and k_i being the molar covolume of the i -th gaseous product:

(49) Sućeska, M. *EXPLO5.3 program*; Zagreb, Croatia, 2009.

(50) Sućeska, M. *EXPLO5.4 program*; Zagreb, Croatia, 2010.

(51) Sućeska, M. *Mater. Sci. Forum* **2004**, 465–466, 325–330.

(52) Sućeska, M. *Propellants, Explos., Pyrotech.* **1991**, 16, 197–202.

(53) Sućeska, M. *Propellants, Explos., Pyrotech.* **1999**, 24, 280–285.

(54) Hobbs, M. L.; Baer, M. R. *Proceedings of the 10th Symposium (International) on Detonation*, ONR 33395-12, Boston, MA, July 12–16, 1993, p 409.

(48) Pinheiro, G. F.; Lourenco, V. L.; Iha, K. *J. Therm. Anal. Calorim.* **2002**, 67, 445–452.

Table 5. Energetic Properties and Detonation Parameters

	1	2	3	4	5	7	8	RDX
Formula	CH ₄ N ₆ O ₃	CHN ₅ O ₃	CH ₄ N ₆ O ₄	C ₂ H ₆ N ₈ O ₃	C ₂ H ₇ N ₉ O ₃	C ₂ H ₈ N ₁₀ O ₃	C ₂ H ₉ N ₁₁ O ₃	C ₃ H ₆ N ₆ O ₆
FW (g mol ⁻¹)	148.11	131.07	164.11	190.16	205.18	220.20	235.16	222.12
IS ^a (J)	7	N.D.	4	>40	20	40	25	7.5
FS ^b (N)	120	N.D.	60	252	112	120	72	120
ESD ^c (J)	0.25	N.D.	0.05	0.20	0.20	0.20	0.20	0.1–0.2
N ^d (%)	56.75	52.23	51.22	58.94	61.45	63.62	65.52	37.84
Ω ^e (%)	-10.80	6.10	0.00	-33.66	-35.09	-36.33	-37.42	-21.61
T _{Dec} ^f (°C)	173	~120	157	211	185	174	153	210
ρ ^g (g cm ⁻³)	1.730	1.940	1.85	1.698	1.697	1.687	1.639	1.80
Δ _f H _m ^{oh} kJ mol ⁻¹	152.0	308.6	218.7	136.7	256.4	361.0	471.5	70
Δ _f U ^{oij} kJ kg ⁻¹	1135.0	2439.3	1438.5	829.6	1364.3	1757.5	2125.6	417
<i>Calculated Values by EXPLO5^o</i>								
Δ _{Ex} U ^{oij} kJ kg ⁻¹	5509 (5627)	6124 (6221)	6535 (6521)	4570 (4580)	4886 (4927)	5158 (5145)	5376 (5355)	6038 (6125)
T _{det} ^k (K)	4218 (4094)	5092 (4949)	4763 (4596)	3500 (3380)	3601 (3491)	3654 (3542)	3749 (3604)	4368 (4236)
P _{CJ} ^l (GPa)	32.2 (32.8)	40.4 (41.6)	39.0 (41.0)	26.6 (27.4)	28.5 (29.0)	29.2 (29.9)	29.4 (29.2)	34.1 (34.9)
V _{Det} ^m (m s ⁻¹)	8885 (8767)	9447 (9283)	9499 (9381)	8201 (8270)	8514 (8503)	8686 (8639)	8768 (8617)	8906 (8748)
V _o ⁿ (L kg ⁻¹)	858 (828)	730 (725)	827 (816)	830 (821)	847 (836)	863 (848)	878 (858)	793 (739)

^a BAM drophammer. ^b BAM impact. ^c Electrical spark sensitivity. ^d Nitrogen content. ^e Oxygen balance. ^f Decomposition temperature from DSC (5 °C min⁻¹). ^g Density from X-ray diffraction. ^h Calculated molar enthalpy of formation. ⁱ Energy of formation. ^j Total energy of detonation. ^k Explosion temperature. ^l Detonation Pressure. ^m Detonation velocity. ⁿ Volume of detonation products. ^o Explo5.03 (Explo5.04).

$$pV/RT = 1 + xe^{\beta x} \quad x = (\kappa \sum X_i k_i) / [V(T + \theta)]^{\alpha}$$

$$\alpha = 0.5, \beta = 0.176, \kappa = 14.71, \theta = 6620$$

(EXPLO 5.03)

$$\alpha = 0.5, \beta = 0.96, \kappa = 17.56, \theta = 4950$$

(EXPLO 5.04)

The detonation parameters calculated with the EXPLO5 program are summarized in Table 5.

The ammonium (1), diaminoguanidinium (7), and triaminoguanidinium (8) salts of nitrotetrazolate-2*N*-oxide show detonation properties (detonation velocity and pressure) similar to those of RDX making both of these compounds potential green replacements for RDX. The thermal stabilities of the ammonium and diaminoguanidinium salts are acceptable for this use; however triaminoguanidinium may prove to be insufficient. The acid (2) and hydroxylammonium salt (3) have detonation characteristics outperforming HMX, one of the most powerful secondary explosives in use; however, their thermal stabilities and the extremely deliquescent nature of the free acid will likely preclude application. When the nitrogen-rich nitrotetrazolate-2*N*-oxides are compared to the corresponding nitrotetrazolates²¹ a marked performance increase is seen. When detonation velocities are compared, the magnitude of the increase ranges from almost 1000 ms⁻¹ for the ammonium salt to only 300 ms⁻¹ for the triaminoguanidinium salt. The lower gains in energetic performance for the substituted guanidines are a result of the lower improvement of density when compared with the ammonium salts.

Sensitivities. For initial safety testing, the impact, friction, and electrostatic discharge sensitivity tests of the prepared nitrogen-rich salts were carried out.^{55,56} The impact sensitivity

tests were carried out according to STANAG 4489⁵⁷ and were modified according to instruction⁵⁸ using a BAM (Bundesanstalt für Materialforschung⁵⁶) drophammer.⁵⁹ The friction sensitivity tests were carried out according to STANAG 2287⁶⁰ and were modified according to instruction⁶¹ using a BAM friction tester. Due to the extremely deliquescent nature of the acid 2 sensitivity tests were unable to be carried out with any semblance of accuracy as water is extremely efficient at reducing the sensitivity of energetic materials. The sensitivities of the salts range from sensitive to insensitive according to the UN Recommendations on the Transport of Dangerous Goods.⁶² Electrostatic sensitivity tests were performed on all materials using a small scale electric spark tester ESD 2010EN (OZM Research⁶³) operating with a “Winspark 1.15” Software package.⁶⁴ At the sensitive side of the scale are the ammonium (1) and hydroxylammonium (3) salts with impact sensitivities of 4 and 7 J, respectively. This is slightly lower than and comparable to RDX, respectively. In contrast the (substituted) guanidinium salts (4–8) have sensitivities much safer than that of RDX

(57) NATO standardization agreement (STANAG) on explosives, *impact sensitivity tests*, no. 4489, Ed. 1, Sept. 17, 1999.

(58) WIWEB-Standardarbeitsanweisung 4-5.1.02, Ermittlung der Explosionsgefährlichkeit, hier der Schlagempfindlichkeit mit dem Fallhammer, Nov. 8, 2002.

(59) <http://www.reichel-partner.de>.

(60) NATO standardization agreement (STANAG) on explosives, *friction sensitivity tests*, no. 4487, Ed. 1, Aug. 22, 2002.

(61) WIWEB-Standardarbeitsanweisung 4-5.1.03, Ermittlung der Explosionsgefährlichkeit oder der Reibeempfindlichkeit mit dem Reibeapparat, Nov. 8, 2002.

(62) Impact: Insensitive > 40 J, less sensitive ≥ 35 J, sensitive ≥ 4 J, very sensitive ≤ 3 J; Friction Insensitive > 360 N, less sensitive = 360 N, sensitive < 360 N and > 80 N, very sensitive ≤ 80 N, extremely sensitive ≤ 10 N. According to the UN Recommendations on the Transport of Dangerous Goods.

(63) Skinner, D.; Olson, D.; Block-Bolten, A. *Propellants, Explos., Pyrotech.* **1998**, *23*, 34–42.

(64) <http://www.ozm.cz/testinginstruments/small-scale-electrostatic-discharge-tester.htm>.

(55) Sućeska, M. *Test Methods for Explosives*; Springer: New York, 1995; p 21 (impact), p 27 (friction).

(56) www.bam.de.

ranging from 20 to greater than 40 J. Such sensitivities are desired for the safe explosives used in insensitive munitions (IMs). In all cases with the exception of the aminoguanidinium salt (**5**) all salts of nitrotetrazolate-2*N*-oxide are less sensitive than the corresponding nitrotetrazolate salt.¹⁷

Conclusions

It is possible to oxidize the nitrotetrazolate anion to the nitrotetrazolate-2*N*-oxide anion under mild, aqueous conditions in high yield. Upon protonation, the nitrotetrazolate-2*N*-oxide anion forms 2-hydroxy-5-nitrotetrazole. Nitrogen-rich nitrotetrazolate-2*N*-oxide salts can be formed via metathesis reactions starting from the now-easily available ammonium nitrotetrazolate-2*N*-oxide, and the molecular and crystal structures of these materials were determined for the first time. Multinuclear NMR, IR, and Raman spectroscopy proved to be valuable tools in characterizing these salts. Computational calculations show energetic, nitrogen-rich nitrotetrazolate-2*N*-oxides to have lower heats of formation than their nitrotetrazolate counterparts.

The nitrotetrazolate-2*N*-oxides exhibit higher densities than nitrotetrazolates due to the greater numbers of intermolecular interactions allowed by the *N*-oxides. Due to high experimentally determined densities, nitrogen-rich nitrotetrazolate-2*N*-oxides are high-performance energetic materials. Decomposition temperatures range from 153 to 211 °C indicating the nitrotetrazolate-2*N*-oxide anion has the ability to form thermally stable energetic materials with appropriate cation pairing, despite being slightly less thermally stable than the corresponding nitrotetrazolates. The experimentally determined sensitivities of the nitrotetrazolate-2*N*-oxides are in general lower than those for the nitrotetrazolates, ranging from sensitivities comparable to that of RDX to insensitive.

Experimental Section

All reagents and solvents were used as received (Sigma-Aldrich, Fluka, Acros Organics) if not stated otherwise. Ammonium nitrotetrazolate hemihydrate was prepared according to the literature procedure.²¹ Melting and decomposition points were measured with a Linseis PT10 DSC using heating rates of 5 °C min⁻¹, which were checked with a Büchi Melting Point B-450 apparatus. ¹H, ¹³C, and ¹⁵N NMR spectra were measured with a JEOL instrument. All chemical shifts are quoted in ppm relative to TMS (¹H, ¹³C) or nitromethane (¹⁵N). Infrared spectra were measured with a Perkin-Elmer Spektrum One FT-IR instrument. Raman spectra were measured with a Perkin-Elmer Spektrum 2000R NIR FT-Raman instrument equipped with a Nd:YAG laser (1064 nm). Elemental analyses were performed with a Netsch STA 429 simultaneous thermal analyzer. Sensitivity data were determined using a BAM drophammer and a BAM friction tester. The electrostatic sensitivity tests were carried out using an Electric Spark Tester ESD 2010 EN (OZM Research) operating with the "Winspark 1.15" software package.

CAUTION! 5-Nitrotetrazole-2*N*-oxide (**2**) and its salts (**1**, **3–8**) are all energetic compounds with sensitivity to various stimuli. While we encountered no issues in the handling of these materials, proper protective measures (face shield, ear protection, body armor, Kevlar gloves, and earthed equipment) should be used at all times.

Ammonium 5-Nitrotetrazolate-2*N*-oxide (ANTX, **1).** Ammonium nitrotetrazolate hemihydrate (1.5 g, 11 mmol) was dissolved in 25 mL of distilled water. The solution was heated to 40 °C, and 21.0 g (34 mmol) of oxone were added in small portions over 1 h. The suspension was stirred at 40 °C for three days followed by the addition of sufficient water to dissolve all solids. The solution was chilled, and 10 mL of concentrated sulfuric acid were added dropwise. The yellow solution was extracted with 30 mL portions of ether 5 times or until the aqueous layer was colorless. The ether extracts were combined and dried over anhydrous magnesium sulfate followed by

evaporation of the ether under vacuum to an oil. The oil was dissolved in 10 mL of distilled water producing a yellow solution, which was chilled, and 5.5 mL of ammonia were added dropwise keeping the solution cold. The solution was evaporated under vacuum, and the yellow solid obtained was recrystallized from acetonitrile yielding 1.20 g (88%) of ammonium nitrotetrazolate-2*N*-oxide. Mp: 165 °C, 173 °C (dec); IR (cm⁻¹) $\tilde{\nu}$ = 3154 (m), 3022 (m), 2867 (m), 2684(w), 2508 (w), 2325 (w), 2269 (w), 2142 (w), 2084 (w), 1846 (w), 1776 (w), 1698 (w), 1678 (w), 1625 (w), 1538 (s), 1470 (m), 1459 (m), 1428 (s), 1411 (s), 1373 (s), 1316 (s), 1270 (s), 1251 (m), 1235 (s), 1192 (m), 1143 (w), 1092 (m), 1061 (m), 1003 (m), 846 (m), 773 (m), 699(w), 660 (m); Raman (1064 nm): $\tilde{\nu}$ = 2516 (2), 2325 (2), 1560 (3), 1544 (1), 1497 (1), 1442 (5), 1414 (100), 1380 (2), 1315 (19), 1274 (3), 1237 (3), 1099 (85), 1064 (10), 1005 (97), 850 (2), 766 (4), 608 (4), 485 (5), 431 (2), 227 (6); ¹H NMR (DMSO-*d*₆) δ (ppm) = 7.30 (s, 4H, NH₄); ¹³C NMR (DMSO-*d*₆) δ (ppm) = 158.4 (s, 1C, CN₅O₃). ¹⁵N NMR (DMSO-*d*₆) δ (ppm) = -28.8 (s, 1N, N3), -30.1 (s, 1N, N5, NO₂), -33.3 (s, 1N N2, N-O), -75.6 (s, 1N, N4), -103.4 (s, 1N, N1), -360.3 (s, 1N, N6, NH₄); *m/z*: (FAB-) 130.1; (CN₅O₃) *m/z*: (FAB+) 18.1 (NH₄); EA (CH₄N₆O₃, 148.08 g mol⁻¹) calcd: C, 8.11; N, 56.75; H, 2.72%. Found: C, 8.09; N, 56.30; H, 2.68%. BAM impact: 7 J; BAM friction: 120 N; ESD: 250 mJ.

5-Nitrotetrazole-2*N*-oxide = 5-Nitro-2-hydroxytetrazole (**2**).

ANTX (0.50 g, 3.4 mmol) was dissolved in 10 mL of distilled water, and an excess of concentrated sulfuric acid was added (~5 mL) slowly while the solution chilled in an ice bath. The yellow solution was extracted with 5 × 10 mL portions of ether, and the ether extracts dried over magnesium sulfate. After evaporation of ether under vacuum, 0.38 g of HNTX was obtained (86%). IR (cm⁻¹) $\tilde{\nu}$ = 3422 (w, br), 2666 (m, br), 1710 (w, br), 1574 (s), 1471 (m), 1418 (m), 1360 (m), 1321 (m), 1248 (m), 1140 (s), 1078 (s), 1034 (s), 890 (m), 845 (s), 757 (w), 676 (w); Raman (1064 nm): $\tilde{\nu}$ = 2953 (8), 1580 (15), 1544 (4), 1473 (27), 1422 (100), 1362 (5), 1325 (13), 1252 (15), 1179 (21), 1081 (14), 1036 (83), 849 (11), 773 (8), 761 (19), 586 (5), 571 (2), 549 (3), 461 (7), 412 (11), 369 (3), 327 (3), 237 (8); ¹H NMR (THF-*d*₈) δ (ppm) = 12.99 (s, 1H, O-H); ¹³C NMR (THF-*d*₈) δ (ppm) = 162.1 (s, 1C, CN₅O₃); ¹⁵N NMR (THF-*d*₈) δ (ppm) = -18.0 (s, 1N, N3), -34.4 (s, 1N, N5, NO₂), -64.1 (s, 1N N2, N-O), -72.6 (s, 1N, N4), -94.2 (s, 1N, N1), -360.3 (s, 1N, N6, NH₄); EA (CN₅O₃H, 99.05 g mol⁻¹) calcd: C, 12.13; N, 70.70; H, 1.02%. Found: not determinable due to high sensitivity. Impact, Friction, and ESD sensitivity: not determinable due to high deliquescency.

Hydroxylammonium 5-Nitrotetrazolate-2*N*-oxide (HxNTX,

3). ANTX (1.0 g, 6.8 mmol) was dissolved in 10 mL of distilled water, and the solution was passed through a column of Amberlyst15 ion-exchange resin loaded with hydroxylammonium cation at a slow rate (~1 h). The yellow column effluent was evaporated to dryness and recrystallized from acetonitrile yielding 0.84 g (88%) of HxNTX after drying under high vacuum. Mp: 149 °C, 157 (dec); IR (cm⁻¹) $\tilde{\nu}$ = 3224 (m), 3134 (m), 3033 (m), 2931 (m), 2815 (m), 2698 (m), 2522 (w), 1620 (w), 1591 (w), 1551 (s), 1512 (s), 1471 (s), 1459 (m), 1419 (vs), 1383 (m), 1315 (s), 1229 (s), 1164 (s), 1104 (m), 1058 (m), 1009 (s), 849 (s), 775 (s), 696 (w), 658 (m); Raman (1064 nm): $\tilde{\nu}$ = 2528 (2), 1592 (1), 1549 (3), 1473 (12), 1460 (6), 1425 (45), 1318 (100), 1234 (2), 1172 (5), 1112 (84), 1060, (21), 1010 (91), 855 (4), 765 (6), 604 (5), 487 (4), 277 (4); ¹H NMR (DMSO-*d*₆) δ (ppm) = 10.06 (s, br, 4H, NOH₄); ¹³C NMR (DMSO-*d*₆) δ (ppm) = 158.0 (s, 1C, CN₅O₃); ¹⁵N NMR (DMSO-*d*₆) δ (ppm) = -27.8 (s, 1N, N3), -29.5 (s, 1N, N5, NO₂), -32.4 (s, 1N, N2, N-O), -74.7 (s, 1N, N4), -102.7 (s, 1N, N1), -298.9 (N6, NH₄O+); *m/z*: (FAB-) 130.1 (CN₅O₃); *m/z*: (FAB+) 34.0 (NH₄O); EA (CN₆H₄O₄, 164.08) calcd: C, 7.32; N, 51.22; H, 2.46%; Found: C, 7.18; N, 50.75; H, 2.18%; BAM impact: 4 J; BAM friction: 60 N; ESD: 50 mJ.

Guanidinium 5-Nitrotetrazolate-2*N*-oxide (GNTX, **4).** ANTX (0.500 g, 3.4 mmol) was dissolved in 50 mL of ethanol. Guanidine carbonate (0.305 g, 1.7 mmol) was added, and the solution was refluxed for 18 h. The yellow solution was evaporated under vacuum

to 15 mL and chilled to 0 °C yielding 0.47 g of GNTX after filtration. The filtrate was concentrated to half volume yielding another 0.10 g of GNTX after cooling and filtration for a combined yield of 88%. Mp: 198 °C, 211 °C (dec); IR (cm⁻¹) $\tilde{\nu}$ = 3446(m), 3403 (m), 3359 (m), 3271 (m), 3201 (m), 2851 (w), 2790 (w), 2505 (w), 2177(w), 1661 (s), 1566 (m), 1537 (m), 2472 (s), 1460 (m), 1431(s), 1392(m), 1319(s), 1226 (m), 1082 (m), 1051(m), 1003(m), 844 (m), 786 (s), 739 (w), 703 (w), 688(w); Raman (1064 nm): $\tilde{\nu}$ = 3274 (2), 1648 (1), 1576 (1), 1552 (3), 1474 (2), 1424 (100), 1411 (8), 1317 (11), 1090 (29), 1052 (10), 1011 (8), 1003 (49), 787 (3), 762 (2), 613 (2), 535 (4), 484 (3), 432 (2), 236 (2), 122 (28); ¹H NMR (DMSO-*d*₆) δ (ppm) = 6.87 (s, broad, 6H, NH); ¹³C NMR (DMSO-*d*₆) δ (ppm) = 158.2 (s, 1C, C(NH₂)₃), 157.6 (s, 1C, CN₅O₃); ¹⁵N NMR (DMSO-*d*₆) δ (ppm) = -28.7 (s, 1N, N3), -29.9 (s, 1N, N, NO₂), -31.5 (s, 1N, N2, N-O), -75.4 (s, 1N, N4), -103.8 (s, 1N, N1), -306.5 (s, 3N, N6/N7/N8, C(NH₂)₃); *m/z*: (FAB-) 130.1 (CN₅O₃); *m/z*: (FAB+) 60.1 (CN₃H₆); EA (C₂N₈H₆O₃, 190.12) calcd: C, 12.63; N, 58.94; H, 3.18%. Found: C, 12.77; N, 58.43; H, 3.14%; BAM impact: > 40 J; BAM friction: 252 N; ESD: 0.20 mJ.

Aminoguanidinium 5-Nitrotetrazolate-2*N*-oxide (AGNTX, 5). ANTX (0.70 g, 4.7 mmol) was dissolved in 20 mL of ethanol, and to this was added 0.64 g (4.7 mmol) of aminoguanidine bicarbonate; the solution was then refluxed for 18 h. The solution had some crystals present after refluxing, and hot ethanol was added until dissolution followed by filtration while hot. The filtrate was allowed to slowly cool to 0 °C yielding after filtration 0.66 g of crystalline AGNTX. Evaporation of the filtrate to half volume under vacuum followed by chilling to 0 °C yielded 0.25 g more of AGNTX for a combined yield of 94%. Mp: 167 °C, 185 °C (dec); IR (cm⁻¹) $\tilde{\nu}$ = 3413 (m), 3360 (m), 3226 (m), 3170 (m), 2851 (w), 2634 (w), 2508 (w), 2163 (w), 1669 (vs), 1648 (s), 1599 (m), 1540 (s), 1473 (s), 1460 (m), 1433 (s), 1395 (m), 1318 (s), 1232 (m), 1198 (m), 1108 (m), 1086 (m), 1054(w), 1008 (m), 971 (w), 935 (s), 843(m), 784 (m), 742 (w), 702 (w), 656 (w); Raman (1064 nm): $\tilde{\nu}$ = 3361 (2), 3267 (2), 1681 (1), 1563 (2), 1541 (3), 1475 (4), 1425 (100), 1320 (11), 1232 (2), 1090 (37), 1055 (15), 1009 (69), 970 (3), 942 (1), 850 (1), 787 (3), 761 (4), 613 (3), 509 (2), 482 (4), 235 (3); ¹H NMR (DMSO-*d*₆) δ (ppm) = 8.53 (s, 1H C-NH-N), 7.22 (s, broad, 2H, C-NH₂), 6.76 (s, broad, 2H, C-NH₂), 4.64 (s, 2H, N-NH₂); ¹³C NMR (DMSO-*d*₆) δ (ppm) = 159.2 (s, 1C, C(NH₂)₂(NHNH₂)), 157.8 (s, 1C, CN₅O₃); ¹⁵N NMR (DMSO-*d*₆) δ (ppm) = -29.3 (s, 1N, N3), -29.9 (s, 1N, N, NO₂), -33.5 (s, 1N, N2, N-O), -75.8 (s, 1N, N4), -103.3 (s, 1N, N1), -307.6 (s, 1N C-NH-NH₂), -314.1 (s, 2N, C-NH₂), -326.3 (s, 1N, C-NH-NH₂); *m/z*: (FAB-) 130.1 (CN₅O₃); *m/z*: (FAB+) 75.1 (CN₃H₇); EA (C₂N₈H₆O₃, 205.14) calcd: C, 11.71; N, 61.45; H, 3.44%; Found: C, 11.65; N, 61.45; H, 3.34%. BAM impact: 20 J; BAM friction: 112 N; ESD: 0.25 mJ.

Silver 5-Nitrotetrazolate-2*N*-oxide (AgNTX, 6). ANTX (1.50 g, 10 mmol) was dissolved in 15 mL of distilled water. While stirring, a solution of 1.72 g (10 mmol) of silver nitrate in 10 mL of distilled water was added dropwise. The yellow suspension was stirred for 30 min, filtered, and rinsed with 10 mL of distilled water. After drying in the dark 1.99 g (82%) of AgNTX were obtained. IR (cm⁻¹) $\tilde{\nu}$ = 1560 (m), 1550 (m), 1494 (m), 1464 (w), 1432 (s), 1470 (s), 1405 (s), 1375 (m), 1325 (s), 1314 (s), 1232 (m), 1105 (w), 1064 (w), 1054 (w), 1027 (w), 1016 (w), 848 (w), 834 (w), 794 (m), 783 (m), 775 (s), 752 (w), 694 (w), 690 (w), 654 (w); ¹³C NMR (DMSO-*d*₆) δ (ppm) = 157.0 (s, 1C, CN₅O₃); ¹⁵N NMR (DMSO-*d*₆) δ (ppm) = -31.0 (s, 1N, N5, NO₂), -31.9 (s, 1N, N3), -35.3 (s, 1N, N2, N-O), -82.7 (s, 1N, N4), -105.7 (s, 1N, N1); *m/z*: (FAB-) 130.1 (CN₅O₃); *m/z*: (FAB+) 107.9 (Ag). EA (AgCN₅O₃, 213.88 g mol⁻¹) calcd: C, 5.05; N, 29.44%; Found: C, 4.97; N, 29.22%; BAM impact: 5 J; BAM friction: 120 N; ESD: 50 mJ.

Diaminoguanidinium 5-Nitrotetrazolate-2*N*-oxide (DAGNTX, 7). AgNTX (1.00 g, 4.2 mmol) was added to a solution of 1.00 g (4.2 mmol) of diaminoguanidinium iodide in 20 mL of distilled water, and

0.1 mL of 2 M nitric acid was added. The solution was stirred for 3 h and was filtered in the dark. The yellow filtrate was evaporated to dryness under reduced pressure and recrystallized from ethanol yielding 0.65 g (70%) of DAGNTX. Mp: 82 °C, 174 °C (dec); IR (cm⁻¹) $\tilde{\nu}$ = 3451 (m), 3352 (m), 3277 (m), 1667 (s), 1578 (w), 1531 (m), 1468 (m), 1457 (m), 1420 (s), 1414 (s), 1409(s), 1310 (s), 1239 (w), 1223 (m), 1178 (m), 1120 (w), 1082 (w), 1059 (w), 1044 (w), 978 (s), 845 (m), 782 (s), 758 (w), 702 (w), 658 (s); Raman (1064 nm): $\tilde{\nu}$ = 3358 (1), 3302 (2) 1685 (2), 1545 (3), 1407 (100), 1314 (13), 1224 (5), 1184 (2), 1060 (13), 1048 (45), 985 (60), 846 (1), 786 (3), 759 (2), 609 (2), 544 (2), 486 (5), 362 (2), 235 (3); ¹H NMR (DMSO-*d*₆) δ (ppm) = 8.54 (s, broad, 2H C-NH-NH₂), 7.13 (s, broad, 2H, C-NH₂), 4.57 (s, broad, 4H, N-NH₂); ¹³C NMR (DMSO-*d*₆) δ (ppm) = 160.3 (s, 1C, C(NH₂)(NHNH₂)₂), 157.8 (s, 1C, CN₅O₃); *m/z*: (FAB-) 130.1 (CN₅O₃); *m/z*: (FAB+) 90.1 (CN₅H₈); EA (C₂N₁₀H₈O₃, 220.15) calcd: C, 10.91; N, 63.62; H, 3.66%; Found: C, 11.15; N, 62.94; H, 3.56%; BAM impact: 40 J; BAM friction: 120 N; ESD: 0.20 mJ.

Triaminoguanidinium 5-Nitrotetrazolate-2*N*-oxide (TAGNTX, 8). AgNTX (0.65 g, 2.7 mmol) was added to a solution of 0.39 g (2.7 mmol) of triaminoguanidinium chloride and 0.1 mL of 2 M nitric acid in 20 mL of distilled water. The solution was stirred for 3 h and was filtered in the dark. The yellow filtrate was evaporated to dryness under reduced pressure and recrystallized from ethanol yielding 0.44 g (70%) of TAGNTX. Mp: 82 °C, 153 °C (dec); IR (cm⁻¹) $\tilde{\nu}$ = 3359 (w), 3346 (w), 3320 (w), 3186 (w), 1671 (m), 1547 (m), 1467 (w), 1458 (w), 1419 (s), 1386 (w), 1340 (w), 1310 (s), 1226 (m), 1141 (m), 1131 (m), 1071 (w), 1048 (w), 993 (s), 958 (m), 911 (m), 849 (m), 778 (m), 661 (w), 604 (w); Raman (1064 nm): $\tilde{\nu}$ = 3359 (1), 3263 (1), 1689 (2), 1547 (5), 1420 (84), 1314 (13), 1229 (5), 1200 (2), 1148 (2), 1073 (67), 1049 (26), 996 (100), 895 (4), 849 (2), 782 (1), 760 (3), 702 (1), 638 (3), 599 (2), 486 (4), 424 (2), 337 (1), 202 (3), 86 (43); ¹H NMR (DMSO-*d*₆) δ (ppm) = 8.56 (s, broad, 3H C-NH-NH₂), 4.42 (s, broad, 6H, N-NH₂); ¹³C NMR (DMSO-*d*₆) δ (ppm) = 159.0 (s, 1C, C(NHNH₂)₃), 157.1 (s, 1C, CN₅O₃); *m/z*: (FAB-) 130.1 (CN₅O₃); *m/z*: (FAB+) 105.1 (CN₈H₆); EA (C₂N₁₁H₉O₃, 235.17) calcd: C, 10.21; N, 65.52; H, 3.86%. Found: C, 10.53; N, 64.76; H, 3.74; BAM impact: 25 J; BAM friction: 72 N; ESD: 0.20 mJ.

Acknowledgment. Financial support of this work by the Ludwig-Maximilian University of Munich (LMU), the U.S. Army Research Laboratory (ARL), the Armament Research, Development and Engineering Center (ARDEC), the Strategic Environmental Research and Development Program (SERDP), and the Office of Naval Research (ONR Global, title: "Synthesis and Characterization of New High Energy Dense Oxidizers (HEDO) - NICOP Effort") under Contract Nos. W911NF-09-2-0018 (ARL), W911NF-09-1-0120 (ARDEC), W011NF-09-1-0056 (ARDEC), and 10 WP-SEED01-002/WP-1765 (SERDP) is gratefully acknowledged. The authors acknowledge collaborations with Dr. Mila Krupka (OZM Research, Czech Republic) in the development of new testing and evaluation methods for energetic materials and with Dr. Muhamed Suceca (Brodarski Institute, Croatia) in the development of new computational codes to predict the detonation and propulsion parameters of novel explosives. We are indebted to and thank Drs. Betsy M. Rice and Brad Forch (ARL, Aberdeen, Proving Ground, MD) and Mr. Gary Chen (ARDEC, Picatinny Arsenal, NJ) for many helpful and inspired discussions and support of our work. Stefan Huber is also thanked for assistance during sensitivity measurements.

Supporting Information Available: CIF files, selected bond lengths and angles, the methodology and details for heats of formation calculation, and complete ref 41. This material is available free of charge via the Internet at <http://pubs.acs.org>.

JA106892A

Nitrotetrazolate-2*N*-oxides, and the Strategy of *N*-oxide Introduction

Michael Göbel,[†] Konstantin Karaghiosoff,[†] Thomas M. Klapötke,^{†‡} Davin G. Piercey,[†] Jörg Stierstorfer.[†]*

Supporting Information:

Bond Angles and Distances

ANTX (1) Selected bond lengths [Å] and angles [°]: O1-N2 1.3014(14), N2-N3 1.3352(14), N3-N4 1.3352(15), N4-C1 1.3228(14), C1-N1 1.3310(16), N1-N2 1.3267(14), C1-N5 1.4435(16), N5-O2 1.2288(14), N5-O3 1.2233(13), O1-N2-N3 122.47(9), O1-N2-N1 122.62(9), N1-N2-N3 114.90(10), N2-N1-C1 99.38(9), N1-C1-N4 115.56(4), C1-N4-N3 104.97(10), N4-N3-N2 105.19(9), N1-C1-N5 122.81(1), N4-C1-N5 121.63(11), O2-N5-O3 124.91(11), C1-N5-O2 117.12(10), N1-N2-N3-N4 0.15(12), O1-N2-N3-N4 -178.40(9).

HNTX (2) Selected bond lengths [Å] and angles [°]: O1-N2 1.3441(18), N2-N3 1.3172(18), N3-N4 1.324(2), N4-C1 1.3353(19), C1-N1 1.3176(19), N1-N2 1.3140(19), C1-N5 1.451(2), N5-O2 1.2214(18), N5-O3 1.2223(17), O1-N2-N3 122.031(13), O1-N2-N1 121.41(12), N1-N2-N3 115.53(13), N2-N1-C1 98.88(12), N1-C1-N4 115.08(14), C1-N4-N3 104.99(12), N4-

N3-N2 104.51(12), N1-C1-N5 121.97(13), N4-C1-N5 122.94(13), O2-N5-O3 125.99(14),
C1-N5-O2 116.97(12), N1-N2-N3-N4 1.02(16), O1-N2-N3-N4 179.12(12).

HxNTX (3) Selected bond lengths [\AA] and angles [$^\circ$]: O1-N2 1.3061(13), N2-N3 1.3317(15),
N3-N4 1.3357(15), N4-C1 1.3240(17), C1-N1 1.3278(15), N1-N2 1.3176(14), C1-N5
1.4435(16), N5-O2 1.2270(13), N5-O3 1.2155(15), O1-N2-N3 121.92(9), O1-N2-N1
122.72(9), N1-N2-N3 115.35(9), N2-N1-C1 99.11(10), N1-C1-N4 115.98(11), C1-N4-N3
104.34(9), N4-N3-N2 105.22(9), N1-C1-N5 121.55(11), N4-C1-N5 122.46(10), O2-N5-O3
124.34(10), C1-N5-O2 117.19(10).

GNTX (4) Selected bond lengths [\AA] and angles [$^\circ$]: O1-N2 1.286(4), N2-N3 1.338(5), N3-
N4 1.348(5), N4-C1 1.317(5), C1-N1 1.326(5), N1-N2 1.337(5), C1-N5 1.445(6), N5-O2
1.223(4), N5-O3 1.223(4), O1-N2-N3 123.5(3), O1-N2-N1 122.2(3), N1-N2-N3 114.3(3),
N2-N1-C1 99.3(3), N1-C1-N4 116.7(4), C1-N4-N3 104.3(3), N4-N3-N2 105.5(3), N1-C1-N5
119.7(3), N4-C1-N5 123.6(4), O2-N5-O3 124.6(4), C1-N5-O2 117.9(3).

AGNTX (5) Selected bond lengths [\AA] and angles [$^\circ$]: O1-N2 1.2878(17), N2-N3 1.3413(19),
N3-N4 1.345(2), N4-C1 1.318(2), C1-N1 1.333(2), N1-N2 1.331(2), C1-N5 1.441(2), N5-O2
1.2260(18), N5-O3 1.225(2), O1-N2-N3 122.91(15), O1-N2-N1 122.95(15), N1-N2-N3
114.13(14), N2-N1-C1 99.70(15), N1-C1-N4 116.09(18), C1-N4-N3 104.47(15), N4-N3-N2
105.62(14), N1-C1-N5 121.05(17), N4-C1-N5 122.84(17), O2-N5-O3 125.07(18), C1-N5-O2
117.74(16).

DAGNTX (6) Selected bond lengths [\AA] and angles [$^\circ$]: N2-O1 1.273(7), O3-N5 1.252(7),
O2-N5 1.216(4), N5-C1 1.449(6), C1-N1 1.335(9), C1-N4 1.345(7), N4-N3 1.302(9), N3-N2
1.340(5), N2-N1 1.317(8), N6-C2 1.310(2), N6-N7 1.407(2), N8-C2 1.328(2), N8-N9
1.405(2), C2-N10 1.321(2), O2-N5-O3 126.6(4), O2-N5-C1 118.3(3), O3-N5-C1 115.1(5),
N1-C1-N4 114.5(7), N1-C1-N5 122.7(4), N4-C1-N5 122.8(6), N3-N4-C1 105.2(7), N4-N3-

N2 105.9(4), O1-N2-N1 120.1(5), O1-N2-N3A 124.9(4), N1-N2-N3 114.9(5), N2-N1-C1 99.4(5).

TAGNTX (7) Selected bond lengths [Å] and angles [°]: O1-N2 1.2929(12), N2-N3 1.3316(14), N3-N4 1.3384(14), N4-C1 1.3145(15), C1-N1 1.3352(14), N1-N2 1.3289(15), C1-N5 1.4346(16), N5-O2 1.2307(13), N5-O3 1.2138(13), O1-N2-N3 122.77(10), O1-N2-N1 122.89(9), N1-N2-N3 114.28(9), N2-N1-C1 99.31(8), N1-C1-N4 116.08(10), C1-N4-N3 104.33(10), N4-N3-N2 105.99(9), N1-C1-N5 121.49(9), N4-C1-N5 122.42(10), O2-N5-O3 124.21(10), C1-N5-O2 117.64(9).

Heats of Formation. All calculations were carried out using the Gaussian G03W (revision B.03) program package.¹ The enthalpies (H) and free energies (G) were calculated using the complete basis set (CBS) method of Petersson and coworkers in order to obtain very accurate energies. The CBS models use the known asymptotic convergence of pair natural orbital expressions to extrapolate from calculations using a finite basis set to the estimated complete basis set limit. CBS-4 begins with a HF/3-21G(d) geometry optimization; the zero point energy is computed at the same level. It then uses a large basis set SCF calculation as a base energy, and a MP2/6-31+G calculation with a CBS extrapolation to correct the energy through second order. A MP4(SDQ)/6-31+(d,p) calculation is used to approximate higher order contributions. In this study we applied the modified CBS-4M method (M referring to the use of Minimal Population localization) which is a re-parametrized version of the original CBS-4 method and also includes some additional empirical corrections.^{2,3} The enthalpies of the gas-phase species M were computed according to the atomization energy method (eq.1) (Tables 5-7).⁴⁻⁶

$$\Delta_f H^\circ_{(g, M, 298)} = H_{(Molecule, 298)} - \sum H^\circ_{(Atoms, 298)} + \sum \Delta_f H^\circ_{(Atoms, 298)} \quad (1)$$

Table 5. CBS-4M results

	point group	el. state	$-H^{298}$ / a.u.
2	C_s	1A_1	537.283789
NTX⁻	C_s	1A_1	536.798772
NH₄⁺	T_d	1A_1	56.796608
NH₄O⁺	C_s	1A_1	131.863249
G⁺	C_1	1A	205.453192
AG⁺	C_1	1A	260.701802
DAG⁺	C_1	1A	315.949896
TAG⁺	C_3	1A	371.197775
H			0.500991
C			37.786156
N			54.522462
O			74.991202

Table 6. Literature values for atomic ΔH_f^{298} / kcal mol⁻¹

	NIST ⁷
H	52.1
C	171.3
N	113.0
O	59.6

Table 7. Enthalpies of the gas-phase species M.

M	M	$\Delta_f H^\circ(\text{g,M})$ / kcal mol ⁻¹
2	CHN ₅ O ₂	82.0
NTX⁻	CN ₅ O ₂ ⁻	19.8
NH₄⁺	NH ₄ ⁺	151.9

NH₄O⁺	NH ₄ O ⁺	164.1
G⁺	CH ₆ N ₃ ⁺	136.6
AG⁺	CH ₇ N ₄ ⁺	160.4
DAG⁺	CH ₈ N ₅ ⁺	184.5
TAG⁺	CH ₇ N ₄ ⁺	208.8
1	CH ₄ N ₆ O ₃	171.7
3	CH ₄ N ₆ O ₄	184.0
4	C ₂ H ₆ N ₈ O ₃	156.4
5	C ₂ H ₇ N ₉ O ₃	180.2
7	C ₂ H ₈ N ₁₀ O ₃	204.4
8	C ₂ H ₉ N ₁₁ O ₃	228.6

The solid state energy of formation (Table 9) of **2** was calculated by subtracting the gas-phase enthalpy with the heat of sublimation (19.2 kcal mol⁻¹) obtained by the TROUTON rule ($\Delta H_{\text{sub}} = 188 \cdot T_m$; $T_m = 348$ K).^{8,9} In the case of the ionic compounds, the lattice energy (U_L) and lattice enthalpy (ΔH_L) were calculated from the corresponding molecular volumes (Table 8) according to the equations provided by Jenkins *et al.*¹⁰ With the calculated lattice enthalpy (Table 8) the gas-phase enthalpy of formation (Table 7) was converted into the solid state (standard conditions) enthalpy of formation (Table 8). These molar standard enthalpies of formation (ΔH_m) were used to calculate the molar solid state energies of formation (ΔU_m) according to equation 2 (Table 9).

$$\Delta U_m = \Delta H_m - \Delta n RT \quad (2)$$

(Δn being the change of moles of gaseous components)

Table 8. Molecular volumes, lattice energies and lattice enthalpies.

	V_M / nm^3	$U_L / \text{kJ mol}^{-1}$	$\Delta H_L / \text{kJ mol}^{-1}$
1	0.133	563.4	566.9
3	0.147	548.0	551.5

4	0.186	514.8	518.3
5	0.216	494.8	498.3
7	0.222	491.2	494.7
8	0.238	482.4	485.8

Table 9. Solid state energies of formation ($\Delta_f U^\circ$)

	$\Delta_f H^\circ(s) /$ kcal mol ⁻¹	$\Delta_f H^\circ(s) /$ kJ mol ⁻¹	Δn	$\Delta_f U^\circ(s) /$ kJ mol ⁻¹	M / g mol ⁻¹	$\Delta_f U^\circ(s) /$ kJ kg ⁻¹
1	36.3	152.0	6.5	168.1	148.11	1135.0
2	73.7	308.6	4.5	319.7	131.07	2439.3
3	52.2	218.7	7	236.1	164.11	1438.5
4	32.6	136.7	8.5	157.8	190.16	829.6
5	61.2	256.4	9.5	279.9	205.18	1364.3
7	86.2	361.0	10.5	387.0	220.20	1757.5
8	112.6	471.5	11.5	500.0	235.22	2125.6

Notes: Δn being the change of moles of gaseous components

References.

1. Frisch, M. J.; Trucks, G. W.; Schlegel, H. B.; Scuseria, G. E.; Robb, M. A.; Cheeseman, J. R.; Montgomery, J. A.; Vreven, J. T.; Kudin, K. N.; Burant, J. C.; Millam, J. M.; Iyengar, S. S.; Tomasi, J.; Barone, V.; Mennucci, B.; Cossi, M.; Scalmani, G.; Rega, N.; Petersson, G. A.; Nakatsuji, H.; Hada, M.; Ehara, M.; Toyota, K.; Fukuda, R.; Hasegawa, J.; Ishida, M.; Nakajima, T.; Honda, Y.; Kitao, O.; Nakai, H.; Klene, M.; Li, X.; Knox, J. E.; Hratchian, H. P.; Cross, J. B.; Adamo, C.; Jaramillo, J.; Gomperts, R.; Stratmann, R. E.; Yazyev, O.; Austin, A. J.; Cammi, R.;

Pomelli, C.; Ochterski, J. W.; Ayala, P. Y.; Morokuma, K.; Voth, G. A.; Salvador, P.; Dannenberg, J. J.; Zakrzewski, V. G.; Dapprich, S.; Daniels, A. D.; Strain, M. C.; Farkas, O.; Malick, D. K.; Rabuck, A. D.; Raghavachari, K.; Foresman, J. B.; Ortiz, J. V.; Cui, Q.; Baboul, A. G.; Clifford, S.; Cioslowski, J.; Stefanov, B. B.; Liu, G.; Liashenko, A.; Piskorz, P.; Komaromi, I.; Martin, R. L.; Fox, D. J.; Keith, T.; Al-Laham, M. A.; Peng, C. Y.; Nanayakkara, A.; Challacombe, M.; Gill, P. M. W.; Johnson, B.; Chen, W.; Wong, M. W.; Gonzalez, C.; Pople, J. A. Gaussian 03, Revision C.03, Gaussian Inc.: Pittsburgh PA, **2003**.

- Ochterski, J.W.; Petersson, J. A.; Montgomery Jr., J.A. *J. Chem. Phys.* **1996**, *104*, 2598-2619.
- Montgomery Jr. J.A.; Frisch, M. J.; Ochterski J. W.; Petersson, G.A. *J. Chem. Phys.* **2000**, *112*, 6532-6538.
- Curtiss, L. A.; Raghavachari, K.; Redfern, P. C.; Pople, Pople, J. A. *J. Chem. Phys.* **1997**, *106*, 1063-1079.
- Byrd, E. F. C.; Rice, B. M. *J. Phys. Chem. A* **2006**, *110*(3), 1005-1013.
- Rice, B. M.; Pai, S. V.; Hare, J. *Comb. Flame* **1999**, *118*(3), 445-458.
- Linstrom, P. J.; Mallard, W. G., Eds., NIST Chemistry WebBook, NIST Standard Reference Database Number 69, June 2005, National Institute of Standards and Technology, Gaithersburg MD, 20899 (<http://webbook.nist.gov>).
- Westwell, M. S.; Searle, M. S. Wales, D. J.; Williams, D. H. *J. Am. Chem. Soc.* **1995**, *117*, 5013-5015.
- Trouton, F. *Philos. Mag.* **1884**, *18*, 54-57.
- Jenkins, H. D. B.; Roobottom, H. K.; Passmore, J.; Glasser, L. *Inorg. Chem.* **1994**, *41*(9), 2364-2367.

Nitrotetrazolate-2N-oxides and the Strategy of N-Oxide Introduction [*Journal of the American Chemical Society* **2010**, *132*, 17216. DOI: 10.1021/ja106892a]. Michael Göbel, Konstantin Karaghiosoff, Thomas M. Klapötke,* Davin G. Piercey, and Jörg Stierstorfer

Page 17216. Since publication of this article, we have been informed that we were not the first to oxidize nitrotetrazole to its N-oxide. Credit for the first preparation of it and its hydroxylammonium salt belongs to Bottaro et al.¹

Page 17226. In the Acknowledgment, we also would like to thank Dr. Burkhard Krumm for valuable NMR assistance during this work. This was omitted in the original manuscript by accidental oversight.

■ REFERENCES

(1) Bottaro, J. C.; Petrie, M. A.; Penwell, P. E.; Dodge, A. L.; Malhotra, R. *NANO/HEDM Technology: Late Stage Exploratory Effort*; Report No. A466714; SRI International: Menlo Park, CA, 2003; DARPA/AFOSR funded, contract no. F49620-02-C-0030.

DOI: 10.1021/ja111543f

Published on Web 01/28/2011

DOI: 10.1002/zaac.201200049

Synthesis and Characterization of Alkaline and Alkaline Earth Salts of the Nitrotetrazolate-2*N*-oxide Anion

Martin A. C. Härtel,^[a] Thomas M. Klapötke,^{*[a]} Davin G. Piercey,^[a] and Jörg Stierstorfer^[a]

Dedicated to Professor Rudolf Hoppe on the Occasion of His 90th Birthday

Keywords: Tetrazoles; *N*-oxides; Nitrotetrazole; Pyrotechnics; High energy density materials

Abstract. The oxidation of the 5-nitrotetrazolate anion to its 2-oxide (NTX) by Oxone® (2KHSO₅·KHSO₄·K₂SO₄) gives synthetic access to a new class of oxidizing coloring agents for pyrotechnical formulations. via aqueous ion metathesis reactions starting from the ammonium salt alkaline (Na, K, Rb, Cs) and alkaline earth metal salts (Ca, Sr, Ba) were prepared and characterized by ¹H, ¹³C NMR, mass, Raman, and IR spectroscopy, elemental analysis and, where possible, by X-ray diffraction (Na, K, Rb, Cs, Ba). The energetic properties were

characterized with differential scanning calorimetry (DSC), impact and friction BAM tests and electrical spark sensitivity testing. 2*N*-oxidation of the 5-nitrotetrazolate anion is shown to effect positive oxygen balances ranging from 3.0–4.7% and general improvement of safety properties under simultaneous reduction of desensitizing molar hydration water content in comparison to the non-oxidized 5-nitrotetrazolate salts.

Introduction

Currently employed pyrotechnics rely on principles that were discovered with the invention of black powder around 220 BC in China: The mixture of fuel and oxidizer, creating energy upon reaction. In the case of black powder, potassium nitrate is mixed with carbon and sulfur. The exothermicity of deflagration can be used to generate light-emitting species in the presence of coloring agents, which are in general metal salts with preferably oxidizing anions for an improved oxygen balance of the mixture. Cation choice is dictated by the few elements having emission lines in the visible spectra. The visible spectra of light can be partially covered by potassium (violet), rubidium and cesium (bluish-violet), copper (blue and green), barium (green), sodium (yellow), calcium (orange), lithium and strontium (red). Rubidium and cesium are of special interest for their emissions in the far and near infrared, respectively. The primary light-emitting species in the gas-phase are atomic (e.g., Li, Na, Sr, Ba), mono-hydroxide [e.g., Sr⁺OH, Ba⁺OH] or mono-chloride species [e.g., Sr⁺Cl, Ba⁺Cl], Cu⁺Cl]. The chloride species are especially important for the luminescence effect due to their increased volatility, so organic chlorides (e.g. C₂Cl₆ or PVC powder) or potassium perchlorate (PPC) are added to pyrotechnical formulations. The latter one

has found wide-spread use in the pyrotechnical industry as it is a chemically and thermally stable high energy oxidizer, however it is a proven toxin: Water-soluble PPC residues were shown to contaminate drinking water, are teratogenic and inhibit iodide uptake by the thyroid gland.^[1]

While potassium, sodium, and strontium nitrate^[2] have been proposed as PPC replacements, an alternative strategy to green pyrotechnical formulations avoiding the use of PPC was proposed by different groups:^[1] The use of nitrogen-rich compounds that also offer the advantage of smokeless, or smoke-reduced, combustion. Unlike the fuel oxidation process in black powder, this class of energetics derives its energy solely from high heats of formation. In that direction intensive synthetic efforts leading to alkaline and/or alkaline earth salts of the anions tetrazolate,^[3] 5-nitriminotetrazolate, and its *N2*-/*N3*-methylation derivatives,^[3b,4] (2-chloroethyl)-5-nitriminotetrazolate,^[3b,5] 5,5'-hydrazine-1,2-diylbis(tetrazolate),^[6] and 5-nitrotetrazolate^[7] were performed. All of these studies delivered promising candidates for application as coloring agents for pyrotechnical applications, yet they are limited by negative or neutral oxygen balances (Ω_{CO_2}) possibly disabling them from oxidizing non-energetic components of pyrotechnical mixtures and preventing residue-free combustion.

A solution to this problem could be *N*-oxidation of the mentioned energetics, which additionally would provide further advantages. Amine *N*-oxides are a synthetic strategy for increasing density, stability, and performance of energetic materials. They have found use in insensitive explosives like LLM-105 (2,6-diamino-3,5-dinitropyrazine-1*N*-oxide).^[8] The zwitterionic structure and the large dipole moment of *N*-oxide groups

* Prof. Dr. T. M. Klapötke
Fax: +49-89-2180-77492
E-Mail: tmk@cup.uni-muenchen.de

[a] Department of Chemistry
Energetic Materials Research
Ludwig-Maximilian University
Butenandtstr. 5–13 (D)
81377 München, Germany

enable the formation of compounds with high densities^[9] and at the same time increased oxygen balances in comparison to the nonoxide amine. This can be exemplified by the comparison of 2,4,6-trinitropyridine to 2,4,6-trinitropyridine-1*N*-oxide. The *N*-oxidation results in both an increase of density and energetic performance.^[10] *N*-oxidation of the anion used in high nitrogen pyrotechnic compositions may be a method of increasing oxygen balance without the need for addition of other oxidizers.

With the discovery of the feasibility of 2*N*-oxidation of the 5-nitrotetrazolate anion with Oxone® (2KHSO₅·KHSO₄·K₂SO₄) in 2010^[11] we decided to pair the 5-nitrotetrazolate-2*N*-oxide anion with alkaline and alkaline earth metal salt cations (Na⁺, K⁺, Rb⁺, Cs⁺, Ca²⁺, Sr²⁺, Ba²⁺) to generate oxidizing coloring agents with positive oxygen balances, which shall be presented in this article.

Results and Discussion

The alkali metal salts **3**·H₂O, **4**, **5**, **6** as well as barium 5-nitro-2-oxido-tetrazolate monohydrate [BaNTX·H₂O (**9**·H₂O)] could be synthesized directly from ANTX (**1**) using stoichiometric amounts of the corresponding metal hydroxides. For the remaining earth alkali salts CaNTX·3H₂O (**7**·3H₂O) and SrNTX·2H₂O (**8**·2H₂O) the intermediate silver salt AgNTX (**2**) had to be synthesized by aqueous treatment of ANTX (**1**) with an equimolar amount of silver nitrate, which was done by following our previously described procedure.^[11] Using the low solubility of silver halides in water CaNTX·3H₂O (**7**·3H₂O) and SrNTX·2H₂O (**8**·2H₂O) could be synthesized from AgNTX (**2**) by equimolar reactions in water under exclusion of light. The yields for all ion metathesis reactions are in an acceptable range of 82–100%. DSC investigations of the products showed minor impurities of ANTX (**1**) in NaNTX·H₂O (**3**·H₂O) as well as BaNTX·H₂O (**9**·H₂O), which were subsequently also synthesized from AgNTX (**2**). Generally the route via the reaction of AgNTX (**2**) and metal halides proved to be more reliable and should be preferred for lab-scale synthesis of high-purity samples. The lithium and copper salt of NTX were also prepared but extreme deliquescence prevented all further investigation for use in pyrotechnic applications (Scheme 1)



alkali metals ($z = 1$)
 NaNTX **3**·H₂O: MHal = NaCl, 99%
 KNTX **4**: MX = KOH, 91%
 RbNTX **5**: MX = RbOH, 99%
 CsNTX **6**: MX = CsOH, 99%

earth alkali metals ($z = 2$)
 CaNTX **7**·3H₂O: MHal = CaCl₂, 100%
 SrNTX **8**·2H₂O: MHal = SrCl₂·6H₂O, $n = 2$, 93%
 BaNTX **9**·H₂O: MHal = BaCl₂·2H₂O, $n = 1$, 93%

Scheme 1. Synthesis of nitrotetrazolate-2*N*-oxide salts.

All metal salts **3**·H₂O, **4**, **5**, **6**, **7**·3H₂O, **8**·2H₂O, and **9**·H₂O were fully characterized by ¹³C NMR, ¹H NMR, IR, Raman, and mass spectroscopy, elementary analysis and X-ray diffrac-

tion. CaNTX·3H₂O (**7**·3H₂O) and SrNTX·2H₂O (**8**·2H₂O) were not characterized by X-ray diffraction as no measurable crystals could be grown; crystallization attempts gave non-measurable crystals or amorphous solids. The molar contents of hydration water of NaNTX·H₂O (**3**·H₂O), CaNTX·3H₂O (**7**·3H₂O), SrNTX·2H₂O (**8**·2H₂O), and BaNTX·H₂O (**9**·H₂O) were determined by elemental analysis. ¹⁵N NMR, IR and Raman spectroscopic properties of the NTX anion are known in the literature.^[11]

To assign the IR and Raman peaks frequency analysis was used from an optimized structure (B3LYP/cc-pVDZ using the Gaussian 03 software.^[12]). The measured IR and Raman spectra of the metal salts **3**·H₂O, **4**, **5**, **6**, **7**·3H₂O, **8**·2H₂O, and **9**·H₂O were in agreement with the ones of the nitrogen rich salts synthesized previously.^[11] The IR peak arising from N–O stretch and minor contributions of asymmetric NO₂ stretching and *N1*–*N2*–*N3* symmetric tetrazole ring in-phase deformation with a calculated wave number of 1549 cm⁻¹ could be found in the range of 1539 of 1558 cm⁻¹. The Raman spectra are more complex than the ones of the nitrogen-rich salts of the NTX anion,^[11] which only contained three clear diagnostic bands that allowed clear band assignments to the calculated frequencies. The first one, the combined C–NO₂ stretch and asymmetric *C1*–*N4*–*N3* in-phase tetrazole ring stretch has a calculated frequency^[11] of 1431 cm⁻¹. Whereas for the nitrogen-rich salts one clear band shows up, the majority of the metal salts show one to three peaks with relative intensities ranging from 40–100%. Only for KNTX (**4**) the band can be assigned to 1417 cm⁻¹ as well as for SrNTX·2H₂O (**8**·2H₂O) to 1408 cm⁻¹. The second diagnostic band corresponding to *N1*–*N2* stretching, in-phase tetrazole ring deformation and C–NO₂ stretching (calcd. 1060 cm⁻¹)^[11] could be found in the region of 1011–1136 cm⁻¹. The final diagnostic stretch at 971–1025 cm⁻¹ (calcd. 918 cm⁻¹)^[11] corresponds to *N2*–*N3* stretching with a small component of NO₂ asymmetric stretching.

Compounds **3**, **4**, **5**, **6**, and **9**·2MeOH were characterized using low temperature single-crystal X-ray structure determination. The measurements were carried out with an Oxford Xcalibur CCD diffractometer at temperatures of –100 °C. Table 1 summarizes a selection of crystallographic data and refinement details. All crystals were grown by vapor diffusion of diethyl ether into a saturated methanol (**3**, **9**) or acetonitrile (**4**, **5**) solution of the salt, with exception of CsNTX (**6**), which crystallized upon evaporation of an aqueous solution.

NaNTX (**3**) crystallizes in the orthorhombic space group *P*₂₁₂₁ with four molecules in the unit cell. KNTX (**4**), RbNTX (**5**), and CsNTX (**6**) crystallize in the monoclinic space group *P*₂₁/*c* with also four molecules in the unit cell, respectively. BaNTX·2MeOH (**9**·2MeOH) crystallizes in the triclinic space group *P* $\bar{1}$ with two molecules in the unit cell. The increasing unit cell volume of the alkali metal salts from sodium to cesium is in accordance with the increasing ionic radii. Hydration water of the bulk materials was lost during the crystallization processes. The crystals of BaNTX (**9**) contained two equivalents of methanol (BaNTX·2MeOH).

The molecular structures of the anions in **3**–**6** and **9**·2MeOH are similar to those observed for the corresponding guanidi-

Table 1. Crystallographic data and structure refinement details for NaNTX (**3**), KNTX (**4**), RbNTX (**5**), CsNTX (**6**), BaNTX·2MeOH (**9**·2MeOH).

	3	4	5	6	9 ·2MeOH
Formula	NaCN ₅ O ₃	KCN ₅ O ₃	RbCN ₅ O ₃	CsCN ₅ O ₃	Ba(CN ₅ O ₃) ₂ ·2 MeOH
FW /g·mol ⁻¹	153.05	169.16	215.53	262.97	459.53
Crystal system	orthorhombic	monoclinic	monoclinic	monoclinic	triclinic
Space group	<i>P</i> 2 ₁ 2 ₁ 2 ₁	<i>P</i> 2 ₁ / <i>c</i>	<i>P</i> 2 ₁ / <i>c</i>	<i>P</i> 2 ₁ / <i>c</i>	<i>P</i> $\bar{1}$
Color / Habit	colorless block	colorless rod	colorless block	colorless block	colorless rod
Size /mm	0.15 × 0.18 × 0.22	0.18 × 0.21 × 0.39	0.10 × 0.20 × 0.30	0.09 × 0.13 × 0.17	0.09 × 0.15 × 0.19
<i>a</i> /Å	4.7487(2)	10.8115(9)	7.399(4)	7.6278(3)	7.9861(3)
<i>b</i> /Å	8.1452(4)	5.3316(5)	5.368(5)	5.4098(2)	8.5386(3)
<i>c</i> /Å	12.2426(6)	9.1184(8)	14.100(6)	14.9139(6)	11.0838(4)
<i>a</i> /°	90	90	90	90	79.582(3)
<i>β</i> /°	90	95.559(8)	102.145(5)	104.390(4)	82.769(3)
<i>γ</i> /°	90	90	90	90	77.426(3)
<i>V</i> /Å ³	473.539(0)	523.14(4)	547.49(9)	596.11(6)	722.57(6)
<i>Z</i>	4	4	4	4	2
$\rho_{\text{calcd.}}$ /g·cm ⁻³	2.147	2.148	2.615	2.930	2.112
μ /mm ⁻¹	0.273	0.961	8.992	6.165	2.811
<i>F</i> (000)	304	336	408	480	440
$\lambda_{\text{MoK}\alpha}$ /Å	0.71073	0.71073	0.71073	0.71073	0.71073
<i>T</i> /K	173	173	173	173	173
θ Min–max /°	4.2, 27.0	4.3, 26.0	4.5, 26.0	4.4, 26.0	4.3, 26.0
Dataset	–6:6; –10:10; –15: 5	–12:13; –6:3; –11:9	–9:9; –6:6; –17:17	–5:9; –6:6; –18:17	–9:9; –10:10; –13:13
Reflections collected	6303	1849	7512	2928	10870
Independent refl.	627	1020	1067	1176	2824
<i>R</i> _{int}	0.038	0.020	0.034	0.026	0.030
Observed reflections	530	853	928	1040	2593
Parameters	91	92	91	92	210
<i>R</i> ₁ (obs)	0.0239	0.0273	0.0159	0.0198	0.0198
<i>wR</i> ₂ (all data)	0.0558	0.0668	0.0368	0.0459	0.0500
<i>S</i>	0.98	1.05	1.01	1.00	1.06
Resd. dens. /e·Å ⁻³	–0.16, 0.22	–0.26, 0.26	–0.42, 0.27	–0.73, 0.99	–0.29, 1.10
Device type	Oxford Xcalibur3	Oxford Xcalibur3	Oxford Xcalibur3	Oxford Xcalibur3	Oxford Xcalibur3
Solution	SIR-92	SIR-92	SIR-92	SIR-92	SIR-92
Refinement	SHELXS-97	SHELXS-97	SHELXS-97	SHELXS-97	SHELXS-97
Absorption correction	multi-scan	multi-scan	multi-scan	multi-scan	multi-scan

mium salts published recently.^[11] Selected views of the structures are shown in Figures 1–5. Exemplarily the bond lengths and angles of the 2-oxido-5-nitrotetrazolate anion in **4** are given in the caption of Figure 2. The cations show standard coordination spheres numerous described for alkali and alkaline earth metal salts.

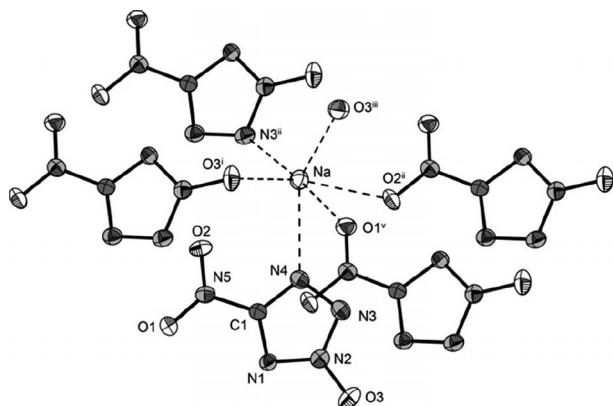


Figure 1. Distorted octahedral coordination mode of one sodium cation in the structure of **3**. Ellipsoids are drawn at the 50% probability level. Symmetry codes: (i) $-x, 0.5+y, 0.5-z$; (ii) $1-x, 0.5+y, 0.5-z$; (iii) $0.5-x, -y, 0.5+z$; (iv) $1-x, -0.5+y, 0.5-z$; (v) $-x, -0.5+y, 0.5-z$.

Klapötke et al. synthesized in 2008 the alkali salts^[7b] of the 5-nitrotetrazolate anion (NT) followed by the alkaline earth

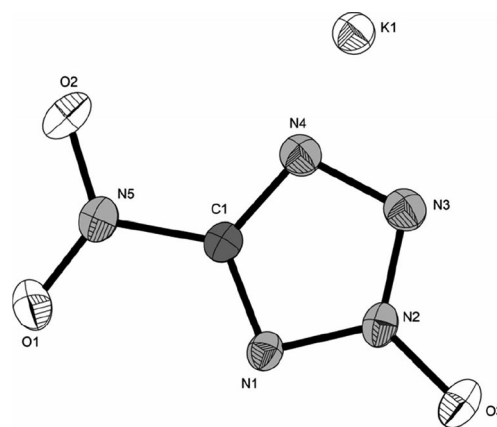


Figure 2. Molecular unit of **4**. Ellipsoids are drawn at the 50% probability level. Selected bond lengths /Å: O1–N5 1.2223(19), O2–N5 1.227(2), O3–N2 1.275(2), N1–C1 1.332(2), N1–N2 1.343(2), N2–N3 1.329(2), N3–N4 1.343(2), N4–C1 1.315(2), N5–C1 1.447(2); selected bond angles /°: O3–N2–N3 122.48(15), O3–N2–N1 123.03(15), N3–N2–N1 114.49(15), N2–N3–N4 105.66(14), C1–N4–N3 104.58(15), C1–N4–K1 116.71(11), N3–N4–K1 99.29(10), O1–N5–O2 124.75(16), O1–N5–C1 117.64(15), O2–N5–C1 117.61(15), N4–C1–N1 116.37(17), N4–C1–N5 121.66(16), N1–C1–N5 121.96(15).

salt^[7a] derivatives in 2009. In order to demonstrate the effect of 2*N*-oxidation the energetic properties of 5-nitrotetrazolate (NT) salts **3a**·2H₂O, **4a**, **5a**, **6a**, **7a**·6H₂O, **8a**·5H₂O, **9a**·5H₂O

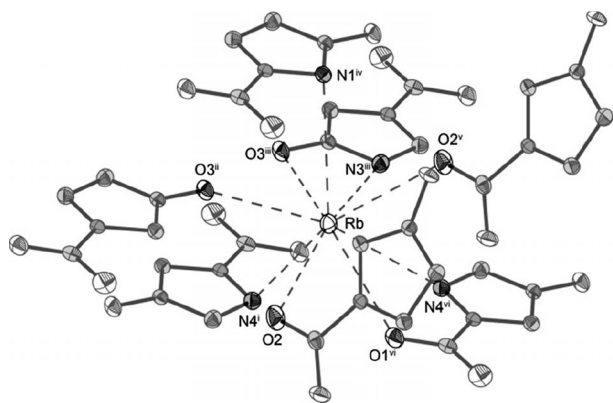


Figure 3. Coordination mode of the rubidium cations in the structure of **5**. Ellipsoids are drawn at the 50% probability level. Symmetry codes: (i) $6; x, 1.5-y, 0.5+z$, (ii) $-x, 0.5+y, 0.5-z$, (iii) $x, 0.5-y, 0.5+z$, (iv) $x, 0.5-y, 0.5+z$, (v) $x, -1+y, z$, (vi) $1-x, -0.5+y, 0.5-z$.

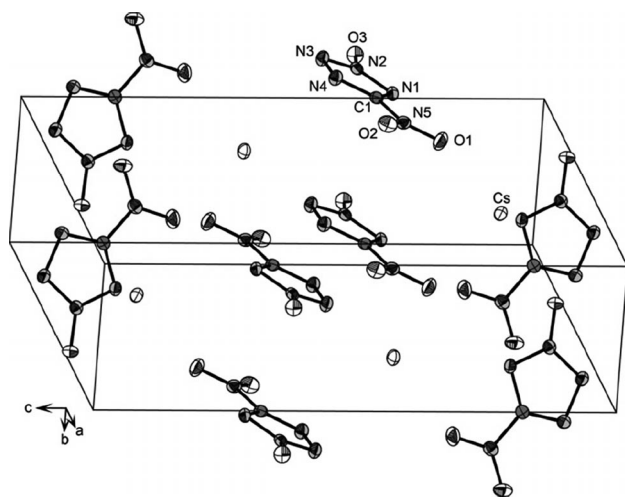


Figure 4. View of the unit cell in the structure of **6** showing the monoclinic $P2_1/c$ symmetry. Ellipsoids are drawn at the 50% probability level.

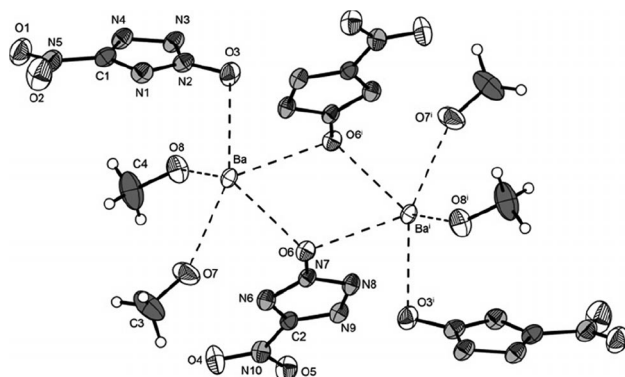


Figure 5. Representation of the dimers formed in the structure of **9**·2MeOH. Ellipsoids are drawn at the 50% probability level. Selected coordination distances /Å: Ba–O3 2.799(4), Ba–O6 2.807(4), Ba–O6ⁱ 2.847(5), Baⁱ–O6 2.847(5), Ba–O7 2.746(3), Ba–O8 2.725(5).

and their 2*N*-oxidation derivatives (NTX) **3**·H₂O, **4**, **5**, **6**, **7**·3H₂O, **8**·2H₂O, **9**·H₂O are compared in Table 2.

Whilst the desensitizing molar hydration water content is effectively reduced by 2*N*-oxidation for all salts, in all cases the effect of 2*N*-oxidation is a reduction of impact and friction sensitivities. Impact sensitivities are in the same magnitude for all salts except for the pair BaNT (**9a**·5H₂O) and BaNTX·H₂O (**9**·H₂O). The series of NTX metal salts **3**·H₂O, **4**, **5**, **6**, **7**·3H₂O, **8**·2H₂O, and **9**·H₂O covers all degrees of sensitivities from insensitive to very sensitive materials concerning impact and friction sensitivities; CsNTX (**6**) is the most sensitive material prepared.^[13]

AgNT (**2a**) was avoided due to its sensitivity properties during the synthesis of nitrogen rich and metal 5-nitrotetrazolate salts,^[7] whereas AgNTX (**2**) has sensitivities similar to those of RDX (1,3,5-trinitroperhydro-1,3,5-triazine) and can be used for large scale synthesis of all other metal salt derivatives. For the electrical spark sensitivities no comparison can be made due to different testing methods when compared with those in the literature.^[7] The melting and decomposition temperatures must be regarded critically as they were measured with heating rates of 5 °C·min⁻¹ for the NTX derivatives **3**·H₂O, **4**, **5**, **6**, **7**·3H₂O, **8**·2H₂O, and **9**·H₂O and 10 °C·min⁻¹ for the NT derivatives **3a**·2H₂O, **4a**, **5a**, **6a**, **7a**·6H₂O, **8a**·5H₂O, and **9a**·5H₂O.^[7] The use of a faster heating rate is known to give higher decomposition temperatures.^[11] Regarding all decomposition and melting temperatures of the metal salts in Table 2 no clear effect of 2*N*-oxidation becomes obvious. The measured densities from X-ray diffraction are significantly raised by 2*N*-oxidation. The oxygen balances for all NTX derivatives **3**·H₂O, **4**, **5**, **6**, **7**·3H₂O, **8**·2H₂O, and **9**·H₂O are positive and improved in comparison to the non-oxidized NT derivatives in a range from 7.4–15.1%. The combustion behaviors of all metal salts of 5-nitrotetrazolate-2*N*-oxide were tested in the context of a possible application as a pyrotechnical colorant. Whilst the hydrated salts burn slowly, the non-hydrated derivatives deflagrate upon flame contact. The color performance is already as expected for such metal salts, but might be improved by additional chlorine sources for commercial applications.

Conclusions

The oxidation of the 5-nitrotetrazolate anion to 5-nitrotetrazole-2*N*-oxide via Oxone® developed by Klapötke et al.^[11] provides synthetic access to alkaline (Na⁺, K⁺, Rb⁺, Cs⁺) and earth alkaline (Ca²⁺, Sr²⁺, Ba²⁺) NTX salts that can be used as oxidizing colorants in pyrotechnical formulations. The crystal structures (besides for CaNTX and SrNTX), spectroscopic and energetic sensitivity properties of these new materials were reported for the first time. The applied synthetic routes to the NTX salts starting from easily accessible ANTX or AgNTX via aqueous ion metathesis reactions and offer excellent yields ranging from 91–100%. The positive oxygen balances in a range of 3.0–4.7% enable the synthesized compounds to oxidize organic chlorine sources in pyrotechnical mixtures that might improve color performance. Additionally 2*N*-oxidation of the 5-nitrotetrazolate anion has proven once more to be a valuable tool for improving the energetic properties in com-

Table 2. Comparison of selected energetic properties of 5-nitrotetrazolate metal salts (**3a–9a**) with their corresponding 2*N*-oxidation derivatives (**3–9**).

Compound	IS ^a /J	FS ^b /N	ESD ^c /mJ	T _m ^d /°C	T _{dec} ^e /°C	ρ _{XRD} ^f /g cm ⁻³	Ω ^g /%
NaNT·2H ₂ O (3a)	>30	~360	N.D.	75 (–H ₂ O)	200	1.731	–9.2
NaNTX·H ₂ O (3)	>40	>288	600	196	220	2.147*	+4.7
KNT (4a)	10	<5	N.D.	168	195	2.027	–10.4
KNTX (4)	10	96	600	140	172	2.148	+4.7
RbNT (5a)	5	<5	N.D.	146	192	2.489	–8.0
RbNTX (5)	>6	144	400	196	206	2.615	+3.7
CsNT (6a)	10	<5	N.D.	158	194	2.986	–6.5
CsNTX (6)	3	48	156	–	188	2.93	+3.0
CaNT·6H ₂ O (7a)	35	84	N.D.	120 (–H ₂ O)	180	N.A.	–4.2
CaNTX·3H ₂ O (7)	>40	360	800	168	180	N.D.	+4.5
SrNT·5H ₂ O (8a)	15	48	N.D.	104 (–H ₂ O)	210	N.D.	–3.9
SrNTX·2 H ₂ O (8)	30	360	800	163	220	N.D.	+4.2
BaNT·5H ₂ O (9a)	2.5–5	<20	N.D.	129 (–H ₂ O)	235	N.D.	–3.5
BaNTX·H ₂ O (9)	40	360	700	–	176	2.112**	+3.9

a) Impact sensitivity (BAM drophammer)^[13]. b) Friction sensitivity (BAM impact)^[13]. c) Electrical spark sensitivity. d) Melting temperature. e) Decomposition temperature. f) Density from X-ray diffraction. N.D. Not determined, N.A.: Not available, *unhydrated crystals, **crystals of dimethanol derivative **9b**. Data for NT derivatives **3a–9a** taken from literature sources^[7]. g) Oxygen balance^[14].

parison to the corresponding non-oxidized derivatives, especially for the reduction of the desensitizing molar hydration water content with simultaneous reduction of the salts sensitivity towards impact and friction and increase of crystal densities. All synthesized salts could find pyrotechnical applications as a result of good color performances.

Experimental Section

General: All reagents and solvents were used as received (Sigma–Aldrich, Fluka, Acros Organics) if not stated otherwise. Ammonium and silver 5-nitrotetrazolate-2*N*-oxide were prepared according to literature.^[11] Melting and decomposition points were measured with a Linseis PT10 DSC using heating rates of 5 K·min⁻¹. ¹H and ¹³C NMR spectra were measured with a JEOL instrument. All chemical shifts are quoted in ppm relative to TMS (¹H, ¹³C). Infrared spectra were measured with a Perkin–Elmer FT-IR Spektrum BXII instrument equipped with a Smith Dura SampilIR II ATR-unit. Transmittance values are described as “strong” (s), “medium” (m) and “weak” (w). Mass spectra were measured with a JEOL MStation JMS 700 instrument. Raman spectra were measured with a Perkin–Elmer Spektrum 2000R NIR FT-Raman instrument equipped with a Nd:YAG laser (1064 nm). The intensities are reported as percentages of the most intensive peak and are given in parentheses. Elemental analyses were performed with a Netsch STA 429 simultaneous thermal analyzer. Sensitivity data were determined using a BAM drophammer and a BAM friction tester. The electrostatic sensitivity tests were carried out with an Electric Spark Tester ESD 2010 EN (OZM Research) operating with the “Winspark 1.15” software package.

CAUTION! The described compounds (**1**, **2**, **3**·H₂O, **4**, **5**, **6**, **7**·3H₂O, **8**·2H₂O, **9**·H₂O) are energetic materials with sensitivity to various stimuli. While we encountered no issues in the handling of these materials, proper protective measures (face shield, ear protection, body armor, Kevlar gloves, and earthed equipment) should be used at all times.

Sodium 5-Nitrotetrazolate-2*N*-oxide Monohydrate (3**·H₂O):** Silver 5-nitrotetrazolate-2*N*-oxide (0.155 g, 0.65 mmol) was suspended in distilled water (5 mL) and sodium chloride (0.038 g, 0.65 mmol) in distilled water (5 mL) was added to the suspension followed by stirring

overnight under exclusion of light. The resulting suspension was filtered obtaining a yellow solution. After evaporation of the solvent and drying under vacuum sodium 5-nitrotetrazolate-2*N*-oxide monohydrate (0.111 g, 99%) was obtained as a yellowish solid. DSC: 120 °C (–H₂O), 196 °C (m.p.), 220 °C (dec.). **IR:** $\tilde{\nu}$ = 3486 (s), 3454 (s), 3269 (w), 2858 (w), 2519 (w), 2168 (w), 1662 (m), 1547 (s), 1468 (m), 1456 (m), 1431 (s), 1394 (m), 1323 (s), 1242 (m), 1104 (w), 1061 (w), 1003 (w), 852 (w), 782 (m), 701 (w), 659 (w) cm⁻¹. **Raman** (1064 nm) $\tilde{\nu}$ = 1561 (5), 1461 (4), 1443 (91), 1411 (100), 1321 (9), 1246 (6), 1100 (67), 1063 (12), 1003 (93), 851 (2), 787 (5), 763 (3), 610 (1), 493 (5), 431 (2) cm⁻¹. **¹H NMR** ([D₆]DMSO): δ = 3.44 (s, hydration-water) ppm. **¹³C NMR** ([D₆]DMSO): δ = 157.6 (s, 1C, CN₅O₃) ppm. **MS** *m/z*: (FAB–) 130.0 (CN₅O₃), *m/z*: (FAB+) 23.0 (Na). **EA** for CH₂N₅NaO₄ (171.05): calcd. C 7.02; H 1.18; N 40.94%; found: C 7.40; H 1.13; N 41.26%. BAM impact: >40 J. BAM friction: >288 N. ESD: 600 mJ.

Potassium 5-Nitrotetrazolate-2*N*-oxide (4**):** Ammonium nitrotetrazolate-2*N*-oxide (0.500 g, 3.38 mmol) was dissolved in distilled water (30 mL). A solution of potassium hydroxide (1.73 mL, aq., 1.95 M, 3.38 mmol) was added and the resulting solution was heated to reflux until the evolution of ammonia had ceased. After evaporation of the solvent and drying under vacuum potassium nitrotetrazolate-2*N*-oxide (0.52 g, 91%) was obtained as a yellow solid. DSC: 140 °C (m.p.); 172 °C (dec.). **IR:** $\tilde{\nu}$ = 3592 (s), 3410 (s), 2859 (w), 2718 (w), 2486 (w), 2186 (w), 1637 (w), 1546 (s), 1475 (m), 1466 (m), 1423 (s), 1395 (s), 1315 (s), 1233 (m), 1176 (m), 1103 (w), 1071 (m), 1051 (m), 995 (m), 842 (m), 794 (m), 777 (m), 707 (w), 657 (m) cm⁻¹. **Raman** (1064 nm) $\tilde{\nu}$ = 1567 (4), 1478 (3), 1435 (14), 1426 (22), 1417 (100), 1405 (11), 1317 (13), 1237 (3), 1074 (75), 1054 (11), 998 (52), 763 (3), 709 (2), 614 (2), 485 (8), 232 (5) cm⁻¹. **¹³C NMR** ([D₆]DMSO): δ = 157.3 (s, 1C, CN₅O₃) ppm. **MS:** *m/z*: (FAB–) 130.1 (CN₅O₃), *m/z*: (FAB+) 39.0 (K). **EA** for KKN₅O₃ (169.14): calcd. C 7.10; N 41.41%; found: C 7.42; H 0.02; N 40.04%. BAM impact: 10 J. BAM friction: 96 N. ESD: 600 mJ.

Rubidium 5-Nitrotetrazolate-2*N*-oxide (5**):** Ammonium nitrotetrazolate-2*N*-oxide (0.526 g, 3.55 mmol) was dissolved in distilled water (30 mL) and a solution of rubidium hydroxide (0.727 g, aq., 50 wt-%, 3.55 mmol) was added. The resulting solution was heated to reflux until the evolution of ammonia had ceased. After evaporation of the solvent and drying under vacuum rubidium nitrotetrazolate-2*N*-

oxide (0.76 g, 99%) was obtained as a yellow solid. DSC: 196 °C (m.p.); 206 °C (dec.). **IR:** $\tilde{\nu}$ = 3584 (w), 3121 (w), 2958 (w), 2845 (w), 2716 (w), 2448 (w), 1844 (w), 1646 (w), 1622 (w), 1595 (w), 1544 (m), 1515 (1), 1472 (m), 1426 (s), 1403 (s), 1313 (s), 1234 (m), 1108 (w), 1046 (m), 974 (m), 844 (m), 791 (m), 774 (m), 704 (w), 660 (m) cm^{-1} . **Raman** (1064 nm) $\tilde{\nu}$ = 1535 (2), 1473 (3), 1427 (28), 1420 (82), 1413 (95), 1400 (40), 1317 (11), 1235 (17), 1047 (62), 978 (100), 846 (1), 785 (1), 759 (2), 711 (4), 663 (1), 614 (2), 490 (6), 386 (1), 240 (4), 207 (2) cm^{-1} . **^{13}C NMR** ($[\text{D}_6]$ DMSO): δ = 157.5 (s, 1C, CN_5O_3) ppm. **MS** m/z : (FAB-) 130.0 (CN_5O_3), m/z : (FAB+) 84.9 (Rb). **EA** for CRbN_5O_3 (215.51) calcd. C 5.57; N 32.50%; found: C 5.96; H 0.01; N 29.24%. BAM impact: >6 J. BAM friction: 144 N. ESD: 400 mJ.

Cesium 5-Nitrotetrazolate-2*N*-oxide (6): Ammonium nitrotetrazolate-2*N*-oxide (0.526 g, 3.55 mmol) was dissolved in distilled water (30 mL) and a solution of cesium hydroxide (1.064 g, aq., 50 wt-%, 3.55 mmol) was added and the resulting solution was heated to reflux until the evolution of ammonia had ceased. After evaporation of the solvent and drying under vacuum cesium nitrotetrazolate-2*N*-oxide (0.90 g, 99%) was obtained as yellow crystals. DSC: 188 °C (dec.). **IR:** $\tilde{\nu}$ = 2362 (w), 1539 (m), 1468 (m), 1424 (s), 1399 (s), 1310 (s), 1230 (m), 1099 (w), 1041 (m), 967 (m), 840 (m), 786 (m), 770 (m), 704 (w), 658 (m), 564 (w) cm^{-1} . **Raman** (1064 nm) $\tilde{\nu}$ = 2800 (1), 2451 (1), 2268 (1), 2198 (1), 1541 (2), 1471 (3), 1426 (17), 1418 (3), 1411 (100), 1398 (50), 1314 (10), 1277 (1), 1231 (19), 1043 (53), 971 (92), 791 (2), 710 (3), 662 (1), 611 (2), 487 (5), 384 (1), 236 (5) cm^{-1} . **^{13}C NMR** ($[\text{D}_6]$ DMSO): δ = 157.3 (s, 1C, CN_5O_3) ppm. **MS** m/z : (FAB-) 130.0 (CN_5O_3), m/z : (FAB+) 132.9 (Cs). **EA** for CCsN_5O_3 (262.95) calcd: C 4.57; N 26.63%; found: C 4.71; N 25.69%. BAM impact: 3 J. BAM friction: 48 N. ESD: 156 mJ.

Calcium 5-Nitrotetrazolate-2*N*-oxide Trihydrate (7·3*H*₂O): Silver 5-nitrotetrazolate-2*N*-oxide (0.803 g, 3.38 mmol) was suspended in distilled water (20 mL) and calcium chloride (0.187 g, 1.69 mmol) was dissolved in distilled water (20 mL). The solution was added to the suspension followed by stirring overnight under exclusion of light. The resulting suspension was filtered to obtain a yellow solution. After evaporation of the solvent and drying under vacuum calcium nitrotetrazolate-2*N*-oxide (0.60 g, 100%) trihydrate was obtained as a yellow solid. DSC: 168 °C (m.p.); 180 °C (dec.). **IR:** $\tilde{\nu}$ = 3597 (s), 3344 (s), 2868 (w), 2553 (w), 2164 (w), 1636 (m), 1622 (m), 1548 (s), 1468 (m), 1453 (m), 1434 (s), 1426 (s), 1389 (m), 1319 (s), 1258 (m), 1246 (m), 1135 (w), 1056 (w), 1026 (w), 850 (w), 777 (m), 703 (w), 658 (w) cm^{-1} . **Raman** (1064 nm) $\tilde{\nu}$ = 1557 (15), 1458 (11), 1439 (91), 1410 (64), 1324 (13), 1257 (1), 1248 (3), 1135 (74), 1058 (15), 1025 (98), 851 (4), 787 (8), 703 (1) 765 (5), 601 (4), 479 (5), 435 (4), 365 (1), 231 (7) cm^{-1} . **^1H NMR** ($[\text{D}_6]$ DMSO): δ = 3.60 (s, hydration-water) ppm. **^{13}C NMR** ($[\text{D}_6]$ DMSO): δ = 157.6 (s, 1C, CN_5O_3) ppm. **MS** m/z : (FAB-) 130.0 (CN_5O_3). **EA** for $\text{C}_2\text{H}_6\text{CaN}_5\text{O}_9$ (353.99) calcd: C 6.78; H 1.71; N 39.54%; found: C 7.42; H 1.57; N 40.25%. BAM impact: >40 J; BAM friction: 360 N; ESD: 800 mJ.

Strontium 5-Nitrotetrazolate-2*N*-oxide Dihydrate (8·2*H*₂O): Silver 5-nitrotetrazolate-2*N*-oxide (0.803 g, 3.38 mmol) was suspended in distilled water (20 mL) and strontium chloride hexahydrate (0.450 g, 1.69 mmol) was dissolved in distilled water (20 mL). The solution was added to the suspension followed by stirring overnight under exclusion of light. The resulting suspension was filtered to obtain a yellow solution. After evaporation of the solvent and drying under vacuum strontium nitrotetrazolate-2*N*-oxide dihydrate (0.60 g, 93%) was obtained as a yellow solid. DSC: 163 °C (m.p.); 220 °C (dec.). **IR:** $\tilde{\nu}$ = 3595 (s), 3547 (s), 3407 (s), 3229 (m), 3123 (m), 2857 (w), 2718 (w), 2363 (w), 2332 (w), 2166 (w), 1630 (m), 1544 (s), 1455 (s), 1430 (s), 1390

(m), 1323 (s), 1255 (m), 1123 (m), 1056 (w), 1013 (w), 850 (w), 778 (m), 696 (w), 659 (m) cm^{-1} . **Raman** (1064 nm) $\tilde{\nu}$ = 1542 (7), 1490 (1), 1466 (5), 1458 (18), 1435 (25), 1408 (101), 1324 (10), 1255 (6), 1123 (70), 1057 (14), 1011 (90), 851 (3), 783 (5), 763 (3), 596 (2), 480 (3), 438 (2), 236 (6) cm^{-1} . **^1H NMR** ($[\text{D}_6]$ DMSO): δ = 3.42 (s, hydration-water) ppm. **^{13}C NMR** ($[\text{D}_6]$ DMSO): δ = 157.3 (s, 1C, CN_5O_3) ppm. **MS** m/z : (FAB-) 130.0 (CN_5O_3), m/z : (FAB+) 89.0 (Sr). **EA** for $\text{C}_2\text{H}_4\text{N}_{10}\text{O}_8\text{Sr}$ (383.74): calcd. C 6.26; H, 1.05; N 36.50; O 33.36; Sr 22.83%; found: C 7.00; H 0.99; N 36.19%. BAM impact: 30 J. BAM friction: 360 N. ESD: 800 mJ.

Barium 5-Nitrotetrazolate-2*N*-oxide Monohydrate (9·*H*₂O): Silver 5-nitrotetrazolate-2*N*-oxide (0.060 g, 0.25 mmol) was suspended in distilled water (20 mL) and barium chloride dihydrate (0.061 g, 0.25 mmol) was dissolved in distilled water (20 mL). The solution was added to the suspension followed by stirring overnight under exclusion of light. The resulting suspension was filtered to obtain a yellow solution. After evaporation of the solvent and drying under vacuum barium 5-nitrotetrazolate-2*N*-oxide monohydrate (0.097 g, 93%) were obtained as a yellow solid. DSC: 176 °C (dec.). **IR:** $\tilde{\nu}$ = 3533 (m), 3547 (m), 2863 (w), 2718 (w), 2543 (w), 2346 (w), 2185 (w), 1579 (m), 1550 (s), 1477 (m), 1429 (s), 1394 (s), 1317 (s), 1241 (m), 1111 (w), 1066 (w), 1014 (w), 852 (w), 817 (w), 783 (m), 729 (w), 701 (w), 656 (w) cm^{-1} . **Raman** (1064 nm) $\tilde{\nu}$ = 1555 (6), 1482 (3), 1446 (47), 1433 (100), 1413 (57), 1317 (14), 1243 (4), 1114 (73), 1071 (5), 1017 (53), 856 (4), 796 (7), 763 (5), 618 (3), 488 (9), 438 (3), 245 (4), 209 (2) cm^{-1} . **^1H NMR** ($[\text{D}_6]$ DMSO): δ = 3.43 (s, hydration-water) ppm. **^{13}C NMR** ($[\text{D}_6]$ DMSO): δ = 157.4 (s, 1C, CN_5O_3) ppm. **MS** m/z : (FAB-) 130.0 (CN_5O_3). **EA** for $\text{C}_2\text{H}_4\text{N}_{10}\text{O}_8\text{Ba}$ (415.43) calcd: C 5.78; H 0.49; Ba 33.06; N 33.72; O 26.96%; found: C 6.05; H 0.58; N 33.53%. BAM impact: 40 J. BAM friction: 360 N. ESD: 700 mJ.

Crystallographic data (excluding structure factors) for the structures in this paper have been deposited with the Cambridge Crystallographic Data Centre, CCDC, 12 Union Road, Cambridge CB21EZ, UK. Copies of the data can be obtained free of charge on quoting the depository numbers CCDC-864043 (3), -864045 (4), -864045(5), -864042 (6), and -864044 (9·2MeOH) (Fax: +44-1223-336-033; E-Mail: deposit@ccdc.cam.ac.uk, <http://www.ccdc.cam.ac.uk>).

Acknowledgement

Financial support of this work by the Ludwig-Maximilians University of Munich (LMU), the U.S. Army Research Laboratory (ARL), the Armament Research, Development and Engineering Center (ARDEC), the Strategic Environmental Research and Development Program (SERDP) and the Office of Naval Research (ONR Global, title: "Synthesis and Characterization of New High Energy Dense Oxidizers (HEDO) - NICOP Effort") under contract nos. W911NF-09-2-0018 (ARL), W911NF-09-1-0120 (ARDEC), W011NF-09-1-0056 (ARDEC) and 10WPSEED01-002/WP-1765 (SERDP) is gratefully acknowledged. The authors acknowledge collaborations with *Dr. Mila Krupka* (OZM Research, Czech Republic) in the development of new testing and evaluation methods for energetic materials and with *Dr. Muhamed Sucesca* (Brodarski Institute, Croatia) in the development of new computational codes to predict the detonation and propulsion parameters of novel explosives. We are indebted to and thank *Drs. Betsy M. Rice* and *Brad Forch* (ARL, Aberdeen, Proving Ground, MD) and *Mr. Gary Chen* (ARDEC, Picatinny Arsenal, NJ) for many helpful and inspired discussions and support of our work. The authors want to thank *St. Huber* for measuring the sensitivities.

References

- [1] G. Steinhauser, T. M. Klapötke, *Angew. Chem. Int. Ed.* **2008**, *47*, 3330–3347.
- [2] G. T. Flegg, T. T. Griffiths, E. L. Charsley, H. Markham, J. J. Rooney, P. D. Howe, *Elimination of Perchlorate Oxidizers for Pyrotechnic Incendiary Compositions*, 38th Int. Annual Conference Of ICT, Karlsruhe, Germany, June 26–29; Karlsruhe, Germany, 2007; p 34/1.
- [3] a) T. M. Klapötke, M. Stein, J. Stierstorfer, *Z. Anorg. Allg. Chem.* **2008**, *634*, 1711–1723; b) T. M. Klapötke, H. Radies, J. Stierstorfer, K. R. Tarantik, G. Chen, A. Nagori, *Propellants Explos. Pyrotech.* **2010**, *35*, 213–219.
- [4] R. Damavarapu, T. M. Klapötke, J. Stierstorfer, K. R. Tarantik, *Propellants Explos. Pyrotech.* **2010**, *35*, 395–406.
- [5] T. M. Klapötke, J. Stierstorfer, K. R. Tarantik, *J. Pyrotech.* **2009**, *28*, 61–67.
- [6] a) M. Ebespacher, T. M. Klapötke, C. M. Sabate, *New J. Chem.* **2009**, *33*, 517–527; b) K. Karaghiosoff, T. M. Klapötke, C. M. Sabaté, *Eur. J. Inorg. Chem.* **2009**, *2*, 238–250.
- [7] a) T. M. Klapötke, C. M. Sabaté, J. M. Welch, *Eur. J. Inorg. Chem.* **2009**, 769–776; b) T. M. Klapötke, C. M. Sabaté, J. M. Welch, *Dalton Trans.* **2008**, *45*, 6372–6380.
- [8] C. Zhang, X. Wang, H. J. Huang, *J. Am. Chem. Soc.* **2008**, *130*, 8359–8365.
- [9] M. S. Molchanova, T. S. Pivina, E. A. Arnautova, N. S. Zefirov, *J. Mol. Struct.* **1999**, *474-515*, *465*, 11–24.
- [10] J. R. Li, J.-M. Zhao, H.-S. Dong, *J. Chem. Crystallogr.* **2005**, *35*, 943–948.
- [11] M. Göbel, K. Karaghiosoff, T. M. Klapötke, D. G. Piercey, J. Stierstorfer, *J. Am. Chem. Soc.* **2010**, *132*, 17216–17226.
- [12] *Gaussian 03*, Revision C.02, M. J. Frisch, G. Trucks, H. B. Schlegel, G. E. Scuseria, M. A. Robb, J. R. Cheeseman, J. A. Montgomery Jr., T. Vreven, K. N. Kudin, J. C. Burant, J. M. Millam, S. S. Iyengar, J. Tomasi, V. Barone, B. Mennucci, M. Cossi, G. Scalmani, N. Rega, G. A. Petersson, H. Nakatsuji, M. Hada, M. Ehara, K. Toyota, R. Fukuda, J. Hasegawa, M. Ishida, T. Nakajima, Y. Honda, O. Kitao, H. Nakai, M. Klene, X. Li, J. Knox, H. P. Hratchian, J. B. Cross, V. Bakken, C. Adamo, J. Jaramillo, R. Gomperts, R. E. Stratmann, O. Yazyev, A. J. Austin, R. Cammi, C. Pomelli, J. W. Ochterski, P. Y. Ayala, K. Morokuma, G. A. Voth, P. Salvador, J. J. Dannenberg, V. G. Zakrzewski, S. Dapprich, A. D. Daniels, M. C. Strain, O. Farkas, D. K. Malick, A. D. Rabuck, K. Raghavachari, J. B. Foresman, J. V. Ortiz, Q. Cui, A. G. Baboul, S. Clifford, J. Cioslowski, B. B. Stefanov, G. Liu, A. Liashenko, P. Piskorz, I. Komaromi, R. L. Martin, D. J. Fox, T. Keith, M. A. Al-Laham, C. Y. Peng, A. Nanayakkara, M. Challacombe, P. M. W. Gill, B. Johnson, W. Chen, M. W. Wong, C. Gonzalez, and J. A. Pople, Gaussian, Inc., Wallingford CT, **2004**.
- [13] Impact: Insensitive > 40 J, less sensitive \geq 35 J, sensitive \geq 4 J, very sensitive \leq 3 J; Friction: Insensitive > 360 N, less sensitive = 360 N, sensitive < 360 N and > 80 N, very sensitive \leq 80 N, extremely sensitive \leq 10 N. According to the UN Recommendations on the Transport of Dangerous Goods.
- [14] Ω /% = $(O - 2C - H/2 - xZ) \cdot 1600/M$. O: number of oxygen atoms, C: number of carbon atoms, H number of hydrogen atoms, Z number of metal atoms, M molecular mass of the compound. Alkali metals: $x = 0.5$, alkaline earth metals: $x = 1$.

Received: February 08, 2012
Published Online: April 26, 2012

DOI: 10.1002/chem.201102064

The Taming of CN_7^- : The Azidotetrazolate 2-Oxide Anion

Thomas M. Klapötke,^{*,[a, b]} Davin G. Piercey,^[a] and Jörg Stierstorfer^[a]

Dedicated to Professor Jürgen Evers on the occasion of his 70th birthday

Abstract: The highly sensitive 5-azido-tetrazolate anion was oxidized to its corresponding *N*-oxide by aqueous oxidation in a buffered oxone solution to the azidotetrazolate 2-oxide anion. After acidic extraction and neutralization with ammonia, the ammonium salt was isolated. Several energetic salts of this novel anion were prepared from the ammonium salt, and in all cases

were found to be of lower sensitivity than the corresponding 5-azidotetrazolate salt while still being highly sensitive towards mechanical stimuli. Explosive performances (detonation velocity,

detonation pressure) of applicable salts were also found to be higher than the non-*N*-oxide variants. Preparation of the free acid 2-hydroxy-5-azidotetrazole was achieved by protonation of the anion and identified by NMR spectroscopy, whereas the majority of the azidotetrazolate 2-oxide salts have unequivocal crystallographic proof.

Keywords: azides • explosives • materials science • oxidation • tetrazoles

Introduction

The synthesis of nitrogen-rich, energetic compounds is a longstanding tradition in the chemical sciences; it attracts scientists as a result of the technical challenges presented in their synthesis and isolation.^[1–3] Such compounds are metastable with regards to their detonation products, with the energy requirement for inducing explosion ranging from as little as a gentle touch to as much as requiring another explosion for initiation. Energetic materials chemistry pushes the limits of the unique molecules that can be created while straddling the line between existence and nonexistence. Nitrogen-rich compounds are candidates for replacing currently used energetic materials (propellants, explosives, pyrotechnics) with “green” replacements because the main combustion/detonation product is harmless molecular nitrogen.^[4–6]

The unique stability of dinitrogen that arises from its strong, short, triple bond means that the decomposition of high-nitrogen compounds with the formation of nitrogen gas is highly favored energetically, thus making nitrogen-rich compounds one intensely pursued strategy in the design of

energetic materials.^[7–9] For a nitrogen-rich material to find practical use as a high explosive, it needs to possess high thermal and mechanical stabilities while concurrently satisfying the demand for ever higher-performing materials. As the nitrogen content of a material rises, the heat of formation also rises, and concurrently the energetic performance. Unfortunately, however, compounds with higher and higher heats of formation are increasingly unstable, both thermally and mechanically. When the five-membered azoles from pyrazole to pentazole are considered, this trend becomes obvious. Pyrazole is not used in energetic materials due to low performance, and the few pentazole derivatives known are unstable under ambient conditions.^[10] With their high nitrogen content and resulting heats of formation, triazoles and especially tetrazoles are very useful heterocyclic backbones for the preparation of high-performance energetic materials.

The tetrazole ring has allowed the preparation of a wide spectrum of energetic compounds from insensitive secondary explosives^[11] to exceedingly sensitive primary explosives^[12] depending on substituents and anion–cation pairing. Of the 5-substituted tetrazoles, 5-azidotetrazole and its salts are comparable or only slightly less sensitive than the most sensitive tetrazoles.^[13] For example, the unquestionably most sensitive tetrazole derivative, diazotetrazole,^[14] explodes in aqueous solution once it crystallizes or the concentration exceeds a few percent, and the lower alkali metal salts of azidotetrazole also explode during crystallization. 1,1'-Azobis(tetrazole) often explodes when manipulated dry, whereas free 5-azidotetrazole can be manipulated dry with only relative safety, yet while still being exceedingly dangerous. 5-Azidotetrazole was first described in patents in 1939,^[15–17] however, not until 2008 was a detailed study of its salts published.^[13]

The oxidation of a tetrazole ring to its 2-oxide has been previously shown by our research group to be an effective

[a] Prof. Dr. T. M. Klapötke, D. G. Piercey, Dr. J. Stierstorfer
Department of Chemistry
Ludwig-Maximilian University of Munich
Butenandtstrasse 5–13 (Haus D), 81377 Munich
Bavaria (Germany)
Fax: (+49) 89-2180-77492
E-mail: tmk@cup.uni-muenchen.de

[b] Prof. Dr. T. M. Klapötke
Center For Energetic Concepts Development (CECD)
University of Maryland
Department of Mechanical Engineering
College Park, Maryland 20742 (USA)

method of reducing the sensitivity of tetrazole-based energetic materials towards mechanical stimuli.^[18] The addition of the single oxygen atom to the ring simultaneously decreases the heat of formation while allowing more intermolecular interactions (as evidenced by the density), both of which are factors that reduce the sensitivity of an energetic material. The increased density relative to the unoxidized form, when combined with the increased oxygen balance makes tetrazole *N*-oxides a useful strategy for increasing energetic performance. The oxygen balance (Ω) is a percentage representation of the oxygen content of a compound, thereby enabling it to oxidize all of its nonoxidizing content to their respective oxides and is easily calculated by Equation (1), in which w is the number of oxygen atoms, x is the number of carbon atoms, y is the number of hydrogen atoms, z is the number of sulfur atoms, and M is the molecular weight:

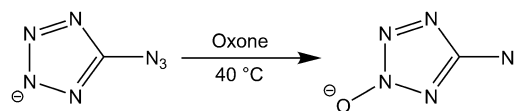
$$\Omega [\%] = (w - 2x - \frac{1}{2}y - 2z) \times 1600/M \quad (1)$$

The only downside observed in our work was the slightly lowered decomposition temperatures.^[18] Unfortunately, this was in contrast to other *N*-oxide based systems in which thermal stability increases.^[19–22] The high performance of azidotetrazole-based energetic materials and their unacceptable sensitivities made this system an interesting candidate for oxidation with anticipated lowered sensitivities and increased performances.

The oxidation of the 5-azidotetrazolate anion under mild aqueous conditions yielded the 5-azidotetrazolate 2*N*-oxide anion. This unique anion was isolated as the ammonium and various other nitrogen-rich and alkali metal salts were rendered by means of metathesis reactions. Characterization included X-ray diffraction, IR, NMR spectroscopy, differential scanning calorimetry (DSC), and impact, friction, and electrostatic discharge; it is as complete as possible. However, a couple of compounds exhibited extensive nonexplosive decomposition during synthesis, and as a result only crystal structures were obtained. All of the salts characterized show lower sensitivities and higher performances relative to their nonoxide analogues. Also of interest is that one prepared salt crystallized as a monohydrate and is completely insensitive towards impact, thus making for the safest compound known that contains the azidotetrazole moiety.

Results and Discussion

Synthesis: The oxidation of the 5-azidotetrazolate anion in a saturated, buffered aqueous Oxone (2KHSO₅·KHSO₄·K₂SO₄ triple salt) solution proceeds easily over three days at 40 °C (Scheme 1). Free acid 5-azido-2-hydroxytetrazole (HAZX, **4**) and its sodium (NaAZX·H₂O, **2**·H₂O), potassium (KAZX, **3**), aminoguanidinium (AGAZX, **5**), and silver (AgAZX, **6**) salts were prepared by simple acid–base chemistry and metathesis reactions with either acid, alkali



Scheme 1. Oxidation of the azidotetrazolate anion to the azidotetrazolate 2-oxide anion.

hydroxide, silver nitrate, or aminoguanidine bicarbonate. Hydroxylammonium azidotetrazolate (HxAzTz, **7**) is a constitutional isomer of **1** and was prepared from 5-azidotetrazole and hydroxylamine in aqueous solution.

After acidification of the reaction solution, ethereal extraction, treatment with ammonia, and recrystallization from acetonitrile, ammonium azidotetrazolate 2-oxide (**1**) was obtained. The crystals produced during recrystallization were suitable for X-ray measurement. Compounds **2** and **3** were prepared by heating to reflux the ammonium salt with the corresponding alkali hydroxide. Evaporation of the solution followed by recrystallization from acetonitrile yielded the pure products. Compound **2** was isolated as a monohydrate, **2**·H₂O, and was completely safe to handle, whereas anhydrous **3** was highly sensitive. Neither compound **2** nor **2**·H₂O formed measurable crystals under any conditions attempted. Long, hairlike fibers were always formed; however, the methanol cocrystal **2**·MeOH was crystallized by the slow diffusion into a methanolic solution of **2**, whereas **3** crystallized upon evaporation. Free acid **4** was prepared by acidification of a solution of **1**, followed by ether extraction and evaporation. Attempts to crystallize this oily material were unsuccessful; however, several times during evaporation the material decomposed nonexplosively for unknown reasons. For this reason, only the NMR spectra are reported. Aminoguanidinium salt **5** was prepared by the treatment of **1** with aminoguanidine bicarbonate in ethanol. Evaporation of the reaction liquors gave a material that was nonexplosive and had only traces of the azidotetrazolate 2-oxide anion remaining within. Diffusion of diethyl ether into a methanolic solution of this material luckily gave a few crystals of pure **5** suitable for X-ray analysis. The reaction of an aqueous solution of **1** with silver nitrate yielded **6** as a highly explosive precipitate, which dry exploded when moved onto a porcelain plate. Compound **7** was prepared by mixing an aqueous solution of hydroxylamine and 5-azidotetrazole. After careful evaporation under ambient conditions, **7** was obtained as a highly sensitive white powder. By diffusion of ether into a solution of **7** in methanol yielded crystals suitable for X-ray measurement.

Spectroscopy: Multinuclear NMR spectroscopy, and particularly ¹³C and ¹⁵N spectroscopy, proved to be a valuable tool for the characterization of the tetrazole and tetrazolates. With the exception of the free acid **4**, all NMR spectra were performed in [D₆]DMSO. We anticipated a high acidity for **4** comparable to our previously reported 2-hydroxy-5-nitrotetrazole, so NMR spectroscopic experiments were performed in [D₈]THF. The anionic azidotetrazolate 2-oxides

all show the single ^{13}C peak near $\delta=151$ ppm, lower than the corresponding azidotetrazolate, which occurs near $\delta=158$ ppm. This trend is comparable to that seen when nitrotetrazolate is oxidized, and the signal shifts upfield. When the ^{15}N spectrum of the azidotetrazolate 2-oxide anion is compared with azidotetrazolate, a loss of nitrogen equivalency is seen between N1 and N4 and between N2 and N3. Unfortunately for N2 and N3, the shifts show up close together at $\delta=-39.1$ and -40.8 ppm (in azidotetrazolate at $\delta=-4.5$ ppm), and although one would rationally expect the largest shift change to belong to N2 where the oxygen has been added, a calculated (MPW1PW91/aug-cc-pVDZ, Gaussian 03^[23]) spectrum says N3 is the most upfield of the two; so for such close signals, precise assignment is avoided. Protonation of the azidotetrazolate-2*N*-oxide anion yields highly acidic **4**, and the ^{13}C NMR spectroscopic shift occurs at $\delta=155$ ppm. The ^1H signal occurs as a broad singlet at $\delta=11.71$ ppm, out of range for an N–H proton because azidotetrazole has its N–H proton at $\delta\approx 7.0$ ppm, thus indicating that, like nitrotetrazolate 2-oxide,^[18] AZX also likely protonates on oxygen to form a 5-azido-2-hydroxytetrazole. Lack of N–H coupling in the ^{15}N spectrum also supports this conclusion, as well as the resonances in the spectrum being similar to other 2-substituted azidotetrazoles. ^{15}N signal assignments were based on a calculated spectrum performed as above and comparison with literature spectra for 2-substituted azidotetrazoles. Unfortunately, assignment for N4 and N2 are unclear as their resonances occur very near each other at $\delta=-81.3$ and -82.9 ppm, thus making precise assignment impossible. Figure 1 shows the ^{15}N spectra that belong to the azidotetrazolate 2-oxide anion and to 5-azido-2-hydroxytetrazole (**4**).

The IR and Raman spectra of all compounds were recorded and assigned using frequency analysis from an optimized structure (B3LYP/cc-pVDZ using the Gaussian 03 software^[23]). All calculations were performed at the DFT level of theory; the gradient-corrected hybrid three-parameter B3LYP^[24,25] functional theory has been used with a correlation consistent cc-pVDZ basis set.^[26–29] The anionic azidotetrazolate 2-oxides generally contain a strong, diagnostic band in the infrared that ranges from 2139 to 2169 cm^{-1} . The calculated value for this band is 2252 cm^{-1} and arises from the azide asymmetric stretch. Another strong band occurs at 1340–1380 cm^{-1} (calcd 1452 cm^{-1}) and this is assigned to the C–N5 covalent azide stretch with minor components of N–O stretching and azide symmetric stretching. The Raman spectra of all salts of azidotetrazolate-2*N*-oxide all adopt a characteristic pattern of three bands. The first at 2152–2159 cm^{-1} (calcd 2252) results from the azide asymmetric stretch. The second at 1493–1499 cm^{-1} (calcd 1452 cm^{-1}) results from the C–N5 covalent azide stretch with minor components of N–O stretching and azide symmetric stretching. The final diagnostic Raman stretch occurs at 1019–1040 cm^{-1} (calcd 1080 cm^{-1}) and is assigned to an asymmetric tetrazole deformation vibration.

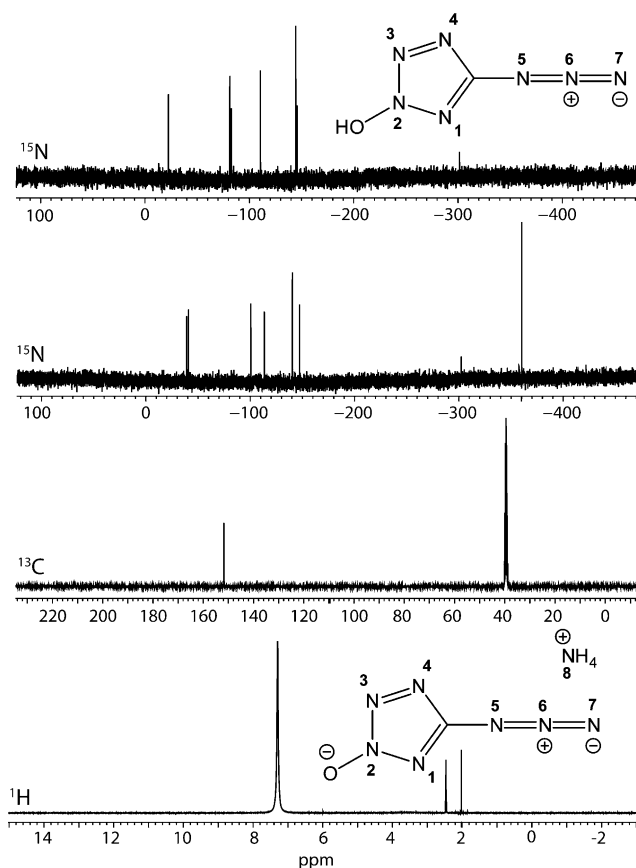


Figure 1. Multinuclear NMR spectroscopy of **1** and **4**.

Relative energy: To support the NMR spectroscopic data in that the azidotetrazolate 2-oxide anion is protonated on the oxygen to form 2-hydroxy-5-nitrotetrazole, the relative energies of N1–H, N3–H, and N4–H ring-protonated species were calculated. The calculations performed were in accordance with the same software, theory, and basis set as described in the vibrational spectroscopy section (Table 1). The relative energies indicate that 5-azido-2-hydroxytetrazole is the lowest-energy species formed from the protonation of the azidotetrazolate 2-oxide anion, similar to what occurred with nitrotetrazolate 2-oxides.

Table 1. Relative energies of protonation sites on the azidotetrazolate 2-oxide anion.^[a]

	O–H	N1–H	N3–H	N4–H
point group	C_1	C_s	C_s	C_s
$-E$ [a.u.]	497.044145	497.031215	497.031624	497.038024
electronic state	$^1A'$	$^1A'$	$^1A'$	$^1A'$
NIMAG	0	0	0	0
zpe [kcal mol^{-1}]	33.7	33.6	33.8	33.3
E_{rel} [Kcal mol^{-1}]	0	8.1	7.9	3.8

[a] $-E$ = electronic energy; NIMAG = number of imaginary frequencies; zpe = zero point energy; E_{rel} = relative energy.

Single-crystal X-ray structure analysis: The low-temperature determination of the crystal structures of **1**, **2**·MeOH, **3**, **5**,

Table 2. X-ray data and parameters of azidotetrazolate 2-oxides.^[a]

	1	2-MeOH	3	5	7
formula	CH ₄ N ₈ O	C ₂ H ₄ N ₇ NaO ₂	CN ₇ OK	C ₂ H ₇ N ₁₁ O	CH ₄ N ₈ O
<i>M_r</i> [g mol ⁻¹]	144.12	181.11	165.18	201.19	144.12
crystal system	orthorhombic	monoclinic	monoclinic	triclinic	monoclinic
space group	<i>P</i> 2 ₁ 2 ₁ (19)	<i>P</i> 2 ₁ / <i>m</i> (11)	<i>P</i> 2 ₁ / <i>n</i> (14)	<i>P</i> $\bar{1}$ (2)	<i>P</i> 2 ₁ / <i>c</i> (14)
color/habit	colorless block	colorless rod	colorless plate	colorless rod	colorless rod
size [mm]	0.17 × 0.21 × 0.23	0.06 × 0.12 × 0.17	0.06 × 0.40 × 0.55	0.13 × 0.17 × 0.30	0.05 × 0.10 × 0.35
<i>a</i> [Å]	7.911(5)	8.8466(8)	3.676(3)	7.7099(4)	3.677(3)
<i>b</i> [Å]	9.562(5)	6.4024(8)	20.793(5)	8.3482(4)	20.885(5)
<i>c</i> [Å]	14.981(5)	13.2145(14)	7.048(7)	13.8979(8)	7.641(7)
α [°]	90	90	90	73.420(5)	90
β [°]	90	92.546(9)	100.755(5)	82.182(4)	98.367(5)
γ [°]	90	90	90	76.385(4)	90
<i>V</i> [Å ³]	1133.2(10)	747.72(14)	529.3(7)	830.96(8)	580.5(7)
<i>Z</i>	8	4	4	4	4
ρ_{calcd} [g cm ⁻³]	1.689	1.609	2.073	1.608	1.649
μ [mm ⁻¹]	0.144	0.184	0.931	0.133	0.140
<i>F</i> (000)	592	368	328	416	296
<i>T</i> [K]	173	173	173	173	173
θ_{min} , θ_{max} [°]	4.3, 26.0	4.2, 25.0	4.2, 26.0	4.1, 26.0	4.7, 26.0
dataset	-9:9; -11:11; -18:9	-10:10; -7:4; -15:14	-3:4; -24:25; -7:8	-9:9; -10:10; -17:17	-4:4; -25:25; -9:7
reflns collected	5818	3556	2722	8398	2928
indep reflns	1293	1422	1041	3265	1132
<i>R</i> _{int}	0.027	0.049	0.032	0.046	0.041
obsd reflns	1140	819	776	1777	700
params	214	124	91	309	107
<i>R</i> ₁ (obsd) ^[b]	0.0235	0.0444	0.0277	0.0369	0.0395
<i>wR</i> ₂ (all data) ^[c]	0.0589	0.1018	0.0608	0.0787	0.0857
GOF ^[d]	0.97	0.83	0.92	0.81	0.85
residual density [e Å ⁻³]	-0.13, 0.15	-0.25, 0.65	-0.20, 0.26	-0.22, 0.17	-0.18, 0.23
solution	SIR-92	SIR-92	SHELXS-97	SHELXS-97	SHELXS-97

[a] Measurements were carried out on a Oxford Xcalibur3 CCD, refined with SHELXL-97, and multiscan absorption correction. λ (MoK α) = 0.71073 Å. [b] $R_1 = \sum ||F_o| - |F_c|| / \sum |F_o|$. [c] $wR_2 = \{ \sum [w(F_o^2 - F_c^2)^2] / \sum [w(F_o)^2] \}^{1/2}$; $w = [\sigma_c^2(F_o^2) + (xP)^2 + yP]^{-1}$ and $P = (F_o^2 + 2F_c^2)/3$; [d] GOF = $\{ \sum [w(F_o^2 - F_c^2)^2] / (n-p) \}^{1/2}$ (n = number of reflections; p = total number of parameters).

and **7** were performed using a Oxford Xcalibur3 diffractometer with a Spellman generator (voltage 50 kV, current 40 mA) and a KappaCCD detector. The data collection and reduction were carried out using the CrysAlisPro software.^[30] The structures were solved either with SIR-92^[31] or SHELXS-97,^[32] refined with SHELXL-97^[33] and finally checked using the Platon^[34] software integrated in the WinGX^[35] software suite. The non-hydrogen atoms were refined anisotropically, and the hydrogen atoms were located and freely refined. The absorptions were corrected by a Scale3 Abspack multiscan method.^[36] In the case of the chiral space group *P*2₁2₁ of **1**, the Friedl pairs were merged. Selected data and parameter of the X-ray determinations are given in Table 2.

The molecular structure of ammonium azidotetrazolate 2-oxide, which crystallizes orthorhombically in the space group *P*2₁2₁, is shown in Figure 2. Its density of 1.689 g cm⁻³ is the highest one of the metal-free salts discussed in this work. It is also higher relative to its isomer **7** (1.649 g cm⁻³), which corroborates the theory of increased density in *N*-oxide compounds.^[18] The geometry of the azidotetrazolate 2-oxide anion is very similar in all compounds within this work. The *N*-oxide is bonded in a distance between 1.280 and 1.311 Å, which is between an N=O double (1.17 Å) and an N–O single bond (1.45 Å), thereby indicat-

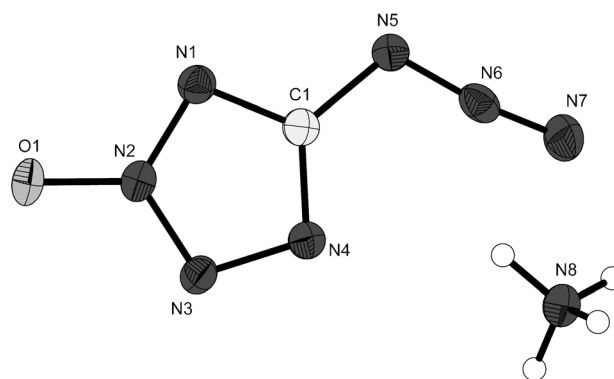


Figure 2. Molecular unit of **1**. Thermal ellipsoids represent the 50% probability level. Hydrogen atoms are drawn as small spheres of arbitrary radius.

ing significant *N*-oxide character. The oxide is also planar with the tetrazole ring, thereby indicating the sp² nature of the N2 to which it is bonded. The azide is angulated (angles 170.9–173.0°) and follows the plane of the aromatic tetrazole ring system. Exact bond lengths are given in Table 3. The structure of **1** is strongly dominated by the hydrogen bonds (Figure 3) of all ammonium hydrogen atoms, with three of

Table 3. Anion bond lengths [Å] in the azidotetrazolate 2-oxide anion.

	1	2·MeOH	3	5	7
O1–N2	1.311(2)	1.280(3)	1.294(3)	1.299(2)	
N1–N2	1.333(2)	1.3533(11)	1.340(3)	1.342(2)	1.355(3)
N1–C1	1.333(2)	1.3368(11)	1.334(3)	1.331(3)	1.322(3)
N2–N3	1.306(2)	1.3005(11)	1.319(3)	1.314(2)	1.304(3)
N3–N4	1.352(2)	1.3550(11)	1.359(3)	1.355(2)	1.345(3)
N4–C1	1.330(2)	1.3186(11)	1.332(3)	1.322(2)	1.328(3)
C1–N5	1.395(2)	1.4007(11)	1.405(3)	1.398(3)	1.391(3)
N5–N6	1.253(2)	1.2240(11)	1.252(3)	1.248(2)	1.249(3)
N6–N7	1.118(2)	1.1254(11)	1.118(3)	1.121(2)	1.125(3)

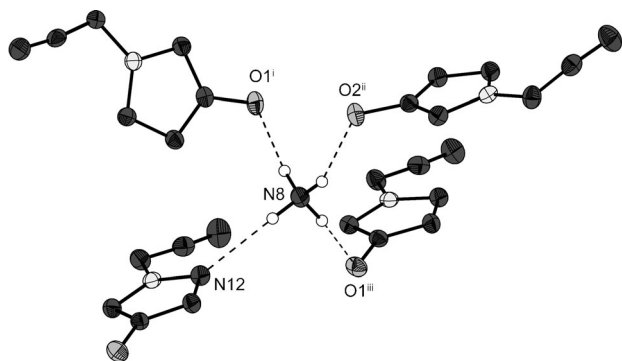


Figure 3. Hydrogen bonding of the ammonium cations. Symmetry codes: i) $-x, 0.5+y, 0.5-z$; ii) $0.5-x, 1-y, -0.5+z$; iii) $0.5-x, -y, -0.5+z$.

them interacting with the oxygen atom of the tetrazolate *N*-oxides.

Compound **2** could only be obtained crystalline as a methanol adduct shown in Figure 4. Its density of 1.609 g cm^{-3} is very low in comparison with other sodium tetrazolates in the literature,^[37] which is probably a result of the inclusion of methanol.

Compound **5**, depicted in Figure 5, crystallizes with the lowest density (1.608 g cm^{-3}) of all compounds investigated

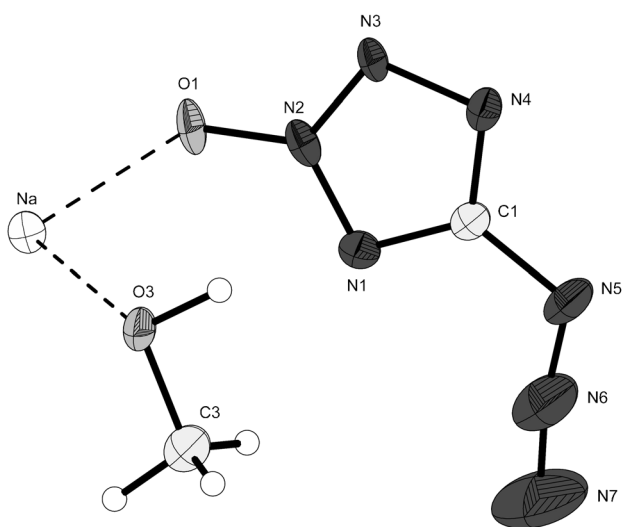


Figure 4. Molecular unit of **2**·MeOH. Thermal ellipsoids represent the 50% probability level.

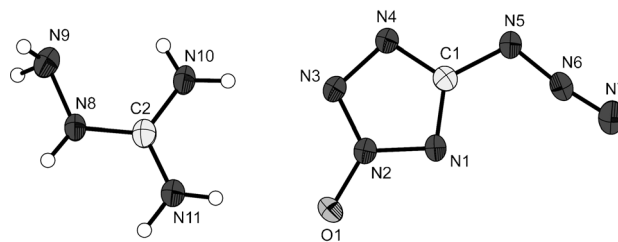


Figure 5. Molecular unit of **5**. Thermal ellipsoids represent the 50% probability level. Hydrogen atoms are drawn as small spheres of arbitrary radius.

in this work. The colorless rods are based on the triclinic crystal system, space group $P\bar{1}$. The structure is strongly dominated by several hydrogen bonds, illustrated in Figure 6. Typical hydrogen-bond graph sets^[38] can be identified, for example, **R(2,2)8**, **R(1,2)3**, **C(2,2)7**, and **C(2,2)8**.

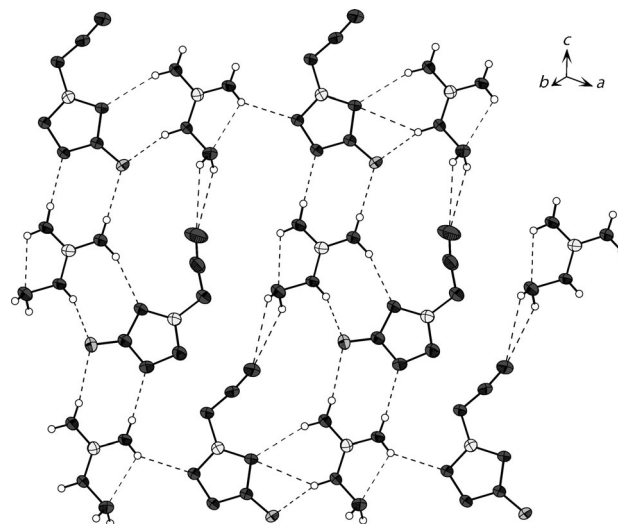


Figure 6. View of the hydrogen-bond motifs within the layers in **5**.

The potassium salt **3** crystallizes in the monoclinic space group $P2_1/n$ with the highest density (2.074 g cm^{-3}) observed in this work. Within the asymmetric unit (Figure 7) the potassium cations are coordinated by the atoms N3 and O1 and show coordination distances of $\text{N3–K}=2.963(3) \text{ Å}$ and

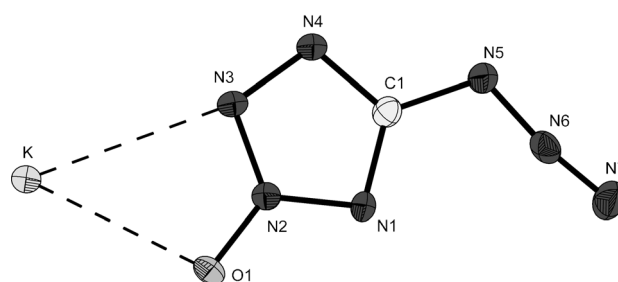


Figure 7. Asymmetric unit of **3**.

O1–K=2.849(3) Å. Within the structure two flight chains along the *a* axis are formed (Figure 8)

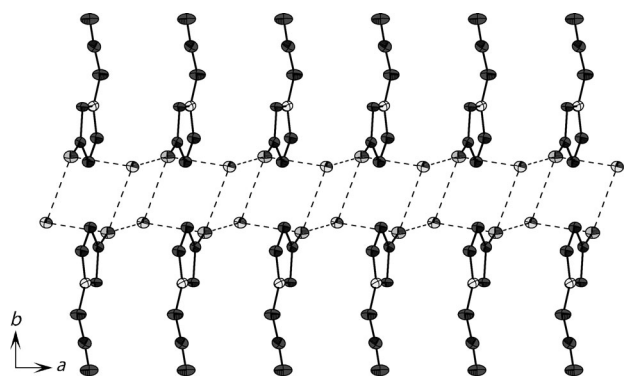


Figure 8. View on the chains along the *a* axis in the structure of **3**.

The isomer of **1**, hydroxylammonium 5-azidotetrazolate (**7**), crystallizes in the monoclinic space group $P2_1/c$. Its molecular structures (Figure 9) are arranged in a wavelike layer structure along the *b* axis. The layers are formed by double flight strands along the *c* axis, which is depicted in Figure 10.

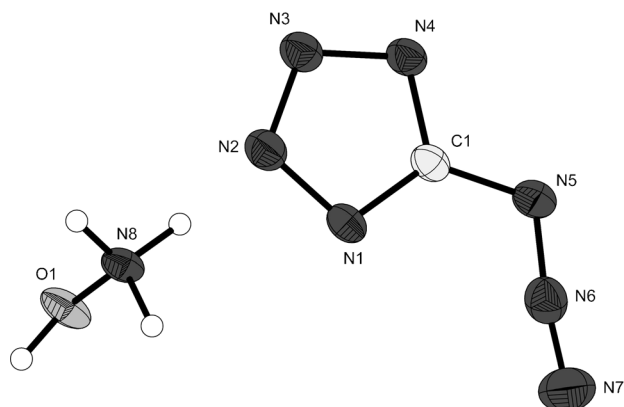


Figure 9. Asymmetric unit of **7**.

Heats of formation: Nitrogen-rich heterocycles, especially those that contain the azide functionality, tend to explode in bomb calorimeters, thereby resulting in insufficient combustion results. Therefore the heats of formation of the metal-free compounds **1**, **5**, and **7** were determined by quantum chemical calculations. For energetic nitrogen-rich compounds, it has been shown appropriate in recent studies^[39–40] to use the atomization method [according to Eq. (2)] based on CBS-4M enthalpies:

$$\Delta_f H^\circ_{(g, M, 298K)} = H_{(molecule, 298K)} - \sum H^\circ_{(atoms, 298K)} + \sum \Delta_f H^\circ_{(atoms, 298K)} \quad (2)$$

The computations were performed with the Gaussian 09 software package.^[41] The obtained gas-phase enthalpies

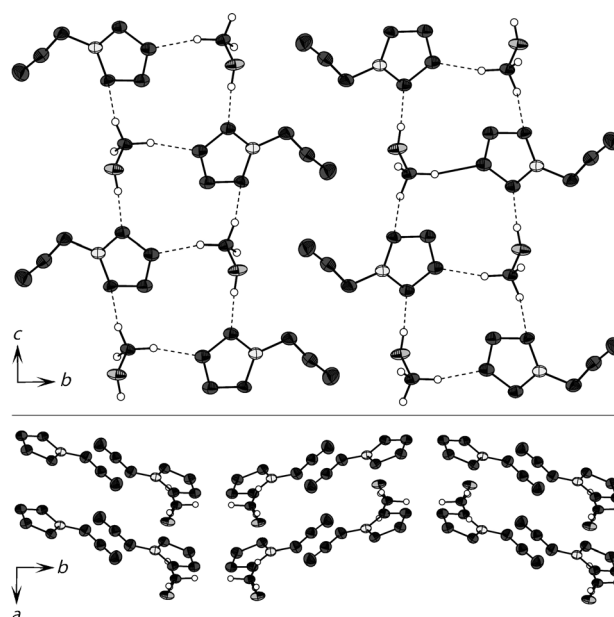


Figure 10. Views along the *a* and *c* axes in the structure of **7**.

were converted into the solid-state enthalpies with Jenkin's equations by using the total molecular volume of the anion-cation pair from the crystal structure (Table 4).

Table 4. CBS-4M calculation results and molecular volumes (V_M) taken from X-ray structures.

M	$-H^{298}$ [a.u.]	$\Delta_f H^\circ(g, M)$ [kcal mol ⁻¹]	V_M [nm ³]
AZX ⁻	495.889863	108.7	
AzTz ⁻	420.796001	113.5	
NH₄⁺	56.796608	151.9	
NH₂O⁺	131.863249	177.9	
AG⁺	260.701802	160.4	
1		260.6	0.142
5		269.1	0.208
7		277.6	0.145

When the heats of formation of the ammonium (**1**) and aminoguanidinium (**5**) salts of azidotetrazolate 2-oxide are compared to the corresponding azidotetrazolates, the solid-state heats of formation are lower by 6 and 20 kJ mol⁻¹, respectively. This trend is comparable to that seen for nitrotetrazolate and its *N*-oxide.^[18]

Detonation parameters: The calculation of the detonation parameters (Table 5) were performed with the program package EXPLO5^[42] using version 5.04 as well as version 5.03 (values in brackets), in which several parameters have been modified. The input was made using the sum formula, energy of formation, and the experimentally determined densities (X-ray). The program is based on the chemical equilibrium, steady-state model of detonation. It uses the Becker–Kistiakowsky–Wilson equation of state (BKW EOS) for gaseous detonation products and Cowan–Fickett's

Table 5. Energetic properties and detonation parameters of AZX salts.

	1	5	7
formula	CH ₄ N ₈ O	C ₂ H ₇ N ₁₁ O	CH ₄ N ₈ O
<i>M_r</i> [g mol ⁻¹]	144.12	201.19	144.12
IS [J] ^[a]	1	N.D.	<1
FS [N] ^[b]	20	N.D.	<5
ESD test [J] ^[c]	0.030	N.D.	0.100
<i>N</i> [%] ^[d]	77.76	76.60	77.76
Ω [%] ^[e]	-33.31	-51.70	-33.31
<i>T_{decomp}</i> [°C] ^[f]	151	N.D.	96
density [g cm ⁻³] ^[g]	1.689	1.608	1.649
Δ _r <i>H_m</i> ^o [kJ mol ⁻¹] ^[h]	534.0	623.3	608.8
Δ _r <i>U</i> ^o [kJ kg ⁻¹] ^[i]	3816.9	3215.1	4335.5
EXPLO 5.04 (5.03)			
-Δ _r <i>U</i> ^o [kJ kg ⁻¹] ^[j]	5668 (5674)	4743 (4770)	6181 (6188)
<i>T_E</i> [K] ^[k]	3960 (4129)	3277 (3396)	4267 (4428)
<i>p_{C-J}</i> [kbar] ^[l]	325 (330)	262 (267)	324 (330)
<i>D</i> [m s ⁻¹] ^[m]	8926 (9167)	8332 (8592)	8959 (9175)
<i>V_{gas}</i> [L kg ⁻¹] ^[n]	830 (842)	820 (840)	831 (844)

[a] Impact sensitivity (BAM drop hammer, 1 of 6). N.D.=not determined. [b] Friction sensitivity (BAM friction test 1 of 6). [c] Electrostatic discharge device (OZM). [d] Nitrogen content. [e] Oxygen balance. [f] Decomposition temperature from DSC ($\beta=5^{\circ}\text{C}$). [g] From X-ray diffraction. [h] Calculated (CBS-4M) heat of formation. [i] Energy of formation. [j] Energy of explosion. [k] Explosion temperature. [l] Detonation pressure. [m] Detonation velocity. [n] Assuming only gaseous products.

equation of state for solid carbon.^[43-46] The calculation of the equilibrium composition of the detonation products is done by applying a modified version of White, Johnson, and Dantzig's free-energy minimization technique. The program is designed to enable the calculation of detonation parameters at the Chapman-Jouguet point. The BKW equation [Eq. (3)] in the following form was used with the BKWN set of parameters (α , β , κ , θ) and with X_i being the mole fraction of the i th gaseous product, and k_i being the molar volume of the i th gaseous product:

$$pV/RT = 1 + xe^{\beta x} \quad x = (\kappa \sum X_i k_i) / [V(T + \theta)]^{\alpha} \quad (3)$$

$$\alpha = 0.5, \beta = 0.176, \kappa = 14.71, \theta = 6620 \text{ (EXPLO 5.03)}$$

$$\alpha = 0.5, \beta = 0.96, \kappa = 17.56, \theta = 4950 \text{ (EXPLO 5.04)}$$

The detonation parameters calculated with the EXPLO5 program are summarized in Table 5.

Compound **1** has a detonation velocity 250 ms⁻¹ higher than the corresponding azidotetrazolate,^[13] and that of compound **5** is 168 ms⁻¹ higher than its analogue that lacks an *N*-oxide. This again confirms that the strategy of *N*-oxide incorporation into tetrazole-based energetic materials is an effective method of increasing their performance.

Compound **7** is of interest because it is a constitutional isomer of **1**. Their performances are almost identical, thereby indicating that the decrease in heats of formation and increase in density balance each other out for compounds of identical oxygen balance. In the next sections, the thermal stabilities and sensitivities will illustrate the superiority of **1** versus **7** and as such the versatility of *N*-oxides as a strategy in energetic material design.

Thermal behavior: The thermal behavior of **1**, **2**, **3**, and **7** were all investigated using a Linseis PT10 differential scanning calorimeter at heating rates of 5°C min⁻¹ with approximately 1–1.5 mg of material. The ammonium salt (**1**) is the most stable; it decomposes at 151°C with no prior melting. Relative to its non-*N*-oxide counterpart, ammonium azidotetrazolate, **1** decomposes 6°C lower. Sodium salt **2**·H₂O loses hydration water at 100°C, undergoes a brief melting event at 118°C, quickly followed by decomposition at 122°C. This decomposition temperature is 33°C lower than its non-*N*-oxide counterpart. Potassium salt **3** decomposes at 138°C with no prior melting, 10°C lower than its non-*N*-oxide counterpart. The overall trend of the azidotetrazolate 2-oxide salts is that they possess slightly lowered decomposition temperatures relative to analogous azidotetrazolate salts, the same trend that was observed for nitrotetrazolate 2-oxide and nitrotetrazolate.

Sensitivities: For initial safety testing, the impact, friction, and electrostatic discharge (ESD) sensitivity of the prepared nitrogen-rich salts were carried out.^[47,48] The impact sensitivity tests were carried out according to STANAG 4489^[49] and were modified according to instruction^[50] using a BAM (Bundesanstalt für Materialforschung^[48]) drop hammer.^[51] The friction sensitivity tests were carried out according to STANAG 2287^[52] and were modified according to instruction^[53] using a BAM friction tester. Electrostatic sensitivity tests were performed on all materials using a small-scale electric spark tester ESD 2010EN (OZM Research^[54]) operating with the Winspark 1.15 software package.^[55] The ammonium salt **1** has an impact sensitivity of 1 J, a friction sensitivity of 10 N, and an ESD sensitivity of 30 mJ. These values place the ammonium salt well within the range of highly sensitive primary explosives according to the UN Recommendations on the Transport of Dangerous Goods.^[56] The electrostatic discharge sensitivity of this compound is in the vicinity of what can be developed by the human body, thus mandating properly grounded handling processes. However, when compared to the impact and friction sensitivities of ammonium azidotetrazolate (<1 J, <5 N), the ability of *N*-oxides to desensitize compounds is again illustrated. Interestingly, **2**·H₂O, sodium azidotetrazolate 2-oxide is completely insensitive towards impact (>40 J) and of low friction and ESD sensitivities (120 N and 0.5 J, respectively). This is despite the fact that it explodes when contacted with a flame, which makes for a very novel, insensitive compound that contains the azidotetrazole moiety. This is in contrast to sodium azidotetrazolate monohydrate, which, despite being hydrated, still possesses very high sensitivities (<1 J impact, <5 N friction). The potassium salt (**3**) has an impact sensitivity of 1.5 J, a friction sensitivity of <5 N, and an ESD sensitivity of 1.3 mJ. Unfortunately, the sensitivities of potassium azidotetrazolate were unmeasured in the literature^[13] due to explosions upon handling, so again our *N*-oxide version is less sensitive. Of interest is the exceedingly high ESD sensitivity of **3**, as 1.3 mJ is easily achieved by the human body, thus making handling exceedingly dangerous. By far

the most sensitive azidotetrazolate 2-oxide salt prepared was the silver salt **6**; this compound exploded repeatedly when attempting to handle and measure sensitivities, so one can say that the impact sensitivity is much less than 1 J, and the friction sensitivity is much less than 5 N. Hydroxylammonium azidotetrazolate (**7**) is an isomer of **1**, which makes for an interesting comparison because they both have similar performances, but **7** is of much higher sensitivity with <1 J impact, <5 N friction, and almost exploding (crackling) when pressed for infrared spectroscopy. Again the lower sensitivity of azidotetrazolate 2-oxide salts is manifested.

Conclusion

From this combined experimental and theoretical work, the following conclusions can be drawn: 1) The CN_7O^- anion can be prepared from azidotetrazolate salts in a mild aqueous oxidation using buffered potassium acetate; 2) azidotetrazolate 2-oxide salts are generally highly sensitive energetic materials; however, while they are less sensitive than the corresponding azidotetrazolate, proper safety measures must still be observed; 3) azidotetrazolate 2-oxides show higher densities, lower heats of formation, and higher performances than the corresponding azidotetrazolates; 4) unfortunately, the thermal stability of azidotetrazolate 2-oxides are lower than the corresponding azidotetrazolate; and 5) sodium azidotetrazolate 2-oxide monohydrate is the safest known compound that contains the azidotetrazole moiety that is insensitive (>40 J) towards impact.

Experimental Section

General: All reagents and solvents were used as received (Sigma–Aldrich, Fluka, Acros Organics) if not stated otherwise. Azidotetrazole was prepared according to the literature procedure. Melting and decomposition points were measured using a Linseis PT10 DSC with heating rates of 5°C min^{-1} , which were checked using a Büchi Melting Point B-450 apparatus. ^1H , ^{13}C , and ^{15}N NMR spectra were measured using a JEOL instrument. All chemical shifts are quoted in ppm relative to TMS (^1H , ^{13}C) or nitromethane (^{15}N). Infrared spectra were measured using a Perkin–Elmer Spektrum One FTIR instrument. Raman spectra were measured using a Perkin–Elmer Spektrum 2000R NIR FT-Raman instrument equipped with a Nd:YAG laser (1064 nm). Elemental analyses were performed using a Netsch STA 429 simultaneous thermal analyser. Sensitivity data were determined using a BAM drophammer and a BAM friction tester. The electrostatic sensitivity tests were carried out using an Electric Spark Tester ESD 2010 EN (OZM Research) operating with the Winspark 1.15 software package.

Caution! All compounds prepared herein are highly energetic compounds highly sensitive to various stimuli. Although we only encountered accidental explosions in the handling of silver salt **6**, proper protective measures (e.g., face shield, ear protection, body armor, Kevlar gloves and earthed equipment) should be used at all times.

Ammonium azidotetrazolate 2-oxide (1): 5-Azidotetrazole (2.00 g, 18 mmol) (**Danger!** Weigh in small portions, dissolve in water and combine. Do not handle 2 g of dry azidotetrazole at one time.) was dissolved in distilled water (90 mL) and NaOH (2 M, 9 mL, 18 mmol) was added followed by potassium acetate (17.1 g, 174 mmol). The solution was

heated to 40°C and oxone (35.1 g, 57 mmol) was added slowly. The resulting suspension was stirred at 40°C for three days, diluted until all solids dissolved, and concentrated sulfuric acid (16.2 mL, 288 mmol) was added upon cooling. The solution was extracted with 5 portions of diethyl ether (100 mL) and NH_3 solution (2 M, 28 mL, 56 mmol) was added to the extracts, followed by stirring and evaporation of the two-phase mixture under a stream of nitrogen. The resulting solid was recrystallized from acetonitrile. The first crop of crystals yielded 0.54 g, and the second yielded 0.24 g for a combined yield of 30%. $^1\text{H NMR}$ ($[\text{D}_6]$ DMSO): $\delta = 7.17$ ppm (s, 4H; NH_4); $^{13}\text{C NMR}$ ($[\text{D}_6]$ DMSO): $\delta = 151.0$ ppm (s, 1C; CN_4); $^{15}\text{N NMR}$ ($[\text{D}_6]$ DMSO): $\delta = -39.1$ (s, 1N; N2 or N3), -40.8 (s, 1N; N2 or N3), -100.5 (s, 1N; N4), -113.4 (s, 1N; N1); -140.4 (s, 1N; N6), -147.3 (s, 1N; N7), -302.2 (s, 1N; N5), -360.2 ppm (s, 1N; N8); IR: $\tilde{\nu} = 3167$ (m) 3012 (m), 2852 (m), 2447 (w), 2278 (w), 2139 (s), 1650 (w), 1540 (w), 1479 (m), 1469 (m), 1432 (m), 1417 (m), 1404 (m), 1372 (m), 1342 (s), 1282 (m), 1232 (m), 1216 (m), 1195 (m), 1135 (m), 1061 (w), 1047 (w), 1020 (w), 997 (w), 970 (w), 854 (w), 830 (w), 806 (w), 791 (w), 765 (m), 743 (w), 724 (m), 685 cm^{-1} (w); Raman IR (1064 nm): $\tilde{\nu} = 3065$ (5), 2858 (1), 2152 (20), 2041 (1), 1684 (3), 1493 (66), 1435 (16), 1407 (6), 1373 (3), 1352 (4), 1234 (20), 1144 (6), 1063 (6), 1022 (100), 814 (12), 768 (2), 727 (6), 686 (1), 596 (13), 517 (7), 433 (2), 362 (14), 280 cm^{-1} (8); DSC (5°C min^{-1}): 151°C (decomp); MS (FAB+): m/z : 18.1 (NH_4^+); MS (FAB-): m/z : 126.0 (CN_7O^-); elemental analysis calcd (%) for $\text{CH}_4\text{N}_8\text{O}$ (144.10 g mol^{-1}): C 8.33, N 77.76, H 2.80; found: too sensitive for measurement; BAM impact: 1 J; BAM friction: 10 N; ESD: 30 mJ.

Sodium azidotetrazolate 2-oxide monohydrate (2·H₂O): Compound **1** (0.240 g, 1.67 mmol) was dissolved in cold water (15 mL). NaOH solution (2 M, 0.83 mL, 1.67 mmol) was added, and the solution was boiled until no more ammonia was released. The solution was allowed to evaporate, and the resulting white powder was recrystallized from acetonitrile to yield **2·H₂O** (0.15 g, 54%). $^1\text{H NMR}$ ($[\text{D}_6]$ DMSO): $\delta = 3.47$ ppm (s, 2H; OH_2); $^{13}\text{C NMR}$ ($[\text{D}_6]$ DMSO): $\delta = 151.0$ ppm (s, 1C; CN_4); IR: $\tilde{\nu} = 3172$ (m), 3519 (m), 3423 (m), 3361 (m), 3258 (w), 2968 (w), 2437 (w), 2365 (w), 2266 (w), 2169 (s), 1653 (w), 1641 (w), 1596 (w), 1506 (m), 1500 (m), 1440 (s), 1383 (s), 1243 (w), 1223 (m), 1156 (w), 1072 (w), 1044 (w), 904 (w), 866 (w), 819 (w), 771 (m), 751 (w), 725 (w), 688 (w), 682 cm^{-1} (w); Raman IR (1064 nm): $\tilde{\nu} = 3357$ (1), 2180 (1), 2151 (9), 1643 (1), 1500 (40), 1485 (2), 1444 (2), 1412 (2), 1394 (4), 1243 (5), 1227 (2), 1158 (4), 1069 (2), 1041 (25), 773 (1), 725 (1), 681 (1), 602 (2), 508 (3), 415 (1), 368 (7), 272 cm^{-1} (3); DSC (5°C min^{-1}): 98°C ($-\text{H}_2\text{O}$), 118°C (decomp); MS (FAB+): m/z : 23.0 (Na^+); MS (FAB-): m/z : 126.0 (CN_7O^-); elemental analysis calcd (%) for $\text{NaCN}_7\text{O}\cdot\text{H}_2\text{O}$ (167.06 g mol^{-1}): C 7.19, N 58.69, H 1.21; found: 7.76, N 55.92, H 1.48; BAM impact: >40 J; BAM friction: 120 N; ESD: 0.500 J

Potassium azidotetrazolate 2-oxide (3): Compound **1** (0.240 g, 1.67 mmol) was dissolved in cold water (15 mL) and KOH solution (2 M, 0.83 mL, 1.67 mmol) was added. The solution was boiled until no more ammonia was released. The solution was allowed to evaporate, thereby yielding **3** (0.22 g, 80%). $^{13}\text{C NMR}$ ($[\text{D}_6]$ DMSO): $\delta = 151.2$ ppm (s, 1C; CN_4); IR: $\tilde{\nu} = 3341$ (w), 2189 (m), 2143 (s), 1492 (m), 1468 (m), 1438 (m), 1386 (s), 1364 (s), 1237 (s), 1195 (m), 1150 (m), 1128 (m), 1056 (m), 1018 (m), 839 (m), 791 (w), 738 (m), 726 (m), 692 cm^{-1} (w); Raman IR (1064 nm): $\tilde{\nu} = 2153$ (14), 1514 (3), 1499 (100), 1440 (6), 1398 (7), 1376 (2), 1239 (17), 1193 (8), 1130 (3), 1058 (2), 1051 (13), 1020 (86), 841 (4), 740 (17), 728 (3), 577 (4), 538 (8), 424 (3), 376 (6), 266 cm^{-1} (5); DSC (5°C min^{-1}): 138°C (decomp); MS (FAB+): m/z : 39.0 (K^+); MS (FAB-): m/z : 126.0 (CN_7O^-); elemental analysis calcd (%) for KCN_7O (165.16 g mol^{-1}): C 7.27, N 59.37; found: too sensitive for measurement; BAM impact: 1.5 J; BAM friction: <5 N; ESD: 1.3 mJ.

5-Azido-2-hydroxytetrazole (4): Compound **1** (0.20 g, 1.39 mmol) was dissolved in distilled water (10 mL) and concentrated sulfuric acid (0.5 mL) was added with stirring in an ice bath. The solution was extracted with ten portions (10 mL each) of diethyl ether, and the ether was dried over magnesium sulfate. The ether solution was filtered and transferred to a Schlenk flask in an ice bath and a stream of nitrogen was used to evaporate the ether. Evaporation using a rotary evaporator led to energetic decomposition. After evaporation, a small amount of oily light yellow liquid was obtained that was dissolved in cool deuterated THF for NMR

spectroscopy. ^1H NMR ($[\text{D}_8]\text{THF}$): $\delta = 11.17$ ppm (s, 1H; OH); ^{13}C NMR ($[\text{D}_8]\text{THF}$): $\delta = 155.0$ ppm (s, 1C; CN_4); ^{15}N NMR ($[\text{D}_8]\text{THF}$): $\delta = -22.4$ (s, 1N; N3), -81.3 (s, 1N; N4 or N2), -82.9 (s, 1N; N4 or N2), -110.6 (s, 1N; N1), -144.6 (s, 1N; N6), -145.8 (s, 1N; N7), -301.4 ppm (s, 1N; N5).

Aminoguanidinium azidotetrazolate 2-oxide (5): Compound **1** (0.240 g, 1.67 mmol) was dissolved in ethanol (10 mL), and aminoguanidine bicarbonate (0.227 g, 1.67 mmol) was added. The solution was heated at reflux overnight and evaporated to yield a nonexplosive, off-white precipitate. ^1H NMR ($[\text{D}_6]\text{DMSO}$): $\delta = 8.81$ (s, 1H; $\text{NH}-\text{NH}_2$), 7.35 and 6.98 ($2 \times$ s, $2 \times 2\text{H}$; CNH_2), 4.67 ppm (s, 2H; $\text{NH}-\text{NH}_2$); ^{13}C NMR ($[\text{D}_6]\text{DMSO}$): $\delta = 164.0$, 158.9 (s, 1C; CN_3H_7), no AZX at ≈ 151 ppm. This unknown solid was dissolved in a small amount of methanol and diethyl ether was allowed to diffuse into it, thereby yielding a small number of crystals of pure **5**.

Silver azidotetrazolate 2-oxide (6): Compound **1** (0.200 g, 1.39 mmol) was dissolved in distilled water (10 mL), and a solution of silver nitrate (0.232 g, 1.39 mmol) in water (10 mL) was added. The solution was stirred for 10 min in the dark and filtered through a tared piece of filter paper. The light yellow precipitate was allowed to dry undisturbed in the dark on the filter paper, thereby yielding **6** (0.227 g, 71%). Further handling led to explosions of the material. IR: $\nu = 2161$ (m), 1504 (s), 1450 (m), 1436 (m), 1383 (s), 1367 (s), 1352 (s), 1251 (m), 1233 (w), 1206 (m), 1155 (w), 1134 (m), 1093 (w), 1074 (w), 1061 (w), 1031 (m), 851 (m), 825 (w), 795 (w), 772 (m), 744 (m), 716 cm^{-1} (m)

Hydroxylammonium azidotetrazolate (7): 5-Azidotetrazole (0.500 g, 4.5 mmol) was dissolved in distilled water (10 mL), and a 50% aqueous hydroxylamine solution (0.276 mL, 4.5 mmol) was added to this. The solution was stirred for 10 min and allowed to evaporate until crystallization, at which point filtration yielded **7** (0.39 g, 60%). ^1H NMR ($[\text{D}_6]\text{DMSO}$): $\delta = 8.77$ ppm (s, 4H; NH_4O); ^{13}C NMR ($[\text{D}_6]\text{DMSO}$): $\delta = 158.4$ ppm (s, 1C; CN_4); IR: $\nu = 3123$ (m), 2888 (m), 2821 (m), 2658 (m), 2444 (m), 2409 (m), 2362 (m), 2258 (m), 2139 (s), 2024 (m), 1623 (m), 1602 (m), 1576 (m), 1566 (m), 1525 (m), 1470 (s), 1462 (s), 1413 (s), 1340 (m), 1247 (m), 1233 (m), 1213 (m), 1141 (w), 1110 (w), 1080 (w), 1001 (m), 913 (m), 787 (m), 735 cm^{-1} (m); Raman IR (1064 nm): $\bar{\nu} = 3160$ (1), 2907 (5), 2680 (2), 2150 (27), 1604 (2), 1578 (2), 1487 (100), 1417 (8), 1338 (2), 1249 (31), 1213 (2), 1144 (5), 1112 (35), 1082 (19), 1005 (26), 790 (13), 737 (5), 552 (32), 424 (12), 342 (16), 302 (40), 214 cm^{-1} (2); DSC (5°C min^{-1}): 96°C (decomp); MS (FAB+): m/z : 34.0 (NH_4O^+); MS (FAB-): m/z : 110.0 (CN_7^-); elemental analysis calcd for $\text{CH}_4\text{N}_8\text{O}$ (144.10 gmol^{-1}): C 8.33, N 77.76, H 2.80; found: too sensitive for measurement; BAM impact: $< 1\text{ J}$; BAM friction: $< 5\text{ N}$; ESD: 0.100 J.

CCDC-827211 (**1**), 827214 (**2-MeOH**), 827213 (**3**), 827215 (**5**) and 827212 (**7**) contain the supplementary crystallographic data for this paper. These data can be obtained free of charge from The Cambridge Crystallographic Data Centre via www.ccdc.cam.ac.uk/data_request/cif.

Acknowledgements

Financial support of this work by the Ludwig-Maximilian University of Munich (LMU), the U.S. Army Research Laboratory (ARL), the Armament Research, Development and Engineering Center (ARDEC), the Strategic Environmental Research and Development Program (SERDP), and the Office of Naval Research (ONR Global, Synthesis and Characterization of New High Energy Dense Oxidizers (HEDO) - NICOP Effort; contract nos. W911NF-09-2-0018 (ARL), W911NF-09-1-0120 (ARDEC), W011NF-09-1-0056 (ARDEC), and 10-WPSEED01-002/WP-1765 (SERDP)) is gratefully acknowledged. The authors acknowledge collaborations with Dr. Mila Krupka (OZM Research, Czech Republic) in the development of new testing and evaluation methods for energetic materials and with Dr. Muhamed Sucesca (Brodarski Institute, Croatia) in the development of new computational codes to predict the detonation and propulsion parameters of novel explosives. We are indebted to and thank Drs. Betsy M. Rice and Brad Forch (ARL, Aberdeen, Proving Ground, MD) and Mr. Gary Chen (ARDEC, Picatinny Arsenal, NJ) for

many helpful and inspired discussions and support of our work. Prof. Dr. Konstantin Karaghiosoff and Dr. Burkhard Krumm are thanked for NMR spectroscopic assistance, Stefan Huber is thanked for measuring the sensitivities, and Dennis Fischer is thanked for many inspirational discussions.

- [1] J. L. Gay-Lussac, *Ann. Chim. Phys.* **1824**, 27, 199.
- [2] J. L. Gay-Lussac, J. Liebig, *Kastners Archiv* **1824**, 11, 58–91.
- [3] J. Berzelius, *Ann. Chem. Pharm.* **1844**, 50, 426–429.
- [4] T. L. Davis, *The Chemistry of Powder and Explosives*, Angriff, Los Angeles, **1943**, pp. 424–430.
- [5] L. V. De Yong, J. J. Campanella, *J. Hazard. Mater.* **1989**, 21, 125–133.
- [6] T. M. Klapötke, C. M. Sabaté, *Heteroat. Chem.* **2008**, 19, 301–305.
- [7] T. Altenburg, T. M. Klapötke, A. Penger, J. Stierstorfer, *Z. Anorg. Allg. Chem.* **2010**, 636, 463–471.
- [8] T. M. Klapötke, C. M. Sabaté, *Z. Anorg. Allg. Chem.* **2009**, 635, 1812–1822.
- [9] N. Fischer, K. Karaghiosoff, T. M. Klapötke, J. Stierstorfer, *Z. Anorg. Allg. Chem.* **2010**, 636, 735–739.
- [10] P. Carlqvist, H. Ostmark, T. J. Brinck, *J. Phys. Chem. A* **2004**, 108, 7463–7467.
- [11] R. Boese, R. T. M. Klapötke, P. Mayer, V. Verma, *Propellants Explos. Pyrotech.* **2006**, 31, 263–268.
- [12] M. H. V. Huynh, M. A. Hiskey, T. J. Meyer, M. Wetzler, *Proc. Natl. Acad. Sci. USA* **2006**, 103, 5409–5412.
- [13] T. M. Klapötke, J. Stierstorfer, *J. Am. Chem. Soc.* **2009**, 131, 1122–1134.
- [14] W. H. Gilligan, M. J. Kamlet (Washington DC, secretary of the Navy), US 4093623, **1978**.
- [15] W. Friedrich, K. Fick (Dynamit AG), DE 719135, **1942**.
- [16] W. Friedrich (Dynamit AG), GB 519069 19400315, **1940**.
- [17] W. Friedrich, K. Fick (Dynamit AG), US 2179783, **1939**; W. Friedrich, K. Fick (Dynamit AG), US 19391114, **1939**.
- [18] M. Göbel, K. Karaghiosoff, T. M. Klapötke, D. G. Piercey, J. Stierstorfer, *J. Am. Chem. Soc.* **2010**, 132, 17216–17226.
- [19] A. M. Churakov, V. A. Tartakovsky, *Chem. Rev.* **2004**, 104, 2601–2616.
- [20] M. N. Glukhovtsev, B. Y. Simkin, V. I. Minkin, *Zh. Org. Khim.* **1988**, 24, 2486–2488.
- [21] S. Inagaki, N. Goto, *J. Am. Chem. Soc.* **1987**, 109, 3234–3240.
- [22] M. Noyman, S. Zilberg, Y. Haas, *J. Phys. Chem. A* **2009**, 113, 7376–7382.
- [23] Gaussian 03, Revision B.04, M. J. Frisch, G. W. Trucks, H. B. Schlegel, G. E. Scuseria, M. A. Robb, J. R. Cheeseman, J. A. Montgomery, Jr., T. Vreven, K. N. Kudin, J. C. Burant, J. M. Millam, S. S. Iyengar, J. Tomasi, V. Barone, B. Mennucci, M. Cossi, G. Scalmani, N. Rega, G. A. Petersson, H. Nakatsuji, M. Hada, M. Ehara, K. Toyota, R. Fukuda, J. Hasegawa, M. Ishida, T. Nakajima, Y. Honda, O. Kitao, H. Nakai, M. Klene, X. Li, J. E. Knox, H. P. Hratchian, J. B. Cross, V. Bakken, C. Adamo, J. Jaramillo, R. Gomperts, R. E. Stratmann, O. Yazyev, A. J. Austin, R. Cammi, C. Pomelli, J. W. Ochterski, P. Y. Ayala, K. Morokuma, G. A. Voth, P. Salvador, J. J. Dannenberg, V. G. Zakrzewski, S. Dapprich, A. D. Daniels, M. C. Strain, O. Farkas, D. K. Malick, A. D. Rabuck, K. Raghavachari, J. B. Foresman, J. V. Ortiz, Q. Cui, A. G. Baboul, S. Clifford, J. Cioslowski, B. B. Stefanov, G. Liu, A. Liashenko, P. Piskorz, I. Komaromi, R. L. Martin, D. J. Fox, T. Keith, M. A. Al-Laham, C. Y. Peng, A. Nanayakkara, M. Challacombe, P. M. W. Gill, B. Johnson, W. Chen, M. W. Wong, C. Gonzalez, J. A. Pople, Gaussian, Inc., Wallingford CT, **2004**.
- [24] A. D. Becke, *J. Chem. Phys.* **1993**, 98, 5648–5652.
- [25] C. Lee, W. Yang, R. G. Parr, *Phys. Rev. B* **1988**, 37, 785–789.
- [26] D. E. Woon, T. H. Dunning Jr, *J. Chem. Phys.* **1993**, 98, 1358–1371.
- [27] R. A. Kendall, T. H. Dunning, Jr., R. J. Harrison, *J. Chem. Phys.* **1992**, 96, 6796–6806.
- [28] T. H. Dunning, Jr., *J. Chem. Phys.* **1989**, 90, 1007–1023.
- [29] K. A. Peterson, D. E. Woon, T. H. Dunning, Jr., *J. Chem. Phys.* **1994**, 100, 7410–7415.

- [30] CrysAlisPro Oxford Diffraction, Version 171.33.41, Oxford, **2009**.
- [31] SIR-92, 1993, A program for crystal structure solution, A. Altomare, G. Casciaro, C. Giacovazzo, A. Guagliardi, *J. Appl. Crystallogr.* **1993**, *26*, 343.
- [32] G. M. Sheldrick, SHELXS-97, Program for Crystal Structure Solution, Universität Göttingen, Göttingen, **1997**.
- [33] G. M. Sheldrick, SHELXL-97, Program for the Refinement of Crystal Structures, University of Göttingen, Göttingen, **1997**.
- [34] A. L. Spek, PLATON, A Multipurpose Crystallographic Tool, Utrecht University, Utrecht, **1999**.
- [35] L. J. Farrugia, *J. Appl. Crystallogr.* **1999**, *32*, 837.
- [36] SCALE3 ABSPACK (1.0.4.gui:1.0.3) (C), Oxford Diffraction, Oxford, **2005**.
- [37] V. Ernst, T. M. Klapötke, J. Stierstorfer, *Z. Anorg. Allg. Chem.* **2007**, *633*, 879–887.
- [38] J. Bernstein, R. E. Davis, L. Shimoni, N.-L. Chang, *Angew. Chem.* **1995**, *107*, 1689–1708; *Angew. Chem. Int. Ed. Engl.* **1995**, *34*, 1555–1573.
- [39] T. M. Klapötke, D. G. Piercy, J. Stierstorfer, *Propellants Explos. Pyrotech.* **2011**, *36*, 160–167.
- [40] T. Fendt, N. Fischer, T. M. Klapötke, J. Stierstorfer, *Inorg. Chem.* **2011**, *50*, 1447–1458.
- [41] Gaussian 09, Revision A.1, M. J. Frisch, G. W. Trucks, H. B. Schlegel, G. E. Scuseria, M. A. Robb, J. R. Cheeseman, G. Scalmani, V. Barone, B. Mennucci, G. A. Petersson, H. Nakatsuji, M. Caricato, X. Li, H. P. Hratchian, A. F. Izmaylov, J. Bloino, G. Zheng, J. L. Sonnenberg, M. Hada, M. Ehara, K. Toyota, R. Fukuda, J. Hasegawa, M. Ishida, T. Nakajima, Y. Honda, O. Kitao, H. Nakai, T. Vreven, J. A. Montgomery, Jr., J. E. Peralta, F. Ogliaro, M. Bearpark, J. J. Heyd, E. Brothers, K. N. Kudin, V. N. Staroverov, R. Kobayashi, J. Normand, K. Raghavachari, A. Rendell, J. C. Burant, S. S. Iyengar, J. Tomasi, M. Cossi, N. Rega, J. M. Millam, M. Klene, J. E. Knox, J. B. Cross, V. Bakken, C. Adamo, J. Jaramillo, R. Gomperts, R. E. Stratmann, O. Yazyev, A. J. Austin, R. Cammi, C. Pomelli, J. W. Ochterski, R. L. Martin, K. Morokuma, V. G. Zakrzewski, G. A. Voth, P. Salvador, J. J. Dannenberg, S. Dapprich, A. D. Daniels, Ö. Farkas, J. B. Foresman, J. V. Ortiz, J. Cioslowski, D. J. Fox, Gaussian, Inc., Wallingford CT, **2009**.
- [42] a) M. Sućeska, EXPLO5.3 program, Brodarski Insitut, Zagreb, **2009**; b) M. Sućeska, Brodarski Insitut, Zagreb, **2010**.
- [43] M. Sućeska, *Mat. Sci. Forum* **2004**, *465–466*, 325–330.
- [44] M. Sućeska, *Propellants Explos. Pyrotech.* **1991**, *16*, 197–202.
- [45] M. Sućeska, *Propellants Explos. Pyrotech.* **1999**, *24*, 280–285.
- [46] M. L. Hobbs, M. R. Baer, *Proceedings of the 10th International Symposium on Detonation*, Boston USA, Office of Naval Research, Arlington, **1993**, p. 409.
- [47] Impact: M. Sućeska, *Test Methods for Explosives*, Springer, New York, **1995**, p. 21; friction: M. Sućeska, *Test Methods for Explosives*, Springer, New York, **1995**, p. 27.
- [48] www.bam.de.
- [49] *NATO Standardization Agreement (STANAG) on Explosives, Impact Sensitivity Tests*, 1st ed., no. 4489, Sept. 17, **1999**.
- [50] WIWEB-Standardarbeitsanweisung 4–5.1.02, Ermittlung der Explosionsgefährlichkeit, hier der Schlagempfindlichkeit mit dem Fallhammer, Nov. 8, **2002**.
- [51] <http://www.reichel-partner.de>.
- [52] *NATO Standardization Agreement (STANAG) on Explosives, Friction Sensitivity Tests*, 1st ed., no. 4487, Aug. 22, **2002**.
- [53] WIWEB-Standardarbeitsanweisung 4–5.1.03, Ermittlung der Explosionsgefährlichkeit oder der Reibeempfindlichkeit mit dem Reibeapparat, Nov. 8, **2002**.
- [54] D. Skinner, D. Olson, A. Block-Bolten, *Propellants Explos. Pyrotech.* **1998**, *23*, 34–42.
- [55] <http://www.ozm.cz/testinginstruments/small-scale-electrostatic-discharge-tester.htm>.
- [56] Impact: Insensitive > 40 J, less sensitive ≥ 35 J, sensitive ≥ 4 J, very sensitive ≤ 3 J. Friction: Insensitive > 360 N, less sensitive = 360 N, sensitive (80–360 N), very sensitive ≤ 80 N, extremely sensitive ≤ 10 N. According to the UN Recommendations on the Transport of Dangerous Goods.

Received: July 5, 2011
Published online: October 4, 2011

A Study of Cyanotetrazole Oxides and Derivatives thereof

Franziska Boneberg, Angie Kirchner, Thomas M. Klapötke,* Davin G. Piercey, Maximilian J. Poller, and Jörg Stierstorfer^[a]

Abstract: In this work we report on the syntheses of energetic salts of cyanotetrazolate-1- and -2-oxides; this offers a unique ability to compare the effects of tetrazole 1- versus 2-oxidation. 5-Cyanotetrazolate-2-oxide can be synthesized by oxidation of the 5-cyanotetrazolate anion with Oxone, while the corresponding 1-oxide was synthesized by the rearrangement of azidoaminofurazan. Both chemical (multinuclear NMR, IR, and Raman spectroscopies, mass spectrometry, etc.) as well as ex-

plosive (impact, friction, and static sensitivities) properties are reported for these energetic salts. Calculated explosive performances using the EXPLO5 computer code are also reported. We furthermore detail the chemistry of these two anions, and their ability to form tetrazole-carboxamides, dihydro-

tetrazines, and tetrazines. The ability to hydrolyze cyanotetrazole oxides to their amides was demonstrated by two copper complexes. Several crystal structures of these species are presented in addition to full chemical characterization. Finally, the unique 1,4-bis(2-*N*-oxidotetrazolate)-1,2,4,5-tetrazine anion was characterized as an energetic material as its ammonium salt.

Keywords: crystal structures • energetic materials • *N*-oxides • tetrazines • tetrazoles

Introduction

The development of new energetic materials for practical use is an area of intense research.^[1–5] Many strategies in the design of new energetic materials have been extensively explored, differing only in the source of energy content. Traditional energetic materials such as RDX (1,3,5-trinitro-1,3,5-triazacyclohexane) and TNT (2,4,6-trinitrotoluene) rely on the oxidation of a carbon backbone by oxygen present in the molecule, ring- or caged-strained compounds such as octanitrocubane or trinitroazetidine, which introduce additional energy content from their strained bonds and high heat of formation, or nitrogen-rich compounds, for which the energetic driving force originates from nitrogen–nitrogen double and single bonds to produce nitrogen gas.

However, these energetic strategies have drawbacks: nitroaromatics and nitramines are toxic,^[6,7] compounds with excessive ring or cage strain have very long synthetic routes,^[8,9] and nitrogen-rich compounds lose thermodynamic and mechanical stability as the number of nitrogen atoms per heterocycle or chain becomes too large.^[10,11,12] A possible solution to the problem of stability of very nitrogen-rich

compounds is the addition of a zwitterionic *N*-oxide to the nitrogen system. The removal of σ electron density can stabilize systems as is seen in 1,2,3,4-tetrazine dioxides,^[13–15] and *N*-oxides also increase densities^[16] and oxygen balances, thus leading to increased energetic performances. Additionally, the increased intermolecular interactions afforded by the very polar *N*-oxide often stabilize these materials towards physical impact, thereby making them safer to handle.^[17,18] The utility of *N*-oxides is illustrated in the variety of energetic materials possessing this functionality such as 5,7-dinitrobenzo-1,2,3,4-tetrazine-1,3-dioxide (DNBTDO),^[19] TKX50,^[20] and dinitroazofuroxan (DDF)^[21] (Figure 1).

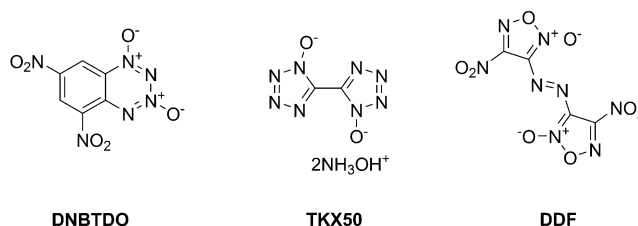


Figure 1. Energetic *N*-oxides.

Within the area of tetrazole-*N*-oxides we have previously detailed the preparation of salts of nitro-,^[17] azido-,^[18] and bistetrazole^[20] oxides, and the general trends for *N*-oxides have held true; they are of higher density, lower sensitivity, and higher performance than the non-oxidized parent compounds; however, they possess a slightly lowered thermal stability. We have been limited previously by the lack of an easy comparison between 1- and 2-tetrazole oxides as nitro-

[a] F. Boneberg, A. Kirchner, Prof. Dr. T. M. Klapötke, D. G. Piercey, M. J. Poller, J. Stierstorfer
Department of Chemistry
Energetic Materials Research
Ludwig-Maximilian University
Butenandtstr. 5–13 (D), 81377 München (Germany)
Fax: (+49) 89-2180-77492
E-mail: tmk@cup.uni-muenchen.de

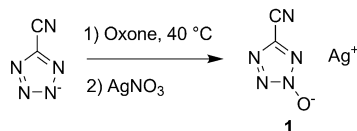
Supporting information for this article is available on the WWW under <http://dx.doi.org/10.1002/asia.201200903>.

and azidotetrazole are known as their 2-oxides, whereas bis-tetrazole is known as its 1-oxide. In this work, we detail the preparation and characterization of both salts of cyanotetrazole 1- and 2-oxides, thereby allowing for the comparison of the effect of N1- versus N2-oxidation. Additionally, we report on the reactions of cyanotetrazole oxides to give tetrazole oxides functionalized with carboxamide, 1,4-dihydro-1,2,4,5-tetrazines, and 1,2,4,5 tetrazine.

Results and Discussion

Synthesis

Prior to this work, the cyanotetrazolate-2-oxide anion was unknown. The preparation of the cyanotetrazolate-2-oxide anion was based on an extrapolation of our previous work.^[17,18] An aqueous solution of sodium 5-cyanotetrazolate was oxidized with potassium peroxymonopersulfate (Oxone) overnight at 40 °C (Scheme 1). By pouring the reac-

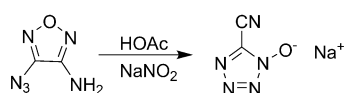


Scheme 1. Oxidation of the cyanotetrazolate anion.

tion mixture into acetone and filtering the precipitate, a crude solution of the cyanotetrazolate-2-oxide in acetone was obtained. After purification by recrystallization, the crude cyanotetrazolate-2-oxide salts were precipitated with silver nitrate, thus yielding pure silver cyanotetrazolate-2-oxide (**1**) as a white powder. In the case of the ammonium salt (**2**), extraction of the crude reaction mixture with ethyl acetate after the addition of aqueous sodium tributylammonium sulfate yielded the tributylammonium salt. Ion exchange led to the isolation of ammonium cyanotetrazolate-2-oxide (**2**) as colorless crystals.

Unlike the cyanotetrazolate-2-oxide, the cyanotetrazolate-1-oxide anion has been reported in one study^[22] as the sodium salt from the reaction of azidoaminofurazan with sodium nitrite (Scheme 2). This sodium salt was precipitated as the silver salt (**3**) by addition of aqueous silver nitrate, or transformed to the ammonium salt (**4**) by ion exchange chromatography performed after extracting the tributylammonium salt from solution.

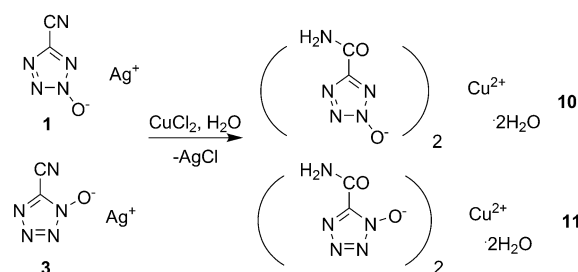
Using silver salts **1** and **3**, metathesis reactions with aminoguanidinium chloride, diaminoguanidinium iodide, or triaminoguanidinium chloride gave the corresponding nitrogen-



Scheme 2. Rearrangement of azidoaminofurazane to the cyanotetrazolate-1-oxide anion.

rich salts (aminoguanidinium cyanotetrazolate-2-oxide (**5**), diaminoguanidinium cyanotetrazolate-2-oxide (**6**), triaminoguanidinium cyanotetrazolate-2-oxide (**7**), aminoguanidinium cyanotetrazolate-1-oxide (**8**), and triaminoguanidinium cyanotetrazolate-1-oxide (**9**)) of the cyanotetrazolate-1 and -2 oxides after filtering off the corresponding silver halide as by-product. Crystals were grown by the slow diffusion of ether into a methanolic solution of the salt.

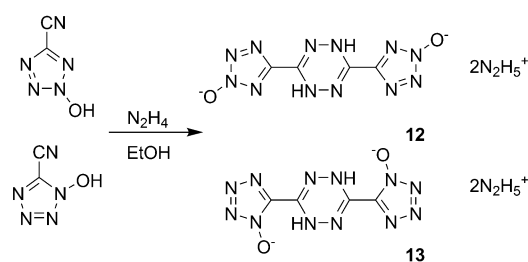
When copper(II) chloride was attempted to be reacted with silver salts **1** and **3**, instead of obtaining the desired salt of cyanotetrazolate oxide, the cyano group of the tetrazole was found to hydrolyze to the amide, thus yielding the copper salts of the carboxamidetetrazole oxides as the dihydrates (Scheme 3). These salts, unlike the other salts, were heated during synthesis, and we suspect that this is the reason for hydrolysis. The hydrolysis of cyanoazoles in aqueous media has been observed previously.^[23]



Scheme 3. Hydrolysis of cyanotetrazole oxides to their amides.

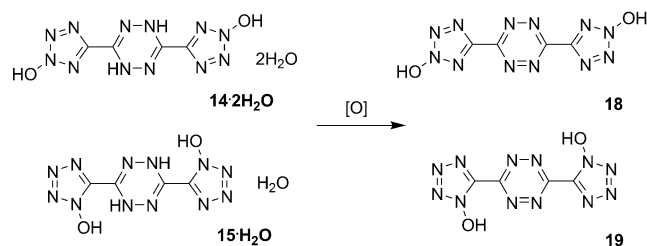
It is known in the literature^[24] that upon treatment of 5-cyanotetrazole with hydrazine in ethanol, a dihydrotetrazine is formed, thereby bridging the tetrazole rings. When cyanotetrazole 1- and 2-oxides were protonated with nitric acid yielding 5-cyano-2-hydroxytetrazole and 5-cyano-1-hydroxytetrazole, the subsequent treatment with hydrazine gave the corresponding dihydrotetrazines as their hydrazinium salts (**12**, **13**; see Scheme 4).

Compounds **12** and **13** were then protonated with hydrochloric acid in water yielding the 1- and 2-hydroxy species as hydrates, **14·2H₂O** and **15·H₂O**. Determination of hydration waters was based on 'best fit' of the elemental analyses. **14·2H₂O** and **15·H₂O** were then deprotonated with ammonia yielding ammonium salts **16** and **17·H₂O**, respectively. With



Scheme 4. Formation of dihydrotetrazines.

the free dihydrotetrazines **14**·2H₂O and **15**·H₂O in hand, the goal was to oxidize them to the corresponding tetrazines (Scheme 5).



Scheme 5. Oxidation of dihydrotetrazines to tetrazines.

Initially, **18** was prepared by bubbling NO₂ through an aqueous solution of **14**·2H₂O. The solution instantly turned deep red due to formation of the tetrazine; however, analysis of the NMR spectra indicated extensive decomposition. When a dilute solution of NO₂ in acetonitrile was added to a slurry of **14**·2H₂O in acetonitrile until no more solid dissolved, a product of higher purity was obtained. The ¹³CNMR spectrum only possessed two resonances, whereas in the ¹HNMR spectrum decomposition was still observed, thus precluding assignment. After addition of the NO₂ solution in acetonitrile, the remaining insolubles were filtered off and the red filtrate was concentrated. Unfortunately, **18** proved to be hygroscopic, and therefore it was dried under high vacuum at 40°C. The obtained red material, when freshly dried, was a highly sensitive explosive: it exploded when a 150 g hammer impacted it from only 1 cm. By reacting this material with aqueous ammonia, the ammonium salt **20** was obtained and fully characterized. Crystals of **20** were grown by diffusing ether into a methanolic solution of **20**. The oxidation of **15**·H₂O to **19** by a similar methodology proved unsuccessful. Oxidation in a manner analogous to that of the 2-oxide led to a red material that lost color upon standing in MeOH or DMSO and decomposed. Attempts using chlorine or ozone as oxidants also failed.

Spectroscopy

Multinuclear NMR spectroscopy, especially ¹³C and ¹⁵N NMR spectroscopy proved to be a useful tool for the characterization of the energetic anions and their salts. In the case of the cyanotetrazolate-1- and 2-oxide anions, the resonance of the tetrazole ring carbon was more downfield for the 2-oxide at 131.1 ppm versus 123.7 ppm for the 1-oxide. The cyano groups exhibit less of a shift difference, with resonances at 112.3 ppm and 110.5 ppm for the 2-oxide and the 1-oxide, respectively. When the cyano groups of both compounds were cyclized to give salts of dihydrotetrazines (**12**, **13**, **16**, and **17**), the 2-oxide possesses resonances at 148.1 and 140.5 ppm and the 1-oxide at 140.4 and 134.3 ppm. Unfortunately, these resonances are too similar to assign them to the tetrazole oxide and to the dihydrote-

tetrazine, respectively. After oxidation of the dihydrotetrazine tetrazole-2-oxide and formation of the ammonium salt **20**, the carbon resonances are found at 158.2 and 150.9 ppm. ¹⁵N NMR spectroscopy was also performed, and the assignment of resonances was made based on a calculated spectrum using MPW1PW91/aug-cc-pVDZ, Gaussian 09.^[25] All resonances were readily assigned with the exception of N2 and N3 in the cyanotetrazolate-2-oxide anion, for which the resonances were too similar to assign them with certainty. Assignments are presented in Figure 2.

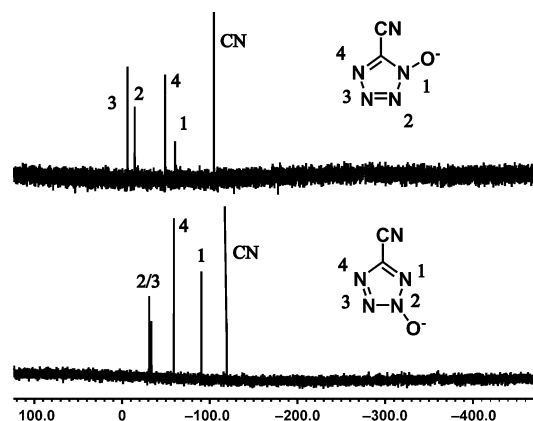


Figure 2. ¹⁵N NMR spectrum of cyanotetrazolate-1 and -2-oxides.

The IR and Raman spectra of all cyanotetrazolate oxide salts were collected and assigned using frequency analysis from an optimized structure of B3LYP/cc-pVDZ calculations using the Gaussian 09 software^[25]. All calculations were performed at the DFT level of theory; the gradient-corrected hybrid three-parameter B3LYP^[26,27] functional theory was used with a correlation-consistent *p*-VDZ basis set.^[28–31]

In the IR spectra, the cyanotetrazolate-1-oxide salts generally contain a strong band around 1406 cm⁻¹. The calculated value for this band is 1503 cm⁻¹ and it arises from N–O stretching. At 2247–2255 cm⁻¹ (calc. 2312 cm⁻¹), the C≡N stretch is seen. At 1429 cm⁻¹ (calc. 1458 cm⁻¹), N1-C1-N4 symmetric tetrazole ring deformation occurs. Finally, the N1-C1-N4 asymmetric tetrazole deformation with minor N–O stretching occurs at 1241–1257 cm⁻¹ (calc. 1278 cm⁻¹).

The IR spectrum of the cyanotetrazolate-2-oxides possesses an N–O O stretch between 1430 and 1674 cm⁻¹ (calc. 1533 cm⁻¹). The C≡N stretch occurs at 2251–2259 cm⁻¹ (calc. 2315 cm⁻¹). Between 950 and 979 cm⁻¹ (calc. 950 cm⁻¹), the tetrazole N2-N3 stretch is observed, and finally between 1133 and 1360 cm⁻¹ (calc. 1401 cm⁻¹), the N3-N4 stretch is seen.

The Raman spectra of all salts of cyanotetrazolate-1-oxide adopt a characteristic pattern of two bands of high intensity. The band between 2249 and 2257 cm⁻¹ (calc. 2312 cm⁻¹) is caused by C≡N stretching. The final stretching occurring at 1458–1465 cm⁻¹ (calc. 1458 cm⁻¹) corresponds to a N1-C1-N4 symmetric tetrazole ring deformation.

In the Raman spectra of the cyanotetrazolate-2-oxide salts, a characteristic pattern of three diagnostic bands is observed. The strongest band at $2256\text{--}2261\text{ cm}^{-1}$ (calc. 2315 cm^{-1}) arises from the $\text{C}\equiv\text{N}$ stretch. The second band corresponds to a tetrazole N2-N3 stretch and occurs between 1001 and 1019 cm^{-1} (calc. 950 cm^{-1}). The final diagnostic stretch ranging from 1436 to 1442 cm^{-1} (calc. 1407 cm^{-1}) belongs to C1-N4 asymmetric tetrazole deformation.

Single Crystal X-ray Analysis

Several herein described compounds (**2**, **4**, **5**, **6**, **7**, **9**, **10**, **11**, and **20**) were also characterized by low-temperature single-crystal X-ray diffraction. Selected data and parameters of the measurements and solutions are gathered in Tables S1 and S2 in the Supporting Information.

Ammonium 2-oxido-5-cyanotetrazolate (**2**) crystallizes in the non-centrosymmetric space group $Pca2_1$ with four cation/anion pairings in the unit cell. In comparison with the corresponding ammonium 1-oxido-5-cyanotetrazolate (**4**) (monoclinic, $P2_1/c$), **2** has a slightly higher density of 1.553 g cm^{-3} (vs. 1.526 g cm^{-3} for **4**). Basically, the oxido-cyanotetrazolate anions are formed as planar anions, in agreement with non-oxidized *2H*-cyanotetrazole.^[32] Within the planar aromatic tetrazolate rings, bond lengths between single and double bonds are observed. The bond lengths between the cyano group and the C1 atom lie between 1.42 and 1.44 \AA , while the CN bond length in the cyano group is between 1.13 and 1.15 \AA . These two bond lengths are not affected by deprotonation as well as oxygenation of the tetrazole ring system. Detailed bond lengths and angles are gathered in Table S3 in the Supporting Information.

The structures of **2** and **4** are dominated by several strong hydrogen bonds involving all hydrogen atoms of the ammonium cations coordinating to the atoms N2 , N4 , and O1 (**2**) and N1 , N2 , N3 , N4 , and O1 (**4**), respectively. Depictions of the molecular units are presented in Figures 3 and 4.

Amino- (**5**) and diaminoguanidinium 2-oxido-5-cyanotetrazolate (**6**), shown in Figures 5 and 6, both crystallize mon-

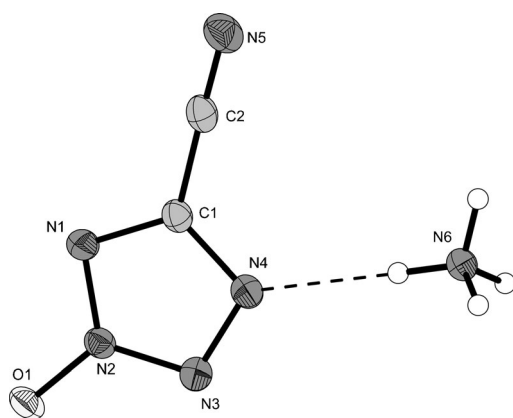


Figure 3. Molecular unit of **2** and its labeling scheme. Ellipsoids are drawn at the 50% probability level.

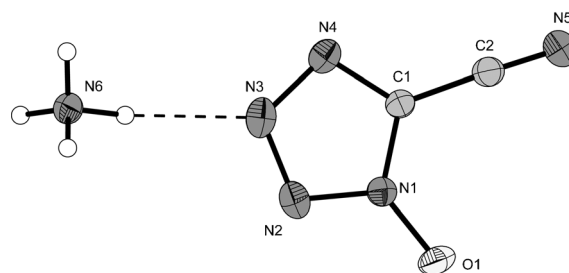


Figure 4. Molecular unit of **4** and its labeling scheme. Ellipsoids are drawn at the 50% probability level.

oclinic in the space groups $P2_1/n$ and $P2_1/c$, respectively. The diaminoguanidinium salt **6** (1.534 g cm^{-3}) shows a slightly higher density in comparison to **5** (1.504 g cm^{-3}). Both structures again are dominated by an intense hydrogen bond network.

The structures of triaminoguanidinium 1- (**9**) and 2-oxido-5-cyanotetrazolate (**7**) could also be determined. The triaminoguanidinium cations follow structures published numerous in the literature such as, for example, triaminoguanidinium nitrate.^[33] The densities of 1.550 g cm^{-3} (**7**) and 1.583 g cm^{-3} (**9**) are higher than those of **2** and **4–6**. The molecular units of both structures are shown in Figures 7 and 8.

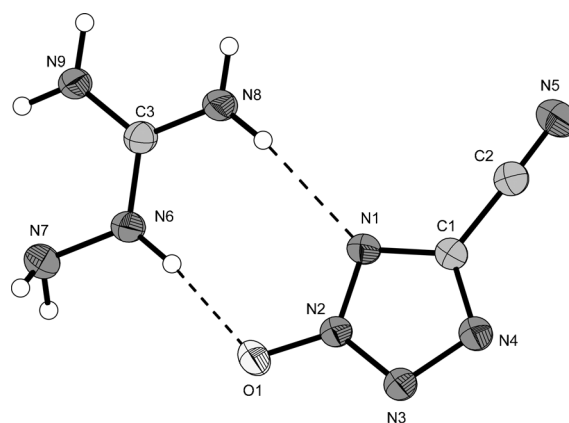


Figure 5. Molecular unit of **5** and its labeling scheme. Ellipsoids are drawn at the 50% probability level.

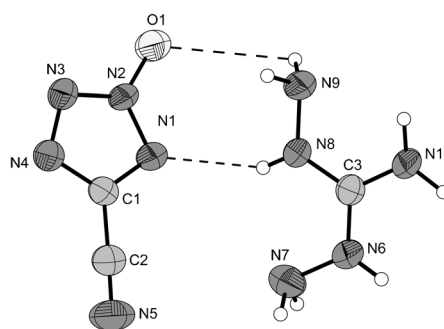


Figure 6. Molecular unit of **6** and its labeling scheme. Ellipsoids are drawn at the 50% probability level.

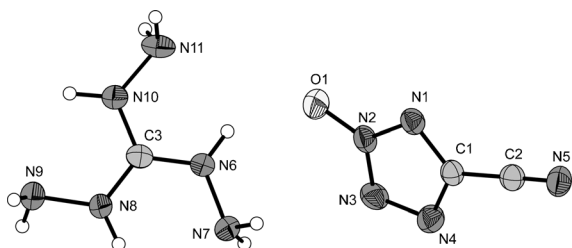


Figure 7. Molecular unit of **7** and its labeling scheme. Ellipsoids are drawn at the 50% probability level.

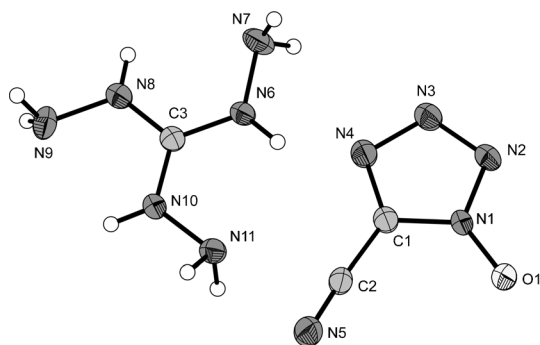


Figure 8. Molecular unit of **9** and its labeling scheme. Ellipsoids are drawn at the 50% probability level.

Single crystals could be obtained after the reaction of 1- and 2-oxido-5-cyanotetrazolate with copper sulfate. In both cases, the corresponding Cu^{II} complexes of the hydrolyzed CN moiety were formed as dihydrates. In both compounds, an expected distorted coordination sphere of d⁹ copper centers was observed; however, the coordination modes of the oxido-tetrazolates were different. In the case of **10** (Figure 9), the bidentate coordination (5-membered ring) is formed by the ring nitrogen atom N1 and the carboxy oxygen atom O1. In the case of **11** (Figure 10), a six-membered ring is formed by coordination of the N-oxide oxygen atom O2 as well as the carboxy oxygen atom O1. The coordi-

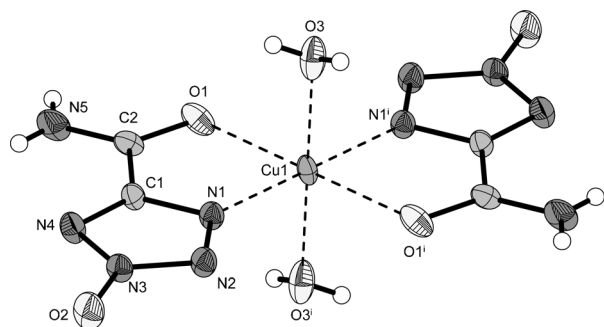


Figure 9. Molecular unit of **10** and its labeling scheme. Ellipsoids are drawn at the 50% probability level. Selected bond lengths [Å]: Cu1–N1 1.957(2), Cu1–O3 2.181(3), Cu1–O1 2.191(2), N1–N2 1.326(3), N1–C1 1.335(3), O2–N3 1.284(3), N3–N2 1.330(3), N3–N4 1.337(3), N5–C2 1.312(4), O1–C2 1.245(4), N4–C1 1.327(4), C1–C2 1.489(4); selected coordination angles [°]: N1–Cu1–O3 90.65(10), N1–Cu1–O1 78.48(8), O3–Cu1–O1 92.32(9).

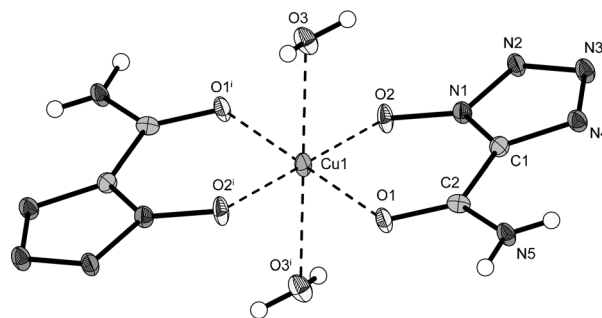


Figure 10. Molecular unit of **11** and its labeling scheme. Ellipsoids are drawn at the 50% probability level. Selected bond lengths [Å]: Cu1–O2 1.935(2), Cu1–O1 1.980(2), Cu1–O3 2.396(3), N5–C2 1.313(4), N4–C1 1.335(4), N4–N3 1.345(3), N3–N2 1.305(4), N2–N1 1.338(3), N1–O2 1.328(3), N1–C1 1.341(4), O1–C2 1.245(4), C2–C1 1.481(4); selected coordination angles [°]: O2–Cu1–O1 94.62(9), O2–Cu1–O3 89.80(10), O1–Cu1–O3 92.51(9).

nation sphere of complex **11** is a typical example of an elongated octahedron formed by Jahn–Teller distortion and described for several copper(II) tetrazolates in the literature.^[34]

Compound **20** could only be obtained crystalline as its trihydrate. A depiction of a molecular unit is given in Figure 11. The asymmetric unit consists of two transected

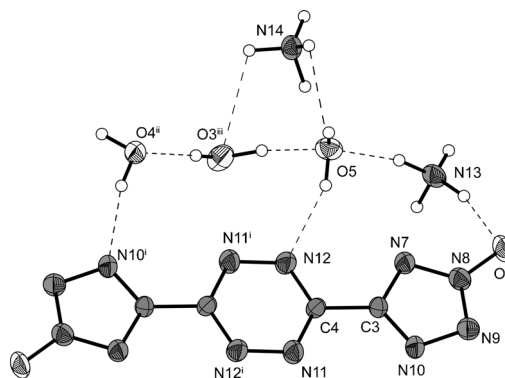


Figure 11. View on one molecular unit of **20** and its labeling scheme. Ellipsoids are drawn at the 50% probability level.

dianions. All water and ammonium protons participate in hydrogen bonds. The density of **20** (1.627 g cm⁻³), which crystallizes in the triclinic space group *P* $\bar{1}$, is the highest observed for the crystalline CHNO compounds within this work. The oxido-tetrazolate dianions have a planar structure similar to that of recently published energetic salts of the 3,6-bis(tetrazole-5-ylate)-1,2,4,5-tetrazine dianion.^[35] The dianions are orientated in bands connected by hydrogen bonds involving crystal water and atom O4. Gaps are filled with the ammonium cations and two further crystal water molecules, as shown in Figure 12.

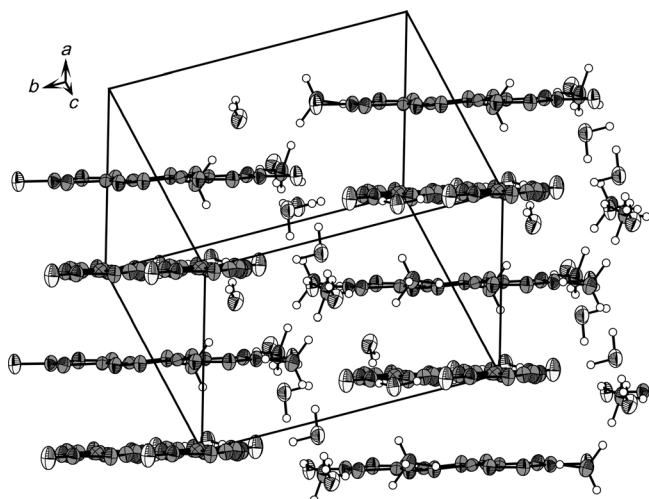


Figure 12. View on the layer-like packing of **20**. One unit cell is drawn.

Energetic Properties

Often, energetic materials tend to explode in bomb calorimetric measurements. Consequently, doubtful combustion energies can potentially be obtained. Therefore, heats of formation of energetic materials are mostly calculated theoretically. In our group, we combine the atomization energy method (Eq. 1) with CBS-4M electronic energies (Table 1), which has been shown suitable in many recently published studies.^[36] CBS-4M energies of the atoms, cations, and anions were calculated with the Gaussian 09 (revision A1) software package^[25] and checked for imaginary frequencies. Values for $\Delta_f H^\circ$ (atoms) were taken from the NIST database.^[37]

$$\Delta_f H^\circ_{(g, M, 298)} = H_{(Molecule, 298)} - \sum H^\circ_{(Atoms, 298)} + \sum \Delta_f H^\circ_{(Atoms, 298)} \quad (1)$$

For calculation of the solid-state energy of formation (Table 2) of **2**, **4–7**, **9**, and **20**, the lattice energy (U_L) and lattice enthalpy (ΔH_L) were calculated from the corresponding molecular volumes (obtained from X-ray elucidations) according to the equations provided by Jenkins and Glasser.^[38]

Table 2. Solid state energies of formation ($\Delta_f U^\circ$).

	$\Delta_f H^\circ$ (g) ^[a] [kJ mol ⁻¹]	V_M ^{b/} nm ³	U_L ^[c] [kJ mol ⁻¹]	ΔH_L ^[d] [kJ mol ⁻¹]	$\Delta_f H^\circ$ (s) ^[e] [kJ mol ⁻¹]	Δn ^[f]	$\Delta_f U^\circ$ (s) ^[g] [kJ mol ⁻¹]	Formula	M [g mol ⁻¹]	$\Delta_f U^\circ$ (s) ^[h] [kJ kg ⁻¹]
2	876.1	0.137	559.0	563.9	312.2	5.5	325.9	C ₂ H ₄ N ₆ O	128.09	2543.3
4	902.5	0.139	556.2	561.2	341.3	5.5	354.9	C ₂ H ₄ N ₆ O	128.09	2770.3
5	911.9	0.204	502.0	507.0	404.9	8.5	426.0	C ₃ H ₇ N ₉ O	185.15	2300.3
6	1013.0	0.217	494.4	499.3	513.6	9.5	537.2	C ₃ H ₈ N ₁₀ O	200.16	2683.0
7	1114.6	0.231	486.4	491.4	623.2	10.5	649.2	C ₃ H ₉ N ₁₁ O	215.18	3016.5
9	1140.9	0.226	489.1	494.0	646.9	10.5	672.9	C ₃ H ₉ N ₁₁ O	215.18	3126.6
20	1411.5*	0.318	1437.4	1452.3	-40.8	16.5	0.1	C ₄ H ₁₄ N ₁₄ O ₅	338.24	0.4

[a] Gas-phase enthalpies of formation (those of the ionic compounds are taken as the respective sums of the non-interacting component ions);* gas-phase enthalpy of three water molecules were subtracted; [b] molecular volume of the molecular unit in the crystal structure; [c] lattice energy calculated by the Glasser–Jenkins equation; [d] lattice enthalpy calculated by the Glasser–Jenkins equation; [e] solid-state molar heat of formation; [f] change of moles of gaseous components; [g] molar energy of formation; [h] energy of formation (mass-dependent).

Table 1. CBS-4M results and gas-phase enthalpies

	Formula	$-H^{298}$ ^[a] /a.u.	$\Delta_f H^\circ$ (g) ^[b] [kJ mol ⁻¹]
HCT2X ^[c]	C ₂ HN ₅ O	425.116700	484.7
CT2X ^{-[d]}	C ₂ HN ₅ O ⁻	424.625696	240.3
HCT1X ^[e]	C ₂ HN ₅ O ⁻	425.105680	513.6
CT1X ^{-[f]}	C ₂ N ₅ O ⁻	424.615667	266.7
TT2X ^{2-[g]}	C ₄ N ₁₂ O ₂ ²⁻	958.510314	864.6
NH₄ ^{+ [h]}	NH ₄ ⁺	56.796608	635.8
AG ^{+ [i]}	CH ₇ N ₄ ⁺	260.701802	671.6
DAG ^{+ [j]}	CH ₈ N ₅ ⁺	315.949896	772.7
TAG ^{+ [k]}	CH ₉ N ₆ ⁺	371.197775	874.3

[a] CBS-4M enthalpy at room temperature; [b] calculated gas-phase heat of formation by using the atomization equation; [c] cyanotetrazolate-2-oxide, protonated; [d] cyanotetrazolate-2-oxide, deprotonated; [e] cyanotetrazolate-1-oxide, protonated; [f] cyanotetrazolate-1-oxide, deprotonated; [g] 1,4-bis(2-*N*-oxidotetrazolate)-1,2,4,5-tetrazine; [h] ammonium; [i] aminoguanidinium cation; [j] diaminoguanidinium cation; [k] triaminoguanidinium cation.

Only these compounds were calculated as they have experimental densities for energetic performance calculations. With the calculated lattice enthalpy (Table 2), the gas-phase enthalpy of formation was converted into the solid-state (standard conditions) enthalpy of formation. These molar standard enthalpies of formation (ΔH_m) were used to calculate the molar solid-state energies of formation (ΔU_m) according to Eq. 2 (Table 2).

$$\Delta U_m = \Delta H_m - \Delta n RT \quad (2)$$

in which Δn denotes the change of moles of gaseous components.

Density is one of the most important parameters for performance calculations. Therefore, only compounds with precise X-ray densities have been studied for their performances. The detonation and propulsion parameters of **2**, **4–7**, **9**, and **20** were calculated using the program EXPLO5 V5.05^[39] and are gathered in Table 3. The program is based on the steady-state model of equilibrium detonation and uses the Becker–Kistiakowsky–Wilson equation of state (BKW E.O.S) for gaseous detonation products and Cowan–Fickett E.O.S. for solid carbon.^[40] The program is designed to enable the calculation of detonation parameters at the Chapman–Jouguet point. The calculations were performed

Table 3. Energetic properties and detonation parameters of **2**, **4–7**, **9**, and **20**.

	2	4	5	6	7	9	20	TNT
Formula	C ₂ H ₄ N ₆ O	C ₂ H ₄ N ₆ O	C ₃ H ₇ N ₉ O	C ₃ H ₈ N ₁₀ O	C ₃ H ₉ N ₁₁ O	C ₃ H ₉ N ₁₁ O	C ₄ H ₁₄ N ₁₄ O ₅	C ₇ H ₅ N ₅ O ₆
Molecular Mass [g mol ⁻¹]	128.09	128.09	185.15	200.16	215.18	215.18	338.24	227.13
IS [J] ^[a]	15	35	40	40	40	40	40	15 ^[41]
FS [N] ^[b]	216	360	324	324	324	216	240	353
ESD-test [J] ^[c]	0.30	0.75	1.5	0.50	0.55	0.50	0.50	3.5
N [%] ^[d]	65.61	65.61	68.09	69.98	71.60	71.60	57.97	18.50
Ω [%] ^[e]	-62.45	-62.45	-73.54	-71.93	-70.63	-70.63	-47.30	-73.96
T _{dec.} [°C] ^[f]	184	172	228	152	160	150	189	290
Density [g cm ⁻³] ^[g]	1.554	1.526	1.504	1.534	1.550	1.583	1.627	1.713(100 K) ^[42]
Δ _f H _m ^o [kJ mol ⁻¹] ^[h]	325.9	354.9	426.0	537.2	649.2	672.9	-40.8	-55.5
Δ _f U ^o [kJ kg ⁻¹] ^[i]	2543.3	2770.3	2300.3	2683.0	3016.5	3126.6	0.4	-168.0
EXPLO5.05:								
-Δ _f U ^o [kJ kg ⁻¹] ^[j]	4609	4831	3957	4277	4559	4666	3715	5258
T _E [K] ^[k]	3288	3412	2842	2971	3060	3084	2746	3663
P _{cl} [kbar] ^[l]	222	220	196	219	237	251	227	235
D [m s ⁻¹] ^[m]	7749	7730	7451	7790	8044	8214	7799	7459
Gas vol. [L kg ⁻¹] ^[n]	762	762	771	788	803	803	840	569
I _s [s] ^[o]	222	228	207	218	227	229	195	205

[a] impact sensitivity (BAM drop hammer, 1 of 6); [b] friction sensitivity (BAM friction tester, 1 of 6); [c] electrostatic discharge device (OZM); [d] nitrogen content; [e] oxygen balance;^[43] [f] decomposition temperature from DSC ($\beta=5^{\circ}\text{C}$); [g] estimated from X-ray diffraction; [h] calculated (CBS-4M) heat of formation; [i] calculated energy of formation; [j] Energy of explosion; [k] explosion temperature; [l] detonation pressure; [m] detonation velocity; [n] assuming only gaseous products; [o] specific impulse calculated at isobaric (60 bar) rocket conditions.

using the maximum densities according to the crystal structures at low temperatures and the calculated energies of formation.

With respect to their detonation performance the best values were obtained for triaminoguanidinium salts **7** and **9**, with **9** being slightly higher (8044 and 8214 ms⁻¹, respectively), thus indicating higher performance for the 1-oxides. However, when ammonium salts **2** and **4** are compared, there is no appreciable difference between the two (7749 and 7730 ms⁻¹, respectively). All compounds prepared are of comparable or higher performance than trinitrotoluene (TNT), but lower than those of the commonly used military explosives like hexogen (RDX) and octogen (HMX).

We also calculated the specific impulse I_s (using the pure compound at 60 bar isobaric rocket conditions), which can be related to the potential use as propellant ingredient. The highest I_s was computed for compounds **4**, **7**, and **9** (228, 227, and 229 s, respectively).

The sensitivities of all compounds were determined by standard methods (see the Experimental Section). The only highly sensitive compound is compound **18**, which when completely dry can explode from only slight impacts. However, due to its high hygroscopicity, this compound's sensitivity rapidly decreases upon standing at ambient conditions. The remainder of compounds in this work are of much lower sensitivity, generally being classified as "less sensitive" to "sensitive" energetic materials according to the UN Recommendations on the Transport of Dangerous Goods.^[44]

Conclusions

The direct oxidation of the cyanotetrazolate anion with Oxone gave the cyanotetrazolate-2-oxide anion. This, along

with the known cyanotetrazolate-1-oxide gave energetic salts of both oxide-containing anions after metathesis reactions. These nitrogen-rich salts show energetic performances in the range of TNT; however, only salts **2** and **5** show thermal stabilities above 180 °C. NMR, IR, and Raman spectroscopies proved useful for characterizing these materials. In the presence of copper, the cyano group of both the 1- and 2-oxides hydrolyze to the corresponding carboxamide. The protonated forms of both cyanotetrazolate-1- and 2-oxides were able to form dihydrotetrazines upon reaction with hydrazine. In the case of the 2-oxide, the dihydrotetrazine can be oxidized to the tetrazine, the ammonium salt of which was fully characterized, illustrating the unique heterocyclic system containing both tetrazole oxides and a 1,2,4,5-tetrazine ring. These compounds may provide base materials or synthetic strategies to new energetic materials.

Experimental Section

General

All reagents and solvents were used as received (Sigma-Aldrich, Fluka, and Acros Organics) unless stated otherwise. Sodium cyanotetrazolate-1-oxide was prepared according to the literature procedure.^[22] Melting and decomposition points were measured with a Linseis PT10 differential scanning calorimeter using heating rates of 5 °C min⁻¹. ¹H, ¹³C and ¹⁵N NMR spectra were measured with a JEOL Eclipse 270 or 400 MHz instrument. All chemical shifts are given in ppm relative to TMS (¹H, ¹³C) or nitromethane (¹⁵N). Infrared spectra were measured with a Perkin-Elmer FT-IR Spectrum BXII instrument equipped with a Smith Dura SampIR II ATR unit. Transmittance values are described as strong (s), medium (m), and weak (w). Mass spectra were measured on a JEOL MStation JMS 700 instrument. Raman spectra were measured with a Perkin-Elmer Spectrum 2000R NIR FT-Raman instrument equipped with a Nd:YAG laser (1064 nm). The intensities are reported as percentages of the most intensive peak and are given in parentheses. Elemental analyses were performed with a Netsch STA 429 simultaneous

thermal analyzer. Sensitivity data were determined using a BAM drop hammer and a BAM friction tester. The electrostatic sensitivity tests were carried out using the electric spark tester ESD 2010 EN (OZM Research) operating with the "Winspark 1.15" software package. XRD was performed on an Oxford Xcalibur3 diffractometer with a Spellman generator (voltage 50 kV, current 40 mA) and a KappaCCD detector using $\text{MoK}\alpha$ radiation ($\lambda = 0.71073 \text{ \AA}$) at low temperature (173 K). The data collection and reduction was carried out using the CrysAlisPro software.^[45] The structures were solved either with SHELXS-97^[46] or SIR-92,^[47] refined with SHELXL-97^[48], and finally checked using the PLATON^[49] software integrated in the WINGX^[50] software suite. All hydrogen atoms were found and freely refined. Friedel pairs of non-centrosymmetric space groups have been merged using the MERG3 command. The absorptions were corrected with a Scale3 Abspack multi-scan method.^[51] CCDC 899950 (2), CCDC 899952 (4), CCDC 899957 (5), CCDC 899956 (6), CCDC 899951 (7), CCDC 899953 (9), CCDC 899955 (10), CCDC 899954 (11), and CCDC 899949 (20) contain the supplementary crystallographic data for this paper. These data can be obtained free of charge from the Cambridge Crystallographic Data Centre via www.ccdc.cam.ac.uk/data_request/cif.

CAUTION! *The described compounds are energetic materials with sensitivity to various stimuli. While we encountered no issues in the handling of these materials, proper protective measures (face shield, ear protection, body armor, Kevlar gloves, and earthened equipment) should be used at all times. Compound 18 is extremely sensitive when dry and should only be handled in small quantities or wet.*

Silver cyanotetrazolate-2-oxide (1)

Sodium cyanotetrazolate-1.5H₂O (5 g, 34.7 mmol) was dissolved in 70 mL of distilled water, and potassium acetate (29.8 g, 304 mmol) was added. The solution was heated to 40 °C, and Oxone (66.8 g, 98 mmol) was added slowly. After stirring of the suspension for 20 h at 40 °C, the solution was poured into 1.6 L of acetone and precipitated salts were filtered off. After evaporation of the solvent under reduced pressure, the remaining solid was dissolved in ethanol. The insoluble residues were filtered off, and the filtrate was evaporated under vacuum. The colorless solid was dissolved in 100 mL of distilled water, and a solution of silver nitrate (5.9 g, 34.7 mmol) in 100 mL of distilled water was added in the dark while stirring. Still in the dark, the colorless suspension was stirred for 15 min, filtered, and washed with 20 mL of distilled water. After drying in the dark, **1** was obtained as a white solid (5.5 g, 73 %). DSC (5 °C min⁻¹): 224 °C (dec); IR: $\tilde{\nu} = 3627$ (w), 3464 (w), 2921 (m), 2242 (m), 1596 (w), 1441 (m), 1428 (m), 1403 (m), 1365 (s), 1340 (m), 1267 (w), 1225 (m), 1090 (w), 1013 (m), 812 (s), 710 cm⁻¹ (s); ¹³C NMR ([D₆]DMSO): $\delta = 132.0$ (s, 1C, CN₄O), 112.3 ppm (s, 1C, CN); MS (FAB⁻) m/z : 110.0 (C₂N₅O); (FAB⁺) m/z 107.0 (Ag); elemental analysis calcd (%) for AgC₂N₅O (217.92): C 11.02, N 32.14, H 0.00; found: C 11.32, N 31.96; H 0.00. BAM impact: 8 J; BAM friction: 240 N; ESD: 50 mJ.

Ammonium cyanotetrazolate-2-oxide (2)

Sodium cyanotetrazolate-1.5H₂O (10 g, 69.4 mmol) was dissolved in 240 mL of distilled water. Next, potassium acetate (59.6 g, 608 mmol) was added and the solution heated to 40 °C. Subsequently, Oxone (120 g, 196 mmol) was added in small portions during the course of 1 h. The suspension was stirred for 20 h at 40 °C, followed by the addition of sufficient water to dissolve all solids. The solution was then allowed to slowly cool down to room temperature, and an excess of sodium tributylammonium sulfate (NaBu₃NHSO₄; 0.8 M, 300 mL) was added. The solution was extracted with ethylacetate (5 × 200 mL), and the combined organic phase was combined and dried over anhydrous magnesium sulfate followed by the evaporation of the solvent under vacuum to give a colorless oil. The oil was mixed with 12 mL of methanol, and the solution was passed through a column of Amberlyst 15 ion exchange resin loaded with ammonium ions. The colorless eluent was evaporated to dryness and recrystallized from acetonitrile to give ammonium 5-cyanotetrazolate-2-oxide as colorless crystals (4.9 g, 55 %). DSC (5 °C min⁻¹): 176 °C (mp), 184 °C (dec); IR: $\tilde{\nu} = 3697$ (w), 3141 (m), 3020 (s), 2918 (w), 2890 (w), 2856 (w),

2544 (w), 2349 (w), 2259 (m), 2179 (w), 2136 (w), 1807 (w), 1708 (w), 1692 (m), 1591 (w), 1546 (w), 1472 (s), 1455 (w), 1438 (s), 1430 (s), 1401 (m), 1387 (m), 1370 (w), 1344 (s), 1226 (s), 1111 (w), 1073 (m), 1013 (m), 792 (m), 723 (m), 698 cm⁻¹ (w); Raman (1064 nm): $\tilde{\nu} = 3047$ (3), 2261 (100), 1700 (1), 1484 (1), 1442 (21), 1389 (8), 1356 (1), 1228 (3), 1109 (14), 1078 (1), 797 (4), 607 (1), 725 (3), 575 (3), 501 (5), 486 (1), 343 cm⁻¹ (1); ¹H NMR ([D₆]DMSO): $\delta = 7.2$ ppm (brs, 4H, NH₄); ¹³C NMR ([D₆]DMSO): $\delta = 132.6$ (s, 1C, CN₄O), 112.2 (s, 1C, CN); MS m/z : (FAB⁻) 110.0 ppm (C₂N₅O); (FAB⁺) m/z : 18.1 (NH₄); elemental analysis calcd (%) for C₂N₅H₄O (128.09): C 18.75, N 65.61, H 3.15; found: C 19.02, N 65.36, H 3.01; BAM impact: 15 J; BAM friction: 216 N; ESD: 300 mJ.

Silver cyanotetrazolate-1-oxide (3)

Sodium cyanotetrazolate-1-oxide (200 mg, 1.4 mmol) was dissolved in 10 mL of distilled water. Under constant stirring in the dark, a solution of silver nitrate (238 mg, 1.4 mmol) in 10 mL water was added, and **3** started to precipitate immediately. The light yellow suspension was stirred for 20 min, filtered under suction, and washed with distilled water. After drying in the dark, **3** was obtained as a white solid (220 mg, 72 %). DSC (5 °C min⁻¹): 201 (T_{dec}); IR: $\tilde{\nu} = 3619$ (w), 3448 (w), 2248 (w), 1572 (w), 1470 (s), 1444 (m), 1427 (m), 1413 (m), 1378 (w), 1330 (w), 1257 (s), 1241 (s), 1225 (w), 1208 (m), 1159 (w), 1096 (w), 1019 (w), 784 (s), 700 cm⁻¹ (w); ¹³C NMR ([D₆]DMSO): $\delta = 123.8$ (s); 110.7 ppm (s); MS (FAB⁻) m/z : 110.0 (C₂N₅O⁻); elemental analysis calcd (%) for AgC₂N₅O (217.92): C 11.02, H 0.00, N 32.14; found: C 11.23; H 0.00, N 31.52; BAM impact: > 4 J; BAM friction: 120 N; ESD: 80 mJ.

Ammonium cyanotetrazolate-1-oxide (4)

Sodium tributylammonium sulfate (30 mL, 0.8 M, 24 mmol) was added to a solution of sodium cyanotetrazolate-1-oxide (0.93 g, 6.6 mmol) in 20 mL of distilled water. After stirring for 30 min, the solution was extracted six times with 15 mL of ethyl acetate. The combined ethyl acetate fractions were then evaporated under reduced pressure. The remaining slightly yellow oil was dissolved in methanol and passed through a column of Amberlyst 15 ion-exchange resin loaded with ammonium cations at a slow rate (ca. 1.5 h). The yellow eluent was evaporated to dryness and recrystallized from 1-propanol to yield **4** as a white solid (0.205 g, 24 %). DSC (5 °C min⁻¹): 160 °C (mp), 172 °C (dec); IR: $\tilde{\nu} = 3171$ (w), 2995 (w), 2829 (w), 2255 (w), 2159 (w), 1695 (w), 1534 (w), 1463 (m), 1429 (s), 1406 (vs), 1241 (s), 1219 (m), 1148 (w), 1080 (w), 1007 (w), 768 (m), 692 cm⁻¹ (w); Raman (1064 nm): $\tilde{\nu} = 2257$ (100), 1466 (50), 1415 (2), 1392 (2), 1246 (3), 1221 (20), 1147 (10), 1091 (6), 1010 (14), 771 (15), 638 (8); 547 (3), 495 (10), 413 (2), 1079 (1), 182 (21), 109 (11), 718 (2), 697 cm⁻¹ (1); ¹³C NMR ([D₆]DMSO): $\delta = 123.9$ (s, -CN₂); 110.8 ppm (s, -CN); ¹H NMR ([D₆]DMSO): $\delta = 7.14$ ppm (s, 4H, NH₄⁺); MS (FAB⁺) m/z : 18.0 (NH₄⁺); (FAB⁻) m/z : 110.0 (C₂N₅O⁻); elemental analysis calcd (%) for NH₄C₂N₅O (128.09): C 18.75, H 3.15, N 65.61; found: C 19.26, H 2.96, N 64.68; BAM impact: 35 J; BAM friction: 360 N; ESD: 0.75 J.

Aminoguanidinium cyanotetrazolate-2-oxide (5)

To a stirred solution of aminoguanidinium chloride (127 mg, 1.15 mmol) in 20 mL of distilled water, finely powdered **1** (250 mg, 1.15 mmol) was added. The suspension was stirred for 30 min and was filtered in the dark. The filtrate was evaporated to dryness to give **5** as colorless crystals (197 mg, 93 %). DSC (5 °C min⁻¹): 228 °C (dec); IR: $\tilde{\nu} = 3540$ (w), 3321 (m), 3262 (m), 3158 (m), 2869 (w), 2774 (w), 2353 (w), 2256 (m), 2198 (w), 1998 (w), 1660 (s), 1613 (w), 1461 (w), 1434 (w), 1421 (w), 1393 (w), 1360 (m), 1326 (w), 1243 (m), 1213 (w), 1512 (w), 1106 (w), 1070 (w), 1049 (w), 1011 (w), 973 (w), 953 (m), 824 (w), 798 (w), 771 (w), 741 (w), 718 (w), 672 cm⁻¹ (w); Raman (1064 nm): $\tilde{\nu} = 3367$ (1), 3334 (1), 3274 (4), 3232 (1), 2259 (100), 1683 (3), 1620 (2), 1569 (1), 1436 (30), 1399 (1), 1379 (1), 1238 (1), 1217 (2), 1095 (10), 1074 (4), 1019 (43), 959 (6), 802 (6), 719 (2), 614 (3), 571 (7), 518 (2), 502 (8), 484 (4), 337 cm⁻¹ (2); ¹H NMR ([D₆]DMSO): $\delta = 8.63$ (s, 1H, C-NH-N), 7.37 (brs, 2H, C-NH₂), 7.04 (brs, 2H, C-NH₂), 4.77 ppm (s, 2H, N-NH₂); ¹³C NMR ([D₆]DMSO): $\delta = 159.4$ (s, 1C, C(NH₂)₂(NHNH₂)), 132.0 (s, 1C, CN₄O),

112.6 ppm (s, 1C, CN); MS (FAB⁻) *m/z*: 110.0 (C₂N₅O); (FAB⁺) *m/z*: 75.1 (CN₄H₇); elemental analysis calcd (%) for CN₄H₇C₂N₅O (200.16): C 19.46, N 68.09, H 3.81; found: C 19.07, N 64.00, H 3.62. BAM impact: 40 J; BAM friction: 324 N; ESD: 1.5 J.

Diaminoguanidinium cyanotetrazolate-2-oxide (6)

Finely powdered **1** (250 mg, 1.15 mmol) was added to a solution of diaminoguanidinium iodide (249 mg, 1.15 mmol) in 20 mL of distilled water. The suspension was slowly shaken by hand for 15 min and filtered in the dark. The filtrate was evaporated to dryness to yield **6** as colorless crystals (193.6 mg, 84%). DSC (5°C min⁻¹): 135°C (mp), 152°C (dec); IR: $\tilde{\nu}$ = 3310 (w), 3234 (s), 3174 (s), 3000 (w), 2889 (w), 2251 (m), 1986 (w), 1913 (8w), 1736 (w), 1668 (s), 1649 (w), 1596 (w), 1461 (w), 1436 (m), 1421 (w), 1394 (m), 1358 (s), 1272 (w), 1232 (m), 1215 (w), 1177 (m), 1120 (w), 1066 (w), 968 (s), 930 (w), 800 (m), 767 (m), 713 cm⁻¹ (w); Raman (1064 nm): $\tilde{\nu}$ = 3791 (2), 3341 (1), 3240 (7), 2256 (100), 1689 (2), 1637 (3), 1437 (24), 1409 (3), 1367 (1), 1322 (1), 1234 (2), 1184 (4), 1090 (12), 1069 (2), 1010 (38), 931 (9), 802 (6), 719 (2), 572 (7), 549 (3), 499 (11), 479 (4), 396 (1), 366 (2), 265 cm⁻¹ (4); ¹H NMR ([D₆]DMSO): δ = 8.54 (brs, 2H, C-NH-NH₂), 7.13 (s, 2H, C-NH₂), 4.58 ppm (s, 4H, N-NH₂); ¹³C NMR ([D₆]DMSO): δ = 160.3 (s, 1C, C(NH₂)(NHNH₂)₂), 131.6 (s, 1C, CN₄O), 112.8 ppm (s, 1C, CN); MS (FAB⁻) *m/z*: 110.0 (C₂N₅O); (FAB⁺) *m/z*: 90.0 (CN₂H₈); elemental analysis calcd (%) for CN₂H₈C₂N₅O (200.16): C 18.00, N 69.98, H 4.03; found: C 18.55, N 67.93, H 4.01. BAM impact: 40 J; BAM friction: 324 N; ESD: 500 mJ.

Triaminoguanidinium cyanotetrazolate-2-oxide (7)

Finely powdered **1** (250 mg, 1.15 mmol) was added to a solution of triaminoguanidinium chloride (161.2 mg, 1.15 mmol) in 20 mL of distilled water in the dark. The suspension was carefully shaken for 15 min, filtered, and rinsed with 10 mL of distilled water in the dark. The filtrate was evaporated to yield **7** as colorless crystals (214.2 mg, 87%). DSC (5°C min⁻¹): 149°C (m.p.), 166°C (dec); IR: $\tilde{\nu}$ = 33614 (w), 3325 (w), 3208 (m), 3119 (w), 2354 (w), 2327 (w), 2256 (m), 1723 (m), 1674 (s), 1587 (w), 1554 (w), 1437 (m), 1400 (m), 1372 (w), 1332 (m), 1246 (w), 1224 (w), 1207 (w), 1133 (s), 1068 (w), 979 (s), 799 (m), 734 (w), 718 cm⁻¹ (w); Raman (1064 nm): $\tilde{\nu}$ = 3234 (10), 2258 (97), 1680 (4), 1644 (2), 1439 (15), 1410 (4), 1384 (3), 1322 (2), 1208 (3), 1140 (6), 1075 814, 1001 (36), 886 (9), 801 (8), 734 (1), 719 (3), 680 (4), 639 (3), 600 (2), 571 (8), 503 (8), 477 (7), 410 (4), 354 cm⁻¹ (3); ¹H NMR ([D₆]DMSO): δ = 8.58 (brs, 3H, C-NH-NH₂), 4.48 ppm (brs, 6H, N-NH₂); ¹³C NMR ([D₆]DMSO): δ = 159.6 (s, 1C, C(NHNH₂)₃), 131.6 (s, 1C, CN₄O), 112.8 ppm (s, 1C, CN); MS (FAB⁻) *m/z*: 109.9 (C₂N₅O); (FAB⁺) *m/z*: 105.1 (C(NHNH₂)₃); elemental analysis calcd (%) for CN₆H₃C₂N₅O (215.18): C 16.74, N 71.6, H 4.21; found: C 16.72, N 70.77, H 4.19. BAM impact: 40 J; BAM friction: 324 N; ESD: 550 mJ.

Aminoguanidinium cyanotetrazolate-1-oxide (8)

To a solution of aminoguanidinium chloride (102 mg, 0.92 mmol) in 20 mL of distilled water, **3** (200 mg, 0.92 mmol) was added in the dark, and the mixture was shaken for 10 min. After filtration, the filtrate was evaporated to dryness to yield **8** as a white solid (0.16 g, 94%). DSC (5°C min⁻¹): 66°C (m.p.), 164°C (dec); IR: $\tilde{\nu}$ = 3467 (w), 3361 (m), 3143 (w), 3060 (w), 2972 (w), 2853 (w), 2643 (w), 2251 (w), 2171 (w), 1655 (vs), 1625 (m), 1463 (m), 1413 (m), 1245 (s), 1221 (m), 1144 (w), 1093 (w), 1007 (w), 973 (w), 889 (w), 772 (m), 682 cm⁻¹ (w); Raman (1064 nm): $\tilde{\nu}$ = 3282 (5), 3229 (1), 3197 (1), 3336 (1), 3355 (1), 2490 (1), 2432 (2), 2253 (98), 2198 (2), 1682 (2), 1631 (5), 1564 (2), 1466 (82), 1417 (3), 1387 (2), 1252 (2), 1223 (35), 1145 (18), 1091 (14), 1009 (18), 973 (21), 776 (25), 717 (2), 694 (1), 639 (12), 550 (4), 492 (15), 416 (3), 360 (2), 246 cm⁻¹ (1); ¹³C NMR ([D₆]DMSO): δ = 159.4 (s, AG⁺); 123.9 (s, CN₄); 110.9 ppm (s, CN); ¹H NMR ([D₆]DMSO): δ = 8.58 (s, 1H, NH-NH₂); 7.01 (brs, 2H, NH₂); 6.99 (brs, 2H, NH₂); 4.51 ppm (brs, 2H, NH-NH₂); *m/z* (FAB⁺): 75.1 (CN₄H₇⁺); *m/z* (FAB⁻): 110.0 (C₂N₅O⁻); elemental analysis calcd (%) for CN₄H₇C₂N₅O (185.15): C 19.46, H 3.81, N 68.09; found: C 19.14, H 3.72, N 64.67; BAM impact: 40 J; BAM friction: 216 N; ESD: 0.5 J.

Triaminoguanidinium cyanotetrazolate-1-oxide (9)

In the dark, **3** (250 mg, 1.15 mmol) was added to a solution of triaminoguanidinium chloride (160 mg, 1.15 mmol) in 20 mL of distilled water. The solution was shaken for about 10 min and filtered. The yellow filtrate was evaporated by blowing a N₂ flow on the liquid surface to afford **9** as colorless crystals (0.19 g, 77%). DSC (5°C min⁻¹): 134°C (m.p.), 150°C (dec); IR: $\tilde{\nu}$ = 3343 (m), 3230 (m), 3095 (w), 3008 (w), 2782 (w), 2659 (w), 2248 (w), 1841 (w), 1674 (vs), 1611 (w), 1590 (w), 1536 (m), 1458 (w), 1418 (m), 1387 (w), 1345 (m), 1246 (s), 1210 (w), 1190 (m), 1131 (s), 1073 (w), 1014 (w), 995 (m), 942 (s), 928 (s), 793 (w), 770 (w), 684 cm⁻¹ (w); Raman (1064 nm): $\tilde{\nu}$ = 3345 (4), 3239 (8), 2249 (98), 2194 (2), 1678 (4), 1646 (1), 1459 (47), 1391 (2), 1350 (3), 1248 (2), 1211 (16), 1202 (3); 1138 (9), 1074 (18), 1011 (10), 880 (10), 771 (15), 696 (1), 647 (10), 548 (4), 494 (12), 429 (6), 313 (1), 257 cm⁻¹ (4); ¹³C NMR ([D₆]DMSO): δ = 159.6 (s, TAG⁺); 123.9 (s, CN₄); 110.8 ppm (s, CN); ¹H NMR ([D₆]DMSO): δ = 8.58 (s, 3H, NH-NH₂); 4.48 ppm (s, 6H, NH-NH₂); MS (FAB⁺) *m/z*: 105.1 (CN₆H₈⁺); (FAB⁻) *m/z*: 110.0 (C₂N₅O⁻); elemental analysis calcd (%) for CN₆H₈C₂N₅O (215.18): C 16.75, H 4.22, N 71.60; found: C 16.87, H 4.12, N 70.13; BAM impact: 40 J; BAM friction: 216 N; ESD: 0.5 J.

Copper(II) bis(carboxamide-tetrazolate-2-oxide) dihydrate (10)

To a solution of copper (II) chloride dihydrate (78 mg, 0.46 mmol) in 15 mL of distilled water, finely powdered **1** (200 mg, 0.92 mmol) was added in the dark. The suspension was carefully shaken by hand for 15 min in the dark followed by filtration. The filtrate was evaporated under heating (40°C) to give **10** as green single crystals (89.3 mg, 55%). IR: $\tilde{\nu}$ = 3854 (w), 3752 (w), 3377 (w), 3341 (w), 3270 (w), 3068 (m), 2782 (w), 2362 (w), 2333 (w), 2206 (w), 1734 (w), 1670 (s), 1590 (m), 1522 (m), 1444 (m), 1406 (w), 1387 (m), 1333 (s), 1246 (m), 1150 (w), 1119 (w), 1069 (w), 999 (w), 981 (w), 894 (w), 872 (w), 822 (m), 784 (w), 703 (m), 687 cm⁻¹ (m); elemental analysis calcd (%) for Cu(C₂N₅H₄O₃)₂ (355.65): C 13.51, N 39.38, H, 2.27; found: C 14.08, N 41.28, H 2.2.

Copper(II) bis(carboxamide-tetrazolate-1-oxide) dihydrate (11)

3 (200 mg, 0.92 mmol) was added to a solution of copper(II) chloride dihydrate (78 mg, 0.46 mmol) in 20 mL of distilled water. The solution was shaken for 10 min and filtered in the dark. The light blue filtrate was evaporated under heating (40°C) to yield **11** as green crystals (124 mg, 0.35 mmol). IR: $\tilde{\nu}$ = 3854 (w), 3746 (w), 3651 (w), 3447 (w), 3377 (w), 3298 (w), 3220 (w), 3170 (w), 2361 (m), 2338 (m), 2111 (w), 1734 (w), 1674 (vs), 1653 (s), 1610 (s), 1560 (w), 1530 (m), 1473 (w), 1457 (w), 1435 (w), 1419 (w), 1378 (m), 1338 (w), 1251 (m), 1208 (m), 1118 (w), 1092 (w), 1016 (w), 820 (w), 784 (m), 732 (w), 706 (m), 684 (w), 668 cm⁻¹ (w); elemental analysis calcd (%) for Cu₂C₄N₁₀O₆H₈ (355.72): C 13.51, H 2.27, N 39.38; found: C 13.78, H 2.23, N 40.63.

Hydrazinium 1,4-bis(2-N-oxidotetrazolate)-dihydro-1,2,4,5-tetrazine (12)

Sodium-5-cyano-tetrazolate-1.5H₂O (5.00 g, 34.7 mmol, 1.0 equiv) was dissolved in 25 mL water. The solution was cooled to 0°C and nitric acid (18.5 mL, 2M, 37.0 mmol, 1.1 equiv) was added. The mixture was stirred for 30 min before it was allowed to warm up to room temperature. The solvent was then removed under reduced pressure at room temperature and the residue was dissolved in ethanol. Remaining solids were filtered off, and the ethanol was evaporated at room temperature under reduced pressure to yield crude 5-cyanotetrazole. The crude product was dissolved in 66 mL water. Subsequently, 2M potassium hydroxide (17.5 mL, 35.0 mmol, 1.0 equiv), potassium acetate (29.80 g, 303.6 mmol, 8.7 equiv), and Oxone (66.03 g, 107.4 mmol, 3.1 equiv) were added. The solution was stirred at 40°C overnight. The solution was then poured into acetone (1.60 L) and stirred, followed by filtration of precipitated salts. After evaporation of the acetone under reduced pressure, the remaining solids were dissolved in hot ethanol. The insoluble remains were filtered off, and the ethanol was removed under reduced pressure. The residue was then dissolved in 15 mL water. The solution was cooled to 0°C before 2M nitric acid (17.4 mL, 34.7 mmol, 1.0 equiv) was added. After stirring the mixture for 30 min, the solvent was evaporated under high vacuum at room temperature. The solid residue was dissolved in dry ethanol, and insoluble remains were filtered off. Next, hydrazine hydrate (2.96 mL,

3.06 g, 60.9 mmol, 1.8 equiv) was added and the mixture was refluxed at about 85 °C for 2 h before additional hydrazine hydrate (2.96 mL, 3.06 g, 60.9 mmol, 1.8 equiv) was added. Subsequently, the mixture was refluxed for another 22 h. The precipitate was filtered off and rinsed with dry ethanol to yield **12** as a white solid (4.38 g, 13.9 mmol, 79.8% relative to the amount of sodium 5-cyanotetrazolate sesquihydrate). DSC: 176 °C (dec.); IR: $\tilde{\nu}$ = 3306 (w), 3272 (w), 3187 (w), 3148 (w), 3079 (w), 2945 (w), 2877 (w), 2649 (w), 2520 (w), 2151 (w), 2119 (w), 1637 (w), 1613 (w), 1545 (w), 1512 (w), 1461 (w), 1448 (w), 1406 (m), 1396 (m), 1372 (s), 1302 (w), 1246 (m), 1193 (w), 1100 (m), 1038 (w), 1014 (w), 993 (w), 972 (m), 864 (w), 783 (m), 749 (w), 724 (w), 701 (w), 650 cm⁻¹ (m); Raman (1064 nm): $\tilde{\nu}$ = 1662 (95), 1625 (8), 1589 (34), 1544 (46), 1515 (2), 1455 (31), 1414 (2), 1399 (6), 1374 (3), 1301 (2), 1237 (9), 1194 (2), 1119 (26), 1051 (5), 1030 (66), 975 (14), 843 (2), 763 (2), 787 (1), 749 (10), 702 (1), 646 (4), 597 (2), 541 (3), 456 (3), 333 cm⁻¹ (3); ¹³C NMR ([D₆]DMSO): δ = 148.10 (s) 140.54 ppm (s); MS (FAB⁺): m/z = 33.1 (N₂H₅⁺), MS (FAB⁻, glycerine): m/z = 251.1 (C₄H₃N₁₂O₂⁻); elemental analysis calcd (%) for (N₂H₅)₂C₄N₁₂O₂H₂ (316.24): N 70.87, C 15.19, H 3.82; found: N 64.81, C 15.49, H 3.62; BAM impact: 35 J; BAM friction: 360 N; ESD 250 mJ.

Hydrazinium 1,4-bis(1-N-oxidotetrazolate)-dihydro-1,2,4,5-tetrazine (**13**)

Sodium cyanotetrazolate-1-oxide (2.00 g, 14.1 mmol, 1.0 equiv) was dissolved in 12 mL of water. The solution was then cooled to 0 °C before 2 M nitric acid (7.04 mL, 14.1 mmol, 1.0 equiv) was added. After stirring the mixture for 30 min, the solvent was evaporated under reduced pressure at room temperature. The solid residue was dissolved in dry ethanol, and insoluble remains were filtered off. Subsequently, hydrazine hydrate (1.20 mL, 1.24 g, 24.7 mmol, 1.8 equiv) was added and the mixture was refluxed at 85 °C for 2 h before another portion of hydrazine hydrate (1.20 mL, 1.24 g, 24.7 mmol, 1.8 equiv) was added. The mixture was refluxed for another 22 h. The precipitate was filtered off and rinsed with dry ethanol to yield **13** as a white solid (1.84 g, 82.5%). DSC: 134 °C (m.p.), 180 °C (dec.); IR: $\tilde{\nu}$ = 3589 (w), 3260 (s), 3183 (m), 3111 (m), 2968 (m), 2909 (m), 2726 (w), 2635 (w), 2298 (w), 2202 (w), 2056 (w), 1988 (w), 1954 (w), 1903 (w), 1653 (m), 1615 (m), 1538 (w), 1514 (s), 1457 (s), 1445 (s), 1411 (m), 1346 (w), 1318 (m), 1243 (s), 1167 (m), 1150 (w), 1103 (s), 1082 (s), 1005 (m), 988 (s), 951 (m), 853 (s), 782 (m), 737 (m), 725 (s), 698 (m), 654 cm⁻¹ (w); Raman (1064 nm): $\tilde{\nu}$ = 3256 (13), 3220 (3), 3002 (3), 2929 (5), 1950 (4), 1907 (3), 1855 (3), 1806 (3), 1770 (3), 1732 (2), 1655 (94), 1594 (43), 1547 (48), 1518 (3), 1473 (28), 1437 (2), 1400 (4), 1354 (4), 1317 (2), 1299 (8), 1277 (2), 1243 (35), 1159 (16), 1143 (2); 1098 (28), 1044 (3), 1014 (16), 989 (2), 974 (4), 845 (16), 760 (6), 736 (11), 698 (5), 634 (7), 599 (3), 542 (4), 432 (7), 408 (2), 377 (3), 331 (3), 281 cm⁻¹ (3); ¹H NMR ([D₆]DMSO): δ = 10.04 (s, N-H), 7.07 ppm (s, N₂H₅⁺); ¹³C NMR ([D₆]DMSO): δ = 140.44 (s), 134.26 ppm (s); MS (FAB⁻, glycerin): m/z = 251.1 (C₄H₃N₁₂O₂⁻); elemental analysis calcd (%) for (N₂H₅)₂C₄N₁₂O₂H₂ (316.24): N 70.87, C 15.19, H 3.82; found: N 65.55, C 15.15, H 3.75; BAM impact: 40 J; BAM friction: > 360 N; ESD: 250 mJ.

1,4-Bis(2-hydroxytetrazole)-dihydro-1,2,4,5-tetrazine dihydrate (**14·2H₂O**)

12 (950 mg, 3.0 mmol, 1.0 equiv) was dissolved in as little hot water as possible, and insoluble remains were filtered off. Subsequently, concentrated hydrochloric acid (37 wt.%, 1.9 mL, 2.26 g, 22.9 mmol, 7.6 equiv) was added and the solution was cooled to 6 °C. The precipitating product was isolated by suction filtration and rinsed with cold water to yield **14·2H₂O** as a white solid (315 mg, 36.3%). DSC: 116 °C (-H₂O), 162 °C (dec.); IR: $\tilde{\nu}$ = 3528 (w), 3421 (w), 3273 (m), 3191 (m), 3107 (w), 2975 (m), 2889 (m), 2525 (m), 2365 (m), 2119 (w), 1984 (w), 1972 (w), 1956 (w), 1629 (w), 1564 (m), 1547 (63), 1539 (m), 1512 (m), 1453 (w), 1446 (w), 1385 (s), 1366 (s), 1239 (s), 1197 (m), 1152 (m), 1129 (m), 1103 (m), 1041 (m), 1015 (m), 993 (s), 856 (m), 771 (s), 694 cm⁻¹ (s); Raman (1064 nm): $\tilde{\nu}$ = 3285 (3), 1665 (98), 1547 (63), 1456 (41), 1385 (3), 1242 (9), 1137 (13), 1038 (49), 974 (7), 842 (4), 767 (1), 750 (9), 633 (4), 599 (1), 543 (3), 463 (1), 416 (1), 331 cm⁻¹ (1); ¹H NMR ([D₆]DMSO): δ = 8.86 (brs, -NH), 4.40 ppm (brs, -OH and hydration water); ¹³C NMR ([D₆]DMSO): δ = 150.39 (s), 139.71 ppm (s); MS (FAB⁻): m/z = 251 (C₄H₃N₁₂O₂⁻); elemental analysis calcd (%) for C₄N₁₂O₂H₄·2H₂O

(288.18): N 58.32, C 16.67, H 2.80; found: N 63.54, C 16.46, H 3.31; BAM impact: 40 J; BAM friction: 360 N; ESD: 250 mJ.

1,4-Bis(1-hydroxytetrazole)-dihydro-1,2,4,5-tetrazine hydrate (**15·H₂O**)

13 (1.84 g, 5.5 mmol, 1.0 equiv) was dissolved in as little hot water as possible, and insoluble material was filtered off. Subsequently, concentrated hydrochloric acid (37 wt.%, 4 mL, 4.76 g, 48.3 mmol, 8.8 equiv) was added and the solution was cooled to 6 °C. The precipitating product was isolated by suction filtration and rinsed with cold water to yield **15·H₂O** as a white solid (0.91 g, 61.1%). DSC: 144 °C (dec.); IR: $\tilde{\nu}$ = 3556 (w), 3329 (m), 3317 (m), 3234 (m), 3190 (m), 3048 (m), 2952 (w), 2933 (w), 2746 (w), 2651 (w), 2623 (w), 2365 (w), 2337 (w), 2198 (w), 2083 (w), 2048 (w), 1831 (w), 1695 (m), 1641 (m), 1594 (m), 1530 (m), 1469 (w), 1433 (s), 1320 (w), 1308 (w), 1265 (w), 1247 (w), 1230 (w), 1191 (w), 1148 (m), 1138 (m), 1114 (w), 1096 (m), 1062 (w), 1037 (m), 1003 (w), 975 (w), 962 (m), 922 (m), 857 (m), 786 (s), 757 (m), 735 (s), 717 (m), 694 (m), 686 cm⁻¹ (m); Raman (1064 nm): $\tilde{\nu}$ = 3243 (4), 1671 (71), 1646 (15), 1567 (95), 1542 (4), 1464 (9), 1411 (1), 1392 (1), 1286 (4), 1244 (17), 1178 (2), 1138 (8), 1090 (15), 1024 (5), 1005 (1), 973 (1), 863 (8), 790 (3), 727 (12), 693 (12), 640 (4), 536 (3), 384 (3), 319 (3), 234 cm⁻¹ (2); ¹H NMR ([D₆]DMSO): δ = 9.78 (brs, N-H), 4.10 ppm (brs, O-H and H₂O); ¹³C NMR ([D₆]DMSO): δ = 138.70 (s), 136.43 ppm (s); MS (DEI⁺): m/z = 252.3 (M⁺); elemental analysis calcd (%) for C₄N₁₂O₂H₄·H₂O (270.17): N 62.21, C 17.78, H 2.24; found: N 59.22, C 17.19, H 2.88; BAM impact: 17 J; BAM friction: 192 N; ESD: 700 mJ.

Ammonium 1,4-bis(2-N-oxidotetrazolate)-dihydro-1,2,4,5-tetrazine (**16**)

14·2H₂O (200 mg, 0.79 mmol) was dissolved in 50 mL of distilled water, and then 2 M ammonia (0.8 mL, 1.59 mmol) was added. Subsequently, the solvent was removed under reduced pressure to yield **16** as a solid (185.5 mg, 82%). IR: $\tilde{\nu}$ = 3262 (m), 3170 (m), 3026 (m), 2853 (m), 2119 (w), 1681 (w), 1604 (w), 1534 (w), 1512 (w), 1430 (m), 1403 (s), 1368 (s), 1274 (w), 1236 (m), 1200 (m), 1154 (w), 1124 (w), 1107 (w), 1048 (w), 1009 (m), 994 (m), 973 (w), 866 (w), 789 (m), 734 (m), 694 cm⁻¹ (w); Raman (1064 nm): $\tilde{\nu}$ = 3264 (3), 3085 (5), 1660 (98), 1536 (64), 1463 (26), 1410 (4), 1395 (1), 1235 (7), 1174 (5), 1122 (37), 1067 (2), 1022 (85), 994 (5), 971 (7), 821 (1), 858 (1), 790 (1), 767 (3), 751 (11), 695 (1), 645 (5), 601 (3), 548 (3), 452 (6), 327 cm⁻¹ (4); ¹H NMR ([D₆]DMSO): δ = 8.3 (s, 2H, -C₂N₄H₂), 7.3 ppm (s, 4H, NH₄); ¹³C NMR ([D₆]DMSO): δ = 148.6 (s, 2C, -CN₄O), 141.1 ppm (s, 2C, -C₂N₄); m/z : (FAB⁻) 251 (C₄H₃N₁₂O₂); m/z : (FAB⁺) 18.1 (NH₄); elemental analysis calcd (%) for (NH₄)₂C₄N₁₂O₂H₂ (286.22): C 16.77, N 68.51, H 3.52; found: C 16.37, N 66.96, H 3.73; BAM impact: 30 J; BAM friction: 360 N; ESD: 500 mJ.

Ammonium 1,4-bis(1-N-oxidotetrazolate)-dihydro-1,2,4,5-tetrazine monohydrate (**17·H₂O**)

To a solution of **15·H₂O** (0.20 g, 0.79 mmol) in about 4 mL distilled water 2 M ammonia (0.83 mL, 1.66 mmol) was added. After that, the mixture was stirred for 0.5 h and the solvent was evaporated under nitrogen flow to afford **17·H₂O** as a white solid (0.22 g, 97%). IR: $\tilde{\nu}$ = 3314 (w), 3268 (m), 3176 (w), 3040 (w), 2897 (w), 2855 (w), 2734 (w), 2633 (w), 1635 (w), 1549 (w), 1510 (m), 1433 (vs), 1415 (s), 1310 (w), 1282 (m), 1231 (m), 1165 (w), 1133 (w), 1093 (m), 1067 (w), 999 (w), 980 (w), 970 (m), 850 (w), 774 (w), 745 (w), 735 (w), 700 cm⁻¹ (w); Raman (1064 nm): $\tilde{\nu}$ = 3274 (2), 3176 (7), 2131 (2), 1653 (98), 1605 (11), 1536 (49), 1467 (21), 1398 (2), 1357 (1), 1289 (10), 1233 (40), 1148 (12), 1089 (17), 1007 (11), 968 (4), 844 (9), 756 (4), 739 (9), 699 (3), 653 (3), 639 (1), 533 (4), 414 (4), 381 (2), 323 (2), 273 cm⁻¹ (1); ¹³C NMR ([D₆]DMSO): δ = 134.8 (s, 2C, -C₂N₄); 140.9 ppm (s, 2C, -CN₄); ¹H NMR ([D₆]DMSO): δ = 10.11 (s, 4H, NH₄⁺); 7.11 ppm (brs, 2H, -NH-); m/z (FAB⁺, NBA): 18.0 (NH₄⁺); m/z (FAB⁻, NBA): 251.0 (C₄H₃N₁₂O₂⁻); elemental analysis calcd (%) for (NH₄)₂C₄N₁₂O₂H₂·H₂O (304.23): C 15.78, H 3.98, N 64.46; found: C 15.80, H 3.96, N 64.54; BAM impact: 40 J; BAM friction: 240 N; ESD: 1.5 J.

1,4-Bis(2-hydroxytetrazole)-1,2,4,5-tetrazine (**18**)

To a suspension of **14·2H₂O** (100 mg, 0.35 mmol, 1.0 equiv) in 100 mL acetonitrile, a solution of nitrogen dioxide in acetonitrile was added

dropwise until the suspension became red and no more of the solid dissolved. The remaining solid was filtered off, and the solution was slowly evaporated under a stream of nitrogen at room temperature. The solid was then dried under high vacuum at 40°C. WARNING: VERY EXPLOSIVE WHEN DRY! ¹³C NMR ([D₆]DMSO): δ=158.4 (s), 154.9 ppm (s); MS (FAB⁻): m/z=249.2 (C₄N₁₂O₂H⁻).

Ammonium 1,4-bis(2-N-oxidotetrazolate)-1,2,4,5-tetrazine monohydrate (20·H₂O)

To a suspension of **14·2H₂O** (100 mg, 0.35 mmol, 1.0 equiv) in 100 mL acetonitrile, a solution of nitrogen dioxide in acetonitrile was added dropwise until the suspension became red and no more of the solid dissolved. The remaining solid was filtered off, and the solution was slowly evaporated under a stream of nitrogen at room temperature. The obtained product was dissolved in water, and then 2 M ammonia (0.37 mL, 0.74 mmol) was added. Afterwards, the solution was evaporated under a stream of nitrogen to yield **20·H₂O** (70 mg, 0.23 mmol) as a red solid after drying under high vacuum. DSC: 95°C (-H₂O), 189°C (dec.); IR: $\bar{\nu}$ =3401 (w), 3165 (m), 3010 (m), 2821 (m), 2361 (w), 2258 (w), 2135 (w), 1831 (w), 1675 (w), 1604 (w), 1570 (w), 1534 (m), 1406 (s), 1354 (s), 1313 (s), 1273 (m), 1263 (m), 1248 (s), 1209 (m), 1098 (w), 1068 (m), 1044 (w), 1011 (m), 992 (m), 921 (w), 825 (w), 787 (m), 781 (m), 742 (w), 703 (w), 676 cm⁻¹ (w); Raman (1064 nm): $\bar{\nu}$ =1997 (1), 1864 (2), 1628 (1), 1516 (100), 1495 (2), 1425 (7), 1391 (3), 1232 (1), 1152 (2), 1100 (29), 1088 (4), 1036 (3), 1002 (17), 988 (5), 820 (4), 764 (1), 601 (1), 465 cm⁻¹ (2); ¹H NMR ([D₆]DMSO): δ=7.29 (brs, NH₄⁺), 3.4 ppm (brs, H₂O); ¹³C NMR ([D₆]DMSO): δ=158.15 (s), 150.92 ppm (s); MS (FAB⁻): m/z=249.1 (C₄N₁₂O₂H⁻); elemental analysis calcd (%) for (NH₄)₂C₄N₁₂O₂·H₂O (302.22): N 64.89, C 15.89, H 3.34; found: N 59.69, C 16.03, H 3.45; BAM impact: 40 J; BAM friction: 240 N; ESD: 500 mJ;

Acknowledgements

Financial support of this work by the Ludwig-Maximilian University of Munich (LMU), the U.S. Army Research Laboratory (ARL), the Armament Research, Development and Engineering Center (ARDEC), the Strategic Environmental Research and Development Program (SERDP), and the Office of Naval Research (ONR Global, title: "Synthesis and Characterization of New High Energy Dense Oxidizers (HEDO) - NICOP Effort ") under contract nos. W911NF-09-2-0018 (ARL), W911NF-09-1-0120 (ARDEC), W011NF-09-1-0056 (ARDEC), and 10 WPSEED01-002/WP-1765 (SERDP) is gratefully acknowledged. The authors acknowledge collaborations with Dr. Mila Krupka (OZM Research, Czech Republic) in the development of new testing and evaluation methods for energetic materials and with Dr. Muhamed Sućeska (Brodarski Institute, Croatia) in the development of new computational codes to predict the detonation and propulsion parameters of novel explosives. We are indebted to and thank Drs. Betsy M. Rice and Brad Forch (ARL, Aberdeen, Proving Ground, MD) and Mr. Gary Chen (ARDEC, Picatinny Arsenal, NJ) for many helpful and inspired discussions and support of our work. The authors want to thank S. Huber for measuring the sensitivities.

- [1] M.-X. Zhang, P. E. Eaton, R. Gilardi, *Angew. Chem.* **2000**, *112*, 422–426; *Angew. Chem. Int. Ed.* **2000**, *39*, 401–404.
- [2] G. H. Tao, B. Twamley, J. M. Shreeve, *J. Mater. Chem.* **2009**, *19*, 5850–5854.
- [3] D. E. Chavez, M. A. Hiskey, D. L. Naud, D. Parrish, *Angew. Chem.* **2008**, *120*, 8431–8433; *Angew. Chem. Int. Ed.* **2008**, *47*, 8307–8309.
- [4] O. S. Bushuyev, P. Brown, A. Maiti, R. H. Gee, G. R. Peterson, B. L. Weeks, L. J. Hope-Weeks, *J. Am. Chem. Soc.* **2012**, *134*, 1422–1425.
- [5] M. H. V. Huynh, M. A. Hiskey, D. E. Chavez, D. L. Naud, R. D. Gilardi, *J. Am. Chem. Soc.* **2005**, *127*, 12537–12543.
- [6] B. Lachance, A. Y. Renoux, M. Sarrazin, J. Hawari, G. I. Sunahara, *Chemosphere* **2004**, *55*, 1339–1348.
- [7] W. McLellan, W. R. Hartley, M. Brower, *Health advisory for hexahydro-1,3,5-trinitro-1,3,5-triazinane*. Technical Report PB90–273533; Office of Drinking Water, U. S. Environmental Protection Agency, Washington DC, 1988.
- [8] N. Sikder, A. K. Sikder, N. R. Bulakh, B. R. Gandhe, *J. Hazard. Mater.* **2004**, *113*, 35–43.
- [9] P. E. Eaton, M. X. Zhang, R. Gilardi, N. Gelber, S. Iyer, R. Surapeneni, *Propellants Explos. Pyrotech.* **2002**, *27*, 1–6.
- [10] P. Carlqvist, H. Östmark, T. Brinck, *J. Phys. Chem. A* **2004**, *108*, 7463–7467.
- [11] Y.-C. Li, C. Qi, S. H. Li, H. J. Zhang, C.-H. Sun, Y.-Z. Yu, S.-P. Pang, *J. Am. Chem. Soc.* **2010**, *132*, 12172–12173.
- [12] T. M. Klapötke, D. G. Piercey, *Inorg. Chem.* **2011**, *50*, 2732–2734.
- [13] M. N. Glukhovtsev, B. Y. Simkin, V. I. Minkin, *Zh. Org. Khim.* **1988**, *24*, 2486–2488.
- [14] S. Inagaki, N. Goto, *J. Am. Chem. Soc.* **1987**, *109*, 3234–3240.
- [15] M. Noyman, S. Zilberg, Y. Haas, *J. Phys. Chem. A* **2009**, *113*, 7376–7382.
- [16] M. S. Molchanova, T. S. Pivina, E. A. Arnautova, N. S. Zefirov, *J. Mol. Struct. (Theochem.)* **1999**, *465*, 11–24.
- [17] M. Göbel, K. Karaghiosoff, T. M. Klapötke, D. G. Piercey, J. Stierstorfer, *J. Am. Chem. Soc.* **2010**, *132*, 17216–17226.
- [18] T. M. Klapötke, D. G. Piercey, J. Stierstorfer, *Chem. Eur. J.* **2011**, *17*, 13068–13077.
- [19] T. M. Klapötke, D. G. Piercey, J. Stierstorfer, M. Weyrauther, *Propellants Explos. Pyrotech.* **2012**, DOI: 10.1002/prop201100151.
- [20] D. Fischer, N. Fischer, T. M. Klapötke, D. G. Piercey, J. Stierstorfer, *J. Mater. Chem.* **2012**, DOI: 10.1039/c2m33646d.
- [21] A. N. Binnikov, A. S. Kulikov, N. N. Makhov, I. V. Orchinnikov, T. S. Pivina, *30th International Annual Conference of ICT*, Karlsruhe, Germany, June 29–July 2, **1999**, p. 58.
- [22] A. M. Churakov, S. L. Ioffe, V. S. Kuz'min, Yu. A. Strelenko, Yu. T. Struchkov, V. A. Tartakovskii, *Khim. Geterotsykl. Soedin.* **1988**, *12*, 1666–1669.
- [23] C. M. Sabaté, E. Jeanne, H. Delalu, *Dalton Trans.* **2012**, *41*, 3817–3825.
- [24] J. Sauer, G. R. Pabst, U. Holland, H.-S. Kim, S. Loebbecke, *Eur. J. Org. Chem.* **2001**, 697–706.
- [25] Gaussian 09, Revision A.1, M. J. Frisch, G. W. Trucks, H. B. Schlegel, G. E. Scuseria, M. A. Robb, J. R. Cheeseman, G. Scalmani, V. Barone, B. Mennucci, G. A. Petersson, H. Nakatsuji, M. Caricato, X. Li, H. P. Hratchian, A. F. Izmaylov, J. Bloino, G. Zheng, J. L. Sonnenberg, M. Hada, M. Ehara, K. Toyota, R. Fukuda, J. Hasegawa, M. Ishida, T. Nakajima, Y. Honda, O. Kitao, H. Nakai, T. Vreven, J. A. Montgomery, Jr., J. E. Peralta, F. Ogliaro, M. Bearpark, J. J. Heyd, E. Brothers, K. N. Kudin, V. N. Staroverov, R. Kobayashi, J. Normand, K. Raghavachari, A. Rendell, J. C. Burant, S. S. Iyengar, J. Tomasi, M. Cossi, N. Rega, J. M. Millam, M. Klene, J. E. Knox, J. B. Cross, V. Bakken, C. Adamo, J. Jaramillo, R. Gomperts, R. E. Stratmann, O. Yazyev, A. J. Austin, R. Cammi, C. Pomelli, J. W. Ochterski, R. L. Martin, K. Morokuma, V. G. Zakrzewski, G. A. Voth, P. Salvador, J. J. Dannenberg, S. Dapprich, A. D. Daniels, Ö. Farkas, J. B. Foresman, J. V. Ortiz, J. Cioslowski, and D. J. Fox, Gaussian, Inc., Wallingford CT, **2009**.
- [26] A. D. Becke, *J. Chem. Phys.* **1993**, *98*, 5648–5652.
- [27] C. Lee, W. Yang, R. G. Parr, *Phys. Rev. B* **1988**, *37*, 785–789.
- [28] D. E. Woon, T. H. Dunning, Jr., R. J. Harrison, *J. Chem. Phys.* **1993**, *98*, 1358–1371.
- [29] R. A. Kendall, T. H. Dunning, Jr., R. J. Harrison, *J. Chem. Phys.* **1992**, *96*, 6796–6806.
- [30] T. H. Dunning, Jr., *J. Chem. Phys.* **1989**, *90*, 1007–1023.
- [31] K. A. Peterson, D. E. Woon, T. H. Dunning, Jr., *J. Chem. Phys.* **1994**, *100*, 7410–7415.
- [32] N. Fischer, T. M. Klapötke, S. Rappenglück, J. Stierstorfer, *Chem-PlusChem* **2012**, DOI: 10.1002/cplu.201200136.
- [33] A. J. Bracuti, *Acta Crystallogr. Sect. B* **1979**, *35*, 760–761.
- [34] T. M. Klapötke, J. Stierstorfer, B. Weber, *Inorg. Chim. Acta* **2009**, *362*, 2311–2320.

- [35] T. M. Klapötke, D. G. Piercey, F. Rohrbacher, J. Stierstorfer, *Z. Anorg. Allg. Chem.* **2012**, DOI: 10.1002/zaac.201200363.
- [36] T. Altenburg, T. M. Klapötke, A. Penger, J. Stierstorfer, *Z. Anorg. Allg. Chem.* **2010**, 636, 463–471.
- [37] P. J. Linstrom and W. G. Mallard, Eds., NIST Chemistry WebBook, NIST Standard Reference Database Number 69, National Institute of Standards and Technology, Gaithersburg MD, 20899, <http://webbook.nist.gov>, (retrieved October 27, **2011**).
- [38] a) H. D. B. Jenkins, H. K. Roobottom, J. Passmore, L. Glasser, *Inorg. Chem.* **1999**, 38, 3609–3620; b) H. D. B. Jenkins, D. Tudela, L. Glasser, *Inorg. Chem.* **2002**, 41, 2364–2367.
- [39] M. Sućeska, EXPLO5.05 program, Zagreb, Croatia, **2012**.
- [40] M. Sućeska, *Propellants Explos. Pyrotech.* **1991**, 16, 197–202.
- [41] R. Mayer, J. Köhler, A. Homburg, *Explosives, 5th ed.*, Wiley-VCH, Weinheim, **2002**.
- [42] R. M. Vrcelj, J. N. Sherwood, A. R. Kennedy, H. G. Gallagher, T. Gelbrich, *Cryst. Growth Des.* **2003**, 3, 1027.
- [43] Calculation of oxygen balance: Ω (%) = $(wO - 2xC - 1/2yH - 2zS)/1600M$. (w: number of oxygen atoms, x: number of carbon atoms, y: number of hydrogen atoms, z: number of sulfur atoms, M: molecular weight).
- [44] Impact: Insensitive, > 40 J; less sensitive, ≥ 35 J; sensitive, ≥ 4 J; very sensitive, ≤ 3 J. Friction: Insensitive, > 360 N; less sensitive = 360 N; sensitive, < 360 N and > 80 N; very sensitive, ≤ 80 N; extremely sensitive, ≤ 10 N. According to the UN Recommendations on the Transport of Dangerous Goods.
- [45] CrysAlisPro, Agilent Technologies, Version 1.171.35.11, **2011**.
- [46] G. M. Sheldrick, SHELXS-97, Program for Crystal Structure Solution, Universität Göttingen, **1997**.
- [47] A. Altomare, G. Cascarano, C. Giacovazzo, A. Guagliardi, *Appl. Crystallogr.* **1993**, 26, 343.
- [48] G. M. Sheldrick, *Shelxl-97, Program for the Refinement of Crystal Structures*, University of Göttingen, Germany, **1994**.
- [49] A. L. Spek, *Platon, A Multipurpose Crystallographic Tool*, Utrecht University, Utrecht, The Netherlands, **1999**.
- [50] L. Farrugia, *J. Appl. Crystallogr.* **1999**, 32, 837–838.
- [51] Empirical absorption correction using spherical harmonics, implemented in SCALE3 ABSPACK scaling algorithm (CrysAlisPro Oxford Diffraction Ltd., Version 171.33.41, **2009**).

Received: September 27, 2012
Published online: ■ ■ ■, 0000

Pushing the limits of energetic materials – the synthesis and characterization of dihydroxylammonium 5,5'-bistetrazole-1,1'-diolate†

Niko Fischer, Dennis Fischer, Thomas M. Klapötke,* Davin G. Piercey and Jörg Stierstorfer

Received 6th June 2012, Accepted 9th August 2012

DOI: 10.1039/c2jm33646d

The safe preparation and characterization (XRD, NMR and vibrational spectroscopy, DSC, mass spectrometry, sensitivities) of a new explosive dihydroxylammonium 5,5'-bistetrazole-1,1'-diolate (TKX-50) that outperforms all other commonly used explosive materials is detailed. While much publicized high-performing explosives, such as octanitrocubane and CL-20, have been at the forefront of public awareness, this compound differs in that it is simple and cheap to prepare from commonly available chemicals. TKX-50 expands upon the newly exploited field of tetrazole oxide chemistry to produce a material that not only is easily prepared and exceedingly powerful, but also possesses the required thermal insensitivity, low toxicity, and safety of handling to replace the most commonly used military explosive, RDX (1,3,5-trinitro-1,3,5-triazacyclohexane). In addition, the crystal structures of the intermediates 5,5'-bistetrazole-1,1'-diol dihydrate, 5,5'-bistetrazole-1,1'-diol dimethanolate and dimethylammonium 5,5'-bistetrazole-1,1'-diolate were determined and presented.

Introduction

The rational design of new energetic materials is a rapidly exploding field^{1–7} with a long traditional rooting in the chemical sciences^{8,9} and a complexity that rivals that of the drug design. While the field has come a long way since the days of Liebig, Berzelius and Gay-Lussac, and the concept of isomerism being determined from explosive silver fulminate and non-explosive silver cyanate,¹⁰ current work in this field still follows the trend of its historic beginnings; that of simultaneous academic and practical interest and advances. In the quest for higher-performing, safer, cheaper, greener, explosive materials, energetic materials chemistry must push the boundaries of the energy

capacity of compounds, which requires new classes of compounds,^{2,11} new synthetic strategies,¹² and advanced computational techniques. For example, the high nitrogen content of many advanced explosives has led to the preparation of new nitrogen–nitrogen bond forming reactions¹² and new heterocyclic systems¹³ in the quest for even higher performance.

In both civilian and military circles, the highest performing explosives make use of the same strategy: cyclic and caged nitramines. Belonging to the oldest class of explosives, those derive their energy from the oxidation of a carbon backbone by containing the oxidizer in the same molecule; RDX (1,3,5-trinitro-1,3,5-triazacyclohexane), HMX (1,3,5,7-tetranitro-1,3,5,7-tetraazacyclooctane) and CL-20 (2,4,6,8,10,12-hexanitro-2,4,6,8,10,12-hexaza-isowurtzitane) all have fatal flaws that mandate replacement with modern explosives. Advanced energetic strategies allow for retention or improvement of the explosive performance, while avoiding the multitude of downsides present in these compounds: toxicity to living organisms (all), difficult and expensive synthesis (HMX, CL-20), high sensitivity to mechanical stimuli (all), and spontaneous changing of properties (CL-20).² New strategies in the design of energetic materials include those with ring or cage strain, high heat of formation compounds, and compounds containing strong dipoles or zwitterionic structures.¹⁴

Unfortunately, the known materials with the highest detonation energy are often highly sensitive due to their unprecedented energy content,⁵ and are made *via* long and expensive pathways with a multitude of steps, making industrial scale-up infeasible. For example, both DDF (dinitroazofuroxane) and ONC (octanitrocubane) possess detonation velocities at the limit of known performances (around 10 000 m s⁻¹), however both are highly

Energetic Materials Research, Department of Chemistry, University of Munich (LMU), Butenandstr. 5-13, D-81377, Germany. E-mail: tmk@cup.uni-muenchen.de; Fax: +49 (0)89 2180 77492; Tel: +49 (0)89 2180 77491

† Electronic supplementary information (ESI) available: 1. Materials and methods; 1.1. NMR spectroscopy; 1.2. vibrational spectroscopy; 1.3. mass spectrometry and elemental analysis; 1.4. differential scanning calorimetry; 1.5. sensitivity testing; 2. experimental work; 2.1. synthesis *via* oxidation of 5,5'-bistetrazole with potassium peroxydisulfate; 2.2. synthesis *via* cyclization of diazidoglyoxime; 2.3. safer synthesis including a multi-step one pot reaction; 3. X-ray diffraction; 3.1. instrument and refinement software; 3.2. crystallographic data and refinement parameters; 3.3. bond lengths, bond angles and hydrogen bonding of TKX-50; 3.4. crystal structures of 5,5'-bistetrazole-1,1'-diol; 3.5. crystal structure of dimethylammonium 5,5'-bistetrazole-1,1'-diolate; 4. explosive performance; 4.1. heat of formation calculations; 4.2. small scale shock reactivity test; 4.3. flame test; 4.4. hot plate test; 5. toxicity assessment; 6. Fast Cook-Off test. cif files. CCDC 872230, 872231, 872232, 884559, 884560 and 884561. For ESI and crystallographic data in CIF or other electronic format see DOI: 10.1039/c2jm33646d

sensitive and have more than 10 synthetic steps with exotic, expensive reagents used.¹⁵

A very promising explosophoric moiety in the design of new energetic materials is the tetrazole ring; the carbon on position 5 of the ring allows the facile attachment of various substituents for energetic tailorability, and the high nitrogen content and heat of formation of the heterocycle lead to high energetic performances. In order to improve the energetic properties of tetrazoles, several recently published studies showed that introduction of N-oxides yields compounds with even higher densities and stabilities, lower sensitivities and better oxygen balances.^{2,7,11} Combining these principles with practical considerations in mind, a simple and secure synthetic pathway to the high performing energetic material dihydroxylammonium 5,5'-bistetrazole-1,1'-diolate (TKX-50) was devised.

Results and discussion

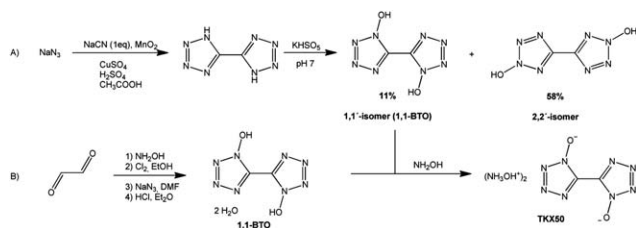
Synthesis (simple and scalable)

There are two major routes (A and B) to the 5,5'-bistetrazole-1,1'-diol (1,1-BTO) moiety (Scheme 1). The first (A) of which, the oxidation of the parent heterocycle with aqueous potassium peroxydisulfate only leads to 1,1-BTO in poor yield (11%). The oxidation of the 5,5'-bistetrazolate anion with peroxydisulfate was carried out in a manner similar to that we have previously reported for 5-nitro- and 5-azidotetrazoles.^{2,7} Unfortunately, this reaction was found to produce the 2,2' isomer as the major product, with only traces of the 1,1' isomer which crystallized upon adding aqueous hydroxylamine.

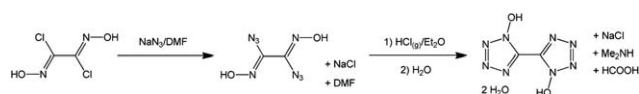
After discovering the outstanding characteristics of TKX-50 as a high explosive, a different route to the precursor 5,5'-bistetrazole-1,1'-diol was necessitated. Tselinskii *et al.*¹⁶ reported on the synthesis of the mentioned precursor 1,1-BTO from the cyclization of diazidoglyoxime under acidic conditions for the first time. Diazidoglyoxime is prepared from dichloroglyoxime in a chloro-azido exchange reaction in DMF with more than 80 % yield, whereas dichloroglyoxime is prepared from glyoxime *via* chlorination in ethanol in high yield.

The problematic step here is the isolation of the highly friction and impact sensitive compound diazidoglyoxime, mandating a revised procedure before industrial-scaled use. The problem was overcome by a procedure combining the formation and cyclization of diazidoglyoxime in one step in solution. Starting from commercially available glyoxal, the reaction process was transformed into a five step, four pot synthesis to isolate TKX-50.

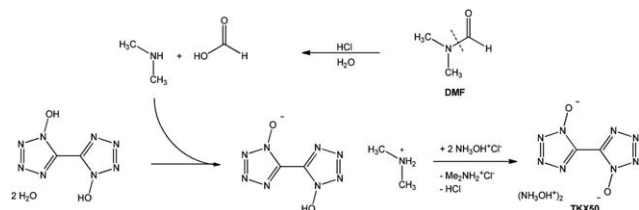
The prepared solution of diazidoglyoxime in DMF (impure with sodium chloride) is directly poured into diethylether and



Scheme 1 Synthesis of TKX-50 *via* oxidation of 5,5'-bistetrazole (A) and *via* cyclization of diazidoglyoxime (B).



Scheme 2 Synthesis of 5,5'-bistetrazole-1,1'-diol in a one pot reaction from dichloroglyoxime.



Scheme 3 Synthesis of TKX-50 from 5,5'-bistetrazole-1,1'-diol isolated from the one pot reaction described in Scheme 2. DMF is cleaved under the acidic conditions to form the dimethylammonium salt of 5,5'-bistetrazole-1,1'-diol, which is then converted into TKX-50.

HCl gas is bubbled through (Scheme 2). After cyclization of the azidooxime in the acidic medium the dimethylammonium salt of 5,5'-bistetrazole-1,1'-diol is formed by a reaction with dimethylamine (formed by hydrolysis of DMF). After isolation and recrystallization of dimethylammonium 5,5'-bistetrazole-1,1'-diolate, it is dissolved in a sufficient amount of boiling water and combined with a solution of hydroxylammonium chloride, from which TKX-50 crystallizes first (Scheme 3).

An alternative procedure using NMP (*N*-methyl-2-pyrrolidone) instead of DMF for the chloro-azido exchange, followed by the same treatment, leads to the free acid 5,5'-bistetrazole-1,1'-diol which is then isolated as its sodium salt tetrahydrate upon the addition of aqueous sodium hydroxide and subsequently treated with hydroxylammonium chloride in water. Starting from dichloroglyoxime, the overall yields of both procedures are very high with 72 % (DMF-route) and 85 % (NMP-route) for the synthesis of TKX-50. For a detailed description of all synthetic routes yielding TKX-50 and for all analytical data please refer to the ESI.†

X-ray diffraction

The crystal structure of TKX-50 was determined at three temperatures (100 K, 173 K, 298 K) in order to detect potential low temperature phase transitions and obtain precise densities (for explosive performance calculations). In addition the crystal structures of the intermediates 5,5'-bistetrazole-1,1'-diol dihydrate (recryst. from either water, MeCN, EtOH or glacial acetic acid), 5,5'-bistetrazole-1,1'-diol dimethanolate (recryst. from methanol) and dimethylammonium 5,5'-bistetrazole-1,1'-diolate (crystallized from H₂O) were determined and are presented in the ESI.† Detailed crystallographic data and parameters of the measurements and solutions are given in Table S1.† The lack of observed phase transitions between 100 K and 298 K is advantageous for energetic materials use as constant properties upon temperature changes result. The density follows the expected trend of decreasing with increased temperature (100 K: 1.918 g cm⁻³ > 173 K: 1.915 g cm⁻³ > 298 K: 1.877 g cm⁻³). TKX-50 crystallizes in the monoclinic space group *P*2₁/*c* with two anion-cation moieties in the unit cell. The molecular moiety of

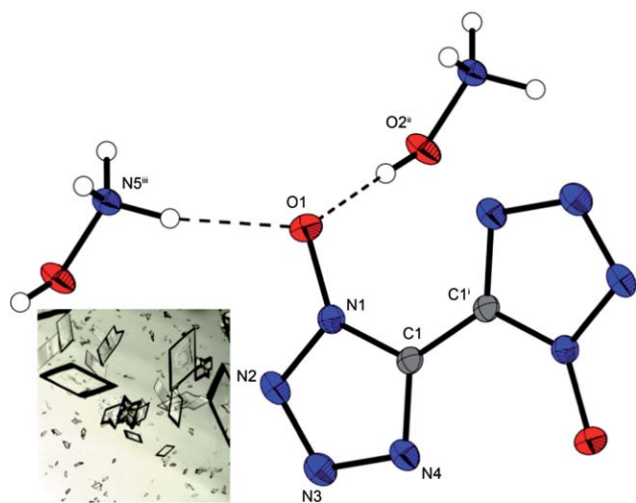


Fig. 1 Representation of the solid state molecular structure of TKX-50 at 100 K. Thermal ellipsoids are drawn at the 50% probability level; symmetry codes: (i) $2 - x, -y, 2 - z$; (ii) $x, 0.5 - y, -0.5 + z$; and (iii) $-1 + x, 0.5 - y, -0.5 + z$.

TKX-50 at 100 K is depicted in Fig. S1.† Its density of 1.918 g cm^{-3} is significantly higher than that of non-oxide dihydroxylammonium 5,5'-bistetrazolate (1.742 g cm^{-3}) recently published.¹⁷ The reason for this may be the strong hydrogen bond network (involving all four hydrogen atoms of the hydroxylammonium cations) (Fig. 1).

Energetic performance

The performance data (Table 1) were calculated with the computer code EXPLO5.05 (latest version). EXPLO5.05 is based on the chemical equilibrium, a steady state model of detonation.

It uses Becker–Kistiakowsky–Wilson's equation of state (BKW EOS) for gaseous detonation products and Cowan–Fickett's equation of state for solid carbon (see ESI†). The input is based on the sum formula, calculated heats of formation (see ESI†) and the maximum densities according to their crystal structures (ESI, Table S1†).

With respect to the detonation velocity (Table 1), TKX-50 shows higher calculated values than all other mass-produced and used explosives like 2,4,6-trinitrotoluene (TNT), RDX, HMX and CL-20. Looking at the detonation pressure, TKX-50 exceeds the values calculated for TNT and RDX and is comparable to HMX, but is slightly lower than for CL-20. Also in terms of potential use as a propellant mixture ingredient TKX-50 shows promising values due to its high nitrogen content. The calculated specific impulse using 60 bar isobaric rocket conditions is 261 seconds, which is slightly better than those of the other compounds in Table 1.

To assess the explosive performance of TKX-50 on a small laboratory scale, a small-scale reactivity test (SSRT) was carried out (see ESI†) in comparison to CL-20 and RDX. Here, a defined volume of the explosive is pressed into a perforated steel block, which is topped with a commercially available detonator (Orica, DYNADET-C2-0ms). Initiation of the tested explosive results in denting a separate aluminium block, which is placed right underneath the steel block (Fig. 2). From measuring the volumes of the dents ($\text{CL-20} \geq \text{TKX-50} \gg \text{RDX}$) (Table 2 in the ESI†), it can be concluded that the small scale explosive performance of TKX-50 exceeds the performance of commonly used RDX and is comparable to that of CL-20.

The performance and safety characteristics for shipping of an explosive can be related to the data obtained from the Koenen test.^{18,19} The explosive is placed in an open-ended, flanged steel tube, which is locked up with a closing plate with variable orifice (0–10 mm), through which gaseous decomposition products are

Table 1 Energetic properties and detonation parameters of prominent high explosives in comparison to TKX-50

	2,4,6-TNT	RDX	β -HMX	ϵ -CL-20	TKX-50
Formula	$\text{C}_7\text{H}_5\text{N}_3\text{O}_6$	$\text{C}_3\text{H}_6\text{N}_6\text{O}_6$	$\text{C}_4\text{H}_8\text{N}_8\text{O}_8$	$\text{C}_6\text{H}_6\text{N}_{12}\text{O}_{12}$	$\text{C}_2\text{H}_8\text{N}_{10}\text{O}_4$
Molecular mass [g mol^{-1}]	227.13	222.12	296.16	438.19	236.15
IS [J] ^a	15 ²¹	7.5 ²¹	7 ²¹	4 ²¹	20
FS [N] ^b	353	120 ²¹	112 ²¹	48 ²¹	120
ESD-test [J] ^c	—	0.20	0.20	0.13	0.10
N [%] ^d	18.50	37.84	37.84	38.3	59.3
Q [%] ^e	−73.96	−21.61	−21.61	−10.95	−27.10
T_m [$^\circ\text{C}$] ^f	81	205 ²²	275 ²⁴	—	—
T_{dec} [$^\circ\text{C}$] ^f	290	210 ²⁴	279 ²⁴	215 ²³	221
Density [g cm^{-3}] ^g	1.713 (100 K) ²⁴ 1.648 (298 K) ²⁵	1.858 (90 K) ²⁶ 1.806 (298 K) ²⁷	1.944 (100 K) ²⁸ 1.904 (298 K) ²⁸	2.083 (100 K) ²⁹ 2.035 (298 K) ²⁹	1.918 (100 K) ³⁰ 1.877 (298 K) ³⁰
Theor. $\Delta_f H^\circ$ [kJ mol^{-1}] ^h	−55.5	86.3	116.1	365.4	446.6
Theor. $\Delta_f U^\circ$ [kJ kg^{-1}] ⁱ	−168.0	489.0	492.5	918.7	2006.4
<i>EXPLO5.05 values</i>					
$-\Delta_E U^\circ$ [kJ kg^{-1}] ^j	5258	6190	6185	6406	6025
T_E [K] ^k	3663	4232	4185	4616	3954
p_{C-J} [kbar] ^l	235	380	415	467	424
D [m s^{-1}] ^m	7459	8983	9221	9455	9698
Gas vol. [L kg^{-1}] ⁿ	569	734	729	666	846
I_S [s] ^o	205	258	258	251	261

^a Impact sensitivity (BAM drophammer (1 of 6)). ^b Friction sensitivity (BAM friction tester (1 of 6)). ^c Electrostatic discharge device (OZM research). ^d Nitrogen content. ^e Oxygen balance ($Q = (xO - 2yC - 1/2zH)M/1600$). ^f Decomposition temperature from DSC ($\beta = 5^\circ\text{C min}^{-1}$). ^g From X-ray diffraction. ^h Calculated (CBS-4M method) enthalpy of formation. ⁱ Calculated energy of formation. ^j Energy of explosion. ^k Explosion temperature. ^l Detonation pressure. ^m Detonation velocity. ⁿ Volume of detonation gases (assuming only gaseous products). ^o Specific impulse using isobaric (60 bar) conditions.

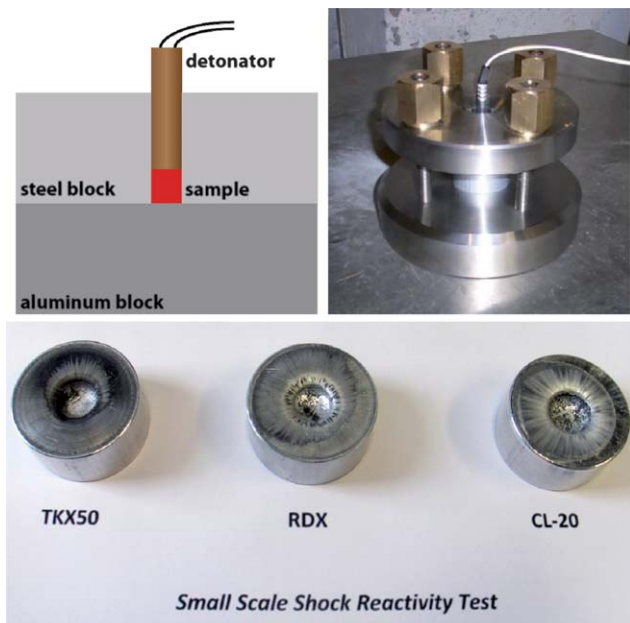


Fig. 2 Small-scale reactivity test of TKX-50, RDX and CL-20. Above pictures: test setup for the SSRT. Below: dented aluminium blocks after initiation of the explosive with a commercial detonator.

vented. A defined volume of 25 mL of the compound is loaded into the flanged steel tube and a threaded collar is slipped onto the tube from below. The closing plate is fitted over the flanged tube and secured with a nut. The decomposition is initiated *via* thermal ignition using four Bunsen burners, which are ignited simultaneously. The test is completed when either rupture of the tube or no reaction is observed after heating the tube for a minimal time period of at least 5 min. In the case of the tube's rupture, the fragments are collected and weighed. The reaction is evaluated as an explosion if the tube is destroyed into three or more pieces. The Koenen test was performed with 23.0 g of TKX-50 using a closing plate with an orifice of 10 mm and caused the rupture of the steel tube into approximately 100 pieces, the size of which reached down to smaller than 1 mm from 40 mm (Fig. 3).

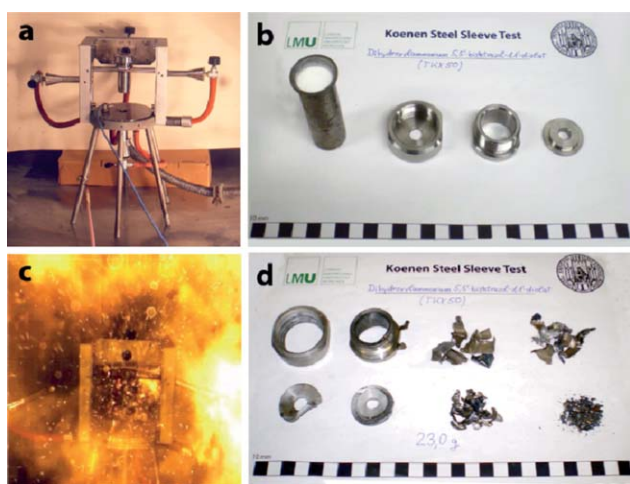


Fig. 3 a) Koenen test experimental setup. (b) Parts of the Koenen steel sleeve before and (d) after the test. (c) Moment of detonation.

TNT destroys the steel tube up to an orifice width of 6 mm, RDX even up to 8 mm.²⁰ In order to get an “Interim Hazard Classification” also a “Fast Cook-Off test” (UN test 3d) was performed in which TKX-50 underwent controlled deflagration (no explosion occurred).

High safety – low sensitivity

Impact sensitivity is a high priority in explosive devices used in the military due to the range of stresses devices may be exposed to. The impact sensitivity of TKX-50 is 20 J which is much lower than those for RDX, HMX and CL-20, which range from 4 to 7.5 J, and all three of which need desensitizing components added for practical use. The low impact sensitivity of TKX-50 shows that it can be used without desensitization.

Friction sensitivity is more important in the manufacturing context, where TKX-50 with 120 N is of comparable or lower sensitivity than any of RDX, HMX or CL-20, increasing the margin of safety in the industrial context. Both the impact and friction sensitivities of TKX-50 as compared to 2,4,6-trinitrotoluene (TNT), RDX, HMX and CL-20 are presented in Table 1.

The human body can generate up to 25 mJ of static electricity, which can easily set off the most sensitive explosives such as lead azide or silver fulminate. TKX-50 has an electrostatic sensitivity of 0.100 J, which is far higher than the human body can generate, allowing a comparable margin of safety when handling, comparable to RDX or HMX.

Thermal stability is important for any explosive in practical use as demanding military requirements need explosives that can withstand high temperatures. For example, a munition sitting in the desert can exceed 100 °C and for general use a component explosive must be stable above 200 °C. TKX-50 with a decomposition onset of 222 °C easily surpasses this requirement (Fig. 4, inset). This stability has been confirmed using a long-term stability test, where the sample is heated in an open glass vessel to a temperature of 75 °C over 48 h to ensure safe handling of the material even at elevated temperatures (Fig. 4, outer curve). The lack of exothermic or endothermic events in the sample temperature or heat flow curve implies that the compound is stable.

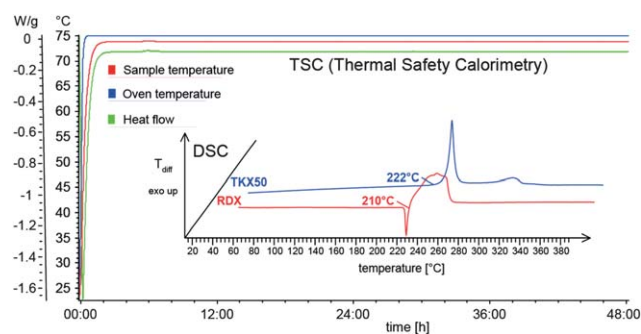


Fig. 4 Outer curve: long term stability (TSC plot) of TKX-50 at a temperature of 75 °C over a period of 48 h. Inner plot: thermal stability of TKX-50 and RDX shown in the DSC plot (heating rate 5 °C min⁻¹).

Toxicity – environmentally friendly

One of the major aims in our search for new “green” energetic materials is the low toxicity of the newly investigated compound

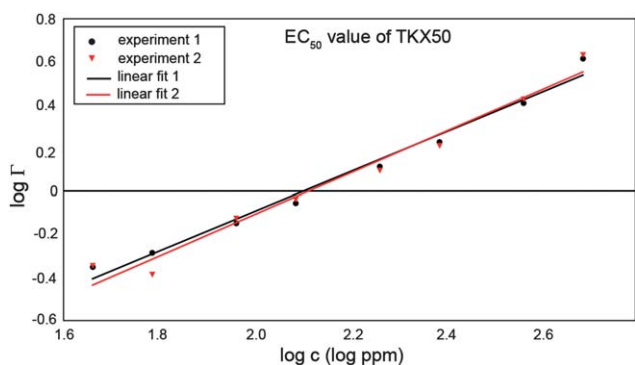


Fig. 5 Toxicity assessment of TKX-50 using a luminescent bacteria inhibition test. Plot of $\log I$ against $\log c$ for determination of the EC_{50} value.

itself, and of its degradation and decomposition products. In recent times the toxicity of energetic materials is a growing concern due to new understandings of the fate of explosives in the environment. The nitramine content of the ubiquitous RDX as well as less used HMX and CL-20 has been shown to be toxic to vital organisms at the base of the food chain, and in addition RDX is a probable human carcinogen. To assess the toxicity of TKX-50 to aquatic life, diluted aqueous solutions of the high explosive were subjected to the luminescent marine bacterium *Vibrio fischeri* using the commercially available bioassay system LUMISTox®. *Vibrio fischeri* is a representative species for other aquatic life and therefore a useful indicator when it comes to groundwater pollution. Being the most important toxicological parameter, the EC_{50} value of the sample was determined. EC_{50} is the effective concentration of the examined compound, at which the bioluminescence of the strain *Vibrio fischeri* is decreased by 50% after a defined period of exposure as compared to the original bioluminescence of the sample before being treated with the differently diluted solutions of the test compound. For RDX we observe an EC_{50} value of 91 ppm after an incubation time of 30 minutes. The herein determined EC_{50} value of TKX-50 of 130 ppm (Fig. 5 and ESI†) lies significantly above the EC_{50} value found for RDX indicating a lower toxicity to *Vibrio fischeri*, and as such, other aquatic life.

Conclusions

We have detailed the preparation of a new explosive, TKX-50 or dihydroxylammonium 5,5'-bistetrazole-1,1'-diolate. This material has exemplified the utility of the tetrazole N-oxide chemistry by providing a new explosive material that is of very high performance (as calculated and demonstrated by SSRT testing), pushing the limits towards the most powerful explosives known, and synthesized in an industrially viable process. Additionally, TKX-50 is of lower sensitivity (mechanically and thermally) than its contemporaries in currently used explosives such as RDX, HMX and CL-20, making increased margins of safety when applied in practical use and devices. Finally, we have demonstrated the lower toxicity of TKX-50 compared to the nitramine RDX, as determined by the EC_{50} value for the decrease in luminescence of *Vibrio fischeri*. All of the characteristics of TKX-50 make it appropriate and exemplary to not just fulfill the long-standing goal of a “green” RDX replacement, but also to replace it with a material of superior performance.

Acknowledgements

Financial support of this work by the Ludwig-Maximilian University of Munich (LMU), the U.S. Army Research Laboratory (ARL), the Armament Research, Development and Engineering Center (ARDEC), the Strategic Environmental Research and Development Program (SERDP) and the Office of Naval Research (ONR) is acknowledged. Furthermore, the authors acknowledge the contributions of Stefan Huber, Susanne Scheutzw, Dr Karin Lux, Sebastian Rest, Marius Reymann and Fabian Wehnekamp.

Notes and references

- 1 M. Göbel, B. H. Tchitchanov, J. S. Murray, P. Politzer and T. M. Klapötke, *Nat. Chem.*, 2009, **1**, 229–235.
- 2 M. Göbel, K. Karaghiosoff, T. M. Klapötke, D. G. Piercy and J. Stierstorfer, *J. Am. Chem. Soc.*, 2010, **132**, 17216–17226.
- 3 H. Gao and J. M. Shreeve, *Chem. Rev.*, 2011, **111**, 7377–7436.
- 4 Y.-C. Li, C. Qi, S.-H. Li, H.-J. Zhang, C.-H. Sun, Y.-Z. Yu and S.-P. Pang, *J. Am. Chem. Soc.*, 2010, **132**, 12172–12173.
- 5 T. M. Klapötke and D. G. Piercy, *Inorg. Chem.*, 2011, **50**, 2732–2734.
- 6 V. Thottempudi and J. M. Shreeve, *J. Am. Chem. Soc.*, 2011, **133**, 19982–19992.
- 7 T. M. Klapötke, D. G. Piercy and J. Stierstorfer, *Chem.–Eur. J.*, 2011, **17**, 13068–13077.
- 8 J. L. Gay-Lussac, *Ann. Chem. Phys.*, 1824, **27**, 199.
- 9 J. Berzelius, *Justus Liebigs Ann. Chem.*, 1844, **50**, 426–429.
- 10 J. L. Gay-Lussac and J. Liebig, *Kastners Archiv.*, 1824, **II**, 58–91.
- 11 A. M. Churakov and V. A. Tartakovskiy, *Chem. Rev.*, 2004, **104**, 2601–2616.
- 12 A. M. Churakov, O. Y. Smirnov, S. L. Ioffe, Y. A. Strelenko and V. A. Tartakovskiy, *Eur. J. Org. Chem.*, 2002, 2342–2349.
- 13 L. A. Burke and P. J. Fazen, *Int. J. Quantum Chem.*, 2009, **109**, 3613–3618.
- 14 R. A. Carboni, J. C. Kauer, J. E. Castle and H. E. Simmons, *J. Am. Chem. Soc.*, 1967, **89**, 2618–2625.
- 15 M.-X. Zhang, P. E. Eaton and R. Gilardi, *Angew. Chem., Int. Ed.*, 2000, **39**, 401–404.
- 16 I. V. Tselinskii, S. F. Mel'nikova and T. V. Romanova, *Russ. J. Org. Chem.*, 2001, **37**, 430–436.
- 17 N. Fischer, D. Izsák, T. M. Klapötke, S. Rappenglück and J. Stierstorfer, *Chem.–Eur. J.*, 2012, **18**, 4051–4062.
- 18 R. C. West and S. M. Selby, *Handbook of Chemistry and Physics*, The Chemical Rubber Co., Cleveland, 48th edn, 1967, pp. D22–D51.
- 19 V. A. Ostrovskii, M. S. Pevzner, T. P. Kofman and I. V. Tselinskii, *Targets Heterocycl. Syst.*, 1999, **3**, 467–526.
- 20 J. Köhler and R. Meyer, *Explosivstoffe*, Wiley-VCH, Weinheim, 9th edn, 1998, pp. 166–168.
- 21 R. Mayer, J. Köhler and A. Homburg, *Explosives*, Wiley-VCH, Weinheim, 5th edn, 2002.
- 22 J. P. Agrawal, *High Energy Materials*, Wiley-VCH, Weinheim, 1st edn, 2010, p. 189.
- 23 R. Turcotte, M. Vachon, Q. S. M. Kwok, R. Wang and D. E. G. Jones, *Thermochim. Acta*, 2005, **433**, 105–115.
- 24 R. M. Vrcelj, J. N. Sherwood, A. R. Kennedy, H. G. Gallagher and T. Gelbrich, *Cryst. Growth Des.*, 2003, **3**, 1027–1032.
- 25 N. I. Golovina, A. N. Titkov, A. V. Raevskii and L. O. Atovmyan, *J. Solid State Chem.*, 1994, **113**, 229–238.
- 26 P. Hakey, W. Ouellette, J. Zubietta and T. Korter, *Acta Crystallogr., Sect. E: Struct. Rep. Online*, 2008, **64**(8), o1428.
- 27 C. S. Choi and E. Prince, *Acta Crystallogr., Sect. B: Struct. Crystallogr. Cryst. Chem.*, 1972, **28**, 2857.
- 28 J. R. Deschamps, M. Frisch and D. Parrish, *J. Chem. Crystallogr.*, 2011, **41**, 966–970.
- 29 N. B. Bolotina, J. M. Hardie, R. L. Speer Jr and A. A. Pinkerton, *J. Appl. Crystallogr.*, 2004, **37**, 808–814.
- 30 X-ray density (for details see CCDC 872231 and 872232).

Pushing the Limits of Energetic Materials - The synthesis and characterization of dihydroxylammonium 5,5'-bistetrazole-1,1'-diolate

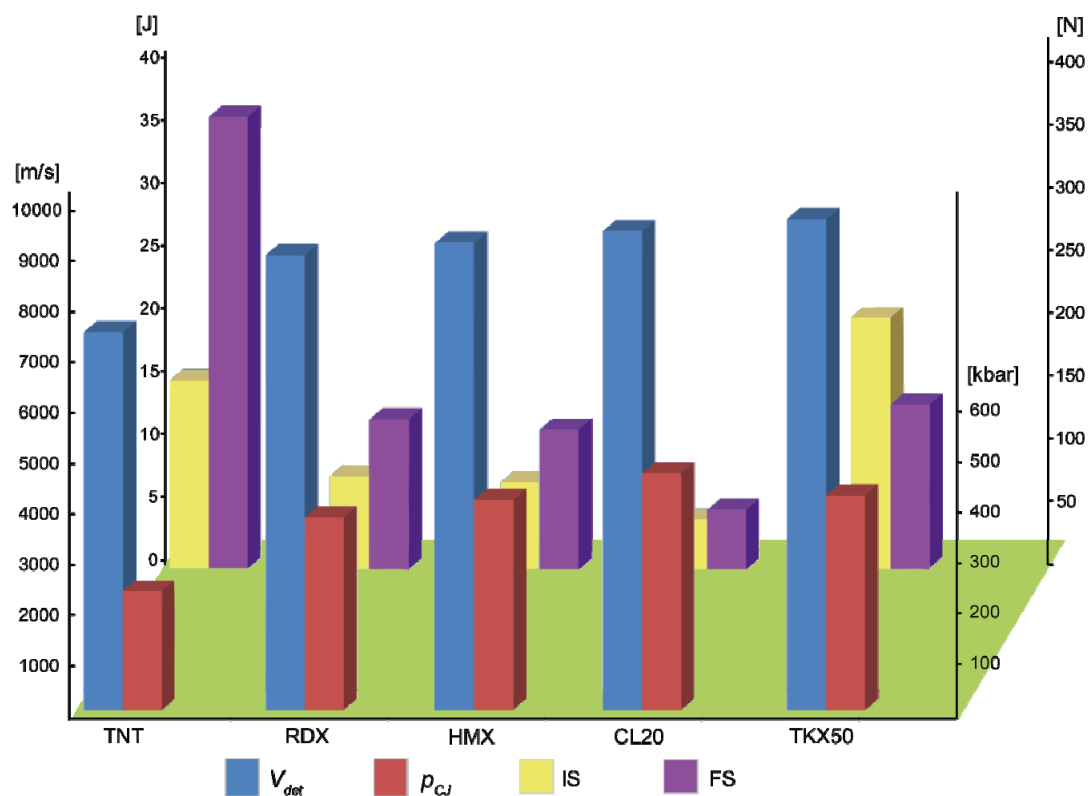
Niko Fischer, Dennis Fischer, Thomas M. Klapötke,* Davin G. Piercey and Jörg Stierstorfer

Energetic Materials Research, Department of Chemistry,

University of Munich (LMU), Butenandtstr. 5-13, D-81377, Germany

Fax: +49 89 2180 77492

E-mail: tmk@cup.uni-muenchen.de



Graphical comparison of the energetic properties of TKX-50 with commonly used explosives (TNT, RDX, HMX, CL-20)

Table of contents

- 1. Materials and Methods**
 - 1.1. NMR spectroscopy**
 - 1.2. Vibrational spectroscopy**
 - 1.3. Mass spectrometry and elemental analysis**
 - 1.4. Differential scanning calorimetry**
 - 1.5. Sensitivity testing**
- 2. Experimental work**
 - 2.1. Synthesis via oxidation of 5,5'-bistetrazole with potassium peroxydisulfate**
 - 2.2. Synthesis via cyclization of diazidoglyoxime**
 - 2.3. Safer synthesis including a multi-step one pot reaction**
- 3. X-ray diffraction**
 - 3.1. Instrument and refinement software**
 - 3.2. Crystallographic data and refinement parameters**
 - 3.3. Bond lengths, bond angles and hydrogen bonding of TKX-50**
 - 3.4. Crystal structures of 5,5'-bistetrazole-1,1'-diol**
 - 3.5. Crystal structure of dimethylammonium 5,5'-bistetrazole-1,1'-diolate**
- 4. Explosive performance**
 - 4.1. Heat of formation calculations**
 - 4.2. Small scale shock reactivity test**
 - 4.3. Flame test**
 - 4.4. Hot plate test**
- 5. Toxicity assessment**
- 6. Fast Cook-Off Test**

1. Materials and Methods

Caution! 5,5'-Bistetrazole-1,1'-diol and its salts are energetic materials with increased sensitivities towards shock and friction. Therefore, proper security precautions (safety glass, face shield, earthened equipment and shoes, Kevlar gloves and ear plugs) have to be applied while synthesizing and handling the described compounds. Specifically, compounds described having the azido group are extremely sensitive and have to be handled very carefully.

All chemicals and solvents were employed as received (Sigma-Aldrich, Fluka, Acros) without further purification unless otherwise stated.

1.1. NMR spectroscopy

^1H and ^{13}C NMR spectra were recorded using a JEOL Eclipse 270, JEOL EX 400 or a JEOL Eclipse 400 instrument. The chemical shifts quoted in ppm in the text refer to tetramethylsilane (^1H , ^{13}C).

1.2. Vibrational spectroscopy

Infrared spectra were measured using a Perkin Elmer Spectrum One FT-IR spectrometer as KBr pellets. Raman spectra were recorded on a Bruker MultiRAM Raman Sample Compartment D418 equipped with a Nd-YAG-Laser (1064 nm) and a LN-Ge diode as detector.

1.3. Mass spectrometry and elemental analysis

Mass spectra of the described compounds were measured at a JEOL MStation JMS 700 using either DEI or FAB technique. To measure elemental analyses a Netsch STA 429 simultaneous thermal analyzer was employed.

1.4. Differential scanning calorimetry

Differential scanning calorimetry (DSC) measurements to determine the melt- and decomposition temperatures of **2–9** (about 1.5 mg of each energetic material) were performed in covered Al-containers containing a hole (0.1 mm) in the lid for gas release and a nitrogen flow of 20 mL per minute on a Linseis PT 10 DSC¹ calibrated with standard pure indium and zinc at a heating rate of 5°C min⁻¹.

1.5. Sensitivity testing

The impact sensitivity tests were carried out according to STANAG 4489² modified instruction³ using a BAM (Bundesanstalt für Materialforschung) drophammer.⁴ The friction sensitivity tests were carried out according to STANAG 4487⁵ modified instruction⁶ using the BAM friction tester. The classification of the tested compounds results from the “UN Recommendations on the Transport of Dangerous Goods”.⁷ Additionally all compounds were tested upon the sensitivity towards electrical discharge using the Electric Spark Tester ESD 2010 EN.⁸

2. Experimental work

2.1. Synthesis of TKX-50 via oxidation of 5,5'-bistetrazole with potassium peroxymonosulfate

5,5'-Bistetrazole (3.00 g, 21.7 mmol) was dissolved in 200 mL of water. Oxone (80.0 g, 109 mmol, 5eq.) was added to the clear solution and the resulting solution was buffered with trisodium phosphate to pH 7. The mixture turned to a pink color, as soon as the pH exceeds a certain value. The mixture was stirred at room temperature for 5 h, was then acidified with conc. sulfuric acid and extracted into diethyl ether. Evaporation of the solvent gave the raw product as a slightly yellow solid, which can be recrystallized from methanol to remove remaining sulfates or phosphates. The reaction yielded a mixture of the 1,1'-isomer, the 2,2'-isomer and the 1,2'-isomer in overall 71% yield (2.60 g, 15.3 mmol) with the 2,2'-isomer being the main product. The isomer mixture (1.70 g, 10 mmol) was

dissolved in 20 mL of hot water. An aqueous solution of hydroxylamine (50% w/w, 1.32 g, 20 mmol) was added and a colorless precipitate formed instantly. The precipitate was redissolved by warming the mixture and the product, which is the dihydroxylammonium salt of the 1,1'-isomer started to precipitate again. It was filtered off and recrystallized from water to remove the salt of the remaining 2,2'-isomer, which showed better solubility in water. Due to the predominant formation of the 2,2'-isomer via the oxidation with oxone, the dihydroxylammonium salt of the 1,1'-isomer could only be obtained in minor yields (0.31 g, 1.3 mmol, 13%).

2.2. Synthesis of TKX-50 via isolation of diazidoglyoxime

Glyoxime

27.5 g (0.69 mol) of NaOH was dissolved in 75 mL of water and the solution was cooled to 0°C in a salt-ice bath. Hydroxylammonium chloride (69.5 g, 1.00 mol) was added while stirring. To the obtained solution glyoxal (72.5 g, 0.50 mol, 40% w/w in H₂O) was added, while the temperature is kept below 10 °C. After complete addition of the glyoxal the solution was further chilled in the salt-ice bath until glyoxime precipitated. The solid was removed by suction filtration and washed with only little ice-water to remove remaining sodium chloride.

¹H NMR (270 MHz, DMSO-*d*₆, 25 °C, ppm) δ: 7.73, 11.61; ¹³C{¹H} NMR (270 MHz, DMSO-*d*₆, 25 °C, ppm) δ: 145.9; EA (found, calc. for C₂H₄N₂O₂, MW = 88.07): C (27.07, 27.28), H (4.69, 4.58), N (31.45, 31.81) %.

Dichloroglyoxime

17.6 g (200 mmol) of glyoxime was suspended in 200 mL of ethanol. Chlorine was bubbled through the suspension at -20 °C until the green suspension turned into a yellowish solution. The solution was allowed to warm up slowly to room temperature meanwhile releasing dissolved chlorine. Then the solvent was removed under vacuum and the remaining solid was resuspended in 50 mL of chloroform, stirred for 15 min at room temperature and filtered yielding 26.6 g (85 %) of the colorless product.

¹H NMR (270 MHz, DMSO-*d*₆, 25 °C, ppm) δ: 13.10; ¹³C{¹H} NMR (270 MHz, DMSO-*d*₆, 25 °C, ppm) δ: 131.2; EA (found, calc. for C₂H₂Cl₂N₂O₂, MW = 156.96): C (15.65, 15.30), H (1.25, 1.28), N (17.49, 17.85) %.

Diazidoglyoxime

784 mg (5 mmol) of dichloroglyoxime was dissolved in 10 mL of dimethyl formamide. At 0 °C 841 mg (12.93 mmol) sodium azide was added. The suspension was stirred for 20 min at 0 °C and 100 mL of water was added. The precipitate was filtered, washed with 20 mL of water and air dried yielding 713 mg (84%) of the colorless product.

DSC (5 °C min⁻¹): 170 °C (dec.); IR (atr, cm⁻¹): $\tilde{\nu}$ = 3209 (w), 2170 (w), 2123 (w), 1622 (w), 1400 (w), 1361 (w), 1286 (m), 1013 (vs), 930 (m), 920 (s), 855 (s), 731 (s); Raman (1064 nm, 300 mW, 25 °C, cm⁻¹): $\tilde{\nu}$ = 2166 (8), 2129 (5), 2091 (3), 1621 (100), 1457 (14), 1390 (12), 1216 (19), 1034 (3), 882 (20), 672 (3), 442 (6); ¹H NMR (270 MHz, DMSO-*d*₆, 25 °C, ppm) δ : 12.08; ¹³C{¹H} NMR (270 MHz, DMSO-*d*₆, 25 °C, ppm) δ : 136.5; EA (found, calc. for C₂H₂N₈O₂, MW = 170.09): C (14.38, 14.12), H (1.46, 1.19), N (66.01, 65.88) %; BAM drophammer: 1.5 J; friction tester: <5 N; ESD: 7 mJ.

5,5'-Bistetrazole-1,1'-diol dihydrate

850 mg (5 mmol) of diazidoglyoxime was suspended in 40 mL of diethyl ether. Gaseous HCl was bubbled through the reaction mixture at 0 to 5 °C while stirring for 2 hours and then the flask was sealed and stirred at room temperature overnight. The solution was allowed to stand for crystallization yielding 760 mg (73 %) of 5,5'-bistetrazole-1,1'-diol dihydrate as pale yellow crystals.

DSC (5 °C min⁻¹): 214 °C (dec.); IR (atr, cm⁻¹): $\tilde{\nu}$ = 3229 (m), 1665 (m), 1411 (w), 1375 (w), 1302 (w), 1208 (w), 1144 (m), 995 (s), 714 (w), 662 (w); Raman (1064 nm, 300 mW, 25 °C, cm⁻¹): $\tilde{\nu}$ = 1608 (100), 1270 (26), 1157 (46), 1133 (38), 1019 (22), 766 (31), 738 (13), 693 (4), 597 (6), 402 (29); ¹H NMR (400 MHz, DMSO-*d*₆, 25 °C, ppm) δ : 6.80; ¹³C{¹H} NMR (400 MHz, DMSO-*d*₆, 25 °C, ppm) δ : 135.8; EA (found, calc. for C₂H₆N₈O₄, MW = 206.12): C (12.01, 11.65), H (2.81, 2.93), N (54.04, 54.36) %; BAM drophammer: >40 J; friction tester: 216 N; ESD: 0.5 J.

Dihydroxylammonium 5,5'-bistetrazole-1,1'-diolate (TKX-50)

5,5'-Bistetrazole-1,1'-diol dihydrate (2.06 g, 10 mmol) was dissolved in 50 mL of warm water. Hydroxylamine (1.32 g, 20 mmol, 50% w/w in H₂O) was added while stirring. Cooling down the solution to room temperature forced the dihydroxylammonium salt to crystallize. It was isolated by suction filtration and air dried. (Yield: 82%).

DSC (5 °C min⁻¹, °C): 221°C (dec.); IR (KBr, cm⁻¹): $\tilde{\nu}$ = 3425 (m), 3219 (s), 3081 (s), 3050 (s), 2936 (s), 2689 (s), 2513 (m), 1599 (m), 1577 (m), 1527 (s), 1426 (s), 1413 (s), 1389 (m), 1352 (m), 1338 (m), 1316 (w), 1236 (vs), 1174 (m), 1145 (w), 1095 (w), 1046 (w), 1029 (w), 1011 (m), m997 (m), 800 (m), 723 (m), 676 (w), 612 (w), 579 (w), 539 (w), 498 (w); Raman (1064 nm, 300 mW, 25 °C, cm⁻¹): $\tilde{\nu}$ = 1616 (100), 1469 (3), 1278 (2), 1239 (25), 1173 (2), 1143 (6), 1116 (10), 1014 (7), 1004 (12), 763 (4), 612 (3), 409 (4), 335 (2), 257 (2), 199 (2); ¹H NMR (400 MHz, DMSO-*d*₆, 25 °C, ppm) δ : 9.66 (s, 8H, NH₃OH); ¹³C{¹H} NMR (400 MHz, DMSO-*d*₆, 25 °C, ppm) δ : 135.5 ((CN₄)₂); m/z (FAB⁺): 34.0 [NH₃OH⁺]; m/z (FAB⁻): 169.1 [C₂HN₈O₂⁻]; EA (found, calc. For C₂H₈N₁₀O₄, MW = 236.15): C (10.50, 10.17), H (3.63, 3.41), N (59.31, 59.31) %; BAM drophammer: 20 J; friction tester: 120 N; ESD: 0.11 J (at grain size <100 μ m).

2.3. Safer synthesis including a multi-step one pot reaction

DMF-route:

Dichloroglyoxim (785 mg, 5 mmol) was dissolved in 10 mL of DMF at room temperature. The solution is cooled to 0°C and NaN₃ (715 mg, 11 mmol) was added. The mixture was stirred for 40 min at 0°C. NaCl precipitated, whereas diazidoglyoxim stayed in solution. The mixture was transferred to a flask containing 100 mL of diethyl ether, which was cooled to 0°C in a salt-ice bath. HCl was bubbled through the suspension maintaining the temperature below 20 °C, until saturation of the diethyl ether indicated by a drop of the temperature back to 0-5 °C was reached. A precipitate, which was formed during the reaction first agglomerates and then was resuspended, once the mixture was saturated with HCl. The flask was stoppered tightly and the reaction mixture was stirred overnight at room temperature under a slight overpressure of HCl, which formed upon warming the mixture to room temperature. The pressure was released and the mixture was poored into an open dish for evaporation either overnight at room temperature or in 1-2 h at 50°C. After most of the diethyl ether was evaporated, 50 mL of water was added resulting in a clear solution. The water was evaporated on a rotary evaporator and the remaining DMF was removed under high vacuum, yielding crude dimethylammonium 5,5'-bistetrazole-1,1'-diolate as a colorless solid. The solid was dissolved in the smallest possible volume of boiling water (app. 10 mL) and hydroxylammonium chloride (750 mg, 10.8 mmol, 2.16 eq.) as a concentrated aqueous solution was added. TKX-50 precipitated from the

solution in 74.6 % yield (882 mg, 3.73 mmol), which was isolated by suction filtration, washed with cold water and air dried.

NMP-route:

Dichloroglyoxime (785 mg, 5 mmol) was dissolved in 10 mL of NMP at room temperature. The solution was cooled to 0 °C and NaN₃ (715 mg, 11 mmol) was added. The mixture was stirred for 40 min at 0 °C. NaCl precipitated, whereas diazidoglyoxime stayed in solution. The mixture was transferred to a flask containing 150 mL of diethyl ether, which was then cooled to 0 °C in a salt-ice bath. HCl was bubbled through the suspension maintaining the temperature below 20 °C, until saturation of the diethyl ether, as indicated by a drop of the temperature back to 0-5 °C, was reached. A thick precipitate, which was formed during the reaction first agglomerated and then was resuspended, once the mixture was saturated with HCl. The flask was stoppered tightly and the reaction mixture was stirred overnight at room temperature under a slight overpressure of HCl, resultant from warming the mixture to room temperature. The pressure was released and the mixture was poured into an open dish for evaporation either overnight at room temperature or in 1-2 h at 50 °C. After evaporation of the diethyl ether and HCl, 50 mL H₂O was added and the mixture was evaporated on a rotary evaporator to completely remove HCl and diethyl ether. The thick, colorless residue containing 5,5'-bistetrazole-1,1'-diol in NMP was taken up in 20 mL of 2M NaOH, whereas the di-sodium salt of 5,5'-bistetrazole-1,1'-diol started to precipitate. The mixture was heated to reflux and upon cooling, the disodium salt precipitated almost quantitatively (90% yield starting from dichloroglyoxime). After isolation of the disodium salt, the solid was dissolved in minimal boiling water (ca. 10 mL) and hydroxylammonium chloride (750 mg, 10.8 mmol, 2.16 eq.) as a concentrated aqueous solution was added. TKX-50 precipitated from the solution in 85.1 % yield (1.00 g, 4.25 mmol), which was isolated by suction filtration, washed with cold water and air dried.

3. X-ray diffraction

3.1. Instrument and refinement software

Suitable single crystal of TKX-50 and its precursors were picked from the crystallization mixture and mounted in Kel-F oil, transferred to the N₂ stream of an Oxford Xcalibur3 diffractometer with a Spellman generator (voltage 50 kV, current 40 mA) and a KappaCCD detector. The data collection was performed using the CRYCALIS CCD software⁹, the data reduction using the CRYCALIS RED software¹⁰. The structures were solved with SIR-92¹¹, refined with SHELXL-97¹² and finally checked using the PLATON software¹³ integrated in the WINGX software suite.¹⁴ The non-hydrogen atoms were refined anisotropically and the hydrogen atoms were located and freely refined. The absorptions were corrected using a SCALE3 ABSPACK multi-scan method.¹⁵ Data and parameters of the X-ray measurements and solutions are gathered in Table S1.

3.2. Crystallographic data and refinement parameters

Table S1. Crystallographic data and refinement parameters

	TKX-50 (100K)	TKX-50 (173K)	TKX-50 (298K)	I-BTO*2H ₂ O	I-BTO*2MeOH	Me ₂ H ₂ N ₂ BTO
Formula	C ₂ H ₈ N ₁₀ O ₄	C ₂ H ₈ N ₁₀ O ₄	C ₂ H ₈ N ₁₀ O ₄	C ₂ H ₆ N ₈ O ₄	C ₄ H ₁₀ N ₈ O ₄	C ₄ H ₆ N ₈ O ₂
Form. weight [g mol ⁻¹]	236.18	236.18	236.18	206.12	234.20	215.20
Crystal system	Monoclinic	Monoclinic	Monoclinic	Monoclinic	Orthorhombic	Orthorhombic
Space Group	<i>P2₁/c</i>	<i>P2₁/c</i>	<i>P2₁/c</i>	<i>C2/m</i> (No. 12)	<i>Pbca</i> (No. 61)	<i>Pbca</i> (No. 61)
Color / Habit	Colorless Blocks	Colorless Block	Colorless Block	Colorless Block	Colorless Block	Colorless Plate
Size, mm	0.25 x 0.30 x 0.40	0.17 x 0.21 x 0.27	0.10 x 0.25 x 0.40	0.13 x 0.18 x 0.20	0.31 x 0.35 x 0.43	0.12 x 0.20 x 0.20
<i>a</i> [Å]	5.4872(8)	5.4260(5)	5.4408(6)	7.7443(3)	7.6818(10)	11.660(2)
<i>b</i> [Å]	11.5472(15)	11.6597(12)	11.7514(13)	6.2459(3)	6.7692(12)	8.7050(17)
<i>c</i> [Å]	6.4833(9)	6.5013(7)	6.5612(9)	8.7000(3)	18.884(3)	18.028(3)
<i>α</i> [°]	90	90	90	90	90	90
<i>β</i> [°]	95.402(12)	95.256(9)	95.071(11)	116.052(2)	90	90
<i>γ</i> [°]	90	90	90	90	90	90
<i>V</i> [Å ³]	408.97(10)	409.58(7)	417.86(9)	378.06(3)	982.0(3)	1829.9(6)
<i>Z</i>	2	2	2	2	4	8
<i>ρ</i> _{calc.} [g cm ⁻³]	1.918	1.915	1.877	1.811	1.584	1.562
<i>μ</i> [mm ⁻¹]	0.173	0.173	0.169	0.166	0.138	0.128
<i>F</i> (000)	244	244	244	212	488	896
<i>λ</i> _{MoKα} [Å]	0.71073	0.71073	0.71073	0.71073	0.71073	0.71073
<i>T</i> [K]	100	173	298	173	173	173
Theta Min-Max [°]	4.7, 27.2	4.7, 27.1	4.7, 27.0	4.4, 27.5	4.2, 26.0	4.2, 25.8
Dataset	-6.7; -11.14; -4:8	-5; 6; -9:14; -8:7	-5; 6; -13:15; -8:8	-10:10; -8:8; -11:11	-9:8; -8:8; -14:23	-14:14; -10: 9; -22:16
Reflections collected	1773	2267	1798	1625	4803	8586
Independent reflections	910	901	911	472	968	1741
<i>R</i> _{int}	0.022	0.024	0.017	0.025	0.068	0.063
Observed reflections	769	681	729	460	555	1244
No. parameters	89	89	89	53	968	173
<i>R</i> ₁ (obs)	0.0342	0.0334	0.0344	0.0458	0.0404	0.0437
<i>wR</i> ₂ (all data)	0.0895	0.0856	0.0915	0.1431	0.0891	0.1201
Goof	1.06	0.97	1.02	1.22	0.84	1.08
Resd. Dens. [e/ Å ³]	-0.31, 0.24	-0.19, 0.23	-0.22, 0.23	-0.26, 0.47	-0.22, 0.29	-0.20, 0.24
Device type	Oxford Xcalibur3 CCD	Oxford Xcalibur3 CCD	Oxford Xcalibur3 CCD	Bruker Kappa CCD	Oxford Xcalibur3 CCD	Oxford Xcalibur3 CCD
Solution	SIR-92	SIR-92	SIR-92	SIR-92	SHELXS-97	SHELXS-97
Refinement	SHELXL-97	SHELXL-97	SHELXL-97	SHELXL-97	SHELXL-97	SHELXL-97
Absorption correction	multi-scan	multi-scan	multi-scan	multi-scan	multi-scan	multi-scan
CCDC	872231	872230	872232	884561	884559	884560

3.3. Bond lengths, bond angles and hydrogen bonding of TKX-50

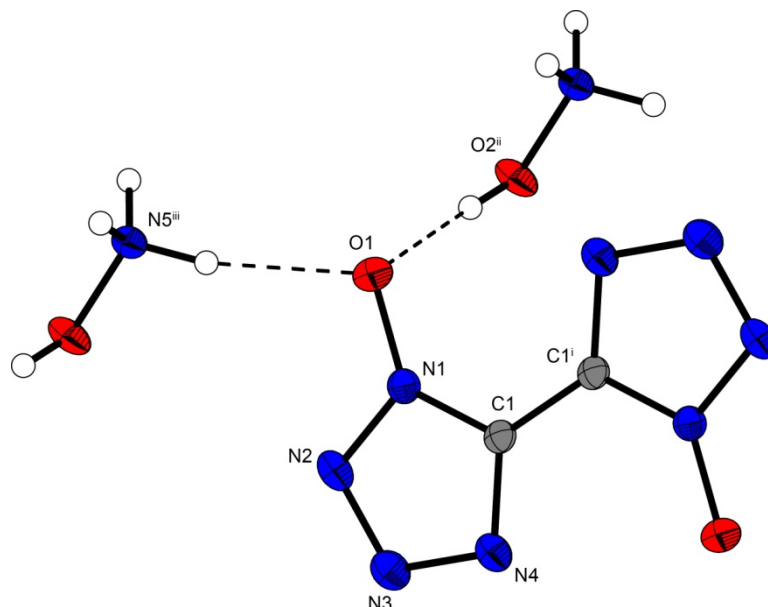


Figure S1. Representation of the solid state molecular structure of TKX-50 at 100 K. Thermal ellipsoids are drawn at the 50% probability level. Selected bond lengths (Å): O1–N1 1.3280(15), N1–N2 1.3424(17), N1–C1 1.3451(18), N2–N3 1.3128(17), N3–N4 1.3513(18), N4–C1 1.3358(19), C1–C1ⁱ 1.445(3), O2–N5 1.4152(15). Selected bond angles (°): O1–N1–N2 122.09(11), O1–N1–C1 129.25(12), N2–N1–C1 108.65(12), N3–N2–N1 106.16(12), N2–N3–N4 111.24(11), C1–N4–N3 105.43(11), N4–C1–N1 108.52(13), N4–C1–C1ⁱ 127.46(16), N1–C1–C1ⁱ 124.02(16); symmetry codes: (i) 2–x, –y, 2–z; (ii) x, 0.5–y, –0.5+z; (iii) –1+x, 0.5–y, –0.5+z. Hydrogen bonds (D–H···A: d(D–H) [Å], d(H···A) [Å], d(D···A) [Å], <(D–H···A) [°]): N5–H5B···O1ⁱ: 0.91(2), 2.15(2), 2.9305(17), 144.1(16); N5–H5B···N4ⁱⁱ: 0.91(2), 2.44(2), 3.0464(18), 124.5(16); N5–H5A···O1 0.93(2), 1.91(2), 2.8327(17), 170.8(18); N5–H5A···N1: 0.93(2), 2.67(2), 3.5481(18), 158.1(15); N5–H5C···O2ⁱⁱⁱ: 0.89(2), 2.21(2), 2.9913(18), 145.9(17); N5–H5C···N3^{iv}: 0.89(2), 2.429(19), 2.9187(17), 115.0(15); O2–H2···O1^v: 0.87(3), 1.74(3), 2.6000(16), 169(3); O2–H2···N1^v: 0.87(3), 2.47(3), 3.2032(16), 142(2); symmetry codes: (i) 1–x, –y, 1–z; (ii) 1+x, y, 1+z; (iii) x, 0.5–y, 0.5+z; (iv) x, y, 1+z; (v) 1+x, y, z.

3.4 Crystal structures of 5,5'-bistetrazole-1,1'-diol

Crystals of 5,5'-bis(1-hydroxy)tetrazole dihydrate (**1,1'BTO·2H₂O**) can be obtained either from water, acetonitrile, glacial acetic acid, ethanol or diethylether. It crystallizes in the monoclinic space group *C2/m* with two molecular units in the unit cell. Its density of 1.811 g cm⁻³ is significantly lower than that of TKX-50 but higher than that of the methanol adduct (1.584 g cm⁻³). The molecular unit is shown in figure S2.

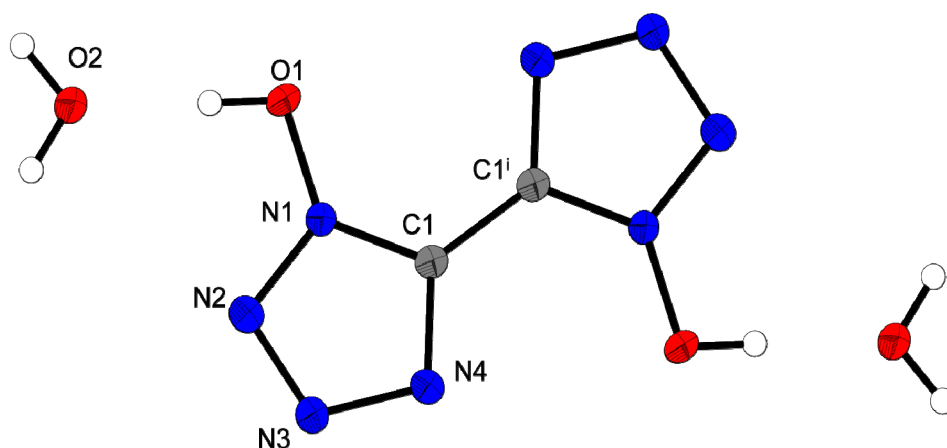


Figure S2 Molecular moiety of 5,5'-bis(1-hydroxy-tetrazole) dihydrate (**1,1'BTO·2H₂O**). Ellipsoids are drawn at the 50 % probability level. (i) 1-x, y, -z. Selected bond lengths (Å): O1–N1 1.340(2), O1–H1 0.84(7), N1–N2 1.332(3), N1–C1 1.338(3), N2–N3 1.304(3), N3–N4 1.353(3), N4–C1 1.334(3), C1–C1ⁱ 1.434(4).

Within the structure layers within the *ac*-plane are formed by an intensive hydrogen bond network depicted Figure S3.

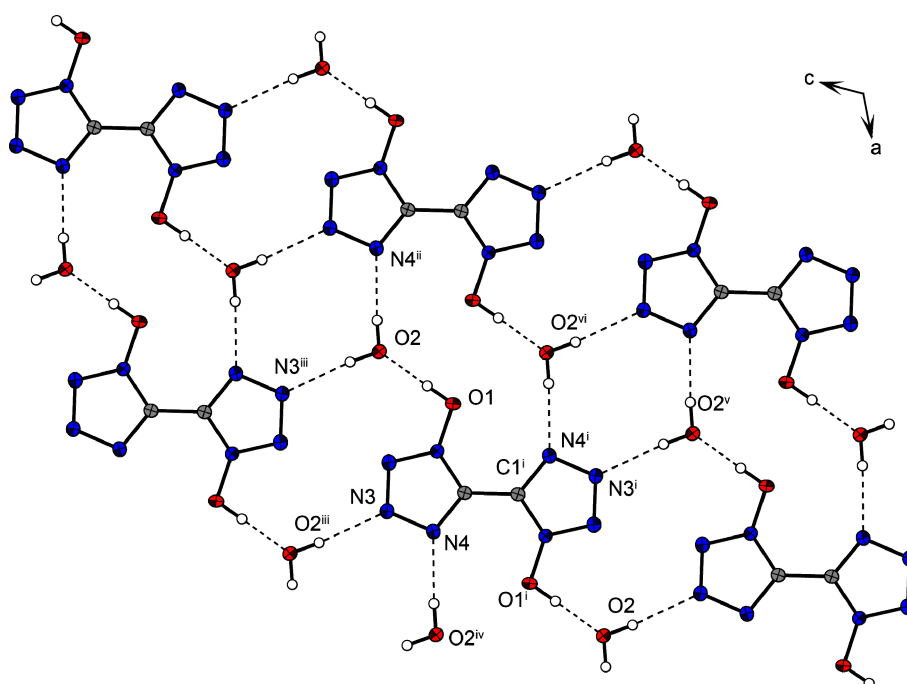


Figure S3 View on a layer within the *ac*-plane showing the intensive hydrogen bond network. Hydrogen bonds (D–H···A: d(D–H) [Å], d(H···A) [Å], d(D···A) [Å], <(D–H···A) [°]): O1–H1···O2 0.84(7), 1.59(8), 2.430(2), 179(8); O2–H2···N4ⁱⁱ 0.84(3), 1.94(3), 2.771(3), 176(5); O2–H3···N3ⁱⁱⁱ 0.830(14), 2.012(11), 2.839(3), 175(4). Symmetry codes: (i) 1-x, y, -z; (ii) -1+x, y, z; (iii) 1-x, y, 1-z; (iv) 1+x, y, z; (v) x, y, -1+z; (vi) -x, y, -z.

Recrystallization from methanol yielded single crystal of 5,5'-bis(1-hydroxy)tetrazole dimethanolate (**1,1'BTO·2MeOH**). The structure of the tetrazolate backbone is similar to that of its dihydrate.

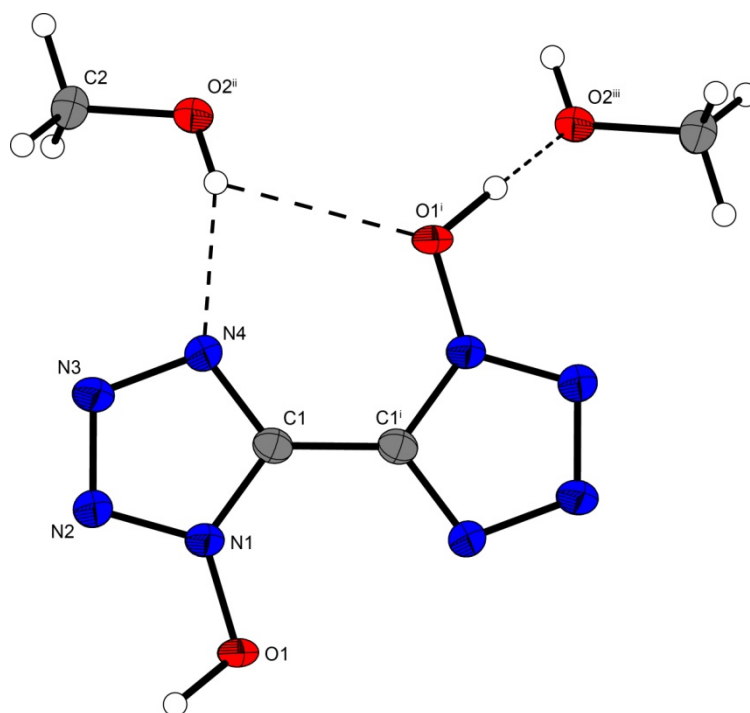


Figure S4 Molecular moiety of **1,1'-BTO · 2MeOH**. Ellipsoids are drawn at the 50 % probability level. Selected bond lengths (Å): O1–N1 1.349(2), O2–C2 1.451(3), N4–C1 1.329(3), N4–N3 1.349(3), N1–N2 1.334(2), N1–C1 1.334(3), N3–N2 1.309(3), C1–C1ⁱ 1.438(4). Symmetry codes: (i) 2-x, -y, 1-z, (ii) 1.5-x, 0.5+y, z; (iii) -0.5+x, -0.5-y, 1-z.

3.5. Crystal structure of dimethylammonium 5,5'-bistetrazole-1,1'-diolate

The dimethylammonium salt formed during the one-pot synthesis of TKX-50 was recrystallized from water. It crystallizes in the orthorhombic space group *Pbca* with eight molecules in the unit cell and a calculated density of 1.562 g cm⁻³.

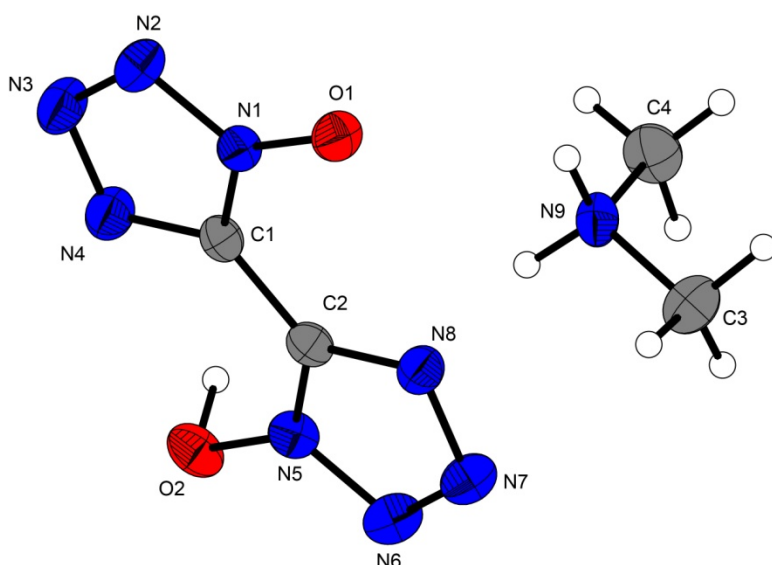


Figure S5 Molecular structure of dimethylammonium 5-(1-hydroxytetrazolyl)-5-(1-oxidotetrazolate). Selected bond lengths (Å): O2–N5 1.346(2), O1–N1 1.333(2), N9–C4 1.472(3), N9–C3 1.480(3), N7–N6 1.300(3), N7–N8 1.361(2), N2–N3 1.310(2), N2–N1 1.337(2), N1–C1 1.335(3), N3–N4 1.350(2), N8–C2 1.331(3), N5–C2 1.340(3), N5–N6 1.342(3), N4–C1 1.333(3), C2–C1 1.445(3)

4. Explosive performance

4.1. Heat of formation calculations

Electronic energies (CBS-4M method) were calculated with the Gaussian09 Revision A.02 software.¹⁶ Gas phase enthalpies of formation were computed using the atomization method (equation 1) often described recently.¹⁷

$$\Delta_f H^\circ_{(g, M, 298)} = H_{(Molecule, 298)} - \sum H^\circ_{(Atoms, 298)} + \sum \Delta_f H^\circ_{(Atoms, 298)} \quad (1)$$

The gas phase enthalpy of formation of TKX-50 was converted into the solid state enthalpy of formation by subtraction of lattice enthalpies ($\Delta_L H = 1515.6 \text{ kJ mol}^{-1}$) calculated according to Jenkins et al.^{18,19} Detonation parameters were calculated with the EXPLO5.05 computer code.^{20,21}

Table S2. CBS-4M calculation results and molecular volume taken from X-ray solution at 100 K.

M	$-H^{298}$ / a.u.	$\Delta_f H^\circ(\text{g,M})$ / kJ mol ⁻¹	V_M / nm ³
C	37.786156	716.7 (NIST value)	
H	0.500991	218.0 (NIST value)	
N	54.522462	472.7 (NIST value)	
O	74.991202	249.2 (NIST value)	
NH₄O⁺	131.863217	687.2	
BTO²⁻	663.687267	587.7	
TKX-50		131.2	0.204

Lastly, the molar standard enthalpies of formation (ΔH_m) were used to calculate the molar solid state energies of formation (ΔU_m) according to equation (2) (Table S2).

$$\Delta U_m = \Delta H_m - \Delta n RT \quad (2) \quad (\Delta n \text{ being the change of moles of gaseous components})$$

4.2. Small scale shock reactivity test

The Small-Scale Shock Reactivity Test (SSRT)^{22,23} was introduced by researchers at IHDIV, DSWC (Indian Head Division, Naval Surface Warfare Center). The SSRT measures the shock reactivity (explosiveness) of energetic materials, often well-below critical diameter, without requiring a transition to detonation. The test setup combines the benefits from a lead block test²⁴ and a gap test.²⁵ In comparison to gap tests, the advantage is the use of a much smaller sample size of the tested explosive (ca. 500 mg). The sample volume V_s is recommended to be 0.284 mL (284 mm³). For our test setup no possible attenuator (between detonator and sample) and air gap (between sample and aluminum block) was used. The used sample weight m_s was calculated using the formula $V_s \times \rho_{\text{Xray}} \times 0.95$. Several tests with commonly used explosives such as TNT, PETN, RDX, HMX and also CL-20 were performed in order to obtain different dents within the aluminum plate. The dent sizes were measured by filling them with powdered SiO₂ and measuring the resulting weight.

Table S3. Results from the Small Scale Shock Reactivity Test (SSRT).

Explosive	weight [mg]	dent [mg SiO ₂]
RDX	504	589
CL-20	550	947
TKX-50	509	857

4.3 Flame test

The flame test is an essential and easy test within for our coworker in order to get first impression of the energetic behavior of a new compound. TKX-50 burns intensively without smoke and significantly residues when brought into an open flame.

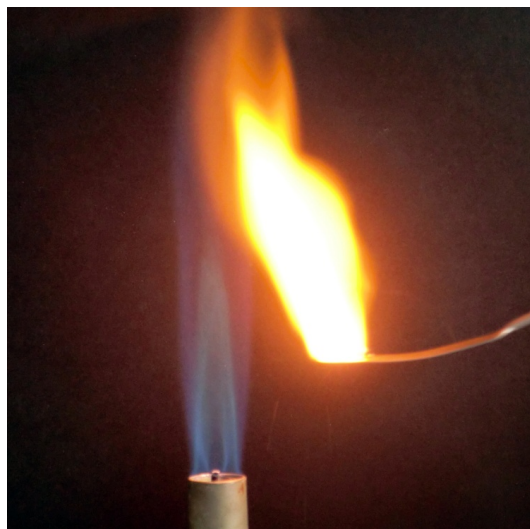


Figure S6 TKX-50 held in the flame on a spatula burns without detonation.

4.4 Hot plate test

Typical secondary explosives deflagrate when heated and show no deflagration-to-detonation transition. Latter case can be heard by fulmination of the compound or deformation of the copper plate of the hot-plate test setup. In the hot-plate test the compound is placed on a 2 mm copper plate and heated with a Bunsen burner below.

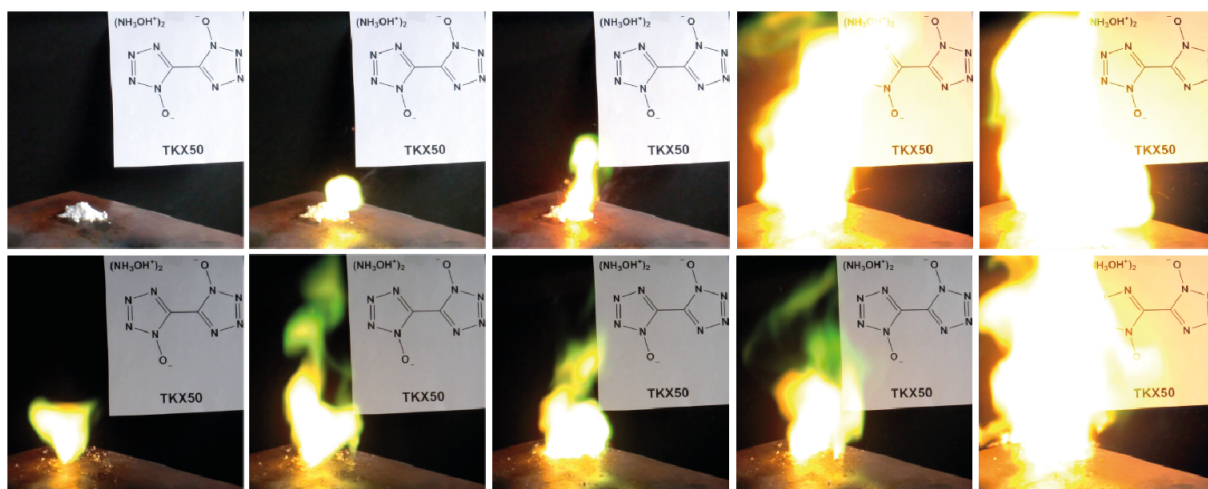


Figure S7 TKX-50 on a copper plate with a Bunsen burner underneath only burns without detonation.

5. Toxicity assessment

The sample dilution sequence corresponds to DIN 38412 L34, which ranges from 1:2 to 1:32 dilution of the compound in the test system. For better reproducibility, all dilution steps were made in duplicate. The change of intensity of bacterial luminescence in the absence (controls) and in the presence (samples) of the tested substances after different incubation times (15 min, 30 min) were recorded. The controls (2% NaCl only) were measured for calculating the correction factor, which is necessary to consider the normal decrease of luminescence without any toxic effect per time. The EC_{50} value can be determined by plotting $\log \Gamma$ against $\log c$, where $\Gamma = \text{inhibition (in \%)} / 100 - \text{inhibition (in \%)}$ and $c = \text{concentration of the test sample}$. The EC_{50} value is identical with the intersection of the resulting graph with the X-axis ($\Gamma = 0$). For better comparison of the resulting toxicities we also determined the toxic effect of RDX to the bacterial strain under the same conditions applied for the toxicity assessment of TKX-50. To imitate the natural environment of the employed marine bacterium as good as possible, the samples need to be diluted with a 2% (w/v) sodium chloride solution. Since RDX is barely soluble in water, a stock solution in acetone was prepared, which was further diluted with the sodium chloride solution to a mixture containing 200 ppm RDX in water/acetone 99/1 (v/v). The poor water solubility of 5,5'-bistetrazole-1,1'-diolates also sets problems during the toxicity tests of TKX-50. Here, an aqueous solution containing 1467 ppm TKX-50 was prepared and sodium chloride was added to adjust the final sodium chloride concentration of the stock solution to 2 % (w/v). Since disodium 5,5'-bistetrazole-1,1'-diolate shows nearly as poor water solubility as TKX-50, no higher concentration of the investigated compound could be used without precipitating disodium 5,5'-bistetrazole-1,1'-diolate tetrahydrate from the stock solution.

6. Fast Cook-Off Test

In order to get an "Interim Hazard Classification" also a fast cook-off test²⁶ (FCO, UN test 3d) was performed in which TKX-50 deflagrated (no explosion occurred). The setup of the FCO is shown in Figure S7. 10 g TKX-50 were loaded in a plastic sample container (unconfined, without cap) and placed in sawdust soaked with kerosene. The kerosene was ignited and the reaction was recorded with a video camera. After ~80 s TKX-50 deflagrated controlled within ~9 s (see supplementary video).



Figure S8 Fast Cook-Off Test of TKX-50

References

1. <http://www.linseis.com>
2. NATO standardization agreement (STANAG) on explosives. *Impact sensitivity tests*. No. 4489, 1st ed., Sept. 17, 1999.
3. WIWEB-Standardarbeitsanweisung 4-5.1.02, Ermittlung der Explosionsgefährlichkeit, hier der Schlagempfindlichkeit mit dem Fallhammer, Nov. 8, 2002.
4. <http://www.bam.de>
5. NATO standardization agreement (STANAG) on explosive. *Friction sensitivity tests*. No. 4487, 1st ed., Aug. 22, 2002.
6. WIWEB-Standardarbeitsanweisung 4-5.1.03, Ermittlung der Explosionsgefährlichkeit oder der Reibeempfindlichkeit mit dem Reibeapparat, Nov. 8, 2002.
7. Impact: Insensitive > 40 J, less sensitive ≥ 35 J, sensitive ≥ 4 J, very sensitive ≤ 3 J; friction: Insensitive > 360 N, less sensitive = 360 N, sensitive < 360 N a. > 80 N, very sensitive ≤ 80 N, extreme sensitive ≤ 10 N; according to the UN recommendations on the transport of dangerous goods.
(+) Indicates: not safe for transport.
8. <http://www.ozm.cz>
9. CrysAlis CCD, Oxford Diffraction Ltd., Version 1.171.27p5 beta (release 01-04-2005 CrysAlis171.NET) (compiled Apr 1 2005,17:53:34).

10. CrysAlis RED, Oxford Diffraction Ltd., Version 1.171.27p5 beta (release 01-04-2005 CrysAlis171.NET) (compiled Apr 1 2005,17:53:34).
11. Altomare, A.; Cascarano, G.; Giacovazzo C.; Guagliardi, A. *J. Appl. Cryst.* **1993**, *26*, 343.
12. Sheldrick, G. M. SHELXL-97. Program for the refinement of crystal structures. University of Göttingen, Germany, 1997.
13. Spek, A. L. PLATON, A multipurpose crystallographic tool, Utrecht University, Utrecht, The Netherlands, 1999.
14. Farrugia, L. J. WinGX suite for small molecule single-crystal crystallography. *J. Appl. Cryst.* **1999**, *32*, 837.
15. SCALE3 ABSPACK - An Oxford Diffraction program (1.0.4,gui:1.0.3) (C), Oxford Diffraction Ltd., 2005.
16. Frisch, M. J. et al, Gaussian 09, Revision A.02, Gaussian, Inc., Wallingford CT, 2009.
17. Fischer, N.; Klapötke, T. M.; Stierstorfer, J.; Wiedemann, C. *Polyhedron* **2011**, *30*, 2374–2386.
18. Jenkins, H. D. B.; Roobottom, H. K.; Passmore, J.; Glasser L. *Inorg. Chem.* **1999**, *38*, 3609–3620.
19. Jenkins, H. D. B.; Tudela, D.; Glasser L. *Inorg. Chem.* **2002**, *41*, 2364–2367.
20. Sucéska, M. *EXPLO5.05 program*. Zagreb, Croatia, 2010.
21. Sucéska, M. *Mater. Sci. Forum* **2004**, *465-466*, 325–330.
22. Felts, J. E.; Sandusky, H. W.; Granholm, R. H. *AIP Conf. Proc.* **2009**, *1195*, 233.
23. Sandusky, H. W.; Granholm, R. H.; Bohl, D. G. IHTR 2701, Naval Surface Warfare Center, Indian Head, MD, 12 Aug 2005.
24. Mayer, R.; Köhler, J. Homburg, A. *Explosives*, 5th ed., Wiley VCH, Weinheim, 2002, 197-200.
25. Mayer, R.; Köhler, J. & Homburg, A. *Explosives*, 5th ed., Wiley VCH, Weinheim, 2002, 148.
26. TB 700-2 NAVSEAINST 8020.8B TO 11A-1-47 DLAR 8220.1, *Joint Technical Bulletin*, Department of Defense ammunition and explosives hazard classification procedures, Headquarters Departments of the Army, the Navy, the Air Force, and the Defense Logistics Agency Washington, DC, 5 January 1998.

Full Paper

The Facile Synthesis and Energetic Properties of an Energetic Furoxan Lacking Traditional “Explosophore” Moieties: (E,E)-3,4-bis(oximomethyl)furoxan (DPX1)

Thomas M. Klapötke,^{*a, b} Davin G. Piercey,^a Joerg Stierstorfer^a^a Department of Chemistry, Energetic Materials Research, Ludwig-Maximilian University Munich, LMU, Butenandtstr. 5–13, 81377 Munich (Germany)
e-mail: tmk@cup.uni-muenchen.de^b Center for Energetic Concepts Development, CECD, Department of Mechanical Engineering, University of Maryland, UMD, College Park, MD 20742 (USA)

Received: May 4, 2010; revised version: September 16, 2010

DOI: 10.1002/prop.201000057

Abstract

Energetic furoxan (E,E)-3,4-bis(oximomethyl)furoxan (DPX1) was synthesized in 75% yield, using a literature procedure, from a precursor readily available in one step from nitromethane. DPX1 was characterized for the first time as an energetic material in terms of calculated performance ($V_{\text{det}} = 8245 \text{ m s}^{-1}$; $p_{\text{C-J}} = 29.0 \text{ GPa}$) and measured sensitivity (impact: 10 J; friction: 192 N; $T_{\text{dec}}: 168^\circ\text{C}$). DPX1 exhibits a sensitivity less than that of RDX, and a performance significantly higher than 2,4,6-trinitrotoluene (TNT).

Keywords: Energetic Materials, Furoxan, Oxime, X-ray

1 Introduction

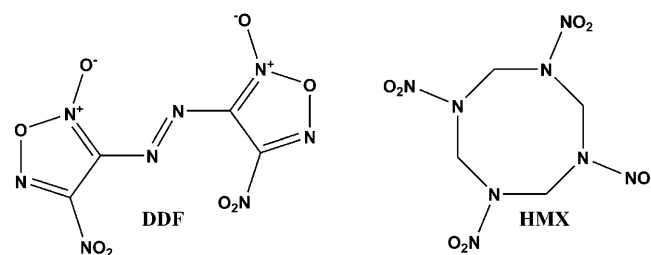
Furoxan (1,2,5-oxadiazole 2-oxide) based energetic materials constitute a recurring trend in the research of new explosives. Their endothermic heat of formation [1] and high nitrogen and oxygen content allow selected substituted furoxans [2] to possess detonation parameters, both calculated and experimental one, reaching levels significantly above that of HMX (Figure 1). The highly energetic nature of furoxans is also resultant from the unique nature of furoxans as being the N-oxide of furazans; forming the N-oxide of the corresponding heterocycle is a known method to increase the crystal density and stability of energetic materials, and as such, their performance [3]. For example, DDF (Figure 1) has an experimental detonation velocity reaching above 10000 m s^{-1} [4].

Unfortunately, the preparation of many new high-performing energetics can be laborious. The preparation of DDF can be seven or more steps depending on the

chosen synthetic precursor [5]. The preparation of octanitrocubane (ONC), another exceedingly high-performance energetic, has more than 10 steps in its synthesis [6].

Fortunately, the synthesis of symmetrical furoxans can be quite facile; dimerization of a nitrile oxide forming a furoxan is a well known reaction, oftentimes unintentional during the use of nitrile oxides in cycloaddition reactions [7,8]. The production of furoxan-containing compounds is often aimed at for their anticancer [9] or NO-releasing [10] properties. To the best of the authors' knowledge, nitrile oxide dimerization to furoxans has not been extensively exploited for the synthesis of energetic molecules.

(E,E)-3,4-bis(oximomethyl)furoxan (DPX1) has been known for over 100 years and was originally termed “isocyanilic acid” [11], but until this publication its explosive properties have never been realized; it has been stated that DPX1 was not explosive [12]. DPX1 was originally discovered as a hydrolysis product of fulminic acid (DPX1, $\text{C}_4\text{H}_4\text{N}_4\text{O}_4$ is a tetramer of fulminic acid, HCNO),

**Figure 1.** Structures of DDF and HMX.

and first prepared in poor yields from dangerous masses of mercury fulminate (1 kg of Hg fulminate would yield 1 g of DPX1) [11]. Since its discovery, new methods of synthesis have been realized, including a convenient method allowing good yields in two steps from nitromethane [13].

Traditional explosophores are well known, and include common chemical functionalities such as nitro, nitramino, azido, perchlorate, nitrate, acetylide, and others. Consisting of only a furoxan ring and aldoximes, DPX1 is of interest as it is calculated to be a better performer than TNT, yet lacks all the traditional energetic functional groups.

In this study we have prepared DPX1 by the literature procedure [13] in good yields from the precursor nitroacetaldehyde oxime, which is available in one step from nitromethane [14]. We report the first modern, spectrochemical measurements of this material, the crystallographic properties, as well as calculated and experimental explosive and thermochemical properties.

2 Experimental Part

2.1 Synthesis

DPX1 was prepared in 75% yield and in high purity from nitroacetaldehyde oxime. Nitroacetaldehyde oxime was prepared from nitromethane via a literature procedure [14] (Scheme 1).

All reagents and solvents were used as received (Sigma–Aldrich, Fluka and Acros Organics). Decomposition temperature measurements were performed on a Linseis DSC at a heating rate of $5^{\circ}\text{C min}^{-1}$. ^1H , ^{13}C , and ^{15}N NMR spectra were recorded using a Jeol Eclipse 400 instrument. All chemical shifts are in ppm relative to TMS (^1H , ^{13}C) or nitromethane (^{15}N). IR spectra were recorded using a PerkinElmer Spektrum One FT-IR instrument. Raman spectra were measured using a PerkinElmer Spektrum 2000R NIR FT-Raman instrument equipped with an Nd-YAG laser (1064 nm). Elemental analyses were performed on a Netzsch STA 429 Simultaneous Thermal Analyser.

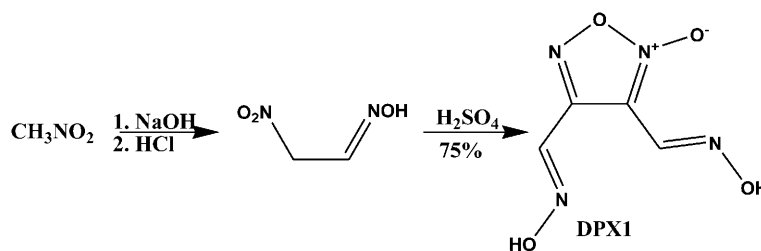
2.2 Synthesis of Nitroacetaldehyde Oxime

According to the literature procedure [14], 40 g of sodium hydroxide (1 mol) was dissolved in 80 mL of distilled water. To this solution 40 g (0.653 mol) of nitromethane was added over 2 h while maintaining the temperature between 45 and 50°C . The solution was stirred at this temperature for 20 min and then the dark red solution was cooled to 0°C , during which time a large mass of solid precipitated, increasing the viscosity of the solution. With efficient stirring and cooling, 85 mL of concentrated hydrochloric acid was added dropwise, keeping the temperature below 5°C . The addition took 1 h, after which the solution was bright yellow with a copious amount of precipitate. The precipitate was filtered and dried under high vacuum for 10 min, and dissolved in 200 mL ether. The ether was dried with a large mass of calcium chloride overnight, after which time the calcium chloride was filtered, rinsed with 200 mL ether, and the ethereal filtrate was evaporated to dryness under vacuum at ambient temperature. 19.23 g (57%) of nitroacetaldehyde oxime was obtained as a mixture of ~60% Z and ~40% E isomer. The material slowly decomposes at room temperature however can be stored indefinitely at -80°C . ^1H NMR (acetone- d_6 , 400.18 MHz, 25°C , TMS) 11.03 and 10.80 (s, 1H, oxime OH, E and Z, respectively), 7.64 ($J=6.0$ Hz) and 7.15 ($J=5.0$ Hz) (t, ^1H , oxime CH, Z and E, respectively), 5.44 ($J=5.0$ Hz) 5.25 ($J=6$ Hz) (d, 2H, nitro CH_2 , E and Z, respectively). ^{13}C NMR (acetone- d_6 , 100.63 MHz, 25°C , TMS) 149.9 and 139.8 (s, 1C, oxime C, Z, and, E respectively), 73.6 and 68.9 s, 1C, C– NO_2 , Z and E, respectively). NMR assignments for E and Z isomers are known in the literature [15]. EA: Calc. for $\text{C}_2\text{H}_4\text{N}_2\text{O}_3$ (MW = 104.07 g mol $^{-1}$): Calc. C 23.08, H 3.87, N 26.92; Found: C 22.94, H 3.73, N 26.97.

2.3 Synthesis of (E,E)-3,4-Bis(oximomethyl)furoxan (DPX1)

Caution! The prepared energetic furoxan is an explosive with sensitivity toward various stimuli. Although we had no problems during synthesis, proper protective equipment should be worn. Extra precautions should be taken when working on larger scale.

According to the literature procedure [13] 13 g (0.12 mol) of freshly-prepared nitroacetaldehyde oxime



Scheme 1. Synthesis of DPX1.

[14] was divided into three approximately equivalent portions. The first third was added slowly to 15 mL concentrated sulfuric acid keeping the temperature below 10 °C. To this solution 6.5 mL of a solution composed of 6 mL 65% oleum and 7 mL concentrated sulfuric acid was added under the same temperature control. The next third of nitroacetaldehyde oxime was added in a similar fashion, followed by the remaining 6.5 mL of oleum solution. The final third of nitroacetaldehyde oxime was added under the same temperature control. The solution was stirred for 10 min below 10 °C followed by removal of the cooling bath. The solution was allowed to self-warm while stirring to 30 °C where it maintained itself for an hour. The solution was then carefully poured over 215 g of crushed ice, and refrigerated for 12 h. After filtration and rinsing with cold water the yield was 8.04 g (75%) of DPX1. Recrystallization from nitromethane yielded crystals suitable for X-ray structure determination. m.p. 168 °C (dec.) (DSC, 5 °C min⁻¹). IR (cm⁻¹): 3365 (m), 3294 (m), 2360 (w), 2340 (w), 1626 (m), 1601 (s), 1498 (m), 1422 (m), 1342 (w), 1320 (w), 1273 (m), 1262 (w), 1131 (w), 1054 (w), 1007 (s), 996 (s), 966 (m), 919 (m), 903 (s), 868 (w), 854 (w), 796 (w), 730 (s), 702 (m). Raman (200 mW, cm⁻¹): 3057 (2), 3002 (2), 1626 (64), 1615 (7), 1592 (100), 1513 (39), 1488 (24), 1438 (11), 1337 (33), 1271 (20), 1129 (32), 1052 (9), 988 (9), 923. ¹H NMR (acetone-*d*₆, 400.18 MHz, 25 °C, TMS): 11.65 (s, 1H), 11.47 (s, 1H), 8.23 (s, 1H), 8.17 (s, 1H). ¹³C NMR (acetone-*d*₆, 100.63 MHz, 25 °C, TMS): 150.3 (1C), 138.9 (1C), 135.7 (1C), 108.7 (1C). ¹⁵N NMR (acetone-*d*₆, 40.55 MHz, 25 °C, CH₃NO₂) 9.01 (s, broad 2N), -7.83 (s, 1N), -26.36 (s, 1N) EA: Calc. for C₄H₄N₄O₄ (MW = 172.10 g mol⁻¹): Calc. C 27.92, H 2.34, N 32.55; Found C 27.45, H 2.37, N 32.21. MS DEI⁺ *m/z* (%) 172.1 (54) [M], 142.1 (18) [M-30], 126.1 (12), 112.1 (100) [M-60], 64.1 (44), 30.1 (41.6). Impact sensitivity: 10 J. Friction sensitivity: 192 N. Electrostatic discharge (ESD) sensitivity: 0.35 J.

3 Results and Discussion

3.1 Synthesis

The precursor nitroacetaldehyde oxide oxime exists as a mixture of E and Z isomers which are in equilibrium [15]. The equilibrium mixture of isomers used in this work was ~60:40 ratio of Z/E, and the 75% final yield of DPX1 which contains oximes only in the E conformation

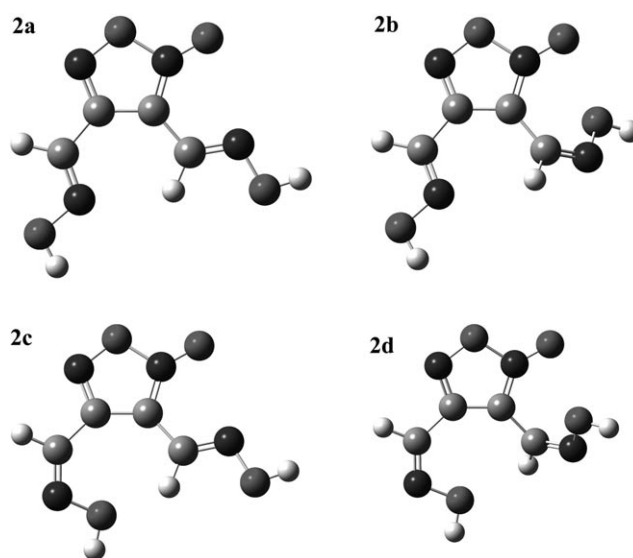


Figure 2. Various isomers of DPX1: E,E-DPX1 (**2a**), E,Z-DPX1 (**2b**), Z,E-DPX1 (**2c**), and Z,Z-DPX1 (**2d**).

indicates the Z-nitroacetaldehyde oxime has isomerized to the E prior to reaction.

3.3.1 Computational Energies

To understand why DPX1 forms solely in the E,E conformation calculations were performed on all (E,E, Z,E, E,Z, and Z,Z) isomers. All calculations were performed using the G03W code [16]. The structures were fully optimized without symmetry constraints at the MPW1PW91 level of theory using a correlation consistent double-zeta cc-pVDZ basis. True minima (*NIMAG*=0) were established and zero point energies calculated via frequency analyses.

The DFT calculations revealed that the only experimentally observed isomer **2a** (E,E-DPX1) is indeed the lowest energy isomer (see Table 1). All structure optimizations were performed without symmetry constraints (in *C*₁ symmetry), but only isomer **2a** optimized to a planar *C*_s structure. Whereas isomer **2c** remained close to planar, isomers **2b** and **2d** optimized to a structure with one of the =N–OH groups almost perpendicular to the plane of the five-membered ring (Figure 1).

Table 1. Relative energies of isomers of DPX1.

	E,E-DPX1	E,Z-DPX1	Z,E-DPX1	Z,Z-DPX1
Figure	2a	2b	2c	2d
- <i>i</i> /a.u.	674.347078	674.342439	674.339906	674.336326
MPW1PW91/cc-pVDZ				
<i>E</i> _{rel} (kJ mol ⁻¹)	0.0	12.1	18.8	28.1
p.g.	<i>C</i> ₁ → <i>C</i> _s	<i>C</i> ₁ → <i>C</i> ₁	<i>C</i> ₁ → <i>C</i> ₁	<i>C</i> ₁ → <i>C</i> ₁
<i>NIMAG</i>	0	0	0	0

3.2 X-Ray Structure

After recrystallization from nitromethane, crystals of DPX1 suitable for single crystal X-ray structure determination were obtained. The molecular structure of the crystalline DPX1 is shown in Figure 3.

The molecular structure was determined using an Oxford Xcalibur3 diffractometer with a Spellman generator (voltage 50 kV, 40 mA current) and a KappaCCD detector. The data collection was performed using the Crysalis CCD software [17]. Data reduction was performed with the Crysalis RED software [18], the structure was solved using the SIR-92 program [19], refined with SHELXL-97 [20] and finally checked with PLATON software [21]. The hydrogen atoms were located and refined. Relevant data and parameters of the X-ray measurements and refinements are given in Table 2.

DPX1 crystallizes in the monoclinic space group $P2_1/n$ with four molecules in the unit cell. The experimentally determined density is 1.744 g cm^{-3} . The bond distances in the furoxan ring are similar to those in other furoxans [22]. Both aldoximes in DPX1 exist in the E configuration, confirming the original confirmation suggested by Grundmann and agreeing with our calculations [13]. Of notable interest is the long O1–N1 distance in DPX1 of 144.79(17) pm; this is the longest bond in the furoxan heterocycle and longer than the O1–N2 bond at 137.53(17) pm. The shortest bond length of the heterocycle is within the N-oxide on N1 where the N1–O2 bond length is 122.61(15) pm. The oximomethyl groups on C2 and C1 deviate from the planarity of the furoxan ring only slightly, for example the torsion angle of $-174.63(14)$ for N2–C2–N4–O4 is twisted 5.37° out of plane. The supercell consists of layers of molecules of DPX1 when viewed along the b axis (Figure 4) with three unique hydrogen bonds, all within the layers. The hydrogen bond between H3a and N3 when considered in duplicate creates a conformationally stable 6-membered ring between neighboring molecules of DPX1 (Figure 5).

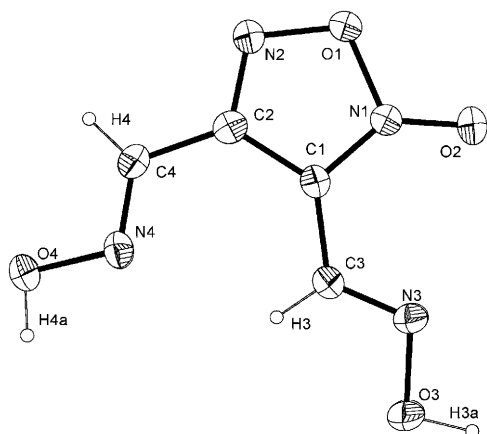


Figure 3. Molecular Structure of DPX1 in the crystalline state. Non-hydrogen displacement ellipsoids are shown at the 50% probability level.

Table 2. Crystal data and structure refinement parameters of DPX1.

Formula	$\text{C}_4\text{H}_4\text{N}_4\text{O}_4$
Formula Mass (g mol^{-1})	172.10
Crystal System	$P2_1/n$
Space Group	Monoclinic
a (pm)	6.5809(6)
b (pm)	11.1829(8)
c (pm)	9.2617(9)
α ($^\circ$)	90
β ($^\circ$)	105.947(10)
γ ($^\circ$)	90
V (pm^3)	655.37(10)
Z	4
ρ_{calc} (g cm^{-3})	1.744
$\lambda_{\text{MoK}\alpha}$ (pm)	71.073
T (K)	200(2)
θ min-max ($^\circ$)	4.30–25.99
Dataset h; k; l	–4; 8; –13; 13; –11; 10
Reflect. coll.	3287
Independ. Refl.	1272
R_{int}	0.0231
No. Parameters	125
R_1/wR_2 (all data)	0.0449/0.0799
R_1/wR_2 ($I > 2\sigma$)	0.0321/0.0768
Goof	0.945
Device type	Oxford Xcalibur3 CCD
Solution	SIR-92
Refinement	SHELXL-97
Absorpt. Corr.	Multi-Scan
CCDC	775100

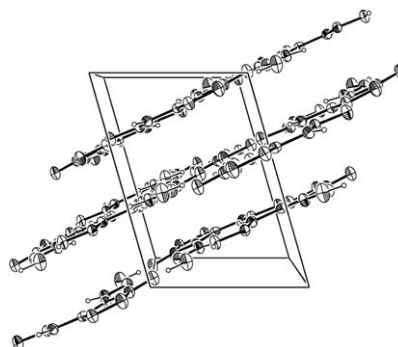


Figure 4. View of unit cell along b axis: repeating planes of molecules. Non-hydrogen displacement ellipsoids are at the 50% probability level.

3.3 Infrared Spectroscopy

DPX1 was analyzed by infrared spectroscopy. Characteristic identified bands are the OH stretching of the oximes at 3365 and 3294 cm^{-1} . Characteristic furoxan ring stretching bands [23] occur at 1422 and 1498 cm^{-1} . The band at 1602 cm^{-1} is appropriate for an oxime and also in the acceptable region for the diagnostic $\text{C}=\text{N}\rightarrow\text{O}$ stretch in a furoxan [24].

3.4 Mass Spectra

An acetone solution of DPX1 allowed detection of the $M+$ peak at $172.1 m/z$ during a DEI^+ experiment. Char-

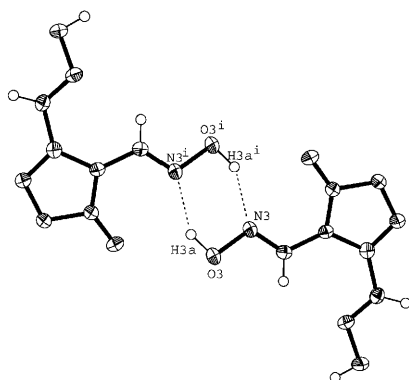


Figure 5. 6-Membered ring formed by hydrogen bonding. Non-hydrogen displacement ellipsoids are at the 50% probability level.

acteristic furoxan fragmentation [25] was observed as M-30 (142.1 m/z) and M-60 (112.1 m/z) corresponding to loss of one and two moles of NO, respectively. The remaining characteristic furoxan cleavage at $[M]/2$ was not observed.

3.5 NMR Spectroscopy

In order to calculate the NMR chemical shifts for ^1H and ^{13}C , the isotropic magnetic shieldings were computed using the Gauge-independent atomic orbital (GIAO) method implemented in G03 [16]. The NMR shielding tensors were calculated using the MPW1PW91/cc-pVDZ optimized structures at the MPW1PW91/aug-cc-pVDZ level of theory using the GIAO method [26–29]. The calculated spectra were compared with the experimental spectra and found to fit generally well.

3.5.1 ^1H NMR

Experimentally, the four protons in DPX1 appear in two general locations, with a pair of proton resonances at each. At 11.65 and 11.47 ppm the resonances corresponding to the oxime O–H protons occur; crystallographic H3a and H4a, respectively. These protons were calculated to occur at 7.1 and 7.0 ppm, respectively, and the relatively large difference is due to the calculated shifts being for a gas phase molecule, whereas in acetone solution the oxime OH protons are freer to ionize. At 8.23 and 8.17 ppm oxime C–H resonances occur; crystallographic H3 and H4, respectively. These were calculated to occur at 8.8 and 8.4 ppm, respectively, closer to experiment due to greatly decreased solvent effects for such less acidic protons. These assignments agree with commonly-available ^1H oxime proton shifts, and computation has revealed that the protons on the side of DPX1 possessing the N-oxide occur at higher chemical shifts.

3.5.2 ^{13}C NMR

The four inequivalent carbons in DPX1 occur as four singlets. The oxime carbons C3 and C4 occur at 135.7 and 138.9 ppm, respectively. These assignments agree very well with the calculated values of 135.1 and 140.8 ppm, respectively. The furoxan ring carbons, C1 and C2, occur at 108.7 and 150.3 ppm, respectively, also agreeing with the calculated values of 105.8 and 147.1. Assignments agree with values reported in the literature for similar compounds [23].

3.5.3 ^{15}N NMR

The spectrum shows three singlet resonances. The oxime nitrogens resonate at 9.01 ppm (broadened signal) as determined by comparison with literature spectra of oximes [30]. The furoxan non N-oxide and N-oxide nitrogens resonate at -7.83 and -26.36 ppm, respectively, as determined by comparison to literature spectra [31].

3.6 Differential Scanning Calorimetry (DSC)

For determination of the thermal stability of DPX1, a DSC experiment was run at a heating rate of 5°C min^{-1} . Exothermic decomposition occurred beginning at 168°C . No melting event was observed prior to decomposition.

3.7 Explosive Properties

3.7.1 Experimental Sensitivities

For initial safety testing, impact, friction, and ESD sensitivities were determined. Impact sensitivity was carried out according to STANAG 4489 [32] and modified according to instruction [33] on a BAM drophammer [34,35]. Friction sensitivity was carried out in accordance with STANAG 4487 [36] and modified according to instruction [37]. Sensitivity toward ESD was determined [38,39] on a small scale electric spark tester ESD 2010EN (OZM Research) operating with the “Winspark 1.15 software package” [40]. DPX1 has an impact sensitivity of 10 J, a friction sensitivity of 192 N and ESD sensitivity of 0.35 J. According to the UN Recommendations on the Transport of Dangerous Goods, DPX1 is classified as sensitive [41].

3.7.2 Computational Properties

3.7.2.1 Theoretical Calculations

All calculations were carried out using the Gaussian G03W (revision B.03) program package [16]. The enthalpies (H) and free energies (G) were calculated using the complete basis set (CBS) method of Petersson and coworkers in order to obtain very accurate energies. The CBS models use the known asymptotic convergence of pair natural orbital expressions to extrapolate from calcula-

Table 3. CBS-4M results.

	Point Group	el. State	$-H_{298}/\text{a.u.}$	NIMAG
DPX1	C_s		673.613761	0
H		$^2A_{1g}$	0.500991	0
C			37.786156	0
N		$^4A_{1g}$	54.522462	0
O			74.991202	0

tions using a finite basis set to the estimated CBS limit. CBS-4 begins with an HF/3-21G(d) geometry optimization; the zero point energy is computed at the same level. It then uses a large basis set SCF calculation as a base energy, and an MP2/6-31+G calculation with a CBS extrapolation to correct the energy through second order. An MP4(SDQ)/6-31+(d,p) calculation is used to approximate higher order contributions. In this study, we applied the modified CBS-4M method (**M** referring to the use of Minimal Population localization) which is a re-parameterized version of the original CBS-4 method and also includes some additional empirical corrections [42]. The enthalpies of the gas-phase species **M** were computed according to the atomization energy method (Eq. 1, Tables 3–5) [43].

$$\Delta_f H_{(g,M,298\text{K})}^\circ = H_{(Molecule,298\text{K})}^\circ - \sum H_{(Atoms,298\text{K})}^\circ + \sum \Delta_f H_{(Atoms,298\text{K})}^\circ \quad (1)$$

The solid state energy of formation (Table 6) of DPX1 was calculated by subtracting the heat of sublimation (83.1 kJ mol^{-1}) obtained by the Trouton rule ($\Delta_{\text{sub}}H = 188 \cdot T_m$, $T_m = 442 \text{ K}$) [45] from the gas-phase enthalpy (Table 5). The molar standard enthalpy of formation ($\Delta_f H^\circ$) was used to calculate the molar solid state energy of formation ($\Delta_f U^\circ$) according to Eq. (2) (Table 6).

Table 4. Literature values for atomic $\Delta_f H^\circ$ (298 K).

	NIST [44] (kcal mol ⁻¹)	(kJ mol ⁻¹)
H	52.1	218.1
C	171.3	717.2
N	113.0	473.1
O	59.6	249.5

Table 5. Enthalpies of the gas-phase species **M**.

M	M	$\Delta_f H_{(g,M,298\text{K})}^\circ$ (kJ mol ⁻¹)
DPX1	$C_4H_4N_4O_4$	+298.86

Table 6. Solid state energies of formation ($\Delta_f U^\circ$).

	$\Delta_f H^\circ(\text{s})$ (kcal mol ⁻¹)	$\Delta_f H^\circ(\text{s})$ (kJ mol ⁻¹)	Δn	$\Delta_f U^\circ(\text{s})$ (kJ mol ⁻¹)	M (g mol ⁻¹)	$\Delta_f U^\circ(\text{s})$ (kJ kg ⁻¹)
DPX1	51.5	215.7	-6	230.6	172.12	1339.83

$$\Delta_f U^\circ = \Delta_f H^\circ - \Delta n RT \quad (2)$$

(Δn being the change of moles of gaseous components).

3.7.2.2 Detonation Parameters

The calculation of the detonation parameters was performed with the program package EXPLO5 (version 5.04) [46]. The program is based on the chemical equilibrium, steady-state model of detonation. It uses the Becker–Kistiakowsky–Wilson’s equation of state (BKW EOS) for gaseous detonation products and Cowan–Fickett’s equation of state for solid carbon [46]. The calculation of the equilibrium composition of the detonation products is done by applying modified White, Johnson, and Dantzig’s free energy minimization technique. The program is designed to enable the calculation of detonation parameters at the *CJ* point. The BKW equation in the following form was used with the BKWN set of parameters ($\alpha, \beta, \kappa, \theta$) as stated below the equations and X_i being the mol fraction of *i*-th gaseous product, k_i is the molar covolume of the *i*-th gaseous product [47]:

$$pV/RT = 1 + xe^{\beta x} x = (\kappa \sum X_i k_i) / [V(T + \theta)]^\alpha$$

$$\alpha = 0.5, \beta = 0.176, \kappa = 14.71, \theta = 6620.$$

The detonation parameters calculated with the EXPLO5 program using the experimentally determined densities (X-ray) are summarized in Table 7 and compared to TNT and RDX.

4 Conclusion

From this combined experimental and theoretical study the following conclusions can be drawn

- (i) DPX1 was synthesized in high yield and purity, with a minimum of steps from commercially available precursors, and its structure in the solid state was determined by single crystal X-ray crystallography.

Table 7. Detonation parameters.

	DPX1	RDX	TNT
ρ (g cm ⁻³)	1.744	1.800	1.654
Ω (%)	-55.78	-21.61	-73.96
Q_v (kJ kg ⁻¹)	-6177	-6125	-5227
T_{ex} (K)	4168	4236	3657
p_{C-J} (GPa)	29.6	34.9	21.6
V_{det} (m s ⁻¹)	8236	8748	7253
V_0 (L kg ⁻¹)	645	739	574

(ii) DPX1 has a predicted detonation velocity of 8236 m s⁻¹ and a detonation pressure of 29.6 GPa, while having an impact sensitivity of 10 J and a friction sensitivity of 192 N; thus it is of lower sensitivity than RDX (Impact: 7 J, Friction: 120 N), while being significantly more powerful than TNT (V_{det} = 7253 m s⁻¹, p_{C-J} = 21.6 GPa). This is despite lacking traditional explosives.

Acknowledgement

Financial support of this work by the Ludwig-Maximilian University of Munich (LMU), the U.S. Army Research Laboratory (ARL), the Armament Research, Development and Engineering Center (ARDEC), the Strategic Environmental Research and Development Program (SERDP), and the Office of Naval Research (ONR Global, title: "Synthesis and Characterization of New High Energy Dense Oxidizers (HEDO) – NICOP Effort") under contract nos. W911NF-09-2-0018 (ARL), W911NF-09-1-0120 (ARDEC), W011NF-09-1-0056 (ARDEC), and 10 WPSEED01-002/WP-1765 (SERDP) is gratefully acknowledged. The authors acknowledge collaborations with Dr. Mila Krupka (OZM Research, Czech Republic) in the development of new testing and evaluation methods for energetic materials and with Dr. Muhamed Sucasca (Brodarski Institute, Croatia) in the development of new computational codes to predict the detonation and propulsion parameters of novel explosives. We are indebted to and thank Dr. Betsy M. Rice and Brad Forch (ARL, Aberdeen, Proving Ground, MD) and Gary Chen (ARDEC, Picatinny Arsenal, NJ) for many helpful and inspired discussions and support of our work. Dr. B. Krumm is also thanked for valuable NMR discussions.

References

- Y. N. Matyushin, V. I. Pepikin, S. P. Golova, T. I. Godovikova, L. I. Khmel'nitskii, Enthalpy of Formation of Dimethylfuroxan and Dimethylfuran. *Russ. Chem. Bull.* **1971**, 20, 162.
- Z. Ilya, K. George, Calculation of Thermochemical and Explosive Characteristics of Furoxanes, *11th Seminar New Trends in Research of Energetic Materials*, Pardubice, Czech Republic, April 9–11, **2008**, Pt. 1 425–433.
- L. Jia-Rong, Z. Jian-Min, D. Hai-Shan, Crystal Structure of 2,4,6-Trinitropyridine and Its N-Oxide, *J. Chem. Crystallogr.* **2005**, 35, 943.
- A. K. Sikder, N. Sikder, A Review of Advanced High Performance, Insensitive and Thermally Stable Energetic Materials Emerging for Military and Space Applications, *J. Hazard. Mater.* **2004**, 112, 1.
- A. N. Binnikov, A. S. Kulikov, N. N. Makhov, I. V. Orchinnikov, T. S. Pivina, 4-Amino-3-Azidocarbonyl Furoxan as an Universal Synthone for the Synthesis of Energetic Compounds of the Furoxan Series, *30th International Annual Conference of ICT*, Karlsruhe, Germany, June 29–July 2, **1999**, p. 58.
- P. E. Eaton, M. X. Zhang, R. Gilardi, N. Gelber, S. Iyer, R. Surapaneni, Octanitrocubane: A New Nitrocarbon, *Propellants, Explos., Pyrotechn.* **2002**, 27, 1.
- N. Arai, M. Iwakoshi, K. Tanabe, K. Narasaka, Generation of Nitrile Oxides from Oxime Derivatives by the Oxidation with Ammonium Hexanitratocerate(IV), *Bull. Chem. Soc. Jpn.* **1999**, 72, 2277.
- Z. X. Yu, P. Caramella, K. N. Houk, Dimerizations of Nitrile Oxides to Furoxans Are Stepwise via Dinitrosoalkene Diradicals: A Density Functional Theory Study, *J. Am. Chem. Soc.* **2003**, 125, 15420.
- M. Boiani, H. Cerecetto, M. Gonzáles, M. Risso, C. Oleazar, O. E. Piro, E. E. Castellano, A. L. Ceráin, O. Ezpeleta, A. Monge-Vega, 1,2,5-Oxadiazole N-Oxide Derivatives as Potential Anti-Cancer Agents: Synthesis and Biological Evaluation, Part IV, *Eur. J. Med. Chem.* **2001**, 36, 771.
- G. Sorba, C. Medana, R. Fruttero, C. Cena, A. D. Stilo, U. Galli, A. Gasco, Water Soluble Furoxan Derivatives as NO Prodrugs, *J. Med. Chem.* **1997**, 40, 463.
- J. Scholvien, Beiträge zur Kenntnis der Knallsäure, *J. Prakt. Chem.* **1885**, 32, 461.
- T. Urbanski, *Chemistry and Technology of Explosives*, Pergamon Press, Oxford **1967**, p. 134.
- C. Grundmann, G. W. Nickel, R. K. Bansal, Nitriloxide XVIII: Das Tetramere der Knallsäure(Isocyanilsäure) und Seine Derivate, *Justus Liebigs Ann. Der Chemie* **1975**, 1029.
- V. E. Matthews, D. G. Kubler, Improved Synthesis of Salts and Esters of Nitroacetic Acid, *J. Org. Chem.* **1960**, 25, 266.
- S. Brownstein, The Structures of Methazonic Acid and Its Anions, *J. Org. Chem.* **1963**, 28, 2919.
- M. J. Frisch, G. W. Trucks, H. B. Schlegel, G. E. Scuseria, M. A. Robb, J. R. Cheeseman, J. A. Montgomery, Jr., T. Vreven, K. N. Kudin, J. C. Burant, J. M. Millam, S. S. Iyengar, J. Tomasi, V. Barone, B. Mennucci, M. Cossi, G. Scalmani, N. Rega, G. A. Petersson, H. Nakatsuji, M. Hada, M. Ehara, K. Toyota, R. Fukuda, J. Hasegawa, M. Ishida, T. Nakajima, Y. Honda, O. Kitao, H. Nakai, M. Klene, X. Li, J. E. Knox, H. P. Hratchian, J. B. Cross, V. Bakken, C. Adamo, J. Jaramillo, R. Gomperts, R. E. Stratmann, O. Yazyev, A. J. Austin, R. Cammi, C. Pomelli, J. W. Ochterski, P. Y. Ayala, K. Morokuma, G. A. Voth, P. Salvador, J. J. Dannenberg, V. G. Zakrzewski, S. Dapprich, A. D. Daniels, M. C. Strain, O. Farkas, D. K. Malick, A. D. Rabuck, K. Raghavachari, J. B. Foresman, J. V. Ortiz, Q. Cui, A. G. Baboul, S. Clifford, J. Cioslowski, B. B. Stefanov, G. Liu, A. Liashenko, P. Piskorz, I. Komaromi, R. L. Martin, D. J. Fox, T. Keith, M. A. Al-Laham, C. Y. Peng, A. Nanayakkara, M. Challacombe, P. M. W. Gill, B. Johnson, W. Chen, M. W. Wong, C. Gonzalez, J. A. Pople, *Gaussian 03*, Revision C.02, Gaussian, Inc., Wallingford CT, **2004**.
- CrysAlis CCD*, Oxford Diffraction Ltd., Version 1.171.27p5 beta (release 01-04-2005 CrysAlis171.NET) (compiled April 1 **2005**, 17:53:34).

- [18] *CrysAlis RED*, Oxford Diffraction Ltd., Version 1.171.27p5 beta (release 01-04-2005 CrysAlis171.NET) (compiled April 1 **2005**, 17:53:34).
- [19] A. Altomare, G. Cascarano, C. Giacovazzo, A. Guagliardi, A Program for Crystal Structure Solution, SIR-92, *J. Appl. Cryst.* **1993**, *26*, 343.
- [20] G. M. Sheldrick, *Program for the Refinement of Crystal Structures, SHELXS-97*, University of Göttingen, Germany **1997**.
- [21] A. L. Spek, *A Multipurpose Crystallographic Tool, PLATON*, Utrecht University, Utrecht, The Netherlands **1999**.
- [22] A. F. Cameron, A. A. Freer, Crystal and Molecular Structure of 3-Methyl-4-Nitrofuroxan, C₃H₃N₃O₄, *Acta Crystallogr.* **1974**, *B30*, 354.
- [23] T. I. Godovikova, S. P. Golova, Y. A. Strelenko, M. Y. Antipin, Y. T. Struchlov, L. I. Khmeľnitskii, Synthesis and Properties of Unsubstituted Furoxan, *Mendeleev Commun.* **1994**, *4*, 7.
- [24] V. I. Kovalenki, V. L. Furer, L. I. Anisimova, E. M. Yagund, Vibration Spectra and Quantum Chemical Calculation of Optoelectronic and Force Parameters of Furoxan and Furoxan, *J. Struct. Chem.* **1994**, *35*, 799.
- [25] K. J. Hwang, I. Jo, Y. A. Shin, S. E. Yoo, J. H. Lee, Furoxans as Potential Nitric Oxide Generator: Mechanistic Speculation on the Electron Impacted Fragmentation, *Tetrahedr. Lett.* **1995**, *36*, 3337.
- [26] K. Wolinski, J. F. Hilton, P. Pulay, Efficient Implementation of the Gauge-independent Atomic Orbital Method for NMR Shift Calculations, *J. Am. Chem. Soc.* **1990**, *112*, 8251.
- [27] K. Wolinski, A. J. Sadlej, Self-consistent Perturbation Theory, *J. Mol. Phys.* **1980**, *41*, 1419.
- [28] R. Ditchfield, Self-consistent Perturbation Theory of Diamagnetism. 1. A Gauge-invariant LCAO (Linear Combination of Atomic Orbitals) Method for NMR Chemical Shifts, *Mol. Phys.* **1974**, *27*, 789.
- [29] R. McWeeny, Perturbation Theory for the Fock-Dirac Density Matrix, *Phys. Rev.* **1962**, *126*, 1028.
- [30] R. E. Botto, P. W. Westerman, J. D. Roberts, ¹⁵N Nuclear Magnetic Resonance Spectroscopy. Natural – Abundance ¹⁵N Spectra of Aliphatic Oximes, *Org. Magn. Reson.* **1978**, *11*, 510.
- [31] P. Cmoch, B. Kamiński, K. Kamińska-Trela, L. Stefaniak, G. A. Webb, Furoxan Rearrangement of some Pyridofuroxan Derivatives Studied by ¹H, ¹³C, ¹⁴N, ¹⁵N, and ¹⁷O NMR Spectroscopy, *J. Phys. Org. Chem.* **2000**, *13*, 480.
- [32] *NATO Standardization Agreement (STANAG) on Explosives, Impact Sensitivity Tests*, no. 4489, Ed. 1, Brussels, September 17, **1999**.
- [33] WIWEB-Standardarbeitsanweisung 4-5.1.02, Ermittlung der Explosionsgefährlichkeit, hier der Schlagempfindlichkeit mit dem Fallhammer, Erding, November 8, **2002**.
- [34] <http://www.bam.de>.
- [35] <http://www.reichel-partner.de>.
- [36] *NATO Standardization Agreement (STANAG) on Explosives, Friction Sensitivity Tests*, no. 4487, Ed. 1, Brussels, August 22, **2002**.
- [37] WIWEB-Standardarbeitsanweisung 4-5.1.03, Ermittlung der Explosionsgefährlichkeit oder der Reibeempfindlichkeit mit dem Reibeapparat, Erding, November 8, **2002**.
- [38] S. Zeman, V. Pelikán, J. Majzlík, Electric Spark Sensitivity of Nitramines. Part II. A Problem of 'Hot Spots', *Cent. Eur. J. Energ. Mater.* **2006**, *3*, 45.
- [39] D. Skinner, D. Olson, A. Block-Bolten, Electrostatic Discharge Ignition of Energetic Materials, *Propellants, Explos., Pyrotech.* **1998**, *23*, 34.
- [40] <http://www.ozm.cz/testinginstruments/small-scale-electrostatic-discharge-tester.htm>.
- [41] Impact: Insensitive >40 J, less sensitive ≥35 J, sensitive ≥4 J, very sensitive ≤3 J; Friction Insensitive >360 N, less sensitive =360 N, sensitive <360 N a. >80 N, very sensitive ≤80 N, extremely sensitive ≤10 N. According to: *UN Recommendations of the Transport of Dangerous Goods. Manual of Tests and Criteria* (Fourth revised ed.), New York and Geneva, United Nations, **2002**, ST/SG/AC.10/11/Rev 4.
- [42] a) J. W. Ochterski, G. A. Petersson, J. A. Montgomery Jr., A Complete Basis Set Model Chemistry V. Extension to Six or More Heavy Atoms, *J. Chem. Phys.* **1996**, *104*, 2598; b) J. A. Montgomery Jr., M. J. Frisch, J. W. Ochterski G. A. Petersson, A Complete Basis Set Model Chemistry VII. Use of the Minimum Population Localization Method, *J. Chem. Phys.* **2000**, *112*, 6532.
- [43] a) L. A. Curtiss, K. Raghavachari, P. C. Redfern, J. A. Pople, Assessment of Gaussian-2 and Density Functional Theories for the Computation of Enthalpies of Formation, *J. Chem. Phys.* **1997**, *106*(3), 1063; b) E. F. C. Byrd, B. M. Rice, Improved Prediction of Heats of Formation of Energetic Materials Using Quantum Chemical Methods, *J. Phys. Chem. A* **2006**, *110*(3), 1005–1013; c) B. M. Rice, S. V. Pai, J. Hare, Predicting Heats of Formation of Energetic Materials Using Quantum Chemical Calculations, *Comb. Flame* **1999**, *118*(3), 445–458.
- [44] P. J. Linstrom, W. G. Mallard, Eds., *NIST Chemistry Web-Book*, NIST Standard Reference Database Number 69, National Institute of Standards and Technology, Gaithersburg MD, 20899, <http://webbook.nist.gov> (retrieved March 30, 2010).
- [45] a) M. S. Westwell, M. S. Searle, D. J. Wales, D. H. Williams, Empirical Correlations between Thermodynamic Properties and Intermolecular Forces, *J. Am. Chem. Soc.* **1995**, *117*, 5013–5015; b) F. Trouton, IV. On Molecular Latent Heat, *Philos. Mag.* **1884**, *18*, 54–57.
- [46] M. Sućeska, *EXPLO5.04 Program*, Zagreb, Croatia, **2010**.
- [47] a) M. Sućeska, Calculation of Detonation Parameters by EXPLO5 Computer Program, *Mater. Sci. Forum* **2004**, *465*, 325; b) M. Sućeska, Calculation of Detonation Properties of C–H–N–O explosives, *Propellants, Explos., Pyrotech.* **1991**, *16*, 197; c) M. Sućeska, Evaluation of Detonation Energy from EXPLO5 Computer Code Results, *Propellants, Explos., Pyrotech.* **1999**, *24*, 280; d) M. L. Hobbs, M. R. Baer, Calibration of the BKW-EOS with a Large Product Species Data Base and Measured C-J Properties, *Proc. of the 10th Symp. (International) on Detonation*, ONR 33395-12, Boston, MA, July 12–16, **1993**, p. 409.

Davin Piercey

University of Munich
Butenandtstrasse 5-13 (Haus D)
D-81377 Munich
Germany

dpich@cup.uni-muenchen.de

Peer Reviewed Publications:

1. Bie, H.; Moore, S. H. D.; **Piercey, D. G.**; Tkachuk, A. V.; Zelinska, O. Ya.; Mar, A. "Ternary rare-earth titanium antimonides: Phase equilibria in the RE-Ti-Sb (RE = La, Er) systems and crystal structures of RE₂Ti₇Sb₁₂ (RE = La, Ce, Pr, Nd) and RETi₃(Sn_xSb_{1-x})₄ (RE = Nd, Sm)" *Journal of Solid State Chemistry* **2007**, *180*, 2216-2224.
2. Tkachuk, A. V.; **Piercey, D. G.**; Mar, A. "Ternary Zirconium Tin Antimonide ZrSn_{2-x}Sb_x (0.2 < x < 0.8), Different from the Parent Binaries ZrSn₂ and ZrSb₂" *Inorganic Chemistry* **2007**, *46*, 2877-2882.
3. Shaune L. McFarlane, Leah S. Coumont, **Davin G. Piercey**, Robert McDonald, and Jonathan G. C. Veinot. "One-Pot Synthesis of a Thermally Stable Blue Emitter: Poly[spiro(fluorene-9,9-(2-phenoxyxanthene)]". *Macromolecules*. **2008**, *41* (21), 7780-7782.
4. Shaune L. McFarlane, **Davin G. Piercey**, Leah S. Coumont, Ryan T. Tucker, Michael D. Fleischauer, Michael J. Brett, Jonathan G. C. Veinot. "Towards Thermally, Oxidatively, and Spectrally Stable Polyfluorene-Based Materials: Aromatic Ether-Functionalized Polyfluorene". *Macromolecules*. **2009**, *42* (3), 591-598.
5. **Davin G. Piercey**, Thomas M. Klapötke. "Nanoscale Aluminum-Metal Oxide (Thermite) Reactions for Application in Energetic Materials" *Central European Journal of Energetic Materials*. **2010**. 7 [2] 115-130.
6. Niko Fischer, Thomas M. Klapötke, **Davin Piercey**, Susanne Scheutzow, Jörg Stierstorfer. "Diaminouronium Nitriminotetrazolates – Thermally Stable Explosives" *Zeitschrift für anorganische und allgemeine Chemie*. **2010**, *636*, 2357-2363.
7. Michael Göbel, Konstantin Karaghisoff, Thomas M. Klapötke, **Davin G. Piercey**, Jörg Stierstorfer. "Nitrotetrazolate-2N-oxides, and the Strategy of N-oxide Introduction" *Journal of the American Chemical Society*. **2010**. *132* (48), 17216-17226.
8. Thomas M. Klapötke, **Davin G. Piercey**, Jörg Stierstorfer. "The Facile Synthesis and Energetic Properties of an Energetic Furoxan Lacking Traditional 'Explosophore' Moieties: (E,E)-3,4-bis(oximomethyl)furoxan (DPX1)" *Propellants, Explosives, Pyrotechnics*. **2011**. 36[2], 160-167.
9. Valentina Cauda, Christian Argyo, **Davin G. Piercey**, Thomas Bein, "Liquid Phase Calcination of Colloidal Mesoporous Silica in High-Boiling Solvents" *Journal of the American Chemical Society*, **2011**, 133[17] 6484-6486.

10. Thomas M. Klapötke, **Davin G. Piercey**. "1,1'-azobis(tetrazole): A Highly Energetic Nitrogen-Rich Compound with a N10 Chain" *Inorganic Chemistry*. **2011**. 50[7] 2732-2734.
11. Thomas M. Klapötke, **Davin G. Piercey**, Jörg Stierstorfer. "The Taming of CN7-: The Azidotetrazolate-2-Oxide Anion. *Chemistry a European Journal*. **2011**. 17[46] 13068-13077.
12. Denis Fischer, Thomas M. Klapötke, **Davin G. Piercey**, Jörg Stierstorfer. "Copper salts of halotetrazoles: laser-ignitable primary explosives" *Journal of Energetic Materials*. **2012**. 30[1] 40-54.
13. Niko Fischer, Thomas M. Klapötke, **Davin G. Piercey**, Jörg Stierstorfer. "Hydroxylammonium 5-Nitriminotetrazolates" *Zeitschrift fuer Anorganische und Allgemeine Chemie*. **2012**. 638[2], 302-310.
14. Thomas M. Klapötke, **Davin G. Piercey**, Jörg Stierstorfer. "Amination of Energetic Anions: High-Performing Energetic Materials" *Dalton Transactions*. **2012**. 41, 9451-9459.
15. Martin Härtel, Thomas M. Klapötke, **Davin G. Piercey** and Jörg Stierstorfer. "Synthesis and Characterization of Alkaline and Alkaline Earth Salts of the Nitrotetrazolate-2N-oxide Anion". *Zeitschrift fuer Anorganische und Allgemeine Chemie*. **2012**. 638, 2008-2014.
16. Dennis Fischer, Niko Fischer, Thomas M. Klapötke, **Davin G. Piercey**, Jörg Stierstorfer. "Pushing the Limits of Energetic Performance" *Journal of Materials Chemistry* **2012**, 22, 20418-20422.
17. Thomas M. Klapötke, **Davin G. Piercey**, Jörg Stierstorfer, Michael Weyrauther. "The Synthesis and Energetic Properties of 5,7-Dinitrobenzotetrazine-1,3-Dioxide." *Propellants, Explosives, Pyrotechnics*, **2012**, 37, 527-535.
18. Thomas M. Klapötke, **Davin G. Piercey**, Florian Rohrbacher, Jörg Stierstorfer. "Synthesis and Characterization of Energetic Salts of the 3,6-Bis(tetrazole-5-ylate)-1,2,4,5-Tetrazine Dianion" *Zeitschrift fuer Anorganische und Allgemeine Chemie*. **2012**. 638, 2235-2242
19. Thomas M. Klapötke, **Davin G. Piercey**, Jörg Stierstorfer. "The 1,4,5-Triaminotetrazolium Cation: A Highly Nitrogen Rich Moiety" *European Journal of Inorganic Chemistry*. **2012**, DOI: 10.1002/ejic.201200964, Early View.
20. Franziska Boneberg, Angie Kirchner, Thomas M. Klapötke, **Davin G. Piercey**, Jörg Stierstorfer. "A Study of Cyanotetrazole Oxides and Derivatives Thereof" *Chemistry An Asian Journal*. **2012**, Accepted, DOI 10.1002/asia.201200903.
21. Thomas M. Klapötke, **Davin G. Piercey**, Jörg Stierstorfer. "The 1,3-Diamino-1,2,3-triazolium Cation: A Highly Energetic Moiety." *European Journal of Inorganic Chemistry*, **2012**, accepted, DOI:10.1002/ejic.201201237.

Patents:

1. Jonathan Veinot, Shaune Lee McFarlane, Leah Coumont, **Davin Piercey**. "Aromatic Ether-Containing Spirofluorenexanthene Monomers, Methods for Their Preparation and Polymerization Thereof". U.S. Provisional Patent Application No. 61/138,360. Filed December 17, **2008**.

- Jonathan Veinot, Shaune Lee McFarlane, Leah Coumont, **Davin Piercey**. "Aromatic Ether-Containing Fluorene Monomers, Processes for Their Preparation and Polymerization Thereof". U.S. Provisional Patent Application No. 61/138,370. Filed December 17, **2008**.
- Thomas M. Klapötke, **Davin G. Piercey**, John W. Fronabarger, Michael D. Williams "A Simple One-Pot Synthesis of Copper(I) nitrotetrazolate from 5-aminotetrazole" **2012**. Patent in Progress, provisional patent number 61/680766.
- Dennis Fischer, Niko Fischer, Thomas M. Klapötke, **Davin G. Piercey**, Jörg Stierstorfer. "New explosives-secondary explosive with great performance and low sensitivity." **2012**. Patent in Progress

Book Chapters:

- Davin G. Piercey**, Thomas M. Klapötke, Amino and nitro tetrazoles: High nitrogen heterocycles, in "Inorganic Experiments", 2nd edn., J. D. Woollins (Ed.), Wiley-VCH, Weinheim, **2010**, p413-415.
- Davin G. Piercey**. "Nanothermites", chapter in "*Chemistry of High-Energy Materials*" Thomas M. Klapötke, de Gruyter, Berlin **2011**.

Education:

LUDWIG-MAXIMILIANS UNIVERSITY OF MUNICH, Munich, Bavaria, Germany
-PhD Energetic Materials Chemistry-synthesis of new primary and secondary explosives.
 -01/2010 to present

UNIVERSITY OF ALBERTA, Edmonton, Alberta, Canada

- Bachelor of Science with Honors, in Chemistry, with First Class Honors.

- 09/2005 to 04/2009.

- Latest year grade point average (on a 4 point scale): 4.0 (A)

- Latest 2 years grade point average (on a 4 point scale): 3.9

- Grade point average for all completed courses in university (on a 4 point scale): 3.5

- A+ in all undergraduate organic chemistry courses.

HARRY AINLAY COMPOSITE HIGH SCHOOL, Edmonton, Alberta, Canada

- 9/2002-6/2005

-Graduated with honors with distinction (Greater than 90% final average)

-100% final grade in Grade 12 chemistry (Chemistry 30)

Presentations:

- ORAL: Thomas M. Klapötke, **Davin G. Piercey**, Jörg Stierstorfer. "Advanced Energetic Materials: Compounds and Strategies" 94th Canadian Chemistry Conference and Exhibition, Calgary, Canada, May 26-30, 2012.
- POSTER: Thomas M. Klapötke, **Davin G. Piercey**, Jörg Stierstorfer. "The Taming of Azidotetrazole: The Azidotetrazolate-2-oxide Anion" 94th Canadian Chemistry Conference and Exhibition, Calgary, Canada, May 26-30, 2012.

3. ORAL: Michael Göbel, Konstantin Karaghiosoff, Thomas M. Klapötke, **Davin G. Piercey**, Jörg Stierstorfer. "The Nitrotetrazolate-2N-Oxide Anion: New Energetic Materials and Chemistry" 94th Canadian Chemistry Conference and Exhibition, Montreal, Canada, June 5-9, 2011.
4. POSTER: Thomas M. Klapötke, **Davin G. Piercey**. "Synthesis and Properties of a Highly-Energetic Compound Containing a Chain of Ten Nitrogen Atoms" 94th Canadian Chemistry Conference and Exhibition, Montreal, Canada, June 5-9, 2011.
5. POSTER: Thomas M. Klapötke, **Davin G. Piercey**. "A Highly Energetic Compound Containing a Ten-Nitrogen Chain" New Trends in the Research of Energetic Materials. Pardubice, Czech Republic, April 13-15, 2011.
6. ORAL: Michael Göbel, Konstantin Karaghiosoff, Thomas M. Klapötke, **Davin G. Piercey**, Jörg Stierstorfer. "Energetic salts and chemistry of the nitrotetrazolate-2N-oxide anion" New Trends in the Research of Energetic Materials. Pardubice, Czech Republic, April 13-15, 2011.
7. POSTER: **Piercey, Davin G.**; Klapötke, Thomas M.; Mayr, Norbert T.; Scheutzow, Susanne; Stierstorfer, Jörg. Silver Nitriminotetrazolate: A Promising Primary Explosive. New Trends in the Research of Energetic Materials. Pardubice, Czech Republic, April 21-23, 2010.
8. POSTER: **Piercey, Davin G.**; Klapötke, Thomas M.; Mayr, Norbert T.; Scheutzow, Susanne; Stierstorfer, Jörg. Silver Nitriminotetrazolate: A Promising Primary Explosive. Western Canadian Undergraduate Chemistry Conference 2009. Kamloops, British Columbia, May 7-9th, 2009.
9. ORAL: **Piercey, Davin G.**; McFarlane, Shaune L.; Coumont, Leah S.; Veinot, Jonathan G. C. A Promising Blue-Emitting Polymer for Application in Optoelectronic Devices. Western Canadian Undergraduate Chemistry Conference 2009. Kamloops, British Columbia, May 7-9th, 2009.
10. POSTER: Coumont, Leah S.; McFarlane, Shaune L.; **Piercey, Davin G.**; Veinot J. G. C. Synthesis of Novel Fluorene-Based Materials for Polymer Light-Emitting Diode Applications. US-Japan POLYMAT 2008 Summit. Ventura Beach, California, Aug 8-13th, 2008.
11. POSTER: McFarlane, Shaune; Veinot, J. G. C.; Coumont, L. S.; **Piercey, D. G.**; Glover, L. A.; Sirtonski, M.; Ruhl, J.; Chisholm, R. A.; McDonald, R.; Tucker, R. T.; Fleischauer, M. D.; Brett, M. Towards stable blue-emitting polyfluorene materials: spiroxanthene and aromatic-ether containing materials. US-Japan POLYMAT 2008 Summit. Ventura Beach, California, Aug 8-13th, 2008.
12. POSTER: Sirtonski, Matthew R.; McFarlane, Shaune; Coumont, Leah S.; **Piercey, Davin G.**; Veinot, J. G. C. Polymer Blends as a Method of Improving the Optoelectronic Properties of PFO. US-Japan POLYMAT 2008 Summit. Ventura Beach, California, Aug 8-13th, 2008.
13. POSTER: Coumont, Leah S.; McFarlane, Shaune L.; **Piercey, Davin G.**; Veinot J. G. C. Synthesis of Novel Fluorene-Based Materials for Polymer Light-Emitting Diode Applications. 91st CSCCE National Meeting, Edmonton, Alberta, May 24 to May 28, 2008.
14. POSTER: McFarlane, Shaune; Coumont, L. S.; **Piercey, D. G.**; Glover, L. A.; Sirtonski, M.; Ruhl, J.; Chisholm, R. A.; McDonald, R.; Tucker, R. T.; Fleischauer, M. D.; Brett,

- M. Veinot, J. G. C.; Towards spectral stability in polyfluorene-based materials. 91st CSCCE National Meeting, Edmonton, Alberta, May 24 to May 28, 2008.
15. POSTER: Sirtonski, Matthew R.; McFarlane, Shaune; Coumont, Leah S.; **Piercey, Davin G.**; Glover, Lydia A.; Fleischauer, M. D.; Veinot, J. G. C. Synthesis and Characterization of Novel Aromatic-Ether Containing Polyfluorenes. 91st CSCCE National Meeting, Edmonton, Alberta, May 24 to May 28, 2008.
16. POSTER: Coumont, Leah S.; McFarlane, Shaune L.; **Piercey, Davin G.**; Veinot, Jonathan G. C. Synthesis of novel fluorene-based materials for polymer light-emitting diode applications. Western Canadian Undergraduate Chemistry Conference, Winnipeg, Manitoba, May 3 to May 5, 2008.

Conference Proceedings:

1. **Piercey, Davin G.**; Klapötke, Thomas M.; Mayr, Norbert T.; Scheutzow, Susanne; Stierstorfer, Jörg. Silver Nitriminotetrazolate: A Promising Primary Explosive. New Trends in the Research of Energetic Materials. Pardubice, Czech Republic, Proceedings of the seminar, April 21-23, **2010**. 625-629.
2. Thomas M. Klapötke, **Davin G. Piercey**. "A Highly Energetic Compound Containing a Ten-Nitrogen Chain" New Trends in the Research of Energetic Materials. Pardubice, Czech Republic, Proceedings of the seminar, April 13-15, **2011**. 1 752-762.
3. Michael Göbel, Konstantin Karaghiosoff, Thomas M. Klapötke, **Davin G. Piercey**, Jörg Stierstorfer. "Energetic salts and chemistry of the nitrotetrazolate-2*N*-oxide anion" New Trends in the Research of Energetic Materials. Pardubice, Czech Republic, Proceedings of the seminar, April 13-15, **2011**. 1, 163-194.
4. Thomas M. Klapötke, **Davin G. Piercey**, Jörg Stierstorfer, "Energetic Salts of the Azidotetrazolate-2-oxide Anion" New Trends in the Research of Energetic Materials. Pardubice, Czech Republic, Proceedings of the seminar, April 18-20, **2012**. Accepted, In press.

Popular Press/Media Highlights:

TECHNOLOGY TRANSFER BLOG

- "New Explosives-secondary explosive with great performance and low sensitivity." 2012.
- Response to work with TKX50: Patent advertising
- <http://www.technology-transfer-blog.com/inventions-physical-sciences/36-innovations/234-new-explosives-secondary-explosive-with-great-performance-and-low-sensitivity>

INORGANIC CHEMISTRY MOST READ E-ALERTS

- "1,1'-Azobis(tetrazole): A Highly Energetic Nitrogen-Rich Compound with a N₁₀ Chain"
- For having the 3rd most read article in inorganic chemistry in 2011.
- <http://c.acs.org/cyvzc/454149/0/676891/13308/0/D/0/0/kieq.html>

NATURE CHEMISTR BLOGROLL: BOOM!

- "Exploding Myths and Exploding Compounds" April 20, 2011
- In response to my work 1,1'-azobis(tetrazole)
- <http://www.nature.com/nchem/journal/v3/n5/full/nchem.1041.html>

CHEMISTRY WORLD

- “The explosive potential of nitrogen compounds” by Laura Howes, March 16, 2011.
- In response to my work 1,1'-azobis(tetrazole)
- www.rsc.org/chemistryworld/news/2011/March/16031102.asp

C&EN: THE SAFETY ZONE

- “A highly Energetic Nitrogen-Rich Compound” by Jylian Kemsley March 9, 2011.
- In response to my work 1,1'-azobis(tetrazole)
- cenblog.org/the-safety-zone/2011/03/a-highly-energetic-nitrogen-rich-compound/

INFINIFLUX

- “More Explosions” By Joel Kelly, March 9, 2011.
- In response to my work 1,1'-azobis(tetrazole)
- infiniflux.blogspot.com/2011/03/more-explosions.html

TOC ROFL

- “In case you were wondering what the properties of this little bugger were” March 8, 2011.
- In response to my work 1,1'-azobis(tetrazole)
- tocrofl.tumblr.com/post/3733875286/in-case-you-were-wondering-what-the-properties-of#notes

ARS TECHNICA

- “New explosives get bigger bang for the buck with extra oxygen” By: Yun Xie, Nov 2010.
- In response to my work with the nitrotetrazolate-2*N*-oxide anion
- arstechnica.com/science/news/2010/11/adding-oxygen-for-stronger-explosives.ars

THINGS I WON'T WORK WITH: IN THE PIPELINE

- “Things I Won't work with: Nitrotetrazole Oxides” By Derek Lowe, Nov 15, 2010.
- In response to my work with the nitrotetrazolate-2*N*-oxide anion
- pipeline.corante.com/archives/2010/11/15/things_i_wont_work_with_nitrotetrazole_oxides.php

INFINIFLUX

- “I value my eyebrows and hearing, thank you very much” By Joel Kelly, Nov 13, 2010.
- In response to my work with the nitrotetrazolate-2*N*-oxide anion
- infiniflux.blogspot.com/2010/11/i-value-my-eyebrows-and-hearing-thank-you.html